TECHNISCHE UNIVERSITÄT MÜNCHEN

Anorganisch-Chemisches Institut

# Metalla Affinity Labels – a New Route to Organometallic Enzyme Hybrids

## Thomas Reiner

Vollständiger Abdruck der von der Fakultät für Chemie der Technischen Universität München zur Erlangung des akademischen Grades eines

Doktors der Naturwissenschaften

genehmigten Dissertation.

Vorsitzender:            Univ.-Prof. Dr. K. Köhler

Prüfer der Dissertation:
  1.  Univ.-Prof. Dr. Dr. h.c. mult. W. A. Herrmann
  2.  Univ.-Prof. Dr. M. Groll
  3.  Univ.-Prof. Dr. J. Buchner

Die Dissertation wurde am 02.04.2009 bei der Technischen Universität München eingereicht und durch die Fakultät für Chemie am 11.05.2009 angenommen.

*For my parents.*

*They have taught me that knowledge is not a duty, but a gift.*

This thesis originated in the time between May 2006 and April 2009 at the Anorganisch-Chemisches Institut of Technische Universität München.

My special thanks go to

**Dr. Jörg Eppinger**

My spiritus rector, thanks for this both challenging as well as fascinating topic, your absolute trust in my skills, thank you for the interest which you had in my work and for all these invaluable scientific discussions, which were crucial for the success of this thesis.

Special thanks also go to

**Professor Dr. Dr. h. c. mult. Wolfgang A. Herrmann**

Thank you very much for the possibility to work in your chair and for the excellent infrastructure which I was allowed to use. Thank you also so much for the interest in my research and for all the support which I was granted.

# Abbreviations

| | |
|---|---|
| abs. | absolute |
| Ac | acetyl |
| ACN | acetonitrile |
| AcOH | acetic acid |
| AcOEt | acetic acid ethyl ester |
| Ar | aryl |
| BAPNA | α-N-Benzoyl-DL-arginine *p*-nitroanilide |
| BuLi | butyl lithium |
| Boc | di-*tert*-butyl dicarbonate |
| Bzl | benzyl |
| Cp | cyclopentadienyl |
| Cp* | pentamethyl cyclopentadienyl |
| CV | cyclic voltametry |
| $\delta$ | chemical shift (ppm) |
| DAST | (diethylamino)sulfur trifluoride |
| DCM | dichloromethane |
| DMF | dimethylformamide |
| DMSO | dimethylsulfoxide |
| eq. | equivalent |
| EDCI | 1-ethyl-3-(3-dimethylaminopropyl) carbodiimide hydrochloride |
| $Et_3N$ | triethylamine |
| EtOH | ethanol |
| $Et_2O$ | diethyl ether |
| ESI | electron spray ionization |
| GC | gas chromatography |
| h | hour(s) |
| HOPfp | 2,3,4,5,6-pentafluorophenole |
| HSQC | heteronuclear spin quantum correlation |
| $^{i}$Pr | Isopropyl |
| M | molar |
| m-Al | metalla affinity label |
| Me | methyl |
| MeOH | methanol |

| | |
|---|---|
| MHz | megahertz |
| min | minute(s) |
| mL | milliliter(s) |
| MS | mass spectrometry |
| NHS | N-hydroxy succinimide |
| NMR | nuclear magnetic resonance |
| *o* | ortho |
| OAc | acetate |
| O$^t$Bu | tert.-butanolate |
| OMEH | organometallic enzyme hybrid |
| TsOH | toluene sulfonyl |
| *p* | para |
| Ph | phenyl |
| ppm | parts per million |
| PS | polystyrene |
| py | pyridine |
| RT | room temperature |
| s | second(s) |
| SS-DCC | N-Cyclohexylcarbodiimide, N'-methyl polystyrene |
| Suc | succinimide |
| TFA | trifluoro acetic acid |
| THF | tetrahydrofurane |
| TOF | turn over frequency |

# Table of Contents

# A | General Introduction

# 1. Synthesis of enantiomerically pure compounds

The synthesis of enantiomerically pure compounds has attracted considerable interest during the last decades. Enantiomerically pure compounds form the crucial basis for a plethora of bulk and fine chemicals, among them pharmaceuticals,[1,2,3,4] fertilizers,[5,6,7] vitamins[8], flavors[9,10] or for example functionalized materials.[11] Developing and improving ways to access enantiomerically pure compounds is one of the scientific challenges of our time, as these compounds need to be synthesized on the one hand in the highest possible purity and on the other hand economically and ecologically friendly. There are three fundamental routes for the generation of enantiomerically pure compounds:

(I)     Enantiomer separation, both chemical as well as enzymatically

(II)    Conversion with a chiral precursor, derived from the chiral pool of naturally occurring enantiomerically pure compounds

(III)   Enantioselective reactions, both stoichiometric or catalytic

The separation of racemic mixtures of enantiomers obtained from unselective reactions is neither ecologically nor economically worthwhile, as enantiomeric mixtures can only be separated with considerable effort from each other. Furthermore, one of the enantiomers will in most cases be of no use for any application. The chiral pool of naturally occurring enantiomerically pure compounds provides only a restricted number of enantiomers, from which in most cases only one enantiomer is available. Therefore, the most multifaceted, economically and ecologically friendly route is enantioselective reactions. Asymmetric catalysis, which can be conducted heterogeneously, homogeneously or enzymatically, is definitely superior to stoichiometric reactions, which do not offer a very broad spectrum of different reactions. Modern asymmetric catalysis offers a plethora of efficient techniques to synthesize enantiopure substrates. The two major options are transition metals catalysts[12] or biocatalysis.[13]

## 1.1. Enantioselective homogeneous catalysis

During the last three decades, transition metal catalyzed reactions have attracted considerable attention in modern synthetic chemistry.[12] Transition metals as for example palladium, rhodium or ruthenium have been applied as highly efficient catalysts. For example, the pioneering work of Wilkinson and coworkers should be mentioned, who were the first to have found a soluble rhodium hydrogenation catalyst for sterically unhindered olefins (figure A1, **A1**).[14] William S. Knowles and coworkers improved this catalyst by introducing a chiral inner sphere environment through application of optically active ligands (**A2**).[15] Further examples for successful asymmetric catalysis are – amongst a large variety of others – for example the works of Noyori and coworkers (**A3**)[16,17,18] or Sharpless and coworkers (**A4**).[19,20,21]



**A1**                          **A2**                          **A3**                          **A4**
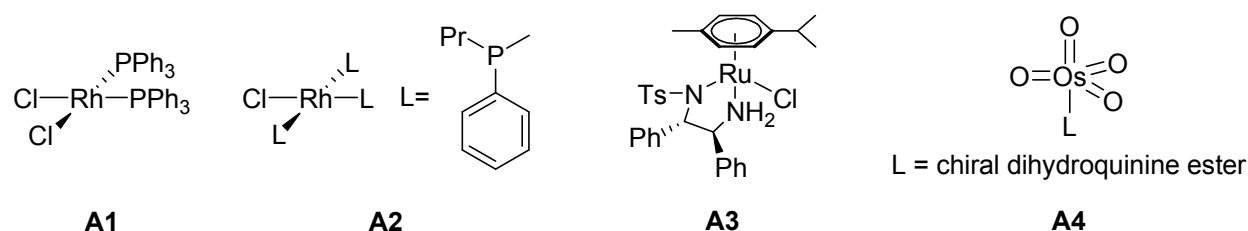
*Figure A1:* Homogeneous transition metal catalysts designed by Wilkinson *et al.*,[14] Knowles *et al.*,[15] Noyori *et al.*[18] and Sharpless *et al.*[19]

In spite of the enormous progress during the last decades, there have always been attempts to design and predict the performance of chiral ligands and homogeneous catalysts rationally. William S. Knowles himself commented this question by saying:

*„Since achieving 95% ee only involves energy differences of about 2 kcal, which is no more than the barrier encountered in a simple rotation of ethane, it is unlikely that before the fact one can predict what kind of ligand structures will be effective.“*[22]

Furthermore, not only the ligand structure, but also many reaction parameters (for example solvents, ions and counter ions, temperature, pressure or buffers) affect the nature of the inner and outer sphere coordination of homogeneous catalysts. Therefore, all these parameters have to be taken into account when interpreting the performance of one of these catalysts.[23]

Overall, while homogeneous catalysts have an enormous potential, their development is difficult and depends to a considerable amount to serendipity.

## 1.2. Enzymatic catalysis

Biocatalysis represents a complementary tool for the generation of enantiomerically pure compounds.[13] The performance of biocatalysts in many cases exceeds the results obtained for homogeneous catalysts in terms of regio- chemo- and stereoselectivity.[24] In addition to their inner coordination sphere, enzymes possess a well-defined outer coordination sphere – the protein scaffold. From the evolutionary standpoint, nature has optimized the chemical environment of biocatalysts for millions of years, and therefore optimized their efficiency and selectivity. In many cases, the outer coordination sphere provokes that the enzyme's active center can only be accessed through a narrow channel, which facilitates the high selectivity.[25] This outer sphere attribute is difficult to mimic and poses one of the major difficulties in the design of homogeneous catalysts. For example, virtually any center in a steroid can be selectively hydroxylated by choosing the appropriate microorganism.[13,24] For example, progesterone is being hydroxylated in the 11α-position by *Rhizopus arrhizus* or *Aspergillus niger*,[24,26] whereas lithiocholic acid is hydroxylated by *Fusarium equiseti* in 7β-position (figure A2).[27]



progesterone
*Rhizopus arrhizus*
*Aspergillus niger*

lithocholic acid
*Fusarium equiseti*
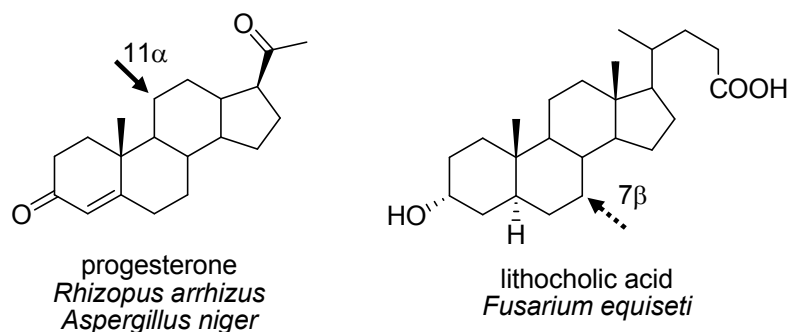
**Figure A2:** Microbial hydroxylation of steroids.[24]

Nevertheless, enzymes are much more restricted in terms of their application depth. In most cases, they are only active in aqueous solutions, highly specific in terms of the substrates which can be used, and catalyze only one type of reaction. A further problem is their lack of stability to variations of pH values or temperature. One possibility to overcome these problems is the punctual or random exchange of their native amino acids sequence.[28] Directed evolution combines techniques to generate enzyme mutants with efficient screening methods, which evaluate their performance in a short amount of time.[29,30] Currently, this concept seems to be promising to overcome disadvantages of biocatalysts.

## 1.3. Enzymatic and homogeneous catalysis – a comparison

The decision, whether the synthesis of a compound should be conducted by transition metal catalysts or biocatalysts is often of essential interest, as both classes of compounds not only show distinct differences in their behavior, but even seem to be diametral in terms of many of their features and properties (table A1). In the area of homogeneous catalysis, there have been considerable achievements during the last decades.[12,31,32,33,34] Nevertheless, to achieve asymmetric induction with homogeneous catalysts, appropriate ligand systems have to be applied, which stabilize one of the two possible diastereomeric transition states and therefore render predominately one product enantiomer. The advantage of homogeneous catalysts is their high tolerance in terms of reaction conditions and their broad spectrum of reactions which can be catalyzed. Enzymatic catalysis uses the native, chiral environment of enzymes to yield asymmetric products in very high yields and optical purities. Its applicability is hampered by its small spectrum of possible reactions and the low tolerance reaction conditions, as for example solvents, temperature or acidic/basic aqueous solutions (table A1).

***Table A1:*** Comparison of features of asymmetric enzymatic and homogeneous catalysis.[35,36]

|  | enzymatic catalysis | homogeneous catalysis |
| --- | --- | --- |
| reaction repertoire | small | large |
| substrate scope | small | large |
| second coordination sphere | well defined | ill defined |
| enantiomers | single enantiomer | both enantiomers |
| optimization | genetic | chemical |
| catalyst recovery | straightforward | difficult |
| turnover numbers | large | modest |
| reaction conditions | mild | harsh |
| reaction medium | mostly aqueous | aqueous and organic |

As presented in table A1, both enzymatic as well as homogeneous catalysis have their own specific advantages. A blend of their properties may be achieved via the synthesis of organometallic enzyme hybrids. They potentially combine the broad spectrum of possible reactions of homogeneous catalysts with the advantages of enzymatic catalysis. Therefore, the synthesis of this type of bioorganometallic hybrid system has more and more emerged into the focus of interest.[35,36,37]

## 1.4. Organometallic Enzyme Hybrids (OMEHs) – artificial Enzymes

Besides amino acid side chains, which are responsible for the formation of secondary and tertiary structures, and which may be activated if positioned in the appropriate electronical environment, nature also relies on cofactors and/or metal ions for the generation of a specific catalytic activity.[38] Presumably one third of all enzymes use metals. Several metallo-enzymes conduct highly difficult reactions (e.g. selective C-H activation or $N_2$ fixation) by stabilizing highly optimized stereo-electronic states within the catalytic cycle.

An interesting aspect of bioorganometallic chemistry arises from the combination of transition metals, which are predominantly applied in modern asymmetric homogeneous catalysis, and their interaction with enzyme scaffolds. In this area of research, the first successful experiment was conducted 1956 by Akabori and coworkers.[39] They obtained a promising enantiomeric excess, after having coated silk with palladium particles and applied the composite material in asymmetric hydrogenation reactions.

Enormous progress has been achieved since. Artificial enzymes have been created through alternation of the active sites of enzymes to accommodate transition metals.[40] Furthermore, also other macromolecular structures of biomolecules have been exploited to serve as chiral scaffolds for hybrid systems, as for example DNA[41] or antibodies.[42] These systems facilitate the combination of features, which have been formerly unique for either homogeneous catalysts or biocatalysts. Highly multifold is the class of organometallic enzyme hybrids (OMEHs).[36] They can be generated via chemical or biological modification of an enzyme and incorporation of an organometallic system into the active site of an enzyme. The enzyme itself serves as chiral ligand, thus facilitating regio- and/or stereoselectivity. It is worthwhile to divide organometallic enzyme hybrids into different classes, as Steinreiber *et al.* did recently.[36] In a first breakdown, artificial metalloenzymes can be divided by:

 

(I)     The type of metal introduced

(II)    The biomolecular scaffold

(III)   The anchoring strategy

In spite of the fact that the concept of organometallic enzyme hybrids is an efficient technique, there are not many publications dealing with this topic. Nevertheless, the variety of reactions which can be catalyzed, reaches deeply into the organometallic homogeneous catalysis. Besides chiral hydrogenations, asymmetric C-C bond formations or oxidations have been realized.[36] Table A1 summarizes an overview on reactions which have been catalyzed by organometallic enzyme hybrids.

**Table A2:** Reactions catalyzed by metalloenzymes.[36]

| reaction type | metal-complex | biomolecule host | anchoring strategy |
|---|---|---|---|
| hydrogenation | Rh-biotin | (strept)avidin | supramolecular[43,44,45,46,47] |
| | Rh | papain | covalent[45,46,48] a |
| | Rh-diphosphine | antibody | supramolecular[49] |
| | Pd | apo-ferritin | supramolecular[50] |
| ketone reduction | M-biotin (M = Ru, Ir, Rh) | (strept)avidin | supramolecular[51] |
| alcohol oxidation | Zn-Cu exchange | carboxypeptidase | dative[52] a |
| | M-biotin (M = Ru, Ir, Rh) | (strept)avidin | supramolecular[53] a |
| sulfoxidation | Mn, Fe-corrole | bovine serum albumin | dative[54] |
| | Cr, Mn–Schiff base | myoglobin | dative[55] |
| | Mn–Schiff base | myoglobin | covalent[56] |
| | $MO_4^{n-}$ (M=V, Mo, Re, Se, W) | hydrolases, ferritin | dative[57] |
| epoxidation | Mn-Schiff base | papain | covalent[45,58] |
| | Zn-Mn exchange | carbonic anhydrase | dative[59] |
| dihydroxylation | $OsO_4$ | bovine serum albumin | dative[60] |
| peroxidation | Se | subtilisin | covalent[61] a |
| | Fe-porphycene | myoglobin | dative[62] a |
| | Fe-hemin | DNA, RNA | supramolecular[63] a |
| hydrolysis | Cu-phenantroline | adipocyte lipid-binding protein | covalent[64,65] |
| Diels-Alder cycloaddition | Cu-Phtalocyanine | bovine serum albumin | dative[47,66] |
| | Cu-bidentate diimines | DNA | supramolekular[67] |
| hydroformylation | Rh | human serum albumin | dative[68] |
| acyl-transferase | Se | subtilisin | covalent[69] a |
| transamination | Cu-pyridoxamine | ribonuclease S | supramolekular[70] |
| DNA-cleavage | Cu-phenantroline | DNA-binding proteins | covalent[71] |
| | Zn | peptide-fragment with Rh-intercalator | covalent[72] |
| | Eu, Ce, Cu | helix-turn-helix / Ca-binding motive | covalent[73] |
| | Ce | complementary peptide nucleic acid | supramolecular[74] |

(a) no selectivity reported.

OMEHs differ by the reaction catalyzed, which is defined by the kind of metal centre introduced into the active site of the enzyme, the biological host (the protein scaffold surrounding the metal centre) and the anchoring strategy used for the fusion of both. The kind of interaction, the anchoring strategy, is possibly the most important criteria of discrimination between different organometallic enzyme hybrids.[36] There are in general three different strategies to anchor the organometallic species into the chiral protein scaffold:

(I)     Supramolecular anchoring

(II)    Dative anchoring

(III)   Covalent anchoring

## 1.4.1. Supramolecular anchoring[75]

Supramolecular anchoring describes all non-covalent interactions (e.g. hydrogen bonds, *Van-der-Waals* bonding) between organometallic catalyst species and enzyme.[76] The pioneer in this anchoring strategy was Whitesides *et al.*, who showed that an achiral rhodium(I) catalyst can be employed as an enantioselective hydrogenation catalyst by anchoring after biotinylation and reaction with (strept)avidin.[43] Ward *et al.* improved this technique by structural variations of the organometallic system and directed evolution of the enzyme scaffold, and successfully applied this system in the catalytic asymmetric transfer hydrogenation of olefins and ketone reduction.[44,51] In this context also the transporter proteins human and bovine serum albumin need to be noted. These proteins have the remarkable property to bind a large number of guest molecules. A variety of different organometallic enzyme hybrids have been designed based on these protein scaffolds (see table A1 for details).

## 1.4.2. Dative anchoring

Kaiser *et al.* were the first to modify the active site of an enzyme by dative modification. Hereby, copper instead of zinc was coordinated in the active site of carboxypeptidase A (CPA).[52] The first example of observed enantioselectivities with an organometallic enzyme hybrid were reported by Kokubo *et al.* in 1983.[60] He coordinated osmium tetroxide by dative anchoring to bovine human serum albumin. In the presence of *tert-*

Butylhydroperoxide as an oxidation agent, OsO₄@BSA has remarkable properties as a dihydroxylation catalyst (scheme A1). The authors assume, that $OsO_4$ is anchored by coordination of the transition metal center to two lysine residues in the hydrophobic enzyme active site of bovine serum albumin. For the dihydroxylation of α-methylstyrene, an enantioselectivity of 68% (S) was reported.
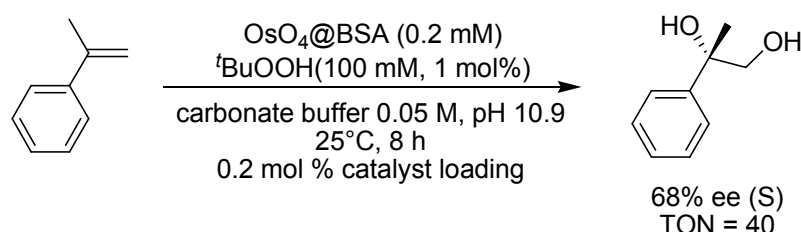


**Scheme A1:** Enantioselective dihydroxylation of olefins by OsO₄@BSA.[60]

### 1.4.3. Covalent anchoring

In 1977, it was also Kaiser *et. al.* who were the first to report covalent anchoring.[77] Via the modification of an amino acid residue with appropriately modified coenzyme analogoues, he created novel catalytic functions. The thiol group of flavopapain Cys25 was modified, converting a protease into a highly active oxidoreductase.
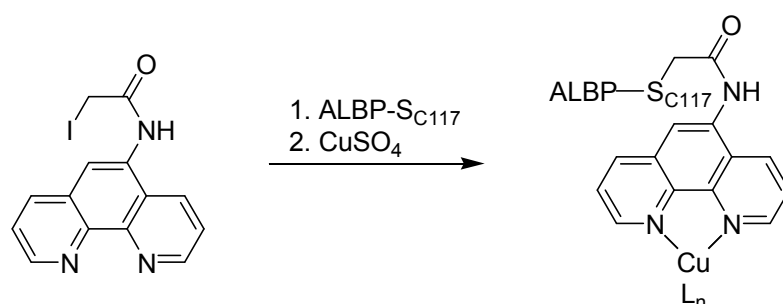


**Scheme A2:** preparation of Cu(II)Phen@ALBP.[64]

Also Distefano and coworkers were successful in covalent anchorage of organometallic catalysts to proteins.[64] They anchored 1,10-phenantroline covalently to adipocyte lipid-binding protein (ALBP) via an iodomethyl ketone. The sole cysteine residue in the protein reacts with iodoacetamido-1,10-phenantroline, resulting in covalent bond formation. After addition of copper(II), the organometallic enzyme hybrid Cu(II)Phen@ALBP is yielded. It was successfully applied in the asymmetric hydrolysis of non-activated amino acid esters.
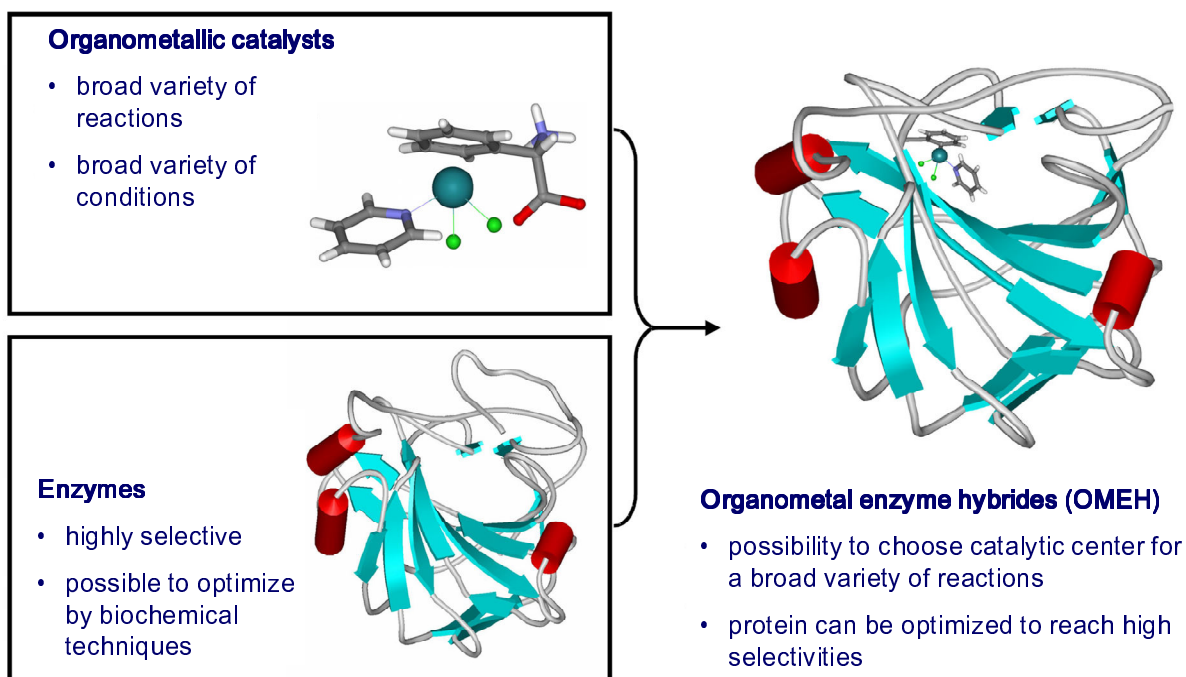
***Figure A3:*** Modification of an enzyme with a homogeneous organometallic catalyst, yielding an organometallic enzyme hybrid.

Furthermore, several other methodologies were published for covalent anchoring by Reetz,[45,47] Lu,[56] van Koten[78] and Salmian.[79] Overall, diverse covalent anchoring strategies can be applied as phosphonic acid esters, halo methyl ketones, Michael-type acceptors or other reactive groups can be utilized, rendering a wide spectrum of protein scaffolds they can be reacted with.

Generally, the fusion of homogeneous and enzymatic catalysis has developed into a vivid research area during the last decades. Especially during the last years, organometallic enzyme hybrids have drawn enormous attention due to reported novel activities and high selectivities.[36] Their catalytic and synthetic potential and applicability seems to be high, as they combine advantages of both organometallic catalysts and enzymes. On the one hand, they feature the enormous scope of reactions, which can be catalyzed by homogeneous catalysis, and on the other hand, their performance can be optimized rationally via directed evolution[29,30,51] and is not as much subject to serendipity[22] as the finding of good chiral ligand systems.

# 2. Cysteine and serine proteases

## 2.1. Properties and Mechanism of cysteine and serine proteases

Proteases or proteolytic enzymes represent by number the largest groups of enzymes. They selectively catalyze the hydrolysis of enzymes, and play a crucial role in numerous physiological processes such as digestion, blood coagulation, wound healing fertilization or for example cell differentiation. Uncontrolled, unregulated or undesired proteolysis can lead to many disease states. Amongst them emphysema, stroke, viral infections, cancer, Alzheimer's disease, inflammation or arthritis. Therefore, inhibition of proteases and thus regulation of proteases has a considerable potential for therapeutic intervention in numerous disease states.[80] This has resulted in extensive investigation of both the mechanism as well as the inhibition of proteases. Based on their catalytically active amino acid side chains, proteases can be separated in four major classes: Aspartatic, serine, cysteine and metalloproteases. By now, there are more than 450 peptidase (endopeptidase and exopeptidase) amino acid sequences available from more than 1400 organisms (bacteria, archaea, archezoa, protozoa, fungi, plants, animals, and viruses), which have been organized in families and clans by Rawlings and Barrett.[81] Their effort has lead to the development of the MEROPS[82] database, which now includes a frequently updated listing of all peptidase sequences.[83]
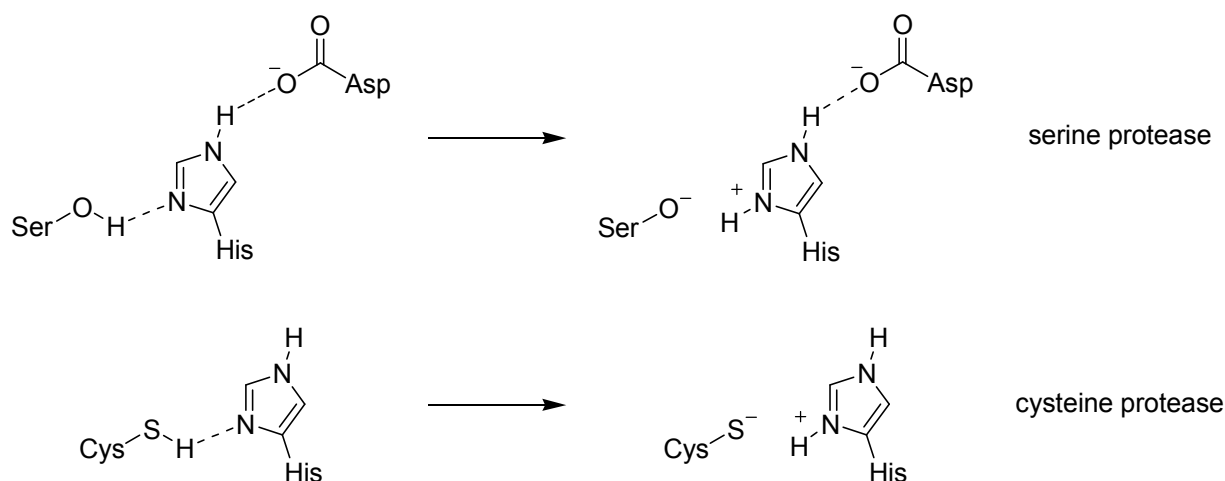


***Scheme A3:*** Mechanism of deprotonation in the active sites of serine and cysteine proteases.[80]

Serine and Cysteine-proteases are both readily available and cheap enzymes,[84] which have many characteristics in common. They feature in their active site a strong

nucleophile (serine or cysteine residue). Their nucleophilicity is strongly enhanced by a basic histidine group in close proximity. For serine proteases, the nucleophilicity is further enhanced by an aspartatic acid (scheme A3). Hydrolysis of a peptide bond is an energetically favored, yet extremely slow process.[85] Through their nucleophilic center, serine and cysteine proteases dramatically speed up this process, facilitated by the nature of their active site.
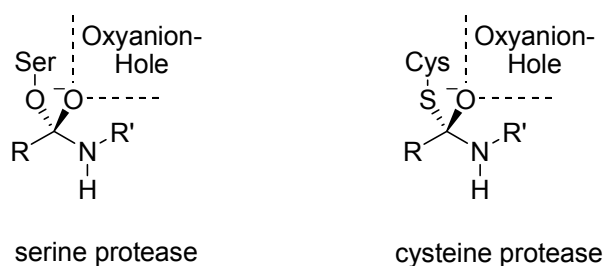


**Figure A4:** Transition states of serine and cysteine proteases during the hydrolytic cleavage of peptides.[80]

The strongly nucleophilic serine or cysteine residues attack carbonyl carbons of ester or amide bonds, resulting in hydrolytic cleavage of these groups. During this process, a tetrahedral intermediate is being formed (figure A4).[80] Thereafter, the negatively charged oxygen in the oxyanion hole is being protonated, and after addition of water, deacylation takes place. Proteases of the same family mainly differ in the design of their oxyanion hole and the amino acid residues involved in peptide hydrolysis. These different amino acid residues are casual for the selectivity of different types of proteases. Although they have almost identical active centers, the chiral enzyme environment of the active site pocket is different for every protease. In terms of organometallic enzyme hybrids, this difference is an enormous feature. Upon anchoring of an organometallic center to different kinds of serine or cysteine proteases, in spite of a possibly identical anchoring strategy, their active sites would lead to different enantioselectivities. The biotin (strept)avidin technology has to rely on only avidin and streptavidin as protein scaffolds, making it dependent to a big extend to directed evolutionary techniques to optimize yields and enantiomeric excesses.[51] Furthermore, a limited number of enzymes available also leads to a limited number of reaction conditions, under which these enzymes can be applied. Due to the number of cysteine and serine proteases, there is an enormous diversity of conditions, under which these enzymes can be applied,[24] among them enzymes, which also can be applied under rather harsh conditions.[86] Therefore, cysteine and serine proteases are an ideal platform for the design of organometallic enzyme hybrids.

## 2.2. Inhibition of cysteine and serine proteases

To immobilize an organometallic catalyst in the active site of a serine or cysteine protease, an appropriate anchoring strategy has to be found. As these two classes of enzymes are crucial for a broad spectrum of physiological processes (section 2.1), there has been intensive research during the last decades to selectively target and therefore alter their active centers.[80,87] Many inhibitors form covalent bonds with the active site cysteine or serine nucleophile and therefore lead to deactivation of the enzyme. The first specific irreversible inhibitors for serine and cysteine proteases were designed by taking a well binding substrate and attaching a reactive warhead to that substrate structure. The early warheads used were alkylating agents such as diazo compounds or haloketones. Nowadays, there is a large number of reacitve groups available, which can result in covalent bond formation. Amongst them, there are acyloxymethyl ketones, epoxides, epoxysuccinyl peptides, acylating agents (e.g. aza-peptides, carbamates, β-lactams, heterocyclic inhibitors), phosphonylation agents (phosphonyl fluorides, peptide phosphonates), sulfonylating agents (sulfonyl fluorides) and others.[80] Table A3 gives a brief overview on the different moieties available.

In this context, the focus lies on the scope and mechanism of succinyl epoxides (potent cysteine protease inhibitors) as well as phosphonyl fluorides, sulfonyl fluorides and peptide phosphonates (potent serine protease inhibitors).

### 2.2.1. Succinyl epoxides

The first representative of this family of inhibitors, E-64, was isolated first by Hanada *et al.* from *Aspergillus japonicus* TPR-64 in 1978.[88] Shortly after, it was synthesized *in vitro*.[89] Similar to the majority of inhibitors for cysteine proteases, a tetraedric product is being formed via covalent bond formation, like during substrate hydrolysis. In general, inhibitors of this class are based on the high electrophilicity of their reactive group. The inhibitory potential of E-64 and its derivatives was also confirmed for various other cysteine proteases.[90] Due to their low toxicity, they have become standard tools for biological and biophysical studies of these proteine, as for example for titration of their active centers.[89,90,91] The binding mode of E-64 was determined by NMR spectroscopy[92] as well as X-Ray diffraction.[93,94]

**Table A3:** Selection of covalent inhibitors for cysteine and serine proteases.[80]

| inhibition via | reactive group | example |
| --- | --- | --- |
| alkylation | halomethylketones |  |
| | diazomethylketones |  |
| | acyloxymethylketones |  |
| | epoxides |  |
| | vinyl sulfones and other Michael acceptors |  |
| acylation | aza-peptides |  |
| | carbamates and thiocarbamates |  |
| | β-lactams |  |
| | heterocycles |  |
| phosphonylation and sulfonylation | peptide phosphonates |  |
| | phosphonyl fluorides |  |
| | sulfonyl fluorides |  |

In the case of E-64, the C2-atom of the oxirane is attacked by the thiol via a $S_N2$ reaction, resulting in the peptide to rest in a propeptide-like binding mode.[94] The leucine residue rests in the $S_2$ subsite, whereas the carboxylic acid group lies in the oxyanion hole. The hydrophobic groups of the inhibitor rest in the area around the $S_3$ subsite (figure A5).
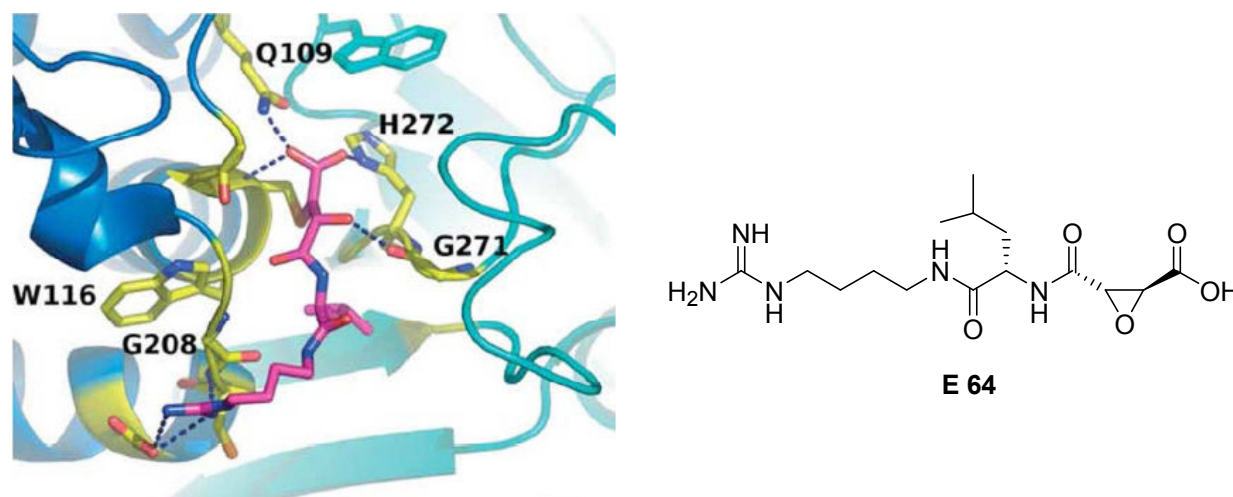


*Figure A5:* X-Ray diffraction based ribbon representation of E-64 in the active site of an enzyme (left) and Lewis-structure of E-64 (right).[93,94]

Today, a large variety of E-64 derivatives is available to induce selectivity. All of them inhibit cysteine proteases through alkylation of the active center cysteine. Nevertheless, for E-64 derivatives, the nucleophilic attack not necessarily takes place at the C2 atom of the oxirane ring. It depends on the orientation of the epoxysuccinyl peptide in the active center, and therefore can also take place at the C3 atom (Scheme A4).[80]
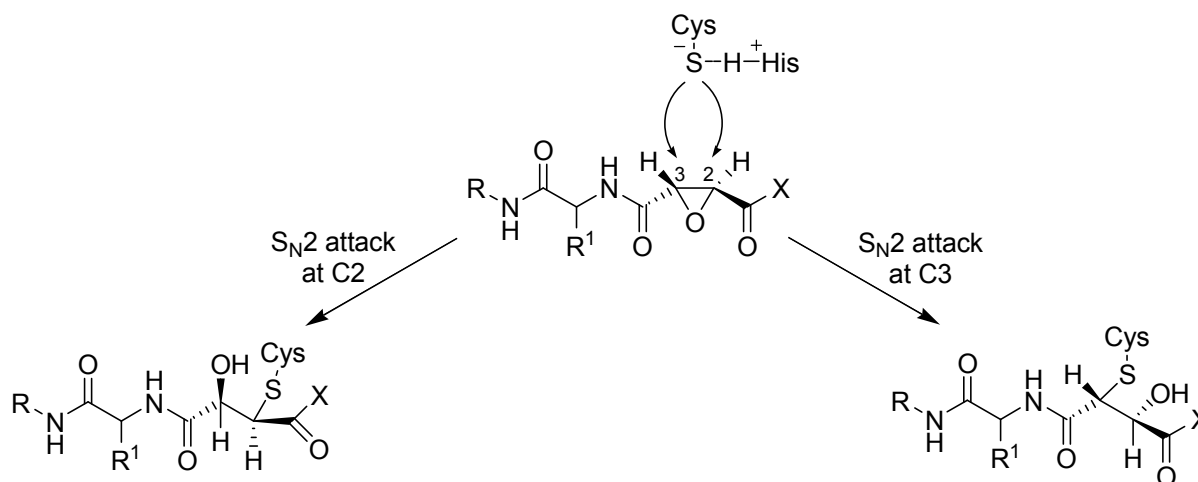


*Scheme A4:* Inhibition pathways of epoxy succinates in cysteine proteases.[80]

## 2.2.2. Phosphonyl fluorides

Phosphonyl fluorides and their effect on *in vivo* processes have been known for about one century. Classical phosphonyl fluorides, which inhibit both cysteine and serine proteases, are diisopropyl fluoro phosphine (DFP), isopropylmethyl phosphonofluoridate (sarin) and 1,2,2-trimethylpropylmethyl phosphonofluoridate (soman). Their lack of a peptidic substrate part (unlike E-64 and its derivatives) makes them unselective towards a particular serine protease. Due to the ubiquitous appearance of serine proteases in living systems (in particular acetylcholinesterase), this renders them extremely toxic. Nevertheless, using a phosphonylfluoride warhead, a large number of serine proteases could be addressed, making them a useful tool for the identification and classification of new serine proteases.



DFP                          sarin                          soman
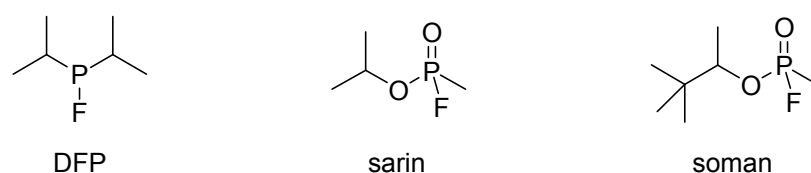
***Figure A7:*** Common representatives of phosphonyl fluorides.

The covalent and irreversible inhibition of serine proteases by phosphonyl fluorides most likely involves nucleophilic replacement of the fluoride group by the active center serine group, yielding a stable enzyme inhibitor complex (scheme A5).
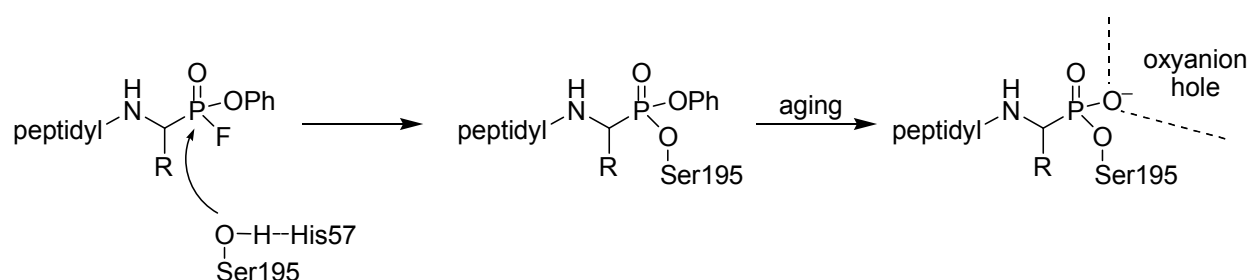


***Scheme A5:*** Inactivation of serine proteases by phosphonyl fluorides.[80]

## 2.2.3. Sulfonyl fluorides

Sulfonyl fluorides have been well investigated as inhibitors of serine proteases since their discovery by Fahney and Gold in 1963.[80] They are suitable for the inhibition of most serine proteases such as chymotrypsin,[95,96] trypsin,[96,97] elastase[98] or fibrinolytic serine proteases.[99] Two prominent members of this class of compounds are phenylmethyl-sulfonylfluoride (PMSF) and 4-(2-aminoethyl)benzenesulfonyl (AEBSF). Sulfonyl fluorides are rather unspecific, and especially PMSF is a general serine

protease inhibitor, which has also been shown to inhibit the cysteine protease papain at a pH of 7.[100] Both PMSF and AEBSF are commercially available. In addition, AEBSF is more stable in physiological medium than PMSF and widely used as a broad-spectrum serine protease inhibitor.
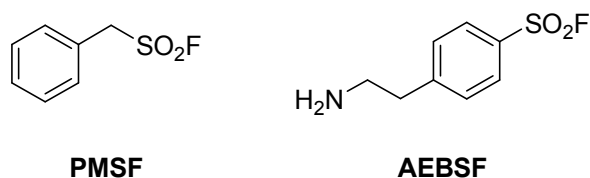


**PMSF**                                    **AEBSF**

*Figure A8:* PMSF and AEBSF, two potent fluoro sulfonyl based serine protease inhibitors.[80]

The mode of inhibition by sulfonyl fluorides is similar to the inhibition by phosphonyl fluorides. They inhibit for example serine protease α-chymotrypsin by $S_N2$ nucleophilic attack of the active site serine residue Ser195, yielding a sulfonyl enzyme derivative (scheme A6). These sulfonyl derivatives are stable for long periods of time except at high pH values.[101] Their low specificy can be increased by additional substituents on the arene ring, also increasing their potency. For example, sulfonyl fluoride inhibitors with a fluoro acyl group can interact with the S1 binding site (scheme A6). This increases the inhibitor's specificy to one particular type of protease.[80]
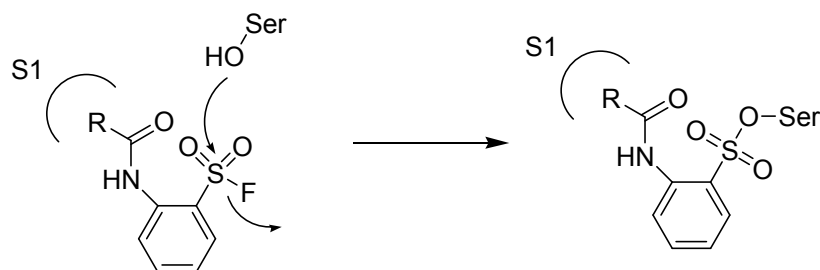


*Scheme A6:* Mechanism of inhibition of serine proteases by sulfonyl fluorides.[80]

## 2.2.4. Peptide phosphonates

Besides phosphonyl fluorides and sulfides, peptide phosphonates are also members of the large group of serine protease inhibitors. They have been developed originating from DFP (figure A7). In contrast to phosphonyl fluorides, peptide phosphonates are less toxic and labile to hydrolysis, making them easier to handle. Furthermore, their peptidic part makes them more selective to specific kinds of proteases. Oleksyszyn *et al.* rendered outstanding services in the synthesis and the development of (α-aminoalkyl)phosphonate diphenyl esters, a group of inhibitors which is extremely multifaceted in terms of their possible variations.[102] In spite of the low electronegativity

of the phenoxy substituents, the phosphorous atom is electrophilic enough to be attacked by the hydroxyl group of the active center's serine residue. Selectivity can be triggered sophisticatedly by attachment of a short peptide sequence to the diphenyl phosphonate group, similar to the peptide sequences in E-64 derivatives. Oleksyszyn *et al.* proposed a mechanism for the covalent inhibition of serine proteases, which is similar to the mechanism for phosphonyl and sulfonyl fluorides (scheme A7). Herein, the hydroxy group of serine attacks the central phosphorous atom, forming a pentacoordinate intermediate.[103] In the next step, one of the phenoxy groups leaves, giving rise to a stable phosphonylated derivative. This derivative undergoes a slow aging process, resulting in the loss of the second phenoxy group. A phosphonic acid monoester is being formed with one of the phosphonate oxygens reaching into the oxyanion hole. The geometry of the phosphorous atom was determined to be tetrahedral by $^{31}P$ NMR measurements.[103] Peptide phosphonate Suc-Val-Pro-Phe$^P$(OPh)$_2$ shows two signals at 19.59 and 18.75 ppm in $^{31}P$ NMR, which can be assigned to its two diastereomers. When reacted with chymotrypsin, these two signals vanish, giving rise to a broad signal at 25.98 ppm, corresponding to the Ser195 phosphonate ester. The signal shift by more than 6 ppm is indicative for a tetrahedral geometry at the phosphorus atom. Also X-Ray diffraction studies confirmed the mode of inhibition and the tetrahedral geometry.[104]
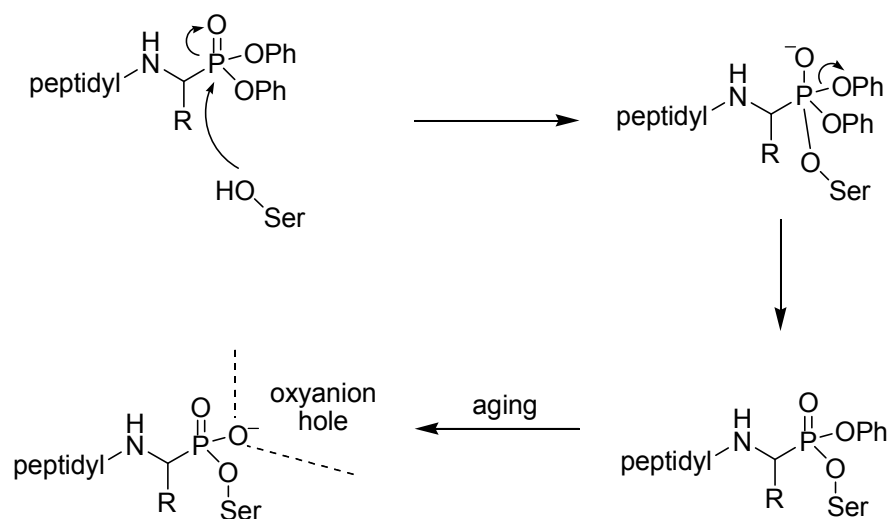


**Scheme A7:** Proposed mechanism of inhibition by peptide phosphonate esters.[80]

Very effective and easily accessible peptide phosphonate inhibitors for α-chymotrypsin can be synthesized on the basis of (α-aminobenzoyl)phosphonate diphenyl ester Z-$^P$(OPh)$_2$.[103] By removal of the Z protection group and attachment of amino acids or peptide sequences, a countless number of different inhibitors can be designed, which –

although having the same mode of inhibition – differ in terms of their selectivities. Table A4 has some representative inhibition data.[103]

**Table A4:** Rate constants ($k_{obsd}$/[I]) for inactivation of serine proteases by diphenyl [α-(N-benzyloxy carbonylamino)alkyl]phosphonates Z-NHCH(R)P(O)(OPh)$_2$ [103] a

| peptide phosphonate | [I] (µM) | $K_{obsd}$/[I] (M$^{-1}$ s$^{-1}$) |
|---|---|---|
| Z-Ala$^P$(OPh)$_2$ | 8.2 | NI$^b$ |
| Z-Val$^P$(OPh)$_2$ | 7.8 | NI$^b$ |
| Z-Leu$^P$(OPh)$_2$ | 7.9 | 81 |
| Z-Met$^P$(OPh)$_2$ | 8.6 | 30 |
| Z-Phe$^P$(OPh)$_2$ | 8.2 | 1200 |

(a) Conditions were as follows: 0.1 M HEPES and 0.5 M NaCl, pH 7.5 at 25 °C. Chymotrypsin concentration 1.6 µM (b) NI, less than 5% inhibition after 1 h.

In summary, peptidyl epoxides, phosphonyl and sulfonyl fluorides and peptidyl phosphonates can be used for the covalent inhibition of a large number of different cysteine and serine proteases. When attached to homogeneous organometallic catalysts, these reactive groups could prove to be highly useful. Their covalent anchoring and strong inhibitory potential of the enzyme active centers guarantees embedment of the catalyst systems in a chiral environment. Furthermore, the large number of different enzymes and reactive motifs leads to numerous different combinations, all of them providing different chiral environments for organometallic catalysts. This leads to different enantioselectivities, making promising candidates of organometallic enzyme hybrids easy and primarily fast to identify.

# 3. Metalla affinity label derived organometallic enzyme hybrids

## 3.1. Motivation - a novel approach to organometallic enzyme hybrids

There are several possibilities for the generation of organometallic enzyme hybrids, which can be classified in terms of the protein scaffold used and the way how a catalyst is anchored on it (section 1.3). Current results clearly prove the potential, which lies behind the combination of chiral protein scaffolds and homogeneous catalysts. Nevertheless, the synthesis of organometallic enzyme hybrids can be challenging, and is not necessarily leading to the desired outcome, which is the generation of enantiomeric excesses through asymmetric catalysis (section 1.3, table A2). This is due to the fact, that the behavior of the organometallic catalyst is different for different organometallic scaffolds, and in case of a non-optimal combination of metal center and protein scaffold chiral induction is low.

Therefore, a novel concept for the generation of organometallic enzyme hybrids seems to be advantageous. A concept, which should facilitate a simple access and a straight forward design of a large number or organometallic enzyme hybrids, from whose promising candidates can be obtained quickly at a large scale, and which therefore overcomes the problem of low chiral induction. The promising candidates should then be optimized for a certain application, condition or even substrate by directed evolution, as it has been shown before,[29,30,51] yielding tailor-made organometallic enzyme hybrids.

For the catalytically active metal center as well as the biological macromolecule, there are countless possibilities of which can be chosen off. From these potential candidates, a combination needs to be picked, which fulfills the catalytical requirements and yields – in the ideal case – only one enantiomer. Concerning the protein scaffold, cysteine and serine proteases make an ideal choice, as there is an enormous number of them commercially available, many of them at low costs.[84] Furthermore, their properties and stabilities have been well investigated, and the structure of numerous representatives has been determined via X-Ray diffraction.[105] Availability of analytical data is crucial for localization of an organometallic catalyst in the enzyme and for probing its protein environment, which serves as basis for a rational supported optimization.

A versatile homogeneous organometallic catalyst also needs to meet some fundamental requirements. It should be coordinated to its ligands firmly, minimizing leaching during catalysis. It also should be highly active – as its concentration is limited by the enzyme's solubility. And furthermore, it needs to be stable to aqueous buffered solutions, as the enzyme must be maintained in a mild environment to guarantee the stability of the tertiary structure of the protein scaffold. Group 8 and group 9 $\eta^6$-arene and $\eta^5$-Cp coordinated complexes meet all these requirements. They are stable under a broad range of conditions, temperatures and aqueous solutions and have been tested successfully for their performance as catalysts in various reactions. Furthermore, their $\eta^6$- and $\eta^5$-ligands are firmly coordinated to the metal centre, making them ideal points to anchor reactive moieties to.
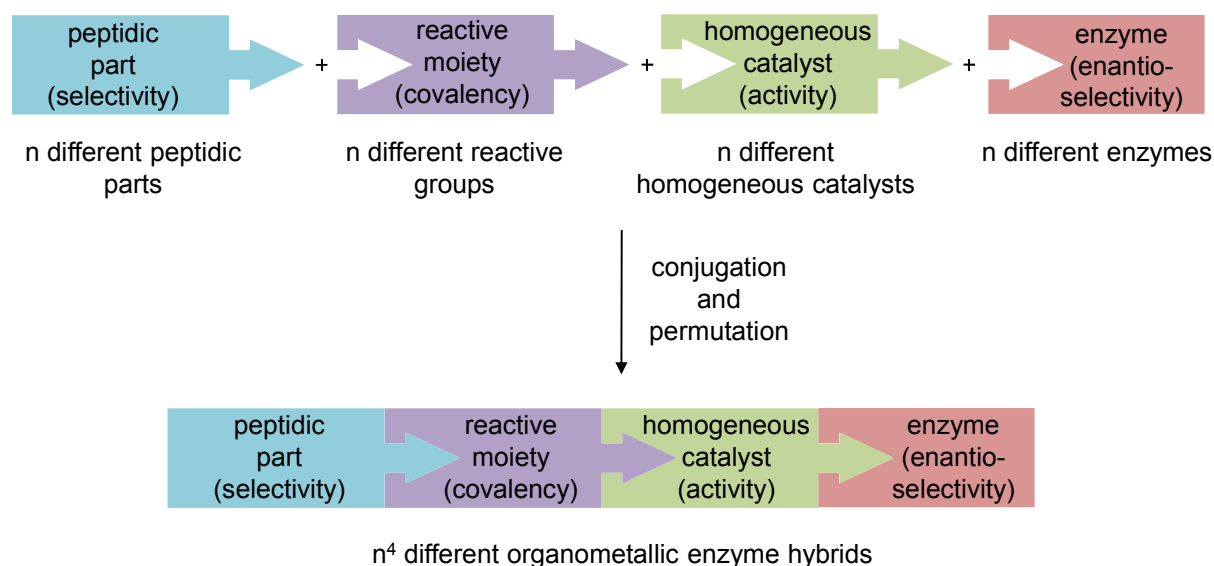


*Figure A8:* The advantages of a modular system for the generation of organometallic enzyme hybrids.

This leads to the most important question in terms of a novel concept of organometallic enzyme hybrids – the anchoring strategy. Basically, there are three different possibilities (section 1.3). For each one of them, there is at least one example, which has been successfully applied in asymmetric synthesis. The only common principle is that the anchoring must be strong enough to withstand catalytic conditions. Nevertheless, the best results have been reached for supramolecular and covalent anchorage of organometallic catalysts.

They also seem to guarantee best, that there are no catalytically active centers outside the chiral enzyme active site, which would lead to decreased enantioselectivities. It therefore is necessary to design the anchor in a way, that perfectly fits the active site of

an enzyme or a class of enzymes. As strong supramolecular anchoring is only found for a limited number of enzymes (mainly biotin (strept)avidin), covalent anchoring seems to be the method of choice. The need of a covalent anchoring also strongly supports the use of cysteine and serine proteases, as there have been many different reactive groups developed, which inhibit these two classes of proteases covalently and specifically (section 2.2).

In addition, also supramolecular interactions have to be taken into account. If the organometallic catalyst is bound to the enzyme at only one point, its position in the enzyme pocket is not well determined. By combining supramolecular and covalent anchoring, the organometallic catalyst has a multi-point anchorage in the active site of the enzyme and its position becomes directed, resulting all metal centers to be in the same chiral protein environment and therefore maximizing the enantiomeric excess obtained.

Furthermore, it would be ideal, if the concept of organometallic enzyme hybrids could be broken down not only to two different building blocks (protein scaffold and organometallic anchor), but to four. Designing the organometallic anchor in a way, that allows easy-to-perform permutation of different homogeneous catalysts, directing peptidic parts and reactive covalent anchors, would give rise to a building block system, with which a library of organometallic enzyme hybrids can be designed of which the best candidates can be chosen off and optimized via directed evolution (figure A8).
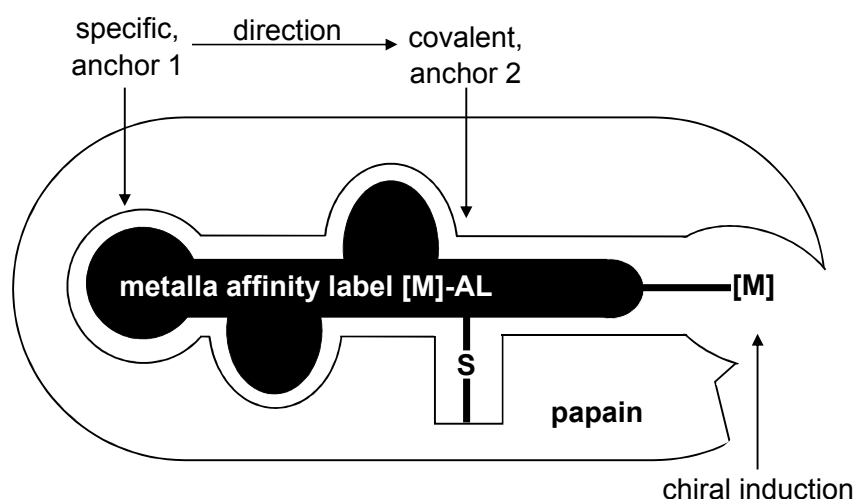


*Figure A9:* Taking advantage of both supramolecular and covalent anchoring – metalla affinity label derived organometallic enzyme hybrids.

Therefore, a novel concept of organometallic enzyme hybrids can be realized, if the following requirements are met:

(I)   The anchor should be able to form a covalent bond via a reactive moiety to guarantee a stable protein-linker complex.

(II)  A peptidic part ensures specific anchorage at the enzyme active site, eliminating the possibility of random immobilization of the homogeneous catalyst on the enzyme surface.

(III) In combination, both the peptidic part and the reactive moiety lead to a directed embedment of the homogeneous catalyst, giving rise to a highly defined environment for the homogeneous catalyst.

(IV)  The system should be modular, providing a variety of organometallic catalysts, peptidic sequences, reactive moieties and enzymes. Hence, a large variety of organometallic enzyme hybrids can be created fast and easy, from which promising candidates can be chosen of for directed evolution.

Overall, this concept can be realized by the synthesis of metalla affinity labels, which are derived from covalent inhibitors (affinity labels) such as E-64 and its derivatives. They consist of a directing peptidic part, and a group which allows covalent attachment. If now a homogeneous catalyst is attached to an affinity label, this is giving rise to a metalla affinity label, which is embedded in the active site of an enzyme via first covalent attachment (firmly fixing the organometallic catalyst) and second supramolecular interaction (guaranteeing the directed embedment of the catalyst). Figure A9 depicts the concept of metalla affinity labels and their embedment into an enzyme. It shows schematically the directed position of the metal centre in the active site of the enzyme and the resulting close proximity to the chiral environment of the protein scaffold. This close and defined proximity induces selectivity and renders the possibility to facilitate asymmetric catalysis.

## 3.2. Scope of the thesis

The objective of this thesis is the development of a novel synthetic and modular route to organometallic enzyme hybrids, as well as their application in asymmetric catalysis. To achieve this aim certain requirements have to be met:

(I)     Homogeneous achiral catalysts with pendant functional groups have to be designed and their activity and potency in aqueous media confirmed.

(II)    The catalysts have to be conjugated to peptidic organic molecules and reactive groups, yielding metalla affinity labels.

(III)   The metalla affinity labels have to be reacted with enzymes and their applicability as asymmetric catalysts confirmed.

As catalytically active metal centers, group 8 and group 9 metal centers were chosen. They are in general stable to air and moisture, and have been successfully applied as catalysts in a variety of different reactions.[106] The metal centers need to have a pendant linker functionality attached to one of their ligands, in order to facilitate conjugation to other metalla affinity label building blocks. For the attachment of the pendant linker group, $\eta^6$-arene and $\eta^5$-Cp* ligands seem to be an excellent choice. They exhibit a strong ligand-metal interaction, making leaching unfavorable. In Addition to that, enzymes scaffolds as well as catalysts have been applied successfully in asymmetric hydrogenations, making this reaction favorable to test the performance of the hybrid systems.[43-48,106,107]



<div align="center">
native enzyme     metalla affinity label     organometallic enzyme hybrid
</div>
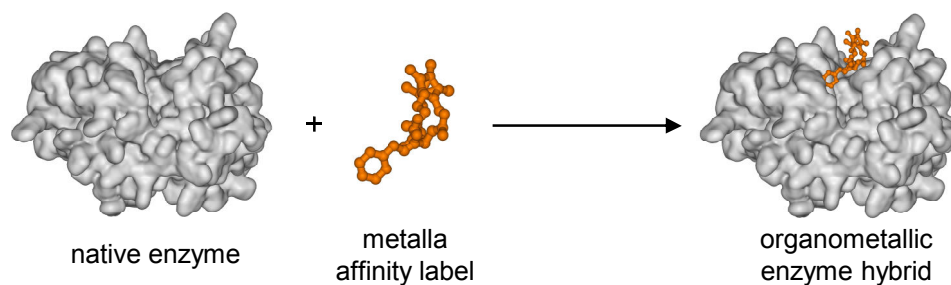
*Scheme A8:* Generation of organometallic enzyme hybrids from metalla affinity labels and enzymes.

Furthermore, methods have to be found to link the organometallic homogeneous catalysts to reactive groups and peptide sequences. During coupling reactions, the inner sphere coordination of the homogeneous catalyst must not be altered. As a linking group, peptide bonds seem to be a promising choice as they can be formed under numerous different conditions.[108] Peptide bond formation conditions also must not lead

to side reactions of the reactive groups of a metalla affinity label. These reactive groups are meant to form covalent bonds in the active centers of enzymes. As reactive groups, oxirane rings, sulfonyl fluorides, phosphonyl fluorides, and diphenyl phosphonates are advantageous, since they have been investigated in detail and can be applied to a plethora of different cysteine and serine proteases for covalent anchorage (section 2). By conjugation with homogeneous catalysts and peptidic parts, metalla affinity labels are obtained, which resemble trifunctional catalysts, able to embed a homogeneous transition metal catalyst in a chiral protein environment (section 3.1).
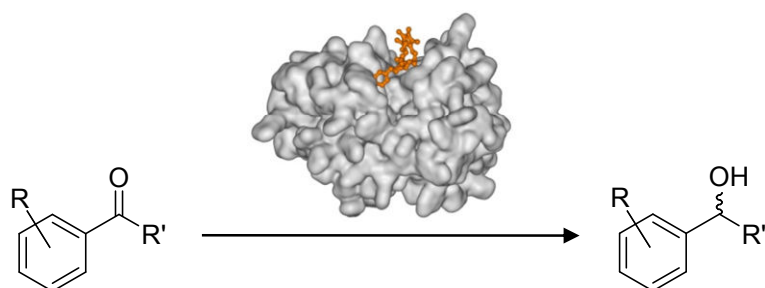


**Scheme A9:** Asymmetric hydrogenation reactions employing organometallic enzyme hybrids.

For the generation of organometallic enzyme hybrids, the generated metalla affinity labels need to be reacted with enzyme scaffolds. Cysteine and serine proteases are a suitable choice as enzyme scaffolds. They have been well investigated during the last decades and are commercially available in a large number, making the generation of numerous organometallic enzyme hybrids possible.[80] Formation of hybrid complexes can be conducted via standard methods described in literature (scheme A8).[102-104,109]

After confirmation of the covalent and selective inhibition of cysteine and serine proteases by metalla affinity labels, conditions have to be found, which are optimal for first the activity of the organometallic catalyst embedded in the active site and second for the stability of the organometallic enzyme hybrid. Both is crucial for the performance of the hybrid system, as the enzyme stability guarantees the enantioselectivity and high transition metal catalyst activity is responsible for sufficiently fast conversion of the substrates (scheme A9).

The successful generation of organometallic enzyme hybrids via metalla affinity labels represents a novel approach for the generation of this class of compounds. Furthermore, it can be seen as a modular system, with which a large number of organometallic enzyme hybrids can be generated and screened for their performance in asymmetric catalysis.

# 4. References

[1]     S. K. Teo, W. A. Colburn, W. G. Tracewell, K. A. Kook, D. I. Stirling, M. S. Jaworsky, M. A. Scheffler, S. D. Thomas, O. L. Laskin, *Clinical Pharmacokinetics* **2004**, *43*, 311-327.

[2]     T. Eriksson, S. Bjorkman, P. Hoglund, *European Journal of Clinical Pharmacology* **2001**, *57*, 365-376.

[3]     K. Nishimura, Y. Hashimoto, S. Iwasaki, *Chemical & Pharmaceutical Bulletin* **1994**, *42*, 1157-1159.

[4]     S. C. Stinson; *Chem. Eng. News* **1999**; *77, 57.*

[5]     S. Alvarez, R. Alvarez, A. R. de Lera, *Tetrahedron: Asymmetry* **2004**, *15*, 839-846.

[6]     E. J. Corey, M. C. Noe, A. Guzman-Perez, *Tetrahedron Letters* **1995**, *36*, 4171-4174.

[7]     G. T. Brooks, T. R. Roberts, *Pesticide Chemistry and Bioscience: The Food-environment Challenge*, Woodhead Publishing Ltd., **1999**, 1st Ed.

[8]     H.-U. Blaser, F. Spindler, *Top. Catal.* **1998**, *4*, 275-282.

[9]     R. Noyori, *Chemtech* **1992,** *22*, 360-367.

[10]    E. Brenna, C. Fuganti, S. Serra, *Tetrahedron: Asymmetry* **2003**, *14*, 1-42.

[11]    G. Jannes, V. Dubois, *Chiral Reaction in Heterogeneous Catalysis*, Springer US, **1995**, 1st Ed.

[12]    (a) *Comprehensive Asymmetric Catalysis*, Vol. I ± III (Eds.: E. N. Jacobsen, A. Pfaltz, H. Yamamoto), Springer, Berlin, **1999**; (b) H. Brunner, W. Zettlmeier, *Handbook of Enantioselective Catalysis with Transition Metal Compounds*, Vol. I ± II, VCH, Weinheim, **1993**; (c) R. Noyori, *Asymmetric Catalysis in Organic Synthesis*, Wiley, New York, **1994**; (d) *Catalytic Asymmetric Synthesis* (Ed.: I. Ojima), VCH, Weinheim, **1993**.

[13]    (a) H. G. Davies, R. H. Green, D. R. Kelly, S. M. Roberts, *Biotransformations in Preparative Organic Chemistry: The Use of Isolated Enzymes and Whole Cell Systems in Synthesis*, Academic Press, London, **1989**; (b) C. H. Wong, G. M. Whitesides, *Enzymes in Synthetic Organic Chemistry*, Pergamon, Oxford, **1994** (Tetrahedron Organic ChemistrySeries , Vol. 12); (c) *Enzyme Catalysis in Organic Synthesis: A Comprehensive Handbook*, Vol. I-II (Eds.: K. Drauz, H.

Waldmann), VCH, Weinheim, **1995**; (d) K. Faber, *Biotransformations in Organic Chemistry*, 3rd ed., Springer, Berlin, **1997**.

[14]   J. A. Osborn, F. H. Jardine, J. F. Young, G. Wilkinson, *J. Chem. Soc. A* **1966**, 1711-1732.

[15]   W. S. Knowles, *Angew. Chem., Int. Ed.* **2002**, *41*, 1998-2007.

[16]   H. Nozaki, S. Moriuti, H. Takaya, R. Noyori, *Tetrahedron Lett.* **1966**, *7*, 5239-5244.

[17]   R. Noyori; *Angew. Chem. Int. Ed.* **2002**, *41*, 2008-2022.

[18]   K.-J. Haack, S. Hashiguchi, A. Fujii, T. Ikariya, R. Noyori, *Angew. Chem. Int. Ed.* **1997**, *36*, 285-288.

[19]   K. B. Sharpless, *Angew. Chem. Int. Ed.* **2002**, *41*, 2024-2032.

[20]   E. N. Jacobsen, I. Marko, E. S. Mungall, G. Schroeder, K. B. Sharpless, *J. Am. Chem. Soc.* **1988**, *110*, 1968-1970.

[21]   H. C. Kolb, M. S. Van Nieuwenhze, K. B. Sharpless, *Chem. Rev.* **1994**, *94*, 2483-2547.

[22]   W. S. Knowles, *Acc. Chem. Res.* **1983**, *16*, 106-112.

[23]   E. M. Vogl, H. Groger, M. Shibasaki, *Angew. Chem. Int. Ed.* **1999**, *38*, 1570-1577.

[24]   *Biotransformations in Organic Chemistry*, 4th Ed. (Ed.: K. Faber), Springer, Berlin, **1999**.

[25]   R. MacKinnon, *Angew. Chem. Int. Ed.* **2004**, *43*, 4265-4277.

[26]   J. Fried, R. W. Thoma, J. R. Gerke, J. E. Herz, M. N. Donin, D. Perlman, *J. Am. Chem. Soc.* **1952**, *74*, 3692-3693.

[27]   S. Sawada, S. Kulprecha, N. Nilubol, T. Yoshida, S. Kinoshita, H. Taguchi, *Appl. Environ. Microbiol.* **1982**, *44*, 1249-1252.

[28]   D. H. Moffet, M. H. Hecht, *Chem. Rev.* **2001**, *101*, 3191-3203.

[29]   (a) M. T. Reetz, M. Rentzsch, A. Pletsch, M. Maywald, *Chimia* **2002**, *56*, 721-723; (b) M. T. Reetz, *Proc. Natl. Acad. Sci.* **2004**, *101*, 5716-5722; (c) M. T. Reetz, *Tetrahedron* **2002**, *58*, 6595-6602; (d) M. T. Reetz, *Angew. Chem. Int. Ed.* **2001**, *40*, 284-310; (e) M. T. Reetz, *Angew. Chem. Int. Ed.* **2002**, *41*, 1335-1338.

[30]   M. T. Reetz, A. Zonta, K. Schimossek, K. Liebeton, K. E. Jaeger, *Angew. Chem. Int. Ed.* **1998**, *36*, 2830-2832.

[31]   W. A. Herrmann, L. J. Goossen, C. Köcher, G. R. J. Artus, *Angew. Chem. Int. Ed.* **1996**, 35, 2805-2807.

[32]   J.-L. Herisson, Y. Chauvin, *Macromol. Chem.* **1971**, 141, 161-176.

[33]   R.R. Schrock, *J. Organometal. Chem.* **1986**, 300, 249-262.

[34]   S.T. Nguyen, L.K. Johnson, R.H. Grubbs, *J. Am. Chem. Soc.* **1992**, 114, 3974-3975.

[35]   T.R. Ward, *Chem. Eur. J.* **2005**, *11*, 3798-3804.

[36]   J. Steinreiber, T. R. Ward, *Coord. Chem. Rev.* **2008**, *252*, 751-766.

[37]   O. Pamies, J.-E. Bäckvall, *Chem.Rev.* **2003**, *103*, 3247-3261.

[38]   J. M. Berg, L. Stryer, J. L. Tymoczko, *Biochemie*, Spektrum Verlag, **2007**, 6th Ed..

[39]   S. Akabori, S. Sakurai, Y. Izumi, Y. Fujii, *Nature* **1956**, *178*, 323-324.

[40]  C. M. Thomas, T. R. Ward, *Appl. Organometal. Chem.* **2005**, *19,* 35-39.

[41]   G. Roelfes, B. L. Feringa, *Angew. Chem. Int. Ed.* **2005**, *44*, 3230-3232.

[42]   R. Ricoux, E. Girgenti, J.-P. Mahy, *Rec. Res. Dev. Biochem.* **2003**, *4*, 757-778.

[43]   M. E. Wilson, G. M. Whitesides, *J. Am. Chem. Soc.* **1978**, *100*, 306-307.

[44]   (a) C.-C. Lin, C.-W. Lin, A. S. C. Chan, *Tetrahedron: Asymmetry* **1999**, *10*, 1887-1893; (b) T. R. Ward, *Chem. Eur. J.* **2005**, *11*, 3798-3804; (c) J. Collot, J. Gradinaru, N. Humbert, M. Skander, A. Zocchi, T. R. Ward, *J. Am. Chem. Soc.* **2003**, *125*, 9030-9031; (d) M. Skander, N. Humbert, J. Collot, J. Gradinaru, G. Klein, A. Loosli, J. Sauser, A. Zocchi, F. Gilardoni, T. R.Ward, *J. Am. Chem. Soc.* **2004**, *126*, 14411-14418; (e) J. Collot, N. Humbert, M. Skander, G. Klein, T. R. Ward, *J. Organomet. Chem.* **2004**, *689*, 4868-4871; (f) M. Skander, C. Malan, A. Ivanova, T. R. Ward, *Chem. Commun.* **2005**, 4815-4817; (g) G. Klein, N. Humbert, J. Gradinaru, A. Ivanova, F. Gilardoni, U. E. Rusbandi, T. R. Ward, *Angew. Chem. Int. Ed.* **2005**, *44*, 7764-7767; (h) U. E. Rusbandi, C. Lo, M. Skander, A. Ivanova, M. Creus, N. Humbert, T. R. Ward, *Adv. Synth. Catal.* **2007**, *349*, 1923-1930.

[45]   M. T. Reetz, M. Rentzsch, A. Pletsch, M. Maywald, *Chimia* **2002**, *56*, 721-723.

[46]   M. T. Reetz, J. J.-P. Peyeralans, A. Maichele, Y. Fu, M. Maywald, *Chem. Commun.* **2006**, 4318-4320.

[47]   M. Reetz, M. Rentzsch, A. Pletsch, M. Maywald, P. Maiwald, J. J.-P. Peyralans, A. Maichele, Y. Fu, N. Jiao, F. Hollmann, R. Mondière, A. Taglieber, *Tetrahedron* **2007**, *63*, 6404-6414.

[48]   (a) L. Panella, J. Broos, J. Jin, M. W. Fraaije, D. B. Janssen, M. Jeronimus-Stratingh, B. L. Feringa, A. J. Minnaard, J. G. De Vries, *Chem. Commun.* **2005**, 5656-5658; (b) J. G. de Vries, L. Lefort, *Chem. Eur. J.* **2006**, *12*, 4722-4734.

[49]   H. Yamaguchi, T. Hirano, H. Kiminami, D. Taura, A. Harada, *Org. Biomol. Chem.* **2006**, *4*, 3571-3573.

[50]   T. Ueno, M. Suzuki, T. Goto, T. Matsumoto, K. Nagayama, Y.Watanabe, *Angew. Chem. Int. Ed.* **2004**, *43*, 2527-2530.

[51]   (a) C. Letondor, N. Humbert, T. R. Ward, *Proc. Natl. Acad. Sci. U.S.A.* **2005**, *102*, 4683-4687; (b) C. Letondor, A. Pordea, N. Humbert, A. Ivanova, S. Mazurek, M. Novic, T. R. Ward, *J. Am. Chem. Soc.* **2006**, *128*, 8320-8328.

[52]   K. Yamamura, E. T. Kaiser, *J. Chem. Soc., Chem. Commun.* **1976**, 830-831.

[53]   C. M. Thomas, C. Letondor, N. Humbert, T. R. Ward, *J. Organomet. Chem.* **2005**, *690*, 4488-4491.

[54]   A. Mahammed, Z. Gross, *J. Am. Chem. Soc.* **2005**, *127*, 2883-2887.

[55]   (a) M. Ohashi, T. Koshiyama, T. Ueno, M. Yanase, H. Fujii, Y. Watanabe, *Angew. Chem. Int. Ed.* **2003**, *42*, 1005-1008; (b) T. Ueno, T. Koshiyama, M. Ohashi, K. Kondo, M. Kono, A. Suzuki, T. Yamane, Y. Watanabe, *J. Am. Chem. Soc.* **2005**, *127*, 6556-6562; (c) T. Ueno, T. Koshiyama, S. Abe, N. Yokoi, M. Ohashi, H. Nakajima, Y. Watanabe, *J. Organomet. Chem.* **2007**, *692*, 142-147.

[56]   J. R. Carey, S. K. Ma, T. D. Pfister, D. K. Garner, H. K. Kim, J. A. Abramite, Z. Wang, Z. Guo, Y. Lu, *J. Am. Chem. Soc.* **2004**, *126*, 10812-10813.

[57]   (a) F. van de Velde, L. Konemann, F. van Rantwijk, R. A. Sheldon, *Chem. Commun.* **1998**, 1891-1892; (b) F. van deVelde, L. Könemann, F. van Rantwijk, R. A. Sheldon, *Biotechnol. Bioeng.* **2000**, *67*, 87-96; (c) F. van de Velde, I. W. C. E. Arends, R. A. Sheldon, *Top. Catal.* **2000**, *13*, 259-265; (d) F. van de Velde, I. W. C. E. Arends, R. A. Sheldon, *J. Inorg. Biochem.* **2000**, *80*, 81-89.

[58]   M. T. Reetz, *Tetrahedron* **2002**, *58*, 6595-6602.

[59]     (a) K. Okrasa, R. J. Kazlauskas, *Chem. Eur. J.* **2006**, *12*, 1587-1596; (b) A. Fernandez-Gacio, A. Codina, J. Fastrez, O. Riant, P. Soumillion, *ChemBioChem* **2006**, *7*, 1013-1016.

[60]     T. Kokubo, T. Sugimoto, T. Uchida, S. Tanimoto, M. Okano, *J. Chem. Soc., Chem. Commun.* **1983**, 769-770.

[61]     (a) I. M. Bell, M. L. Fisher, Z. P. Wu, D. Hilvert, *Biochemistry* **1993**, 32, 3754; (b) I.M. Bell, D. Hilvert, *Biochemistry* **1993**, *32*, 13969-13973.

[62]     T. Hayashi, D. Murata, M. Makino, H. Sugimoto, T. Matsuo, H. Sato, Y. Shiro, Y. Hisaeda, *Inorg. Chem.* **2006**, *45*, 10530-10536.

[63]     (a) P. Travascio, Y. Li, D. Sen, *Chem. Biol.* **1998**, *5*, 505-517; (b) P. Travascio, A. J. Bennet, D. Y.Wang, D. Sen, *Chem. Biol.* **1999**, *6*, 779-787.

[64]     D. Qi, C.-M. Tann, D. Haring, M. D. Distefano, *Chem. Rev.* **2001**, *101*, 3081-3111.

[65]     R. R. Davies, M. D. Distefano, *J. Am. Chem. Soc.* **1997**, *119*, 11643-11652.

[66]     M. T. Reetz, N. Jiao, *Angew. Chem. Int. Ed.* **2006**, *45*, 2416-2419.

[67]     (a) G. Roelfes, B. L. Feringa, *Angew. Chem. Int. Ed.* **2005**, *44*, 3230-3232; (b) G. Roelfes, A. J. Boersma, B. L. Feringa, *Chem. Commun.* **2006**, 635-637; (c) G. Roelfes, *Mol. Biosyst.* **2007**, *3*, 126-135.

[68]     (a) M. Marchetti, G. Mangano, S. Paganelli, C. Botteghi, *Tetrahedron Lett.* **2000**, *41*, 3717-3720; (b) C. Bertucci, C. Botteghi, D. Giunta, M. Marchetti, S. Paganelli, *Adv. Synth. Catal.* **2002**, *344*, 556-562; (c) S. Crobu, M. Marchetti, G. Sanna, *J. Inorg. Biochem.* **2006**, *100*, 1514-1520.

[69]     Z.-P. Wu, D. Hilvert, *J. Am. Chem. Soc.* **1989**, *111*, 4513-4514.

[70]     R. S. Roy, B. Imperiali, *Protein Eng.* **1997**, *10*, 691-698.

[71]     (a) M. M. Meijler, O. Zelenko, D. S. Sigman, *J. Am. Chem. Soc.* **1997**, *119*, 1135-1136; (b) C. B. Chen, L. Milne, R. Landgraf, D. M. Perrin, D. S. Sigman, *ChemBioChem* **2001**, *2*, 735-740.

[72]     (a) M. P. Fitzsimons, J. K. Barton, *J. Am. Chem. Soc.* **1997**, *119*, 3379-3380; (b) K. D. Copeland, M. P. Fitzsimons, R. P. Houser, J. K. Barton, *Biochemistry* **2002**, 41, 343-356.

[73]     (a) R. T. Kovacic, J. T. Welch, S. J. Franklin, *J. Am. Chem. Soc.* **2003**, *125*, 6656-6662; (b) J. T. Welch, W. R. Kearney, S. J. Franklin, *Proc. Natl. Acad. Sci.*

*U.S.A.* **2003**, *100*, 3725-3730; (c) S. W.Wong-Deyrup,Y. Kim, S. J. Franklin, *J. Biol. Inorg. Chem.* **2006**, *11*, 17-25; (d) S. Lim, S. J. Franklin, *Protein Sci.* **2006**, *15*, 2159-2165; (e) S. B. Shields, S. J. Franklin, *Biochemistry* **2004**, *43*, 16086-16091.

[74]   (a) Y. Kitamura, M. Komiyama, *Nucleic Acids Res.* **2002**, *30*, e102/1-e102/6; (b) W. Chen, Y. Kitamura, J. M. Zhou, J. Sumaoka, M. Komiyama, *J. Am. Chem. Soc.* **2004**, *126*, 10285-10291; (c) W. Chen, M. Komiyama, *ChemBioChem* **2005**, *6*, 1825-1830; (d) Y. Yamamoto, A. Uehara, A. Watanabe, H. Aburatani, M. Komiyama, *ChemBioChem* **2006**, *7*, 673-677; (e) Y. Yamamoto, M. Mori, Y. Aiba, T. Tomita, W. Chen, J.-M. Zhou, A. Uehara, Y. Ren, Y. Kitamura, M. Komiyama, *Nucleic Acids Res.* **2007**, *35*, e53/1-e53/8.

[75]   R. Krämer, *Angew. Chem. Int. Ed.* **2006**, *45*, 858-860.

[76]   J. M. Lehn, *Science* **1993**, *260*, 1762-1763.

[77]   H. L. Levine, Y. Nakagawa, E. T. Kaiser, *Biochem. Biophys. Res. Commun.* **1977**, *76*, 64-70.

[78]   C. A. Kruithof, M. A. Casado, G. Guillena, M. R. Egmond, A. van der Kerk-van Hoof, A. J. R. Heck, R. J. M. K. Gebbink, G. van Koten, *Chem. Eur. J.* **2005**, *11*, 6869-6877.

[79]   P. Haquette, M. Salmain, K. Svedlung, A. Martel, B. Rudolf, J. Zakrzewski, S. Cordier, T. Roisnel, C. Fosse, G. Jaouen, *ChemBioChem* **2007**, *8*, 224-231.

[80]   J. C. Powers, J. L. Asgian, Ö. D. Ekici, K. E. James, *Chem. Rev.* **2002**, *102*, 4639-4750.

[81]   (a) N. D. Rawlings, A. J. Barrett, *Biochem. J.* **1993**, *290*, 205-218; (b) N. D. Rawlings, A. J. Barrett, *Methods Enzymol.* **1994**, *244*, 461-486.

[82]   http://merops.co.uk

[83]   N. D. Rawlings, E. O'Brien, A. J. Barrett, *Nucleic Acids Res.* **2002**, *30*, 343-346; (b) A. J. Barrett, N. D. Rawlings, E. O'Brien, *J. Struct. Biol.* **2001**, *134*, 95-102.

[84]   for example: http://www.sigmaaldich.com

[85]   R. Wolfenden, M. J. Snider, *Acc. Chem. Res.* **2001**, *34*, 938-945.

[86]   (a) M. Ferrer, O. Golyshina, A. Beloqui, P. N. Golyshin, *Curr. Opin. Microbiol.* **2007**, *10*, 207-214; (b) D. W. Hough, M. J.  Danson, *Curr. Opin. Chem. Biol.*

**1999**, *3*, 39-46; (c) D. C. Demirjian, F. Moris-Varas, C. S. Cassidy, *Curr. Opin. Chem. Biol.* **2001**, *5*, 144-151.

[87]    (a) D. L. Mykles, *Methods Cell Biol.* **2001**, *66*, 247-287; (b) H. U. Demuth, *J. Enzyme Inhib.* **1990**, *3*, 249-278; (c) D. Bromme, J. Kaleta, *Curr. Pharm. Des.* **2002**, *8*, 1639-1658; (d) C. M. Kam, D. Hudig, J. C. Powers, *Biochim. Biophys. Acta* **2000**, *1477*, 307-323.

[88]    K. Hanada, M. Tamai, M. Yamagishi, S. Ohmura, J. Sawada, I. Tanaka, *Agric. Biol. Chem.* **1978**, *42*, 523-528.

[89]    K. Hanada, M. Tamai, S. Ohmura, J. Sawada, T. Seki, I. Tanaka, *Agric. Biol. Chem.* **1978**, *42*, 529-536.

[90]    K. Hanada, M. Tamai, S. Morimoto, T. Adachi, S. Ohmura, J. Sawada, I. Tanaka, *Agric. Biol. Chem.* **1978**, *42*, 537-541.

[91]    (a) A. J. Barrett, A. A. Kembhavi, M. A. Brown, H. Kirschke, C. G. Knight, M. Tamai, K. Hanada, *Biochem. J.* **1982**, *201*, 189-198; (b) T. Inaba, Y. Hirayama, N. Fujinaga, *Agric. Biol. Chem.* **1979**, *43*, 655-656; (c) H. Sugita, S. Ishiura, K. Suzuki, K. Imahori, *J. Biochem.* **1980**, *87*, 339-341; (d) T Towatari, K. Tanaka, D. Yoshikawa, N. Katunuma, *J. Biochem.* **1978**, *84*, 659-671.

[92]    Y. Yabe, D. Guillaume, D. H. Rich, *J. Am. Chem. Soc.* **1988**, *110*, 4043-4044.

[93]    (a) K. I. Varughese, F. R. Ahmed, P. R. Carey, S. Hasnain, C. P. Huber, A. C. Storer, *Biochem.* **1989**, *28*, 1330-1332; (b) A. Fujishima, Y. Imai, T. Nomura, Y. Fujisawa, Y. Yamamoto, T. Sugawara, *FEBS Lett.* **1997**, *407*, 47-50.

[94]    K. I. Varughese, Y. Su, D. Cromwell, S. Hasnain, N.-H. Xuong, *Biochem.* **1992**, *31*, 5172-5176.

[95]    (a) B. R. Baker, J. A. Hurlbut, *J. Med. Chem.* **1969**, *12*, 221-224. (b) B. R. Baker, J. A. Hurlbut, *J. Med. Chem.* **1969**, *12*, 118-122.

[96]    D. Fahrney, A. M. Gold, *J. Am. Chem. Soc.* **1963**, *85*, 997-1000.

[97]    B. R. Baker, E. H. Erickson, *J. Med. Chem.* **1969**, *12*, 112-117.

[98]    M. O. Lively, J. C. Powers, *Biochim. Biophys. Acta* **1978**, *525*, 171-179.

[99]    R. Laura, D. J. Robison, D. H. Bing, *Biochemistry* **1980**, *19*, 4859-4864.

[100]   J. R. Whitaker, J. Perez-Villasenor, *Arch. Biochem. Biophys.* **1968**, *124*, 70-78.

[101]   (a) A. M. Gold, D. Fahrney, *Biochemistry* **1964**, *3*, 783-791. (b) A. M. Gold, *Biochemistry* **1965**, *4*, 897-901.

[102] J. Oleksyszyn, J. C. Powers, *Biochem. Biophys. Res. Commun.* **1989**, *161*, 143-149.

[103] J. Oleksyszyn, J. C. Powers, *Biochemistry* **1991**, *30*, 485-493.

[104] J. A. Bertrand, J. Oleksyszyn, C.-H. Kam, B. Boduszek, S. Presnell, R. R. Plaskon, F. L. Suddath, J. C. Powers, L. D. Williams, *Biochemistry* **1996**, *35*, 3147-3155.

[105] For X-Ray diffractional data, please see the RCSB Protein Data Bank (http://www.rcsb.org).

[106] C. Daguenet, R. Scopelliti, P.J. Dyson, *Organometallics* **2004**, *23*, 4849-4857.

[107] (a) I. Ogatha, R. Iwata, *Tetrahedron* **1973**, *29*, 2753; (b) J. Ros, E. de la Encarnación, Á. Alvarez-Larena, J.F. Piniella, I. Moldes, *J. Organomet. Chem.* **1998**, *566*, 165-174.

[108] T. W. Greene, P. G. M. Wuts, *Protective Groups in Organic Synthesis*, John Wiley & Sons, Inc., 3rd Ed. New York, **1999**.

[109] (a) M. M. Fernandez, D. S. Clark, H. W. Blanch, Biotech. Bioeng. 1991, 37, 967-972; (b) K. Matsumoto, K. Mizoue, K. Kitamura, W.-C. Tse, C. P. Huber, T. Ishida, *Biopolymers (Peptide Science)*, **1999**, *51*, 99-107.

# B | Results and Discussion

# B1. Synthesis and application of $\eta^6$-arene Ru(II) complexes

## 1. Introduction

The well established stability of sandwich complexes of late transition metals towards oxygen, water or even under physiological conditions[1] has triggered wide spread interest in the application of such systems as biological probes[2,3] as well as pharmacologically active compounds (**B1**, **B2**).[4,5,6] In particular, the labeling of aromatic side chains of unprotected amino acids and peptides by introduction of CpM and Cp*M-moieties (M = d6-metal cation) has been an active field with pivotal contributions by the groups of Moriart,[7]Pearson,[8] Sheldrick[9] and others.[10] The transition to half-sandwich complexes adds an further dimension to the chemistry of these systems due to the introduction of potentially labile coordination sites. Specifically, half sandwich arene ruthenium(II) complexes conquered a plethora of applications. In particular the *in vivo* and *in vitro* cytotoxicity of this class of compounds has recently triggered intense research activity targeting the design of selective organometallic anti cancer agents.[11,12] (**B3**) They also have attracted considerable attention due to a wide range of applications including building blocks for supramolecular structures,[13] catalysts for transfer hydrogenations,[14,15,16] (**B4**, **B5**) hydrogenations[17] or C-C couplings.[18] Finally, half sandwich ruthenium complexes were successfully applied as catalytically active metal centers in organometallic enzyme hybrids.[19] Ruthenium $\eta^6$-arene complexes with pendant carboxylate groups,[20] alcohols,[21] or even amino acids[3,9,22] have been synthesized (**B6**). There are also several examples of $\eta^6{:}\eta^1$-arenes which include an additional tether at the metal centre comprising functional groups such as alcohols,[23] amides[15] or carbenes.[24] Nevertheless, half sandwich ruthenium complexes of biogenic amino acids have not been reported yet. The only example of non biogenic amino acids comprising a $\eta^6$-arene ruthenium metal centre was reported by Beck *and coworkers* in 2001.[22] In addition, none of the reported motifs exhibits an open coordination site which is required for a metal centered catalytic activity. Furthermore, organometallic complexes comprising ruthenium metal centers have been investigated as hydrogenation catalysts for several decades. In particular, Iwata and coworkers were the first to use $\eta^6$-arene ruthenium(II) complexes as catalysts for hydrogenations in 1973.[25]
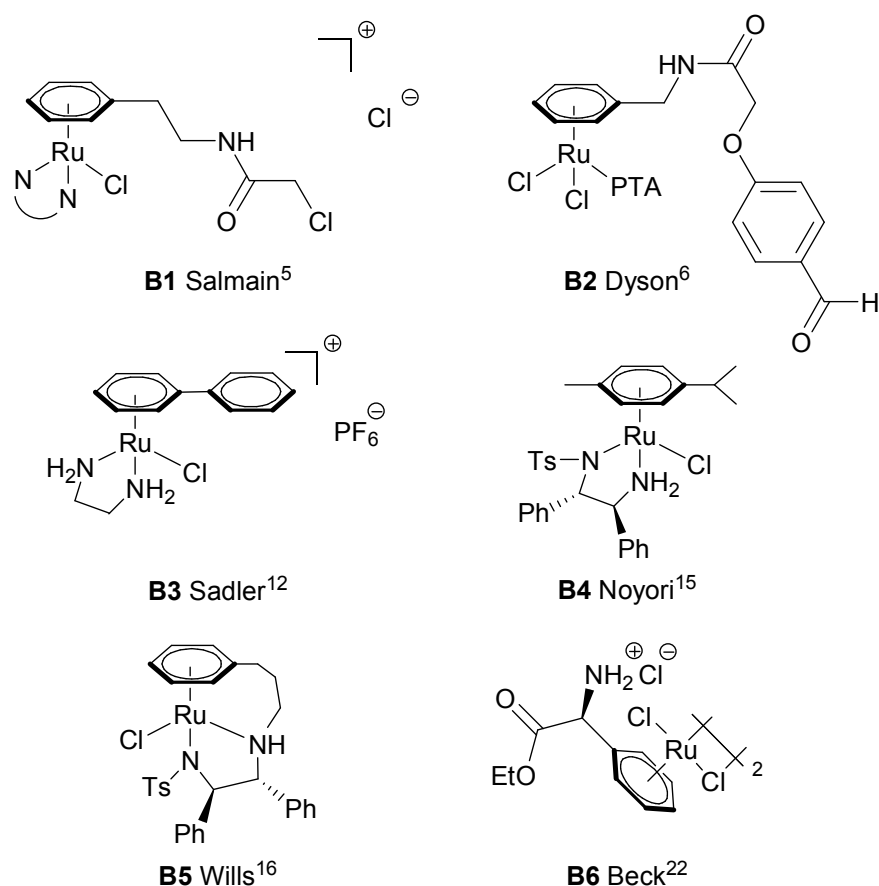
**Figure B1:** Various $\eta^6$-arene Ru(II) half sandwich complexes applied in the selective inhibition of enzymes (**B1**), biological probes (**B2**), tumor therapy (**B3**) or catalysis (**B4**, **B5**). Complex (**B6**) represents the only Ru(II) half-sandwich complex with $\eta^6$-coordination of an amino acid side chain and unprotected amino group.

In this early report, $[(\eta^6\text{-benzene})RuCl_2]_2$ was employed in the hydrogenation of 1-pentene. Pentane was obtained in 22 % yield after 4 h reaction time at a temperature of 20 °C and at a pressure of $p(H_2) = 20$ bar. In 1998, Moldes and coworkers reported the catalytic hydrogenation of styrene (Scheme B1).[26] They employed $\eta^6$-arene ruthenium(II) catalysts, depicted in Figure B2. These catalysts yielded 97 % of ethylbenzene after 80 h at a temperature of 90 °C and at a pressure of 20 bar $H_2$ (substrate / catalyst = 200 / 1). They also reported, that the performance of $[(\eta^6\text{-cymene})RuCl_2]_2$ does not improve significantly upon increasing the hydrogen pressure at a temperature of 80 °C.[26]
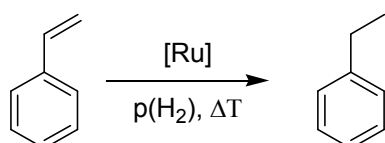


**Scheme B1:** Hydrogenation of styrene employing ruthenium catalysts.
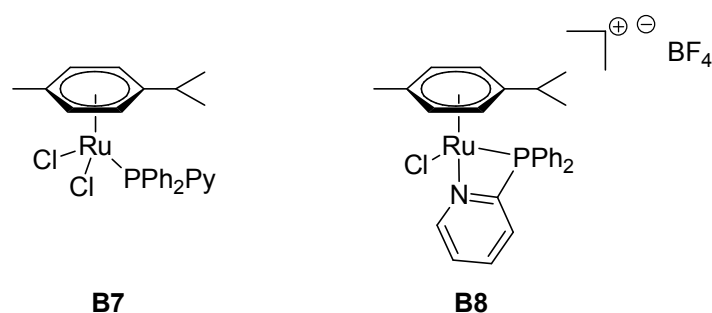
*Figure B2:* Hydrogenation catalysts employed by Moldes and coworkers.[26]

The application of mononuclear $\eta^6$-arene ruthenium(II) complexes in the biphasic hydrogenation was described by Dyson and coworkers in 2004.[27] The use of water as a second phase is facile, as water not only represents a cheap and environmentally justifiable solvent, but also is easy to handle.[28,29] Furthermore, water has shown to lead to catalyst activation in some cases.[27]
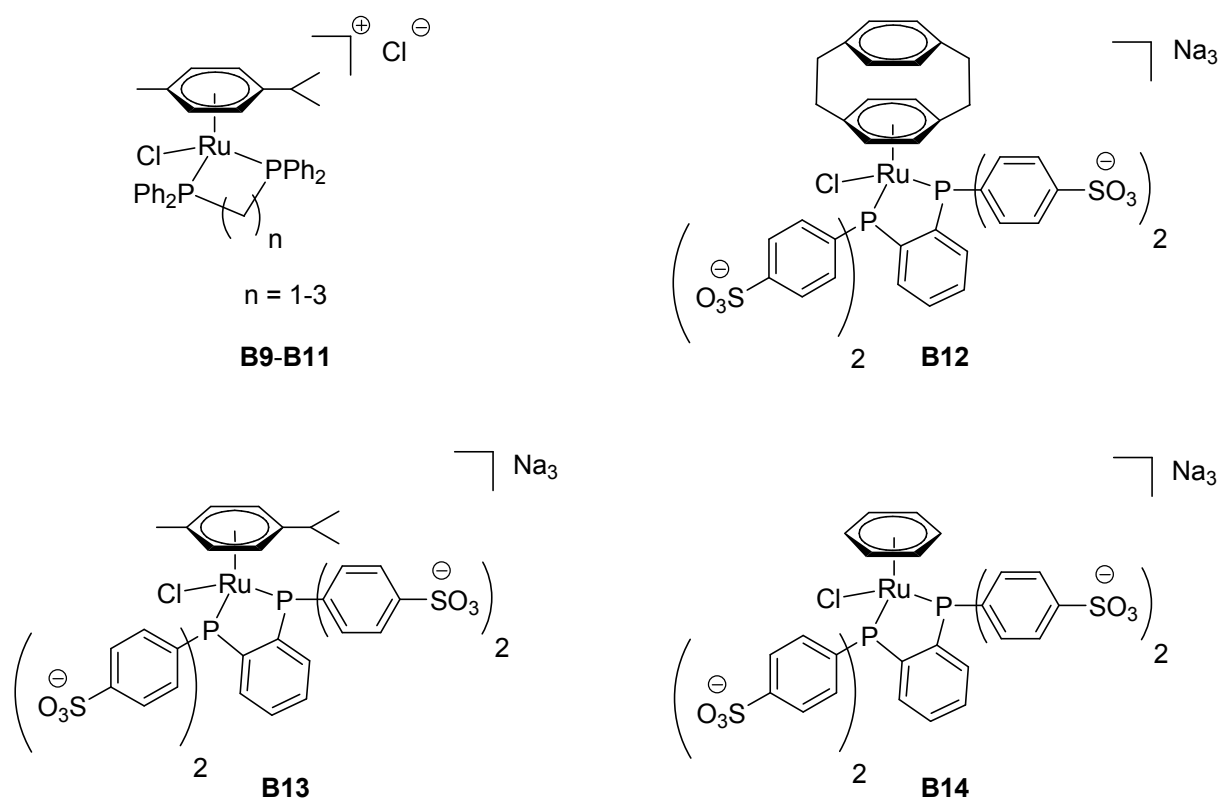


*Figure B3:* Mononuclear $\eta^6$-arene ruthenium(II) catalysts applied by Dyson and coworkers.[27]

As catalysts for the hydrogenation of styrene, Dyson and coworkers used the $\eta^6$-arene ruthenium(II) complexes depicted in figure B2. Their structure varies in comparison to the catalysts described above by their bidentate phosphane ligands.[27]

All catalysts applied by Dyson and coworkers yielded 100% conversion of styrene to ethylbenzene after 2 h (conditions: 100 °C, $p(H_2)$ = 45 bar; substrate / catalyst = 2000 / 1; solvent: toluene / water). The solubility of the catalysts in aqueous solution had a tremendous effect on their performance, obvious upon comparison of their activities. Catalysts without sulfonic acid substituted bidentate phosphane ligands (**B9**-**B11**) yielded 50 % ethylbenzene after about 80 min. The much more water soluble catalysts, whose phosphane ligands were substituted with sulfonic acid groups (**B12**-**B14**), yielded 50 % ethylbenzene already after about 40-50 min.[27]

Therefore, it seems interesting to take advantage of the $\eta^6$-arene arene substituent to introduce functional groups, which should modulate the solubility and therefore the performance of this class of catalysts. In the study presented here, 40 different di- and mononuclear ruthenium(II) complexes were designed, comprising five different kinds of functional groups (alcohol, amine, acetamide, carboxylic acid, carboxylic acid ester) and linker lengths ranging from one to five $CH_2$-groups. The behavior of the pendant linkers was investigated, and the reactivity of amino acid linkers closely analyzed. The ruthenium(II) catalysts were screened for their performance in the catalytic hydrogenation and transfer hydrogenation of olefins. Furthermore, osmium(II) complexes with pendant linkers were designed and ruthenium(II) complexes immobilized via their linker functionalities.

## 2. Synthesis of ruthenium(II) catalysts with pendant linkers

### 2.1. Synthesis of 1,4-cyclohexadiene precursors

The established route for the synthesis of $\eta^6$-arene ruthenium(II) complexes is facilitated by the oxidation of 1,4-cyclohexadiene and its derivatives by Ru(III)Cl$_3$ and its simultaneous reduction and coordination to Ru(II).[22] This method was first described by Winkhaus *et al.* in 1967.[30] All $\eta^6$-arene ruthenium(II) complexes designed in this study comprise an arene ligand, which is coordinated to the metal centre via this strategy. The necessary 1,4-cyclohexadiene derivatives were designed by the well-known *Birch*-Reduction.

This reaction facilitates the generation of 1,4-cyclohexadienes from their corresponding arenes. For this purpose, the aromatic educt is suspended in liquid ammonia, in which thereafter an alkaline metal (Li or Na, in this study Li was used exclusively) is dissolved. Upon addition of a proton source (in this study, ethanol was used) the aromatic ring system is reduced via two consecutive one electron reductions, yielding the 1,4-cyclohexadiene derivatives.[31]

One of the advantages of this reaction strategy is the sole formation of 1,4- or 2,5-cyclohexadiene derivatives, whereas conjugated double bonds are not formed. The reaction is straight forward and tolerates a wide variety of different functional groups on the aromatic ring system. Furthermore, with the substrates employed in this study, only 1,4-cyclohexadiene derivatives were obtained. This was confirmed by $^1$H NMR and $^{13}$C NMR spectroscopy. In all cases, two different signals with the ratio of 2 / 1 were observed for the three olefinic protons at about 6.0 – 5.5 ppm. The four CH$_2$ protons were observed significantly upshifted, at about 2.8-2.5 ppm. The *Birch*-Reduction is therefore a facile protocol for the generation of 1,4-cyclohexadiene derivatives, making time consuming bottom up synthesis obsolete. [32] Nevertheless, one should note that this reaction requires close attention, as a considerable amount of liquid ammonia as well as alkaline metals and protic solvents are needed. Failures and misjudgment can therefore lead to violent reactions.

To determine the influence of different functional groups of pendant linkers on the performance of ruthenium(II) catalysts, phenylalkyl amines, phenylalkyl alcohols and phenylalkyl carboxylic acids were used as substrates in the *Birch*-Reduction. Linker

lengths varied from one to five $CH_2$ groups to determine their influence on the catalyst performance. Scheme B2 depicts the different substrates used. For yields, see table B1.
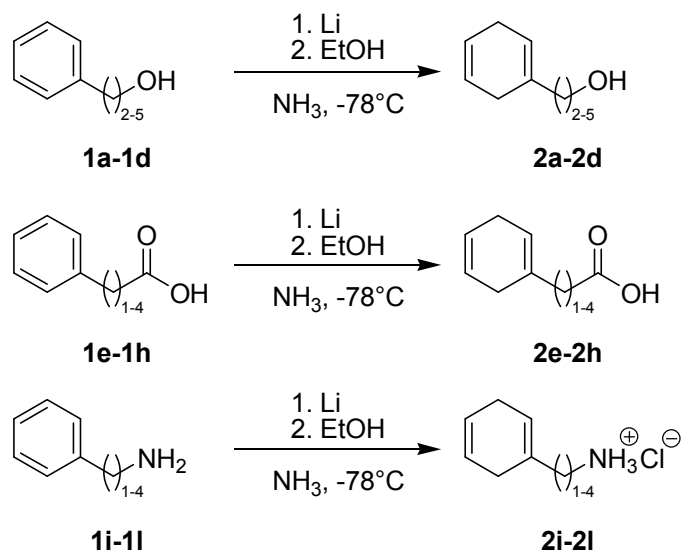


**Scheme B2:** Functionalized phenylalkyl derivatives employed as substrates in the Birch-Reduction.

All employed alkylarenes **1a**-**1l** are commercially available and were used without further purification (scheme B2). They yield their corresponding 1,4-cyclohexadiene derivatives **2a**-**2l** in moderate to high yields (table B1). In all cases, reaction conditions themselves were the same. Nevertheless, work-up procedures varied depending on the functional group.

For alcohols **2a**-**2d**, the reaction mixture was evaporated to dryness under reduced pressure, the remaining solids suspended in a minimum amount of water and extracted with dichloromethane. After removal of water from the organic phase with $MgSO_4$, the alcohols were received upon evaporation of the solvent.

For amines and carboxylic acids **2e**-**2l**, the reaction mixture was evaporated to dryness under reduced pressure, the remaining solids suspended in a minimum amount of water and acidified with hydrochloric acid (pH 1-2). The products were collected by recrystallization at -18 °C. Alkylamines **2i**-**2l** were yielded as their corresponding ammonium chloride salts. Extraction with dichloromethane was also carried out for **1i**, yielding 1,4-cyclohexadiene-1-benzyl amine as a slightly yellowish oil.

The identity and purity of all products **2a**-**2l** was confirmed by $^1$H NMR and $^{13}$C NMR spectroscopy. IR spectra of products **2e**-**2h** show strong carbonyl resonances between 1710 und 1690 cm$^{-1}$.

*Table B1:* Variety of products yielded by birch reduction of functionalized aryls.

| entry | educt | FG | n = | product | yield [%] |
|-------|-------|-----|-----|---------|-----------|
| 1 | **1a** | -OH | 2 | **2a** | 32 |
| 2 | **1b** | -OH | 3 | **2b** | 73 |
| 3 | **1c** | -OH | 4 | **2c** | 73 |
| 4 | **1d** | -OH | 5 | **2d** | 82 |
| 5 | **1e** | -COOH | 1 | **2e** | 78 |
| 6 | **1f** | -COOH | 2 | **2f** | 77 |
| 7 | **1g** | -COOH | 3 | **2g** | 44 |
| 8 | **1h** | -COOH | 4 | **2h** | 29 |
| 9 | **1i** | $-NH_3^+Cl^-$ | 1 | **2i** | 62 |
| 10 | **1j** | $-NH_3^+Cl^-$ | 2 | **2j** | 51 |
| 11 | **1k** | $-NH_3^+Cl^-$ | 3 | **2k** | 76 |
| 12 | **1l** | $-NH_3^+Cl^-$ | 4 | **2l** | 94 |

Furthermore, $\eta^6$-arene ruthenium(II) complexes with pendant donor functionalities can undergo intramolecular as well as intermolecular (polymerization) coordination. To examine this effect during catalysis, the amines **2i**-**2l** were converted into their corresponding acetamides. This extends the library of 1,4-cyclohexadiene derivatives to be employed for complex synthesis by compounds **2m**-**2p**, whose nitrogen donor has a significantly lower nucleophilicity (scheme B3).



**2i-2l**                                                    **2m-2p**
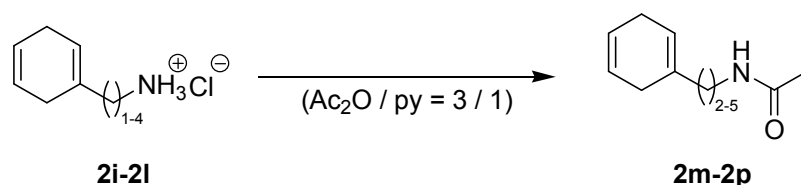
*Scheme B3:* Acetylation of 1,4-cyclohexadiene derivatives with acetic acid anhydride.

This straight forward synthesis results in product yields of up to 96% (table B2). As solvents for acetylation a mixture of pyridine (base) and acetylation reagent (acetic anhydride) were used. The products **2m**-**2p** can easily be isolated by removing the volatiles of the reaction mixture under reduced pressure and subsequent extraction from a mixture of water and dichloromethane. The product identity and purity was confirmed by $^1$H NMR and $^{13}$C NMR spectroscopy. IR spectra of compounds **2e**-**2h** showed strong resonances at 1650-1630 cm$^{-1}$ and 1570-1515 cm$^{-1}$. These resonances are lying in the expected range of acetamides. Furthermore, typical diene resonances were observed between 1000 cm$^{-1}$ and 600 cm$^{-1}$.

***Table B2:*** Variety of products yielded by acetylation of 1,4-cyclohexadiene-1-ammonium chlorides.

| entry | FG | n = | product | yield [%] |
|-------|------|-----|---------|-----------|
| 1 | -NHAc | 1 | **2m** | 71 |
| 2 | -NHAc | 2 | **2n** | 96 |
| 3 | -NHAc | 3 | **2o** | 77 |
| 4 | -NHAc | 4 | **2p** | 81 |

By the same method, 1,4-cyclohexadiene-1-benzyl ammonium chloride **2i** was converted to the corresponding trifluoroacetamide **2q**. This was facilitated by employing trifluoroacetic acid instead of acetic acid. All other reaction conditions and work-up procedures were identical to the ones described for **2m**-**2p**. The structural identity and purity of 1,4-Cyclohexadiene **2q** was confirmed by $^1$H NMR, $^{13}$C NMR and $^{19}$F NMR spectroscopy, elemental analysis as well as IR spectroscopy.
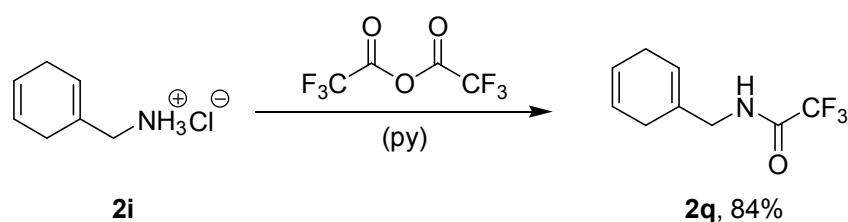


***Scheme B4:*** Conversion of 1,4-cyclohexadiene-1-benzyl ammonium chloride **2i** to 1,4-cyclohexadiene-1-benzyl trifluoroacetamide **2q**.

In $^{13}$C NMR spectra, compound **2q** comprises a quartet at 157.7 ppm with a coupling constant of 36.9 Hz, resembling the CO carbon atom. The $CF_3$ group is downshifted dramatically compared to a $CH_3$ group and observed as a quartet at 116 ppm with a coupling constant of 287.5 Hz. In $^{19}$F spectra, only one single peak at -75.92 ppm is observed, lying in the expected range for a $CF_3$ groups. $^1$H NMR spectra revealed the NH resonance also to be shifted significantly. It was observed at 7.38 ppm, whereas the NH resonance of the corresponding acetylamide **2m** was observed at 5.52 ppm. This shift of almost 1.9 ppm can be accounted to the strong electron withdrawing effect of a $CF_3$ group.

## 2.2. Synthesis of dinuclear ruthenium complexes

Halide bridged half sandwich complexes of ruthenium and osmium have been investigated for several decades.[33,34] However, d6 metal centers have a high tendency to coordinate nucleophiles such as primary amines. For the coordination of arenes with nucleophilic amines, we chose the approach by Beck *et al.*,[22] who reported $\eta^6$-arene coordinated *(R)*-2,5-dihydrophenylglycine to a ruthenium(II) centre. This was achieved by esterification of the terminal carboxylate group of *(R)*-2,5-dihydrophenylglycine and simultaneous shielding of the terminal amino group from the ruthenium. By conducting the reaction in 2 M hydrochloric acid, the amino group is protonated under these conditions and thus does not coordinate to the Lewis acidic metal center. By using these two approaches, dinuclear complexes **3a-t** were synthesized, featuring non
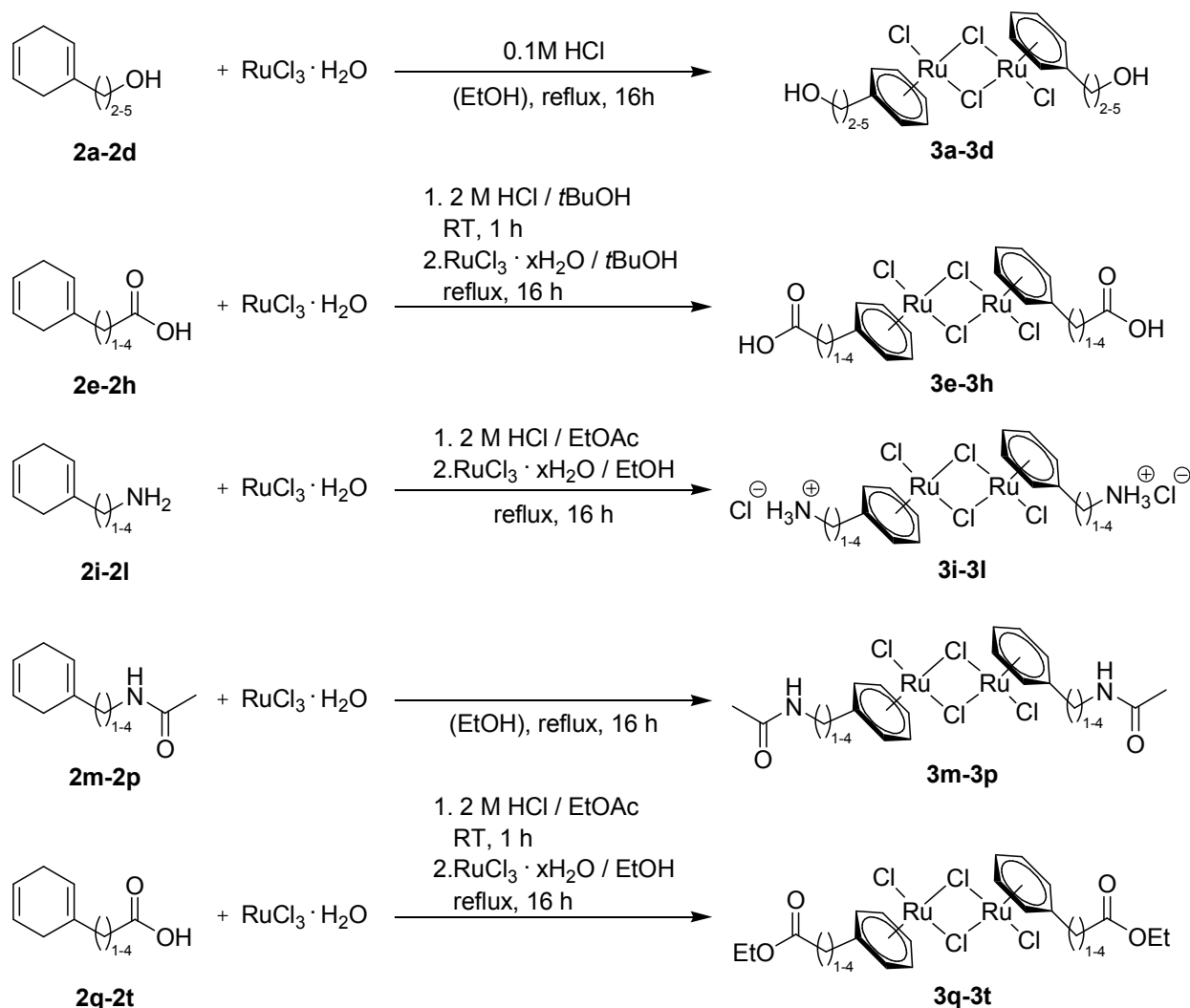


**Scheme B5:** Synthesis of $\eta^6$-aryl Ruthenium(II) dimeric complexes having different functionalities. For yields and solvents, see table 1.

coordinated alcohols, ammonium chlorides, N-acetyl-amides and carboxylic esters with 1 to 4 $CH_2$ groups (Scheme B5). Product yields are listed in table B3. In all cases, five equivalents of the corresponding 1,4-cyclohexadiene-derivative were reacted with one equivalent of $RuCl_3 \cdot n\ H_2O$ by refluxing in the reaction solution over night. The product was recovered by sequential recrystallization and filtration (from the reaction medium) at -18 °C and was then washed with ethanol and pentane. Despite the well-optimized synthesis of halide-bridged dinuclear $\eta^6$-arene ruthenium(II) complexes, elaboration becomes more complicated due to the pendant linker functionalities. To prevent coordination of nucleophilic functional groups to the metal centre, different strategies had to be applied, depending on the functional group (see table B3 for details).

**Table B3:** Synthesis of functionalized $\eta^6$-aryl Ruthenium(II) dimeric complexes.[a]

| entry | ligand | FG | $(CH_2)_n$ | solvent | product | yield [%] |
|:---:|:---:|:---:|:---:|:---:|:---:|:---:|
| 1 | **2a** | -OH | 2 | 0.1M HCl in EtOH | **3a** | 87 |
| 2 | **2b** | -OH | 3 | 0.1M HCl in EtOH | **3b** | 77 |
| 3 | **2c** | -OH | 4 | 0.1M HCl in EtOH | **3c** | 89 |
| 4 | **2d** | -OH | 5 | 0.1M HCl in EtOH | **3d** | 77 |
| 5 | **2e** | -COOH | 1 | 2 M HCl in *t*BuOH | **3e** | 70 |
| 6 | **2f** | -COOH | 2 | 2 M HCl in *t*BuOH | **3f** | 41 |
| 7 | **2g** | -COOH | 3 | 2 M HCl in *t*BuOH | **3g** | 78 |
| 8 | **2h** | -COOH | 4 | 2 M HCl in *t*BuOH | **3h** | 65 |
| 9 | **2i** | $-NH_3^+Cl^-$ | 1 | 2 M HCl in EtOAc / EtOH | **3i** | 83 |
| 10 | **2j** | $-NH_3^+Cl^-$ | 2 | 2 M HCl in EtOAc / EtOH | **3j** | 88 |
| 11 | **2k** | $-NH_3^+Cl^-$ | 3 | 2 M HCl in EtOAc / EtOH | **3k** | 86 |
| 12 | **2l** | $-NH_3^+Cl^-$ | 4 | 2 M HCl in EtOAc / EtOH | **3l** | 89 |
| 13 | **2m** | -NHAc | 1 | EtOH | **3m** | 68 |
| 14 | **2n** | -NHAc | 2 | EtOH | **3n** | 92 |
| 15 | **2o** | -NHAc | 3 | EtOH | **3o** | 84 |
| 16 | **2p** | -NHAc | 4 | EtOH | **3p** | 84 |
| 17 | **2e** | -COOEt | 1 | 2 M HCl in EtOAc / EtOH | **3q** | 83 |
| 18 | **2f** | -COOEt | 2 | 2 M HCl in EtOAc / EtOH | **3r** | 80 |
| 19 | **2g** | -COOEt | 3 | 2 M HCl in EtOAc / EtOH | **3s** | 85 |
| 20 | **2h** | -COOEt | 4 | 2 M HCl in EtOAc / EtOH | **3t** | 88 |

(a) see scheme B5 for synthetic details.

The low nucleophilicity of 1,4-cyclohexadiene alkyl alcohols **2a**-**2d** was further reduced by addition of 0.1 M HCl to the ethanolic reaction solution. This ensures a strongly acidic initial pH and hinders alcohol coordination at the metal centre, yielding the

dinuclear complexes **3a**-**3d**. Hydrochloric acid was not added during the synthesis of complexes **3m**-**3p**, as the acetyl group, with which the amine was functionalized, is not nucleophilic enough to lead to side reactions. This however is not true for the amino-functionalized complexes **3i**-**3l**. The high nitrophilicity of ruthenium(II) metal centers made it necessary to conduct the synthesis in 2 M HCl in ethanol. This ensures the amino group to be protonated during the synthesis. The amino group is therefore, lacking a free electron pair, not able to coordinate to the metal centre. Consistently, all complexes **3i**-**3l** were obtained as ammonium chloride salts, which was proven from $^1$H NMR spectrometry as well as elemental analysis. In $^1$H NMR spectra, the peaks corresponding to the NH$_3$ protons were observed between 8.8 and 7.9 ppm as a broad singulet with an integral of 3. This clearly indicates the amine to be protonated. The peak assignment was confirmed by $^1$H$^1$H COSY NMR spectroscopy. In all cases, elemental analysis fitted the values calculated for the di-HCl adducts. In the case of 1,4-cyclohexadiene derivatives with carboxylic acid functional groups, two different methods were applied. Carboxylic acids can be undertaken a convenient acid catalyzed esterification. This was facilitated by stirring **2e**-**2h** in a 2M solution of HCl in acetic acid ethyl ester for 1 h at room temperature (Scheme B6). The resulting ethyl ester was not isolated. For the synthesis of complexes **3e-3h**, comprising pendant linkers with carboxylic acid functional groups, a different method was applied (scheme B5, table B3). The reaction was conducted in 2 M hydrochloric acid in *tert*-butanole. In contrast to the synthesis of carboxylic esters **3q-3t**, carried out in acetyl ethyl ester and ethanol, reaction in *tert*-butanole does not lead to esterification due to instability of *tert*-butanole ethyl esters at low pH values (scheme B7).
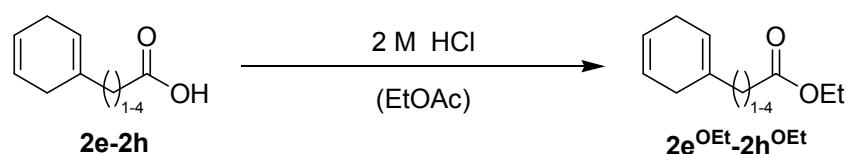


**Scheme B6:** Acid catalyzed esterification of 1,4-cyclohexadiene derivatives **2e**-**2h**.

The colors of the synthesized dimeric halide bridged ruthenium(II) complexes **3a**-**3t** range from deep green over orange to deep red. $^1$H and $^{13}$C NMR spectra were collected without exceptions in DMSO-d$_6$. This is due to the fact, that complexes **3a**-**3t** are virtually insoluble to only slightly soluble in aprotic and protic apolar as well as polar solvents. In general, donor solvents such as H$_2$O and DMSO cleave the *μ*-chloro bridges of the dinuclear complexes, yielding mononuclear complexes of much higher

solubility. All dinuclear $\eta^6$-arene ruthenium complexes synthesized by the procedures described in scheme B5 and table B3 were obtained in good to excellent yields 92%-94%). In each case, the products obtained were analytically pure. Nevertheless, yields were lower for **3f**. This can be attributed to the high solubility of this complex in ethanol, reducing yields first during recrystallization from the reaction mixture and second during work-up. Consequently, yields could be improved by applying longer recrystallization times and cold ethanol to rinse the resulting precipitate.
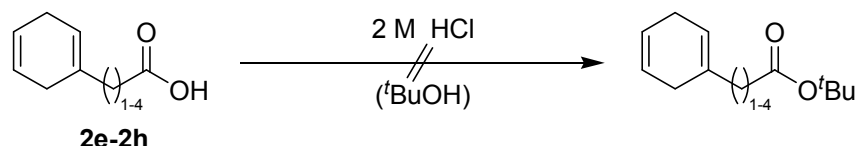


***Scheme B7:*** Esterification of 1,4-cyclohexadiene derivatives **2e**-**2h** does not take place in $^t$BuOH.

The identities and purities of complexes **3a**-**3t** have been confirmed by $^1$H NMR, $^{13}$C NMR, elemental analysis and IR spectroscopy. When necessary, $^1$H$^1$H COSY NMR spectra were recorded to assign the different alkyl $CH_2$ groups of the pendant linkers.

For all complexes **3a**-**3t** $^1$H NMR spectra confirmed the rearomatization of the 1,4-cyclohexadiene derivative. While in $^1$H NMR spectra of **2a**-**2p** signals with an integral of 3 were observed between 5.0 and 5.5 ppm, resembling the olefinic CH protons, the $^1$H NMR spectra of their corresponding $\eta^6$-arene complexes **3a**-**3t**, showed signals with the intensity of 5, shifted downfield by about 0.5-1.2 ppm (resonances observed between 6.5 and 5.5 ppm). The signals observed for the arene system can clearly be distinguished from non-coordinated alkylarenes **1a**-**1l**, where the arene signals are observed at around 7 ppm. The upfield shift of coordinated $\eta^6$-arene signals can be attributed to the strong electron withdrawing effect of transition metal centers, resulting in a deshielding of the proton nuclei.

This effect can also clearly be seen in $^{13}$C NMR spectra. The olefinic peak signals of 1,4-cyclohexadiene derivatives **2a**-**2p** are observed between 130-120 ppm, the quaternary carbon is observed around 130 ppm. The two $CH_2$ ring carbons appear around 25-30 ppm. In $^{13}$C spectra of dinuclear $\eta^6$-arene complexes **3a**-**3t**, all five arene CH carbons are observed at about 83-89 ppm, whereas the quaternary carbon is observed around 105 ppm. Again, rearomatization is clearly visible. Furthermore, the upfield shift of $\eta^6$-arene complexes **3a**-**3t** compared to non-coordinated arenes **1a**-**1l** was observed. Arene signals for the functionalized aryls are observed at values around

120-130 ppm for the CH carbons and 140 ppm for the quarternary carbon (see figure B4 for a representative $^{13}$C NMR spectrum).

IR spectra of $\eta^6$-arene complexes **3a**-**3t** show aromatic bands between 900-700 cm$^{-1}$. Hydroxy functionalized complexes **3a**-**3d** show clearly identifiable vibrational frequencies resulting from the hydroxyl group between 1076-1047 cm$^{-1}$. In case of carboxylic acids **3e**-**3h**, CO stretching frequencies between 1750 cm$^{-1}$ to 1725 cm$^{-1}$ are observed. In comparison to non-coordinated 1,4-cyclohexadiene derivatives, the wavenumber increases by about 30 cm$^{-1}$. Acetamide functionalized complexes **3m**-**3p** show vibrational frequencies at 1680-1630 cm$^{-1}$, 1570-1515 cm$^{-1}$ and 1380 – 1350 cm$^{-1}$. These deformational frequencies lie in the expected range for acetamides. Carboxylic acid ethyl ester complexes **3s**-**3t** show strong bands between 1743 cm$^{-1}$ and 1728 cm$^{-1}$, resembling the CO stretching frequencies.
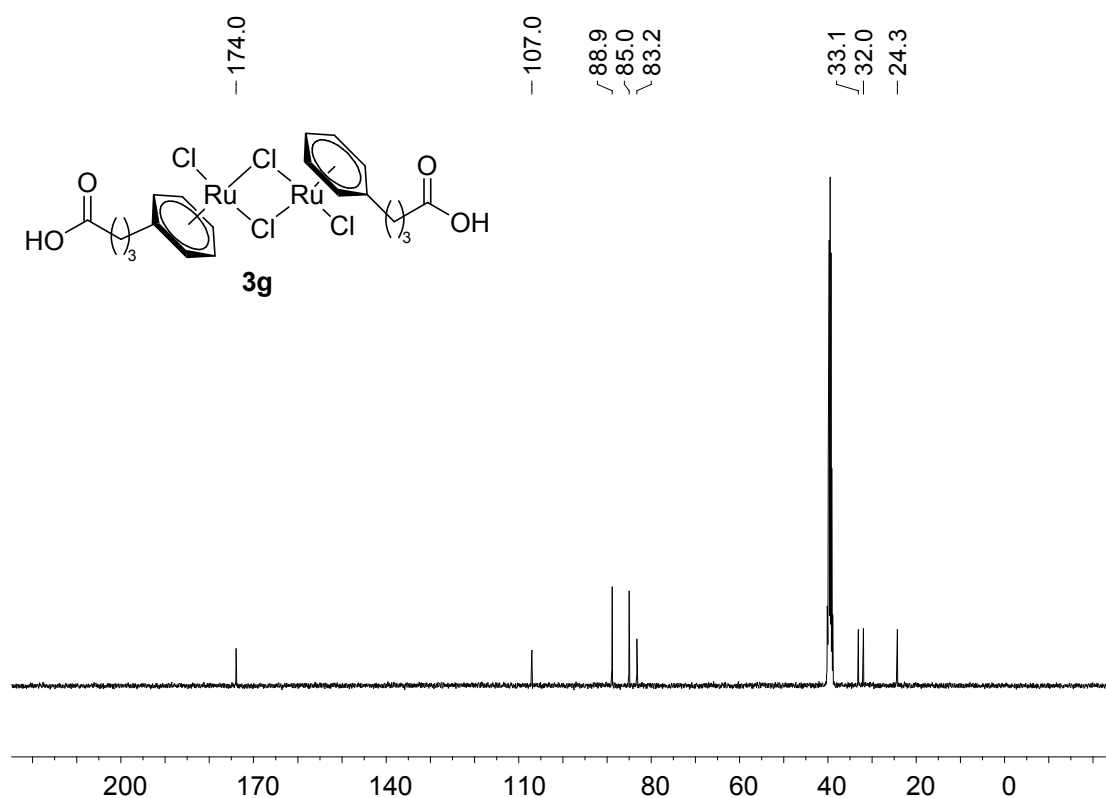


***Figure B4:*** Representative $^{13}$C NMR spectrum of dinuclear $\eta^6$-arene complexes **3a**-**3t**. Depicted: Spectrum of **3g**. $^{13}$C NMR (100.5 MHz; 25 °C; DMSO-d$_6$).

## 2.3. Synthesis of mononuclear ruthenium catalysts

To generate catalytically more potent organometallic systems, complexes **3a**-**3t** were converted to their 18 electron monodentate triphenylphosphine analogues **4a**-**4t**. Cleavage of dinuclear $\eta^6$-arene ruthenium(II) complexes by donor ligands was described by Smith and coworkers already in 1974.[35] Süss-Fink and coworkers as well as Therrien and coworkers reported other complexes of this class in which triphenylphosphine always acts as a ligand.[36,37,38,39]
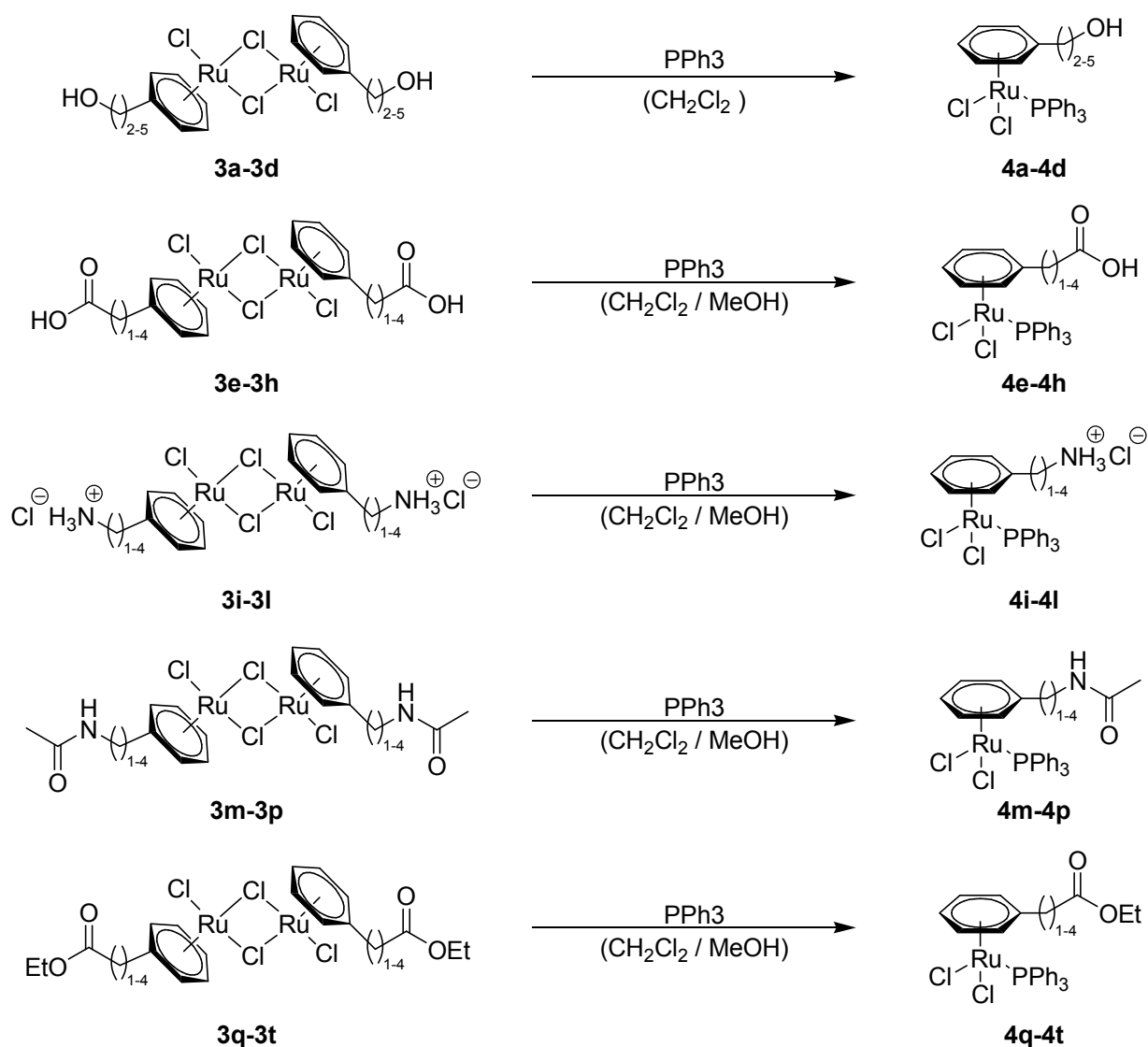
**Scheme B8:** Cleavage of dinuclear $\eta^6$-aryl Ruthenium(II) complexes using triphenylphosphine. For reaction conditions and yields see table B4.

Preparation of this class of organometallic complexes follows a simple preparative procedure. Compared to the method of Smith and coworkers, only the solvent was changed.[35] Conversion occurs readily and without side product formation in either a

mixture of dichloromethane or dichloromethane / methanol = 1 / 1, depending on the solubilities of the di- and mononuclear species (see scheme B8 and table B4 for details). Excess of triphenylphosphine was washed with diethylether in which complexes **4a**-**4t** are in general virtually insoluble. All complexes **3a**-**3t** and **4a**-**4t** are stable to air for at least several months and do not need to be stored under argon. Therefore, a small library of mononuclear $\eta^6$-aryl Ru (II)PPh$_3$ complexes can be generated, which are potential catalysts in the hydrogenation of olefins. Furthermore, by the large variety of functional groups as well as chain lengths, influences of these structural criteria can be investigated.

***Table B4:*** Synthesis of functionalized mononuclear $\eta^6$-aryl Ruthenium complexes, reaction conditions and yields.

| entry | reactant | FG | $(CH_2)_n$ | solvent | time | product | yield [%] |
|:---:|:---:|:---:|:---:|:---:|:---:|:---:|:---:|
| 1 | **3a** | -OH | 2 | DCM | 2h | **4a** | 52 |
| 2 | **3b** | -OH | 3 | DCM | 1h | **4b** | 95 |
| 3 | **3c** | -OH | 4 | DCM | 2h | **4c** | 93 |
| 4 | **3d** | -OH | 5 | DCM | 1h | **4d** | 97 |
| 5 | **3e** | -COOH | 1 | DCM/MeOH | 1 h | **4e** | 60 |
| 6 | **3f** | -COOH | 2 | DCM | 2 h | **4f** | 77 |
| 7 | **3g** | -COOH | 3 | DCM/MeOH | 30 min | **4g** | 81 |
| 8 | **3h** | -COOH | 4 | DCM | 2 h | **4h** | 61 |
| 9 | **3i** | -NH$_3^+$Cl$^-$ | 1 | DCM/MeOH | 3 h | **4i** | 79 |
| 10 | **3j** | -NH$_3^+$Cl$^-$ | 2 | DCM/MeOH | 3 h | **4j** | 59 |
| 11 | **3k** | -NH$_3^+$Cl$^-$ | 3 | DCM/MeOH | 3 h | **4k** | 67 |
| 12 | **3l** | -NH$_3^+$Cl$^-$ | 4 | DCM/MeOH | 30 min | **4l** | 88 |
| 13 | **3m** | -NHAc | 1 | DCM/MeOH | 20 min | **4m** | 93 |
| 14 | **3n** | -NHAc | 2 | DCM/MeOH | 20 min | **4n** | 99 |
| 15 | **3o** | -NHAc | 3 | DCM/MeOH | 30 min | **4o** | 78 |
| 16 | **3p** | -NHAc | 4 | DCM/MeOH | 20 min | **4p** | 89 |
| 17 | **3q** | -COOEt | 1 | DCM/MeOH | 1 h | **4q** | 83 |
| 18 | **3r** | -COOEt | 2 | DCM/MeOH | 2 h | **4r** | 47 |
| 19 | **3s** | -COOEt | 3 | DCM/MeOH | 30 min | **4s** | 91 |
| 20 | **3t** | -COOEt | 4 | DCM/MeOH | 30 min | **4t** | 90 |

Nevertheless, due to the differences in solubility of the dinuclear complexes **3a**-**3t**, not only the solvent mixture, but also reaction times had to be set individually, ranging from 30 min to 120 min (table B4). All complexes were obtained in good to quantitative yields

(52-99 %). Low yields can mainly be attributed to the low but yet increased solubility of some complexes in diethylether as seen, for example, for **4a**. Work-up procedures need to be optimized in this case. The identity and purity of complexes **4a**-**4t** have been confirmed by $^1$H NMR, $^{13}$C NMR, elemental analysis and IR spectroscopy. When necessary, $^1$H$^1$H COSY NMR spectra were recorded to assign the different alkyl CH$_2$ groups of the pendant linkers. In $^1$H NMR spectra of all complexes, thriphenylphosphine is clearly identified as a novel ligand. All spectra show two multiplets at between 7.0 and 7.8 ppm with an integral ratio of 9 / 6. These multiplets can be assigned to the six *ortho*-CH protons as well as the nine *meta*- and *para*-CH protons of the triphenylphosphine ligand. In $^1$H NMR spectra of their corresponding dinuclear complexes **3a**-**3t**, no peaks were observed in this range.
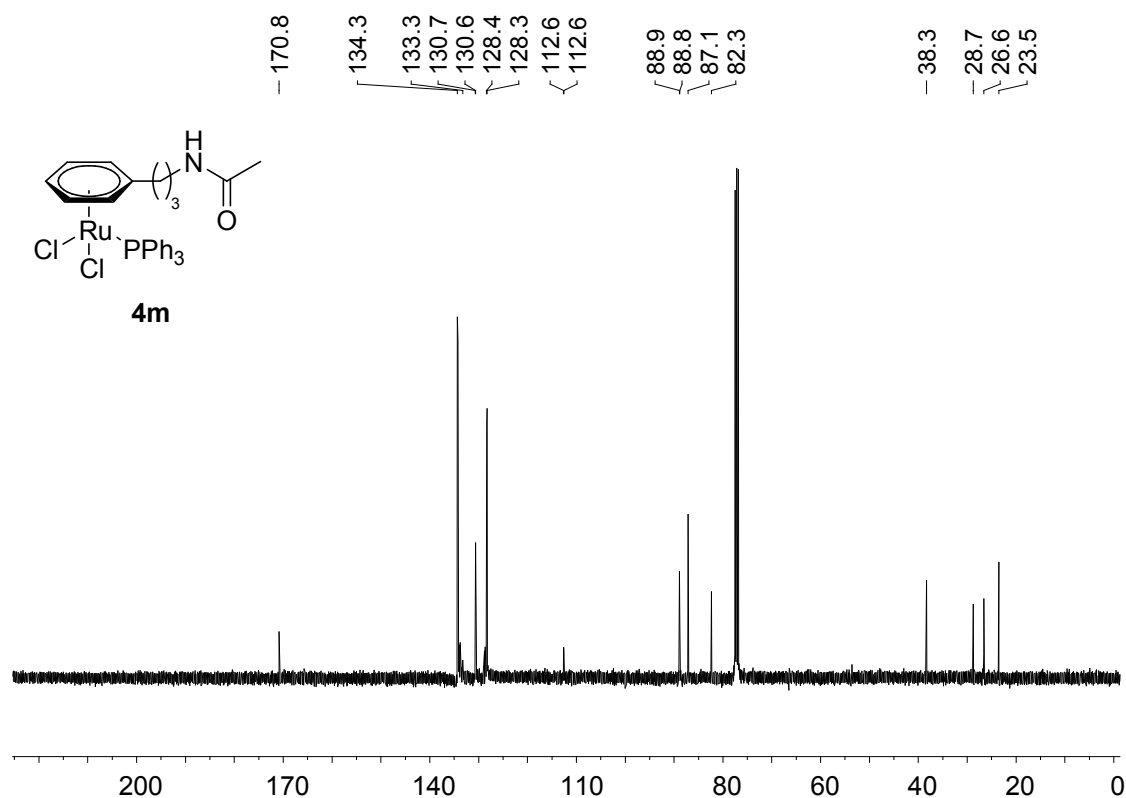


***Figure B5:*** Representative $^{13}$C NMR spectrum of mononuclear η$^6$-arene complexes **4a**-**4t**. Depicted: Spectrum of **4m**. $^{13}$C NMR (100.5 MHz; 25 °C; CDCl$_3$).

Furthermore, $^1$H NMR spectra of **4a**-**4t** comprise signals of the coordinated η$^6$-arene ligand between 4.5 ppm and 5.5 ppm with an integral of 5. In most cases, differentiation between *ortho*- *meta*- and *para*-CH protons is possible, resulting in integral ratios of 2 / 2 / 1. Coupling constants of the coordinated CH protons are typically between 4.5 and 7.5 Hz. Compared to $^1$H spectra of dinuclear complexes **3a**-**3t**, these signals are significantly upshifted by about 1 ppm.

Also in $^{13}$C NMR spectra of complexes **4a-4t**, introduction of a triphenylphosphine ligand leads to significant changes in peak patterns. All spectra confirm triphenylphosphine as a novel ligand. Its aromatic carbon peaks are observed as four distinct signals at 134 ppm ($J_{PC}$ = 10 Hz), 133 ppm ($J_{PC}$ = 47-49 Hz), 130 ppm ($J_{PC}$ < 3 Hz), and 128 ppm ($J_{PC}$ = 10 Hz). The coupling constants are in accordance to values reported before.[40] In $^{13}$C NMR spectra of dinuclear complexes **3a-3t**, no peaks are observed in this range. Furthermore, the coordinated $\eta^6$-arene carbon atoms for catalysts **4a-4t** are observed in the ranges 100-115 ppm (quaternary carbon atom) and 80-95 ppm (CH carbons). These shifts are in accordance to shifts observed for complexes **3a-3t**. Nevertheless, for mononuclear complexes, six signals are observed for the coordinated $\eta^6$-arene carbons. The additional two signals can be attributed to doublet formation, resulting from $^3J_{PC}$ couplings. Coupling constants lie in the range between 4.5 Hz and 10 Hz (see figure B5 for a representative $^{13}$C NMR spectrum).

In all $^{31}$P NMR spectra, the signal corresponding to the coordinated triphenylphosphine phosphorous was observed as a singulet in the range between 27 ppm and 29 ppm. Therefore, the signal of triphenylphosphine shifts, compared to the not coordinated ligand, by more than 30 ppm. This also clearly confirms successful coordination.

In IR spectra, characteristic signals essentially correspond to the signals observed for complexes **3a-3t**. Vibrational CO resonances for acetamides **4m-4p** appear between 1645 cm$^{-1}$ and 1671 cm$^{-1}$. The carboxylic acid ethyl ether complexes **4q-4t** show CO bond stretching frequencies ranging from 1726 cm$^{-1}$ to 1733 cm$^{-1}$. In case of carboxylic acids **4e-4h**, CO stretching frequencies between 1740 cm$^{-1}$ to 1710 cm$^{-1}$ are found. However, $\eta^6$-arene complexes **4a-4t** show differences in the range of their aromatic bands between 900-700 cm$^{-1}$. In comparison to their precursors **3a-3t**, these bands are significantly stronger due to the additional aromatic rings introduced by the triphenylphosphine.

All complexes **4a-4t** have an intense red to orange color and show different solubility properties due to their $\eta^6$-arene functional groups. Ammonium chlorides are significantly more soluble in polar protic media than carboxylic esters or for example alcohols. Due to solubility problems, NMR spectra for **4i-4k** were carried out in CD$_3$COD instead of CDCl$_3$. This was also done for complex **4f**. It has a much lower solubility in dichloromethane than its corresponding ethyl ester **4n**. Even from a mixture of CD$_3$COD / CDCl$_3$ = 1 / 1, **4f** readily crystallizes within several hours (figure B6).
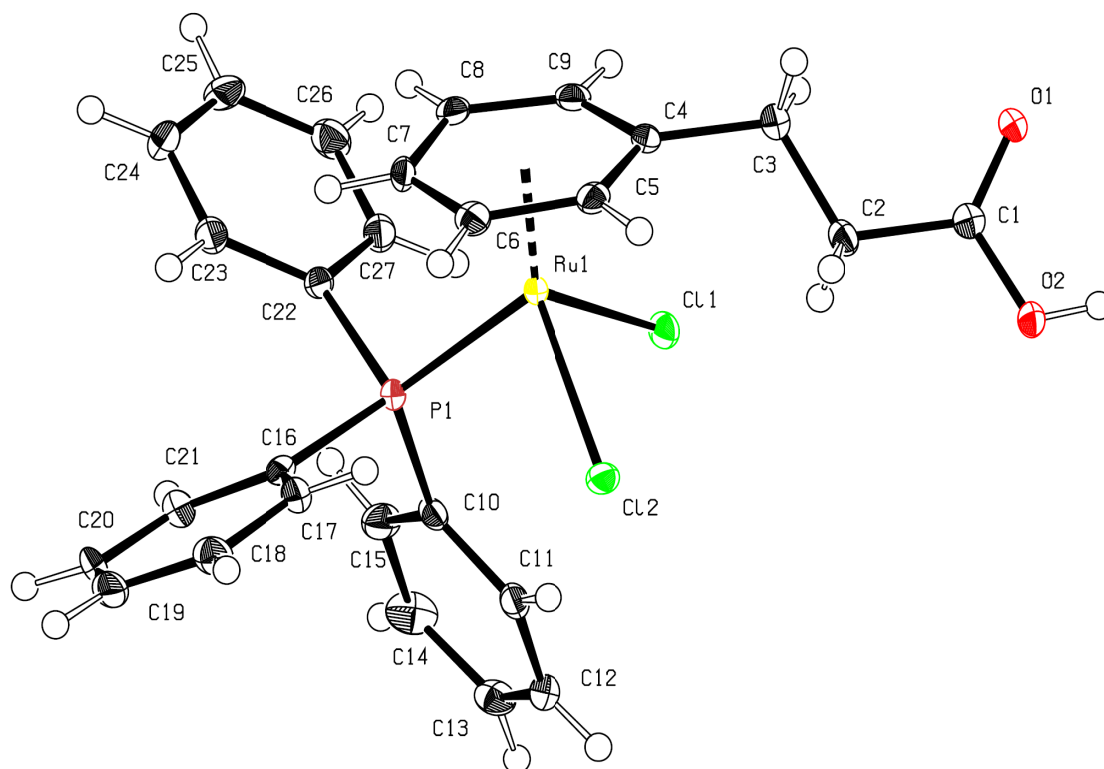
***Figure B6:*** ORTEP representation of **4f**. (50% thermal ellipsoids). Selected bond lengths (Å) and angles (deg): Ru(1)-C(4) 2.252(2), Ru(1)-C(5) 2.241(3), Ru(1)-C(6) 2.191(3), Ru(1)-C(7) 2.186(3), Ru(1)-C(8) 2.208(2), Ru(1)-C(9) 2.184(2), C(1)-O(1) 1.224(3), C(1)-O(2) 1.325(3), Ru(1)-Cl(1) 2.4140(6), Ru(1)-Cl(2) 2.4099(6), Ru(1)-P(1) 2.3643(7), O(1)-C(1)-O(2) 121.9(2), Cl(1)-Ru(1)-Cl(2) 87.13(2), Cl(1)-Ru(1)-P(1) 86.74(2), Cl(2)-Ru(1)-P(1) 91.09(2).

Complex **4f** crystallized in the *P2₁/n* space group. All bond lengths and angles are lie in the expected range. Bond distances between transition metal centre and $\eta^6$-arene ring range from 2.252(2) - 2.186(3) Å. They are similar to bond lengths observed for crystal structures of other functionalized $\eta^6$-arene complexes (**3i^DMSO**, figure B8). As observed for the **3i^DMSO** crystal, the Ru(1)-C(4) bond (geminal carbon) is slightly enlonged 2.252(2) Å compared to the other Ru-C$_{arene}$ bonds. The shortest bond is Ru(1)-C(7) (C$_{para}$) with a bond lengths of only 2.186(3) Å. Ru-Cl bond lengths are very similar, ranging from 2.4099(6) to 2.4140(6) Å. The complex forms a piano stool-type tetrahedral geometry. The Cl(1)-Ru(1)-Cl(2) angle (121.9(2) °) is significantly larger than the two P(1)-Ru(1)-Cl angles (86.74(2) ° and 87.13(2) °). This is due to the higher steric approach of the chlorine ligands compared to the triphenylphosphine. The crystal structure of **4f** clearly confirms, that the pendant carboxylic acid linker does not coordinate to the metal centre, as indicated by NMR and IR spectra and elemental analysis.
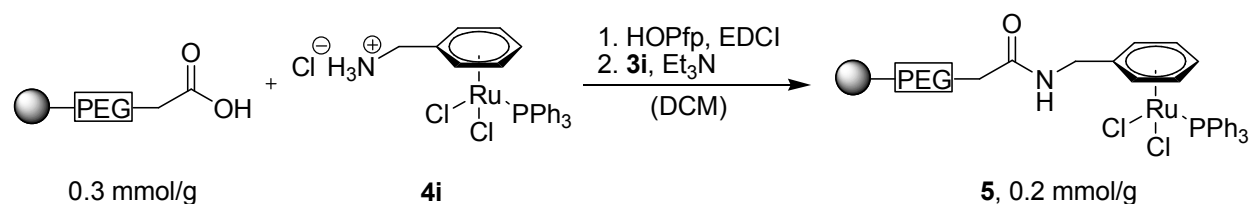
**Scheme B9:** Immobilization of [(η^6-benzylammonium)(PPh₃)RuCl₂]Cl **3i**. Complex 3i was immobilized on a composite polystyrene and 3.000-4.000 MW PEG resin in which the ends of the PEG chains had been functionalized with carboxyl groups. Immobilization was facilitated via the formation of a pentafluorophenol active ester.

To evaluate the possibility of catalyst immobilization on a solid phase support, a carboxy functionalized polystyrene / polyethylene glycol resin (NovaBiochem) was converted into its corresponding pentafluorophenol active ester. This active ester is readily cleft in the presence of triethylamine by complex **4i**, yielding the light orange catalyst resin **5** (scheme B9). Its structural identity was confirmed by $^{31}$P MAS NMR, infrared spectrometry and elemental analysis. Magic Angle Spinning revealed a single phosphorous peak at 28.6 ppm. For educt complex **4i**, one phosphorous peak at 28.6 was observed in $^{31}$P NMR spectrometry in deuterated chloroform, indicating the ruthenium centre to be structurally unaltered.
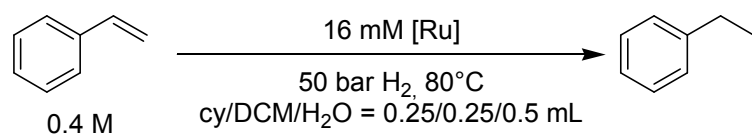


**Scheme B10:** Stability test of catalyst systems under hydrogenation conditions. Catalyst/Substrate = 1/25. The experiment was carried out under constant hydrogen pressure, both phases of the reaction solution were analyzed via ESI MS.

IR spectrometry also indicated product formation. The IR spectrum of the educt resin shows a CO bond stretching frequency at 1717 cm$^{-1}$. This signal can be attributed to the carboxylic acid. In the product resin **5**, this signal has vanished, giving rise to an amide bands 1520 cm$^{-1}$. Other amide bands, which would be expected in the range between 1680 cm$^{-1}$ 1630 cm$^{-1}$ could not be observed due to signal overlay resulting from the composite PEG resin. Nevertheless, this value lies in the expected range for acetamide bands,[40] thus indicating the immobilization of catalyst **4i** to have been successful. In elemental analysis, ruthenium, phosphorous and chlorine were found in a stoichiometry of 1 / 1 / 2 and a concentration of 0.2 mmol/g, confirming the success of the immobilization.

**Table B5:** Masses and species observed for selected catalysts in ESI MS spectra.[a]

| entry | catalyst | masses obs. [m/z] | species obs. [m/z] | abundance [%] |
|---|---|---|---|---|
| 1 | **4b** | 497.0 | $[M-Cl-HCl-H_2]^+$ | 55 |
|   |    | 534.9 | $[M-Cl]^+$ | 50 |
|   |    | 1105.0 | $[2M-Cl]^+$ | 20 |
| 2 | **4e** | 495.8 | $[2M-2HCl-CO_2+AcN]^+$ | 100 |
|   |    | 1090.7 | $[2M-2HCl+Na]^+$ | 65 |
|   |    |        | $[4M-4PPh_3-3HCl-Cl]^+$ |    |
|   |    | 455.0 | $[2M-2HCl-CO_2]^+$ | 60 |
| 3 | **4l** | 548.0 | $[M-Cl-HCl]^+$ | 100 |
|   |    | 285.9 | $[M-PPh_3-Cl-HCl]^+$ | 85 |
|   |    | 1130.8 | $[2M-Cl-2HCl]^+$ | 65 |
|   |    | 1209.7 | $[2M-Cl-HCl+AcN]^+$ | 45 |
| 4 | **4n** | 299.9 | $[M-PPh_3-Cl]^+$ | 100 |
|   |    | 561.9 | $[M-Cl]^+$ | 60 |
| 5 | **4r** | 576.9 | $[M-Cl]^+$ | 100 |
|   |    | 541.1 | $[M-Cl-HCl]^+$ | 95 |
|   |    | 315.0 | $[M-PPh_3-Cl]^+$ | 90 |
|   |    | 355.7 | $[M-PPh_3-Cl+AcN]^+$ | 85 |

(a) Measurements were carried out in approx. 0.02 M solution of catalyst in acetonitrile. Main metal containing peaks are displayed. Organic peaks have been omitted for clarity (e.g. $PPh_3$).

To test the stability of the $\eta^6$-arene ring under catalytic conditions, a standard biphasic experiment was conducted (scheme B10). As catalysts, complexes **4b**, **4e**, **4l**, **4n** and **4r** were employed in catalyst loadings of 4 mol%. High catalyst loadings and therefore high concentrations enabled analysis of the metal species formed during the catalyst cycle via ESI MS. Before tested in catalysis, the complexes were analyzed in ESI MS to determine the educt peak values. Analytical data gained during that experiment revealed the complexes to be intact and possible to be measured by ESI MS. There was a tendency of loosing triphenylphosphine observed, which happens during the measurement, as to be concluded from the NMR spectra, in which neither free triphenylphosphine nor a set of signals fitting the complexes' dinuclear precursors (**4b**, **4e**, **4l**, **4n**, **4r**) can be detected.

***Table B6:*** Masses and species observed for selected catalysts after catalytic runs in ESI MS spectra.[a]

| entry | catalyst | masses obs. [m/z] | species obs. [m/z] | abundance [%] |
|---|---|---|---|---|
| 1 | **4b** | 952.9[c] | $[3M-HCl-3Cl+2OH+\eta^6\text{-ligand}]^+$ | 35 |
| | | 764.9[c] | $[2M-HCl-2Cl+OH+\eta^6\text{-ligand}+styrene]^+$ | 20 |
| | | 730.0[c] | $[2M-2HCl-2Cl+OH+\eta^6\text{-ligand}+styrene]^+$ | 15 |
| 5 | **4e** | 1021.8[b] | $[2M-Cl+H_2O]^+$ | 20 |
| | | 975.8[c] | $[3M-3PPh_3-2Cl+OH+styrene]^+$ | 15 |
| 3 | **4l** | 625.1[b] | $[2M-2PPh_3-2HCl-Cl+H_2O]^+$ | 100 |
| | | 879.0[c] | $[2M-PPh_3-4HCl-Cl+2OH+2Na+H_2]$ | 100 |
| | | 913.8[c] | $[2M-PPh_3-2HCl-3Cl+4OH+2Na]$ | 85 |
| 2 | **4n** | 1061.9[c] | $[4Ru+7OH+3styrene+2\eta^6\text{-ligand}]^+$ | 50 |
| | | 1000.9[c] | $[4Ru+7OH+3styrene+\eta^6\text{-ligand}]^+$ | 50 |
| | | 942.9[c] | $[4Ru+7OH+4styrene]^+$ | 40 |
| 4 | **4r** | 576.9[b] | $[M-Cl]^+$ | 10 |
| | | 1189.5[b] | $[2M-Cl]^+$ | 10 |
| | | 541.1[b] | $[M-Cl-HCl]^+$ | 5 |
| | | 1121.8[c] | $[3M-3PPh_3-5Cl-3CH_2CH_3+Na+3styrene]^+$ | 100 |
| | | 890.9[c] | $[3M-3PPh_3-4Cl-3CH_2CH_3+2H_2O]^+$ | 40 |
| | | 857.9[c] | $[3M-3PPh_3-6Cl-3CH_2CH_3+2OH+styrene]^+$ | 40 |
| | | 609.0[c] | $[2M-2PPh_3-Cl-2CH_2CH_3+2H]^+$ | 20 |

(a) Catalyst/Styrene = 1/25. Main metal containing peaks are listed. Organic peaks observed (e.g. $PPh_3O$) are omitted for clarity. Catalysts were employed in a concentration of 16 mM. (b) ESI MS spectrum of organic phase (c) ESI MS spectrum of aqueous phase.

Analysis of the organic and inorganic phases of the catalyst solutions after substrate conversions (70-80 °C, 35 min) have revealed different sets of signals (table B6). Therefore, we assume the catalysts **4a**-**4t** to be precursors for the active species formed during the catalytic cycle. Only for complex **4r** residual signals resembling the initial organometallic species were observed in ESI MS spectra (576.9, $[M-Cl]^+$ and 1189.5 $[2M-Cl]^+$). An interesting finding in ESI spectra was a peak of 279.1 (m/z) resembling triphenylphosphine oxide. As the catalytic runs were performed without purging the autoclave with nitrogen or argon, triphenylphosphine could have been oxidized by air present in the autoclave. Formation of triphenylphosphine could be a sign for either catalyst activation or deactivation as triphenylphosphine oxide can not serve as a catalyst ligand any more. Metal containing peaks were assigned by their isotope patterns. In general they appear at higher molecular weights than those of the initial catalysts (Tab. 4), which can be assigned to the formation of species of higher nuclearity. This may be either a sign for formation of hydride bridged species in

solution[41] or indicate the presence of undercoordinated species which agglomerate under ESI MS conditions. Furthermore, several peaks can only be explained by taking styrene into account, which can form a $\pi$-bond to the metal centre via its olefinic ethylene or a $\eta^6$-arene piano stool bond via its aromatic ring. Formation of a $\eta^6$-arene bond implies cleavage of the initial functionalized $\eta^6$-arene ligand. This is possible to happen, as has been reported in literature.[17] Nevertheless, if this was a dominant process, metal containing peaks observed in ESI MS spectra should be the same for all catalysts employed. Yet, no single peak in ESI spectra was observed twice. Therefore, the $\eta^6$-arene ligand of the complex employed plays a role in catalyst performance, in spite of its ability to be cleaved by styrene.

Another possibility to test the $\eta^6$-arene ligand stability is by testing catalyst resin **5** under catalytic conditions and evaluate leaching of the transition metal centre (Fig. 4). Catalyst was employed in a concentration of 1 mol ‰ with respect to styrene. After 2 h, catalyst resin **5** yielded 79% of phenylethanole, detected by GC FID. The catalyst resin was filtered off and washed with dichloromethane and water. Elemental analysis revealed the content of Ru to be 0.9 % (0.1 mmol/g), whereas it initially was 1.8 % (0.2 mmol/g). This proves the $\eta^6$-arene ligand cleavage to take place, yet indicating that the cleavage is not a dominant process.

Therefore, the synthesized library consisting of complexes **4a**-**4t** can be tested for their performance under hydrogenation conditions, as the different substituents must have an effect on their behavior in terms of their dispersion in the two different phases, the nucleophilic properties of the functional groups and the resulting electronic features of the metal centre.

## 3. Synthesis osmium(II) complexes with pendant linkers

As reported above, the dimeric $\mu$-chloro-bridged complex **3c** is readily formed upon conversion of 4'-(2,5-dihydrophenyl)butanole with $RuCl_3 \cdot n\ H_2O$. Under very similar reaction conditions, the dimeric $\mu$-chloro-bridged complex **6** is obtained when $OsCl_3 \cdot n\ H_2O$ is used instead of ruthenium (scheme B11). The products are obtained as brown powders in good yields and excellent purity, if the reaction is carried out under an atmosphere of argon. For the osmium complex **6**, use of dry ethanol is mandatory to achieve satisfactory product formation. Complexes **3c** and **6** are moderately soluble in alcohols yet dissolve readily in donor solvents such as water and DMSO.



**2c**

**3c**: M = Ru (89 %)
**6**:   M = Os (70 %)
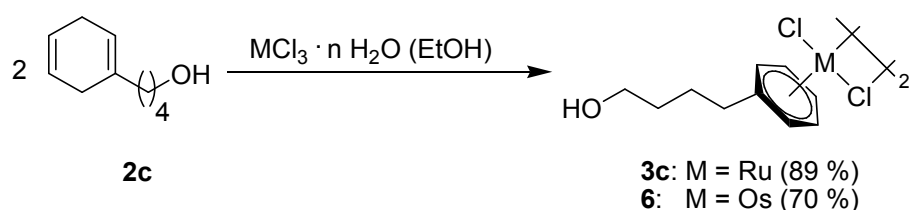
**Scheme B11:** Synthesis of dinuclear halide bridged $\eta^6$-arene complexes **3c** and **6**.

Complexes **3c** and **6** were characterized by elemental analysis, $^1H$ NMR, $^{13}C$ NMR and IR spectroscopy. The resonances for the $\eta^6$-arene moieties show a typical upfield shift compared to non-coordinated arenes. $^{13}C$ NMR resonances for the arene carbons of monomeric **3c**$^{DMSO}$ and **6**$^{DMSO}$ in DMSO-$d_6$ are observed between 109 ppm and 75 ppm. (Figure B7). For the osmium(II) complex **6**, signals appear about 7 to 8 ppm more upfield, compared to the analogous ruthenium(II) complex **3c**. This indicates a weaker ring current for the Os(II) compound, which might be explained by an increased transfer of electron density from ligand $\pi$-system to metal centered orbitals, since the interacting 6s and 5d orbitals (osmium) are lower in energy than the respective 5s and 4d orbitals (ruthenium).[42] There are no spectroscopic indications of an interaction between the alcohol function and the metal centre. For the Ru(II) complex **3c**, the O$H$-resonance observed by $^1H$ NMR in DMSO-$d_6$ is nearly identical to that of 4'-phenylbutanole with a triplet around $\delta$ = 4.4 ppm and a $^3J_{HH}$ coupling constant of the expected 5 Hz.[43] The corresponding signal for Os(II) derivative **6** appears slightly broadened and shifted upfield at $\delta$ = 3.8 ppm. Once synthesis of the complexes is completed, they may be handled under air. They are stable for several months without any apparent signs of decomposition. Even in a combination of 1 M of hydrochloric acid in water and DMSO, no change of the arene resonances was detected over a period of several days.
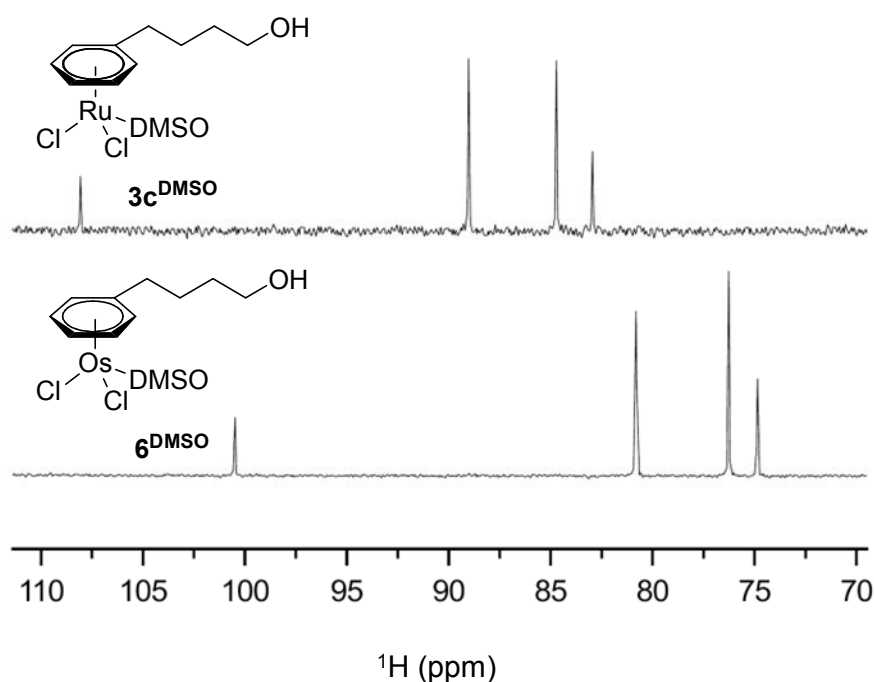
***Figure B7:*** Aromatic $^{13}C$ NMR resonances of complexes **3c**$^{DMSO}$ and **6**$^{DMSO}$ (100.5 MHz, 300 K, DMSO-$d_6$).

While synthesis of alcohol functionalized $\eta^6$-arene complexes is straight forward, conversion of $\omega$-(2,5-dihydrophenyl)alkyl amines with Os(III)Cl$_3$ under the same condition does not afford any identifiable product. This may be attributed to the high affinity of the amine tethers towards electrophilic cationic $d^6$ metal centers impairing arene-coordination. Hence, to suppress undesired binding of the amino function by protonation, 2,5-dihydrobenzyl amine was dissolved in a 2 M solution of HCl in ethyl acetate prior to addition of the metal chloride (scheme B12). Under the acidic reaction conditions, Ru(II) complex **3i** formed in good yields as an ochre powder.
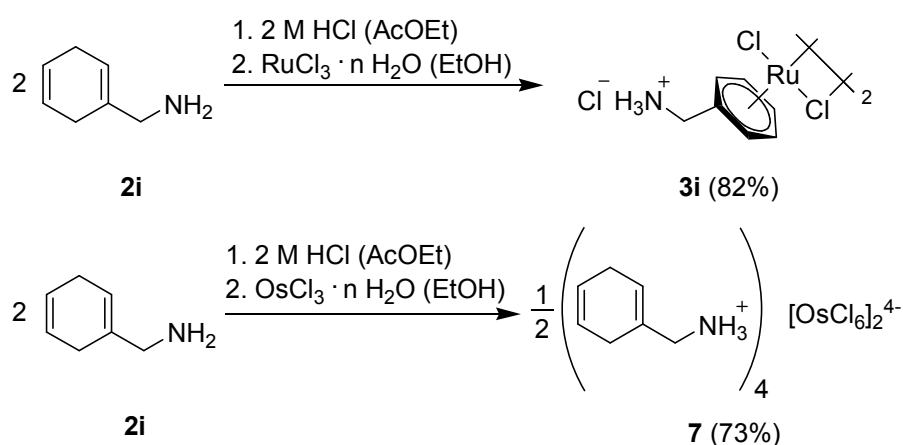


***Scheme B12:*** Synthesis of compounds **3i** and **7**.

It is virtually insoluble in aprotic media like dichloromethane and acetone and only slightly soluble in alcohols yet dissolves readily in donor solvents such as water and DMSO. According to ^{1}H and ^{13}C NMR spectrometry as well as elemental analysis and IR, complex **3i** was obtained as hydrochloride salt. The ammonium protons give rise to a distinct singlet at $\delta$ = 8.80 ppm in ^{1}H NMR. Resonances corresponding to aromatic carbons appear between 93.4 ppm and 86.9 ppm in ^{13}C NMR, which again represents a typical upfield shift in comparison to non-coordinated arenes. Complex **3i**[DMSO] crystallized from a concentrated solution in DMSO-$d_6$ within several days at room temperature (figure B8). The molecular structure was derived by single crystal X-ray diffraction and solved in the centrosymmetric space group $P2_1/c$. It reveals a $\eta^6$-arene Ru(II) dichloride motive, which is electronically saturated by an DMSO ligand featuring typical S-coordination.[44] In the solid state, each ammonium hydrogen is part of a N-H-Cl hydrogen bond. An intramolecular interaction with Cl(2) is evident from distance ($R_{H-Cl(2)}$ = 2.73(1) Å) and angle ($\angle_{N-H-Cl(2)}$ = 162.2(1) °) criteria.[45] Two additional short intermolecular hydrogen bonds connect the ammonium moieties and the chloride counter ions by a two-dimensional zig-zag motive ($d_{H-Cl}$ = 2.28(1) / 2.25(1) Å).
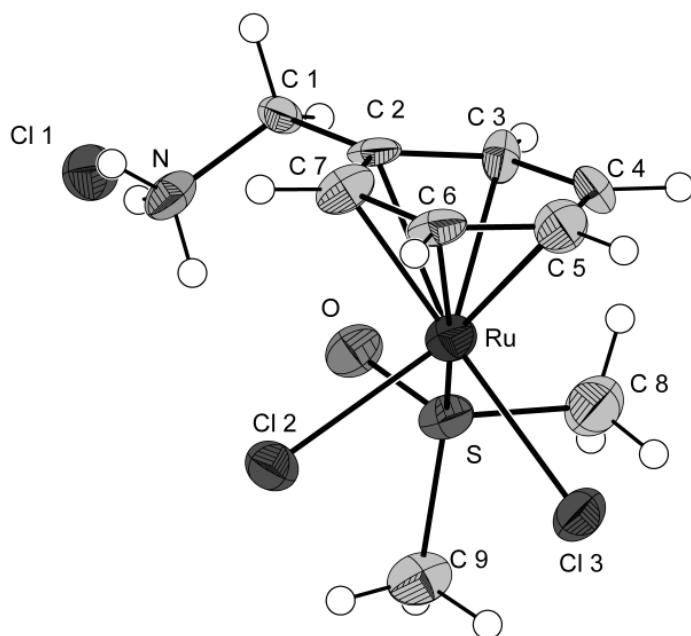


***Figure B8:*** ORTEP drawing of complex **3i**[DMSO] (50% thermal ellipsoids). Selected bond lengths (Å) and angles (deg): Ru-C(2) 2.204(8), Ru-C(3) 2.184(9), Ru-C(4) 2.219(8), Ru-C(5) 2.191(10), Ru-C(6) 2.162(9), Ru-C(7) 2.144(8), C(2)-C(1)-N 112.6(7), Cl(2)-Ru-Cl(3) 88.57(9), Cl(2)-Ru-S 85.49(9), Cl(3)-Ru-S 84.80(9).

In contrast to synthesis of Os(II) complex **6**, conversion of 2,5-dihydrobenzyl ammonium chloride with Os(III) chloride under acidic conditions reproducibly yields the Os(IV) salt **7** as deep red crystals in good yields (scheme B12). The crystalline reaction product consists of the well known, stable osmat(IV) dianion $[OsCl_6]^{2-}$, counterbalanced by two 2,5-dihydrobenzylammonium cations. $^1H$ and $^{13}C$ NMR spectra of the reaction mixture only exhibit signals corresponding to the 2,5-dihydrobenzyl ammonium cation. Absence of aromatic or $\eta^6$-arene signals clearly indicates, that oxidation of the ligand precursor by Os(III) chloride does not take place und these conditions.
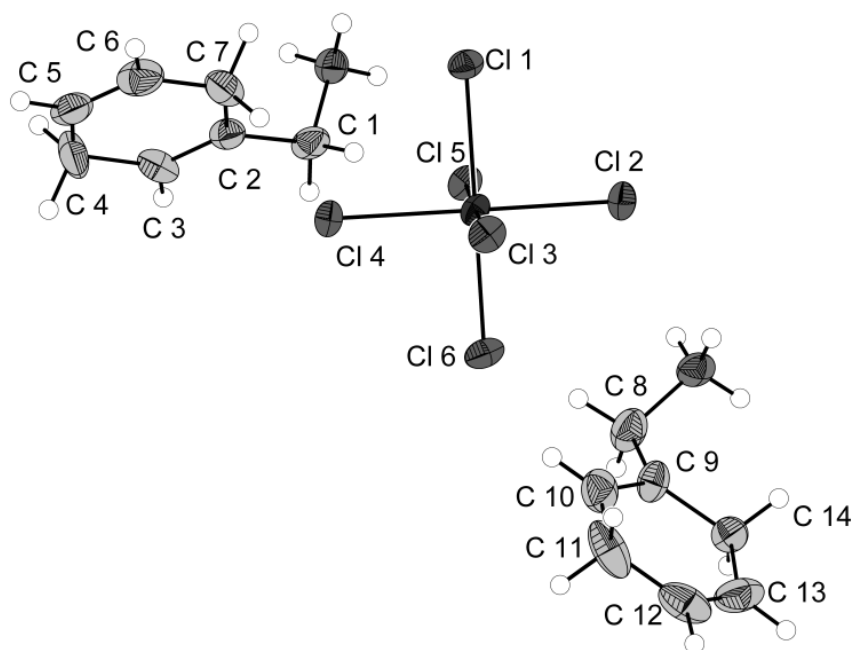


***Figure B9:*** ORTEP drawing of complex **7** (50% thermal ellipsoids). Selected bond lengths (Å) and angles (deg): Os-Cl(1) 2.3588(5), Os-Cl(2) 2.3427(6), Os-Cl(3) 2.3110(4), Os-Cl(4) 2.3386(6), Os-Cl(5) 2.3391(4), Os-Cl(6) 2.3249(5), C(2)-C(3) 1.3298(2), C(3)-C(4) 1.4751(3), C(4)-C(5) 1.4490(3), C(5)-C(6) 1.3309(2), C(6)-C(7) 1.4699(3), C(7)-C(2) 1.4696(3).

Product **7** was crystallized from the reaction mixture (figure B9). The structure, which was solved in space group *P2$_1$/c,* features the octahedral $[OsCl_6]^{2-}$ dianion surrounded by two hydrogen bonded 2,5-dihydrobenzylammonium cations ($R_{H-Cl}$ = 2.48(1) Å). Os-Cl bond length are significantly elongated for the two chloride ligands Cl(1) ($R_{Os-Cl(1)}$ = 2.3588(5) Å) and Cl(2) ($R_{Os-Cl(2)}$ = 2.3427(6) Å) which are participating in hydrogen bonding, if compared to the average of the other four Os-Cl bonds (R = 2.3284). In agreement with NMR, alternating C-C bond lengths indicate the cations to be 2,5-dihydrobenzyl ammonium and not benzyl ammonium. Distances for C(2)-C(3) and C(5)-C(6) are 1.398(2) and 1.3309(2) Å, respectively, thus being long for an alkene bond. The remaining four C-C bond lengths measured range from 1.4490(3) to 1.4751(3) Å,

which are slightly shortened values for C-C single bonds. This is a clear indication for the 2,5-dihydrobenzylammonium cations to be disordered in the crystal structure.

Formation of Os(IV) compound **7** under acidic conditions, which are well suited for the synthesis of $\eta^6$-arene complexes may be attributed to the well established tendency of 5d vs. 4d transition metals to prefer higher oxidation states.[46] Since rigorous exclusion of oxygen did not change the outcome of the reaction the most likely oxidant is added hydrochloric acid. However, direct conversion of the 2,5-dihydrobenzyl amine and successive conversion with osmium(III) chloride only yielded a black tar, which showed a plethora of signals in the aromatic region in $^1$H and $^{13}$C NMR when dissolved in DMSO. The occurrence of aromatic signals indicates C-H and possibly benzylic C-N activation processes, yet formation of $\eta^6$-arene complexes was not detected.

Overall, complexes **3c** and **6** as well as **3i** and **7** reveal a distinct reactivity difference for ruthenium and osmium during the conversion of the respective metal(III) chlorides with 2,5-dihydro arenes comprising donor-functionalized side chains. In contrast to clean formation of the Ru(II) $\eta^6$-benzyl ammonium complex **5**, the corresponding Os(II) compound did not form due to either predominant oxidation to Os(IV) or unspecific C-H activation. However, utilizing an alcohol functionalized 2,5-dihydro arene, synthesis of the first example of a $\eta^6$-arene complex of osmium(II) with a pendant donor was achieved. Stability against air, moisture, water and acid in combination with an enhanced solubility in aqueous media qualify such compounds as potential precursors for biological probes in drug development.

# 4. Synthesis of $\eta^6$:$\eta^1$-arene ruthenium phenylalanine complexes

## 4.1. Reactivity of $\eta^6$:$\eta^1$-arene ruthenium complexes

The synthesis of complexes that combine the chemical properties of biogenic amino acids and the versatile features of catalytically active metal centers were investigated. The synthesis of various novel chloro-bridged $\eta^6$-phenylalanine ethyl ester as well as $\eta^6$:$\eta^1$-phenylalanine and $\eta^6$:$\eta^1$-phenylalanine ethyl ester complexes, their characteristics in $^1$H and $^{13}$C NMR spectroscopy and their application in the transfer hydrogenation of ketones was investigated.
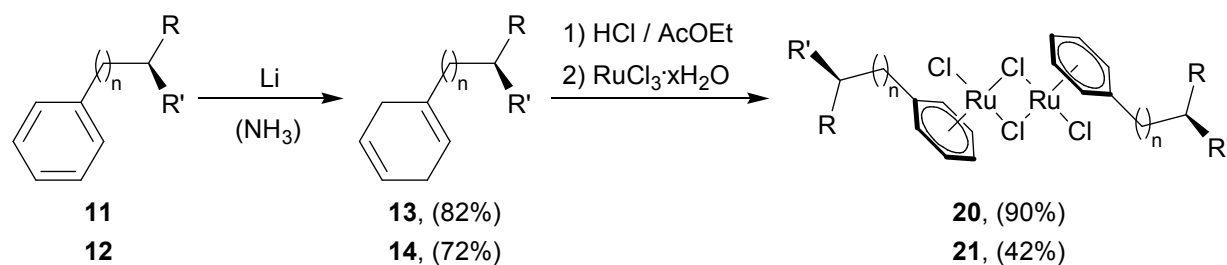


**11, 13:**    n = 1, R = COO$^-$, R' = NH$_3^+$
**12, 14:**    n = 0, R = COO$^-$, R' = NH$_3^+$
  **20:**      n = 1, R = COOEt, R' = NH$_3^+$
  **21:**      n = 0, R = COOEt, R' = NH$_3^+$

***Scheme B13:*** Synthesis of $\eta^6$-arene ruthenium complexes **20** and **21**[22].

The distinct orientation of carboxylic and amino moiety which is characteristic for α-amino acids is well suited to chelate cationic metal centers. Hence, a decrease in binding affinity of these functionalities is essential to achieve a side-chain selective derivatization. Beck *et al.* recently described an elegant procedure avoiding tedious protection/deprotection strategies by a simple *in situ* protonation (amino group) and esterification (carboxy group) in acidic solutions.[22] Applying this strategy, the dihydro derivates **13**[47] and **14**,[48] which were prepared from the artificial amino acid phenylglycine as well as the biogenic amino acid L-phenylalanine, respectively, can be converted with ruthenium(III) chloride hydrate in refluxing ethanol to the corresponding $\eta^6$-arene ruthenium(II) complexes **20** and **21** in (scheme B13). 2,5-dihydro-phenylalanine **13** was crystallized from the reaction solution with 0.5 equivalents of HCl (figure B10). All distances and bond angles were in the expected range. Crystal data and details for the structure determination are listed in table C33.
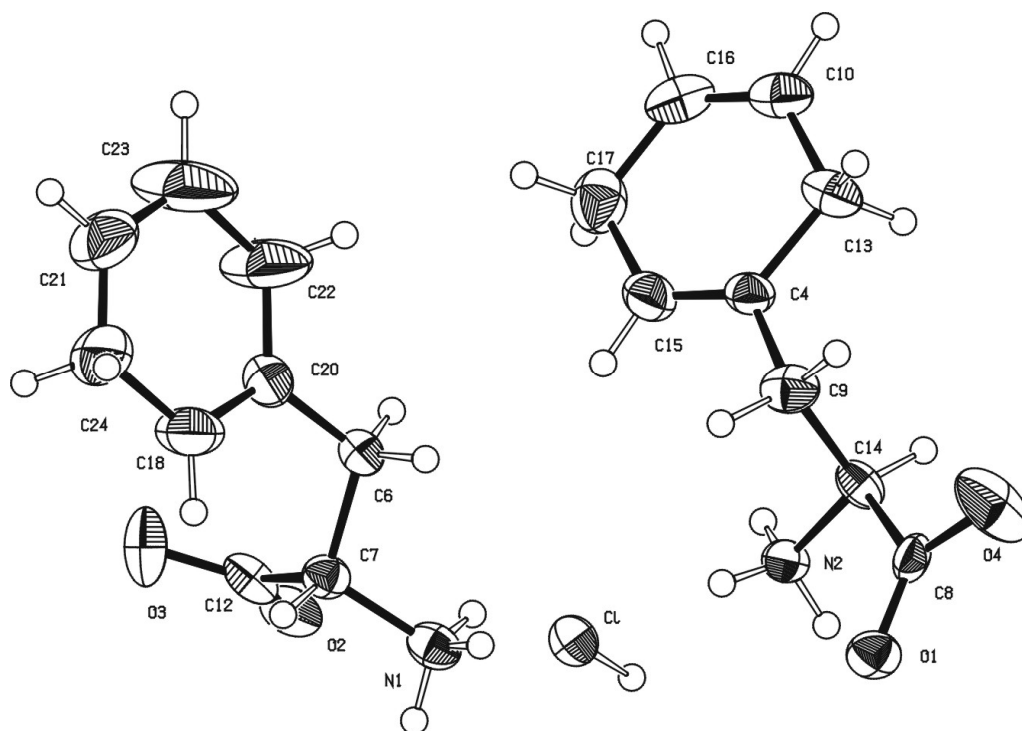
**Figure B10:** ORTEP-representation of 1,4-dihydro-L-phenylalanine **13**

$^t$BuOH esters are highly labile under the strongly acidic reaction conditions. Therefore, a change in reaction medium from AcOEt / EtOH to $^t$BuOH prevents formation of acetic esters. Therefore, coordination of the acetate group should not take place. Nevertheless reaction of 2,5-dihydro-phenylglycine **14** with RuCl$_3$ · nH$_2$O in the presence of $^t$BuOH does not lead to the expected pendant amino acid. Instead, decarboxylation of phenylglycine at the α-CH position, resulting in the formation of the dimeric μ-chloro-bridged η$^6$-benzylammionium ruthenium(II) complex **3i** was observed (scheme B14). However, decarboxylation does not take place, when 2,5-dihydro-phenylalanine **13** is employed instead of 2,5-dihydro-phenylglycine **14** in this case, the monomeric η$^6$:η$^1$-phenylalaine complex **22**, exhibiting a free carboxylic acid, is obtained. It was isolated in high yields as a bright yellow powder. Decarboxylation of 2,5-dihydro-phenylglycine **14** might be due to the higher acidity of this ligand in α-position, resulting from the electron withdrawing effect induced by coordination of the arene ring to the Ru(II) metal centre.
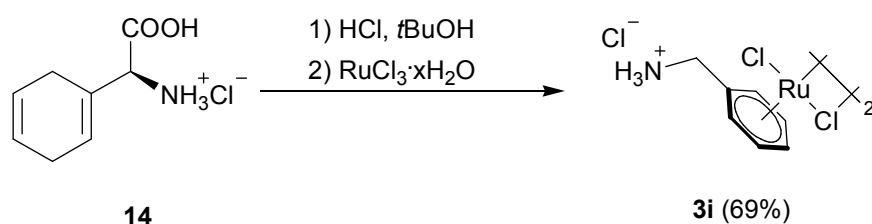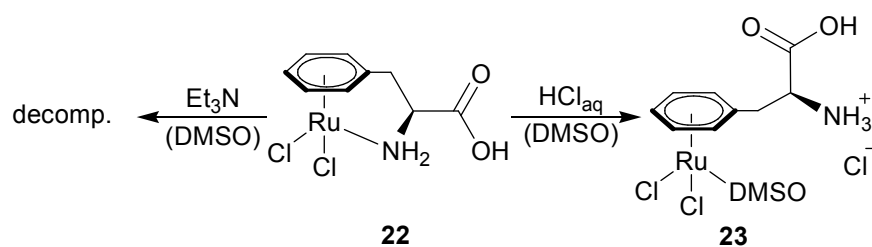


**Scheme B14:** Synthesis of η$^6$-arene ruthenium complex **3i** from 2,5-dihydro-L-phenylglycine in $^t$BuOH.
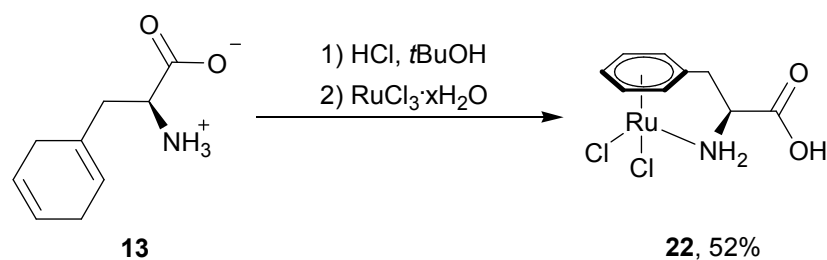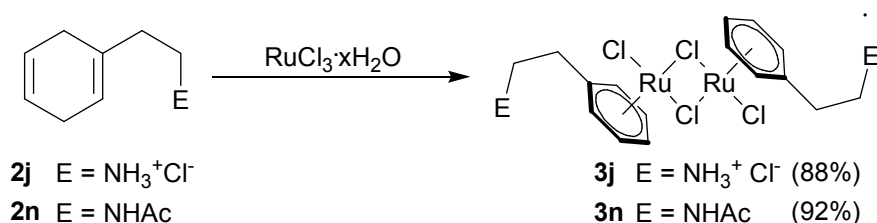
**Scheme B15:** Synthesis of $\eta^6$:$\eta^1$-arene ruthenium complex **22** from 2,5-dihydro-L-phenylalanine in *t*-butanole.

Complex **22** is obtained as a monomer, as the amine tether coordinates to the metal centre (scheme B15). The IR spectra of the ruthenium(II) complexes **20**, **21** and **22** reveal strong absorptions between 1741 and 1746 cm$^{-1}$, which correspond to the respective CO stretching frequencies.[49] While IR spectra of **22** in chloroform solution exhibit one carbonyl absorption at 1741 cm$^{-1}$, preparations in KBr pellets display two sharp bands in the carbonyl region at 1734 cm$^{-1}$ and 1726 cm$^{-1}$. The same two bands are present in nujol, hence halide exchange during sample preparation can be ruled out as possible reason for the double band structure. Therefore, this feature is attributed to the presence of two distinct conformations in solid state. The $^1$H and $^{13}$C NMR spectra of the dimeric complexes **20**, **21** and **3i** only show a single set of signals. Complex **22** is only slightly soluble in organic solvents except of DMSO-$d_6$, where it decomposes by losing the $\eta^6$-arene coordination. $^1$H NMR spectra of **22** proved the coordination of the amine to the metal centre, as there were two signals for the NH$_2$ protons observed. One of them was observed in the region of 4.75-4.62 ppm and the other at 4.06 ppm. Each signal integrates to one proton. In contrast, the ammonium resonance of **3i** is observed as a single signal, a broad singulet at 8.80 ppm. This signal integrates to three protons. To avoid decomposition, $^{13}$C MAS NMR spectra of **22** were recorded. These spectra exhibited a double set of signals for complex **22**.



**Scheme B16:** Reactivity of **22** towards acidic (HCl) and base (Et$_3$N).

**2j** E = NH$_3^+$Cl$^-$
**2n** E = NHAc

**3j** E = NH$_3^+$ Cl$^-$ (88%)
**3n** E = NHAc (92%)

**Scheme B17:** Synthesis of η$^6$-arene ruthenium complex **3j**[51,52] and **3n** via rearomatization of cyclohexadiene derivatives **2j**[50] and **2n**.

This might be due to packing effects in solid state, where for example different hydrogen bonding patterns lead to stereoelectronic changes for the ruthenium complex **22**, as it was observed with IR spectra in nujol and KBr. Decomposition of complex **22** is faster in the presence of 4% triethylamine in DMSO, whereas in the presence of 4% HCl$_{conc}$, no decomposition was observed. Furthermore, addition of HCl leads to protonation of the amine tether and therefore dissociation of amine and metal centre. This results in the formation of **23**, the first example of a non-functionalized η$^6$-arene phenylalanine ligand coordinated to a ruthenium metal centre (scheme 16). $^{13}$C NMR spectra of **23** exhibited only a single set of signals, the ammonium signal in $^1$H NMR spectra was observed as a broad singulet at 8.72 ppm. The optical rotatory power of **23** was determined to be [α]$_D^{22}$ +44.0 (c = 0.58 in HCl$_{conc}$ / DMSO = 1 / 25). This value lies in the range of non-coordinated L-phenylalanine, thus ruling out the η$^6$-arene ligand to undergo racemization under the reaction conditions. This also proves the double set of signals observed for **22** in $^{13}$C MAS NMR spectra not to origin from two different enantiomers present in solid state.
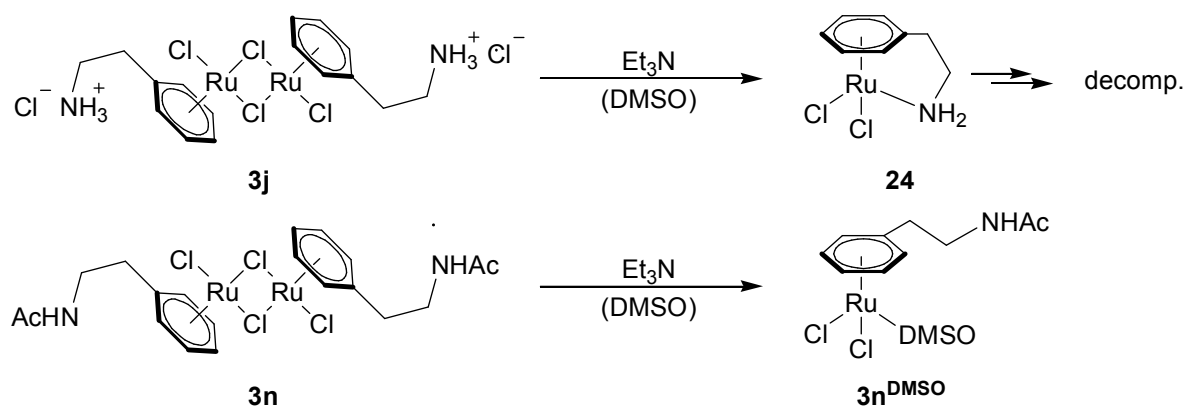


**Scheme B18:** Reactivity under basic conditions is depending on the side chain functionality in complexes **3j** and **3n**.

To determine the influence of the pendant amine group of complex **22** in Et$_3$N / DMSO, two model compounds were synthesized, the literature known complex **3j**[51,52] and its acetamide analogue, complex **3n**. Both were obtained as brown and ochre powders in high yields from their 2,4-dihydro cyclohexadiene derivatives (88 % for **3j**, 92 % for **3n**, both scheme B17). In case of **3j**, the NH$_3^+$ resonance was observed as a broad singulet at 8.15 ppm in $^1$H NMR spectra. The amide signal of **3n** was observed as a multiplet at 7.94 ppm in $^1$H NMR spectra.
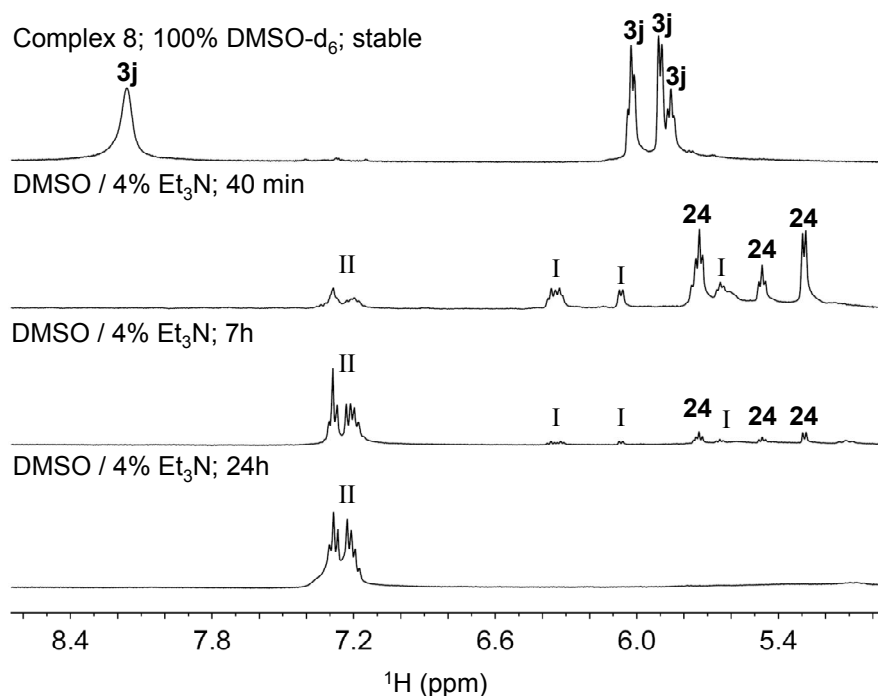


**Figure B11:** $^1$H NMR spectra of complex **3j** in Et$_3$N / DMSO-$d_6$ (1 / 25) at different reaction times (**I**: unisolated intermediate. **II**: liberated arene ligand).

Both complexes **3j** and **3n** form deep red solutions in DMSO-$d_6$ and are stable under aerobic conditions for days without any signs of decomposition. Upon addition of triethylamine, the color of complex **3j** instantly changes from red to yellow resulting from the formation of complex **24** (scheme B18). Complex **24** was synthesized via a different route before.[53] $^1$H NMR spectra reveal the ammonium signal to have vanished and given rise to a NH$_2$ resonance at 4.39 ppm. The resonances of the coordinated arene ring also shift by up to 0.5 ppm, revealing the metal centre coordination to change. When triethylamine is added to a solution of complex **3n** in DMSO-$d_6$, there is no change in $^1$H NMR spectra as well as $^{13}$C NMR spectra observed (scheme B18). Therefore, only pendant primary amines are able to coordinate to the metal centre in the presence of triethylamine (Et$_3$N/DMSO-$d_6$ = 1/25). Furthermore, this coordination of the amine tether results in complex **24** to be highly unstable (figure B11).

In $^1$H NMR, decomposition intermediate **I** can be observed after five minutes. It was not further analyzed, yet, compound **I** has a coordinated arene ring system, as the arene signals are downshifted in comparison to non-coordinated arenes (6.4 – 5.1 ppm). Approximately 20 % of complex **24** has decomposed after 40 min. The intermediate **I** is giving rise to non $\eta^6$-arene coordinated ligand **II**, appearing at 7.4 – 6.9 ppm. After 24 h, the decomposition was found to be complete, resulting in the sole observation of rearomatized non-coordinated ligand **II** (figure B11). This finding is in accordance with observations made for $\eta^6$:$\eta^1$-coordinated complex **22**, which is unstable in DMSO-$d_6$ and highly unstable in DMSO-$d_6$ containing Et$_3$N. It becomes stable upon addition of HCl, resulting in a loss of its amine $\eta^1$ coordination and giving rise to complex **23**. The initially DMSO-$d_6$ stable complex $\eta^6$-arene coordinated complex **3j** becomes unstable upon addition of Et$_3$N, yielding the likewise unstable $\eta^6$:$\eta^1$-coordinated complex **24**. It therefore is assumed that the coordinated amine tether and the resulting strained ring system amine-ruthenium-arene are crucial for the instability and consequential dissociation of arene and metal.
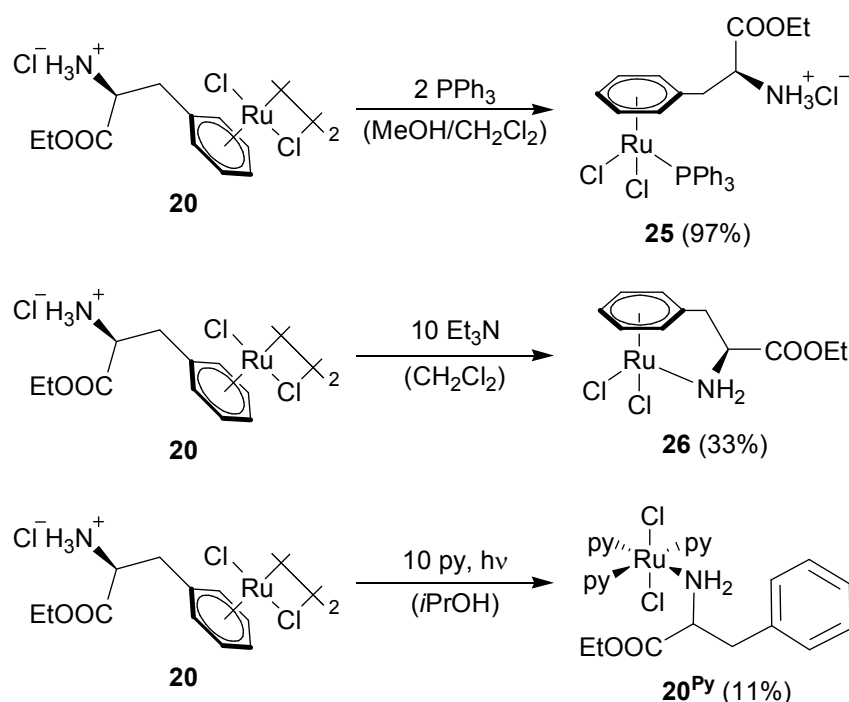


**Scheme B19:** Reactivity of dinuclear $\eta^6$-arene complex **20** towards different nucleophiles.

To determine the reactivity of dimeric complex **20**, it was reacted with different nucleophiles. Reaction with triphenylphosphine in a mixture of methanol and dichloromethane yielded the highly soluble adduct **25** in near-quantitative yield (97 %, scheme B19). No coordination of the pendant amino group was observed. The R-NH$_3^+$ resonance was observed as a broad singulet 8.77 ppm. The deep red

solid is stable in organic solvents such as methanol without decomposition. When **20** was suspended in dichloromethane and triethylamine was added, the color of the reaction mixture changed from orange to bright yellow within 2 h, resulting from the formation of $\eta^6$:$\eta^1$-coordinated complex **26**. The yield for this reaction was only 33 % on account of the necessity of removing triethylamine from the reaction mixture by washing the complex in $CH_2Cl_2$, in which it is slightly soluble.
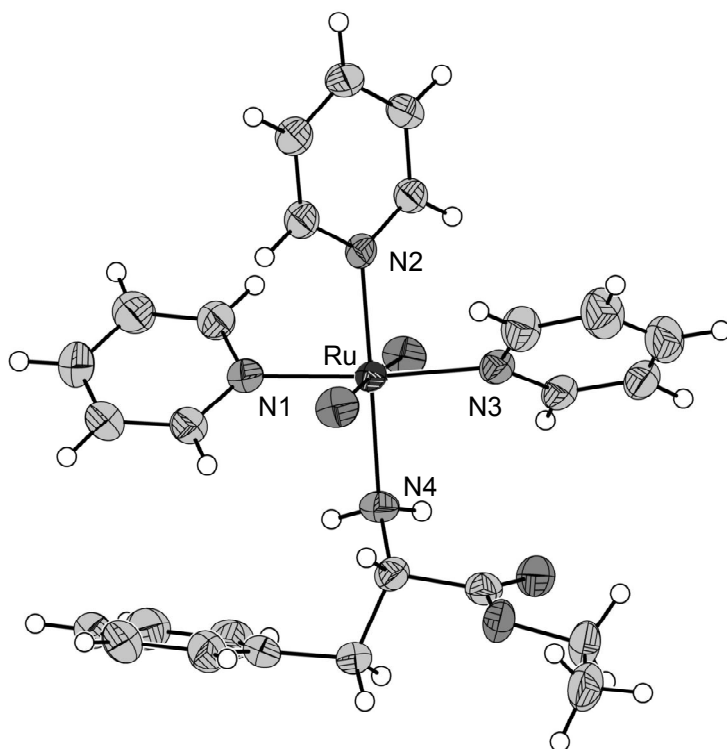


***Figure B12:*** ORTEP representation of complex **20**$^{Py}$ (50 % thermal ellipsoids). Selected bond lengths (Å): Ru-N1 2.102(3), Ru-N2 2.053(3), Ru-N3 2.090(3), Ru-N4 2.164(3).

Due to its ethyl ester group, it exhibits higher solubility to dichloromethane as well as chloroform, compared to the carboxylic acid analogue **22**. Therefore, $^1$H and $^{13}$C NMR spectra of **25** were able to be recorded in $CDCl_3$. In $^1$H NMR spectra, two signals were observed for the diastereotopic $NH_2$ protons. One of them as a triplet at 4.57 ppm and one as a multiplet at 3.82 ppm. This is in accordance with the signals observed for the amine proton resonances observed for the carboxylic acid analogue, complex **22**. Complex **26** is, in accordance to other $\eta^6$:$\eta^1$-coordinated complexes, unstable in protic solvents such as methanol and coordinating solvents, as for example DMSO. When complex **20** is reacted with reagent pyridine, no selective product formation is observed. The complex quickly reacts with the basic as well as coordinating reagent, resulting in the formation of different decomposition products.

One of the decomposition products, complex **20**[Py], was crystallized from the reaction mixture, confirming the observations made above for $\eta^6$:$\eta^1$-coordinated complexes (figure B12). The $\eta^6$-arene coordination is lost, resulting in an octahedral geometry for the transition metal centre, which is coordinated by two chlorine anions in trans position, three pyridine and one L-phenylalanine ethyl ester, coordinated via the amine. All bond lengths and angles of the crystallized complex **20**[Py] are in the expected range. Standard crystallographic data is displayed in table C35.

The Ru-N4 (2.1640(3) Å) bond is longer than the other Ru-N bonds (2.053(3)-2.102(3) Å). This could be addressed to a stronger pyridine-ruthenium interaction compared to ruthenium phenylalanine. This explains the finding of a second species in the reaction solution, the octahedral complex [(py)$_4$RuCl$_2$], which already has been crystallized before.[54]

## 4.2. Synthesis of η⁶:η¹-arene Ru(II) complexes with diamine ligands

Complex **20** was also reacted with the chelating diamine derivatives N-*p*-tosyl ethylenediamine **15**[55] and 1,4-di-N-*p*-tosylethylenediamine **16**[56] (scheme B20). Their identity and purity has been confirmed by $^1$H NMR, $^{13}$C NMR, IR spectrometry and elemental analysis. As the synthesis of both compounds is straight forward as well as self-explanatory, their synthesis will not be explained in detail. Synthetic procedures are listed in the experimental section. Furthermore, 1,4-di-N-*p*-tosylethylenediamine **16** was also crystallized from diethylether at room temperature, yielding clear needles (figure B13). All distances and bond angles were in the expected range. Crystal data and details for the structure determination are listed in table C34.
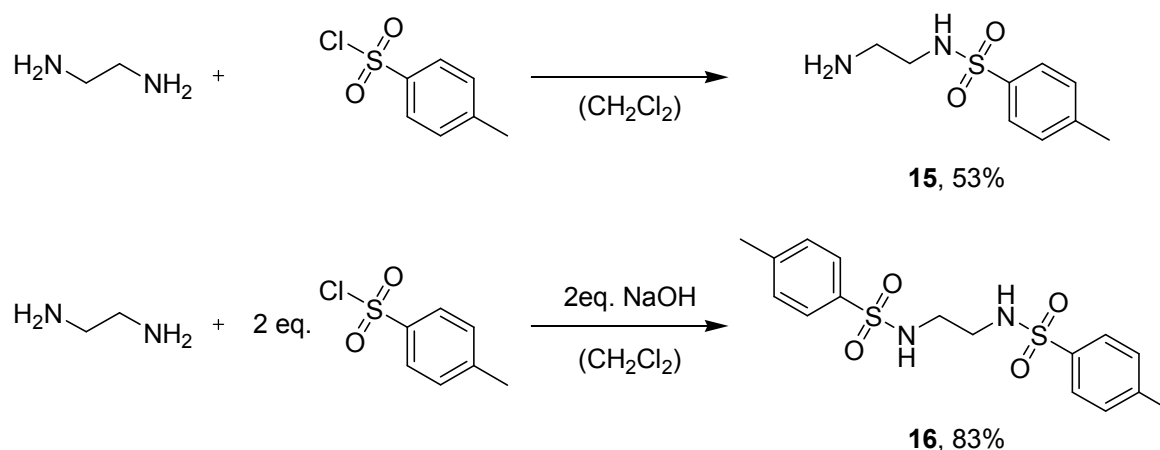


***Scheme B20:*** Synthesis of ethylene diamine derivatives **15**[55] and **16**.[56]

Coordination of compounds **15** and **16** to the dimeric η⁶-arene complex **20** was carried out in ethanolic solution, resulting in complexes **27** and **28** (scheme B21). Triethylamine was added to deprotonate the ligand as well as to neutralize the evolving hydrochloric acid. It also leads to coordination of the α-amino group of the phenylalanine ligand. As observed earlier, this yields a five membered heterocycle, resulting from the η⁶:η¹-coordinated chelating phenylalanine ethyl ester ligand. In general, complexes **27** and **28** possess highly different solubility properties. While complex **27** can be dissolved in dichloromethane and side products, such as triethylammoniumchloride, can be extracted with water, the monocationic complex **28** itself is highly soluble in water. In order to remove triethylamine from **28**, the complex was dissolved in cold dry tetrahydrofurane and triethylammoniumchloride was filtered off.
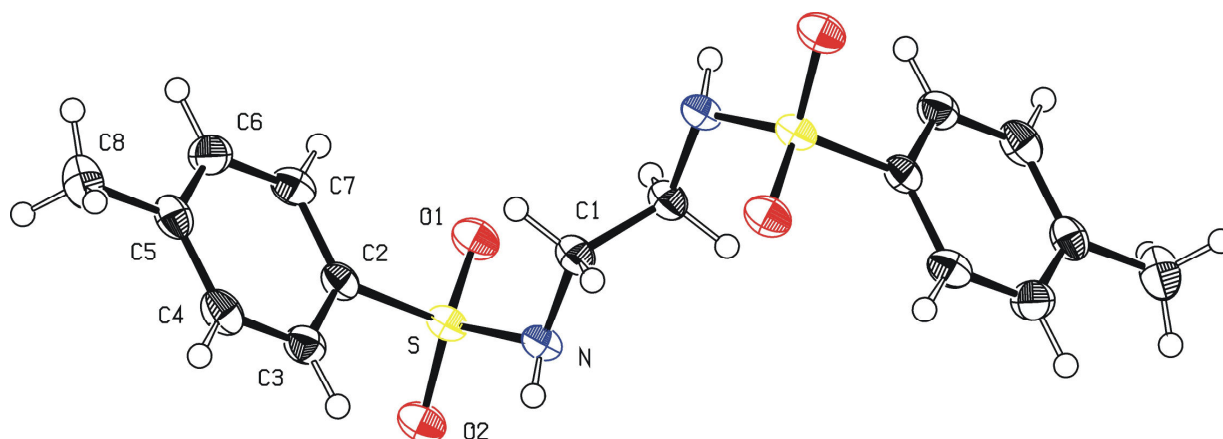
***Figure B13:*** ORTEP-representation of 1,4-di-N-*p*-tosylethylenediamine **16**

Both complexes are stable in solution and in solid state when exposed to light, oxygen or water. When dissolved in a mixture of acetonitrile, water and triethylamine, the ethyl ester is saponified without altering the inner coordination sphere of the metal complexes, yielding complexes **29** and **30** (scheme B22). This can be explained by the shielding effect of the ethylene diamine chelating ligands, which can reduce the tendency of arene dissociation from the ruthenium(II) centre. Complex **28** dissolves in water as well as dichloromethane, whereas the internal salt **30** is insoluble in dichloromethane, and only slightly soluble in water. Complex **30** crystallizes readily from DMSO at room temperature. NMR spectra were recorded in DMSO-$d_6$ / $CD_3COOD$ (9 / 1). The deuterated acetic acid protonates the phenylalanine carboxylate group and strongly increases solubility, thus preventing crystallization. A very interesting feature of $^{13}C$ NMR experiments is the detection of three α-*CH* signals for the ($S_{Ru}/S_{\alpha\text{-}CH}$) diastereomer (71.9, 71.8, 71.7 ppm) and three α-*CH* signals for the ($R_{Ru}/S_{\alpha\text{-}CH}$) diastereomer (71.5, 71.4, 71.3 ppm).
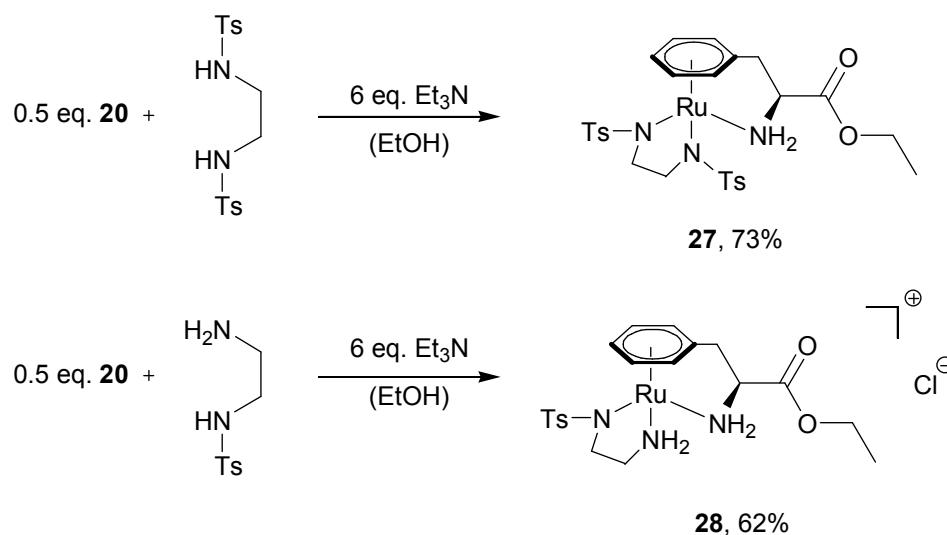


***Scheme B21:*** Conversion of **20** with ethylene diamine ligands, yielding complexes **27** and **28**.
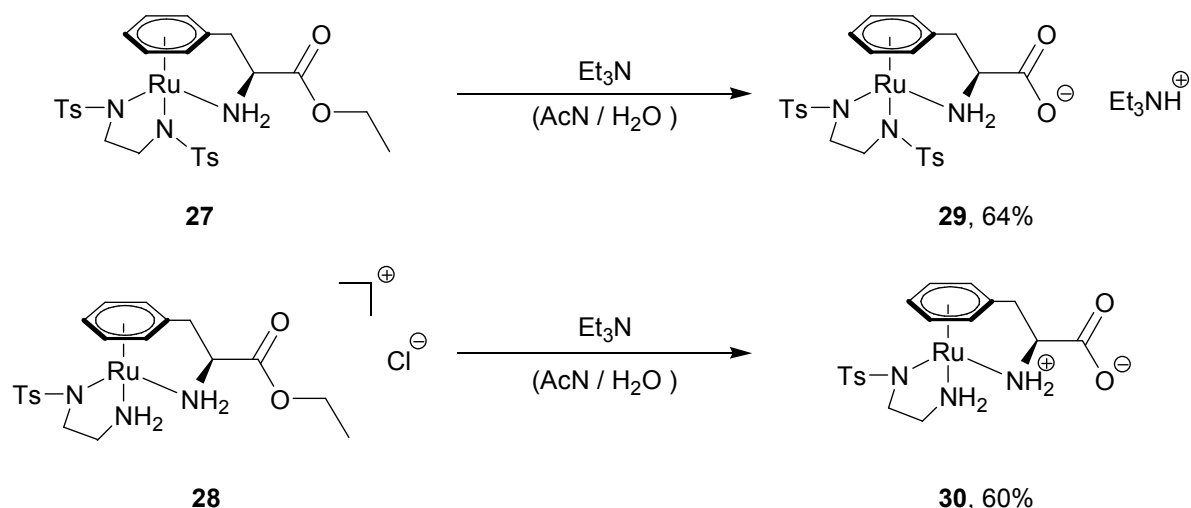
**Scheme B22:** Saponification of complexes **27** and **28** with triethylamine gives complexes **29** and **30**.

When recorded in DMSO-$H_6$ / $CH_3COOH$ (9 / 1), only one signal for ($S_{Ru}$/$S_{\alpha-CH}$)-$\alpha$-$CH$ and one signal for ($R_{Ru}$/$S_{\alpha-CH}$)-$\alpha$-$CH$ was observed. A reason for the observation of three $\alpha$-$CH$ signals can be attributed to slow exchange of one or two protons with deuterons. This was also confirmed with ESI mass spectrometry. For this purpose, ESI MS spectra of both the complexes in deuterated and non-deuterated acetic acid (in both cases, 10 % acetic acid in DMSO was used) were recorded. Different isotopic patterns for samples dissolved in deuterated and not deuterated solvents were detected. The pattern observed for complex **30** dissolved in non deuterated solvent resembles the calculated one, whereas the one in deuterated solvent contains considerable amounts of a species having a molar mass increased by 1 g/mol as well as 2 g/mol. This proves the slow proton-exchange of the primary amine functions. The described effect was not observed for the primary amine of the ethylenediamine ligand. All amine-bound hydrogen atoms show different $^1$H NMR shifts which were assigned by $^1$H$^1$H-COSY experiments. For all complexes **27-30**, two chemically inequivalent protons were observed that are connected to the $\alpha$-nitrogen. The basic nature of the coordinated nitrogen and the different ligands and available counter ions lead to the formation of a cationic ruthenium complex in case of **28** and an anionic complex in case of **29**. In infrared spectra of complexes **27** and **28**, the absorptions of the ester functions can clearly be identified at 1738 and 1736 cm$^{-1}$, respectively. The IR spectra of complexes **29** and **30** provide no evidence of ester functions, instead, carboxylic acid signals at 1610 and 1619 cm$^{-1}$ arise.
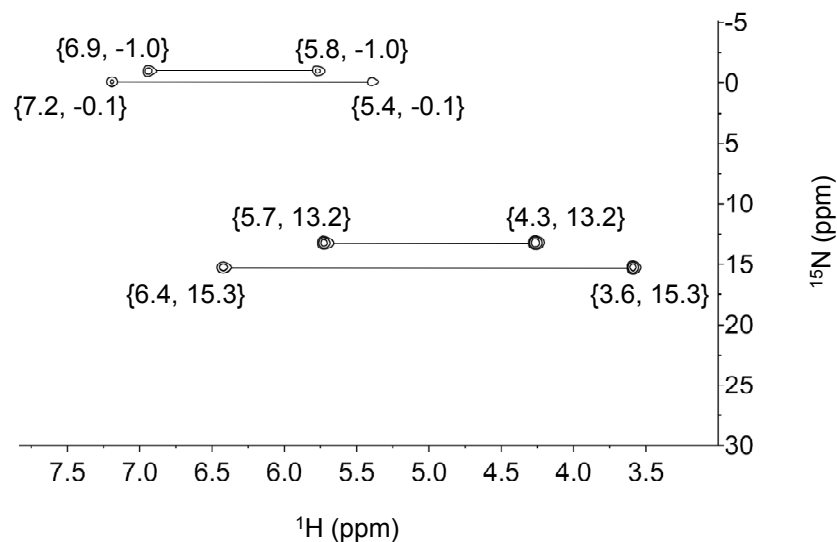
*Figure B14:* $^1H^{15}N$-HSQC of complex **28** (500 MHz, 25°C, CDCl$_3$, natural abundance).

Both complexes **27** and **29** have a single set of signals, as there is only one chiral centre present in these systems at the α-CH carbon. In complexes **28** and **30**, the ruthenium centre acts as a second stereocentre, resulting in diastereomeric compounds. Hence, two sets of signals were observed for these systems in NMR spectra. As the complexes have different not interconnected spin systems, no complete assignment of both the (*S*)-Ru and (*R*)-Ru complex was possible. Only different spin systems could be assigned that are separated from each other. The diastereomers of **28** were distributed in a ratio of 3:2, whereas the ratio between *R* and *S* was 1:1 for complex **30**, indicating the ethylenediamine ligand to be flexible. One diastereomer might be disfavored in complex **28**, as the bulky ethyl ester group disfavors one of the conformations. Complex **30**, containing the much smaller carboxylate group, does not display any preference for one of the conformations. In case of complex **28**, a $^1H^{15}N$-HSQC NMR-spectrum was recorded (figure B14). It confirmed the data collected in $^1H$, $^1H^1H$-COSY and $^{13}C$ NMR spectra. In this system, there are four inequivalent nitrogen atoms, two atoms belonging to the ($S_{Ru}/S_{α-CH}$)- and two to the ($R_{Ru}/S_{α-CH}$)-conformation. Each of these nitrogen atoms has two inequivalent protons, which are shifted to each other by values of up to 2.8 ppm on the $^1H$ NMR scale. The structure of complex **30** was confirmed by X-Ray crystallography (figure B15). Standard crystallographic data is being displayed in table C36. It cocrystallized in the λ-($S_{Ru}$, $S_{α-CH}$)- and δ-($R_{Ru}$, $S_{α-CH}$) configuration. There was no racemization observed at the α-position of the phenylalanine ligand.
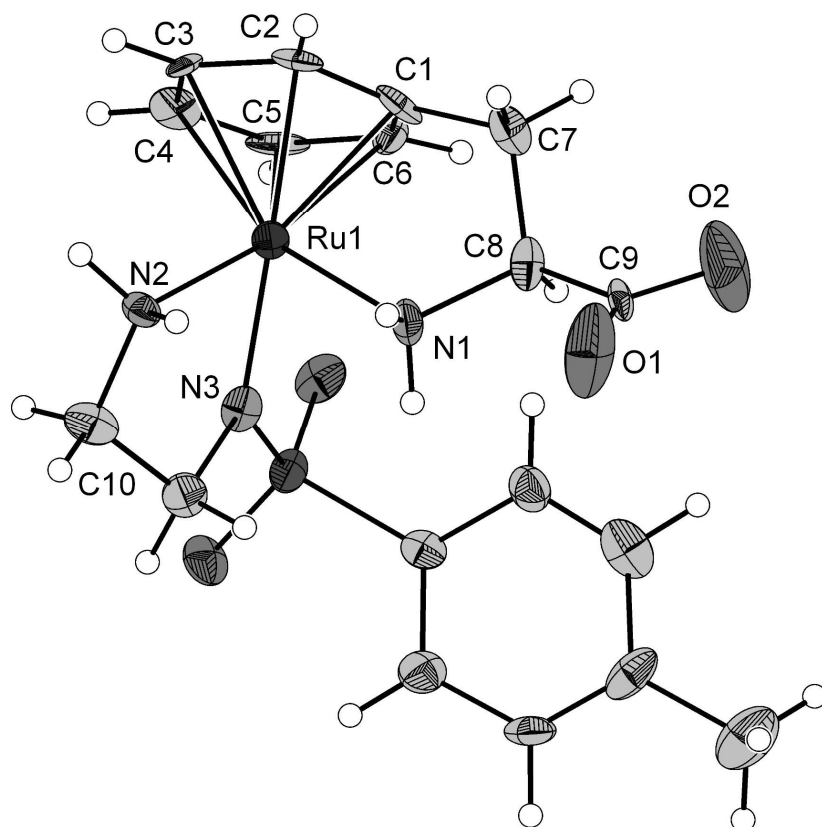
***Figure B15:*** ORTEP representation of complex **30** (50 % thermal ellipsoids). Selected bond lengths (Å) and angles (deg) ($R_{Ru}/S_{\alpha-CH}$): Ru1-C1 2.086(12), Ru1-C2 2.171(17), Ru1-C3 2.186(14), Ru1-C4 2.158(17), Ru1-C5 2.166(12), Ru1-C6 2.186(10), Ru1-N1 2.157(12), Ru1-N2 2.105(7), Ru1-N3 2.079(13), C9-O1 1.198(14), C9-O2 1.240(1), Ru1-N1-C8 110.7(6) Ru1-N2-C10 111.2(7) ($R_{Ru}/S_{\alpha-CH}$): Ru2-C1 2.131(12), Ru2-C2 2.161(9), Ru2-C3 2.197(12), Ru2-C4 2.238(15), Ru2-C5 2.165(16), Ru2-C6 2.149(16), Ru2-N1 2.137(11), Ru2-N2 2.142(7), Ru2-N3 2.135(13), C9-O1 1.209(17), C9-O2 1.292(15), Ru2-N1-C8 111.4(6) Ru2-N2-C10 111.6(7). [57]

Complex **30** crystallized, as indicated by $^1$H and $^{13}$C NMR spectroscopy, as an internal salt. The tosylated nitrogen N1 and the carboxyl functionality are deprotonated, which is clearly demonstrated by torsional angle values and CO bond lengths respectively (footnote of figure B15). Thus, the two terminal amines (N2, N3) are neutral and therefore each bound to two protons. Furthermore, the coordinated aromatic system is tethered by a C2-bridge that causes a hard conformational strain. An analysis of the crystal structure revealed that the angle between two planes consisting of carbon atoms C2, C3, C4, C5 and C6 on the one and carbon atoms C1, C2 and C6 on the other hand form an angle of 9.16 (96) degrees. Noyori and coworkers presented an organometallic ruthenium(II) complex similar to the system described here, containing a (1*S*,2*S*)-N-p-toluenesulfonyl-1,2-diphenylethylene-diamine, a $\eta^6$-bound cymene and a chlorine ligand.[15] They found Rh-N bond distances of 2.117(9) Å for the coordinated $RNH_2$- and 2.144(8) Å for the coordinated TsNR-function. These values are lying in the range of the ones found for complex

**30**, indicating N2 to be bound to two protons. Noyori and coworkers deprotonated their organometallic system, which eliminates HCl. The formerly protonated $RNH_2$ loses one proton. For the resulting RNH-group, a bond distance of 1.897(6) Å is now found, which is significantly shorter than the bond length found for complex **30**. The TsNR-Ru bond also shortens due to the higher electrophilicity of the metal centre, being now 2.065(6) Å long. These findings also indicate the nitrogen atoms N1 and N2 in complex **30** to be protonated twice and the nitrogen atom N4 to be not protonated. The crystal structure of complex **30** therefore supports the NMR experiments described above.

# 5. Biphasic hydrogenations employing $\eta^6$-arene Ru(II) catalysts

Catalysts **4a**-**4t** were tested for their performance in the catalytic hydrogenation of styrene (scheme B23). For this reaction set up, an autoclave with sample outlet was used, allowing to take samples from the reaction mixture and determine turn over frequencies (table B7). Experiments showed that there is no direct correlation between linker lengths and turn over frequencies. There also is no straight forward correlation between the type of functional group linked to the catalysts and its turn over frequencies. Nevertheless, catalysts **4j** and **4k**, having high solubilities in water as well as low solubilities in organic solvents, have very low activities. Therefore, in spite high solubility in water has been reported to have a positive effect on catalyst activity, solubility in organic solvents is necessary to hydrogenate styrene.[17]

*Table B7:* Catalytic runs employing different mononuclear ruthenium complexes.

| entry | catalyst | FG | $(CH_2)_n$ | $TOF_{max}$ [h$^{-1}$] | $t_{ini}$ [min] | $t_{max}$ [min] | yield [%] |
|---|---|---|---|---|---|---|---|
| 1 | **4a** | -OH | 2 | 1280 | 30 | 73 | 100 |
| 2 | **4b** | -OH | 3 | 1940 | 0 | 41 | 96 |
| 3 | **4c** | -OH | 4 | 800 | 55 | 80$^a$ | 76 |
| 4 | **4d** | -OH | 5 | 1330 | 114 | 120$^a$ | 92 |
| 5 | **4e** | -COOH | 1 | 4290 | 0 | 120 | 96 |
| 6 | **4f** | -COOH | 2 | 2000 | 0 | 100$^a$ | 97 |
| 7 | **4g** | -COOH | 3 | 700 | 55 | 100$^a$ | 92 |
| 8 | **4h** | -COOH | 4 | 1360 | 0 | 59 | 100 |
| 9 | **4i** | -NH$_3^+$Cl$^-$ | 1 | 3330 | 0 | 89 | 99 |
| 10 | **4j** | -NH$_3^+$Cl$^-$ | 2 | 950 | 56 | 101$^a$ | 68 |
| 11 | **4k** | -NH$_3^+$Cl$^-$ | 3 | 1540 | 0 | 101$^a$ | 35 |
| 12 | **4l** | -NH$_3^+$Cl$^-$ | 4 | 2220 | 0 | 80 | 100 |
| 13 | **4m** | -NHAc | 1 | 2730 | 0 | 52 | 100 |
| 14 | **4n** | -NHAc | 2 | 4290 | 0 | 32 | 100 |
| 15 | **4o** | -NHAc | 3 | 1580 | 43 | 73 | 99 |
| 16 | **4p** | -NHAc | 4 | 1710 | 27 | 56 | 100 |
| 17 | **4q** | -COOEt | 1 | 2070 | 34 | 64 | 100 |
| 18 | **4r** | -COOEt | 2 | 1370 | 0 | 120$^a$ | 91 |
| 19 | **4s** | -COOEt | 3 | 2500 | 0 | 40 | 100 |
| 20 | **4t** | -COOEt | 4 | 920 | 46 | 79 | 100 |

(a) in these cases $t_{max}$ marks the last data point measured. Reaction was not necessarily complete.
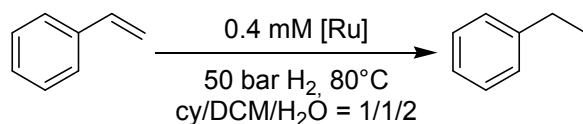
***Scheme B23:*** Hydrogenation of Styrene. Catalyst/Substrate = 1/1000. Conversions and yields were determined against a diethyleneglycol dibutyl ether standard by gas chromatography. Catalytic runs were carried out under constant pressure, sampling during catalysis was facilitated through a sealable pipe.

Catalysts able to dissolve in both phases seem to be the best choice to yield high turnover frequencies. In general, turn over frequencies between 700 h$^{-1}$ for catalyst **4g** and 4290 h$^{-1}$ for catalysts **4n** and **4e** were observed. This shows a great dependency of the type of the $\eta^6$-arene ligand for the catalyst performance. Also initial values for the catalysts vary between 0 minutes and 144 minutes. This could be due to a different speed of active species formation depending on the nature of the pendant linker bound to the $\eta^6$-arene ligand and therefore the metal centre.

***Table B8:*** Catalytic runs employing buffered aqueous solutions.

| entry | catalyst | pH | TOF$_{max}$ [h$^{-1}$] | t$_{ini}$ [min] | t$_{max}$ [min] | yield [%] |
|-------|----------|-----|----------------------|-----------------|-----------------|-----------|
| 1 | **4b** | 2.5 | n.o. | n.o. | 120$^a$ | 10 |
| 2 | **4b** | 6.5 | 440 | 62 | 120$^a$ | 66 |
| 3 | **4b** | 10.5 | 5450 | 19 | 31 | 100 |
| 4 | **4l** | 2.5 | n.o. | n.o. | 120$^a$ | 42 |
| 5 | **4l** | 6.5 | 1880 | 26 | 45 | 96 |
| 6 | **4l** | 10.5 | 1360 | 20 | 51 | 98 |

Additionally, catalysts **4b** and **4l** were tested in buffered aqueous solutions at pH values of 2.5, 6.5 and 10.5 (table B8). These experiments revealed that with catalyst **4b** catalysis at low pH values extremely slows down activity. In contrast, activity goes up at a pH of 10.5. When catalysis is carried out at this pH, its turn over frequency increases to 5450 h$^{-1}$ and only 31 minutes are needed until the reaction is complete. With complex **4l**, turn over frequencies also extremely decrease at a pH of 2.5. They speed up at higher pH values. Yet, turn over frequencies are higher at pH 6.5 than at 10.5. This might be due to its different solubility properties in aqueous and organic solvents from complex **4b**, making transfer between the two phases easier at pH 6.5 than at 10.5.

***Table B9:*** Catalytic runs employing different substrates.

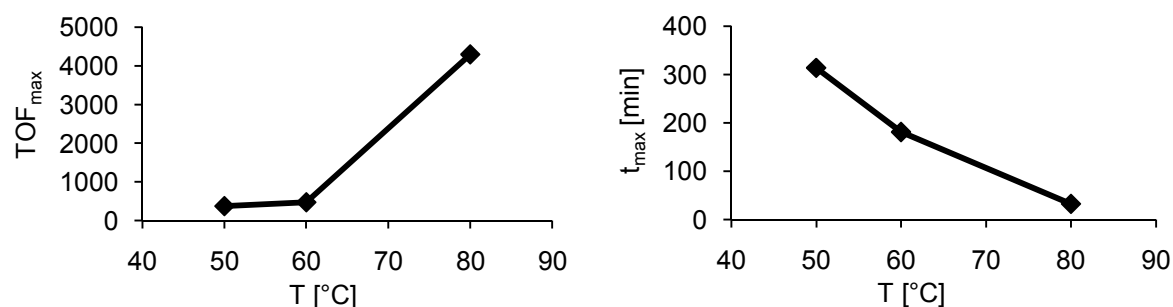| entry | catalyst | substrate | TOF$_{max}$ | t$_{ini}$ [min] | t$_{max}$ [min] | yield [%] |
|-------|----------|-----------|-------------|-----------------|-----------------|-----------|
| 1 | **4b** | 1-octene | 3160 | 36 | 50 | 100 |
| 2 | **4b** | Cyclooctene | 6670 | 35 | 49 | 98 |

***Figure B16:*** Effect of different temperatures in the catalytic hydrogenation of styrene employing catalyst **4n**.

Complex **4b** was also tested for its ability to hydrogenate the non-aromatic substrates 1-octene and cyclooctene (table B9). With these substrates, turn over frequencies of up to 6670 $h^{-1}$ were reached. This proves that employment of an aromatic substrate is not necessary. Catalysis employing complex **4n** was tested under different temperatures. With these experiments, a strong dependency of temperature and turn over frequency was detected. When temperature is decreased by 20°C to 60°C, it drops to around 10 %. When the catalysis is carried out at only 50°C, turn over frequency drops to 9% compared to the reaction at 80 °C. Time intervals necessary to reach complete conversion also increase significantly by lowering the temperature (figure B16). In contrast to TOFs, where the decrease of activity appears to be exponential with decreased temperature, time values of completion seem to decrease almost linearly.
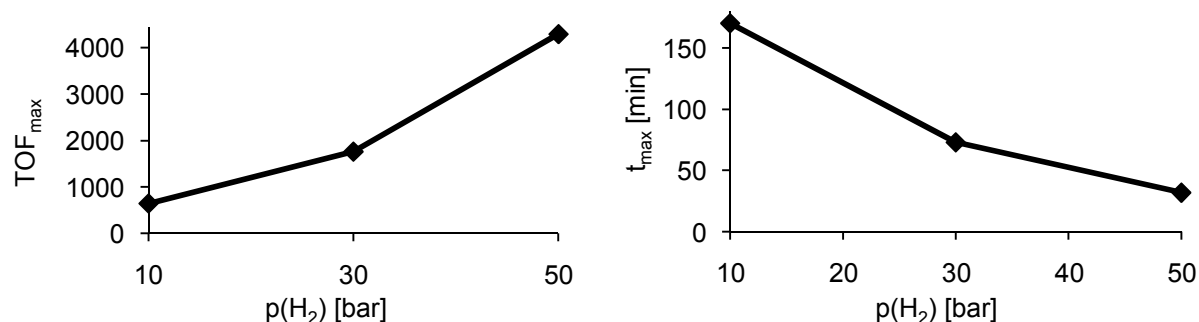


***Figure B17:*** Effect of different pressures in the catalytic hydrogenation of styrene employing catalyst **4n**.

Catalyst **4n** was also tested for its turn over frequencies and time values of complete conversion at different pressures (figure B17). The reaction was carried out not only at 50 bar $H_2$, but also at 30 bar and 10 bar. As to be seen in figure B17, dependency of time and turn over frequency is almost linear in respect to the $H_2$ pressure applied. It has been reported before, that solubility of dihydrogen in water depends linearly on the $H_2$ pressure.[58] Therefore, we assume a first order dependency of the concentration of hydrogen applied and the catalysis speed.

# 6. Transfer hydrogenations employing η⁶:η¹-arene Ru(II) catalysts

The coordination chemistry of complexes **20**, **26, 27** and **28** is well reflected by their catalytic activity and enantioselectivity in the transfer hydrogenation of ketones. As a model substrate, acetophenone was chosen. The reaction was carried out at room temperature in 2-propanole as solvent and hydrogen-donating species (scheme B24). All investigated systems showed different behavior under the applied reaction conditions.
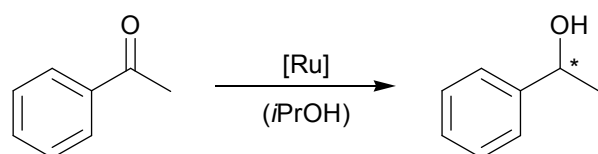


***Scheme B24:*** Hydrogenation of Acetophenone. The reaction was carried out at room temperature using a 1.4 M. solution of acetophenone (10 mM) in 2-propanole. Reaction time = 12.5 d. Yield was determined by gas chromatography. Complex **20**: substrate:KOH:catalyst = 1000/100/1; Complexes **26**,**27**,**28**: substrate/KOH/catalyst = 1000/100/2; Ees were determined by chiral gas chromatography.[59]

Their activity under reaction conditions fits the results above. The most active catalyst is complex **28**, however, this complex has in its initial form no free coordination sites which can interact with a substrate (table B10, entry 4). This indicates the η⁶-arene ring to be cleaved by the base under the applied reaction conditions, releasing free coordination sites. Complex **20** shows low activity in the conversion of acetophenone to 2-phenylethanole (table B10, entry 1). The observed activity supports the assumption, that during reaction, the deprotonated amine coordinates to the metal centre, as having been shown above (scheme B19). The observed activity for complex **20** is smaller by more than a magnitude of 10 compared to complex **28**. An explanation for the differences in activity might be addressed to a steric approach. Both the amine of the phenylalanine ligand as well as the primary amine of the ethylene diamine ligand act as proton acceptors in transfer hydrogenation. In this process, the ethylene diamine appears to be much more catalytically active than the amine group present at the phenylalanine ligand. This might be the reason for the significant difference in activities for N-*p*-tosyl ethylenediamine containing complex **20** (table B10, entry 4) and complexes **26**, **27** and **28**, which are not coordinated to this ligand (table B10, entries 1-3). Enantiomeric excesses were highly different for the tested ruthenium complexes. The most active complex **28** only gave essentially racemic mixtures (ee = 2 % (*R*), table B10, entry 4), which can be accounted to the low chiral information, which is transmitted

when catalysis is predominantly mediated via the achiral ethylenediamine ligand. Enantiomeric excesses were significantly higher for complexes **20**, **26** and **27**, ranging from 17 % to 52 % (table B10, entries 1-3). The best results were obtained with complex **14**, which possesses, in contrast to complexes **20** and **26**, the sterically demanding 1,4-di-N-*p*-tosylethylenediamine, which might increase the steric information transmitted by the chiral phenylalanine ligand. The enantiomeric excesses observed also indicate that the catalytic activity is mediated via the ethylene diamine rather than the phenylalanine ligand.

***Table B10:*** Hydrogenation results for the catalytic hydrogenation of acetophenone.[a]

| entry | complex | time [d] | yield [%] | ee [%] |
|-------|---------|----------|-----------|--------|
| 1 | **20** | 12.5 | <2 | 20 (*S*) |
| 2 | **26** | 12.5 | <2 | 17 (*S*) |
| 3 | **27** | 12.5 | <2 | 52 (*S*) |
| 4 | **28** | 12.5 | 27 | 1 (*R*) |

(a) Conditions: The reaction was carried out at room temperature using a 1.4 M. solution of acetophenone (10 mM) in 2-propanole. Reaction time = 12.5 d. Yields were determined by gas chromatography. Complex **20**: substrate:KOH:catalyst = 1000/100/1; Complexes **26**,**27**,**28**: substrate/KOH/catalyst = 1000/100/2; Ees were determined by chiral gas chromatography.[59]

However, reactions employing potassium isopropanolate instead of potassium hydroxide resulted in a completely different behavior of catalysts **20**, **27** and **28**. In this case, no conversion of acetophenone was detected within 24 h for ethylene diamine derivative coordinated catalysts **27** and **28**, whereas catalyst **20** showed moderate activity (15 % yield). This can be accounted to the fact, that **27** and **28** do not have an open coordination site, whereas **20** has two labile-coordinated chlorine anions, which can be exchanged during catalysis. Therefore, dissociation of the $\eta^6$-arene ring is negligible in the absence of hydroxide anions. This excludes the possibility of complexes **27** and **28** to be active in catalysis, as these two species do not have an open coordination site, with which the substrate could interact with.

# B2. Synthesis and derivatization of η⁵-half sandwich complexes

## 1. Introduction

Half sandwich complexes of the late transition metals have become ubiquitous in organometallic chemistry.[60] Among the many developments, side chain functionalization particularly has added new facets to the chemistry of this class of compounds.[61,62,63] The emerging reactivity patterns have been utilized to tailor solubility,[63,64] control the electronic properties of the metal centre via hemi-labile coordination,[64,65,66,67] introduce chirality,[68] or to accelerate catalytic reactions by a bifunctional mechanism.[69] Compounds with pendant amino groups have attracted considerable attention, with (2-dimethylamino)ethyl tethered η⁵-cyclopentadienyl derivatives of Ru, Rh, or Ir being prominent examples.[63,69] A field of growing interest has become the conjugation of late transition metal complexes comprising appropriate functional groups with biological and bioactive compounds such as hormones,[70] vitamins,[71,72] peptides,[73] enzymes[74] or DNA.[75] A common conjugation reaction utilizes primary amine and carboxylic acid groups to form a peptide bond. While a broad range of functionalized sandwich complexes exist,[76] half sandwich complexes of late transition metals bearing carboxy functionalized side chains[77,78,79] or pimary amine derivatives are particularly rare.[79,80]

The few examples existing for group 9 metals have been synthesized via salt metathesis of Cp(R)Na and a M(I)X precursor. The elegant synthesis described for [Cp*MCl₂]₂ (M=Rh, Ir)[81] has to date not been applied with Cp-ligands possessing a side chain amine-functionality. This may be attributed to the tedious synthetic access to such ligands.[82] Therefore, the synthesis of late transition metal cyclopentadienyl complexes exhibiting a primary amine tether seemed an interesting and rewarding project, as it can lead to functionalizeable complexes.

This approach resulted in a synthetic route to respective rhodium(III) and iridium(III) compounds, starting from a Cp* tautomere. Further, investigations on the selective derivatization of the side chain's functionality were conducted successfully.

# 2. Synthesis of η⁵-half sandwich rhodium and iridium complexes

For the synthesis of rhodium(III) and iridium(III) complexes with pendant linker functionalities, a Cp* tautomere was chosen, which has already been applied in literature as a η⁵-ligand for titanium complexes.[83,84] Therefore, no major difficulties were observed in ligand synthesis.
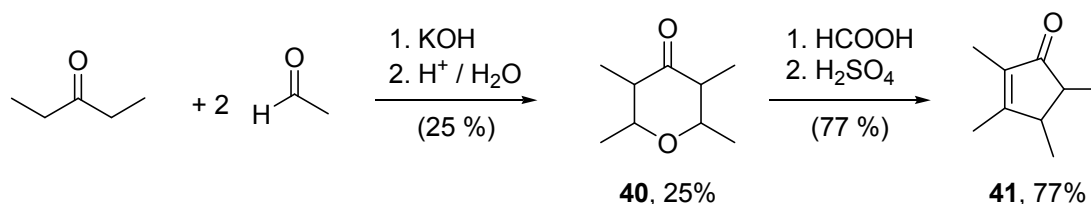


**Scheme B25:** Synthesis of the ligand precursor tetramethylcyclopentenone.[83]

The synthetic route for the synthesis of the ligand precursor tetramethylcyclopentenone **41** was already reported by Fendrick *et al.*[83] Hereby, 3-pentanone and formic acid aldehyde serve as starting materials (scheme B25). In this 2 step synthesis, 2,3,5,6-tetrahydro-2,3,5,6-tetramethyl-4-pyrone **40** is generated first, which was obtained analytically pure after distillation. Nevertheless, its ¹H NMR spectrum is rather challenging due to its four stereocenters, which do not have any preferential conformation.

Also the second step, a proton catalyzed elimination of water is straight forward. The ligand precursor **41** can be isolated, after having been distilled twice, in high purity (> 99 % purity, 77% yield) and was directly used in the following reaction procedures.
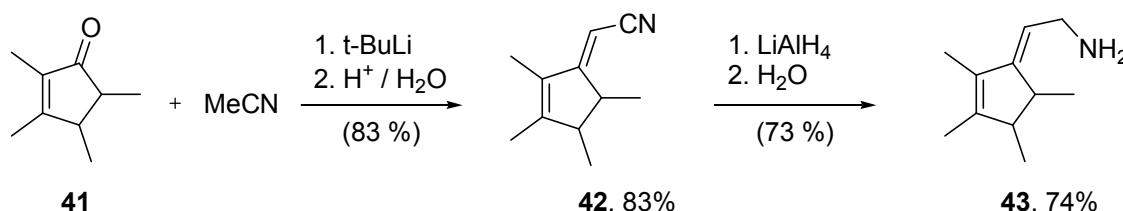


**Scheme B26:** Synthesis of 2-(2,3,4,5-Tetramethylcyclopentadienyl)ethylamine tautomere **43** via the reported route of Leusen *et al.*[84]

The synthesis of 2-(2,3,4,5-Tetramethylcyclopentadienyl)ethylamine tautomere **43** was carried out following the procedure described by Leusen *et al.* (scheme B26).[84] The only differences to the reported procedure was the application of ᵗBuLi for the deprotonation of acetonitrile instead of ⁿBuLi, as better conversions were achieved in

this case. This can be attributed to the higher basicity of the oxygen atom present in lithium alkyl $^t$BuLi and its lower nucleophilicity. Characterization of **43** was carried out via $^1$H NMR spectroscopy. Characteristic peak shifts of the amine linker can be utilized to determine the identity and purity of the compound, as signals of the ring system only shift slightly upon conversion of **42** to **43**. The ligand 2-(2,3,4,5-Tetramethyl-cyclopentadienyl)ethylamine tautomere **43** as well as its precursor **42** are yielded almost exclusively with an exocyclic double bond. This can be explained by the increased acidity of the exocyclic proton during the elimination of water within the conversion of **41**, yielding **42**. Furthermore, the exocyclic double bond is favored, as it facilitates a conjugated double bond system including the nitrile functionality.

The synthesis of nitrogen donor functionalized complexes of group 9 metals with oxidation state III has been investigated in detail by Jutzi and coworkers.[60] He also observed a tendency of the pendant nitrogen donor to coordinate to the metal centre.

Coordination of the tether might deactivate the amine for further functionalizations and cause it to be of no avail in the synthesis of metalla affinity labels. Therefore, a simple strategy was applied to avoid coordination of the amine tether. It was protonated with hydrochloric acid (2 M in dioxane), resulting in **43$^{HCl}$** (scheme B27). The resulting ammonium chloride nitrogen does not feature a free electron pair, which could coordinate to the Lewis acid metal centre. This makes synthesis of pendant non coordinated amine-functionalized Cp* ligands possible. The protonated ligand **43$^{HCl}$** was not isolated and directly applied in the synthesis of $\eta^5$-cyclopentadiene transition metal complexes.
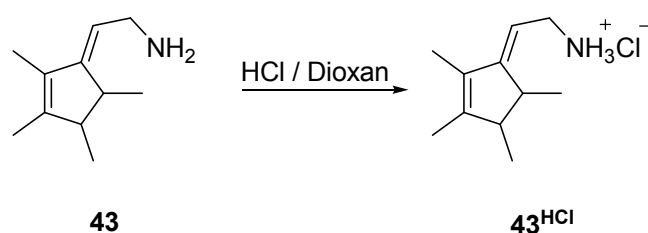


**Scheme B27:** Protonation of **43**, resulting in its ammonium chloride **43$^{HCl}$**.

Formation of a Cp-$\pi$-system necessitates isomerization of the exocyclic double bond of ligand **43**, which represents a well known reactivity of group 9 metals.[85] Refluxing the reaction mixture for four days in ethanol lead to clean formation of rhodium complex **50**, which precipitates in high purity as orange powder (scheme B28). The product can be stored under air for months without detectable decomposition. It exhibits significant

solubility only in strong donor solvents like water or DMSO, which are capable of metal coordination and splitting of the dimeric structure.[65,86]
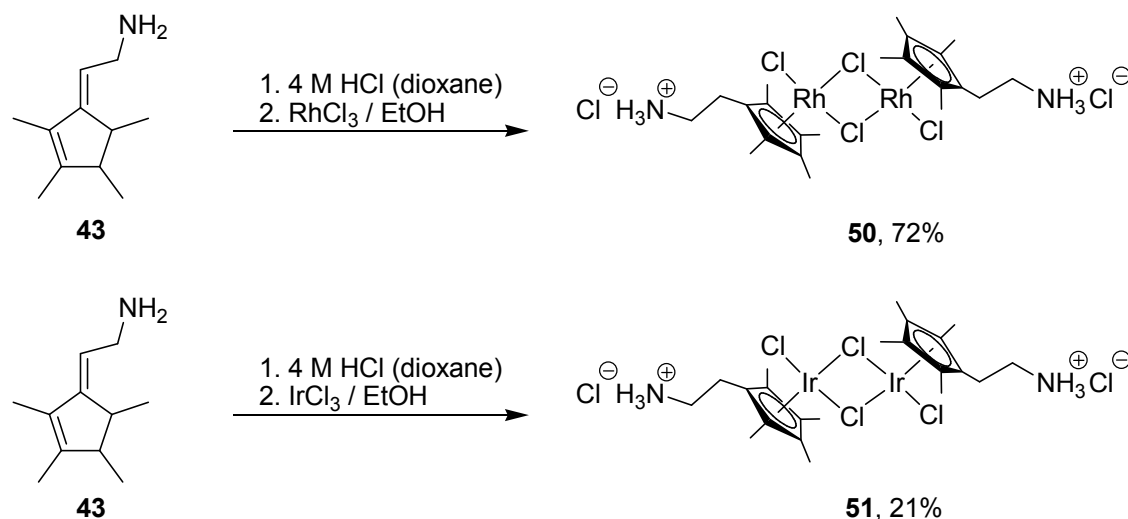


**Scheme B28:** Synthesis of dinuclear $\mu$-chloro bridged group 9 metal complexes **50** and **51**.

Synthesis of the homologous iridium complex **51** (scheme B28) reveals distinct reactivity differences of the two group 9 metals, which are less pronounced for the synthesis of the $\mu$-chloro bridged $\eta^5$-cyclopentadienyl analogues [Cp*MCl$_2$]$_2$ (M=Rh, Ir) under similar conditions,[81] yet have been reported to strongly influence synthesis of [Cp*MCl$_2$]$_2$ from hexamethyl dewar benzene.[87] In contrast to rhodium complex **50**, iridium cyclopentadiene derivative **51** remains dissolved. The markedly increased solubility of complex **51** seems to limit product formation to equilibrium concentration and no additional conversion is observed after 24 hrs. The product was obtained in high purity as bright yellow powder upon removal of solvent and washing with non polar solvents.

^{1}H NMR spectra of complex **50** and **51** in DMSO-d$_6$ are nearly identical. The NH$_3^+$ group gives rise to a broad singlet at $\delta$ = 8.10 (**50**) or $\delta$ = 8.12 (**51**) which integrates to three protons, indicating, that the amine tether does not coordinate to the metal center. This is in contrast to for example alkenyl side chain linkers. They resemble hemi-labile ligands, which are known to coordinate to group 9 metal centers since several decades.[67] Resonances observed for the methyl (two singlets centered at $\delta$ =1.7 ppm) and methylen (triplets at about $\delta$ = 2.9 and $\delta$ = 2.4 ppm) moieties are in agreement with those observed for similar compounds.[65] This also indicates, that there is no equilibrium between these species and an internal salt of the composition

$[(\eta^5\text{-Me}_4\text{Cp}(\text{CH}_2)_2\text{NH}_3)\text{RhCl}_3]$. The methylene resonances were assigned based on $^1\text{H}^1\text{H}$ COSY spectra. The strong downfield shift of the methylene protons adjacent to the nitrogen is also indicative for a protonation of the amino function.[64,66]

$^{13}\text{C}$ NMR reveals $\eta^5$-coordination of the cyclopentadiene system in complexes **50** and **51**, since chemical shifts are in the typical range.[65] For complex **2**, carbon resonances are split into doublets due to a $^1J_{\text{Rh,C}}$ coupling, with coupling constants ranging from 8.1 Hz to 7.3 Hz, which is close to literature data for $[\text{Cp*RhCl}_2\text{PPh}_3]$ **54** ($^1J_{\text{Rh,C}}$ = 6.2 Hz).[87,88] While for both complexes the chemical shifts of the methyl and methylene resonances are very similar, evaluation of $^{13}\text{C}$ NMR spectra reveals clear differences for the cyclopentadienyl signals. In comparison to Rh complex **50** (102.6, 94.0, 93.8), resonances for Ir compound **51** (97.1, 92.2, 85.8) are shifted upfield by 6-8 ppm and cover a broader frequency range (**50**: 8.9 ppm, **51**: 11.3 ppm, see figure B18). This indicates a lower degree of $\pi$-aromatization for the Ir compound.
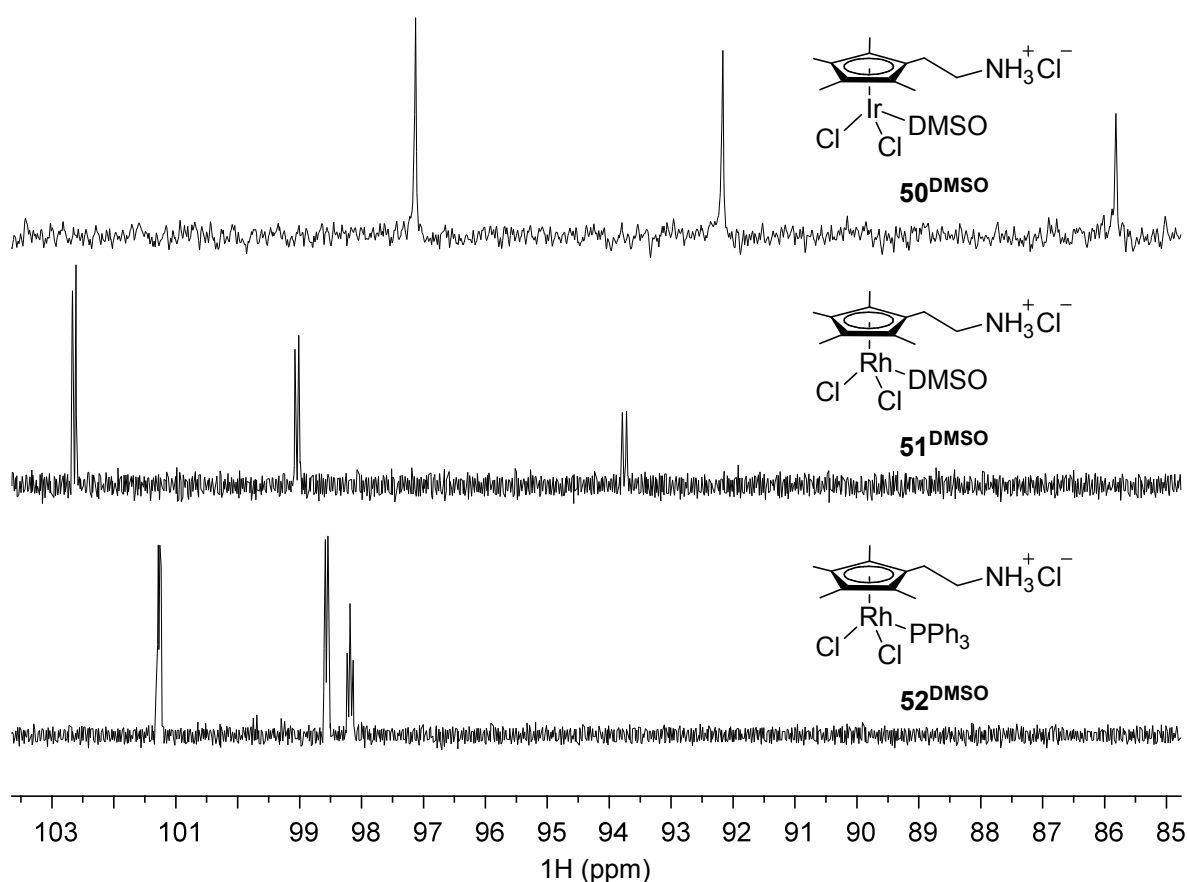


***Figure B18:*** Comparison of the Cp of complexes **50**, **51** and **52** ($^{13}\text{C}$ NMR, DMSO-$d^6$).

While bubbling CO through a DMSO-solution of complex **50** only yielded a transient band at 2066 cm$^{-1}$, coordinated donor solvent was displaced irreversibly upon addition of triphenyl phosphine. Resulting complex **52** can be isolated in quantitative yields after removal of the solvent (scheme B29). $^{31}$P NMR of **52** shows a doublet at 30.3 ppm with a $^{1}J_{Rh,C}$ coupling constant of 144 Hz and thus is similar to that reported for [Cp*RhCl$_2$PPh$_3$] **54** ($\delta$ = 30.6 ppm, $^{1}J_{Rh,C}$ = 144 Hz).[89,90] Despite of the extra PPh$_3$ signals, $^{1}$H NMR of complex **52** resembles that of the precursor **50** with a broad NH$_3^+$ resonance at 8.18 ppm. $^{13}$C NMR reveals the intact $\eta^5$-coordination of the $\pi$-ligand, with a markedly decreased spread of the Cp-carbon signals (101.3, 98.6, 98.2 ppm). These resonances are split by $^{1}J_{Rh,C}$ couplings, ranging from 6.8 to 5.9 Hz and additional $^{2}J_{P,C}$ coupling ranging from 5.9 to 1.5 Hz (figure B18). Further, $^{3}J_{P,C}$ coupling of 1.4 to 0.7 Hz is observed for Cp*-methyl groups.
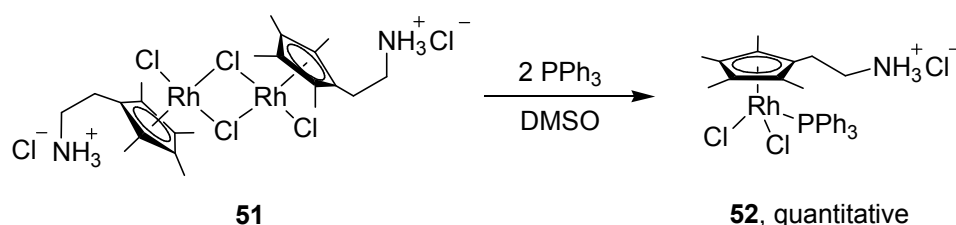


**Scheme B29:** Donor induced splitting of dinuclear complex **51**.

According to spectroscopical data, the nitrogen atom in complexes **50**, **51** and **52** is protonated and does not coordinate to the metal centre. Besides, elemental analysis is in agreement with isolation of HCl adducts. Side chain selective derivatization necessitates deprotonation of the amino group. Yet, it has been shown for similar complexes, that the nucleophilic nitrogen atom coordinates intramolecular to the electrophilic metal center.[65] In **52** however, the triphenyl phosphine prevents immediate coordination of the nucleophilic nitrogen. Correspondingly, reaction with succinic anhydride in dichloromethane under basic conditions leads to peptide bond formation, yielding pure phosphine adduct **53** after acidic workup in 54 % yield (scheme B30).
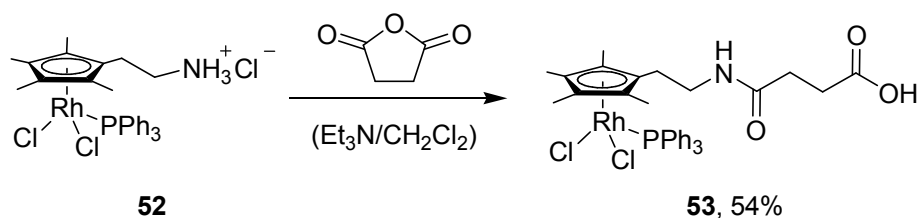


**Scheme B30:** Side-chain selective modification of **53** with succinic anhydride.

Conversion was confirmed by IR spectroscopy due to the presence of bands which can be assigned to carbonic acid ($\tilde{\nu}$(CO) = 1730 cm$^{-1}$) and amide ($\tilde{\nu}$(amide I) = 1647 cm$^{-1}$, $\tilde{\nu}$(amide II) = 1545 cm$^{-1}$) functionalities. The [Cp*Rh(PPh$_3$)Cl$_2$] core of **53** is unaltered as judged by the minor changes in $^1$H, $^{13}$C, $^1$H,$^1$H COSY and $^{31}$P NMR in comparison to precursor **52**. In agreement with the IR data, $^{13}$C NMR shows two carbonyl resonances at $\delta$ = 174.4 ppm and 174.7 ppm, while $^1$H NMR reveals the presence of an amide proton at $\delta$ = 7.60 ppm.

The synthesis of the first example of Cp*Rh(III) and Cp*Ir(III) complexes comprising a primary amine functionality in the side chain can be achieved under acidic reaction conditions employing ligand precursor **1**. If the coordination sphere of the d$^6$ cation is electronically saturated, e. g. by addition of triphenyl phosphine, side chain selective derivatization can be achieved under basic conditions. Hence metal center and side chain functionality can be addressed independently under appropriate conditions. This enables the bifunctional Cp*-derived ligand **1** to covalently conjugate reactive late transition metal cations with functionalities of other molecules, e.g. carboxyl groups.

Therefore, this reactivity allows the synthesis of metalla affinity labels, which themselves can be reacted with enzymes to yield organometallic enzyme hybrids.

# B3. Synthesis and application of organometallic enzyme hybrids

## 1. Introduction

Modern asymmetric catalysis offers efficient techniques to synthesize enantiopure substrates. The two major options are transition metals catalysis[91] or biocatalysis.[92] Besides traditional techniques, the use of organometallic enzyme hybrids has become a quickly emerging field.[93] Inspired by the pioneering work of Wilson and Whitesides[94] on the biotin-streptavidin technology and Reetz *et al.* on the directed evolution of enzymes,[95] there have been considerable achievements in the creation of organometallic enzyme hybrids.[96] In particular, Ward *et al.* not only used the biotin (strept)avidin technique to generate enantioselectivity, but also optimized their organometal protein hybrid system by directed evolution of the enzyme.[97] This opened a new perspective of optimization of organometallic catalysts, ligand synthesis to generate high enantioselectivities becomes redundant. One of the major advantages of the biotin (strept)avidin technique is the efficient inhibition of the streptavidin by coordination of biotin to the (strept)avidin protein binding pocket ($K_a \approx 10^{14}$ M$^{-1}$).[98] Previous results have shown, that selective and directed inhibition is an advantage for the generation of efficient organometal enzyme hybrids.[96,97,98] Success was likewise achieved in the crystallization of organometal enzyme hybrids, both with non-covalent[99] as well as covalent[100] immobilization of the organometallic species. Nevertheless, the biotin (strept)avidin technology has some limitations, which hamper broad applicability. First of all, the non-covalent interaction between biotin (strept)avidin is strong, but limited to one class of proteins. Second, non-covalent interaction always implies the risk of protein conformation to undergo alterations under the applied reaction conditions. This can result in a decrease or loss of binding affinity between substrate and enzyme and lead to the release of active organometallic catalyst into the achiral reaction medium. Furthermore, non covalent enzyme ligand interactions which are equally strong as those found between biotin and (strept)avidin are rare, whereas there are numerous covalent binding moieties, which inhibit whole classes of enzymes.[101] There is a wide range of enzymes, which are extremely stable to increased temperature, varying pH values, organic solvents or denaturing reagents, making covalent inhibition interesting for the synthesis of organometallic enzyme hybrids.[102]

# 2. Concepts and basic principles

## 2.1. Cysteine protease based organometallic enzyme hybrids

To explore a new route for the design of organometallic enzyme hybrids, which allows a wider applicability in terms of conditions, enzymes and metal centers is a challenging project. The route can be realized by choosing an E64 affinity label analogue as a model system, which is known to inhibit cysteine proteases covalently via nucleophilic attack to its epoxide moiety.[103] It was attached to rhodium as well as ruthenium catalysts by peptide bond formation, resulting in metalla affinity labels ([M]-ALs), which inhibit cysteine proteases covalently as well as site specifically. The peptide part of the metalla affinity label in combination with the covalent anchoring ensures it to be orientated in the enzyme's active site pocket and therefore results in a directed anchoring of the transition metal catalyst (figure B19).
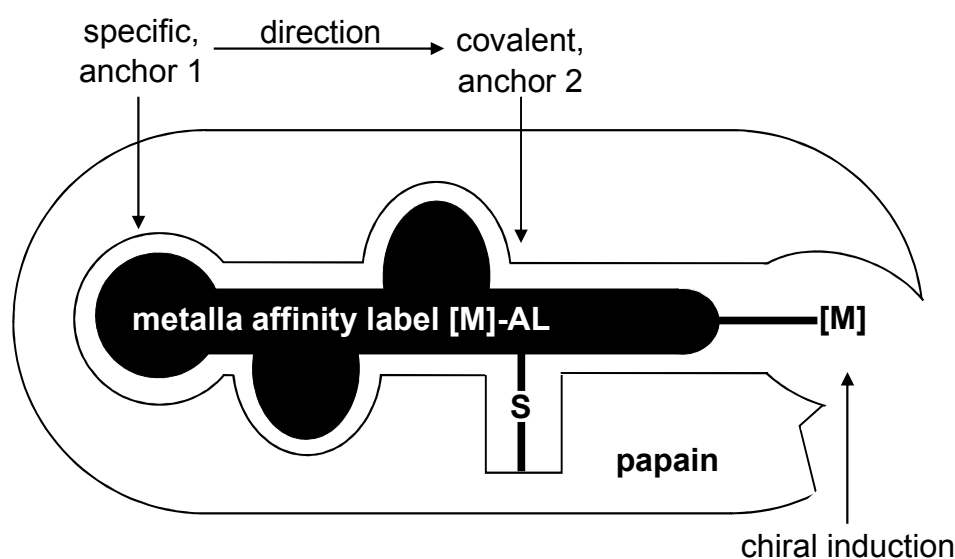


*Figure B19:* Fusion of a metalla affinity label with an enzyme, generating an organometallic enzyme hybrid. The label is bound selectively and covalently into the active site pocket of cysteine proteases.

The resulting metalla affinity labels can be regarded as trifunctional organometallic catalysts, consisting of a peptidic part, which ensures specific interaction of [M]-ALs and the active site pocket and the epoxide moiety, which allows covalent attachment. Combination of both results in a directed orientation of the metalla affinity label's third part, the achiral organometallic catalyst. It is anchored in the active site, allowing asymmetric catalysis through embedment in the chiral protein environment.

The synthetic route to these compounds is another notable feature of our approach. As the peptide bond formation between organometallic catalysts and the affinity label is the last synthetic step, the generation of different [M]-ALs is possible rapidly. Combination of different catalysts, affinity parts and enzymes allows the generation of an organometallic enzyme hybrid library, from which promising candidates can be tested for their performance in asymmetric catalysis in only a short amount of time.

The resulting organometallic enzyme hybrids can be applied in the hydrogenation of ketones, where they have proven the concept described above to be valid (figure B20).
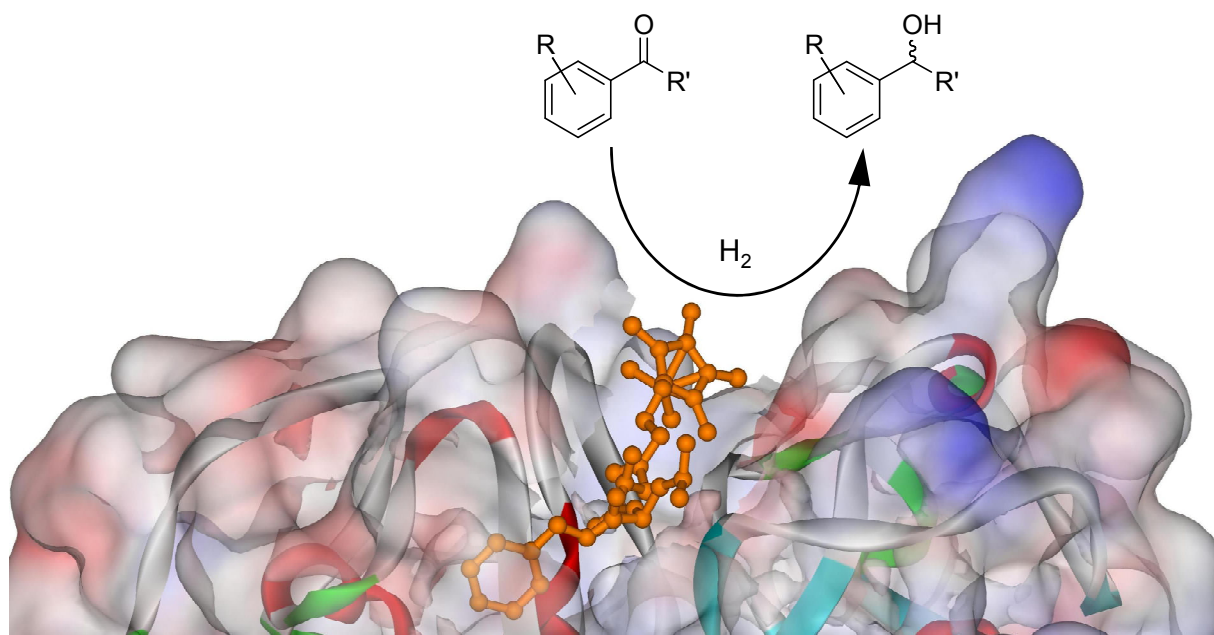


***Figure B20:*** Embedded metalla affinity label in the active site of the cysteine protease papain.

## 2.2. Serine protease based organometallic enzyme hybrids

Nevertheless, not only epoxide groups seem to be profitable moieties, with which a catalyst can be anchored into the active site of a protein. There exists a plethora of reactive functional groups, with which covalent bond formation can be facilitated.[101] In addition, there are also different kinds of proteases, which can be addressed.[101]
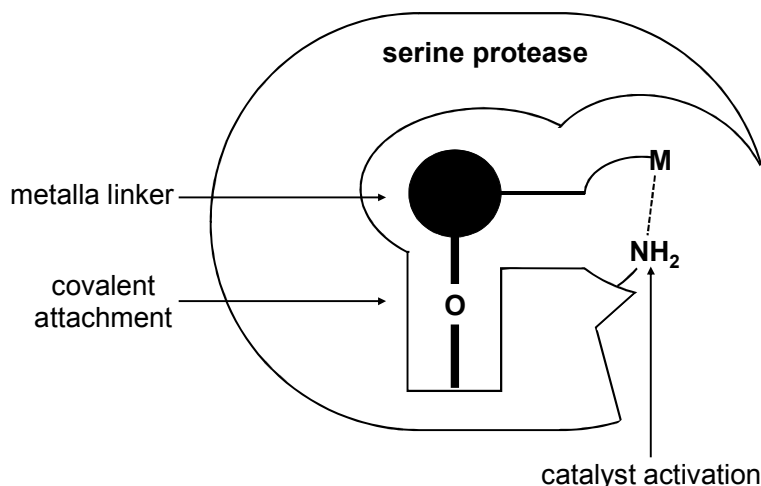


*Figure B21:* Metalla affinity labels employed in the catalytic enzyme-assisted hydrogenation of ketones.

Besides the epoxide containing cysteine protease inhibitor E64, fluorosulfonic acids, fluorophosphonic acids and phosphonic acid esters have proven to be of interest, as they inhibit serine proteases efficiently.[101] Furthermore, not only asymmetric hydrogenations, but also asymmetric transfer hydrogenations can be considered to be of interest for organometallic enzyme hybrid catalysis. Serine proteases trypsin and α-chymotrypsin have shown to be inhibited efficiently by fluoro phosphonic and fluoro sulfonic acids.[97] In both cases, covalent bond formation occurs via the nucleophilic attack of the active center serine residue to the phosphorous or sulfur moiety.
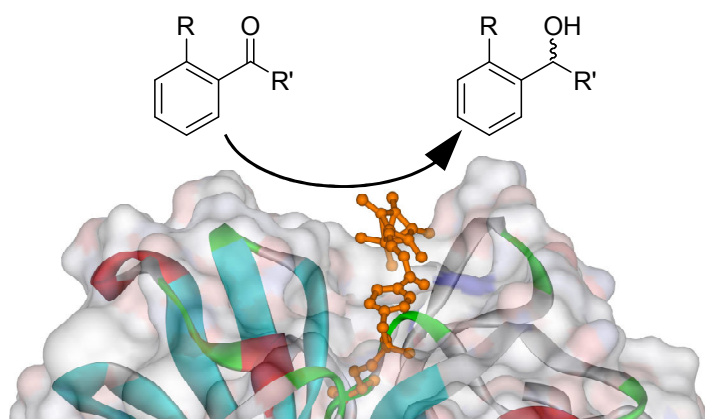


*Figure B22:* Embedded metalla linker in the active site of the serine protease trypsin.

If a derivative of rhodium phosphine catalyst **52** is applied in transfer hydrogenations, the enzyme itself does not only act as a chiral scaffold. It furthermore can actively take part in the catalytic cycle, thus not only being crucial for the generation of enantiomeric excesses, but also for yields. This is due to the necessity of an amine coordinated to the metal centre, as has been described before.[15] This amine may be provided by the enzyme surface.

Therefore, this concept takes not only advantage of the enzyme's chiral scaffold, but also of the activation of phosphine catalysts. It was facilitated trough embedment of the catalyst into the enzyme's active site by first a covalent anchor and second by coordinative bond formation between primary or secondary amines on the enzyme surface and the transition metal centre (Figure B21).

The resulting organometallic enzyme hybrids can therefore be tested for their performance not only in hydrogenation reactions, but also in the catalytic enantioselective transfer hydrogenation (Figure B22).

## 3. Synthesis of E64 derived metalla affinity labels

For the synthesis of an E64 derived metalla affinity label, *L*-leucine and benzylamine were chosen as peptidic part, as they have been proven to bind efficiently into the active site of papain before.[104,105] To build up the affinity label structure, first Boc-*L*-leucine was reacted with benzylamine under formation of a peptide bond between the two compounds (scheme B31). As coupling reagent, EDCI was used. Based on its water solubility, this carbodiimide is the reagent of choice for peptide formation in solution, as, in contrast to the more common DCC, simple extraction of the product makes silica column chromatography obsolete. By addition of the carboxylic acid to the central carbodiimide carbon, an acylisocarbamide is formed, which can be attacked by strong nucleophiles. The resulting peptide **60** was analyzed by $^1$H NMR, $^{13}$C NMR and $^1$H$^1$H COSY NMR spectroscopy. It was further analyzed by IR spectroscopy and elemental analysis. All obtained data fit the expected values, confirming the identity and purity of the compound.



**60**, 79%
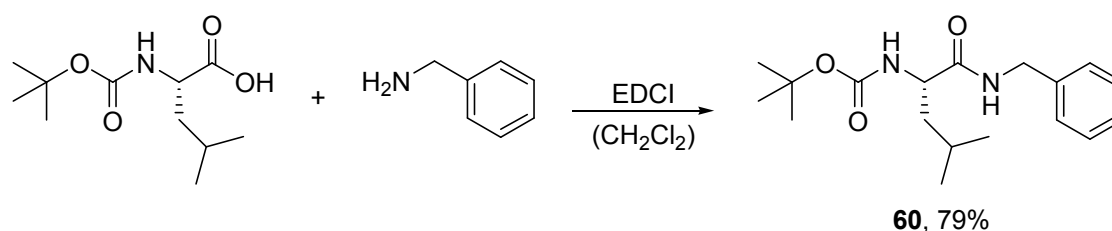
**Scheme B31:** Synthesis of compound **60**.

For further derivatization, its Boc protective group was removed in acidic medium. This was achieved by addition of trifluoro acetic acid.[106] The strong acid protonates the carbonyl group, leading to elimination of $CO_2$ and isobutene. The product purity and identity was confirmed by $^1$H NMR, $^{13}$C NMR, elemental analysis, IR spectroscopy and ESI MS (221.3, [M+H]$^+$). Compound **61** was obtained analytically pure, after silica column chromatography (scheme B32).



**60** **61**, 95%
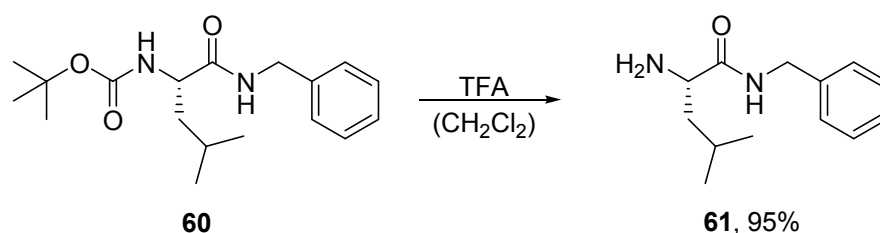
**Scheme B32:** Deprotection of **60**, yielding amine **61**.

In $^{13}$C NMR spectra, only one carbonyl signal is observed for compound **61** (175.0 ppm), whereas there are two different carbonyl signals observed for compound **60** (172.6 ppm and 155.9 ppm).

The second building block in the synthesis of E64 derived metalla affinity labels is the epoxide moiety, which is necessary for the formation of a covalent bond with the active center cysteine sulfur. It was built up from *D*-(-)-diethyl tartrate. The use of diethyl tartrate results in an epoxide motive with (2*S*, 3*S*)-configuration. The absolute configuration of the epoxide is crucial for the inhibitor activity, as the (2*R*, 3*R*) diastereomer of E64 has a significantly decreased inhibitory potential, as has been shown before.[107] Also other investigations have pointed out a preference for the (2*S*, 3*S*)-configuration.[108,109] The synthesis of ethyl(2*S*, 3*S*)-(+)-epoxysuccinate was conducted according to the published reaction sequence by Chehade *et al.*[104] (scheme 33).
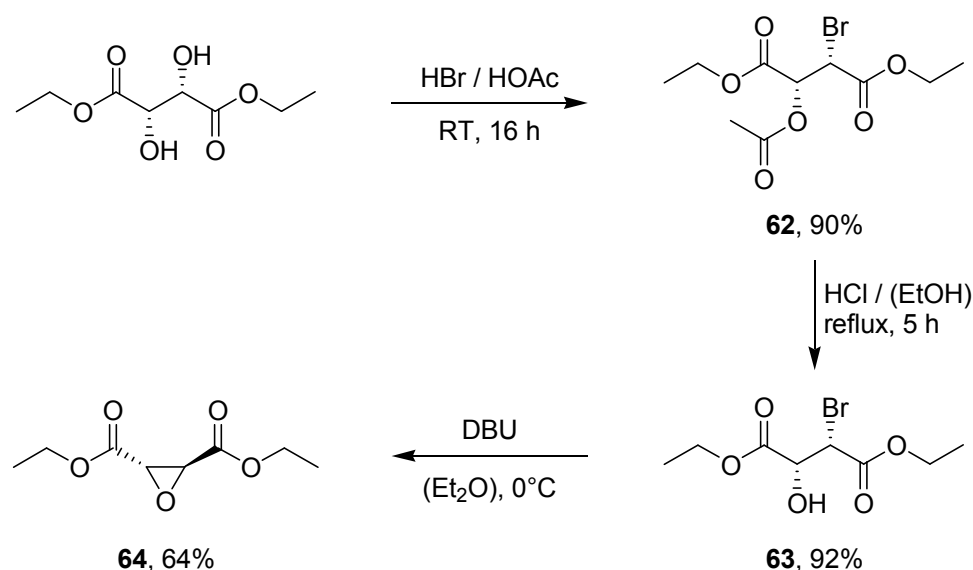


**Scheme B33:** Synthesis of diethyl(2*S*, 3*S*)-(+)-epoxysuccinate **64** from *D*-(-)-diethyl tartrate.[104]

Herefore, the commercially available *D*-(-)-diethyl tartrate was converted into its bromoester **62**, by stirring it in hydrobromic acid (33 % in acetic acid). The subsequent hydrolysis of the acetyl ester was mediated using a solution of hydrochloric acid in ethanol, yielding bromohydrin **63** in 92 % yield. Compound **63** forms diethyl(2*S*, 3*S*)-(+)-epoxysuccinate **64** when stirred with 1,8-diazabicyclo[5.4.0]-undec-7-ene (DBU) in a solution of diethylether at 0 °C. After aqueous workup, **64** is obtained with a yield of 64% and with an overall yield of 53%.

Identity and purity of **64** was confirmed via $^1$H and $^{13}$C NMR spectroscopy. In $^1$H NMR spectra, the two epoxide protons are observed as a single singulet at 3.65 ppm (integral 2). In $^{13}$C NMR spectra, four signals are observed at 166.9 (carbonyl), 62.4 (ethyl-CH$_3$), 14.2 (ethyl-CH$_2$) and 52.2 (epoxide-CH).
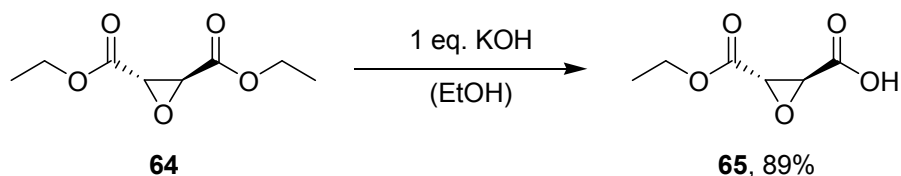


**Scheme B34:** Saponification of diethyl(2*S*, 3*S*)-(+)-epoxysuccinate **64**, yielding ethyl(2*S*, 3*S*)-(+)-epoxy-succinate **65**.[104]

To facilitate a peptide bond formation with peptide **61**, one of the ethyl groups was cleft by basic hydrolysis in ethanol. For this purpose, diethylepoxysuccinate **64** was dissolved in a solution of dry ethanol, containing one equivalent of potassium hydroxide. Applying dry ethanol as well as the stoichiometric amount of potassium hydroxide improves selective cleavage of only one ethyl ester and reduces the risk of the epoxide group being opened trough nucleophilic attack of hydroxide anions. Product compound ethyl(2*S*, 3*S*)-(+)-epoxy-succinate **65** is obtained in 89% yield (scheme B34).
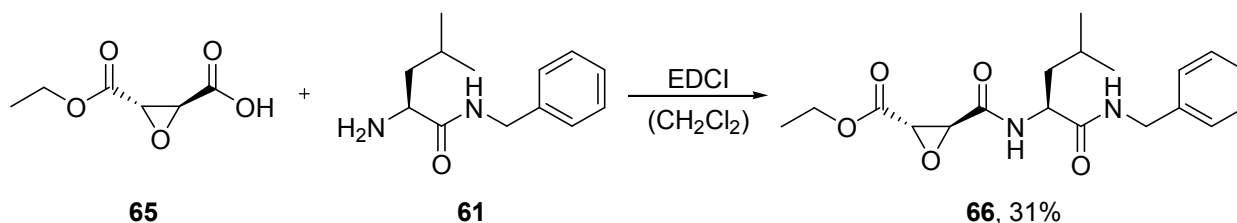


**Scheme B35:** Peptide bond formation between building blocks **65** and **61**, yielding compound **66**.

Ethyl epoxisuccinate **65** was analyzed via $^1$H and $^{13}$C NMR spectroscopy. The integral ratios of epoxide protons to ethyl protons are 2 / 5. For diethylepoxysuccinate **64**, they are 2 / 10. Besides, for **65**, the epoxide proton signals are inequivalent due to loss of $C_2$-symmetry and therefore observed as doublets at 3.71 ppm and 3.70 ppm ($^3J_{HH}$ = 1.2 Hz). In $^{13}$C NMR spectra, they are observed at 52.4 ppm and 51.6 ppm.

The two building blocks ethylepoxysuccinate **65** and peptide **61** were conjugated via peptide bond formation. As described above, water-soluble EDCI was used to facilitate the reaction. Compound **66** was obtained in excellent purity. It was analyzed by $^1$H NMR, $^{13}$C NMR, elemental analysis and IR spectrometry. $^1$H$^1$H COSY spectra were collected to assign the different spin systems. The two epoxide protons are observed

again as doublets at 3.61 ppm and 3.43 ppm ($^3J_{HH}$ = 2.1 Hz). In $^{13}$C NMR, three signals are observed for the carbonyl carbon atoms at 171.5, 166.5 and 166.2 ppm. In $^1$H NMR, the ethyl ester protons are observed at 4.46-4.19 ppm (m, $CH_2$) and 1.30 ppm (t, $^3J_{HH}$ = 7.3 Hz, $CH_3$). In $^{13}$C NMR spectra, they are observed at 62.5 ppm and 14.2 ppm.
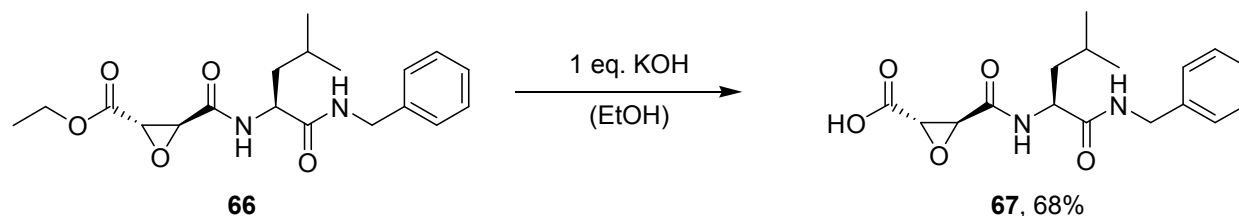


**Scheme B36:** Saponification of compound **66**, yielding [M]-AL precursor **67**.

The final affinity label **67** was obtained by saponification of compound **66**. The reaction was carried out according to saponification of diethyl epoxysuccinate **64**. Again, only one equivalent KOH in dry ethanol was employed to prevent nucleophilic attack to the epoxide moiety. After work-up, metalla affinity label precursor **67** was obtained analytically pure in 68 % yield.
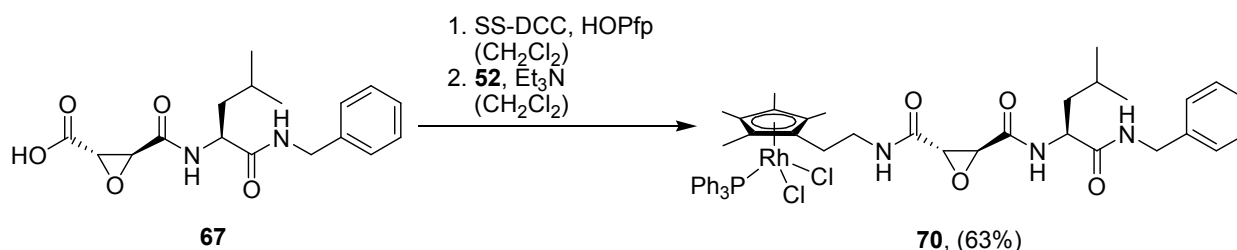
Structural identity was confirmed via elemental analysis IR spectrometry $^1$H NMR, $^{13}$C NMR, and $^1$H$^1$H COSY NMR spectrometry. In $^1$H NMR, the two epoxide protons are observed as doublets at 3.57 ppm and 3.51 ppm ($^3J_{HH}$ = 2.1 Hz). Again, in $^{13}$C NMR, three signals can be assigned to carbonyl carbon atoms. They were observed at 172.7, 168.8 and 166.7 ppm. Neither in $^{13}$C NMR nor $^1$H NMR spectra, signals corresponding to an ethyl ester group were detected, confirming the saponification to have been successful and complete.

However, the crucial step in the synthesis of metalla affinity labels is the assembly of the bioactive inhibitor **67** and organometallic catalyst **52**. Hereby, a peptide bond needs to be formed. During this step, the reactive moiety of the peptidic part must not be altered, as well as the inner coordination sphere of the catalyst. For example, coordination of nucleophilic groups of the inhibitor to the metal centre must not happen. Only the pendant catalyst linker (amine) and the inhibitor linker (carboxylic acid) are to take part in the reaction.

A large number of conditions for the formation of peptide bonds have been described.[110] However, most possibilities need to be ruled out, as the organometallic catalyst **52** as well as the inhibitor **67** are subject to numerous restrictions in terms of work up procedures due to their reactivity (Lewis-acid transition metal centre, nucleophilic epoxide moiety).

One successful technique however was the conversion of inhibitor **67** in its pentafluorophenole active ester (OPfp-ester), which then was reacted with catalyst **52**. As activating reagent for the formation of the active ester, a polystyrene bound carbodiimide resin (NovaBiochem) was used. It is superior to other activating reagents, as it can be filtered off prior to addition of the catalyst and therefore does not result in side-product formation.

A slight excess of triethylamine was added to ensure deprotonation of the pendant amine linker of **52**. Due to the steric approach of the ethyl groups of triethylamine, coordination to the metal centre does not take place. Deprotonation results in the amine being nucleophilic enough to attack the pentafluorophenol active ester, yielding the metalla affinity label [Rh]-Epx **70**. Both reactions, the formation of the pentafluorophenole active ester as well as the peptide bond formation, proceed extremely selective and quantitative. After washing and extraction procedures to remove triethylamminoum chloride and pentafluorophenole, the [Rh]-Epx **70** is yielded analytically pure in 63% yield (scheme 37).



**Scheme B37:** Synthesis of metalla affinity label [Rh]-Epx **70** via pentafluorophenole active ester formation.

The structural identity and purity of [Rh]-Epx **70** was confirmed via elemental analysis, IR spectrometry, ESI MS, $^1$H NMR, $^{13}$C NMR and $^1$H$^1$H COSY NMR spectrometry. In ESI MS spectra, masses of 880.1 ([M-Cl]$^+$) and 618.2 ([M-Cl-PPh$_3$]$^+$) were observed, confirming the mass of the product species. In $^1$H NMR spectrometry, two peaks corresponding to the epoxide moiety could be observed at 3.55 ppm and 3.53 ppm ($^3J_{HH}$ = 1.9 Hz). In $^{13}$C NMR, two peaks at 54.5 ppm and 54.1 ppm were observed for the epoxide. These values are in close proximity to the ones observed before for compounds comprising epoxides. Therefore, the epoxide can be assumed to be still intact. In $^{31}$P NMR, a doublet at 30.0 ppm was observed ($^3J_{PRh}$ = 143 Hz). This shift is extremely close to the one observed for complex **52** (30.3 ppm, $^3J_{PRh}$ = 143 Hz), also indicating the catalyst inner sphere coordination to be intact and the reaction to have been successful.
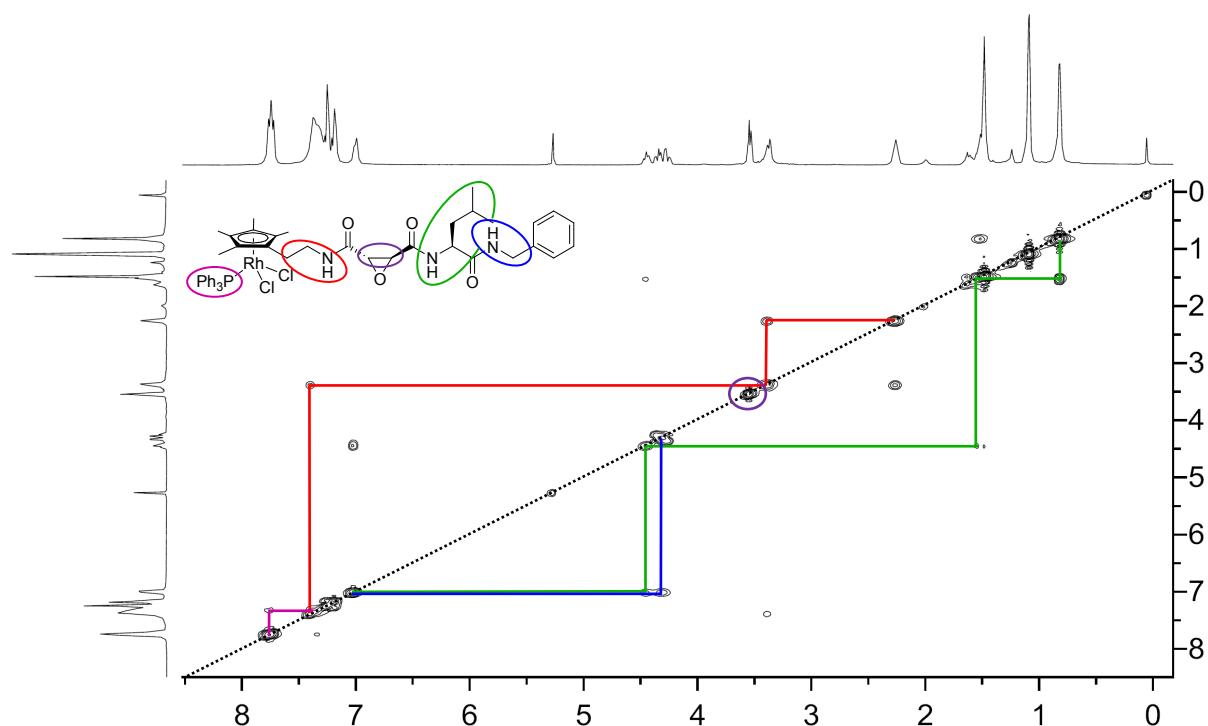
**Figure B23:** Symmetrized $^1H^1H$ COSY NMR spectrum of [Rh]-Epx **70**. Red: pendant linker. Pink: triphenylphosphine signals. Purple: epoxide CH protons. Green: Leucine spin system. Blue: Benzylamine $CH_2$ and NH protons. Not connected by colored lines: a) arene ligand methyl groups (1.1 ppm and 1.5 ppm); b) benzylamine aromatic signals (7.1-7.0 ppm).

Another notable feature of the NMR spectra of **70** is the fact, that only one set of signals is observed for this organometallic system. As it has three stereocenters and racemization of one of them would lead to different diastereomers with different sets of signals, the stereochemistry of **70** is confirmed to be still intact and only one diastereomer was obtained. A $^1H^1H$ COSY spectrum of **70** is shown in figure B23. The spin systems (different colors) can easily be distinguished from each other and therefore a complete assignment of the structure is possible.
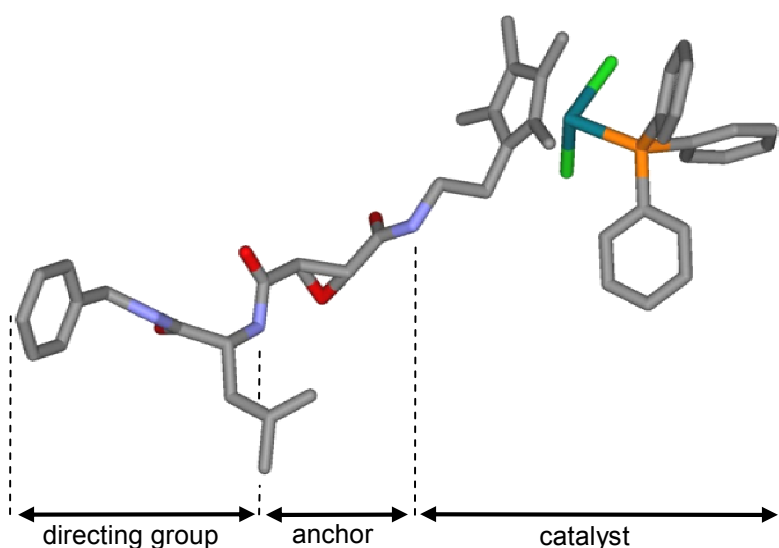


**Figure B24:** Stick-representation of X-Ray structural data of metalla affinity label [Rh]-Epx **70**.

In addition to that, crystals suitable for X-Ray diffraction of [Rh]-Epx **70** were grown from a 0.02 M solution of methanol at -18 °C within several weeks. Figure B24 shows a stick representation of the X-Ray structure. Crystal data and details of the structure determination are listed in table C37. The crystal structure proves the metalla affinity label to have exactly the structural features it was designed to have. Coordination of nucleophilic groups to the metal centre did not take place. The inner sphere coordination remained unaltered. Also the epoxide moiety and all stereocenters are still intact and display the conformation they were meant to have.

Furthermore, figure B24 shows very descriptively the different components of a metalla affinity label:

a) The peptidic directing group, consisting in this case of benzylamine and leucine, which is responsible for targeting the metalla affinity label into the enzyme's active site.

b) The anchoring moiety, in this case an epoxide, which can be opened via nucleophilic attack by the active site cysteine in the enzyme, resulting in covalent anchoring.

c) The initially achiral catalyst itself, which is embedded in the chiral active site upon covalent anchorage, and which can facilitate enantioselective catalysis in this chiral environment.

As mentioned above, the synthesis of metalla affinity labels follows a building block technique, which enables generation of a large variety of different structures in just a short amount of time. To prove this concept, metalla affinity label precursor **67** was not only reacted with rhodium complex **52**, but also with ruthenium complex **4i**. The reaction was conducted analogous to the procedure described above. After work-up procedures, the pure metalla affinity label [Ru]-Epx **71** was isolated in good yields (69%, scheme 38).
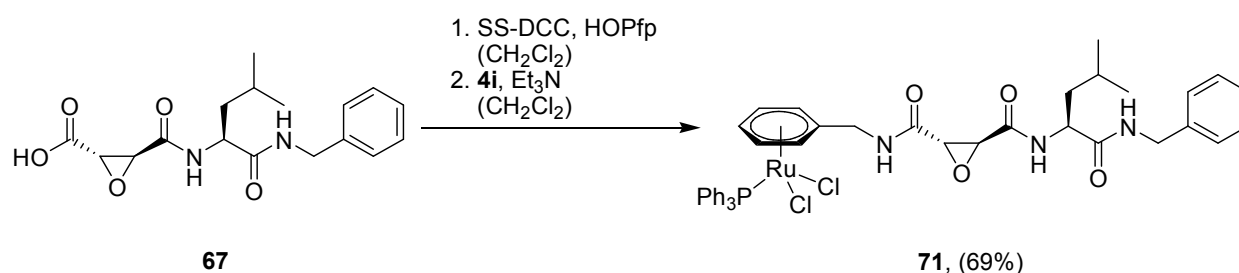


**Scheme B38:** Synthesis of metalla affinity label [Ru]-Epx **70** via pentafluorophenole active ester formation.

Identity and purity of [Ru]-Epx **71** was confirmed via elemental analysis, IR spectrometry, ESI MS, $^1$H NMR, $^{13}$C NMR and $^1$H$^1$H COSY NMR spectrometry. In ESI MS spectra, a mass of 822.1 was observed, corresponding to the [M-Cl]$^+$ fragment.

As observed above, the epoxide moiety was proven to be intact by NMR spectra (3.93 and 3.57 ppm). Yet, coupling constants were too small to be resolved in $^1$H NMR spectra. Nevertheless, $^1$H and $^{13}$C NMR shifts are in close proximity to values observed for epoxide containing compounds. In $^{31}$P NMR, a singulet at 27.8 ppm was observed. This shift is very close to the one observed for complex **4i** (28.4 ppm). This confirms the catalyst inner sphere coordination to be intact and the reaction to be successful. An interesting feature of $^1$H NMR and $^{13}$C NMR spectra is, that all 5 coordinated aromatic ring protons and all six coordinated aromatic ring carbons are inequivalent due to the stereoinformation transmitted by the epoxide and L-leucine. Therefore, five different signals are observed in $^1$H NMR for the protons (3 signals for **4i**) and six signals in $^{13}$C NMR (4 signals for **4i**). In addition to that, none of the NH protons is superimposed in the spectra of **71**. Therefore, two triplets were observed, which can be assigned to the benzylamine NH and the pendant linker NH (7.97 ppm and 6.50 ppm each $^3J_{HH}$ = 5.4 Hz). There is also a doublet at 6.76 ppm with a coupling constant of $^3J_{HH}$ = 8.3 Hz, which can be assigned to the leucine NH.

In conclusion, peptide bond formation via pentafluorophenole active esters has proven to be a powerful tool in the synthesis of metalla affinity labels, giving rise to a building block technique, with which many metalla affinity labels can be designed within a short time and only little synthetic effort.

## 4. Synthesis of a competitive enzyme inhibitor analogue

Metalla affinity labels [Rh]-Epx **70** and Ru-[Epx] **71** represent covalent cysteine protease inhibitors. They inhibit the enzyme activity irreversibly by nucleophilic attack of the active center cysteine to the epoxide moiety. To confirm the designed mode of inhibition, a non-covalent inhibitor analogue of [Rh]-Epx **70** was designed, which is structurally identical, but does not comprise the epoxide group (scheme B39).

For this purpose, compound **61** was reacted with succinic acid anhydride. As a base pyridine was used. It was employed stoichiometrically and removes acid, formed during the reaction, from the equilibrium. At the same time, it serves as a nucleophilic catalyst, with which an acetylpyridinium-intermediate is formed.[110]
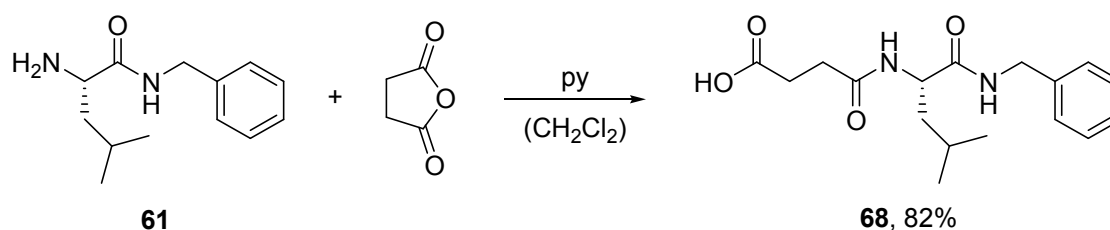


**Scheme B39:** Synthesis of the competitive metalla affinity label precursor **68**.

After purification of the raw product via silica column chromatography, **68** was obtained in 82% yield. Its identity was confirmed via $^1$H NMR, $^{13}$C NMR and $^1$H$^1$H COSY NMR spectroscopy. In addition to that elemental analysis and IR spectroscopy measurements were carried out. In $^{13}$C NMR spectra of **68**, three signals were observed, which can be assigned to carbonyl carbon atoms (176.3, 173.2 and 172.4 ppm). The peptide **61** shows only one signal in that region at 175.0 ppm. In addition to that, the product mass was confirmed by ESI MS spectra, and a mass of 321.1 was observed, which can be assigned to the [M-H]$^+$-fragment.
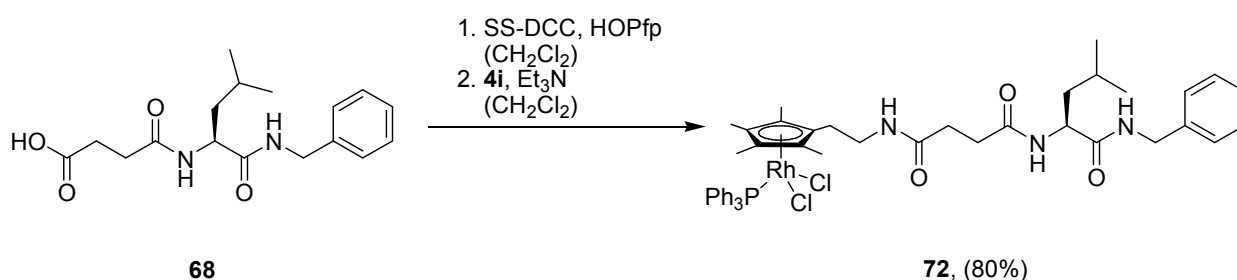


**Scheme B40:** Synthesis of the non-covalent metalla label [Ru]-Deox **72** via pentafluorophenole active ester formation.

To create a non-covalent metalla affinity label, $\eta^5$-cyclopentadienyl derivative rhodium complex **52** was reacted with precursor **68**. For the formation of a peptide bond between the two building blocks, a pentafluorophenol active ester was generated. The reaction was carried out analogue to the synthesis of [Rh]-Epx **70**, where the procedure was described in detail.

Characterization of [Rh]-Deox **72** was conducted using $^1H$ NMR, $^{13}C$ NMR and $^1H^1H$ COSY NMR spectroscopy, IR spectrometry, elemental analysis and ESI mass spectrometry. In ESI spectra two main masses were observed at 866.0 ([M-Cl]$^+$) and 604.2 ([M-Cl-PPh$_3$]$^+$). Compared to the analogue covalent inhibitor [Rh]-Epx **70**, masses decreased by an amount of exactly 14 g/mol (880.1 ([M-Cl]$^+$) and 618.2 ([M-Cl-PPh$_3$]$^+$)). This difference in mass is based on the substitution of one oxygen atom (16 g/mol) by two protons (each 1 g/mol) and therefore indicates the structural integrity of complex **72**. $^1H$ NMR spectroscopy does not show the typical signals from the epoxide moiety, but instead a multiplet originating from the four $CH_2$ protons of succinic acid anhydride (2.60-2.38 ppm). In $^{13}C$ NMR, these $CH_2$ groups appear at 32.1 and 31.7 ppm. $^{31}P$ NMR reveals a doublet at 29.8 ppm ($^3J_{PRh}$ = 142 Hz). This shift is almost identical to the one observed for [Rh]-Epx **70** (30.0 ppm, $^3J_{PRh}$ = 143 Hz). Again, this indicates also the catalyst inner sphere coordination to be intact and the peptide bond formation to have been successful.

## 5. Fluoro phosphonic acid irreversible inhibitors

Besides metalla affinity labels for cysteine proteases, metalla linkers for serine proteases were synthesized. Fluorosulfonic acids, fluorophosphonic acids and phosphonic acid esters have been shown to inhibit serine proteases efficiently in earlier studies.[101] As suitable precursor for a fluorophosphonic metalla linker, a phosphonic acid with an aliphatic side chain **84** was applied.[111] This phosphonic acid ester has been applied by Cravatt and coworkers to generate specific, activity based affinity labels for the identification and characterization of serine hydrolases. Herefore, phosphonic acid **84** was conjugated with biotin or fluorescin.[112] Since both markers were introduced via peptide bond formation, the phosphonic acid **84** represents a precursor for the synthesis of metalla linkers, thus generating an organometallic system, which can be reacted specifically with serine proteases, dramatically widening the scope of enzymes which can be addressed.
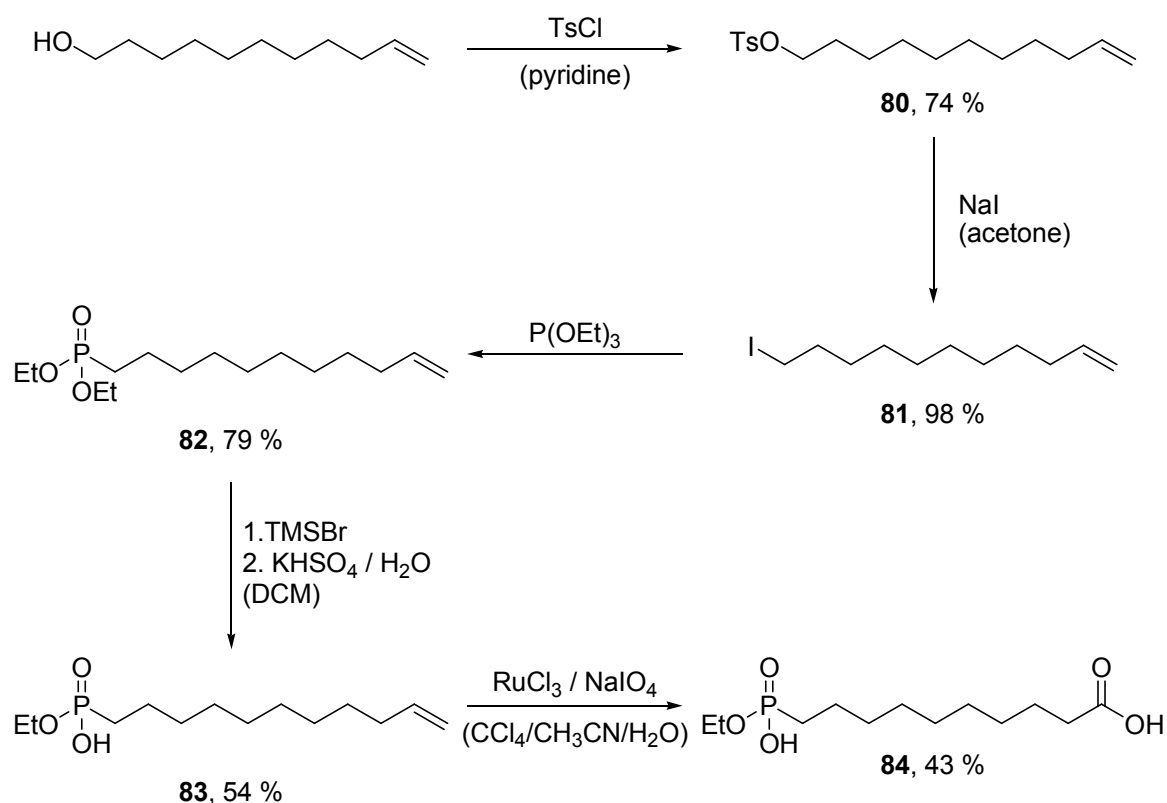


**Scheme B41:** Synthesis of metalla label precursor **84** by the method of Liu *et al.*[111]

Phosphonic acid **84** is received from 10-undecene-1-ol, which is being converted in a five step synthetic route to 1-(Ethoxyhydroxyphosphinyl)-10-undecene **84**, comprising an ethoxy phosphonic acid as well as a carboxylic acid, one of them at each end of the

alkane chain (scheme 41). All reactions were performed analogue to the reported procedures.[111] Product identity and purity was confirmed via standard analytical procedures ($^{1}$H NMR and $^{31}$P NMR spectroscopy). All obtained data is in agreement with literature values. The crucial step in the synthesis of fluoro phosphonic metalla linker [Rh]-PF **90** is the conversion of its precursor **84** with the fluorinating reagent DAST and the subsequent peptide bond formation with organometallic catalyst **52**. Hereby, the ethoxy phosphonic acid is converted into its ethoxy phosphonic acid fluoride and the carboxylic acid into its carboxylic acid fluoride (intermediate **84***, scheme B42).[113]
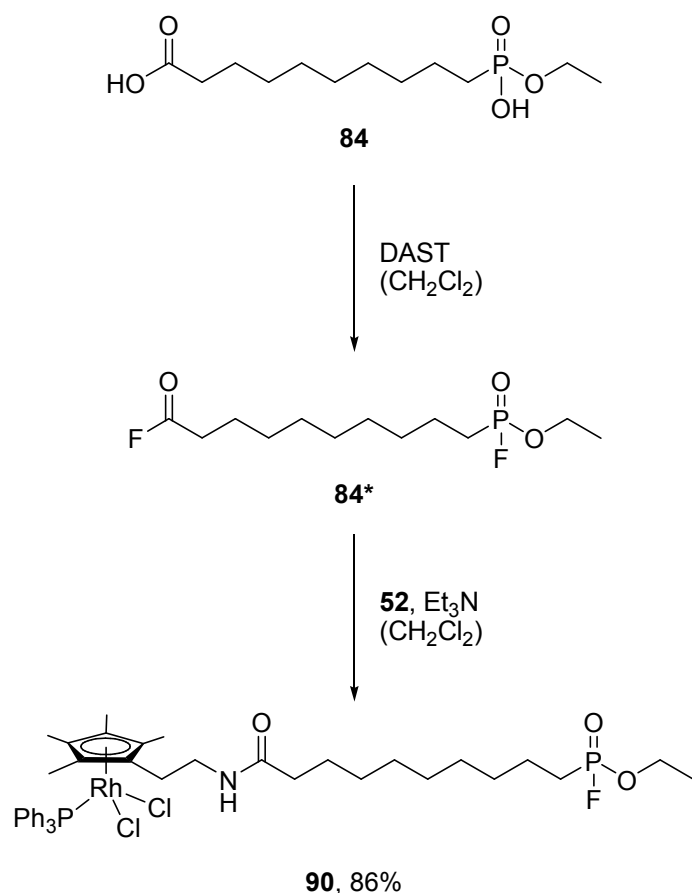


**Scheme B42:** Synthesis of the fluoro phosphonic acid metalla label [Rh]-PF **90** via formation of carboxylic acid fluorides (intermediate **84***).

Characterization of the intermediate **84*** was carried out *in situ* via $^{19}$F and $^{31}$P NMR spectroscopy. In $^{19}$F spectra, a characteristic doublet was observed, originating from a FP coupling (-64.57 ppm, $^{1}J_{FP}$ = 1.07 kHz). Furthermore, a singulet was observed, which can be assigned to a carboxylic acid fluoride 45.55 ppm. Apart from signals originating from DAST, no further signals were observed. In $^{31}$P spectra, a doublet at 32.52 ppm ($^{1}J_{FP}$ = 1.07 kHz) was observed. Therefore, conversion of **84** to **84*** is

regarded to be specific as well as quantitative. For the conversion of **84\*** to metalla linker [Rh]-PF **90**, the carboxylic acid fluoride was placed in a teflon flask and dissolved in dichloromethane. Thereafter, triethylamine and organometallic rhodium complex **52** were added. The reaction was monitored *in situ* by $^{19}$F NMR spectrometry. It was complete after only a few minutes, which can be judged by the fading of the carboxylic acid fluoride signal at 45.55 ppm. Work-up and purification of the raw product was carried out similar to the procedure described for [Rh]-Epx **70**, and succeeds without any difficulties. Triethylammonium chloride and -fluoride can be removed by extraction with brine and water. Minor side products as well as excess **84\*** were removed by precipitating and washing the raw product with diethylether and hexane.
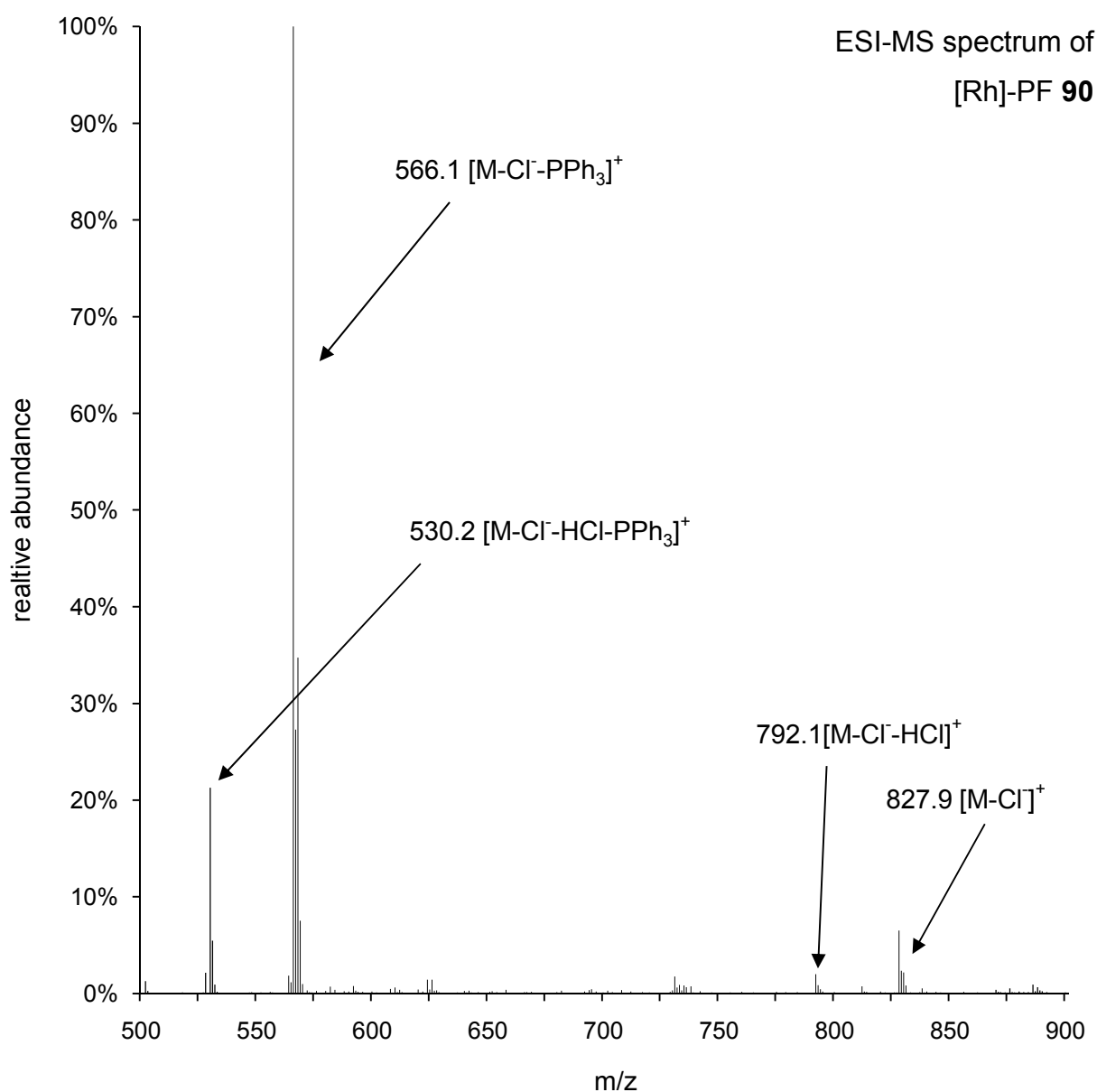


*Figure B25:* ESI-MS spectrum of fluoro phosphonic acid metalla label [Rh]-PF **90** (+c ESI Full MS; 500-900; RT: 0.33-0.57; AV: 10; NL: 7.7E6).

Characterization of [Rh]-PF **90** was carried out by $^1$H NMR, $^{13}$C NMR, $^1$H$^1$HCOSY NMR, $^{19}$F NMR and $^{31}$P NMR spectroscopy. In addition, IR spectra and ESI MS spectra were recorded and the product analyzed by elemental analysis.

In $^1$H NMR spectra, the characteristic peaks originating of the amide bond formed are observed (6.40 ppm, 1 H, t, $^3J_{HH}$ = 5.8). The PF moiety can clearly be observed in $^{19}$F NMR as well as $^{31}$P NMR spectra. In $^{19}$F NMR, a characteristic doublet is observed at -64.57 ppm with a coupling constant of $^3J_{PF}$ = 1.07 kHz. This value is identical to the one observed for **84***, thus indicating the PF bond to be unaltered. In $^{31}$P NMR, two different doublets confirm the reaction to have been successful. One of them was observed at 32.54 ppm ($^1J_{PF}$ = 1.07 kHz) which originates from the PF bond and the other at 29.8 ppm ($^1J_{PRh}$ = 142 Hz), originating from the PRh bond. The doublet at 29.82 ppm is very close to the value observed for organometallic catalyst **52** (30.27 ppm, $^1J_{PRh}$ = 144 Hz).

In ESI MS spectra of [Rh]-PF **90** the expected fragments appear, which can be explained by simple bond cleavages at the transition metal centre in the ESI MS ion source. In every peak observed, one of the chloride ligands was cleft from the molecule, rendering an observed mass reduced by 35 g/mol (827.9, [M-Cl]$^+$). Furthermore, cleavage of an additional HCl easily takes place, reducing the observed mass by additional 36 g/mol (792.1, [M-Cl-HCl]$^+$). The two dominant signals at 566.1 and 530.2 originate from the fragments [M-Cl-PPh$_3$]$^+$ and [M-Cl-HCl-PPh$_3$]$^+$. In these cases, the labile bound triphenylphosphine ligand is cleft from [Rh]-PF **90** in the ion source, reducing the observed masses by 262.3 g/mol. Therefore, all four observed main signal groups originate from the metalla linker [Rh]-PF **90**. The isotopic patterns of the signal groups confirm the absence of a chloride in the fragment 530.2 ([M-Cl-HCl-PPh$_3$]$^+$) and the presence of a chloride in the fragment 566.1 [M-Cl-PPh$_3$]$^+$).

## 6. Fluoro sulfonic acid irreversible inhibitors

Besides fluorophosphonic acids, fluorosulfonic acids can serve as potent inhibitors for serine proteases. Two of the most prominent examples for fluorosulfonic acid covalent inhibitors are PMSF and AEBSF, depicted in figure B26.[101] For rhodium complexes [Rh]-Epx **70** and [Rh]-PF **90**, two different methods have been developed to form a peptide bond between the organometallic and the organic building block. One of the methods is taking advantage of pentafluorophenol active esters, the other of the reactivity of carboxylic acid fluorides. Details of the reaction procedures are described above (sections B3.3 and B3.5). For the generation of fluorosulfonic acids metalla linker [Rh]-SF **91**, both routes were applied to prove their applicability with different reactive moieties (scheme B43).
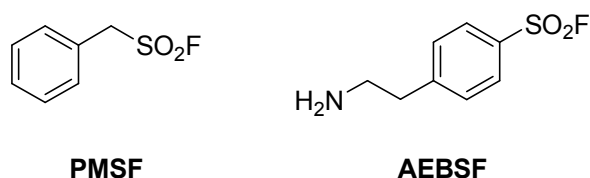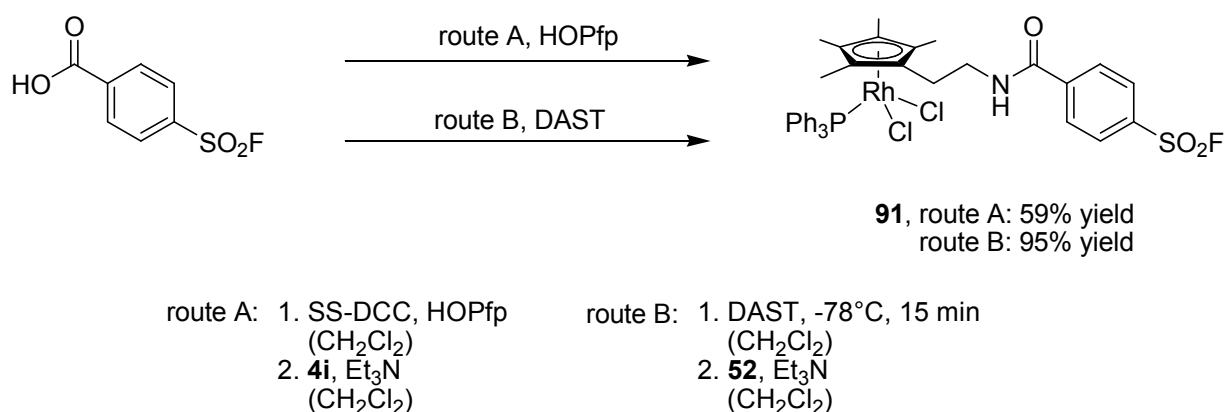


**PMSF**                          **AEBSF**

*Figure B26:* PMSF and AEBSF, two potent fluoro sulfonic acid based serine protease inhibitors.[101]

As organic building block for the generation of fluoro sulfonic acid metalla linkers, the commercially available 4-(fluorosulfonyl)benzoic acid was used. It was shown, that it is possible to convert this carboxylic acid via the polymer bound carbodiimide resin SS-DCC into its pentafluorophenole active ester (route A). This was subsequently reacted with organometallic catalyst **52** in the presence of triethylamine under peptide bond formation. During this reaction, the sulfonic acid was not subject to any side reaction, yielding [Rh]-SF **91** in 59% yield.



**91**, route A: 59% yield
route B: 95% yield

route A:  1. SS-DCC, HOPfp
($CH_2Cl_2$)
2. **4i**, $Et_3N$
($CH_2Cl_2$)

route B:  1. DAST, -78°C, 15 min
($CH_2Cl_2$)
2. **52**, $Et_3N$
($CH_2Cl_2$)

*Scheme B43:* Synthesis of fluoro phosphonic acid metalla **91** via A) pentafluorophenole active ester formation and B) formation of carboxylic acid fluorides.

The carboxylic acid fluoride analogue may also be obtained from 4-(fluorosulfonyl) benzoic acid using DAST (Route B). Subsequent conversion with organometallic catalyst **52** in the presence of triethylamine yields [Rh]-SF **91** (95 % yield). This reaction also succeeded without decomposition of the fluorosulfonic acid. Generally, obtained yields for the metalla linker are significantly higher for route B than for route A, which can be attributed to the quantitative conversion to the carboxylic acid fluoride and its high selectivity to nucleophilic attacks. Furthermore, the lower number of different steps during the reaction might have an impact on higher yields in case of route B.
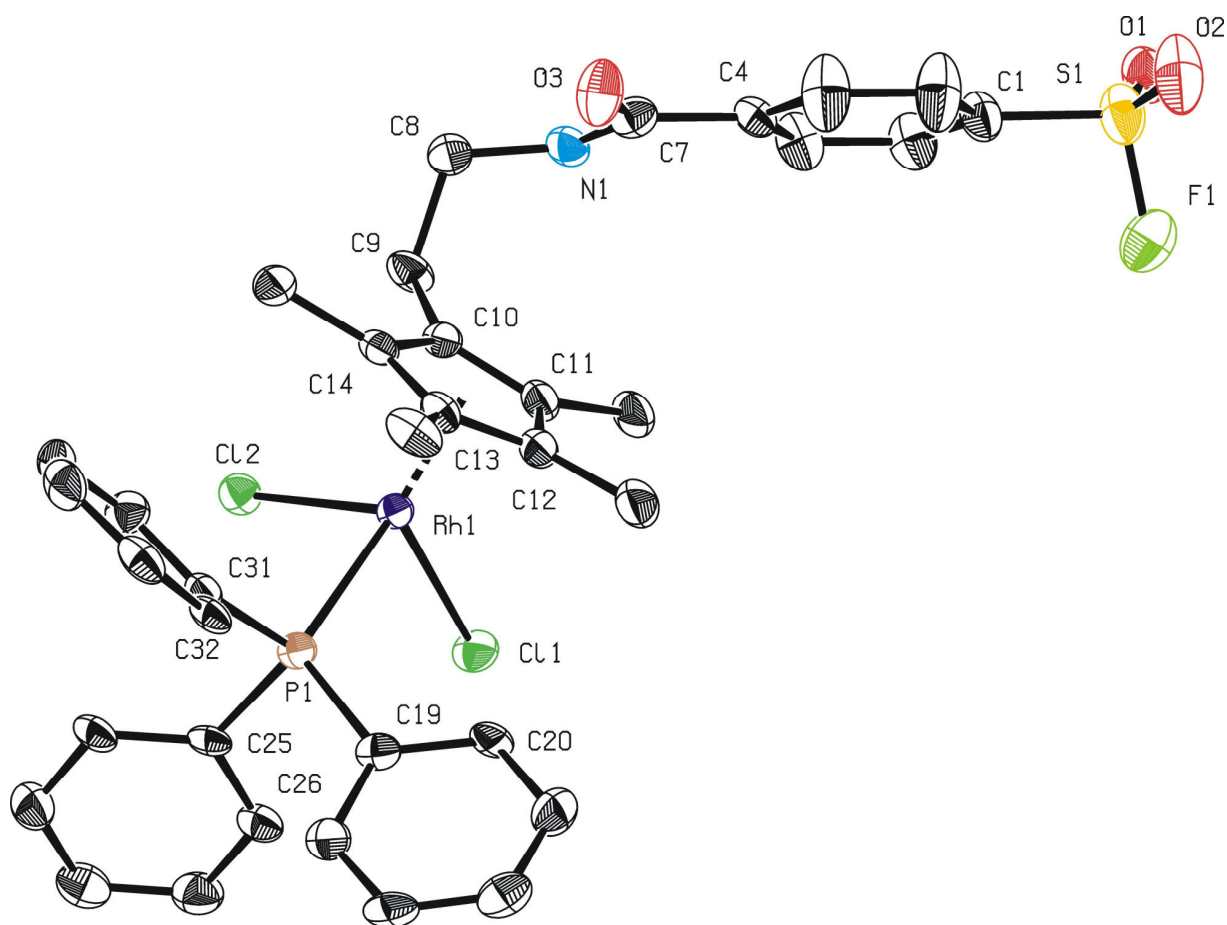


***Figure B27:*** ORTEP representation of conformer 1 of metalla linker [Rh]-SF **91**. Selected bond lengths (Å) and angles (deg): Rh(1)-C(10) 2.199(5), Rh(1)-C(11) 2.226(5), Rh(1)-C(12) 2.186(5), Rh(1)-C(13) 2.190(4), Rh(1)-C(14) 2.161(5), Rh(1)-Cl(1) 2.3883(14), Rh(1)-Cl(2) 2.4061(11), Rh(1)-P(1) 2.3243(14), S(1)-O(1) 1.415(4), S(1)-O(2) 1.407(4), S(1)-F(1) 1.565(4), Cl(1)-Rh(1)-Cl(2) 91.36(4), P(1)-Rh(1)-Cl(1) 87.74(5), P(1)-Rh(1)-Cl(2) 86.92(4), O(1)-S(1)-O(2) 122.0(3), F(1)-S(1)-O(1) 105.2(2), F(1)-S(1)-O(2) 104.9(2).

The metalla label [Rh]-SF **91** was identified via elemental analysis, IR spectroscopy, ^{1}H NMR, ^{13}C NMR, ^{19}F NMR and ^{31}P NMR spectroscopy. In both cases, spectra obtained were identical. The metalla linker was obtained analytically pure. In ^{19}F NMR spectroscopy, only one singulet was observed, which was assigned to the fluoro sulfonic acid fluoride (85.86 ppm). Furthermore, in ^{31}P NMR, the doublet originating

from the triphenylphosphine phosphorous is indicative for the success of the reaction. It was observed at 30.04 ppm ($^1J_{Rh,P}$ = 143 Hz). In $^1$H NMR, a triplet originating from the peptide NH proton was observed at 8.12 ppm with a coupling constant of $^3J_{HH}$ = 5.8 Hz. All observed values are in accordance to the ones obtained for the metalla labels above.
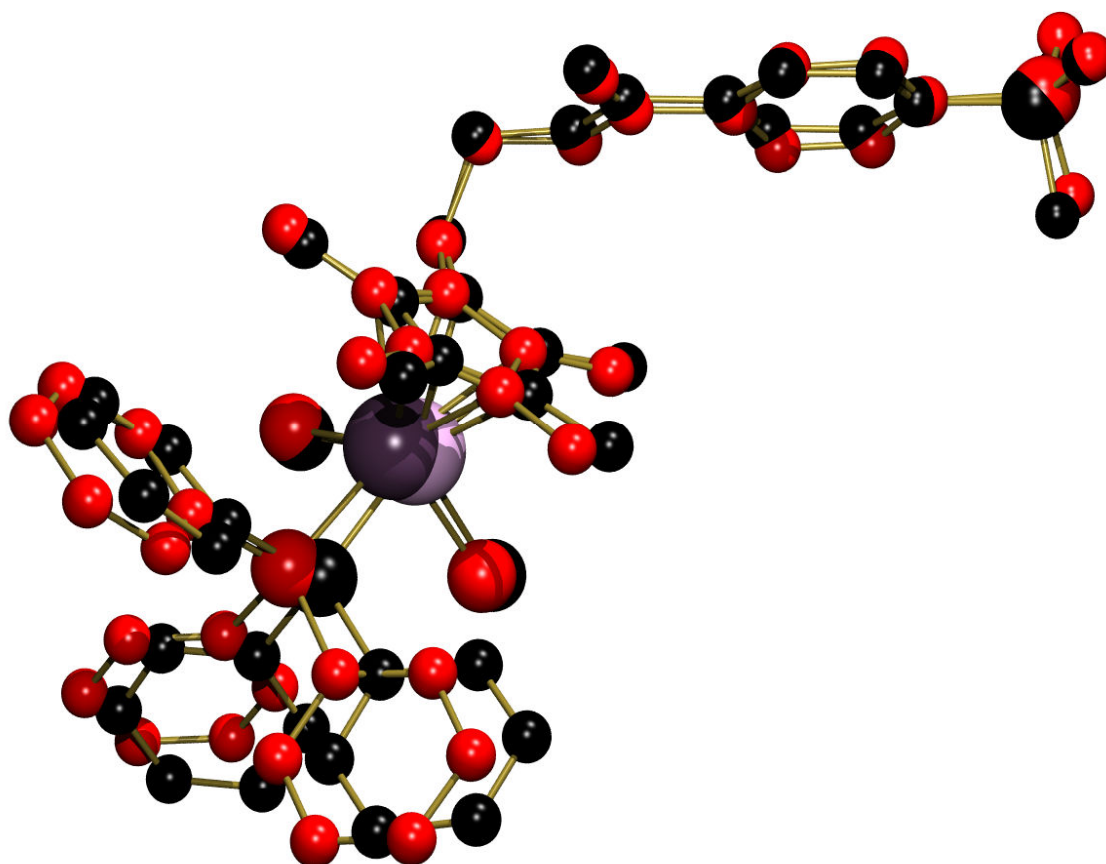


*Figure B28:* Representation of the two different conformations of [Rh]-SF **91** cocrystallized in one cell.

Metalla linker [Rh]-SF **91** was crystallized from a solution of CDCl$_3$ at -18 °C within several months at a concentration of approximately 40 mg/mL (figure B27). The structure shows the formed peptide bond linking organometallic catalyst **52** and the organic fluoro sulfonic acid. No alteration of the metal center inner sphere has taken place, as it was also observed for [Rh]-Epx **70**. Furthermore, the fluoro sulfonic acid is still intact and has not been subject to any nucleophilic additions. All bond lengths and angles are in the expected range. Crystal data and details of the structure determination are listed in table C38.

Metalla linker [Rh]SF **91** crystallized in the *P-1* space group. Bond distances between the transition metal centre and the $\eta^6$-arene ring range from 2.226(5) - 2.161(5) Å. They are similar to bond lengths observed for $\eta^6$-arene complexes **3i**$^{DMSO}$ (figure B8) and **4r** (figure B6). None of the Rh-C bonds is significantly elongated, as it was observed for **3i**$^{DMSO}$ and **4r**. This might be due to the steric demand of the methyl group in the Cp* ring system, making them very similar to the steric demand of the pendant linker group. Also Ru-Cl bond lengths are very similar, ranging from 2.3883(14) - 2.4061(11) Å. The complex forms a piano stool-type tetrahedral geometry. The Cl(1)-Ru(1)-Cl(2) angle (91.36(4) °) is only slightly larger than the two P(1)-Ru(1)-Cl angles (87.74(5) ° and 86.92(4) °). The two F(1)-S(1)-O angles are identical (105.2(2) ° and 104.9 (2) °).

A very interesting feature of the unit cell is the presence of two different conformers of [Rh]-SF **91**. They both resemble the same structure, nevertheless, bond angles and lengths are slightly different. Figure B28 depicts an overly of the two different conformations.
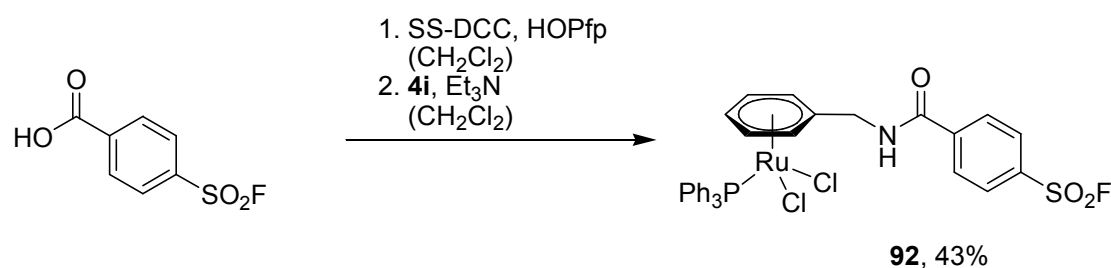


**Scheme B44:** Synthesis of the fluoro sulfonic acid metalla label [Ru]-SF **92** via pentafluorophenole active ester formation.

Not only organometallic rhodium catalyst **52**, but also $\eta^6$-arene ruthenium catalyst **4i** was used for the generation of fluoro sulfonic acid metalla linkers. In this case, the peptide bond formation was achieved via pentafluorophenole active esters, yielding metalla linker [Ru]-SF **92** in 43% yield. Product identity and purity was confirmed via NMR spectroscopy, elemental analysis, IR spectrometry and ESI-MS. $^{19}$F NMR shows one singulet at 66.28 ppm for the fluoro sulfonic acid fluoride. This differs from the value obtained for [Rh]-SF **91** ($^{19}$F NMR: s, 85.86 ppm). The peak is upshifted by almost 20 ppm. In $^{31}$P NMR, this difference would be a clear indication for the fluorides not to belong to identical moieties. However, this is not true for $^{19}$F NMR spectroscopy. $^{19}$F NMR signal shifts are highly sensitive to very small electronic changes, resulting in huge peak shifts. Both peaks observed are in the region in which fluoro sulfonic acids are expected to be. Additionally, ESI MS confirms the metalla linker [Ru]-SF **92** to have

the correct mass (691.9 g/mol, $[M-Cl]^+$). This and all other obtained analytical data confirm that the product formation has been successful.

Due to the lack of a peptidic part, the fluoro sulfonic acid metalla linkers do not have a directing group, and must be seen as "metalla labels" rather than metalla affinity labels. Nevertheless, as the distance between transition metal catalyst and reactive group is rigid and short, the chiral information transmitted by the enzyme's active site pocket can be assumed to be sufficient to allow enantioselective catalysis. Furthermore, nucleophilic moieties on the enzyme surface could substitute labile-bound ligands of the transition metal centre, generating a second anchoring of the metalla linker and thus increasing the performance of the resulting organometallic enzyme hybrid.

## 7. Phosphonic acid esters irreversible inhibitors

Peptide derivatives of (α-aminoalkyl)phosphonate diphenyl esters have proven to be potent inhibitors for serine proteases.[101,114,115] Figure B28 depicts the basic motive, from which this class of inhibitors is derived. For the generation of metalla affinity labels, (α-aminophenyl)phosphonate diphenyl ester was synthesized according to known literature procedures.[116,117]
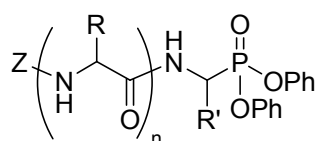
R   = amino acid residue
R'  = alkyl, aryl

***Figure B27:*** Basic motive for (α-aminoalkyl)phosphonate diphenyl esters, a potent class of serine protease inhibitors.[101,114,115]

The synthesis of diphenyl (α-aminobezyl)phosphonate diphenyl ester **86** was achieved via two consecutive reactions, starting from benzaldehyde, triphenylphosphite and benzyl carbamate. The first step was carried out according to the procedure described by Oleksyszyn *et. al.*[116]

**85**, 48%
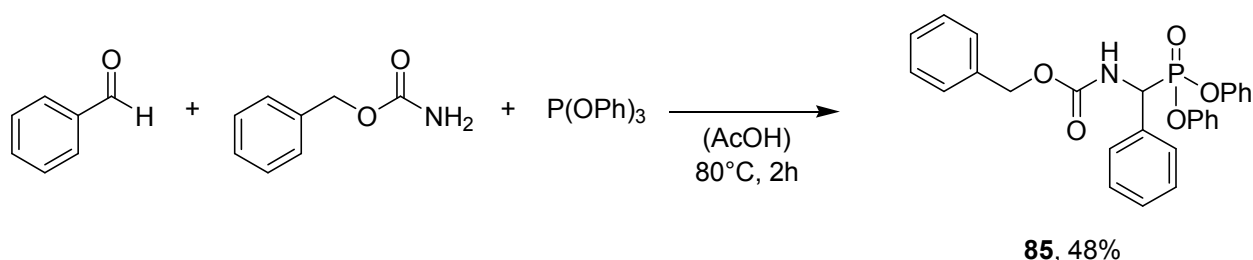
***Scheme B44:*** Synthesis of 1-(N-benzoyloxycarbonyl)-aminobenzylphosphonate diphenylester **85**.[116]

The product of this straight forward synthesis was analyzed by standard NMR spectrometry and IR spectrometry. Analytical data is in agreement with the reported literature values, proving the successful synthesis of 1-(N-benzoyloxycarbonyl)-aminobenzylphosphonate diphenylester **85**.

In the second reaction step, the Z-protection group was removed trough addition of hydrobromic acid (33% in acetic acid). First, the ammonium chloride of **86** is being obtained, which was neutralized by bubbling gaseous $NH_3$ through a suspension of **86** · HCl in diethylether. The product compound **86** was analyzed via $^1$H NMR, $^{13}$C NMR $^{31}$P NMR and IR spectrometry.
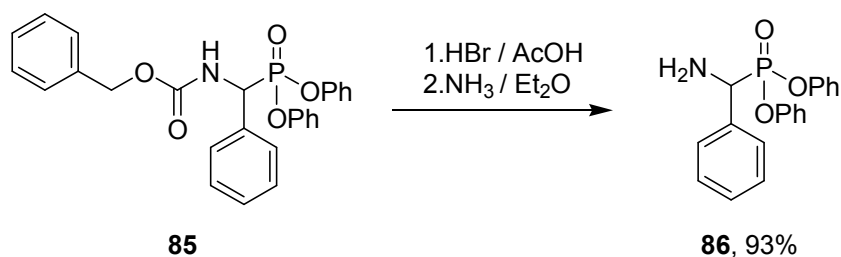
**Scheme B45:** Deprotection of **85**, yielding (α-aminobezyl)phosphonate diphenyl ester **86**.

To facilitate peptide bond formation between (α-aminobezyl)phosphonate diphenyl ester **86** and organometallic linker **52**, a carboxylic acid group has to be introduced, as both building blocks comprise a terminal amine group. A very elegant way of introducing the carboxylic acid is the nucleophilic ring opening of cyclic anhydrides, as for example succinic acid anhydride (scheme 45).

In theory, both compounds **52** and **86** could have been reacted with succinic acid anhydride. Yet, the reaction was conducted with **86** to minimize the loss in organometallic complex **52**, as it is more difficult to access compared to diphenyl phosphonate **86**. The reaction was carried out by dissolving both succinic acid anhydride and **86** in dichloromethane. One equivalent of pyridine was added. Pure product **87** was obtained after precipitation with diethylether from a solution of ethylacetate, as judged by elemental analysis, IR spectrometry, $^1$H NMR, $^{13}$C NMR and $^{31}$P NMR. Furthermore, ESI MS analysis proved compound **87** to have the expected mass (462.2 g/mol, [M+Na]$^+$).
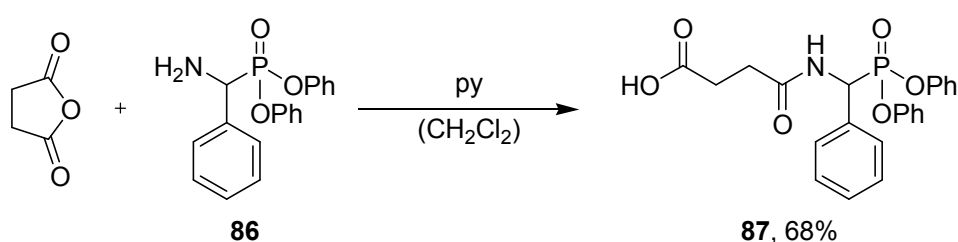


**Scheme B46:** Nucleophilic attack of succinic anhydride to (α-aminobezyl)phosphonate diphenyl ester **86**, yielding the phosphonic acid diphenylester metalla affinity label precursor **87**.

In $^{31}$P NMR, a singulet was observed at 15.1 ppm, which was assigned to the phosphonic ester. For educt **86**, the phosphorous signal shift was 18.4 ppm (singulet). Furthermore, in $^{13}$C NMR, two inequivalent carbonyl signals were observed for **87** (176.3 ppm and 171.8 ppm). Also in IR spectra, two bands were identified, which can be assigned to CO bond stretching frequencies (1677 cm$^{-1}$ and 1653 cm$^{-1}$). In $^1$H NMR, the NH proton was observed as a doublet of doublets. This peak pattern originates from the

NH proton coupling with the α-proton (spin = ½) as well as the phosphorous nucleus (spin = ½).

Nevertheless, the crucial step in the synthesis of diphenyl phosphonate metalla affinity labels is the peptide bond formation between organometallic species (complex **52**) and phosphonate **87**. For this purpose, pentafluorophenole active ester formation was chosen, as both the organometallic as well as the phosphonate building block are subject to numerous restrictions due to their instability (scheme B47). The peptide bond formation via pentafluorophenole active esters is an extremely gentle method and has been successfully applied before. It is described in detail in section B3.3. Diphenyl phosphonate carboxylic acid **87** was converted into its pentafluorophenole ester using a carbodiimide resin as coupling reagent. The resin was filtered off and triethylamine and rhodium complex **52** added. The raw product was purified by precipitation and washed with hexane or pentane and diethylether, yielding the pure metalla affinity label [Rh]-(OPh)$_2$ **93** in 68% yield as a red solid.
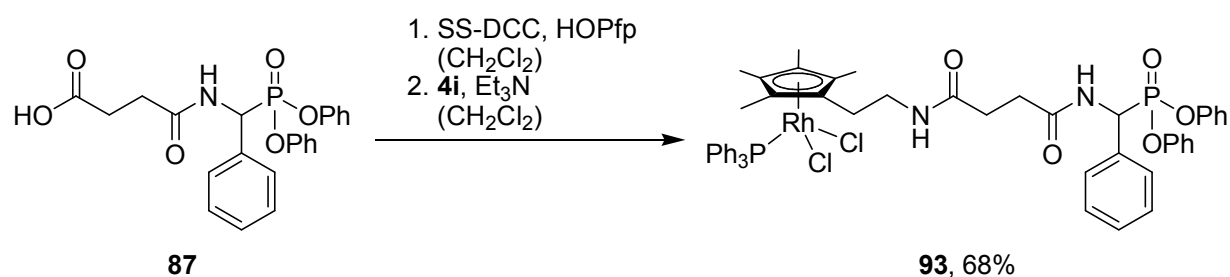


**Scheme B47:** Synthesis of the phosphonic acid diphenylester metalla affinity label [Rh]-(OPh)$_2$ **93** via pentafluorophenole active ester formation.

Identity and purity of [Rh]-(OPh)$_2$ **93** was confirmed by IR spectroscopy, ESI MS, $^1$H NMR, $^{13}$C NMR, $^{31}$P NMR as well as $^1$H$^1$H COSY NMR spectroscopy. IN ESI MS, the typical fragmentation patterns (discussed in detail in section B3.5) were obtained (984.8 [M-Cl]$^+$, 723.1 [M-Cl-PPh$_3$]$^+$). In $^{13}$C NMR, two signals originating from carbonyl carbons were observed (172.6 ppm 172.0 ppm). The signal at 176.3 ppm, which was observed for compound **87**, vanished and gave rise to the significantly upfield-shifted peptide bond carbonyl signal at 172.6 ppm. In $^{31}$P NMR spectra, there was only an insignificant shift of the diphenyl phosphonate signal, proving its electronic properties to be unaltered ([Rh]-(OPh)$_2$ **93**: 14.8 ppm; **87**: 15.1 ppm). Also the coordination sphere of the transition metal centre is intact, as judged by $^{31}$P NMR spectra ([Rh]-(OPh)$_2$ **93**: 29.9 ppm, $^1J_{RhP}$ = 143 Hz; **52**: 30.3 ppm, $^1J_{RhP}$ = 144 Hz).

## 8. Synthesis of an unselective enzyme inhibitor analogue

Besides the covalent and competitive metalla affinity labels [Rh]-Epx **70**, [Ru]-Epx **71** and [Rh]-Deox **72** and metalla linkers [Rh]-PF **90**, [Rh]-SF **91**, [Ru]-SF **92** and [Rh]-(OPh)$_2$ **93**, a covalent and unselective inhibitor was designed. Metalla labels [Rh]-Epx **70** and [Ru]-Epx **71** are both selective, yet only [Rh]-Epx **70** can be embedded covalently into the enzyme's active site pocket. In contrast, [Rh]-OSu **94** represents a covalent, yet unselective linker. It was designed to underline the importance of selective attachment of metalla linkers to enzymes for the generation of enantiomeric excesses. The synthesis of [Rh]-OSu **94** was facilitated by peptide bond formation between organometallic complex **53** and N-hydroxy-succinimide. As coupling reagent, a polymer-bound carbodiimide resin was used. The reaction was conducted similar to the method described earlier (section B3.3). However, in this case, coupling was facilitated with both catalyst **53** and carbodiimide resin present in the reaction mixture at the same time, avoiding pentafluorophenole active esters as intermediates. Furthermore, the use of N-hydroxy succinimide leads to more side reactions, as it represents a much better ligand for rhodium metal centers compared to pentafluorophenole.
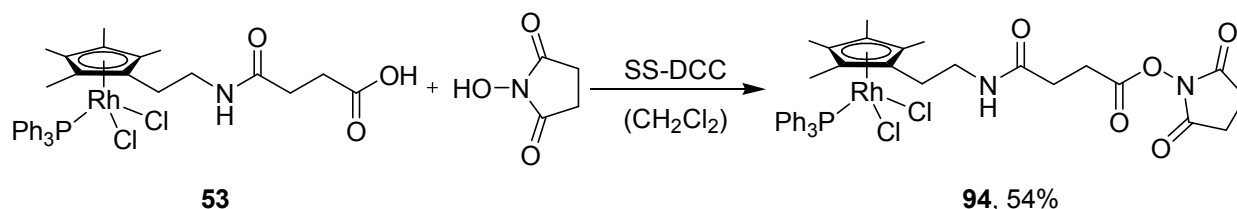


**Scheme B48:** Synthesis of the unspecific metalla linker [Rh]-OSu.

In spite of that, the analytically pure [Rh]-OSu **94** could be isolated. It was characterized via $^1$H NMR, $^{13}$C NMR, $^{31}$P NMR and $^1$H$^1$H COSY NMR spectroscopy as well as IR spectrometry and ESI MS. In $^{31}$P NMR, a doublet at 30.0 ppm with a coupling constant of $^1J_{RhP}$ = 143 Hz was observed. This signal is in very close proximity to the doublet observed for educt catalyst **53** in $^{31}$P NMR (30.1 ppm, $^1J_{RhP}$ = 143 Hz). $^{13}$C NMR spectroscopy revealed three signals originating from carbonyl carbons (170.3, 169.2 and 168.2 ppm). In ESI MS spectra, the correct mass of [Rh]-OSu **94** was detected (760.9 [M-Cl]$^+$ and 498.9 [M-Cl-PPh$_3$]$^+$), proving the conversion to have been successful.

# 9. η⁶-arene complexes of ruthenium as enzyme probes and -inhibitors

It has been shown recently, that inhibitors containing fluorine groups can be used as potent probes for the analysis of enzyme-inhibitor complexes in $^{19}$F NMR spectrometry.[118] In addition to that, non functionalized η⁶-arene complexes of ruthenium were shown to selectively bind to the active site of enzymes. This coordinative binding is mediated by the replacement of labile bound ligands of the ruthenium metal centre by nucleophilic groups on the enzyme surface.[119]

Therefore, η⁶-arene complexes were tested for their inhibitorial activity. Hence, N-trifluoroacetyl-1,4-cyclohexadiene-1-benzyl amide **2q** was reacted with RuCl₃ · n H₂O to give the dinuclear halide bridged η⁶-arene ruthenium complex **8** (scheme B49) in 63% yield. The reaction was conducted as described for the formation of dinuclear N-acetyl η⁶-arene ruthenium(II) complexes **2e**-**2h** (section B2.2.2).
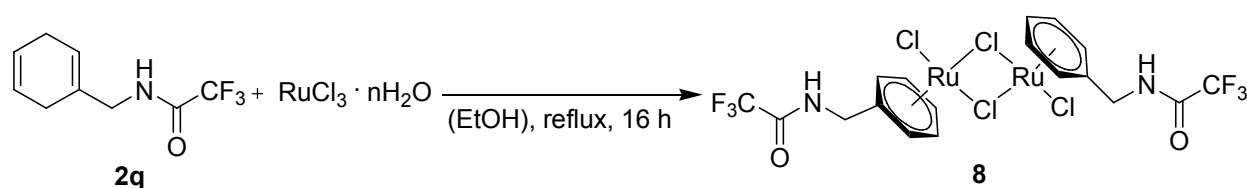


**Scheme B49:** Synthesis of dimeric η⁶-arene ruthenium(II) complex **8**.

Product identity and purity was confirmed via $^{1}$H NMR, $^{13}$C NMR and $^{19}$F NMR spectroscopy as well as elemental analysis and IR spectrometry. All analytical data is as expected. In $^{19}$F NMR, the CF₃ fluorine signals were observed as at -75.92 ppm (singulet). Nevertheless, a notable feature of $^{13}$C NMR spectra of **8** is the fact, that the CF₃ carbon is found dramatically downshifted (due to the strong electron withdrawing effect of fluorine) at 116.0 ppm with a coupling constant of $^{1}J_{FC}$ = 287.5 Hz. The carbonyl carbon is observed at 157.7 ppm as a quartet with a coupling constant of $^{2}J_{FC}$ = 36.9 Hz.

Complex **8** was reacted with IspH, an enzyme which comprises an Fe₃S₄ cluster in the active centre. The enzyme was provided by Michael Groll and coworkers. Complex **8**, being monomeric in solution, was expected to bind into the active center of IspH via replacement of the labile bound chlorine atoms by Fe₃S₄ cluster sulfides. Nevertheless, inhibition of IspH could not be confirmed by NMR spectroscopy due to the detection limit of the NMR spectrometer used (400 MHz) in combination with the limited concentration of IspH available. However, inhibition assays of IspH with complex **8** and other η⁶-arene

ruthenium(II)complexes (**3b**, **3e**, **3i**, **3m**, **3p**, **20**, **22**) as well as transition metal salts gave promising results (figure B29).[120]
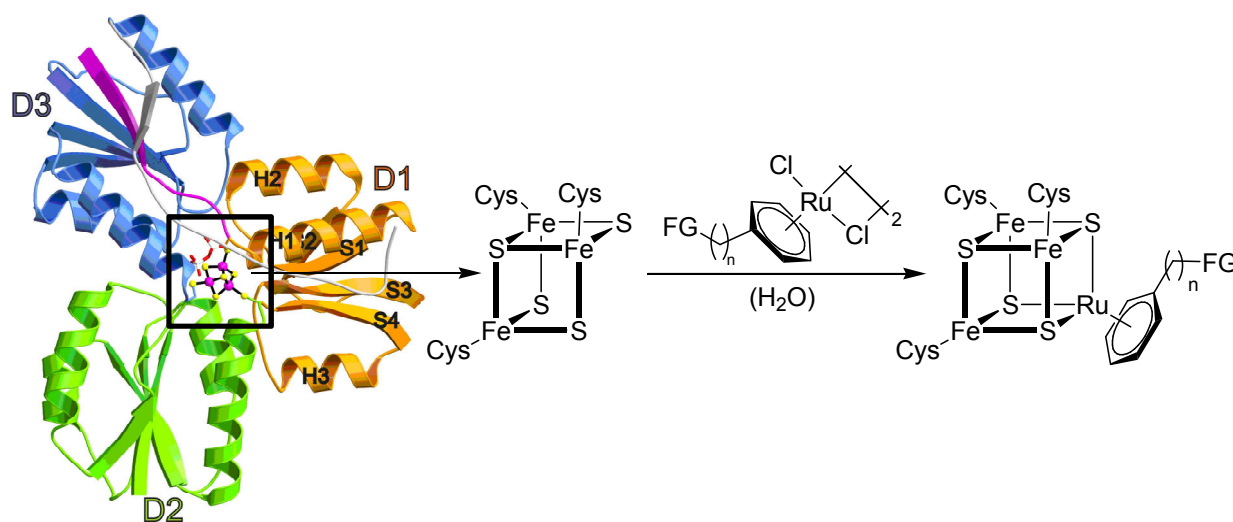


**Figure B29:** Coordination of metal ions as well as ruthenium fragments to the [$Fe_3S_4$] cluster of *E. coli* IspH.[120]

Particularly [($\eta^6$-phenylalanine ethylester)RuCl$_2$]$_2$ · 2 HCl **22** resulted in a decrease of enzyme activity of about 75%. UV/VIS spectroscopy indicated that the incorporation of metal ions or ruthenium fragments to the [$Fe_3S_4$] cluster leads to changes in the absorption spectrum of IspH. Besides absorption in UV region, iron-sulfur proteins display a characteristic absorption band at a wavelength of 400 nm. The intensity of this band increases with incorporation of metal ions. The coordination of metal ions or metal fragments to the iron-sulfur cluster of IspH leads to inhibition of enzyme activity.[120]

Overall, inhibition of $\eta^6$-arene ruthenium(II) complexes with IspH seems to be a promising project for further investigations (figure B30).
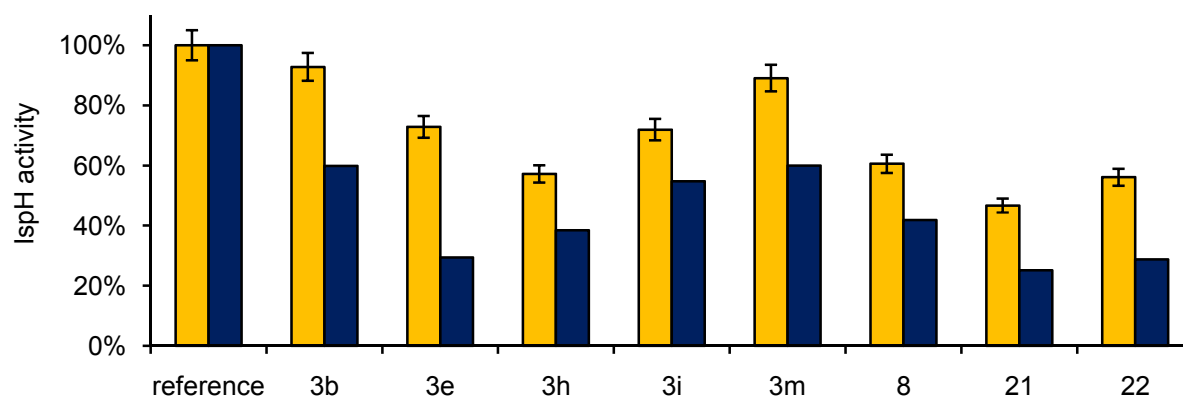


**Figure B30:** Residual activity of IspH after inhibition with different $\eta^6$-arene ruthenium complexes (NMR-assisted inhibition assays). Orange: IspH / Ru = 1 / 1. Blue: IspH / Ru = 1 / 10. [120]

## 10. Synthesis of a redox active fluoro sulfonic acid enzyme inhibitor

Ferrocene labeled biomolecules are favored tools for the electrochemical detection in biosensors. The use of ferrocene and its derivatives as redox-active probes is based on their unique properties like stability in aerobic and aqueous media, straightforwardness of synthesis and the redox behavior of the ferrocene/ferrocenium pair.[121]

For this purpose, a ferrocene bound fluoro sulfonic acid metalla linker [Fc]-SF **95** was designed, which was meant to bind into the active site of bovine pancreatic trypsin. Due to the ferrocene moiety it should then be possible to detect the binding via cyclic voltametry. The [Fc]-SF@trypsin complex should have a different redox potential compared to the unbound [Fc]-SF **95** metalla linker because of their unequal electronic environment.
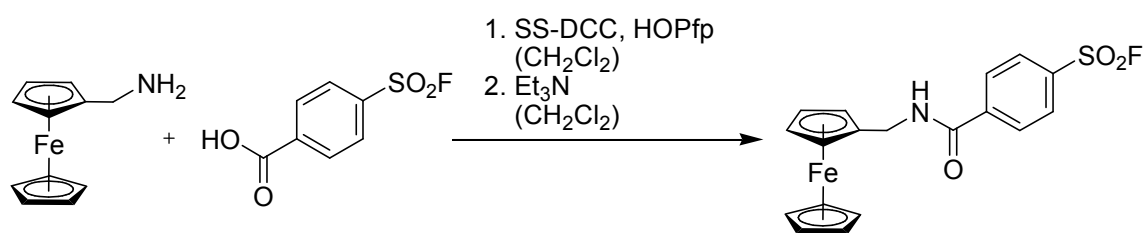


**Scheme B50:** Synthesis of Ferrocene labeled fluoro sulfonic acid [Fc]-SF **95**.

[Fc]-SF **95** was synthesized using the polymer-bound carbodiimide SS-DCC as coupling reagent (the reaction procedure was discussed in detail in section B3.3). In contrast to rhodium complexes **52**, **53** and ruthenium complex **4i**, ferrocene is due to its stability an easy to handle substrate. Its tendency of decomposing is tremendously decreased compared to the catalysts mentioned above. The raw product was purified via silica column chromatography and its identity confirmed via $^1$H NMR, $^{13}$C NMR and $^{19}$F NMR spectroscopy as well as ESI MS. In $^1$H NMR, besides the characteristic signals originating from the cyclopentadienyle ligands and the arene CH protons, the $CH_2$ protons were observed at 4.35 ppm (singulet). The NH proton was observed as a singulet at 6.36 ppm. In $^{19}$F NMR spectroscopy, the fluoro sulfonic acid fluoride is observed at 66.08 ppm as a singulet. This shift is almost identical to the one observed for [Ru]-SF **92** (66.28 ppm, singulet). In the mass spectra as base peak the fragment $[M+H]^+$ with m/z = 401.2 could be observed.

In contrast to the conversion of known water soluble ferrocene labeled affinity labels for cysteine proteases, a complete conversion of [Fc]-SF **95** with trypsin did not succeed. In

solutions containing 10% DMSO, only a small amount of [Fc]-SF **95** remains dissolved, resulting in incomplete formation of [Fc]-SF@trypsin.[121]

In spite of the fact, that in MALDI-TOF spectra only a small amount of labeled trypsin was detected, the cyclic voltamogramme of [Fc]-SF@trypsin immobilized to a HOPG electrode showed a typical redox-potential for ferrocene derivatives (figure B31).[121]
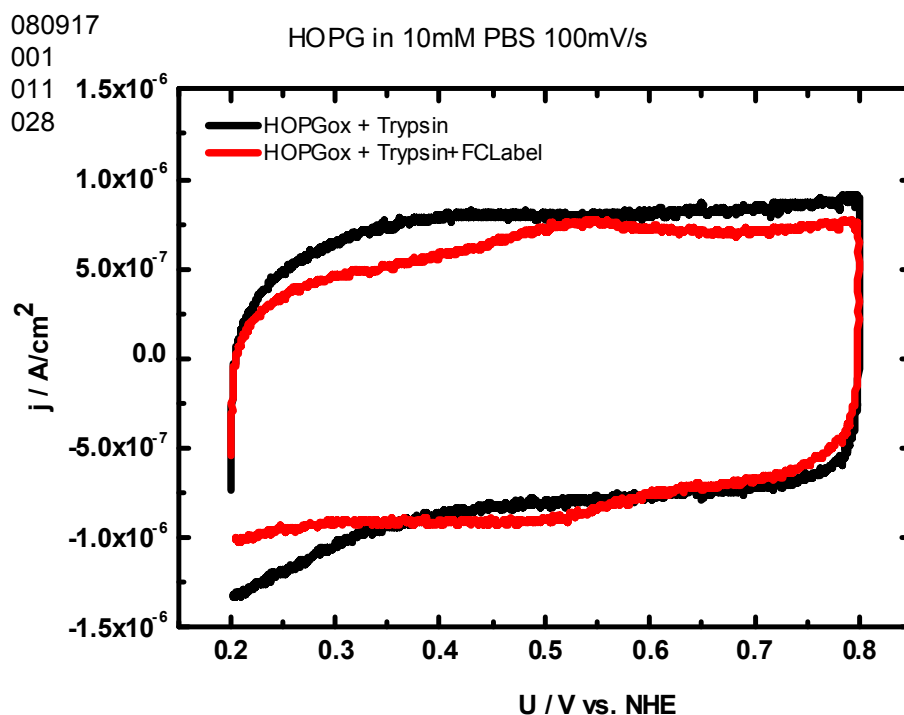


*Figure B31:* Cyclic voltamogramme of trypsin (black) and [Fc]-SF@trypsin (red).

These first measurements indicate, that an improvement in water solubility of the ferrocene label [Fc]-SF **95**, for example by using ferrocenylalanine instead of ferrocenemethylamine, could improve the labeling of the redox active linker to trypsin. This would result in better inhibition and therefore lead to higher intensity of the detected electrochemical peak.[121]

# 11. Organometallic enzyme hybrids derived from cysteine proteases

## 11.1. Formation of organometallic enzyme hybrids

Both metalla affinity labels [Rh]-Epx **70** and [Rh]-Deox **72** can be regarded as multifunctional organometallic catalysts (Figure B32). Both comprise a peptidic part, which directs the label selectively into the active site of the enzyme. This ensures specific interaction of [M]-ALs and the active site pocket. Nevertheless, only [Rh]-Epx **70** has an epoxide moiety, which allows covalent attachment to the enzyme. Therefore, for [Rh]-Epx **70,** this gives rise to a directed orientation of the metalla affinity label's third part, the achiral organometallic catalyst. It is anchored in the active site, allowing asymmetric catalysis through embedment in the chiral protein environment (chapter B3.2.1). In theory, both complexes [Rh]-Epx **70** and [Rh]-Deox **72** could bind to the enzyme via coordination of nucleophilic moieties on the enzyme surface to the Lewis acidic transition metal centre, resulting in random and unspecific interaction of metalla affinity label. If no interaction and therefore no covalent attachment of [Rh]-Deox **72** (which does not have an epoxide moiety) and the cysteine protease is detected, the formation of a coordinative bond between enzyme surface and transition metal centre can be ruled out for both [Rh]-Epx **70** and [Rh]-Deox **72**, as both comprise identical metal centers.
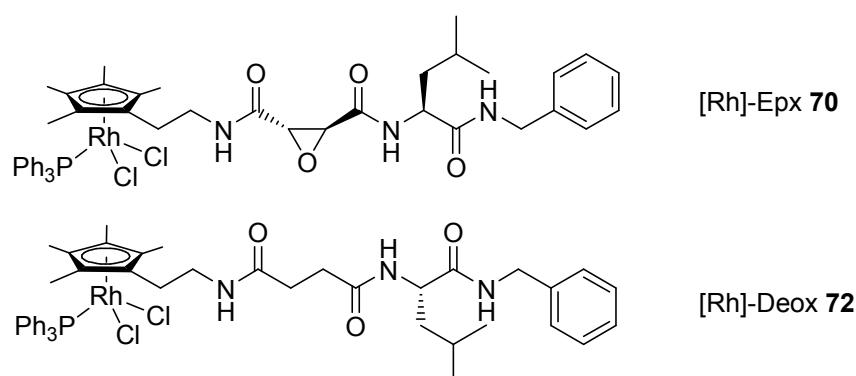


***Figure B32:*** Covalent and non-covalent metalla affinity labels [Rh]-Epx **70** and [Rh]-Deox **72** used for the conversion with cysteine proteases.

There were different methods applied to confirm the designed mode of interaction of metalla affinity labels and the cysteine protease papain. For this purpose, both metalla affinity labels [Rh]-Epx **70** and [Rh]-Deox **72** were stirred with a solution of activated papain. As activation reagents, TCEP or DTT were used. This is necessary, as in commercially available papain, disulfide bridges between the active center cysteine

Cys25 and a Cysteine amino acid deactivate the enzyme and thereby protect it from autocatalytic cleavage. The reducing reagents DTT and TCEP cleave this disulfide bridge and therefore enable inhibition by metalla affinity labels (scheme 51).
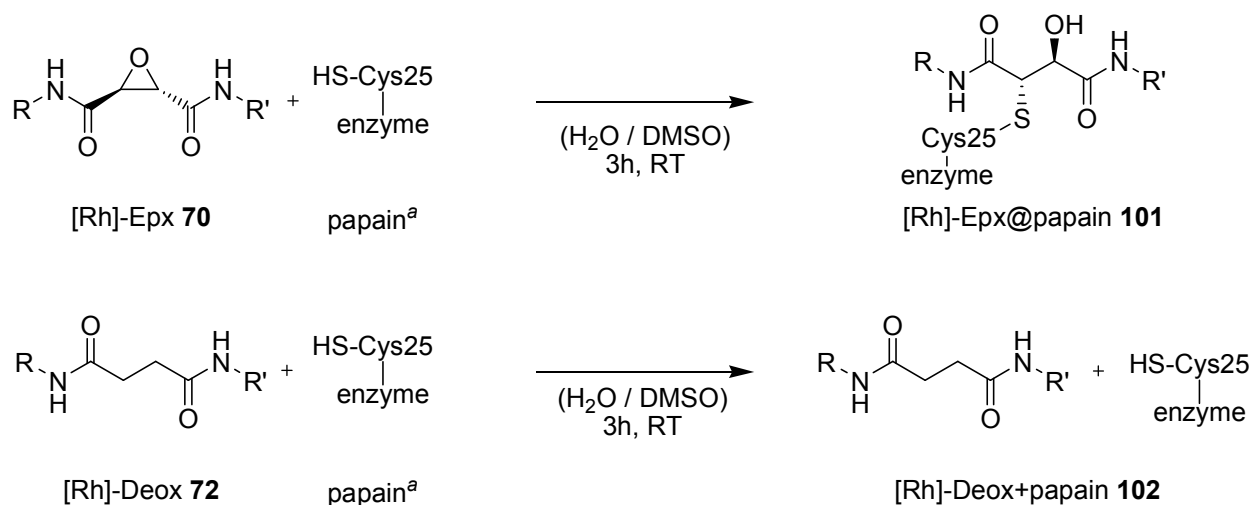


**Scheme B51:** Conversion of metalla affinity labels with cysteine proteases, resulting in the formation of organometallic enzyme hybrids [Rh]-Epx@papain **101** and [Rh]-Deox+papain **102**. (a) papain was activated with TCEP or DTT.

First, the covalent inhibition of papain by [Rh]-Epx **70** was confirmed by MALDI-TOF analysis (figure B33). With native papain, consisting of only one single peptide strand, one single set of peaks with a mass of 23.418 ± 1 kDa was observed. Upon addition of covalent inhibitor [Rh]-Epx **70**, a second set of peaks appeared for the organometallic enzyme hybrid [Rh]-Epx@papain **101** with a mass of 24.015 kDa. The increase of molecular weight by 597 ± 1 Da again confirms the metalla affinity label to bind covalently to papain. Its mass is decreased by the amount of triphenylphosphine and two chlorine atoms, which can be replaced by nucleophilic groups in the enzyme pocket. Interaction of the inner coordination sphere of the metal centre with the environment of the active site further increases the chiral information of the enzyme transferred to the metal centre. Nevertheless, the metal centre is not blocked by its nucleophilic ligands. In the double charged peak region, another peak was observed at 12.064 kDa. Referring to a mass of 24.128 kDa. Difference in 113 Da from [Rh]-Epx@papain **101** could originate from solvent-metal centre interaction as well as coordination of cysteine present in the reaction solution. This proves the metal centre to be able to bind as well as to release ligands present in the reaction solution, which is the fundamental premise for catalytic conversions. Furthermore, no multiple additions of the label to the enzyme were detected. This proves that [Rh]-Epx **70** binds only to one single site of the enzyme via selective inhibition of the enzyme pocket. Peak **I**, the only

impurity observed, originates from papain upon activation with DTT or TCEP. It was found neither to interact with [Rh]-Epx **70** nor [Rh]-Deox **72**, and thus is not relevant for the formation of organometallic enzyme hybrids generated with cysteine protease papain.
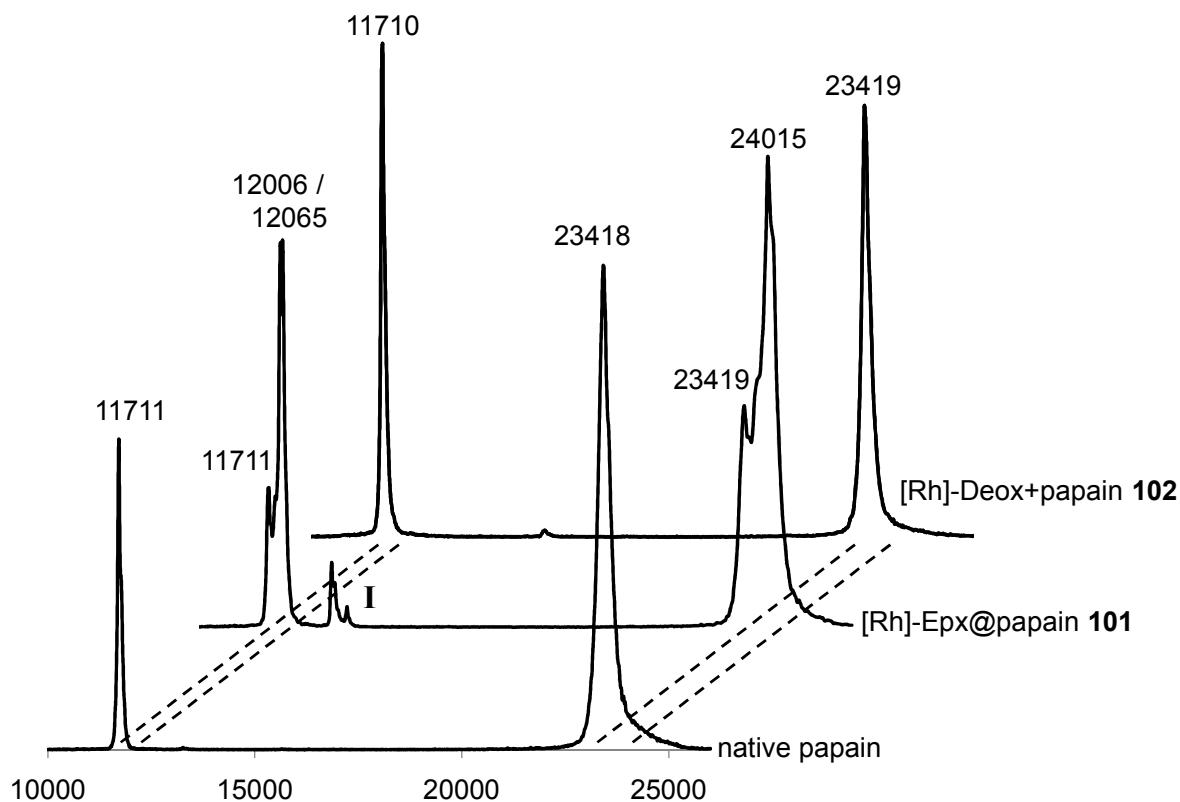


***Figure B33:*** MALDI-TOF mass spectra of [Rh]-Epx@papain **101**, [Rh]-Deox+papain **102** and native papain.

Besides MALDI-TOF spectra, a second method to determine the inhibitor strength of both [Rh]-Epx **70** and [Rh]-Deox **72** was applied. For this purpose, the two metalla labels were reacted with papain (scheme B51) in different concentrations and the residual papain enzyme activity tested in a standard chromogenic assay.[122] Inhibitory assays should yield a stronger inhibition for [Rh]-Epx **70**. As it inhibits papain covalently, it should induce a complete loss in enzyme activity. In contrast, [Rh]-Deox **72** should lead to no or just slight inhibition, as it does not comprise an epoxide moiety, which could facilitate covalent bond formation.

As enzyme substrate, $N_\alpha$-Benzoyl-DL-arginine *p*-nitroanilide (BAPNA) was used. This substrate is cleaved selectively at the arginine-*p*-nitroanilide peptide bond, releasing *p*-nitroanilide into the reaction solution. The amount of *p*-nitroanilide can be quantified by photometric measurements due its high extinction coefficient at 405 nm. From the

amount released per time, the enzymatic activity and therefore the amount of active papain in solution can be measured. Upon addition of increasing concentrations of [Rh]-Epx **70** in solution, the amount of active papain is decreased, resulting in a slower release of *p*-nitroanilide and therefore a lower absorption is measured (scheme B52).
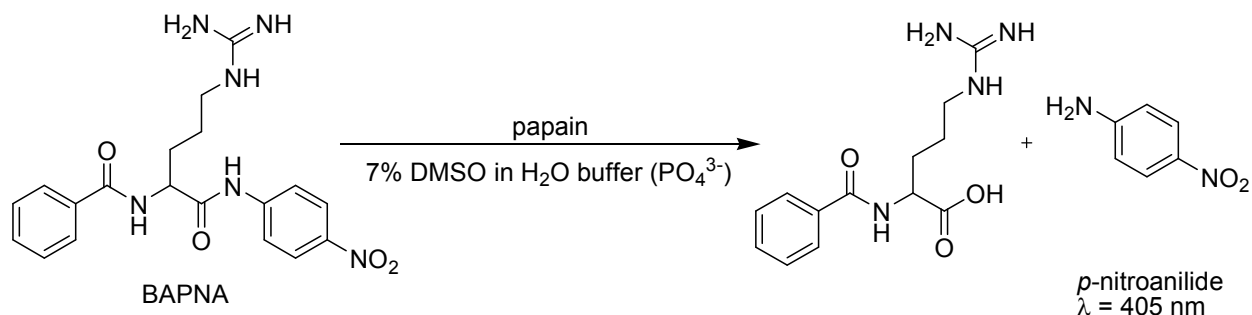


**Scheme B52:** Photometric assays for the determination of enzyme activity of papain in the presence of different concentrations of [Rh]-Epx **70** and [Rh]-Deox **72**.

The results confirm, that enzyme activity decreases linearly with the amount of [Rh]-Epx **70** added (figure B34). It is completely suppressed in a solution containing approx. 1.4 µM [Rh]-Epx **70** and above. This strongly indicates [Rh]-Epx **70** to bind to papain covalently. When the same experiment was repeated with [Rh]-Deox **72**, there was no loss in enzyme activity detected at all. Bond strength between [Rh]-Deox **72** and papain is therefore not strong enough to decrease the enzyme activity. Therefore, inhibition of papain by [Rh]-Epx **70** is attributed to covalent binding of the epoxide moiety, the metal centre is not involved in inhibition of the enzyme.
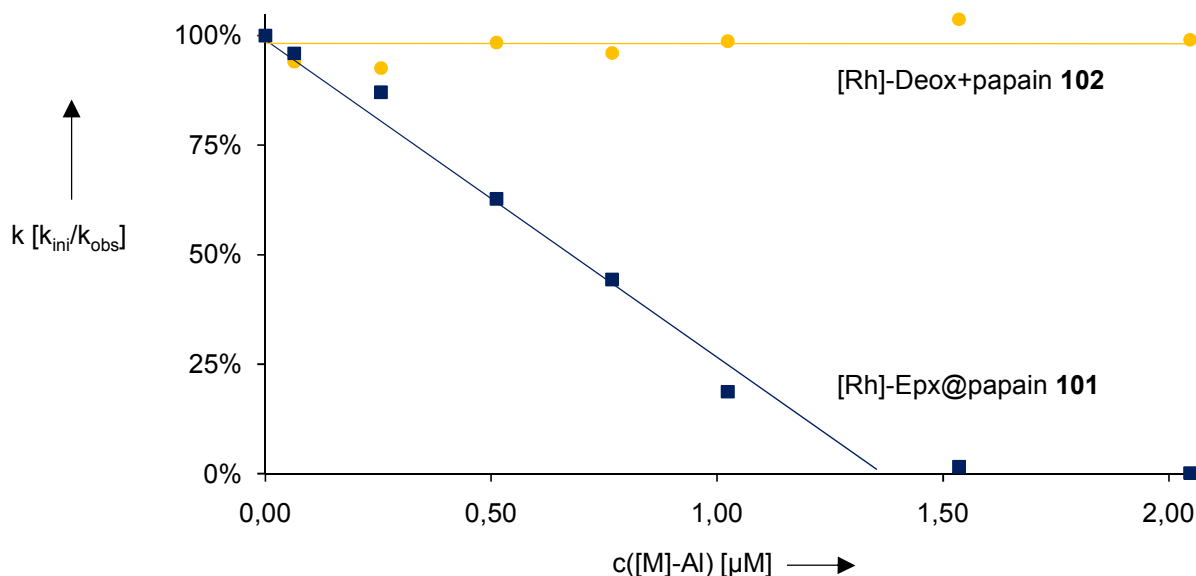


**Figure B34:** Chromogenic assay of papain in the presence of [Rh]-Epx **70** and [Rh]-Deox **72**, employing BAPNA as substrate. The enzyme activity was monitored at 405 nm. Data points were collected at t = 0 (initial absorbance) and t = 125 min.
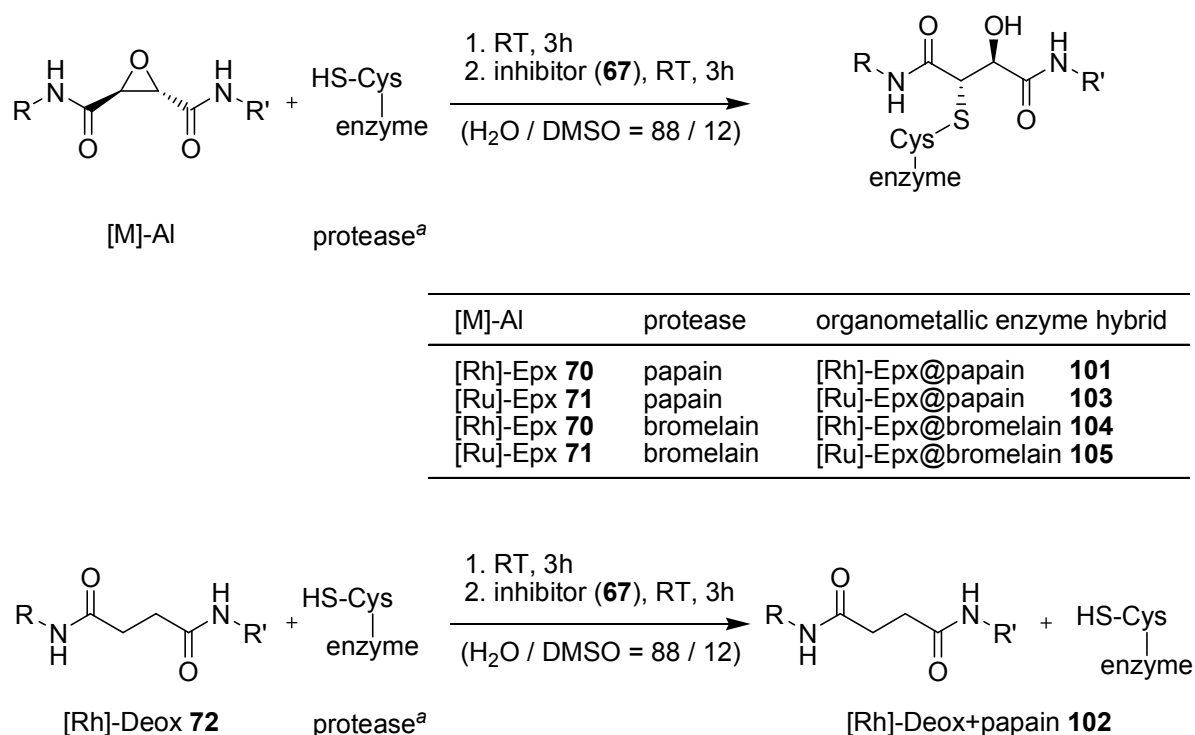
The enzyme activity assays were also used to determine the amount of active enzyme available for conversion with [M]-Al. By adding an understoichiometric amount of [Rh]-Epx **70**, at a concentration where residual activity of the enzyme is still detectable, complete incorporation of the catalyst in the enzyme pocket can be assumed. Therefore, all metal centers are embedded in the chiral environment, and a decrease of enantiomeric excess by catalyst species dissolved in reaction media can be excluded.

In summary, it was confirmed by MALDI-TOF measurements as well as chromogenic assays, that covalent metalla affinity label [Rh]-Epx **70** binds selectively as well as irreversibly into the active site of the enzyme. Experiments with its non-covalent analogue [Rh]-Deox **72** revealed that there was no inhibition and therefore no immobilization of the metalla labels on the enzyme surface via coordination of nucleophilic groups to the transition metal centre.

These experiments strongly support the expected binding mode of metalla affinity labels, and thus confirm the concept of organometallic enzyme hybrids generated via metalla affinity labels (section B3.2.1).

## 11.2. Hydrogenation screening

The concept of metalla affinity labels binding selectively and irreversibly into the active site of cysteine proteases has been confirmed above (section B3.11.1). This results in the organometallic catalyst being embedded in the chiral environment of the enzyme pocket, transforming the initially achiral transition metal catalyst into a catalyst capable of asymmetric induction. As a prototype reaction to test the performance of organometallic enzyme hybrids derived from [Rh]-Epx **70** and [Ru]-Epx **71** and cysteine proteases papain and bromelain, the catalytic hydrogenation of ketones was chosen. [Rh]-Deox **72** was tested as well under the same conditions to determine the effect of the covalent embedment of catalysts in the chiral environment of the enzyme pocket.



| [M]-Al | protease | organometallic enzyme hybrid |
|---|---|---|
| [Rh]-Epx **70** | papain | [Rh]-Epx@papain **101** |
| [Ru]-Epx **71** | papain | [Ru]-Epx@papain **103** |
| [Rh]-Epx **70** | bromelain | [Rh]-Epx@bromelain **104** |
| [Ru]-Epx **71** | bromelain | [Ru]-Epx@bromelain **105** |



**Scheme B53:** Generation of organometallic enzyme hybrids of metalla affinity labels with cysteine proteases, resulting in the formation of organometallic enzyme hybrids [Rh]-Epx@papain **101**, [Ru]-Epx@papain **103**, [Rh]-Epx@bromelain **104** and [Rh]-Deox+papain **105**. (a) papain and bromelain were activated with using reducing agent DTT.

The organometallic catalyst part of metalla labels **70** to **72** was proven to be active in hydrogenation reactions before.[123] Commercially available 2,2,2-trifluoro acetophenone was used as a prototype substrate, as conversions and yields can be monitored easily via standard $^{19}F$ NMR spectrometry. Preparation of the active organometal enzyme hybrid followed a three step protocol. First, commercially available cysteine proteases were stirred gently in a solution of DTT. The reducing agent activates the proteases via

reduction of the active site cysteine moiety. After activation, the metalla affinity label was added. To avoid autolytic cleavage of the protease, residual enzyme activity was suppressed by addition of HO-Eps-Leu-NH-Bzl **67**.[124] This results in a reaction solution, in which first all metalla affinity label is embedded in a chiral environment, and second protease activity is suppressed. Following this protocol, the complexes [Rh]-Epx **70**, [Ru]-Epx **71** and [Rh]-Deox **72** were tested for their performance with papain and bromelain (Scheme B53).
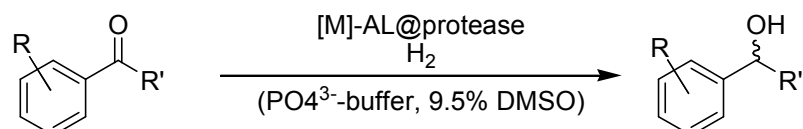


***Scheme B54:*** Enantioselective hydrogenation of ketones employing organometallic enzyme hybrids as catalysts. Please see figure B35 for a list of the different substrates employed. See tables B11-B13 and tables C12-C20 for hydrogenation results.

For hydrogenation reactions, ketone was added to organometallic enzyme hybrid solutions prepared according to the procedure described in scheme B53. The reaction mixture was pressurized ($H_2$) and stirred gently for the desired amount of time (scheme B54). To verify that enantiomeric excesses are generated in the active site of the enzyme, [Rh]-Epx@papain **101**, [Ru]-Epx@papain **103**, [Ru]-Epx@bromelain **104** and [Rh]-Deox+papain **102** as well as [Rh]-Epx **70**, [Ru]-Epx **71** and [Rh]-Deox **72** were tested under standard reaction conditions (table B11). In all cases, yields obtained without applying enzymes as chiral scaffolds were low in comparison to [Rh]-Epx@papain **101** (table B11, entries 8-10). Enantiomeric excesses were considerably lower for [Rh]-Deox+papain **102** (6 %). When the organometallic systems were tested for their performance in absence of enzyme, racemic products were observed in all cases.
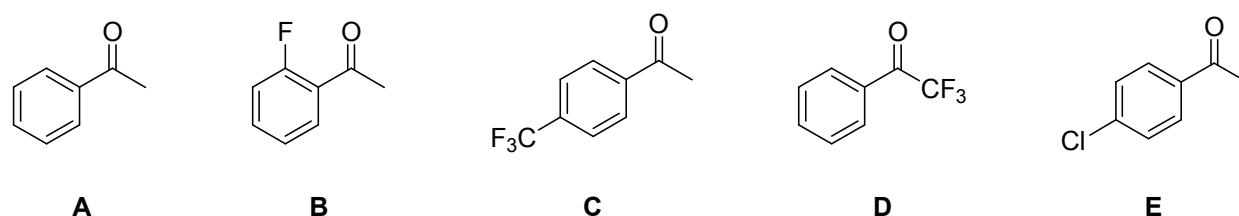


| A | B | C | D | E |

***Figure B35:*** Substrates employed in the catalytic hydrogenation of ketones with cysteine protease based organometallic enzyme hybrids. Please see tables B11-B13 and tables C12-C20 for hydrogenation results.

The increased yield and the slight enantiomeric excess observed (26% yield, 6% ee) with [Rh]-Deox+papain **102** indicates that there is some interaction between [Rh]-Deox **72** and the enzyme. Nevertheless, it also shows the importance of specific and covalent anchoring of the transition metal catalyst into the enzyme, as the corresponding experiment employing [Rh]-Epx@papain **101** yielded 3.2-fold higher yields and 3.8-fold higher enantiomeric excesses.

To underline the modularity of metalla affinity labels covalently bound into cysteine proteases, [Ru]-Epx@papain **103** was tested for its performance in the catalytic hydrogenation of 2,2,2-Trifluoroacetophenone (table 1, entry 3). In this case, a yield of 44 % was observed. Enantiomeric excess was 20 % for the (*S*)-enantiomer.

**Table B11:** Screening of different catalysts and organometallic enzyme hybrids.

| entry | catalyst | substrate | t [h] | p [H$_2$] | yield [%] | ee [%] |
|-------|----------|-----------|-------|-----------|-----------|--------|
| 1 | [Rh]-Epx@papain **101**[a] | D | 96 | 75 | 92 | 20 (*R*) |
| 2 | [Rh]-Epx@papain **101**[a] | D | 65 | 25 | 81 | 23 (*R*) |
| 3 | [Ru]-Epx@papain **103**[a] | D | 96 | 75 | 44 | 20 (*S*) |
| 4 | [Ru]-Epx@papain **103**[a] | D | 65 | 25 | 19 | 25 (*S*) |
| 5 | [Ru]-Epx@bromelain **105**[a] | D | 96 | 75 | 40 | 10 (*S*) |
| 6 | [Ru]-Epx@bromelain **105**[a] | D | 65 | 25 | 12 | 18 (*S*) |
| 7 | [Rh]-Deox+papain **102**[a] | D | 65 | 25 | 26 | 6 (*R*) |
| 8 | [Rh]-Epx **70** | D | 65 | 25 | 4 | 3 (*S*) |
| 9 | [Ru]-Epx **71**[a] | D | 65 | 25 | 5 | < 1 (*S*) |
| 10 | [Rh]-Deox **72** | D | 65 | 25 | 5 | 3 (*S*) |

Total volume of the reaction was 525 µL, substrate / catalyst ratio = 50 / 1. The content of DMSO was 9.5 %. Reaction temperature was 40 °C. Yields were determined by ^{19}F NMR spectroscopy. Enantiomeric excesses were determined by chiral GC. (a) DTT concentration was 0.95 mM.

Predominant formation of the (*S*)-enantiomer instead of the (*R*)-enantiomer is attributed to the change of linker length between epoxide moiety and transition metal centre. This results in a different chiral environment for the catalyst and an inversion of the catalyst selectivity. Metalla label [Ru]-Epx **71** was also tested with the cysteine protease bromelain instead of papain (table 1, entries 5 and 6). The resulting hybrid [Ru]-Epx@bromelain **105** gave yields of 40 % and enantiomeric excesses of 10 % for the (S)-enantiomer.

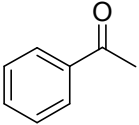*Table B12:* Performance screening of [Rh]-Epx@papain **101** under varying conditions.
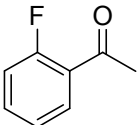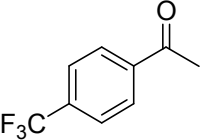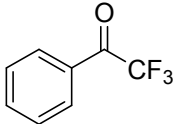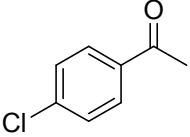
| entry | organometallic enzyme hybrid | substrate | T [°C] | DTT [mM] | pH | p [H$_2$] | yield [%] | ee [%] |
|:---:|:---:|:---:|:---:|:---:|:---:|:---:|:---:|:---:|
| 1 | [Rh]-Epx@papain **101** | **D** | 20 | 3.8 | 6.5 | 25 | 10 | 24 (*R*) |
| 2 | [Rh]-Epx@papain **101** | **D** | 30 | 3.8 | 6.5 | 25 | 16 | 24 (*R*) |
| 3 | [Rh]-Epx@papain **101** | **D** | 40 | 3.8 | 6.5 | 25 | 53 | 24 (*R*) |
| 5 | [Rh]-Epx@papain **101** | **D** | 40 | 2.9 | 6.5 | 25 | 57 | 22 (*R*) |
| 6 | [Rh]-Epx@papain **101** | **D** | 40 | 1.9 | 6.5 | 25 | 58 | 22 (*R*) |
| 7 | [Rh]-Epx@papain **101** | **D** | 40 | 0.95 | 6.5 | 25 | 81 | 23 (*R*) |
| 8 | [Rh]-Epx@papain **101** | **D** | 40 | 0.48 | 6.5 | 25 | 19 | 10 (*R*) |
| 9 | [Rh]-Epx@papain **101** | **D** | 40 | 0.19 | 6.5 | 25 | 36 | 2 (*R*) |
| 10 | [Rh]-Epx@papain **101** | **D** | 40 | 0.01 | 6.5 | 25 | 21 | 2 (*S*) |
| 11 | [Rh]-Epx@papain **101** | **D** | 40 | 0.95 | 6.0 | 25 | 33 | 20 (*R*) |
| 12 | [Rh]-Epx@papain **101** | **D** | 40 | 0.95 | 7.0 | 25 | 39 | 19 (*R*) |
| 13 | [Rh]-Epx@papain **101** | **D** | 40 | 0.95 | 7.5 | 25 | 42 | 15 (*R*) |
| 14 | [Rh]-Epx@papain **101** | **D** | 40 | 0.95 | 6.5 | 10 | 10 | 11 (*R*) |
| 15 | [Rh]-Epx@papain **101** | **D** | 40 | 0.95 | 6.5 | 75 | 89 | 20 (*R*) |

Total volume of the reaction was 525 µL, substrate / catalyst ratio = 50 / 1. The content of DMSO was 0.5 %. Reaction time was 65 h. Yields were determined by ^{19}F NMR spectroscopy. Enantiomeric excesses were determined by chiral GC.

These experiments show the advantages of using the metalla affinity label building block technique for the generation of organometallic enzyme hybrids. Simple change of enzymes or metal centers can invert enantioselectivity. By employing different enzymes, labels or metal centers, potential hybrid catalysts can be screened efficiently and quickly, making the identification of promising catalyst candidates facile, which then can be optimized via directed evolution.[95,97] Organometallic enzyme hybrid [Rh]-Epx@papain **101** showed yields of 10 % and enantiomeric excesses of 24 % at temperatures of 20 °C (table B12, entry 1). When temperature was increased, yields of up to 53 % were obtained without decrease of enantiomeric excess (table B12, entries 2 and 3). The organometallic enzyme hybrid therefore is stable under the conditions applied. The amount of reducing reagent is crucial for activity and selectivity of the organometallic enzyme hybrid (table B12, entries 4 to 10). Concentrations larger than 0.95 mM lead to deactivation of the hybrid, smaller concentrations lead to reduced enantiomeric excesses. This can be explained by the dithiol DTT being able to

coordinate to the metal centre. The thiophilicity of group 8 and 9 transition metals deactivates the catalyst in high concentrations efficiently although enantiomeric excesses observed remain stable. At low concentrations of DTT, not all papain can be activated and therefore made accessible for the [M]-AL. Hence, the catalyst is not embedded efficiently in the chiral environment, yielding lower enantiomeric excesses. The greater the amount of catalyst in solution, the lower the enantiomeric excess observed. A screening of different pH values revealed the organometallic enzyme hybrid to yield optimal results in terms of yield as well as enantiomeric excess at a pH of 6.5 (table B12, entries 7 and 11 to 13). A strong influence on the hybrid catalyst performance was detected in variation of hydrogen pressure (table B12, entries 7, 14 and 15). When a hydrogen pressure of 10 bar was applied, yields dropped from 81 % to 10 %. Enantiomeric excess was also significantly decreased, which can be explained by slight conformational changes of the hybrid at elevated pressures. This observation is supported when catalysis is carried out at 75 bar hydrogen pressure. Yields improve slightly from 81 % to 89 %, whereas the enantiomeric excess decreases from 23 to 20 percent (*R*).

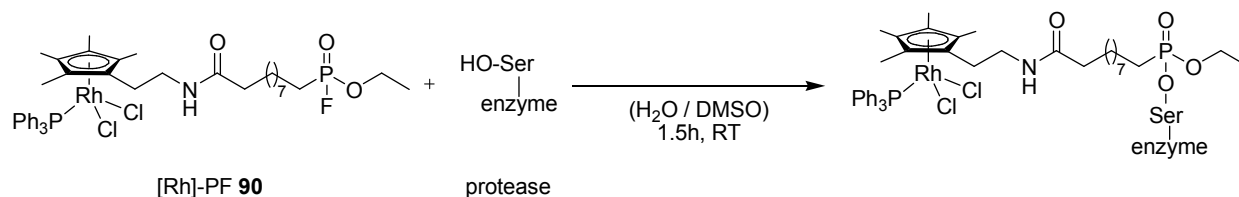**Table B13.** Screening of different prochiral ketones with **1**<sup>Rh</sup>@papain

| Entry | organometallic enzyme hybrid | substrate | yield [%] | ee [%] |
|---|---|---|---|---|
| 1[a] | [Rh]-Epx@papain **101** | | 2 | 37 (*R*) |
| 2[a] | [Rh]-Epx@papain **101** | | 8 | 29 (*R*) |
| 3[b] | [Rh]-Epx@papain **101** | | 16 | 45 (*R*) |
| 4[b] | [Rh]-Epx@papain **101** | | 92 | 20 (*R*) |
| 5[a] | [Rh]-Epx@papain **101** | | 12 | 64 (*R*) |

Total volume of the reaction was 525 µL, substrate / catalyst ratio = 50 / 1. The content of DMSO was 0.5 %. T = 40 °C, p = 75 bar, t = 96 h, c(DTT) = 0.95 mM. [a] yields and enantiomeric excesses were determined by chiral GC. [b] yields were determined by $^{19}$F NMR spectroscopy, enantiomeric excesses were determined by chiral GC.
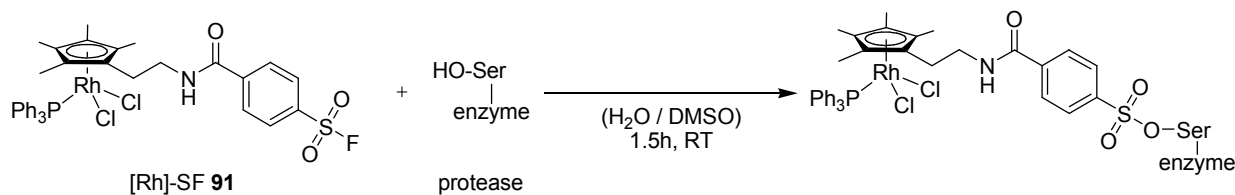
Besides using 2,2,2-Trifluoroacetophenone as a substrate, the performance of [Rh]-Epx@papain **101** was tested with a variety of other ketones (table B13). These experiments show the broad applicability of the organometallic enzyme hybrids. Nevertheless, best results were received for electron withdrawing substituents on the ketone (table B13, entries 3 and 4). Enantiomeric excesses were higher with all tested ketones than for 2,2,2-Trifluoroacetophenone, which results from the higher difference in steric demand of the arene system in comparison to the methyl group. The best results were observed for 4'-chloroacetophenone, for which yields of 12 % and enantiomeric excesses of 64% were obtained with [Rh]-Epx@papain **101**. There have been many other hydrogenation experiments conducted within this screening, which will not be discussed in detail within this context. For a complete list of data obtained, please refer to the experimental section, tables C12-C20.

This screening proves a new concept to generate OMEHs. They have been generated via the exploitation of covalent bond formation between epoxide affinity labels and cysteine proteases. For this purpose, a new type of cysteine protease inhibitors, metalla affinity labels, was designed. They can be reacted selectively, directed and covalently with cysteine proteases, as shown in section B3.11.1. Metalla affinity labels are trifunctional in terms of having a covalent anchor, with which the metalla affinity label is bound to the enzyme, a directing part, which makes attachment to the active site favorable and an achiral transition metal catalyst. Directed and selective covalent bond formation between the metalla affinity label and the cysteine proteases results in the transition metal catalyst being embedded in the chiral active site environment, generating organometallic enzyme hybrids, which were tested in the catalytic hydrogenation of ketones, yielding enantiomeric excesses of up to 64 %.

In addition, this concept can be seen as a building block system, with which a wide range of hybrid systems can be generated in a short amount of time and screened for potential promising candidates. This feature originates from the synthetic route to these compounds, which is another notable feature. As the peptide bond formation between organometallic catalysts and the affinity label is the last synthetic step, the rapid generation of different [M]-ALs is possible. Combination of different catalysts, affinity parts and enzymes allows the generation of an OMEH library, from which promising candidates can be tested for their performance in asymmetric catalysis in only a short amount of time. This widens the spectrum of OMEHs by offering access to new classes of enzymes.

# 12. Organometallic enzyme hybrids derived from serine proteases

## 12.1. Formation of organometallic enzyme hybrids

Both metalla affinity labels and epoxide metalla affinity labels have proven to be suitable for the generation of organometallic enzyme hybrids (section B3.11). Apart from these epoxide-derived metalla affinity labels, fluoro sulfonic acid, fluoro phosphonic acid and diphenyl phosphonate inhibitors (complexes **90**-**94**) were designed, comprising rhodium or ruthenium transition metal centers as catalytically active species. Their reactive moieties and peptidic parts were shown to bind selectively and covalently to the active centers of serine proteases.[101] Confirmation of their applicability as metalla linkers for the generation of organometallic enzyme hybrids would widen the scope of moieties, with which organometallic catalysts can be anchored to enzymes.



*Figure B36:* Phosphonic acid and Sulfonic acid fluoride metalla linkers [Rh]-PF **90** and [Rh]-SF **91**.

For this study, the serine proteases trypsin and α-chymotrypsin were chosen as enzyme scaffolds, as they have shown to be efficiently inhibited by fluoro phosphonic and fluoro sulfonic acids.[101] In both cases, covalent bond formation occurs via the nucleophilic attack of the active center serine residue to the phosphorous or sulfur moiety. Peptide bond formation of the linkable $\eta^5$-rhodium phosphine catalyst **52** with compounds containing fluoro sulfonic and fluorophosphonic acids yielded the linkable organometallic catalysts [Rh]-PF **90** and [Rh]-SF **91** (figure B36). To prove the ability of linkable catalysts [Rh]-PF **90** and [Rh]-SF **91** to act as covalent inhibitors, both were reacted with trypsin as well as α-chymotrypsin under standard reaction conditions and the resulting species were analyzed via MALDI-TOF spectrometry.

| [M]-Al | protease | organometallic enzyme hybrid |
|---|---|---|
| [Rh]-PF **90** | α–chymotrypsin | [Rh]-PF@α–chymotrypsin **106** |
| | trypsin | [Ru]-PF@trypsin                **108** |



| [M]-Al | protease | organometallic enzyme hybrid |
|---|---|---|
| [Rh]-SF **91** | α–chymotrypsin | [Rh]-SF@α–chymotrypsin **107** |
| | trypsin | [Ru]-SF@trypsin                **109** |

***Scheme B55:*** Conversion of organometallic linkers and serine proteases, resulting in the formation of organometallic enzyme hybrids [Rh]-PF@α-chymotrypsin **106**, [Rh]-SF@α-chymotrypsin **107**, [Rh]-PF@ trypsin **108** and [Rh]-PF@ trypsin **109**.

For this purpose, both complexes were dissolved in a solution of one of the enzymes. Activation with a reducing agent was not necessary in this case, as the commercially available serine proteases trypsin and α-chymotrypsin are not deactivated. Conversion of **90** and **91** with enzymes yielded the organometallic enzyme hybrids [Rh]-PF@α-chymotrypsin **106** [Rh]-SF@α-chymotrypsin **107** [Rh]-PF@trypsin **108** [Rh]-SF@trypsin **109**. MALDI-TOF measurements revealed molecular masses correlating to the employed linkers. Masses observed were always higher than the ones of the native enzymes (table B14). Moreover, multiple addition of linker to the enzyme can be ruled out as the corresponding masses are absent. Inhibition of trypsin and α-chymotrypsin was complete for organometallic linker [Rh]-PF **90**, whereas with [Rh]-SF **91**, there was still native enzyme observed. Furthermore, MALDI-TOF spectra revealed a high tendency of the triphenylphosphine to be substituted by other ligands. This feature supports activation of the transition metal catalysts by nucleophilic moieties on the enzyme surface (section B3.2.2) and is in accordance to observations made for cysteine proteases (section B3.11.1). Overall, MALDI-TOF spectra confirm the binding mode of metalla linkers with fluoro sulfonic as well as fluoro phosphonic reactive groups (table B14).

***Table B14:*** Table of species observed in MALDI-TOF spectra in comparison to the native enzymes employed.

| entry | native enzyme / OMEH | obs. Mass [kDa] | $\Delta_{\text{native enzyme}}$ [Da] | species |
|---|---|---|---|---|
| 1 | α-chymotrypsin | 25.443 | | $[M]^+$ |
| | | 12.729 | | $[M]^{2+}$ |
| 2 | [Rh]-PF@α-chymotrypsin **106** | 25.946 | 503 | $[M-PPh_3-Cl-OEt-F]^+$ |
| | | 12.979 | 250 | $[M-PPh_3-Cl-OEt-F]^{2+}$ |
| 3 | [Rh]-SF@α-chymotrypsin **107** | 26.135 | 692 | $[M-2Cl-F]^+$ |
| | | 13.080 | 351 | $[M-2Cl-F]^{2+}$ |
| 4 | Trypsin | 23.303 | | $[M]^+$ |
| | | 11.661 | | $[M]^{2+}$ |
| 5 | [Rh]-PF@trypsin **108** | 23.803 | 500 | $[M-PPh_3-Cl-OEt-F]^+$ |
| | | 11.911 | 250 | $[M-PPh_3-Cl-OEt-F]^{2+}$ |
| 6 | [Rh]-SF@trypsin **109** | 23.733 | 430 | $[M-PPh_3-2Cl-F]^+$ |
| | | 11.879 | 218 | $[M-PPh_3-2Cl-F]^{2+}$ |
| | | 24.003 | 700 | $[M-2Cl-F]^+$ |
| | | 12.018 | 357 | $[M-2Cl-F]^{2+}$ |

Metalla linker [Rh]-PF **90** was as well tested for its ability to covalently inhibit serine protease trypsin via a chromogenic assay. The assay was carried out similar to the one described for cysteine protease papain (section B3.10.1). To confirm the covalent interaction of [Rh]-PF and trypsin, different concentrations of the metalla linker were added to a solution of the enzyme, and after about 10 minutes incubation the enzyme's activity in the enzymatic hydrolysis of BAPNA was measured. This was monitored by UV/VIS detection of the emerging *p*-nitroaniline, which has a strong absorption band at 405 nm (scheme B56). The measured absorption and therefore the concentration of *p*-nitroaniline can be correlated to the activity of residual trypsin and therefore the inhibition strength of [Rh]-PF **90**. Figure B37 clearly shows, that increasing concentration of the metalla linker results in a significant decrease of the enzyme activity. This is a strong indication that the enzyme is covalently inhibited by the metalla linker **90**.
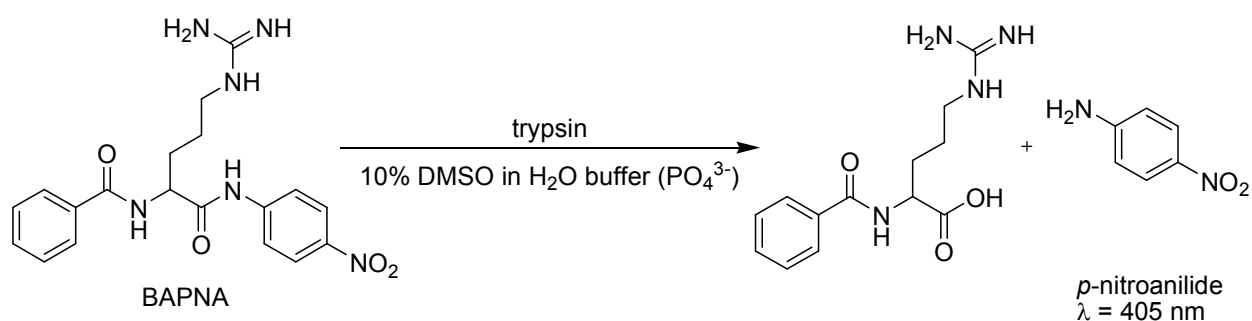
**Scheme B56:** Enzymatic cleavage of BAPNA by serine protease trypsin, releasing *p*-nitroaniline.

As the cleavage of the arginine-*p*-nitroanilide bond is a first order reaction, the obtained values are directly proportional to the enzyme activity (figures B37 and B38). The obtained linear decrease can be used as an indication for the amount of metalla linker, which is necessary for complete suppression of enzyme activity. Nevertheless, the obtained value will be higher than the amount of enzyme employed, as in aqueous solution, fluoro phosphonic acids tend to hydrolyze and therefore are not able to covalently interact and inhibit trypsin any longer.
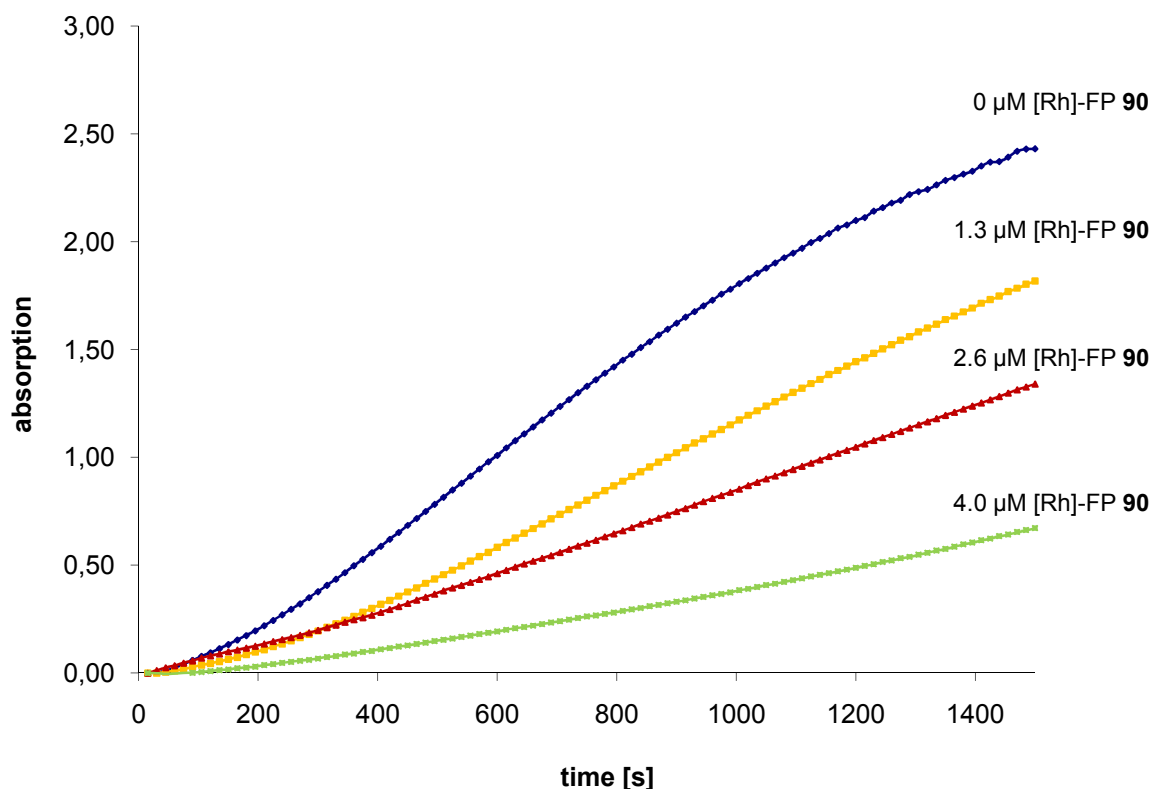


**Figure B37:** Chromogenic assay of trypsin in the presence of different concentrations of [Rh]-PF **90**. Comparison of *p*-Nitroanilide concentration versus time.

According to the results obtained from the chromogenic assay, a minimum concentration of 9.8 µM [Rh]-PF **90** is necessary to completely inhibit the enzyme

activity. The enzyme concentration in solution is approximately 8.6 µM. Therefore, a minimum of 1.14 eq. of [Rh]-mAL are needed to completely inhibit the enzyme activity (figure B38). Nevertheless, the metalla linkers need to be applied under-stoichiometrically. This is crucial, as an excess of metalla liker leads to unbound transition metal centers in solution, which are not embedded in a chiral environment and decrease the enantiomeric excess obtained during catalytic runs.

To overcome autolytic cleavage of the enzyme, PMSF, a potent inhibitor for serine proteases (figure B26) was added after incubation of the enzyme with metalla linkers. Autolytic cleavage would render transition metal centers to loose their chiral environment, as it destroys the structure of the enzyme scaffolds. Addition of PMSF after incubation on the one hand minimizes the amount of catalytically active metal centers in solution and on the other hand eliminates autolytic cleavage, resulting a maximum of metalla linkers **90**-**94** to be embedded in a chiral environment.
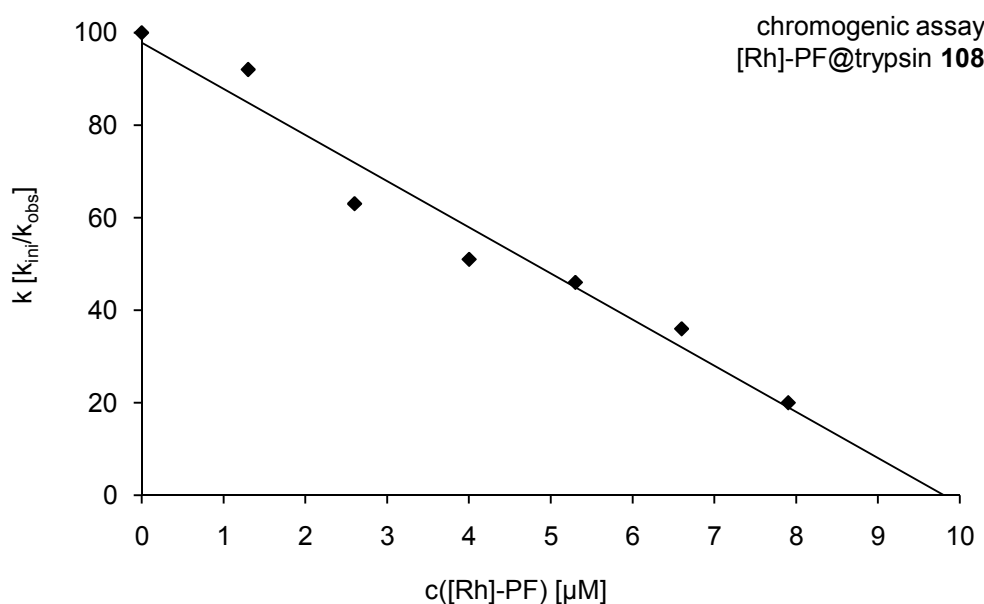


**Figure B38:** Chromogenic assay of trypsin in the presence of different concentrations of [Rh]-PF **90**, employing BAPNA as substrate. The enzyme activity was monitored at 405 nm. Data points were collected at t = 0 (initial absorbance). And t = 15 min.

Overall, chromogenic assays as well as MALDI-TOF spectra have confirmed the covalent inhibition of serine proteases trypsin and α-chymotrypsin by metalla linkers **90**-**94** resulting in organometallic enzyme hybrids **106**-**109**. These results give way for testing the organometallic enzyme hybrids in the catalytic transfer hydrogenation of ketones.

## 12.2. Hydrogenation screening

The concept of fluoro sulfonic and fluoro phosphonic metalla linkers binding selectively and irreversibly to serine proteases has been confirmed (section B3.12.1). Additionally, if labile ligands of the metal centre are replaced by nucleophilic amine or amide residues on the enzyme surface, this should capacitate the organometallic catalyst to facilitate transfer hydrogenations.[125] Furthermore, embedment of the initially achiral transition metal centre in the chiral enzyme active site pocket should lead to enantioselectivity. Both [Rh]-PF **90**, and [Rh]-SF **91** as well as the serine proteases α-chymotrypsin and trypsin were tested for their performance. As a non-covalent analogue of metalla linkers **90** and **91**, the literature known Cp* rhodium(III) complex [Cp*RhPPh$_3$Cl$_2$] **54** was tested.[87,88] As substrates, the prochiral ketones 2'-fluoroacetophenone **B** and 2,2,2-trifluoroacetophenone **D** were applied as substrates (figure B39).
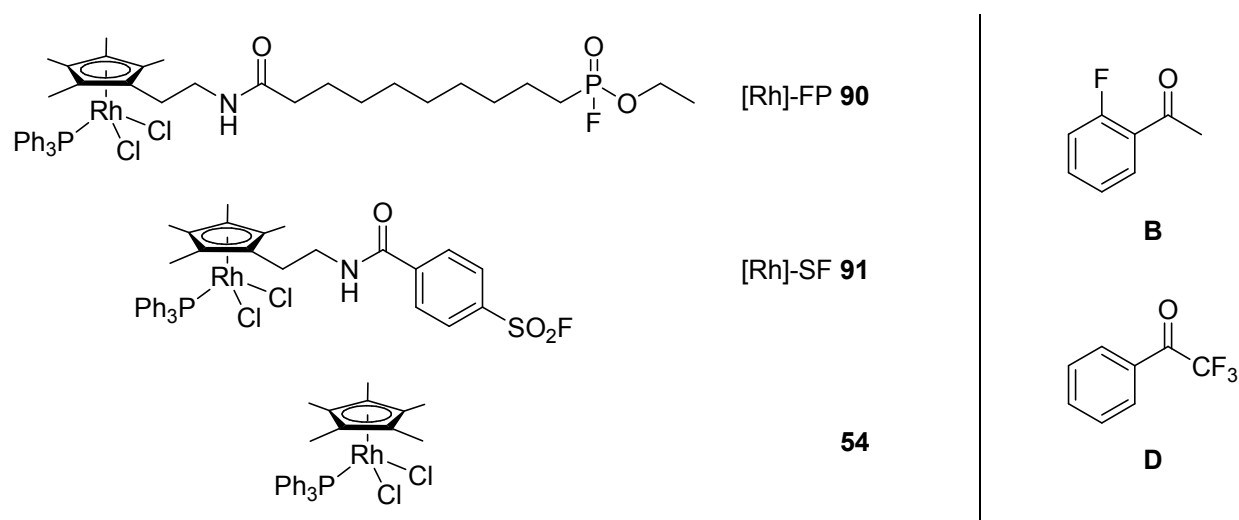


***Figure B39:*** Catalysts ([Rh]-PF **90**, [Rh]-SF **91**) and substrates (**B**, **D**) employed in the catalytic enantioselective transfer hydrogenation of ketones.

The organometallic enzyme hybrid catalysts **106**-**109** were prepared similar to the method described in section B3.11.2. However, no activation reagent is needed for serine proteases. Therefore, an understoichiometric amount of metalla linkers [Rh]-PF **90** and [Rh]-SF **91** was added directly to solutions of α-chymotrypsin or trypsin. To eliminate residual enzyme activity and therefore autolytic cleavage of enzyme present in solution, PMSF was added to the reaction mixture after incubation with the metalla linkers was complete. Finally, an aqueous buffered solution containing sodium formiate was added. The catalytic transfer hydrogenation was initialized by addition of ketone **B**

or **D** (figure B39) to the reaction solution (scheme B57). Homogenous catalyst [Cp*Rh(PPh₃)Cl₂] **54** was treated the same way to guarantee comparability of the transfer hydrogenation results.



| [M]-Al | protease | organometallic enzyme hybrid |
|---|---|---|
| [Rh]-PF **90** | α–chymotrypsin | [Rh]-PF@α–chymotrypsin **106** |
| | trypsin | [Rh]-PF@trypsin          **108** |

| [M]-Al | protease | organometallic enzyme hybrid |
|---|---|---|
| [Rh]-SF **91** | α–chymotrypsin | [Rh]-SF@α–chymotrypsin **107** |
| | trypsin | [Rh]-SF@trypsin          **109** |
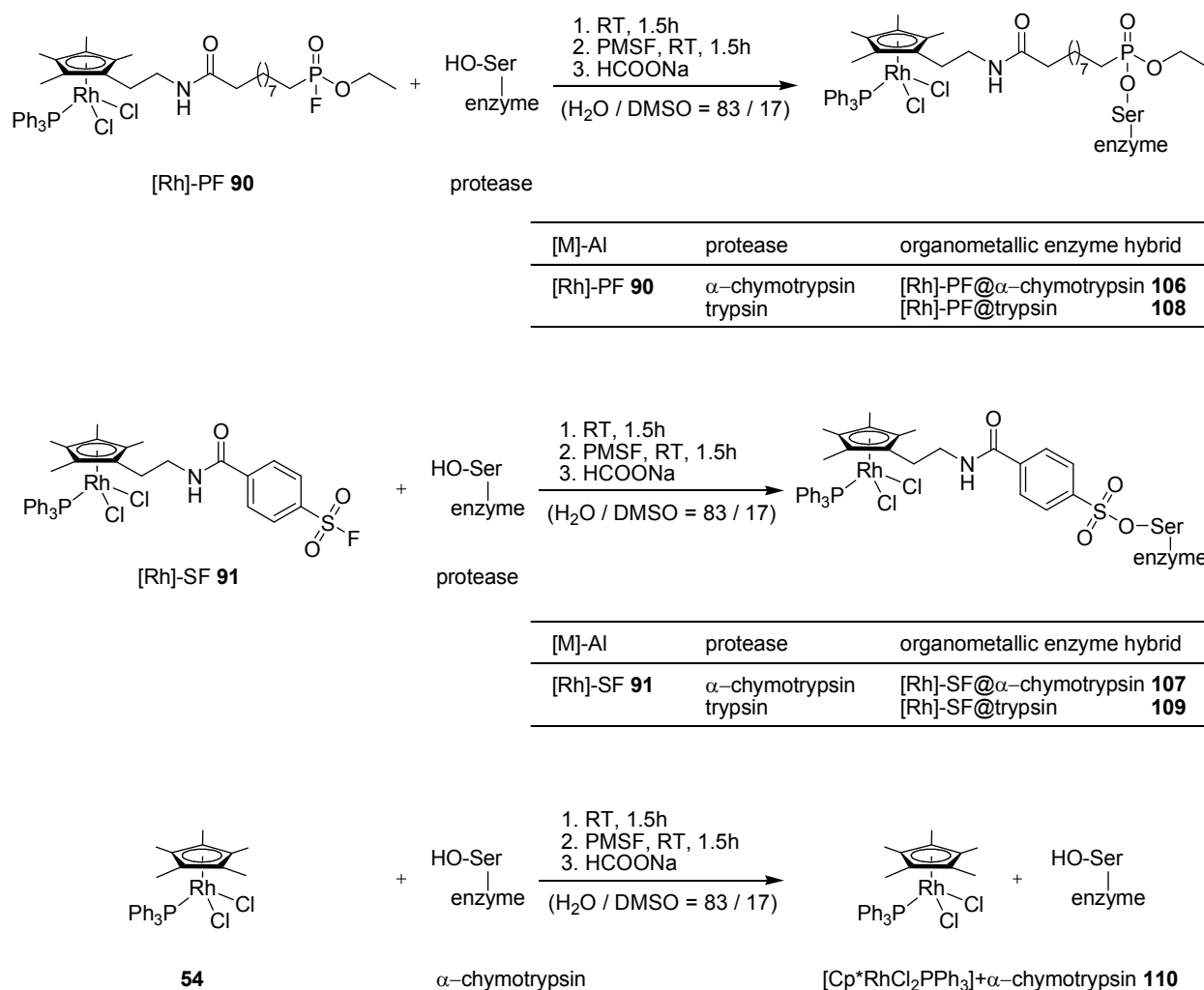
*Scheme B57.* Catalytic transfer hydrogenation of ketones facilitated by linkable organometallic transition metal catalysts and serine proteases.

Organometallic enzyme hybrid [Rh]-SF@α-chymotrypsin **107** was screened under various conditions in order to optimize its performance. For this purpose, different concentrations of formiate buffer were tested, ranging from 1 M to 0.1 M formiate. With higher concentration, increased yields and enantiomeric excesses were observed. This effect might be accounted to small structural changes of the protein scaffold resulting from different ion strengths (table B15, entries 1-3). Significant differences in catalyst performance were observed upon variation of the pH value of the reaction solution. At pH values of 3, yields and enantiomeric excesses were both low (<5 %). With increasing pH, yields increased up to a value of 33 % at a pH of 7 with an enantiomeric excess of 17 %. Enantiomeric excesses of up to 20 % were observed at pH 5, yielding

24 % of 2,2,2-trifluorophenylethanole (table B15, entries 1, 4-6). For increased reaction time, the catalyst performance slightly dropped from 20% to 17% enantiomeric excess. (table B15, entries 1 and 7). Hydrogenations were also carried out with 2'-fluoracetophenone **B** (table B15, entry 8). This experiment revealed the substrate to be hydrogenated much slower than 2,2,2-trifluoroacetophenone **D**. However, the enantioselectivity of [Rh]-SF@α-chymotrypsin **107** was confirmed (16% ee).

*Table B15:* Optimization of reaction conditions employing enzyme hybrid catalyst **107**.

| entry | organometallic enzyme hybrid | substrate | pH | time [h] | formiate [M] | yield [%] | ee [%] |
|-------|------------------------------|-----------|-----|----------|--------------|-----------|--------|
| 1 | [Rh]-SF@α-chymotrypsin **107** | **D** | 5 | 48 | 1.0 | 24 | 20 (*S*) |
| 2 | [Rh]-SF@α-chymotrypsin **107** | **D** | 5 | 48 | 0.4 | 18 | 14 (*S*) |
| 3 | [Rh]-SF@α-chymotrypsin **107** | **D** | 5 | 48 | 0.1 | 10 | 11 (*S*) |
| 4 | [Rh]-SF@α-chymotrypsin **107** | **D** | 8 | 48 | 1.0 | 32 | 13 (*S*) |
| 5 | [Rh]-SF@α-chymotrypsin **107** | **D** | 7 | 48 | 1.0 | 33 | 17 (*S*) |
| 6 | [Rh]-SF@α-chymotrypsin **107** | **D** | 3 | 48 | 1.0 | 4 | 3 (*S*) |
| 7 | [Rh]-SF@α-chymotrypsin **107** | **D** | 5 | 144 | 1.0 | 50 | 17 (*S*) |
| 8 | [Rh]-SF@α-chymotrypsin **107** | **B** | 5 | 144 | 1.0 | 12 | 16 (*S*) |

Total volume of the reaction was 610 µL, substrate / catalyst ratio = 50 / 1. The content of DMSO was 17 vol%. The reaction was carried out at room temperature.

Embedding metalla linker [Rh]-SF **91** did not only result in asymmetric induction, but also in enhanced activity in comparison to the performance of homogenous non-linkable catalyst [Cp*RhPPh$_3$Cl$_2$] **54**.

Catalyst **54** was employed in presence and absence of α-chymotrypsin. In addition to that, metalla linker [Rh]-SF **91** was tested for its performance in absence of α-chymotrypsin (table B16, entries 1-4). Without addition of α-chymotrypsin, only low yields ranging between 3 % and 5 % were obtained (entries 2 and 4). Also when non-linkable complex **54** was tested in the presence of α-chymotrypsin, the observed yield was only 4 % (table B16, entry 3). High yields and enantiomeric excesses were only obtained, when both enzyme and linkable catalyst were present in solution (table B16, entry 1). In all other cases, racemic mixtures of both the (*R*) and the (*S*) enantiomer of 2,2,2-trifluorophenylethanole were obtained.

This confirms that both, the linkable moiety of metalla linker **91** and the protein ligand are crucial not only for the generation of enantiomeric excesses, but also for the

generation of the active catalyst species. Covalent bond formation between linker and enzyme forces the transition metal in close proximity to the enzyme surface. This amplifies the tendency of replacement of labile bound ligands in the transition metal inner sphere by nucleophilic centers on the enzyme surface. By replacement of a chlorine atom or the triphenylphosphine ligand by an amine or amide, the rhodium metal centre should become much more active in transfer hydrogenation reactions, which can easily be concluded from the postulated catalytic cycle.[125] The observed increased activity in case of [Rh]-SF@α-chymotrypsin **107** compared to other catalysts therefore confirms the concept, that the metal centre is localized on the enzyme surface, and ligand exchange has taken place, turning complexes [Rh]-PF **90** or [Rh]-SF **91** into active transfer hydrogenation catalysts (section B3.2.2).

***Table B16:*** Comparison of catalyst performances in dependence of anchoring moiety and presence of enzyme.

| entry | catalyst | substrate | enzyme | linker | yield$^a$ [%] | ee$^a$ [%] |
|:---:|:---:|:---:|:---:|:---:|:---:|:---:|
| 1 | [Rh]-SF@α-chymotrypsin **107** | **D** | yes | yes | 24 | 20 (*S*) |
| 2 | [Rh]-SF **91** | **D** | no | yes | 5 | <1 (*S*) |
| 3 | [Cp*RhCl$_2$PPh$_3$]+α-chymotrypsin **110** | **D** | yes | no | 4 | <1 (*S*) |
| 4 | [Cp*RhCl$_2$PPh$_3$] **54** | **D** | no | no | 3 | <1 (*S*) |

Total volume of the reaction was 610 µL, substrate / catalyst ratio = 50 / 1. The content of DMSO was 17 %. Reaction time was 48 h. The reaction was carried out at room temperature. (a) 2,2,2-trifluoro acetophenone was used as substrate.

Long linker lengths between the rhodium catalyst and the anchoring moiety should lessen enantiomeric excesses, as they allow the catalyst to coordinate to a larger number of different nucleophilic residues on the enzyme and therefore decreases the chiral information transferred. This is supported by employing catalyst [Rh]-PF@ α-chymotrypsin **106** in the catalytic transfer hydrogenation of 2,2,2-trifluoro-acetophenone **D** (table B17, entry 3). Enantiomeric excesses were reduced by a ratio of 2 compared to results obtained with catalyst [Rh]-SF@α-chymotrypsin **107**. Nevertheless, slightly higher enantiomeric excesses of up to 13 % were obtained by using 2'-fluoroacetophenone as substrate (table B17, entry 2). Transfer hydrogenation reactions with enzyme catalyst [Rh]-SF@trypsin **109**, employing trypsin as enzyme, resulted in good yields (29 %), yet, enantiomeric excesses were poor (5 %). This can be accounted to different nucleophilic moieties in the selectivity pockets of the individual enzymes, being in close proximity to the transition metal catalyst. This result again

underlines the advantages of the modular concept of metalla linkers and metalla affinity labels. Without any biological optimizations, yet by simple exchange of the enzyme scaffold, α-chymotrypsin can be concluded to be the more promising candidate for optimization of the hybrid system via directed evolution, as it has been used for different systems before.[96,97]

***Table B17:*** Comparison of different enzyme hybrid catalysts and substrates.

| entry | catalyst | substrate | pH | formiate [M] | yield [%] | ee [%] |
|-------|----------|-----------|-----|--------------|-----------|--------|
| 1 | [Rh]-SF@trypsin **109** | **D** | 5 | 1.0 | 29 | 5 (*S*) |
| 5 | [Rh]-PF@α-chymotrypsin **106** | **D** | 5 | 1.0 | 22 | 9 (*S*) |
| 6 | [Rh]-PF@α-chymotrypsin **106** | **B** | 5 | 1.0 | 5 | 13 (*S*) |

Total volume of the reaction was 610 µL, substrate / catalyst ratio = 50 / 1. The content of DMSO was 17 vol%. The reaction was carried out at room temperature. Reaction time was 48 h.

In addition to screening different reaction conditions and different organometallic enzyme hybrids, their performance in dependence of reaction time was tested. The resulting kinetics are displayed in figure B40. As shown above, 2,2,2-trifluoro-acetophenone **D** is converted significantly faster than 2'-fluoroacetophenone **B**. This is possibly due to the much more electron deficient carbonyl bond in **D**, making it easier for organometallic enzyme hybrid **106** to hydrogenate the substrate.
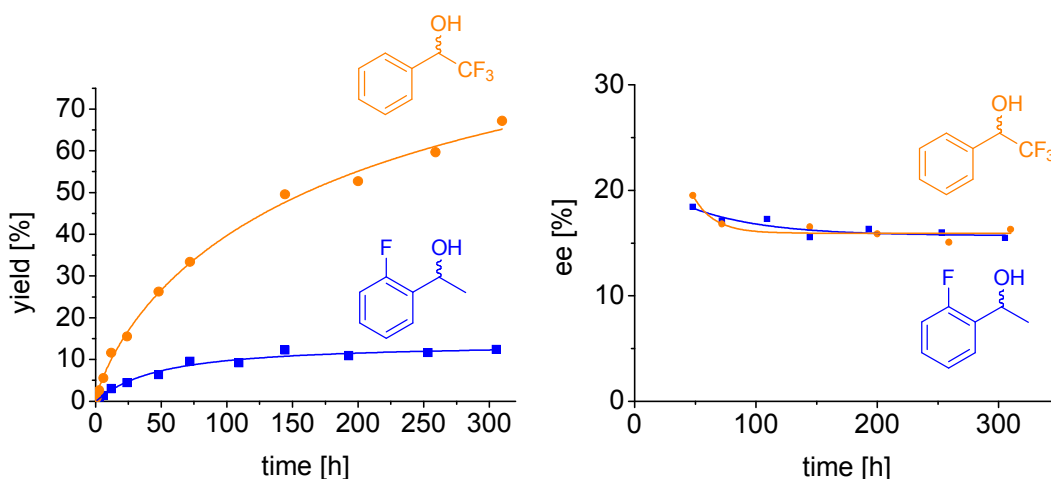


**Figure B40:** Yields and enantiomeric excesses obtained with organometallic enzyme hybrid [Rh]-SF@α-chymotrypsin **107** in the enantioselective transfer hydrogenation of ketones at different reaction times.

For both substrates the enantiomeric excesses observed are initially around 18-20% and only decrease slightly over time. This might be accounted to the enzyme losing its chiral information, which is a result of the enzyme slowly losing its tertiary structure in

the reaction solution. This was to be expected due to the high ion strength of formiate present (500 mM). Nevertheless, even after more than 300 h of reaction time, enantiomeric excesses only decreased by less than 5%. There were several other hydrogenation experiments conducted within this screening, which proved the stability of the respective organometallic enzyme hybrid catalysts. For a complete list of data obtained, please refer to the experimental section, tables C21-C25.

In conclusion, transfer hydrogenation experiments with bifunctional organometallic linkers, consisting of rhodium triphenylphosphine catalysts and anchoring moieties, have confirmed to be applicable as inhibitors for serine proteases. The resulting enzyme hybrid catalysts were applied in the catalytic transfer hydrogenation of ketones, giving up to 70 % yield and enantiomeric excesses up to 20 %.

Furthermore, the enzyme not only acts as scaffold, transferring chiral information, but also activates the transition metal catalyst. This most likely takes place through embedment of the catalyst by first covalent ancourage (mediated by the reactive group) and second by coordinative bond formation between primary or secondary amines on the enzyme surface and the transition metal centre. It is therefore crucial not only for the enantioselectivity, but also for the generation of yields. This and the use of fluoro sulfonic and fluoro phosphonic acids as anchoring moieties for serine proteases are a novel feature for organometallic enzyme hybrids, broadening the scope and applicability of this technology.

## 13. References

[1]     (*a*) G. Winkhaus, H. Singer, *J. Organomet. Chem.* **1967**, *7*, 487-491; (*b*) G. Winkhaus, H. Singer, M. Kricke, *Z. Naturforsch.* **1966**, *21b*, 1109-1110; (*c*) R. A. Zelonka, M. C. Baird, *J. Organomet. Chem.* **1972**, *44*, 383-389; (*d*) R. A. Zelonka, M.C. Baird, *Can. J. Chem.* **1972**, *50*, 3063-3072; (*e*) M. A. Bennett, G. B. Robertson, A. K. Smith, *J. Organomet. Chem.* **1972**, *43*, C41-C43; (*f*) M. A. Bennett, A. K. Smith, *J. Chem. Soc. Dalton Trans.* **1974**, 233-241; (*g*) A. N. Nesmeyanov, A. Z. Rubezhov, *J. Organomet. Chem.* **1979**, *164*, 259-275; (*h*) T. Arthur, T. A. Stephenson, *J. Organomet. Chem.* **1981**, *208*, 369-387; (*i*) E. L. Muetterties, J. R. Bleeke, E. J. Wucherer, *Chem. Rev.* **1982**, *82*, 499-525; (*j*) R. M. Moriarty, U. S. Gill, Y. Y. Ku, *J. Organomet.. Chem.* **1988**, *350*, 157-190; (*k*) M. A. Bennett, *Coord. Chem. Rev.* **1997**, *166*, 225-254.

[2]     D. B. Grotjahn *Coord. Chem. Rev.* **1999**, *190-192*, 1125-1141.

[3]     R. Krämer, *Angew. Chem. Int. Ed.* **1996**, *35*, 1197-1199.

[4]     (*a*) K. Severin, R. Bergs, W. Beck, *Angew. Chem. Int. Ed.* **1998**, *37*, 1634-1654; (*b*) G. Jaouen, A. Vessières, *Acc. Chem. Res.* **1993**, *26*, 361-369; (*c*) P. Köpf-Maier, H. Köpf, *Chem. Rev.* **1987**, *87*, 1137-1152; (*d*) R. Alberto, *J. Organomet. Chem.* **2007**, *692*, 1179-1186; (*e*) D. S. Williams, G. E. Atilla, H. Bregman, A. Arzoumanian, P. S. Klein, E. Meggers, *Angew. Chem. Int. Ed.* **2005**, *44*, 1984-1987; (*f*) H. Bregman, P. J. Carroll, E. Meggers, *J. Am. Chem. Soc.* **2006**, *128*, 877-884; (*g*) J. É. Debreczeni, A. N. Bullock, G. E. Atilla, D. S. Williams, H. Bergman, S. Knapp, E. Meggers, *Angew. Chem. Int. Ed.* **2006**, *45*, 1580-1585; (*h*) C. Streu, E. Meggers, *Angew. Chem. Int. Ed.* **2006**, *45*, 5645-5648.

[5]     P. Haquette, B. Talbi, S. Canaguier, S. Dagorne, C. Fosse, A. Martel, G. Jaouen, M. Salmain, *Tetrahedron Lett.* **2008**, *49*, 4670-4673.

[6]     W. H. Ang, E. Daldini, L. Juillerat-Jeanneret, P. J. Dyson, *Inorg. Chem.* **2007**, *46*, 9048-9050.

[7]     R. M. Moriarty, Y.-Y. Ku, U. S. Gill, *Chem. Commun.* **1987**, 1837-1838.

[8]     A. J. Pearson, K. Lee, *J. Org. Chem.* **1994**, *59*, 2304-2313.

[9]     (*a*) W. S. Sheldrick, A. Gleichmann, *J. Organomet. Chem.* **1994**, *470*, 183-187; (*b*) A. J. Gleichmann, J. M. Wolff, W. S. Sheldrick, *J. Chem. Soc., Dalton Trans.* **1995**, 1549-1554; (*c*) J. M. Wolff, A. J. Gleichmann, C. Schmidt, W. S. Sheldrick,

*J. Inorg. Biochem.* **1995,** *59*, 219; (*d*) J. M. Wolff, W. S. Sheldrick, *J. Organomet. Chem.* **1997**, *531*, 141-149; (*e*) J. M. Wolff, W. S. Sheldrick, *Chem. Ber. Recueil* **1997**, *130*, 981-988; (*f*) D. A. Herebian, C. S. Schmidt, W. S. Sheldrick, C. van Wüllen, *Eur. J. Inorg. Chem.* **1998**, 1991-1998. (*g*) R. Stodt, S. Gencaslan, A. Frodl, C. Schmidt, W. S. Sheldrick, *Inorg. Chim. Acta* **2003**, *355*, 242-253; (*h*) R. Stodt, S. Gencaslan, I. M. Müller, W. S. Sheldrick, *Eur. J. Inorg. Chem.* **2003**, 1873-1882.

[10]   (*a*) R. S. Koefod, K. R. Mann, *J. Am. Chem. Soc.* **1990**, *112*, 7287–7293; (*b*) J. W. Janetka, D. H. Rich, *J. Am. Chem. Soc.* **1995**, *117*, 10585–10586; (*c*) R. M. Fairchild, K. T. Holman, *Organometallics* **2007**, *26*, 3049-3053.

[11]   (*a*) R. H. Fish, G. Jaouen, *Organometallics* **2003**, *22*, 2166-2177; (*b*) R. E. Morris, R. E. Aird, P. del S. Murdoch, H. Chen, J. Cummings, N. D. Hughes, S. Parsons, A. Parkin, G. Boyd, D. I. Jodrell, P. J. Sadler, *J. Med. Chem.* **2001**, *44*, 3616-3621; (*c*) R. E. Aird, J. Cummings, A. A. Ritchie, M. Muir, R. E. Morris, H. Chen, P. J. Sadler, D. I. Jodrell, *Br. J. Cancer* **2002**, *86*, 1652-1657. (*d*) S. J. Dougan, P. J. Sadler, *Chimia* **2007**, *61*, 704-715; (*e*) R. Schuecker, R. O. John, M. A. Jakupec, V. B. Arion, B. K. Keppler, *Organometallics*; (*f*) W. F. Schmid, R. O. John, V. B. Arion, M. A. Jakupec, B. K. Keppler, *Organometallics* **2007**, *26*, 6643-6652.

[12]   (*a*) A. F. A. Peacock, A. Habtemariam, R. Fernandez, V. Walland, F. P. A. Fabbiani, S. Parsons, R. E. Aird, D. I. Jodrell, P. J. Sadler, *J. Am. Chem. Soc.* **2006**, *128*, 1739-1748; (*b*) A. F. A. Peacock, S. Parsons, P. J. Sadler, *J. Am. Chem. Soc.* **2007**, *129*, 3348-3357; (*c*) H. Kostrhunova, J. Florian, O. Novakova, A. F. A. Peacock, P. J. Sadler, V. Brabec, *J. Med. Chem.* **2008**, *51*, 3635–3643; (*d*) J. C. Gray, A. Habtemariam, M. Winnig, W. Meyerhof, P. J. Sadler, *J. Biol. Inorg. Chem.* **2008**, *13*, 1111-1120.

[13]   K. Severin, *Chem. Commun.* **2006**, 3859-3867.

[14]   (*a*) W. Baratta, W. A. Herrmann, R. M. Kratzer, P. Rigo, *Organometallics* **2000**, *19*, 3664-3669; (*b*) W. Baratta, E. Herdtweck, W. A. Herrmann, P. Rigo, J. Schwarz, *Organometallics* **2002**, *21*, 2101-2106; (*c*) S. Gladiali, E. Alberico, *Chem. Soc. Rev.* **2006**, *35*, 226-236.

[15]    K.-J. Haack, S. Hashiguchi, A. Fujii, T. Ikariya, R. Noyori *Angew. Chem. Int. Ed.* **1997**, *36*, 285-288.

[16]    (*a*) J. Hannedouche, G. J. Clarkson, M. Wills, *J. Am. Chem. Soc.* **2004**, *126*, 986-987; (*b*) A.M. Hayes, D.J. Morris, G.J. Clarkson, M. Wills, *J. Am. Chem. Soc.* **2005**, *127*, 7318-7319; (*c*) D.J. Morris, A.M. Hayes, M. Wills, *J. Org. Chem.* **2006**, *71*, 7035-7044.

[17]    C. Daguenet, R. Scopelliti, P.J. Dyson, *Organometallics* **2004**, *23*, 4849-4857.

[18]    (*a*) L. Ackermann, A. Althammer, R. Born, *Angew. Chem. Int. Ed.* **2006**, *45*, 2619-2622; (*b*) A. Fürstner, L. Ackermann, *Chem. Comm.* **1999**, 95-96.

[19]    (*a*) M. Creus, A. Pordea, T. Rossel, A. Sardo, C. Letondor, A. Ivanova, I. LeTrong, R. E. Stenkamp, T. R. Ward, *Angew. Chem. Int. Ed.* **2008**, *47*, 1400-1404; (*b*) J. Steinreiber, T. R. Ward, *Coord. Chem. Rev.* **2008**, *252*, 751-766.

[20]    R. Stodt, S. Gencaslan, I. M. Müller, W. S. Sheldrick, *Eur. J. Inorg. Chem.* **2003**, 1873-1882.

[21]    (*a*) J. Soleimannejad, A. Sisson, C. White, *Inorg. Chim. Acta* **2003**, *352*, 121-128; (*b*) G. Marconi, H. Baier, F. W. Heinemann, P. Pinto, H. Pritzkow, U. Zenneck, *Inorg. Chim. Acta* **2003**, *352*, 188-200; (*c*) J. Soleimannejad, C. White, *Organometallics* **2005**, *24*, 2538-2541.

[22]    H. Dialer, P. Mayer, K. Polborn, W. Beck, *Eur. J. Inorg. Chem.* **2001**, 1051-1055.

[23]    T. Ohnishi, Y. Miyaki, H. Asano, H. Kurosawa, *Chem. Lett.* **1999**, *28*, 809-810.

[24]    (*a*) B. Çetinkaya, S. Demir, I. Özdemir, L. Toupet, D. Sémeril, C. Bruneau, P. H. Dixneuf, *New J. Chem.* **2001**, *25*, 519-521; (*b*) B. Çetinkaya, S. Demir, I. Özdemir, L. Toupet, D. Sémeril, C. Bruneau, P. H. Dixneuf, *Chem. Eur. J.* **2003**, *9*, 2323-2330; (*c*) I. Özdemir, S. Demir, Bekir Çetinkaya, L. Toupet, R. Castarlenas, C. Fischmeister, P. H. Dixneuf, *Eur. J. Inorg. Chem.* **2007**, 2862-2869.

[25]    I. Ogatha, R. Iwata, *Tetrahedron* **1973**, *29*, 2753.

[26]    J. Ros, E. de la Encarnación, Á. Alvarez-Larena, J. F. Piniella, I. Moldes, *J. Organomet. Chem.* **1998**, *566*, 165-174.

[27]    C. Daguenet, R. Scopelliti, P. J. Dyson, *Organometallics* **2004**, *23*, 4849-4857.

[28]    F. Joó, J. Kovács, A. C. Bényei, Á. Kathó, *Angew. Chem. Int. Ed.* **1998**, *37*, 969.

[29]    F. Joó, *Acc. Chem. Res.* **2002**, 35, 738.

[30]   G. Winkhaus, H. Singer, *J. Organomet. Chem.* **1967**, *7*, 487-491.

[31]   R. Brückner, *Reaktionsmechanismen. Organische Reaktionen, Stereochemie, moderne Synthesemethoden*, Spektrum Akademischer Verlag **2004**.

[32]   T. Reiner, *Master Thesis*, Technische Universität München, **2006**.

[33]   (a) G. Winkhaus, H. Singer, *J. Organomet. Chem.* **1967**, *7*, 487-491; (b) G. Winkhaus, H. Singer, M. Kricke, *Z. Naturforsch.* **1966**, *21b*, 1109-1110; (c) R. Zelonka, M. C. Baird, *J. Organomet. Chem.* **1972**, *44*, 383-389; (d) R. A. Zelonka, M. C. Baird, *Can. J. Chem.* **1972**, *50*, 3063-3072; (e) M. A. Bennett, G. B. Robertson, A. K. Smith, *J. Organomet. Chem.* **1972**, *43*, C41-C43; (f) M. A. Bennett, A. K. Smith, *J. Chem. Soc. Dalton Trans.* **1974**, 233-241; (g) A. N. Nesmeyanov, A. Z. Rubezhov, *J. Organomet. Chem.* **1979**, *164*, 259-275; (h) M. A. Bennett, *Coord. Chem. Rev.* **1997**, *166*, 225-254.

[34]   T. Arthur, T. A. Stephenson, *J. Organomet. Chem.* **1981**, *208*, 369-387.

[35]   M. A. Bennet, A. K. Smith, *J. Chem. Soc., Dalton Trans.* **1974**, 233-241.

[36]   L. Vieille-Petit, B. Therrien, G. Süss-Fink, *Eur. J. Inorg. Chem.* **2003**, *20*, 3707-3711.

[37]   L. Vieille-Petit, S. Unternährer, B. Therrien, G. Süss-Fink, *Inorg. Chem. Acta* **2003**, *355*, 335-339.

[38]   L. Vielle-Petit, G. Süss-Fink, B. Therrien, T. R. Ward, H. Stckli-Evans, G. Labat, L. Karmazin-Brelot, A. Neels, T. Buergi, R. G. Finke, C. M. Hagen, *Organometallics* **2005**, *24(25)*, 6104-6119.

[39]   G. Süss-Fink, B. Therrien, *Inorg. Chem. Acta* **2006**, *359*, 4350-4354.

[40]   M. Hesse, H. Meier, B. Zeeh, *Spektroskopische Methoden in der organischen Synthese*, Thieme, 6th Ed., **2002**.

[41]   G. Süss-Fink, B. Therrien, L. Vieille-Petit, M. Tschan, V. B. Romakh, T. R. Ward, M. Dadras, G. Laurenczy, *J. Organomet. Chem.* **2004**, *689*, 1362-1369.

[42]   J. B. Mann, T. L. Meek, E. T. Knight, J. F. Capitani, L. C. Allen, *J. Am. Chem. Soc.* **2000**, *122*, 5132-5137.

[43]   H. E. Gottlieb, V. Kotlyar, A. Nudelman, *J. Org. Chem.* **1997**, *62*, 7512-7515.

[44]   (a) M. Chandra, D. S. Pandey, M. C. Puerta, P. Valerga *Acta Crystallogr., Sect.E:Struct.Rep.Online* **2002**, *E58*, m28-m29; (b) T. J.Beasley, R. D.Brost, C. K. Chu, S. L.Grundy, S. R.Stobart, *Organometallics* **1993**, *12*, 4599-4606.

[45]  W. C. Hamilton, J. A. Ibers, *Hydrogen bonding in solids. Methods of Molecular Structure Determination*, W. A. Benjamin Inc. New York **1968**.

[46]  T. Sixt, W. Kaim, W. Preetz, *Z. Naturforsch. B* **2000**, *55*, 235-237.

[47]  A. Skolaut, J. Rétey, *Arch. Biochem. Biophys.* **2001**, *393*, 187-191.

[48]  G. Zvilichovsky, V. Gurvich, *Tetrahedron* **1995**, *51*, 5479-5490.

[49]  Due to decarboxylation, the IR spectrum of **5** does not exhibit any CO bond stretching frequencies.

[50]  R. Grewe, H.-W. Otto *Chem. Ber.* **1959**, *92*, 644-651.

[51]  Y. Miyaki, T. Onishi, H. Kurosawa, *Inorg. Chim. Acta* **2000**, *300-302*, 369-377.

[52]  C. Scolaro, T. J. Geldbach, S. Rochat, A. Dorcier, C. Gossens, A. Bergamo, M. Cocchietto, I. Tavernelli, G. Sava, U. Rothilsberger, P. J. Dyson, *Organometallics*, **2006**, *25*, 756-765.

[53]  M. Melchart, A. Habtemariam, O. Novakova, S. A. Moggach, F. P. A. Fabbiani, S. Parsons, V. Brabec, P. J. Sadler, *Inorg. Chem.* **2007**, *46*, 8950-8962.

[54]  (*a*) W.-T. Wong, T.-C. Lau, *Acta Cryst. Sect. C* **1994**, *C50*, 1406-1407; (*b*) M. R. J. Elsegood, D. A. Tocher, *Acta Cryst. Sect. C* **1995**, *C51*, 40-42.

[55]  A. Dijksman, J.M. Elzinga, Y.-X. Li, I. W. C. E. Arends, R. A. Sheldon, *Tetrahedron: Asymmetry* **2002**, *13*, 879-884.

[56]  Y. Fukudome, H. Naito, T. Hata, H. Urabe, *J. Am. Chem. Soc.* **2008**, *130*, 1820-1821.

[57]  The structure was also solved in space group *P*-1, as suggested by checkcif. This leads to higher R-values and significant disordering, resulting in the necessity of introducing a split model. Also, the solvent molecules cannot be refined. Furthermore, a partial inversion of chirality at the α-CH phenylalaine takes place.

[58]  (a) P. W. Atkins, *Physical Chemistry*, Wiley VCH, New York, **1994**; (b) R. R. Raposo, E. Calviño, M. A. Esteso, J. Electroanal. Chem. 2008, 617, 157-163; (c) U. J. Jáuregui-Haza, E. J. Pardillo-Fontdevila, A. M. Wilhelm, H. Delmas, *Lat. Am. App. Res.* **2004** *34*, 71-74.

[59]  Enantiomer separations were carried out using a Varian capillary column, fused silica 25 m x 0.25 mm, coated cp chirasil-dex CB df = 0.25.

[60]  (a) P. Jutzi, U. Siemeling, *J. Organomet. Chem.* **1995**, *500*, 175-185; (b) C. Janiak, H. Schumann, *Adv. Organomet. Chem.* **1991**, *33*, 291-393; (c) N. J. Coville, K. E. du Plooy, W. Pickl, *Coord. Chem. Rev.* **1992**, *116*, 1-267.

[61]  P. Jutzi, J. Dahlhaus, *Synthesis* **1993**, 684-686.

[62]  (a) P. Jutzi, J. Dahlhaus, M. O. Kristen, *J. Organomet. Chem.* **1993**, *450*, C1-C3; (b) P. Jutzi, J. Dahlhaus, M. J. Bangel, *J. Organomet. Chem.* **1993**, *460*, C13-C15.

[63]  C. Müller, V. Derk, P. Jutzi, *J. Organomet. Chem.* **2000**, *600*, 127-143.

[64]  (a) A. I. Philippopooulos, N. Hadjiliadis, C. E. Hart, B. Donnadieu, P. C. McGowan, R. Poilblanc, *Inorg. Chem.* **1997**, *36*, 1842-1849; (b) P. C. McGowan, C. E. Hart, B. Donnadieu, R. Poilblanc, *J. Organomet. Chem.* **1997**, *528*, 191-194; (c) P. K. Chan, W. K. Leong, K. I. Krummel, M. V. Garland, *Eur. J. Inorg. Chem.* **2006**, 1568-1572.

[65]  P. Jutzi, M. O. Kristen, B. Neumann, H.-G. Stammler, *Organometallics* **1994**, *13*, 3854-3861.

[66]  (a) A. I. Philippopoulos, B. Donnadieu, R. Poilblanc, N. Hadjiliadis, *J. Organomet. Chem.* **1999**, *582*, 286-291; (b) A. I. Philippopoulos, R. Poilblanc, N. Hadjiliadis, *Inorg. Chim. Acta* **1998**, *283*, 24-29.

[67]  (a) J. Okuda, K. H. Zimmermann, E. Herdtweck, *Chem. Ber.* **1989**, *122*, 1645-1647; (b) J. Okuda, K. H. Zimmermann, *Angew. Chem. Int. Ed.* **1991**, *30*, 430-431; (c) K. H. Zimmermann, R. S. Pilato, I. T. Horváth, J. Okuda, *Organometallics* **1992**, *11*, 3935-3937.

[68]  F. K. Cheung, C. Lin, F. Minissi, A. L. Crivillé, M. A. Graham, D. J. Fox, M. Wills, *Org. Lett.* **2007**, *9*, 4659-4662.

[69]  (a) J. A. Ayllon, S. F. Sayers, S. Sabo-Etienne, B. Donnadieu, B. Chaudret, E. Clot, *Organometallics* **1999**, *18*, 3981-3990; (b) T. Matsubara, K. Hirao, *Organometallics* **2001**, *20*, 5759-5868; (c) Y. F. Lam, C. Q. Yin, C. H. Yeung, S. M. Ng, G. Jia, C.P. Lau, *Organometallics* **2002**, *21*, 1898-1902; (d) S. Fuqiang, *Organometallics* **2006**, *25*, 4034-4037.

[70]  (a) M. Cais, E. Slovin, L. Snarsky, *J. Organomet. Chem.* **1978**, *160*, 223-230; (b) B. Ferber, S. Top, A. Vessières, R. Welter, G. Jaouen, *Organometallics* **2006**, *25*, 5730-5739.

[71]   M. E. Wilson, G. M. Whitesides, *J. Am. Chem. Soc.* **1978**, *100*, 306-307.

[72]   (a) G. Klein, N. Humbert, J. Gradinaru, A. Ivanova, F. Gilardoni, U. E. Rusbandi, T. R. Ward, *Angew. Chem. Int. Ed.* **2005**, *44*, 7764-7767. (b) M. Creus, T. R. Ward, *Org. Biomol. Chem.* **2007**, *5*, 1835-1844.

[73]   J. Lemke, N. Metzer-Nolte, *Eur. J. Inorg. Chem.* **2008**, 3359-3366.

[74]   P. Haquette, B. Talbi, S. Canaguier, S. Dagorne, C. Fosse, A. Martel, G. Jaouen, M. Salmain, *Tet. Lett.* **2008**, *49*, 4670-4673.

[75]   W. A. Wlassoff, G. C. King, *Nucleic Acids Res.* **2002**, *30*, e58/1-e58/7.

[76]   For reviews see: (a) G. Jaouen, A. Vessières, I. S. Butler, *Acc. Chem. Res.* **1993**, *26*, 361-369; (b) K. Severin, R. Bergs, W. Beck, *Angew. Chem. Int. Ed.* **1998**, *37*, 1635-1654; (c)  D. B. Grotjahn, *Coord. Chem. Rev.* **1999**, *190-192*, 125; (d) R. Alberto, *J. Organomet. Chem.* **2007**, *692*, 1179-1186.

[77]   Y.-F. Xu, Y. Shen, Z. Pang, *J. Organomet. Chem.* **2004**, *689*, 823-832.

[78]   (a) J. A. Miguel-Garcia, P. M. Maitlis, *J. Chem. Soc., Chem. Commun.* **1990**, 1472-1473; (b) J. A. Miguel-Garcia, H. Adams, N. A. Bailey, P. M. Maitlis, *J. Chem. Soc., Dalton Trans.* **1992**, 131-137; (c) R. Stodt, S. Gencaslan, I. M. Müller, W. S. Sheldrick, *Eur. J. Inorg. Chem.* **2003**, 1873-1882.

[79]   (a) H. Dialer, P. Mayer, K. Polborn, W. Beck, *Eur. J. Inorg. Chem.* **2001**, 1051-1055; (b) H. Dialer, W. Steglich, W. Beck, *Tetrahedron* **2001**, *57*, 4855-4861;

[80]   (a) Y. Miyaki, T. Onishi, H. Kurosawa, *Inorg. Chim. Acta* **2000**, *300*, 369-377; (b) C. Scolaro, T. J. Geldbach, S. Rochat, A. Dorcier, C. Gossens, A. Bergamo, M. Cocchietto, I. Tavernelli, G. Sava, U. Rothlisberger, P. J. Dyson, *Organometallics* **2006**, *25*, 756-765; (c) A. Casini, C. Gabbiani, F. Sorrentino, M. P. Rigobello, A. Bindoli, T. J. Geldbach, A. Marrone, N. Re, C. G. Hartinger, P. J. Dyson, L. Messori, *J. Med. Chem.* **2008**, *51*, 6773-6781.

[81]   C. White, A. Yates, P. M. Maitlis, D. M. Heinekey, *Inorg. Synth.* **1992**, *29*, 228-234.

[82]   (a) A. Avey, D. R. Tyler, *Organometallics* **1992**, *11*, 3856-3863; (b) O. Segnitz, M. Winter, K. Merz, R. Fischer, *Eur. J. Inorg. Chem.* **2000**, 2077-2085.

[83]   C. M. Fendrick, L. D. Schertz, V. W. Day, T. J. Marks, *Organometallics* **1988**, *7*, 1828-1838.

[84] D. van Leusen, D. J. Beetstra, B. Hessen, J. H. Teuben, *Organometallics* **2000**, *19*, 4084-4089.

[85] S. Carrà, R. Ugo, *Inorg. Chim. Acta, Rev.* **1967**, *1*, 49-63.

[86] (a) A. I. Philippopoulos, R. Bau, R. Poilblanc, N. Hadjiliadis, *Inorg. Chem.* **1998**, *37*, 4822-4827; (b) E. Nakatani, Y. Takai, H. Kurosawa, *J. Organomet. Chem.* **2007**, *692*, 278-285.

[87] (a) J. W. Kang, K. Moseley, P. M. Maitlis, *J. Am. Chem. Soc.* **1969**, *91*, 5970-5977; (b) B. L. Booth, R. N. Haszeldine, M. Hill, *J. Organomet. Chem.* **1969**, *16*, 491-496.

[88] B. Paz-Michel, M. Cervantes-Vazquez, M. A. Paz-Sandoval, *Inorg. Chim. Acta* **2008**, *361*, 3094-3102.

[89] V. Tedesco, W. von Philipsborn, *Mag. Res. Chem.* **1996**, *34*, 373-376.

[90] W. D. Jones, V. L. Kuykendall, *Inorg. Chem.* **1991**, *30*, 2615-2622, and references therein.

[91] (a) *Comprehensive Asymmetric Catalysis*, Vol. I ± III (Eds.: E. N. Jacobsen, A. Pfaltz, H. Yamamoto), Springer, Berlin, **1999**; (b) H. Brunner, W. Zettlmeier, *Handbook of Enantioselective Catalysis with Transition Metal Compounds*, Vol. I ± II, VCH, Weinheim, **1993**; (c) R. Noyori, *Asymmetric Catalysis in Organic Synthesis*, Wiley, New York, **1994**; (d) *Catalytic Asymmetric Synthesis* (Ed.: I. Ojima), VCH, Weinheim, **1993**.

[92] (a) H. G. Davies, R. H. Green, D. R. Kelly, S. M. Roberts, *Biotransformations in Preparative Organic Chemistry: The Use of Isolated Enzymes and Whole Cell Systems in Synthesis*, Academic Press, London, **1989**; (b) C. H. Wong, G. M. Whitesides, *Enzymes in Synthetic Organic Chemistry*, Pergamon, Oxford, **1994** (Tetrahedron Organic ChemistrySeries , Vol. 12); (c) *Enzyme Catalysis in Organic Synthesis: A Comprehensive Handbook*, Vol. I-II (Eds.: K. Drauz, H. Waldmann), VCH, Weinheim, **1995**; (d) K. Faber, *Biotransformations in Organic Chemistry*, 3rd ed., Springer, Berlin, **1997**.

[93] (a) J. Steinreiber, T. R. Ward, *Coord. Chem. Rev.* **2008**, *252*, 751-766; (b) D. Qi, C.-M. Tann, D. Haring, M. D. Distefano, *Chem. Rev.* **2001**, *101*, 3081-3111.

[94] M. E. Wilson, G. M. Whitesides, *J. Am. Chem. Soc.* **1978**, *100*, 306-307.

[95]    (a) M. T. Reetz, M. Rentzsch, A. Pletsch, M. Maywald, *Chimia*, **2002**, *56*, 721-723; (b) M. T. Reetz, *Proc. Natl. Acad. Sci.* **2004**, *101*, 5716-5722; (c) M. T. Reetz, *Tetrahedron* **2002**, *58*, 6595-6602; (d) M. T. Reetz, *Angew. Chem. Int. Ed.* **2001**, *40*, 284-310; (e) M. T. Reetz, *Angew. Chem. Int. Ed.* **2002**, *41*, 1335-1338.

[96]    (a) M. Reetz, M. Rentzsch, A. Pletsch, M. Maywald, P. Maiwald, J. J.-P. Peyralans, A. Maichele, Y. Fu, N. Jiao, F. Hollmann, R. Mondière, A. Taglieber, *Tetrahedron* **2007**, *63*, 6404-6414; (b) J. R. Carey, S. K. Ma, T. D. Pfister, D. K. Garner, H. K. Kim, J. A. Abramite, Z. Wang, Z. Guo, Y. Lu, *J. Am. Chem. Soc.* **2004**, *126*, 10812-10813; (c) R. R. Davies, M. D. Distefano, *J. Am. Chem. Soc.* **1997**, *119*, 11643-11652; (d) L. Panella, J. Broos, J. Jin, M. W. Fraaije, D. B. Janssen, M. Jeronimus-Stratingh, B. L. Feringa, A. J. Minnaard, J. G. de Vries, Chem. Comm. 2005, 5656-5658; (e) J. G. de Vries, L. Lefort, *Chem. Eur. J.* **2006**, *12*, 4722-4734; (f) P. Haquette, M. Salmain, K. Svedlung, A. Martel, B. Rudolf, J. Zakrzewski, S. Cordier, T. Roisnel, C. Fosse, G. Jaouen, *ChemBioChem* **2007**, *8*, 224-231; (g) J. Pierron, C. Malan, M. Creus, J. Gradinaru, I. Hafner, A. Ivanova, A. Sardo, T. R. Ward, *Angew. Chem. Int. Ed.* **2008**, *47*, 701-705; (h) C. A. Kruithof, H. P. Dijkstra, M. Lutz, A. L. Spek, M. R. Egmond, R. J. M. Klein Gebbink, G. van Koten, *Eur. J. Inorg. Chem.* **2008**, 4425-4432.

[97]    (a) G. Klein, N. Humbert, J. Gradinaru, A. Ivanova, F. Gilardoni, U. E. Rusbandi, T. R. Ward, *Angew. Chem. Int. Ed.* **2005**, *44*, 8864-7767; (b) M. Creus, T. R. Ward, *Org. Biomol. Chem.* **2007**, *5*, 1835-1844. (c) T. R. Ward, *Angew. Chem. Int. Ed.* **2008**, *47*, 7802-7803.

[98]    (a) T. R. Ward, *Chem. Eur. J.* **2005**, *11*, 3798-3804; (b) *"Avidin–Biotin Technology": Methods Enzymol.* **1990**, 184, whole volume.

[99]    M. Creus, A. Pordea, T. Rossel, A. Sardo, C. Letondor, A. Ivanova, I. LeTrong, R. E. Stenkamp, T. R. Ward, *Angew. Chem. Int. Ed.* **2008**, *47*, 1400-1404.

[100]   P. Haquette, B. Talbi, S. Canaguier, S. Dagorne, C. Fosse, A. Martel, G. Jaouen, M. Salmain, *Tetrahedron Lett.* **2008**, *49*, 4670-4673.

[101]   J. C. Powers, J. L. Asgian, Ö. D. Ekici, K. E. James, *Chem. Rev.* **2002**, *102*, 4639-4750.

[102]  (a) M. Ferrer, O. Golyshina, A. Beloqui, P. N. Golyshin, *Curr. Opin. Microbiol.* **2007**, *10*, 207-214; (b) D. W. Hough, M. J. Danson, *Curr. Opin. Chem. Biol.* **1999**, *3*, 39-46; (c) D. C. Demirjian, F. Moris-Varas, C. S. Cassidy, *Curr. Opin. Chem. Biol.* **2001**, *5*, 144-151.

[103]  (a) Y. Yabe, D. Guillaume, D. H. Rich, *J. Am. Chem. Soc.* **1988**, *110*, 4043-4044; (b) K. I. Varughese, F. R. Ahmed, P. R. Carey, S. Hasnain, C. P. Huber, A. C. Storer, *Biochemistry* **1989**, *28*, 1330-1332; c) K. Matsumoto, D. Yamamoto, H. Ohishi, K. Tomoo, T. Ishida, M. Inoue, T. Sadatome, K. Kitamura, H. Mizuno, *FEBS Lett.* **1989**, *245*, 177-180.

[104]  K. A. H. Chehade, A. Baruch, S. H. L. Verhelst, M. Bogyo, *Synthesis* **2005**, *2*, 240-244.

[105]  F. Sarabia, A. Sánchez-Ruiz, S. Chammaa, *Bioorg. Med. Chem.* **2005**, *13*, 1691-1705.

[106]  T. W. Greene, P. G. M. Wuts, *Protective Groups in Organic Synthesis*, John Wiley & Sons, Inc., 3rd Ed. New York, **1999**.

[107]  C. Parkes, A. A. Kembhavi, A. J. Barrett, *Biochem. J.* **1985**, *230*, 509-516.

[108]  M. Tamai, C. Yokoo, M. Murata, K. Oguma, K. Sota, E. Sato, Y. Kanaoka, *Chem. & Pharm. Bull.* **1987**, *35*, 1098-1104.

[109]  C. Giordano, R. Calabretta, C. Gallina, V. Consalvi, R. Scandurra, F. Chiaia Noya,C. Franchini, *Eur. J. Med. Chem.* **1993**, *28*, 917-926.

[110]  A. Francis, C. Sundberg, R. J. Sundberg, *Advanced Organic Chemistry Part B: Reactions and Synthesis*, Springer, **2007**, 2nd edition.

[111]  Y. Liu, M. P. Paricelli, B. F. Cravatt, *PNAS* **1999**, *96*, *26*, 14694-14699.

[112]  (a) D. Kidd, Y. Liu, B. F. Cravatt, *Biochemistry* **2001**, *40*, 4005-4015; (b) M. J. Evans, B. F. Cravatt, *Chem.Rev.* **2006**, *106*, 3279-3301.

[113]  R. P. Singh, J. M. Shreeve, *Synthesis* **2002**, *17*, 2561-2578.

[114]  A. Mucha, P. Kafarski; *Tetrahedron* **2002**, *58*, 5855-5863.

[115]  J. Oleksyszyn, J. C. Powers, *Biochemistry*, **1991**, *30*, 485-493.

[116]  J. Oleksyszyn, L. Subotkowska, P. Mastalerz, *Synthesis* **1979**, 985-986.

[117]  H. Hoffmann, H. Förster, *Mh. Chem.* **1968**, *99*, 380-388.

[118]  G. Papeo, P. Giordano, M. G. Brasca, F. Buzzo, D. Caronni, F. Ciprandi, N. Mongelli, M. Veronesi, A. Vulpetti, C. Dalvit, *J. Am. Chem. Soc.* **2007**, *129*, 5665-5672.

[119]  I. W. McNae, K. Fishburne, A. Habtemariam, T. M. Hunter, M. Melchart, F. Wang, M. D. Walkinshaw, P. J. Sadler, *Chem. Commun.* **2004,** 1786-1787.

[120]  I. Span, *Diplomarbeit*, Technische Universität München, **2008**.

[121]  A. Schlichtiger, *PhD thesis*, Technische Universität München, **2009**.

[122]  (a) S. Tokura, N. Nishi, J. Noguchi, *J. Biochem.* **1971**, *69*, 599-600; (b) E. Salih, J. P. G. Malthouse, D. Kowlessur, M. Jarvis, M. O'Driscoll, K. Brocklehurst, *Biochem. J.* **1987**, *247*, 181-193; (c) M. M. Fernandez, D. S. Clark, H. W. Blanch, *Biotech. Bioeng.* **1991**, *37*, 967-972.

[123]  (a) P. J. Dyson, D. J. Ellis, G. Laurenczy, *Adv. Synth. Catal.* **2003**, *345*, 211-215; (b) T. J. Geldbach, G. Laurenczy, R. Scopelliti, P. J. Dyson, *Organometallics* **2006**, *25*, 733-742; (c) A. B. Chaplin, P. J. Dyson, *Organometallics* **2007**, *26*, 4357-4360; (d) P. Govindaswamy, J. Canivet, B. Therrien, G. Suess-Fink, P. Stepnicka, J. Ludvik, *J. Organomet. Chem.* **2007**, *692*, 3664-3675; (e) A. D. Selmeczy, W. D. Jones, *Inorg. Chim. Acta* **2000**, *300-302*, 138-150.

[124]  B. J. Gour-Salin, P. Lachance, M.-C. Magny, C. Plouffe, R. Ménard, A. C. Storer, *Biochem. J.* **1994**, *299*, 389-392.

[125]  M. Yamakawa, H. Ito, R. Noyori, *J. Am. Chem. Soc.* **2000**, *122*, 1466-1478.

# C | Experimental

# 1.    General

## 1.1.  Schlenk technique

All organometallic conversions were conducted using standard Schlenk technique. Organic reactions were carried out under Schlenk conditions, if it was necessary. As inert gas, Argon was used (welding argon 4.6), which was applied without further purification. Dry solvents were only used if it was necessary. Sealed glass equipment was secured with mercury-free pressure-relief valves (Normag Glassware). The Schlenk-line had a two-way system, it was attached to both a rotary vane pump (approx. $1 \cdot 10^{-2}$ - $3 \cdot 10^{-1}$ mbar) and an argon inlet.

## 1.2.  Glove-Box technique

Highly air and moisture-sensitive compounds were prepared and handled in a Glove-Box (MBraun), which had an Argon inert gas atmosphere (welding argon 4.6). They were stored at -45°C.

## 1.3.  Solvent preparation

Diethylether, hexane, pentane, dichloromethane, tetrahydrofurane, acetonitrile, toluene, and benzene were obtained from a solvent drying plant (MBraun, MB SPS). Methanol and ethanol were stirred over sodium and thereafter distilled and stored under inert atmosphere. Triethylamine was stirred for 24 h over $LiAlH_4$ and thereafter distilled and stored under inert atmosphere. Dimethylsulfoxide was stirred for 24 h over $CaH_2$ and thereafter distilled and stored under inert atmosphere.[1]

## 1.4.  Analytical methods

***NMR spectrometry:*** For NMR measurements, the following spectrometers were used: JEOL JNM-GX 400 ($^1$H NMR 400.13 MHz, $^{13}$C NMR 100.53 MHz), T = 300 K, or BRUKER DRX 500 ($^1$H NMR 500.13 MHz, $^{13}$C NMR 125.76 MHz), T = 300 K. Signals were calibrated to the residual proton resonance respectively the natural abundance $^{13}$C resonance of the solvent (DMSO-$d_6$, $\delta_H$ = 2.50 and $\delta_C$ = 39.52 ppm; CDCl$_3$, $\delta_H$ = 7.26 and $\delta_C$ = 77.16 ppm; CD$_3$OD, $\delta_H$ = 3.31 and $\delta_C$ = 49.00 ppm; CD$_3$CN, $\delta_H$ = 1.97 and $\delta_C$ = 1.32 ppm / 118.26 ppm; H$_2$O $\delta_H$ = 4.79 ppm). $^{31}$P NMR spectra were calibrated to an external standard (phosphoric acid). Signal multiplicities are abbreviated as: s (singlet), d (dublet), t (triplet), m (multiplet), br (broad), "q" (quartet / pseudo quartet), "quint" (quintet / pseudo quintet).

***MAS NMR spectrometry:*** MAS NMR spectra: Bruker Avance 300 ($^{13}$C NMR 75.43 MHz), T = 300 K. Supervising senior scientist: Dr. G. Raudaschl-Sieber.

***Gas chromatography:*** Achiral gas chromatographies were carried out on a Varian 1200L quadrupole MS/MS. All substrates were analyzed using standard temperature protocols.

***Chiral gas chromatography:*** Enantiomer separations were carried out on a HP 5890A equipped with a flame ionization detector. For this purpose, a Varian capillary column (fused silica 25 m x 0.25 mm, coated cp chirasil-dex CB df = 0.25) was used.

***Table C1:*** Temperature program for enantiomer separations for 2,2,2-trifluorophenylethanole, 2'-flurophenylethanole, phenylethanole and 4'-trifluoromethylphenylethanole.

| ramp [°C/min] | T [°C] | hold [min] |
|---|---|---|
|  | 90 | 8 |
| 4 | 130 | 20 |
| 10 | 180 | 2 |

***Table C2:*** Temperature program for enantiomer separations 4'-chlorophenylethanole.

| ramp [°C/min] | T [°C] | hold [min] |
|---|---|---|
|  | 90 | 8 |
| 4 | 130 | 20 |
| 10 | 190 | 25 |

***Optical rotation:*** Optical rotation values were determined on a Perkin-Elmer Polarimeter 341. Cell length: 1 dm; T = 24 °C; λ = D.

***ESI mass spectrometry:*** FAB MS spectra were recorded on a Finnigan-MAT 90 mass spectrometer (Xenon). Supervising technician: R. Dumitrescu.

***ESI mass spectrometry:*** ESI MS spectra were recorded on a LCQ classic (Thermo Electron). Supervising technician: B. Cordes.

***MALDI-TOF spectrometry:*** MALDI-TOF spectra were recorded on a Bruker Ultraflex TOF/TOF with a SOUT-MTP ion source. Samples were prepared in α-cyano-hydroxy-cinnamic acid. (337 nm, ~100 µJ, 1 ns pulse width). Supervising technician: H. Krause.

***Elemental analysis:*** Elemental analyses were obtained from the Microanalytical Laboratory of Technische Universität München. Supervising technician: U. Ammari.

*IR spectrometry:* IR spectra were recorded on a Jasco FT/IR-460 PLUS and prepared as KBr pallets, Nujol suspension between KBr plates or $CHCl_3$ solutions in a KBr cell. Wavelengths $\tilde{\nu}$ are noted in $cm^{-1}$. Absorption bands are abbreviated as follows: w (weak), m (medium), s (strong), vs (very strong), sh (shoulder).

*Photometric measurements:* Photometric measurements were carried out on a Genios 96 well plate reader. Absorptions were read at 405 nm and variances corrected to the initial base line values.

*X-Ray spectroscopy:* Crystals suitable for X-Ray diffractions were obtained from saturated solution crystallization, diffusion crystallization, solvent evaporation crystallization or temperature gradient crystallization. X-Ray structural analyses were carried out in the laboratories of Dr. E. Herdtweck, Dr. F. Kraus and M.Sc. F. Kiefer. Diffraction data were collected on an Oxford Xcalibur3 and Nonius Kappa CCD diffractometer using Mo$K_\alpha$ radiation ($\lambda$ = 0.71073 Å, graphite monochromator). A Cryojet Controller from Oxford Diffractions allowed measurements at 150 K. The absorption correction (empirical) of the Oxford Xcalibur3 data set was carried out using the program CrysAlis RED (Oxford Diffraction Ltd). The structures were solved by Direct Methods and refined by least-squares and difference Fourier analysis, using least-squares cycles based on $F^2$ using SHELXTL[2]; SHELXS-86"[3], SHELXL[3] or PLATON [4] software packages. R-Values are defined as follows (($\sigma F_o$) = standard deviation of $F_o$):

$$R = \frac{\sum \left\| F_0 \right| - \left| F_c \right\|}{\sum \left| F_0 \right|}$$

$$R_w = \left[ \frac{\sum_w \left( \left| F_0 \right| - \left| F_c \right| \right)^2}{\sum_w \left| F_0 \right|} \right]^{\frac{1}{2}}$$

$$w = \left[ \sigma^2 \left( F_0 \right) \right]^{-1}$$

# 2. Synthetic procedures

## 2.1. List of commercially available precursors

The following reactants and reagents, which are numbered in the text flow, were obtained commercially and used without further purification:

**Table C3:** Reactants and reagents numbered in the text flow:

| entry | substance number | substance name | CAS number |
|---|---|---|---|
| 1 | **1a** | 2-phenyl-1-ethanol | 60-12-8 |
| 2 | **1b** | 3-phenyl-1-propanol | 122-97-4 |
| 3 | **1c** | 4-phenyl-1-butanol | 3360-41-6 |
| 4 | **1d** | 5-phenyl-1-pentanol | 10521-91-2 |
| 5 | **1e** | 2-phenyl-1-acetic acid | 103-82-2 |
| 6 | **1f** | hydrocinnamic acid | 501-52-0 |
| 7 | **1g** | 4-phenyl-1-butyric acid | 1821-12-1 |
| 8 | **1h** | 5-phenyl-1-valeric acid | 2270-20-4 |
| 9 | **1i** | benzylamine | 100-46-9 |
| 10 | **1j** | 2-phenyl-1-ethylamine | 64-04-0 |
| 11 | **1k** | 3-phenyl-1-propylamine | 2038-57-5 |
| 12 | **1l** | 4-phenyl-1-butylamine | 13214-66-9 |
| 13 | **11** | L-phenylalanine | 63-91-2 |
| 14 | **12** | L-phenylglycine | 2935-35-5 |

The following reactants and reagents, which are not numbered in the text flow, were obtained commercially and used without further purification:

**Table C4:** Reactants and reagents not numbered in the text flow (alphabetical list).[a]

| entry | substance name | CAS number |
|---|---|---|
| 1 | acetic acid anhydride | 108-24-7 |
| 2 | acetic aldehyde | 75-07-0 |
| 3 | BAPNA | 911-77-3 |
| 4 | benzaldehyde | 100-52-7 |
| 5 | benzyl carbamate | 621-84-1 |
| 6 | bromelain | 37189-34-7 |
| 7 | α-chymotrypsin | 9004-07-03 |

(a) standard reagents and reactants as well as solvents and gasses are not listed.

***Table C4 - continued:*** Reactants and reagents not numbered in the text flow (alphabetical list).[a]

| entry | substance name | CAS number |
|---|---|---|
| 8 | DAST | 38078-09-0 |
| 9 | DBU | 6674-22-2 |
| 10 | DTT | 3483-12-3 |
| 11 | EDCI | 25952-53-8 |
| 12 | ethylene diamine | 107-15-3 |
| 13 | Boc-L-Leucine | 13139-15-6 |
| 14 | SS-DCC | 01-64-0211[b] |
| 15 | 4-(fluorosulfonyl)-benzoic acid | 455-26-5 |
| 16 | N-Hydroxy succinimide | 6066-82-6 |
| 17 | $IrCl_3 \cdot n\ H_2O$ | 10025-83-9 |
| 18 | $LiAlH_4$ | 16853-85-3 |
| 19 | $NaIO_4$ | 7790-28-5 |
| 20 | $OsCl_3 \cdot n\ H_2O$ | 13444-93-4 |
| 21 | papain | 9001-73-4 |
| 22 | pentafluorophenole | 771-61-9 |
| 23 | PMSF | 329-98-6 |
| 24 | 3-pentanone | 96-22-0 |
| 25 | $RhCl_3 \cdot n\ H_2O$ | 20765-98-4 |
| 26 | $RuCl_3 \cdot n\ H_2O$ | 14898-67-0 |
| 27 | succinic acid anhydride | 108-30-5 |
| 28 | TCEP | 51805-45-9 |
| 29 | *p*-toluenesulfonyl chloride | 98-59-9 |
| 30 | triethylamine | 121-44-8 |
| 31 | triethylphosphite | 122-52-1 |
| 32 | trifluoroacetic acid anhydride | 407-25-0 |
| 33 | trimethylsilylbromide | 2857-97-8 |
| 34 | triphenylphosphine | 603-35-0 |
| 35 | triphenylphosphite | 101-02-0 |
| 36 | trypsin | 9002-07-07 |
| 37 | 10-undecenole | 112-43-6 |

(a) standard reagents and reactants as well as solvents and gasses are not listed. (b) NovaBiochem Cat. No.

## 2.2. 1,4-Cyclohexadiene derivatives[5]

**General procedure for the synthesis of 1',4'-cyclohexadiene-1-alkyl-alcohols:** The corresponding aryl-alcohol **1a**-**1d** (35 mmol) was placed in a flask fitted with gas inlet, and pressure relief valve and cooled to -78 °C. Then, liquid ammonia (250 mL) was condensed in the flask under constant stirring, before lithium (3 g) was added slowly to the reaction mixture. The deep blue mixture was maintained at -78°C for 30 minutes, before cold dry ethanol was carefully added until the blue color vanished. The ammonia was allowed to evaporate overnight and the remaining volatiles removed in vacuo. The residual white solid was suspended in a minimum amount of water and extracted with dichloromethane. The organic phase was dried over $MgSO_4$ and volatiles removed under reduced pressure.

*1',4'-cyclohexadiene-1-ethanole* (**2a**):
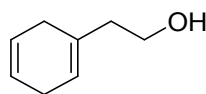


Yellowish oil. Yield: 11.2 mmol, 32%. - **$^1$H NMR** (400 MHz, 25°C, CDCl$_3$): $\delta$ = 5.66 (m, 2 H, C(6)*H* / C(7)*H*), 5.48 (m, 1 H, C(4)*H*), 3.68 (t, $^3J_{HH}$ = 7.1, 2H, C(1)*H$_2$*), 2.68-2.55 (m, 4H, C(5)*H$_2$* / C(8)*H$_2$*), 2.20 (t 2H, $^3J_{HH}$ = 6.4, C(2)*H$_2$*). - **$^{13}$C NMR** (100.5 MHz; 25 °C; CDCl$_3$): $\delta$ = 131.5 (*C*(3)), 124.2 / 124.1 (*C*(6) / *C*(7)), 121.3 (*C*(4)), 60.2 (*C*(1)), 40.4 (*C*(2)), 28.9, 26.8 (*C*(5) / *C*(8)).

*1',4'-cyclohexadiene-1-propanole* (**2b**):
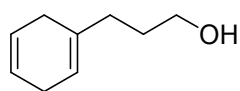


Yellowish oil. Yield: 25.5 mmol, 73%. - **$^1$H NMR** (400 MHz, 25°C, CDCl$_3$): $\delta$ = 5.68 (m, 2 H, C(7)*H* / C(8)*H*), 5.43 (m, 1 H, C(5)*H*), 3.62 (t, $^3J_{HH}$ = 6.2, 2H, C(1)*H$_2$*), 2.66-2.56 (m, 4H, C(6)*H$_2$* / C(9)*H$_2$*), 2.02 (t 2H, $^3J_{HH}$ = 7.5, C(3)*H$_2$*), 1.83 (s, 1H, O*H*), 1.67 (tt, 2 H, $^3J_{HH}$ = 7.1, C(2)*H$_2$*). - **$^{13}$C NMR** (100.5 MHz; 25 °C; CDCl$_3$): $\delta$ = 134.6 (*C*(4)), 124.4 / 124.3 (*C*(7) / *C*(8)), 118.8 (*C*(5)), 62.8 (*C*(1)), 33.8 / 30.3 / 29.0 / 26.8 (*C*(2) / *C*(3) / *C*(6) / *C*(9)).

*1',4'-cyclohexadiene-1-butanole* (**2c**):[6]
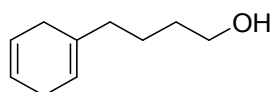


Yellowish oil. Yield: 25.6 mmol, 73%. - **$^1$H NMR** (400 MHz, 25°C, CDCl$_3$): $\delta$ = 5.69 (m, 2 H, C(8)$H$ / C(9)$H$), 5.41 (m, 1 H, C(6)$H$), 3.64 (t, $^3J_{HH}$ = 6.4, 2H, C(1)$H_2$), 2.67-2.55 (m, 4H, C(7)$H_2$ / C(10)$H_2$), 1.98 (t, 2H, $^3J_{HH}$ = 7.3, C(4)$H_2$), 1.59-1.44 (m, 4 H, $^3J_{HH}$ = 7.1, C(2)$H_2$ / C(3)$H_2$). - **$^{13}$C NMR** (100.5 MHz; 25 °C; CDCl$_3$): $\delta$ = 134.9 (*C*(5)), 124.4 /124.4 (*C*(8) / *C*(9)), 118.7 (*C*(6)), 63.0 (*C*(1)), 37.3 / 32.5 / 29.0 / 26.9 / 23.5 (*C*(2) / *C*(3) / *C*(4) / *C*(7) / *C*(10)).

*1',4'-cyclohexadiene-1-pentaneole* (**2d**):
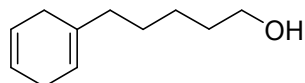


Yellowish oil. Yield: 28.7 mmol, 82%. - **$^1$H NMR** (400 MHz, 25°C, CDCl$_3$): $\delta$ = 5.66 (m, 2 H, C(9)$H$ / C(10)$H$), 5.37 (m, 1 H, C(6)$H$), 3.57 (t, $^3J_{HH}$ = 6.6, 2H, C(1)$H_2$), 2.66-2.52 (m, 4H, C(8)$H_2$ / C(11)$H_2$), 2.31 (s, 1H, O$H$), 1.93 (t 2H, $^3J_{HH}$ = 7.3, C(5)$H_2$), 1.52 (tt, $^3J_{HH}$ = 6.6, C(2)$H_2$), 1.40 (tt, $^3J_{HH}$ = 7.9, C(4)$H_2$), 1.30 (tt, $^3J_{HH}$ = 7.5 / C(3)$H_2$). - **$^{13}$C NMR** (67.9 MHz; 25 °C; CDCl$_3$): $\delta$ = 135.0 (*C*(6)), 124.4 /124.3 (*C*(9) / *C*(10)), 118.3 (*C*(7)), 62.8 (*C*(1)), 37.5 / 32.7 / 29.0 / 27.2 / 26.8 / 25.5 (*C*(2) / *C*(3) / *C*(4) / *C*(5) / *C*(8) / *C*(11)).

**General procedure for the synthesis of 1',4'-cyclohexadiene-1-alkyl-carboxylic acids:** The corresponding aryl-carboxylic acid **1m**-**1p** (35 mmol) was placed in a flask fitted with gas inlet, and pressure relief valve and cooled to -78 °C. Then, liquid ammonia (250 mL) was condensed in the flask under constant stirring, before lithium (3 g) was added slowly to the reaction mixture. The deep blue mixture was maintained at -78°C for 30 minutes, before cold dry ethanol was carefully added until the blue color vanished. The ammonia was allowed to evaporate overnight and the remaining volatiles removed in vacuo. The residual white solid was dissolved in a minimum amount of water, acidified with hydrochloric acid (pH 1-2), and recrystallized at -18°C over night. The resulting product was collected by filtration and dried in vacuo.

*1',4'-cyclohexadiene-1-acetic acid* (**2e**):
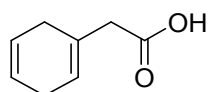


White crystals. - Yield: 27.3 mmol, 78 %. - **$^1$H NMR** (400 MHz; 25 °C; CDCl$_3$): $\delta$ = 11.03 (br, 1 H, COO*H*), 5.68 (m, 2 H, C(6)*H* / C (7)*H*), 5.62 (m, 2 H, C(4)*H*), 3.01 / 2.71 (m, 6 H, C(2)*H*$_2$ / C(5)*H*$_2$ / C(8)*H*$_2$). - **$^{13}$C NMR** (100.5 MHz; 25 °C; CDCl$_3$): $\delta$ = 178.4 (*C*(1)), 127.9 (*C*(3)), 124.0 / 123.9 / 123.9 (*C*(4) / *C*(6) / *C*(7)), 42.9 (*C*(2)), 29.1 / 26.9 (*C*(5) / *C*(8)). - **IR** (KBr): $\tilde{v}$ = 1696 vs (CO), 1425 m, 1404 m, 1350 m, 1248 s, 974 m, 964 s cm$^{-1}$.

*1',4'-cyclohexadiene-1-propanoic acid* (**2f**):
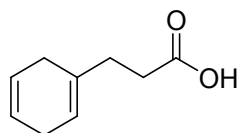


White crystals. - Yield: 27.0 mmol, 77 %. - **$^1$H NMR** (400 MHz; 25 °C; CDCl$_3$): $\delta$ = 11.56 (br, 1 H, COO*H*), 5.69 (m, 2 H, C(7)*H* / C (8)*H*), 5.45 (m, 2 H, C(4)*H*), 2.69-2.57 (m, 4 H, C(6)*H*$_2$ / C(9)*H*$_2$), 2.49 / 2.28(t, 2 H, $^3J_{HH}$ = 7.7 Hz, C(2)*H*$_2$ / C(3)*H*$_2$). - **$^{13}$C NMR** (100.5 MHz; 25 °C; CDCl$_3$): $\delta$ = 180.2 (*C*(1)), 133.2 (*C*(4)), 124.3 / 124.1 (*C*(7) / *C*(8)), 119.3 (*C*(5)), 32.4 / 32.0 / 29.1 / 26.8 (*C*(2) / *C*(3) / *C*(6) / *C*(9)). - **IR** (KBr): $\tilde{v}$ = 1697 vs (CO), 1685, vs, 1438 w, 1412 w, 1331 m, 1290 m, 1227 s, 960 s cm$^{-1}$.

*1',4'-cyclohexadiene-1-butanoic acid* (**2g**):
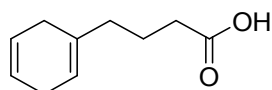


White crystals. - Yield: 15.4 mmol, 44 %. - **$^1$H NMR** (400 MHz; 25 °C; CDCl$_3$): $\delta$ = 11.57 (br, 1 H, COO*H*), 5.69 (m, 2 H, C(8)*H* / C (9)*H*), 5.43 (m, 2 H, C(6)*H*), 2.69-2.55 (m, 4 H, C(7)*H*$_2$ / C(10)*H*$_2$), 2.34 / 2.01 (t, $^3J_{HH}$ = 7.5, C(2)*H*$_2$ / C(4)*H*$_2$),1.76 (tt, $^3J_{HH}$ = 7.5, C(4)*H*$_2$). - **$^{13}$C NMR** (100.5 MHz; 25 °C; CDCl$_3$): $\delta$ = 180.5 (*C*(1)), 133.8 (*C*(5)), 124.3 / 124.3 (*C*(8) / *C*(9)), 119.6 (*C*(6)), 36.7 / 33.6 / 28.8 / 26.9 / 22.3 (*C*(2) / *C*(3) / *C*(4) / *C*(7) / *C*(10)). - **IR** (KBr): $\tilde{v}$ = 1696 vs, 1429 m, 1282 m, 1214 w, 959 m cm$^{-1}$.

*1',4'-cyclohexadiene-1-pentanoic acid* (**2h**):
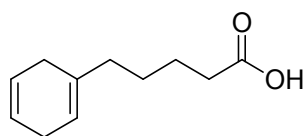


White crystals. - Yield: 10.2 mmol, 29 %. - **$^1$H NMR** (400 MHz; 25 °C; CDCl$_3$): $\delta$ = 11.57 (br, 1 H, COO*H*), 5.72 (m, 2 H, C(9)*H* / C (10)*H*), 5.41 (m, 2 H, C(7)*H*), 2.67-2.54 (m, 4 H, C(8)*H*$_2$ / C(11)*H*$_2$), 2.36 / 1.97 (t, $^3J_{HH}$ = 7.3, C(2)*H*$_2$ / C(5)*H*$_2$), 1.63 / 1.46 (tt, $^3J_{HH}$ = 7.5, C(3)*H*$_2$ / C(4)*H*$_2$). - **$^{13}$C NMR** (100.5 MHz; 25 °C; CDCl$_3$): $\delta$ = 180.1 (*C*(1)), 134.6 (*C*(6)), 124.4 / 124.4 (*C*(9) / *C*(10)), 118.8 (*C*(7)), 37.2 / 34.1 / 29.0 / 26.9 / 26.8 / 24.5 (*C*(2) / *C*(3) / *C*(4) / *C*(5) / *C*(8) / *C*(11)). - **IR** (KBr): $\tilde{v}$ = 1710 vs, 1408 m, 1316 w, 1254 m, 1202 m, 962 m, 931m cm$^{-1}$.

**General procedure for the synthesis of 1',4'-cyclohexadiene-1-alkyl-ammonium chlorides:** The corresponding arylamine **1i**-**1l** (35 mmol) was placed in a flask fitted with gas inlet, and pressure relief valve and cooled to -78 °C. Then, liquid ammonia (250 mL) was condensed in the flask under constant stirring, before lithium (3 g) was added slowly to the reaction mixture. The deep blue mixture was maintained at -78°C for 30 minutes, before cold dry ethanol was carefully added until the blue color vanished. The ammonia was allowed to evaporate overnight and the remaining volatiles removed in vacuo. The residual white solid was dissolved in a minimum amount of water and acidified with hydrochloric acid (pH 6). The solvent volume was reduced to 20% under reduced pressure and the reaction mixture recrystallized at -18°C over night. The resulting product was collected by filtration and dried in vacuo.

*1',4'-cyclohexadiene-1-benzyl ammonium chloride* (**2i**):[7]
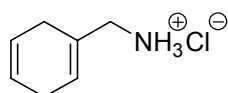


White solid. - Yield: 21.7 mmol, 62%. - **$^1$H NMR** (400 MHz; 25 °C; D$_2$O): $\delta$ = 5.84 (m, 1 H, C(3)*H*), 5.78 (m, 2 H, C(5)*H* / C (6)*H*), 3.52 (s, 2 H, C(1)*H*$_2$), 2.72-2.65 (m, 4 H, C(4)*H*$_2$; C(7)*H*$_2$). - **$^{13}$C NMR** (100.5 MHz; 25 °C; D$_2$O): $\delta$ = 127.9 (*C*(2)), 125.1 / 124.5 (*C*(5) / *C*(6)), 123.6 (*C*(3)), 44.6 (*C*(1)), 26.9 / 26.0 (*C*(4) / *C*(7)).

*1',4'-cyclohexadiene-1-ethyl ammonium chloride* (**2j**):[8]
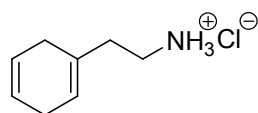


White solid. - Yield: 17.9 mmol, 51%. - **$^1$H NMR** (400 MHz; 25 °C; D$_2$O): $\delta$ = 5.78 (m, 2 H, C(6)$H$ / C(7)$H$), 5.65 (m, 1 H, C(4)$H$), 3.12 (t, 2 H, $^3J_{HH}$ = 6.8 Hz, C(1)$H_2$), 2.72-2.65 (m, 4 H, C(5)$H_2$; C(8)$H_2$), 2.36 (t, 2 H, $^3J_{HH}$ = 6.8 Hz, C(2)$H_2$). - **$^{13}$C NMR** (100.5 MHz; 25 °C; D$_2$O): $\delta$ = 130.3 (C(3)), 124.8 / 124.5 (C(6) / C(7)), 123.1 (C(4)), 37.5 / 34.6 / 27.8 / 26.4 (C(1) / C(2) / C(5) / C(8)).

*1',4'-cyclohexadiene-1-propyl ammonium chloride* (**2k**):
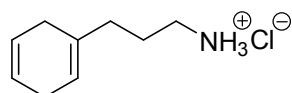


White solid. - Yield: 26.6 mmol, 76%. - **$^1$H NMR** (400 MHz; 25 °C; D$_2$O): $\delta$ = 5.82 (m, 2 H, C(7)$H$ / C(8)$H$), 5.60 (m, 1 H, C(5)$H$), 3.01 (t, 2 H, $^3J_{HH}$ = 7.3 Hz, C(1)$H_2$), 2.70-2.65 (m, 4 H, C(6)$H_2$; C(9)$H_2$), 2.12 (m, 2 H, C(3)$H_2$), 1.82 (tt, 2 H, $^3J_{HH}$ =6.4 Hz, C(2)$H_2$). - **$^{13}$C NMR** (100.5 MHz; 25 °C; D$_2$O): $\delta$ = 134.3 (C(4)), 125.0 / 124.9 (C(7) / C(8)), 120.0 (C(5)), 39.5 / 33.6 / 28.2 / 26.4 / 24.7 (C(1) / C(2) / C(3) / C(6) / C(9)).

*1',4'-cyclohexadiene-1-butyl ammonium chloride* (**2l**):
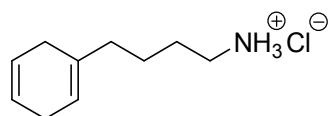


White solid. Yield: 32.9 mmol, 94%. - **$^1$H NMR** (400 MHz; 25 °C; D$_2$O): $\delta$ = 5.76 (m, 2 H, C(8)$H$ / C(9)$H$), 5.51 (m, 1 H, C(6)$H$), 3.00 (t, 2 H, $^3J_{HH}$ = 6.8 Hz, C(1)$H_2$), 2.67-2.59 (m, 4 H, C(7)$H_2$; C(10)$H_2$), 2.02 (t, 2 H, $^3J_{HH}$ = 7.3 Hz, C(4)$H_2$), 1.65 (tt, 2 H, $^3J_{HH}$ = 7.3 Hz, C(2)$H_2$),1.49 (tt, 2 H, $^3J_{HH}$ = 6.9 Hz, C(3)$H_2$). - **$^{13}$C NMR** (100.5 MHz; 25 °C; D$_2$O): $\delta$ = 135.3 (C(5)), 125.1 / 125.0 (C(8) / C(9)), 119.3 (C(6)), 39.8 / 36.3 / 28.5 / 26.7 / 26.6 / 23.8 (C(1) / C(2) / C(3) / C(4) / C(7) / C(10)).

**General procedure for the synthesis of N-Acetyl-1',4'-cyclohexadiene-1-alkyl-amines:** Under an atmosphere of argon, 1',4'-cyclohexadiene-1-alkyl-ammonium chloride **2i**-**2l** (3.5 mmol) was dissolved in a mixture of acetic anhydride and pyridine (4 mL acetic anhydride / pyridine = 3 / 1) and stirred at 0°C for 2 h. Solvent was evaporated under reduced pressure, the residue dissolved in water (5 mL) and extracted with dichloromethane (3 x 5 mL). The organic phase was dried over MgSO4 and dried under reduced pressure.

*N-acetyl-1',4'-cyclohexadiene-1-benzyl amine* (**2m**):
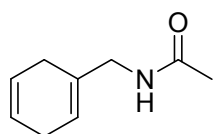


Yellowish solid. - Yield: 2.49 mmol, 71 %. - $^1$**H NMR** (400 MHz; 25 °C; CDCl$_3$): $\delta$ = 5.69 (m, 2 H, C(7)*H* / C (8)*H*), 5.58 (m, 1 H, C(5)*H*), 5.52 (br, 1 H, N*H*), 3.77 (d, $^3J_{(H,H)}$ = 5.8, 2 H, C(3)*H*$_2$), 2.69-2.58 (m, 4 H, C(6)*H*$_2$; C(9)*H*$_2$), 2.00 (s, 3 H, C(2)*H*$_2$). - $^{13}$**C NMR** (100.5 MHz; 25 °C; CDCl$_3$): $\delta$ = 170.3 (*C*(1)), 132.0 (*C*(4)), 124.1 / 124.0 (*C*(7) / *C*(8)), 121.0 (*C*(5)), 45.4 (*C*(3)), 27.4 / 26.7 (*C*(6) / *C*(9)), 23.4 (*C*(2)). - **IR** (KBr): $\tilde{v}$ = 1637 vs (CO), 1558 sh, 1443 m, 1395 m, 1369 m, 1287 m, 1262 m, 1239 w, 1024 s, 968 m, 872 w, 802 s cm$^{-1}$.

*N-acetyl-1',4'-cyclohexadiene-1-ethyl amine* (**2n**):
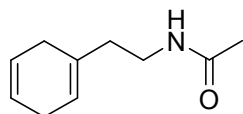


Yellowish solid. - Yield: 3.36 mmol, 96 %. - $^1$**H NMR** (400 MHz; 25 °C; CDCl$_3$): $\delta$ = 5.68 (m, 2 H, C(8)*H* / C (9)*H*), 5.57 (br, 1 H, N*H*), 5.47 (m, 1 H, C(6)*H*), 3.33 (dt, $^3J_{(H,H)}$ = 6.4 Hz, C(3)*H*$_2$), 2.70-2.55 (m, 4 H, C(7)*H*$_2$; C(10)*H*$_2$), 2.14 (t, 2 H, $^3J_{(H,H)}$ = 6.8, C(4)*H*$_2$), 1.94 (s, 3 H, C(2)*H*$_2$). - $^{13}$**C NMR** (100.5 MHz; 25 °C; CDCl$_3$): $\delta$ = 170.1 (*C*(1)), 132.0 (*C*(5)), 124.2 / 124.1 (*C*(8) / *C*(9)), 121.0 (*C*(6)), 37.1 / 37.1 / 28.7 / 26.9 / 23.4 (*C*(2) / *C*(3) / *C*(4) / *C*(7) / *C*(10)). - **IR** (KBr): $\tilde{v}$ = 1650 vs, 1564 s, 1454 m, 1363 s, 1293 m, 1261 m, 1197 m, 1099 s, 961 s, 798 m cm$^{-1}$.

*N-acetyl-1',4'-cyclohexadiene-1-propyl amine* (**2o**):
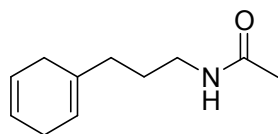


Yellowish solid. - Yield: 2.70 mmol, 77 %. - **$^1$H NMR** (400 MHz; 25 °C; CDCl$_3$): $\delta$ = 5.69 (m, 2 H, C(9)*H* / C (10)*H*), 5.53 (br, 1 H, N*H*), 5.43 (m, 1 H, C(7)*H*), 3.23 (dt, $^3J_{(H,H)}$ = 6.8, $^3J_{(H,H)}$ = 7.1 Hz, C(3)*H$_2$*), 2.67-2.54 (m, 4 H, C(8)*H$_2$*; C(11)*H$_2$*), 1.99 (t, 2 H, $^3J_{(H,H)}$ = 7.7, C(5)*H$_2$*), 1.95 (s, 3 H, C(2)*H$_2$*), 1.62 (tt, 2 H, $^3J_{(H,H)}$ = 7.4, C(4)*H$_2$*). - **$^{13}$C NMR** (100.5 MHz; 25 °C; CDCl$_3$): $\delta$ = 170.2 (*C*(1)), 134.3 (*C*(6)), 124.4 / 124.3 (*C*(9) / *C*(10)), 119.2 (*C*(7)), 39.6 / 35.0 / 29.0 / 27.3 / 26.9 / 23.5 (*C*(2) / *C*(3) / *C*(4) / *C*(5) / *C*(8) / *C*(11)). - **IR** (KBr): $\tilde{v}$ = 1635 vs, 1559 s, 1440 m, 1369 m, 1301 m, 1183 w, 1101 w, 1042 w, 958 m, 801 w cm$^{-1}$.

*N-acetyl-1',4'-cyclohexadiene-1-butyl amine* (**2p**):
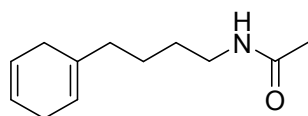


Yellowish solid. - Yield: 2.84 mmol, 81 %. - **$^1$H NMR** (400 MHz; 25 °C; CDCl$_3$): $\delta$ = 5.84 (br, 1 H, N*H*), 5.66 (m, 2 H, C(10)*H* / C (11)*H*), 5.37 (m, 1 H, C(8)*H*), 3.20 (dt, $^3J_{(H,H)}$ = 6.22 Hz, C(3)*H$_2$*), 2.66-2.50 (m, 4 H, C(9)*H$_2$*; C(12)*H$_2$*), 1.95-1.92 (m, 4 H, C(2)*H$_2$*, C(6)*H$_2$*), 1.49-1.38 (m, 4 H, C(4)*H$_2$*, C(5)*H$_2$*). - **$^{13}$C NMR** (100.5 MHz; 25 °C; CDCl$_3$): $\delta$ = 170.3 (*C*(1)), 134.6 (*C*(7)), 124.3 / 124.3 (*C*(9) / *C*(10)), 118.7 (*C*(8)), 39.6 / 37.1 / 29.3 / 28.9 / 26.8 / 24.6 / 23.3 (*C*(2) / *C*(3) / *C*(4) / *C*(5) / *C*(6) / *C*(9) / *C*(12)). - **IR** (KBr): $\tilde{v}$ = 1652 vs, 1557 s, 1435 s, 1370 s, 1295 s, 1104 m, 958 w, 804 w cm$^{-1}$.

*N-trifluoroacetyl-1',4'-cyclohexadiene-1-benzyl amine* (**2q**):
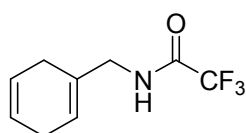


To a stirred, cooled solution (0 °C) of 1',4'-Cyclohexadiene-1-benzyl ammonium chloride **2i** (400 mg, 3.74 mmol) in dichloromethane (8 mL) first pyridine (880 µL) and then slowly a solution of trifluoroacetic acid anhydride  (1.03 mL) in dichloromethane (2 mL)

was added. The reaction mixture was stirred for 2 h at 0 °C and over night at room temperature. Then, water was slowly added (8 mL) and the reaction mixture extracted with dichloromethane (3 x 10 mL). The organic phase was dried over MgSO4 and volatiles removed under reduced pressure, yielding an ivory powder. Yield: 84% (647 mg, 3.16 mmol). - **$^1$H NMR** (400 MHz; 25 °C; CDCl$_3$): $\delta$ = 6.44 (m, 1 H, N*H*), 5.69 (m, 2 H, C(7)*H* / C (8)*H*), 5.65 (m, 1 H, C(5)*H*), 3.87 (d, $^3J_{(H,H)}$ = 6.2, 2 H, C(3)*H*$_2$), 2.73-2.58 (m, 4 H, C(6)*H*$_2$; C(9)*H*$_2$). - **$^{13}$C NMR** (100.5 MHz; 25 °C; CDCl$_3$): $\delta$ = 157.4 (q, $^2J_{FC}$ = 36.9, *C*(1)), 130.1 (*C*(4)), 124.0 / 123.5 / 122.9 (*C*(5) / *C*(7) / *C*(8)), 116.0 (q, $^1J_{FC}$ = 287.5, *C*(2)), 45.6 (*C*(3)), 27.2 / 26.6 (*C*(6) / *C*(9)). - **$^{19}$F NMR** (376.2 MHz; 25 °C; CDCl$_3$): $\delta$ = -75.72. - **IR** (KBr): $\tilde{v}$ = 3291 s, 3098 w, 2887 m, 2862 w, 2828 m, 1699 vs (C=O), 1560 s, 1435 m, 1367 m, 1251 s, 1181 vs cm$^{-1}$. - **EA** C$_9$H$_{10}$F$_3$NO (750.27): calcd. C 52.68, H 4.91, N 6.83; found C 52.28, H 4.89, N 6.56.

## 2.3. Dimeric ruthenium complexes with pendant functionalized linker

**General procedure for the synthesis of dinuclear ruthenium complexes with $\eta^6$-arylalcohol-ligands:** The cyclohexadiene-derivative **2a**-**2d** (5.75 mmol) was stirred with HCl$_{conc.}$ in Ethanol (60 mL, approx. 0.1 M). To this solution, RuCl$_3$ · nH$_2$O (300 mg, 1.15 mmol) was added and the resulting solution heated for 16 h at 80°C. The suspension was reduced to half the volume in vacuo, cooled to -10 °C for 48 h, filtered and the precipitate washed with cold pentane and ethanol (each 3 x 5 mL) and dried in vacuo.

*[($\eta^6$-2'-phenylethanole)RuCl$_2$]$_2$* (**3a**): [9]
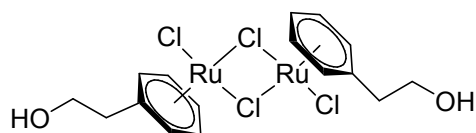


Dark red powder. - Yield: 294.3 mg (87%). - **$^1$H NMR** (400 MHz, 25 °C, DMSO-d$_6$): δ = 5.97 (t, $^3J$ = 5.8, 2 H, C$_{meta}H$), 5.77 (d, $^3J$ = 5.6, 2 H, C$_{ortho}H$), 5.74 (d, $^3J$ = 5.2, 1 H, C$_{para}H$), 4.79 (s, 1 H, -O$H$), 3.69 (t, $^3J$ = 6.0, 2 H, 1'-C$H_2$), 2.57 (t, $^3J$ = 6.2, 2 H, 2'-C$H_2$). - **$^{13}$C NMR** (100.5 MHz, 25 °C, DMSO-d$_6$): δ = 105.1, 88.4, 86.1, 83.6 (C$_{arom}$), 59.9 (1'-C$H_2$), 36.2 (2'-C$H_2$). – **IR** (KBr): $\tilde{v}$ = 1515 w, 1453 s, 1413 w, 1396 s, 1235 w, 1140 s, 1051 vs, 1006 w, 864 s, 855 s cm$^{-1}$. - **EA** C$_{16}$H$_{20}$Cl$_4$O$_2$Ru$_2$ (588.281): calcd. C 32.67, H 3.43; found C 32.68, H 3.42.

*[($\eta^6$-3'-phenylpropanole)RuCl$_2$]$_2$* (**3b**): [10]
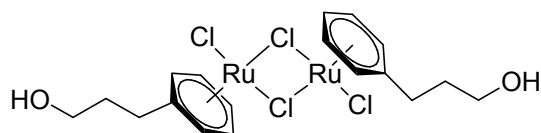


Red powder; - Yield: 363.0 mg (77%). - **$^1$H NMR** (400 MHz, 25 °C, DMSO-d$_6$): δ = 5.97 (t, $^3J$ = 5.2, 2 H, C$_{meta}H$), 5.73 (m, 3 H, C$_{ortho}H$, C$_{para}H$), 4.56 (t, $^3J$ = 4.0, 1 H, -O$H$), 3.44 (m, 2 H, 1'-C$H_2$), 2.47 (t, $^3J$ = 8.0, 2 H, 3'-C$H_2$), 1.72 (tt, $^3J$ = 6.8, $^3J$ = 6.0, 2 H, 2'-C$H_2$). - **$^{13}$C NMR** (67.9 MHz, 25 °C, DMSO-d$_6$): δ = 107.9, 88.9, 84.9, 83.0 (C$_{arom}$), 60.0 (1'-C$H_2$), 32.1 (3'-C$H_2$), 29.5 (2'-C$H_2$). - **IR** (KBr): $\tilde{v}$ = 3069 w, 3052 s, 2949 w 2874 w, 1515

w, 1449 vs, 1414 s, 1367 s, 1215 w, 1053 vs, 1019 s, 869 s cm$^{-1}$. - **EA** $C_{18}H_{24}Cl_4O_2Ru_2$ (616.334): calcd. C 35.08, H 3.92; found C 35.29, H 3.80.

*[($\eta^6$-4'-phenylbutanole)RuCl$_2$]$_2$* (**3c**):
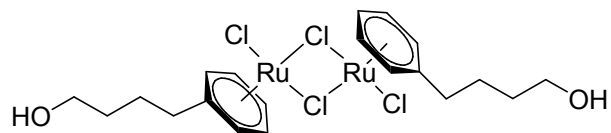


Brown powder; - Yield: 330.0 mg (89%). - **$^1$H NMR** (400 MHz, 25 °C, DMSO-d$_6$): $\delta$ = 5.98 (t, $^3J$ = 5.6, 2 H, C$_{meta}$H), 5.74 (m, 3 H, C$_{ortho}$H, C$_{para}$H), 4.42 (t, $^3J$ = 5.2, 1 H, -OH), 3.41 (tt, $^3J$ = 5.2 $^3J$ = 6.0, 2 H, 1'-CH$_2$), 2.44 (t, $^3J$ = 7.6, 2H, 4'-CH$_2$) , 1.72 (tt, $^3J$ = 7.2, $^3J$ = 6.0, 2 H, 3'-CH$_2$), 1.47 (tt, $^3J$ = 6.8, $^3J$ = 5.2, 2 H, 2'-CH$_2$). - **$^{13}$C NMR** (100.5 MHz, 25 °C, DMSO-d$_6$): $\delta$ = 108.1, 89.0, 84.7, 83.0 (C$_{arom}$), 60.3 (1'-CH$_2$), 32.4 (4'-CH$_2$), 32.0 (2'-CH$_2$), 25.6 (3'-CH$_2$). - **IR** (KBr): $\tilde{v}$ = 3060 s, 3046 w, 2930 s, 2874 w, 1442 w, 1405 w, 1076 s, 981 w, 868 w, 858 w cm$^{-1}$. - **EA** $C_{20}H_{28}Cl_4O_2Ru_2$ (644.387): calcd. C 37.28, H 4.38; found C 37.08, H 4.24.

*[($\eta^6$-5'-phenylpentanole)RuCl$_2$]$_2$* (**3d**): [11]
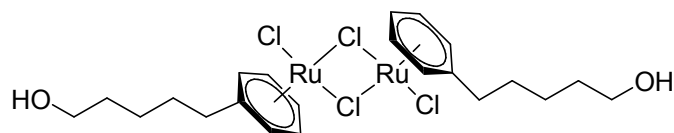


Red powder; - Yield: 297.0 mg (77%). - **$^1$H NMR** (400 MHz, 25 °C, DMSO-d$_6$): $\delta$ = 5.97 (t, $^3J$ = 5.8, 2 H, C$_{meta}$H), 5.74 (d, $^3J$ = 6.0, 2 H, C$_{ortho}$H), 5.72 (d, $^3J$ = 6.4, 1 H, C$_{para}$H), 4.36 (t, $^3J$ = 4.8, 1 H, -OH), 3.38 (m, 2 H, 1'-CH$_2$), 2.43 (t, $^3J$ = 7.6, 2H, 5'-CH$_2$) , 1.58 (tt, $^3J$ = 8.0, $^3J$ = 7.2, 2 H, 4'-CH$_2$), 1.43 (tt, $^3J$ = 7.6, $^3J$ = 6.4, 2 H, 2'-CH$_2$), 1.34 (m, 2 H, 3'-CH$_2$). - **$^{13}$C NMR** (100.5 MHz, 25 °C, DMSO-d$_6$): $\delta$ = 108.0, 89.0, 84.7, 83.0 (C$_{arom}$), 60.5 (1'-CH$_2$), 32.6 (5'-CH$_2$), 32.2 (4'-CH$_2$), 28.7 (2'-CH$_2$), 25.2 (3'-CH$_2$). - **IR** (KBr): $\tilde{v}$ = 3062 vs, 3052 vs, 2938 vs, 2861 vs, 1516 w, 1491 w, 1448 vs, 1407 s, 1390 s, 1147 s, 1047 vs, 871 s cm$^{-1}$. - **EA** $C_{22}H_{32}Cl_4O_2Ru_2$ (672.440): calcd. C 39.29, H 4.80; found C 39.31, H 4.72.

**General procedure for the synthesis of dinuclear ruthenium complexes with η⁶-arylcarboxyl-ligands:** The cyclohexadiene-derivative **2q**-**2t** (5.75 mmol) was stirred with a solution of 20 mL of HCl in *tert*BuOH (approx. 2 M) until the ligand completely dissolved. To this solution, $RuCl_3 \cdot nH_2O$ (300 mg, 1.15 mmol) and 40 mL of *tert*BuOH was added and the resulting solution heated for 16 h at 80°C. The suspension was reduced to half the volume in vacuo, filtered and the precipitate washed with cold pentane and ethanol (each 3 x 5 mL) and dried in vacuo.

*[(η⁶-2'-phenyl acetic acid)RuCl₂]₂* (**3e**):
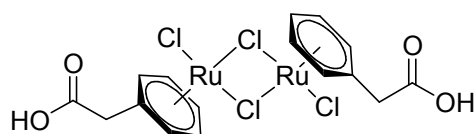


Ochre powder; - Yield: 249.4 mg (70%). - **¹H NMR** (400 MHz, 25 °C, DMSO-d₆): $\delta$ = 12.80 (s, 1 H, COO*H*), 6.01 (t, $^3J$ = 6.0, 2 H, C$_{meta}$*H*), 5.90 (d, $^3J$ = 6.0, 2 H, C$_{ortho}$*H*), 5.83 (t, $^3J$ = 5.6, 1 H, C$_{para}$*H*), 3.49 (s, 2 H, C*H₂*). - **¹³C NMR** (100.5 MHz, 25 °C, DMSO-d₆): $\delta$ = 170.8 (*C*OOH), 98.9, 88.4, 87.2, 84.6 (*C*$_{arom}$), 38.0 (*C*H₂). - **IR** (KBr): $\tilde{v}$ = 1734 vs (C=O), 1452 s, 1416 s, 1363 vs, 1229 vs, 1136 vs cm⁻¹. - **EA** $C_{16}H_{16}Cl_4O_4Ru_2$ (616.248): calcd. C 31.18, H 2.62; found C 31.16, H 2.52.

*[(η⁶-3'-phenyl propanoic acid)RuCl₂]₂* (**3f**):
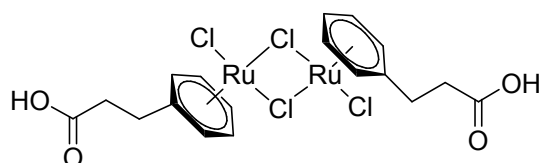


Red powder; Yield: 151.7 mg (41%). - **¹H NMR** (400 MHz, 25 °C, DMSO-d₆): $\delta$ = 12.30 (s, 1 H, COO*H*), 5.99 (t, $^3J$ = 5.8, 2 H, C$_{meta}$*H*), 5.81 (d, $^3J$ = 6.0, 2 H, C$_{ortho}$*H*), 5.76 (t, $^3J$ = 5.6, 1 H, C$_{para}$*H*), 2.66 (m, 4 H, 1'-C*H₂*, 2'-C*H₂*). - **¹³C NMR** (67.9 MHz, 25 °C, DMSO-d₆): $\delta$ = 173.3 (*C*OOH), 105.6, 88.3, 85.7, 83.7 (*C*$_{arom}$), 32.6 (1'-*C*H₂), 27.8 (2'-*C*H₂). - **IR** (KBr): $\tilde{v}$ = 1701 vs (C=O), 1444 s, 1424 s, 1323 w, 1281 w, 1227 s, 960 w, 858 w cm⁻¹. - **EA** $C_{18}H_{20}Cl_4O_4Ru_2$ (644.301): calcd. C 33.55, H 3.13; found C 33.89, H 3.29.

*[(η⁶-4'-butyric acid)RuCl₂]₂* (**3g**):
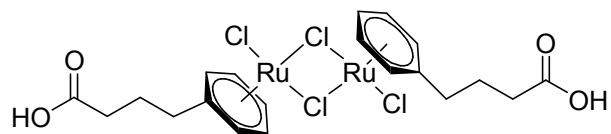


Red powder; - Yield: 302.2 mg (78%). - **¹H NMR** (400 MHz, 25 °C, DMSO-d₆): $\delta$ = 12.11 (s, 1 H, COO*H*), 5.99 (t, $^3J$ = 5.6, 2 H, C$_{meta}$*H*), 5.75 (m, 3 H, C$_{ortho}$*H*, C$_{para}$*H*), 2.45 (t, $^3J$ = 7.8, 2 H, 3'-C*H₂*), 2.30 (t, $^3J$ = 7.4, 2 H, 1'-C*H₂*), 1.82 (tt, $^3J$ = 8.0, $^3J$ = 7.2, 2 H, 2'-C*H₂*). - **¹³C NMR** (100.5 MHz, 25 °C, DMSO-d₆): $\delta$ = 174.0 (*C*OOH), 107.0, 88.9, 85.0, 83.2 (*C*$_{arom}$), 33.1 (1'-*C*H₂), 32.0 (3'-*C*H₂), 24.3 (2'-*C*H₂). - **IR** (KBr): $\tilde{v}$ = 1700 vs (C=O), 1447 s, 1430 w, 1406 s, 1284 w, 1246 vs, 1210 w, 940 w, 871 w cm⁻¹. - **EA** C₂₀H₂₄Cl₄O₄Ru₂ (672.354): calcd. C 35.73, H 3.60; found C 35.96, H 3.66.

*[(η⁶-5'-valeric acid)RuCl₂]₂* (**3h**):
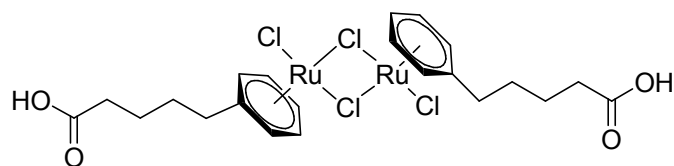


Orange powder; Yield: 261.6 mg (65%). - **¹H NMR** (400 MHz, 25 °C, DMSO-d₆): $\delta$ = 12.03 (s, 1 H, COO*H*), 5.98 (t, $^3J$ = 5.4, 2 H, C$_{meta}$*H*), 5.74 (m, 3 H, C$_{ortho}$*H*, C$_{para}$*H*), 2.45 (t, $^3J$ = 6.6, 2 H, 4'-C*H₂*), 2.24 (t, $^3J$ = 6.0, 2 H, 1'-C*H₂*), 1.57 (m, 4 H, 2'-C*H₂*, 3'-C*H₂*). - **¹³C NMR** (100.5 MHz, 25 °C, DMSO-d₆): $\delta$ = 174.3 (*C*OOH), 107.7, 89.0, 84.7, 83.0 (*C*$_{arom}$), 33.4 (1'-*C*H₂), 32.2 (4'-*C*H₂), 28.3 (3'-*C*H₂), 24.1 (2'-*C*H₂). - **IR** (KBr): $\tilde{v}$ = 1708 vs (C=O), 1447 s, 1426 w, 1411 w, 1402 s, 1310 w, 1222 vs, 929 w, 872 w cm⁻¹. - **EA** C₂₂H₂₈Cl₄O₄Ru₂ (700.407): calcd. C 37.73, H 4.03; found C 37.83, H 3.95.

**General procedure for the synthesis of dinuclear ruthenium complexes with η⁶-arylammoniumchloride-ligands:** The cyclohexadiene-derivative **2i-2l** (5.75 mmol) was stirred with a solution of 20 mL of HCl in ethyl acetate (approx. 2 M). To this solution, RuCl₃ · nH₂O (300 mg, 1.15 mmol) and 40 mL of EtOH was added and the resulting solution heated for 16 h at 80°C. The suspension was reduced to half the volume in vacuo, cooled to -10°C for 48 h, filtered and the precipitate washed with cold pentane and ethanol (each 3 x 5 mL) and dried in vacuo.

*[(η⁶-benzylammonium)RuCl₂]₂Cl₂* (**3i**):
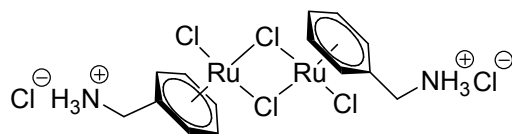


Ochre powder; - Yield: 300.7 mg (83%). - **¹H NMR** (400 MHz, 25 °C, DMSO-d₆): $\delta$ = 8.80 (s, 3 H, N$H_3^+$), 6.23 (d, $^3J$ = 6.0, 2 H, C$_{ortho}H$), 6.13 (t, $^3J$ = 5.8, 2 H, C$_{ortho}H$), 5.98 (t, $^3J$ = 5.6 1 H, C$_{para}H$), 3.81 (s, 2 H, C$H_2$). - **¹³C NMR** (100.5 MHz, 25 °C, DMSO-d₆): $\delta$ = 93.4, 89.3, 87.3, 86.9 (C$_{arom}$), 40.6 (C$H_2$). - **IR** (KBr): $\tilde{v}$ = 1562 vs, 1493 vs, 1376 w, 1211 s, 1141 w, 1106 w, 1038 w, 868 vs cm⁻¹. - **EA** C₁₄H₂₀Cl₆N₂Ru₂ (631.180): calcd. C 26.64, H 3.19, N 4.44; found C 26.90, H 3.40, N 4.27.

*[(η⁶-2'-phenylethylammonium)RuCl₂]₂Cl₂* (**3j**): [10]
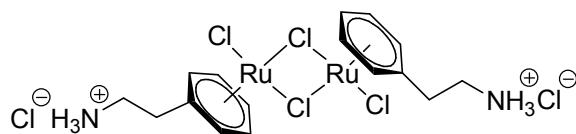


Brown powder, - Yield: 332.0 mg (88%). - **¹H NMR** (400 MHz, 25 °C, DMSO-d₆): $\delta$ = 8.15 (s, 3 H, N$H_3^+$), 6.02 (t, $^3J$ = 5.8, 2 H, C$_{meta}H$), 5.90 (d, $^3J$ = 5.6, 2 H, C$_{ortho}H$), 5.86 (t, $^3J$ = 5.6 1 H, C$_{para}H$), 3.16 (m, 2 H, 1'-C$H_2$), 2.78 (t, $^3J$ = 7.6, 2 H, 2'-C$H_2$). - **¹³C NMR** (100.5 MHz, 25 °C, DMSO-d₆): $\delta$ = 101.1, 87.6, 87.2, 84.9 (C$_{arom}$), 37.8 (1'-C$H_2$), 30.4 (2'-C$H_2$). - **IR** (KBr): $\tilde{v}$ = 1583 s, 1485 s, 1455 vs, 1423 s, 1143 s, 1024 w, 996 w, 945 w, 854 s cm⁻¹. - **EA** C₁₆H₂₄Cl₆N₂Ru₂ (659.233): calcd. C 29.15, H 3.67, N 4.25; found C 29.53, H 3.62, N 4.26.

*[(η⁶-3'-phenylpropylammonium)RuCl₂]₂Cl₂* (**3k**):
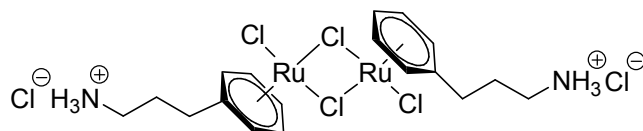


Green powder; - Yield: 341.2 mg (86%). - **¹H NMR** (400 MHz, 25 °C, DMSO-d₆): $\delta$ = 8.04 (s, 3 H, N$H_3^+$), 6.01 (t, $^3J$ = 5.2, 2 H, C$_{meta}H$), 5.79 (m, 3 H, C$_{ortho}H$, C$_{para}H$), 2.85 (m, 2 H, 1'-C$H_2$), 2.54 (t, $^3J$ = 7.4, 2 H, 3'-C$H_2$), 1.90 (m, 2 H, 2'-C$H_2$). - **¹³C NMR** (100.5 MHz, 25 °C, DMSO-d₆): $\delta$ = 106.3, 88.8, 85.1, 83.5 (C$_{arom}$), 38.2 (1'-CH₂), 29.3 (3'-C$H_2$), 26.5 (2'-C$H_2$). - **IR** (KBr): $\tilde{v}$ = 1597 s, 1486 vs, 1450 s, 1417 w, 1136 w, 1041 w, 965 w,

855 s cm$^{-1}$. - **EA** $C_{18}H_{28}Cl_6N_2Ru_2$ (687.286): calcd. C 31.46, H 4.11, N 4.08; found C 31.56, H 4.02, N 3.92.

*[(η$^6$-4'-phenylbutylammonium)RuCl$_2$]$_2$Cl$_2$ (3l)*:
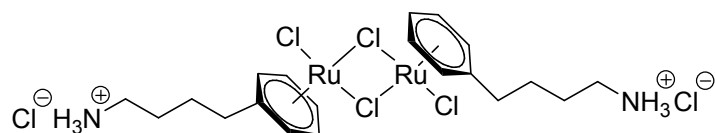


Orange powder; - Yield: 365 mg (89%). - **$^1$H NMR** (400 MHz, 25 °C, DMSO-d$_6$): $\delta$ = 7.94 (s, 3 H, N$H_3^+$), 6.01 (t, $^3J$ = 5.6, 2 H, C$_{meta}H$), 5.78 (d, $^3J$ = 6.4, 2 H, C$_{ortho}H$), 5.75 (d, $^3J$ = 5.6, 1 H, C$_{para}H$), 2.80 (m, 2 H, 1'-C$H_2$), 2.46 (t, $^3J$ = 7.2, 2 H, 4'-C$H_2$), 1.63 (m, 4 H, 2'-C$H_2$, 3'-C$H_2$). - **$^{13}$C NMR** (100.5 MHz, 25 °C, DMSO-d$_6$): $\delta$ = 107.4, 88.9, 84.9, 83.2 ($C_{arom}$), 38.4 (1'-CH$_2$), 31.8 (4'-CH$_2$), 26.5 (3'-CH$_2$), 25.5 (2'-CH$_2$). - **IR** (KBr): $\tilde{v}$ = 1590 s, 1569 w, 1468 vs, 1460 vs, 1147 w, 1120 s, 982 w, 860 s cm$^{-1}$. - **EA** $C_{20}H_{32}Cl_6N_2Ru_2$ (715.339): calcd. C 33.58, H 4.51, N 3.92; found C 33.67, H 4.40, N 3.92.

**General procedure for the synthesis of dinuclear ruthenium complexes with η$^6$-arylacetamide-ligands:** To a stirred solution of cyclohexadiene-derivative **2e**-**2h** (6.90 mmol) in Ethanol (50 mL) RuCl$_3$ · nH$_2$O (300 mg, 1.15 mmol) was added and the resulting solution heated for 16 h at 80°C. The suspension was reduced to half the volume in vacuo, cooled to -10°C for 48 h, filtered and the precipitate washed with cold pentane and ethanol (each 3 x 5 mL) and dried in vacuo.

*[(η$^6$-N-acetyl-benzylamine)RuCl$_2$]$_2$ (3m)*:
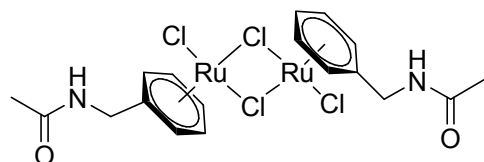


Ochre powder; - Yield: 251.1 mg (68%). - **$^1$H NMR** (400 MHz, 25 °C, DMSO-d$_6$): $\delta$ = 8.34 (t, $^3J$ = 6.0, 1 H, N$H$), 6.05 (t, $^3J$ = 6.0, 2 H, C$_{meta}H$), 5.81 (d, $^3J$ = 6.4, 2 H, C$_{ortho}H$), 5.78 (d, $^3J$ = 6.0, 1 H, C$_{para}H$), 4.11 (d, $^3J$ = 6.4, 2 H, C$H_2$), 1.87 (s, 3 H, C$H_3$). - **$^{13}$C NMR** (100.5 MHz, 25 °C, DMSO-d$_6$): $\delta$ = 170.0 ($C$ONH), 103.1, 88.6, 85.0, 84.1 ($C_{arom}$), 65.7 (CH$_2$), 22.4 (CH$_3$). - **IR** (KBr): $\tilde{v}$ = 1682 vs (C=O), 1534 s, 1448 w, 1421 w, 1286 w, 1271

w cm$^{-1}$. - **EA** $C_{18}H_{22}Cl_4N_2O_2Ru_2$ (642.331): calcd. C 33.66, H 3.45, N 4.36; found C 33.34, H 3.54, N 4.12.

*[($\eta^6$-N-acetyl-2'-phenylethylamine)RuCl$_2$]$_2$* (**3n**):
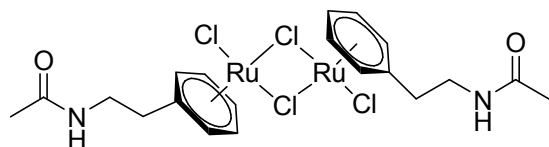


Ochre powder; - Yield: 354.7 mg (92%). - **$^1$H NMR** (400 MHz, 25 °C, DMSO-d$_6$): $\delta$ = 7.94 (m, 1 H, N*H*), 5.98 (t, $^3J$ = 5.6, 2 H, C$_{meta}H$), 5.76 (m, 3 H, C$_{ortho}H$, C$_{para}H$), 3.34 (m, 2 H, 1'-C*H*$_2$), 2.56 (t, $^3J$ = 6.8, 2 H, 2'-C*H*$_2$), 1.78 (s, 3 H, C*H*$_3$). - **$^{13}$C NMR** (100.5 MHz, 25 °C, DMSO-d$_6$): $\delta$ = 169.4 (*C*ONH), 104.3, 88.3, 86.0, 84.0 (*C*$_{arom}$), 38.0 (2'-*C*H$_2$), 32.8 (1'-*C*H$_2$), 22.6 (*C*H$_3$). - **IR** (KBr): $\tilde{v}$ = 1643 vs (C=O), 1567 br, 1446 s, 1376 s, 1297 vs, 1254 w, 1194 w, 1153 w, 1103 w cm$^{-1}$. - **EA** $C_{20}H_{26}Cl_4N_2O_2Ru_2$ (670.385): calcd. C 35.83, H 3.91, N 4.18; found C 35.38, H 3.91, N 4.07.

*[($\eta^6$-N-acetyl-3'-phenylpropylamine)RuCl$_2$]$_2$* (**3o**):
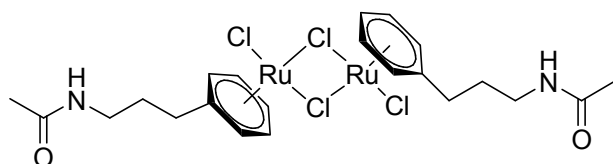


Ochre powder; - Yield: 336 mg (84%). - **$^1$H NMR** (400 MHz, 25 °C, DMSO-d$_6$): $\delta$ = 7.90 (m, 1 H, N*H*), 5.99 (t, $^3J$ = 4.8, 2 H, C$_{meta}H$), 5.74 (m, 3 H, C$_{ortho}H$, C$_{para}H$), 3.07 (dt, $^3J$ = 6.4, $^3J$ = 5.6, 2 H, 1'-C*H*$_2$), 2.44 (t, $^3J$ = 7.2, 2 H, 3'-C*H*$_2$), 1.79 (s, 3 H, C*H*$_3$), 1.71 (tt, $^3J$ = 7.2, $^3J$ = 6.4, 2 H, 2'-C*H*$_2$). - **$^{13}$C NMR** (100.5 MHz, 25 °C, DMSO-d$_6$): $\delta$ = 169.2 (*C*ONH), 107.5, 88.89, 84.9, 83.1 (*C*$_{arom}$), 37.9 (1'-*C*H$_2$), 30.1 (2'-*C*H$_2$), 28.8 (3'-*C*H$_2$), 22.6 (*C*H$_3$). - **IR** (KBr): $\tilde{v}$ = 1645 vs (C=O), 1558 vs, 1450 s, 1367 w, 1297 s, 1150 w, 1101 w cm$^{-1}$. - **EA** $C_{22}H_{30}Cl_4N_2O_2Ru_2$ (698.438): calcd. C 37.83, H 4.33, N 4.01; found C 37.54, H 4.31, N 3.96.

*[(η$^6$-N-acetyl-4'-phenylbutylamine)RuCl$_2$]$_2$* (**3p**):
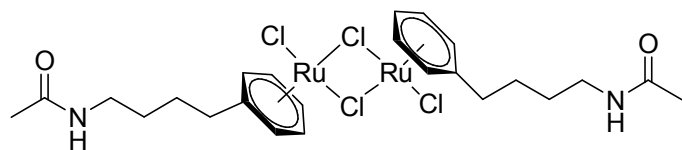


Brown powder; - Yield: 336 mg (84%). - **$^1$H NMR** (400 MHz, 25 °C, DMSO-d$_6$): $\delta$ = 7.82 (m, 1 H, N$H$), 5.99 (t, $^3J$ = 6.0, 2 H, C$_{meta}H$), 5.75 (d, $^3J$ = 5.6, 2 H, C$_{ortho}H$), 5.73 (d, $^3J$ = 6.0, 1 H, C$_{para}H$), 3.04 (dt, $^3J$ = 6.4, 2 H, 1'-C$H_2$), 2.43 (t, $^3J$ = 7.6, 2 H, 4'-C$H_2$), 1.78 (s, 3 H, C$H_3$), 1.57 (tt, $^3J$ = 7.2, $^3J$ = 7.2, 2 H, 3'-C$H_2$), 1.43 (tt, $^3J$ = 7.2, $^3J$ = 6.8, 2 H, 2'-C$H_2$). - **$^{13}$C NMR** (100.5 MHz, 25 °C, DMSO-d$_6$): $\delta$ = 169.1 (*C*ONH), 107.8, 89.0, 84.8, 83.0 (*C*$_{arom}$), 38.1 (1'-*C*H$_2$), 32.2 (4'-*C*H$_2$), 28.8 (3'-*C*H$_2$), 26.4 (2'-*C*H$_2$), 22.6 (*C*H$_3$). - **IR** (KBr): $\tilde{v}$ = 1652 / 1636 (C=O), 1559 vs, 1450 s, 1370 w, 1299 s, 1214 w, 1150 w cm$^{-1}$. - **EA** C$_{24}$H$_{34}$Cl$_4$N$_2$O$_2$Ru$_2$ (726.491): calcd. C 39.68, H 4.72, N 3.86; found C 39.13, H 4.57, N 3.73.

**General procedure for the synthesis of dinuclear ruthenium complexes with η$^6$-arylcarboxyl-ethylester-ligands:** The cyclohexadiene-derivative **2m**-**2p** (5.75 mmol) was stirred with a solution of 20 mL of HCl in ethyl acetate (approx. 2 M) for 1 h. To this solution, RuCl$_3$ · nH$_2$O (300 mg, 1.15 mmol) and 40 mL of EtOH was added and the resulting solution heated for 16 h at 80°C. The suspension was reduced to half the volume in vacuo, cooled to -10°C for 48 h, filtered and the precipitate washed with cold pentane and ethanol (each 3 x 5 mL) and dried in vacuo.

*[(η$^6$-2'-phenyl acetyl ethyl ester)RuCl$_2$]$_2$* (**3q**):
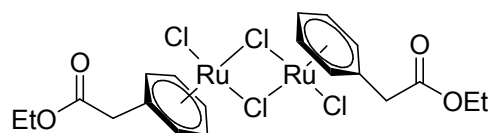


Red powder; - Yield: 323 mg (83%). - **$^1$H NMR** (400 MHz, 25 °C, DMSO-d$_6$): $\delta$ = 6.03 (t, $^3J$ = 5.8, 2 H, C$_{meta}H$), 5.93 (d, $^3J$ = 5.6, 2 H, C$_{ortho}H$), 5.84 (t, $^3J$ = 5.6, 1 H, C$_{para}H$), 4.11 (q, $^3J$ = 7.2, 2 H, C$H_2$-CH$_3$), 3.57 (s, 2 H, 1'-C$H_2$), 1.20 (t, $^3J$ = 7.0, 3 H, CH$_2$-C$H_3$). - **$^{13}$C NMR** (100.5 MHz, 25 °C, DMSO-d$_6$): $\delta$ = 169.4 (*C*OOEt), 98.2, 88.4, 87.2, 84.8 (*C*$_{arom}$), 60.8 (*C*H$_2$-CH$_3$), 37.6 (1'-*C*H$_2$), 14.0 (CH$_2$-*C*H$_3$). - **IR** (KBr): $\tilde{v}$ = 1743 vs sh

(C=O), 1450 w, 1420 w, 1369 w, 1336 s, 1220 s, 1177 vs, 1032 w cm$^{-1}$. - **EA** C$_{20}$H$_{24}$Cl$_4$O$_4$Ru$_2$ (672.354): calcd. C 35.73, H 3.60; found C 35.73, H 3.72.

*[(η$^6$-3'-phenyl propanoic acid ethyl ester)RuCl$_2$]$_2$* (**3r**):
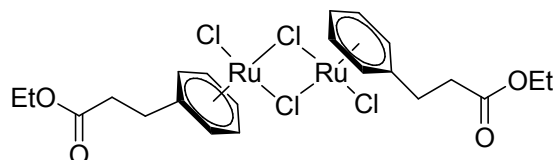


Red powder. Yield: 321 mg (80%). - **$^1$H NMR** (400 MHz, 25 °C, DMSO-d$_6$): $\delta$ = 5.99 (t, $^3J$ = 5.8, 2 H, C$_{meta}$H), 5.82 (d, $^3J$ = 5.6, 2 H, C$_{ortho}$H), 5.77 (t, $^3J$ = 5.4, 1 H, C$_{para}$H), 4.07 (q, $^3J$ = 7.1, 2 H, C$H_2$-CH$_3$), 2.72 (m, 4 H, 1'-C$H_2$, 2'-C$H_2$), 1.17 (t, $^3J$ = 7.0, 3 H, CH$_2$-C$H_3$). - **$^{13}$C NMR** (100.5 MHz, 25 °C, DMSO-d$_6$): $\delta$ = 171.9 (COOEt), 105.1, 88.2, 85.9, 83.9 (C$_{arom}$), 60.1 (CH$_2$-CH$_3$), 32.4 (2'-CH$_2$), 27.7 (1'-CH$_2$), 14.1 (CH$_2$-CH$_3$). - **IR** (KBr): $\tilde{v}$ = 1728 vs (C=O), 1449 w, 1418 w, 1378 w, 1248 w, 1203 s, 1172 s, 867 w cm$^{-1}$. - **EA** C$_{22}$H$_{28}$Cl$_4$O$_4$Ru$_2$ (700.407): calcd. C 37.73, H 4.03; found C 37.55, H 3.87.

*[(η$^6$-4'-butyric acid ethyl ester)RuCl$_2$]$_2$* (**3s**):
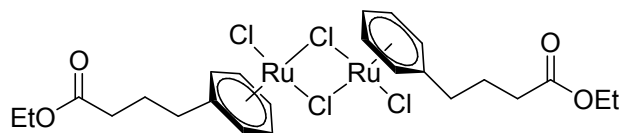


Red powder; - Yield: 354.8 mg (85%). - **$^1$H NMR** (400 MHz, 25 °C, DMSO-d$_6$): $\delta$ = 5.99 (t, $^3J$ = 5.6, 2 H, C$_{meta}$H), 5.74 (m, 3 H, C$_{ortho}$H, C$_{para}$H), 4.04 (q, $^3J$ = 7.1, 2 H, C$H_2$-CH$_3$), 2.46 (t, $^3J$ = 7.8, 2 H, 3'-C$H_2$), 2.37 (t, $^3J$ = 7.4, 2 H, 1'-C$H_2$), 1.84 (tt, $^3J$ = 7.6, 2 H, 2'-C$H_2$), 1.18 (t, $^3J$ = 7.0, 3 H, CH$_2$-C$H_3$). - **$^{13}$C NMR** (100.5 MHz, 25 °C, DMSO-d$_6$): $\delta$ = 172.4 (COOEt), 106.9, 88.9, 85.1, 83.3 (C$_{arom}$), 59.9 (CH$_2$-CH$_3$), 33.0 (3'-CH$_2$), 31.9 (1'-CH$_2$), 24.2 (2'-CH$_2$), 14.1 (CH$_2$-CH$_3$). - **IR** (KBr): $\tilde{v}$ = 1734 vs (C=O), 1447 w, 1376 w, 1318 w, 1304 w, 1196 s, 1176 s, 1155 s, 1035 w, 870 w cm$^{-1}$. - **EA** C$_{24}$H$_{32}$Cl$_4$O$_4$Ru$_2$ (728.460): calcd. C 39.57, H 4.43; found C 39.35, H 4.19.

*[(η$^6$-5'-valeric acid ethyl ester)RuCl$_2$]$_2$* (**3t**):
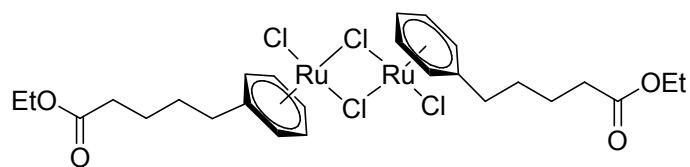


Orange powder; - Yield: 381.6 mg (88%). - **$^1$H NMR** (400 MHz, 25 °C, DMSO-d$_6$): $\delta$ = 5.98 (t, $^3J$ = 5.4, 2 H, C$_{meta}$H), 5.74 (m, 3 H, C$_{ortho}$H, C$_{para}$H), 4.04 (q, $^3J$ = 7.3, 2 H, CH$_2$-CH$_3$), 2.45 (t, $^3J$ = 6.4, 2 H, 4'-CH$_2$), 2.31 (t, $^3J$ = 6.0, 2 H, 1'-CH$_2$), 1.59 (m, 4 H, 2'-CH$_2$, 3'-CH$_2$), 1.17 (t, $^3J$ = 7.2, 3 H, CH$_2$-CH$_3$). - **$^{13}$C NMR** (100.5 MHz, 25 °C, DMSO-d$_6$): $\delta$ = 172.7 (COOEt), 107.6, 89.0, 84.8, 83.1 (C$_{arom}$), 59.7 (CH$_2$-CH$_3$), 33.2 (4'-CH$_2$), 32.1 (1'-CH$_2$), 28.1 (3'-CH$_2$), 24.0 (2'-CH$_2$), 14.1 (CH$_2$-CH$_3$). - **IR** (KBr): $\tilde{v}$ = 1734 vs (C=O), 1450 s, 1415 w, 1378 w, 1310 w, 1271 w, 1179 s, 1033 w, 871 w cm$^{-1}$. - **EA** C$_{26}$H$_{36}$Cl$_4$O$_4$Ru$_2$ (756.514): calcd. C 41.28, H 4.80; found C 41.10, H 4.72.

## 2.4. Monomeric ruthenium complexes with pendant functionalized linker

**General procedure for the synthesis of mononuclear ruthenium catalysts with $\eta^6$-alcohol-ligands:** To a suspension of dinuclear ruthenium(II) complex **3a-3d** (0.15 mmol) in dry dichloromethane (7.5 mL), triphenylphosphine was added (0.30 mmol) and the mixture stirred at RT for 2.5 h. The suspension was filtered, the solvent removed, the residue washed with diethyl ether (3 x 5 mL) and dried in vacuo.

*[($\eta^6$-2'-phenylethanole)(PPh$_3$)RuCl$_2$]* (**4a**): [12]
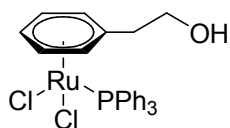


Orange solid; - Yield: 87 mg (52%). - **$^1$H NMR** (400 MHz, 25 °C, CDCl$_3$): $\delta$ = 7.75-7.71 (m, 6 H, C$_{arom'}$H), 7.42-7.37 (m, 9 H, C$_{arom'}$H), 5.60 (d, $^3J$ = 5.2, 2 H, C$_{ortho}$H), 5.02 (t, $^3J$ = 4.8, 2 H, C$_{meta}$H), 4.69 (m, 1 H, C$_{para}$H), 4.10 (t, $^3J$ = 5.2, 2 H, 1'-C$H_2$), 2.89 (m, 2 H, 2'-C$H_2$) 2.25 (s, 1 H, -O$H$). - **$^{13}$C NMR** (100.5 MHz, 25 °C, CDCl$_3$): $\delta$ = 134.3 (d, $J_{PC}$ = 9.2 Hz, C$_{PPh3}$), 133.4 (d, $J_{PC}$ = 47.7 Hz, C$_{ortho'}$), 130.6 (d, $J_{PC}$ = 2.3 Hz, C$_{para'}$), 128.3 (d, $J_{PC}$ = 10.0 Hz, C$_{meta'}$), 108.7 (d, $^2J_{PC}$ = 8.5 Hz, C$_{arom}$), 92.1 (d, $^2J_{PC}$ = 4.6 Hz, C$_{arom}$), 86.2(C$_{arom}$), 83.0 (C$_{arom}$), 61.0 (1'-CH$_2$), 35.5 (2'-CH$_2$). - **$^{31}$P NMR** (161.8 MHz, 25 °C, CDCl$_3$): $\delta$ = 28.35 (s). - **IR** (KBr): $\tilde{v}$ = 1480 s, 1435 vs, 1408 w, 1185 w, 1093 vs, 1048 s, 843 w, 763 w, 750 s cm$^{-1}$. - **EA** C$_{26}$H$_{25}$Cl$_2$OPRu (556.426): calcd. C 56.12, H 4.53; found C 55.51, H 4.18.

*[($\eta^6$-3'-phenylpropanole)(PPh$_3$)RuCl$_2$]* (**4b**): [10]
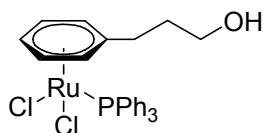


Orange solid; - Yield: 163 mg (95%). - **$^1$H NMR** (400 MHz, 25 °C, CDCl$_3$): $\delta$ = 7.74-7.69 (m, 6 H, C$_{arom'}$H), 7.41-7.35 (m, 9 H, C$_{arom'}$H), 5.35 (d, $^3J$ = 5.2, 2 H, C$_{ortho}$H), 5.13 (t, $^3J$ = 4.6, 2 H, C$_{meta}$H), 4.52 (m, 1 H, C$_{para}$H), 3.76 (t, $^3J$ = 5.8, 2 H, 1'-C$H_2$), 2.78 (t, $^3J$ = 7.4, 2

H, 3'-C$H_2$), 2.20 (s, 1 H, -O$H$), 1.94 (t, $^3J$ = 6.4, $^3J$ = 6.0, 2 H, 2'-C$H_2$). - $^{13}$**C NMR** (67.9 MHz, 25 °C, CDCl$_3$): $\delta$ = 134.3 (d, $J_{PC}$ = 9.2 Hz, $C_{PPh3}$), 133.6 (d, $J_{PC}$ = 47.7 Hz, $C_{ortho'}$), 130.6 (d, $J_{PC}$ = 1.5 Hz, $C_{para'}$), 128.3 (d, $J_{PC}$ = 10.0 Hz, $C_{meta'}$), 112.7 (d, $^2J_{PC}$ = 6.9 Hz, $C_{arom}$), 88.7 (d, $^2J_{PC}$ = 5.4 Hz, $C_{arom}$), 88.0($C_{arom}$), 82.0 ($C_{arom}$), 61.4 (1'-C$H_2$), 30.9 (3'-C$H_2$), 28.6 (2'-C$H_2$). - $^{31}$**P NMR** (161.8 MHz, 25 °C, CDCl$_3$): $\delta$ = 28.83 (s). - **IR** (KBr): $\tilde{v}$ = 1481 s, 1436 vs, 1262 w, 1193 w, 1092 vs, 1064 s, 1029 w, 924 w, 855 w, 751 s cm$^{-1}$. – **EA** C$_{27}$H$_{27}$Cl$_2$OPRu (570.452): calcd. C 56.85, H 4.77; found C 56.38, H 4.83. - **ESI-MS** m/z (%) = 497.0 [M-Cl-HCl-H$_2$]$^+$ (55), 534.9 [M-Cl]$^+$ (50), 1105.0 [2M-Cl]$^+$ (20).

*[($\eta^6$-4'-phenylbutanole)(PPh$_3$)RuCl$_2$]* (**4c**):
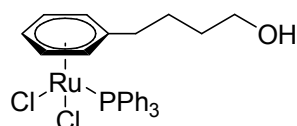


Orange solid; - Yield: 167 mg (93%). - $^1$**H NMR** (400 MHz, 25 °C, CDCl$_3$): $\delta$ = 7.73-7.69 (m, 6 H, $C_{arom'}H$), 7.39-7.33 (m, 9 H, $C_{arom'}H$), 5.26 (d, $^3J$ = 5.6, 2 H, $C_{ortho}H$), 5.17 (t, $^3J$ = 4.8, 2 H, $C_{meta}H$), 4.55 (t, $^3J$ = 4.8, 1 H, $C_{para}H$), 3.64 (t, $^3J$ = 5.8, 2 H, 1'-C$H_2$), 2.63 (t, $^3J$ = 7.6, 2H, 4'-C$H_2$) , 2.28 (s, 1 H, -O$H$), 1.71 (tt, $^3J$ = 7.6, $^3J$ = 6.8, 2 H, 3'-C$H_2$), 1.64 (tt, $^3J$ = 6.8, $^3J$ = 6.4, 2 H, 2'-C$H_2$). - $^{13}$**C NMR** (67.9 MHz, 25 °C, CDCl$_3$): $\delta$ = 134.1 (s, $C_{PPh3}$), 133.4 (d, $J_{PC}$ = 46.9 Hz, $C_{ortho'}$), 130.4 (s, $C_{para'}$), 128.1 (d, $J_{PC}$ = 10.0 Hz, $C_{meta'}$), 112.3 (d, $^2J_{PC}$ = 6.2 Hz, $C_{arom}$), 88.3 (m, $C_{arom}$), 81.6 (d, $^2J_{PC}$ = 9.2 Hz, $C_{arom}$), 61.8 (1'-C$H_2$), 32.2 (4'-C$H_2$), 31.9 (2'-C$H_2$), 25.0 (3'-C$H_2$). - $^{31}$**P NMR** (161.8 MHz, 25 °C, CDCl$_3$): $\delta$ = 28.45 (s). - **IR** (KBr): $\tilde{v}$ = 1481 s, 1435 vs, 1261 w, 1187 w, 1093 vs, 1027 s, 854 w, 801 w, 748 s cm$^{-1}$. - **EA** C$_{28}$H$_{29}$Cl$_2$OPRu (584.479): calcd. C 57.54, H 5.00; found C 57.21, H 5.03.

*[($\eta^6$-5'-phenylpentanole)(PPh$_3$)RuCl$_2$]* (**4d**):
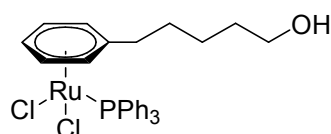


Orange solid; - Yield: 174 mg (97%). - $^1$**H NMR** (400 MHz, 25 °C, CDCl$_3$): $\delta$ = 7.75-7.71 (m, 6 H, $C_{arom'}H$), 7.41-7.36 (m, 9 H, $C_{arom'}H$), 5.24 (d, $^3J$ = 5.2, 2 H, $C_{ortho}H$), 5.16 (t, $^3J$ = 4.8, 2 H, $C_{meta}H$), 4.56 (t, $^3J$ = 4.8, 1 H, $C_{para}H$), 3.63 (t, $^3J$ = 6.4, 2 H, 1'-C$H_2$), 2.63 (t, $^3J$ = 7.6, 2H, 5'-C$H_2$) , 1.66 (tt, $^3J$ = 7.6, 2 H, 4'-C$H_2$), 1.58 (m, 2 H, 2'-C$H_2$), 1.46 (tt, $^3J$ =

8.0, $^3J$ = 6.8, 2 H, 3'-C$H_2$). - **$^{13}$C NMR** (67.9 MHz, 25 °C, CDCl$_3$): δ = 134.2 (d, $J_{PC}$ = 10.0 Hz, $C_{PPh3}$), 133.5 (d, $J_{PC}$ = 46.9 Hz, $C_{ortho'}$), 130.5 (s, $C_{para'}$), 128.2 (d, $J_{PC}$ = 10.0 Hz, $C_{meta'}$), 112.4 (d, $^2J_{PC}$ = 6.2 Hz, $C_{arom}$), 88.4 (s, $C_{arom}$), 81.8 (d, $^2J_{PC}$ = 3.0 Hz, $C_{arom}$), 62.5 (1'-C$H_2$), 32.7 (5'-C$H_2$), 32.4 (4'-C$H_2$), 28.9 (2'-C$H_2$), 25.5 (3'-C$H_2$). - **$^{31}$P NMR** (161.8 MHz, 25 °C, CDCl$_3$): δ = 28.35 (s). - **IR** (KBr): $\tilde{v}$ = 1481 s, 1435 vs, 1261 w, 1186 w, 1092 vs, 1029 w, 846 w, 802 w, 748 s cm$^{-1}$. - **EA** C$_{29}$H$_{31}$Cl$_2$OPRu (598.506): calcd. C 58.20, H 5.22; found C 57.64, H 5.18.

**General procedure for the synthesis of mononuclear ruthenium catalysts except complexes with η$^6$-alcohol-ligands:** To a suspension of dinuclear ruthenium(II) complex **3e**-**3t** (0.15) in methanol / dichloromethane (1 / 1, 7.5 mL), triphenylphosphine was added (0.33 mmol) and the mixture stirred at RT for 1.0 h. The suspension was filtered, the solvent removed, the residue washed with diethyl ether (3 x 5 mL) and dried in vacuo.

*[(η$^6$-2'-phenyl acetic acid)(PPh$_3$)RuCl$_2$]* (**4e**):
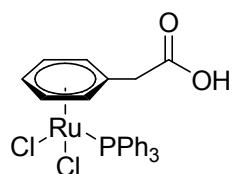


Red solid; - Yield: 102.6 mg (60%). - **$^1$H NMR** (400 MHz, 25 °C, CDCl$_3$): δ = 7.72-7.68 (m, 6 H, $C_{arom'}H$), 7.46-7.37 (m, 9 H, $C_{arom'}H$), 5.41 (d, $^3J$ = 5.2, 2 H, $C_{ortho}H$), 5.23 (t, $^3J$ = 5.2, 2 H, $C_{meta}H$), 4.69 (t, $^3J$ = 5.0, 1 H, $C_{para}H$), 3.78 (s, C$H_2$). - **$^{13}$C NMR** (100.5 MHz, 25 °C, CDCl$_3$): δ = 174.3 (*COOH*), 134.3 (d, $J_{PC}$ = 9.2 Hz, $C_{PPh3}$), 133.7 (d, $J_{PC}$ = 38.4 Hz, $C_{ortho'}$), 130.8 (d, $J_{PC}$ = 2.3 Hz, $C_{para'}$), 128.4 (d, $J_{PC}$ = 10.7 Hz, $C_{meta'}$), 111.2 (s, $C_{arom}$), 89.9 (d, $^2J_{PC}$ = 5.4 Hz, $C_{arom}$), 88.8 (s, $C_{arom}$), 82.1 (s, $C_{arom}$), 38.3 (C$H_2$). - **$^{31}$P NMR** (161.8 MHz, 25 °C, CDCl$_3$): δ = 28.54 (s). - **IR** (KBr): $\tilde{v}$ = 1728 vs (C=O), 1482 w, 1434 vs, 1180 w, 1157 w, 1093 vs cm$^{-1}$. - **EA** C$_{26}$H$_{23}$Cl$_2$O$_2$PRu (570.409): calcd. C 54.75, H 4.06; found C 55.24, H 4.29. - **ESI-MS** m/z (%) = 455.0 [M-2HCl-CO$_2$]$^+$ (60), 495.8 [2M-2HCl-CO$_2$+AcN]$^+$ (100), 1090.7 [2M-2HCl+Na]$^+$ (65).

*[(η⁶-3'-phenyl propanoic acid) (PPh₃)RuCl₂]* (**4f**):
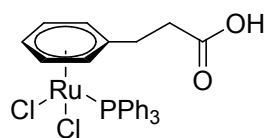


Red solid; - Yield: 134.9 mg (77%). - **¹H NMR** (400 MHz, 25 °C, CD₂Cl₂): $\delta$ = 7.71-7.66 (m, 6 H, $C_{arom'}H$), 7.46-7.37 (m, 9 H, $C_{arom'}H$), 5.28 (t, $^3J$ = 5.6, 2 H, $C_{ortho}H$), 5.21 (t, $^3J$ = 5.7, 2 H, $C_{meta}H$), 4.61 (t, $^3J$ = 5.4, 1 H, $C_{para}H$), 2.85 (t, $^3J$ = 7.0, 2 H, 2'-$CH_2$), 2.66 (t, $^3J$ = 7.2 2 H, 1'-$CH_2$). - **¹³C NMR** (100.5 MHz, 25 °C, CDCl₃ / CD₃OD): $\delta$ = 175.0 ($C$OOH), 134.7 (d, $J_{PC}$ = 9.2 Hz, $C_{PPh3}$), 133.7 (d, $J_{PC}$ = 47.6 Hz, $C_{ortho'}$), 131.2 (s, $C_{para'}$), 128.7 (d, $J_{PC}$ = 10.8 Hz, $C_{meta'}$), 111.1 (d, $^2J_{PC}$ = 6.2 Hz, $C_{arom}$), 89.2 (s, $C_{arom}$), 82.4 (d, $^2J_{PC}$ = 3.8 Hz, $C_{arom}$), 33.3 (1'-$CH_2$), 28.4 (2'-$CH_2$). - **³¹P NMR** (161.8 MHz, 25 °C, CD₂Cl₂): $\delta$ = 28.53 (s). - **IR** (KBr): $\tilde{v}$ = 1710 vs (C=O), 1483 w, 1436 s, 1405 s, 1261 s, 1239 s, 1187 w, 1093 vs, 1026 s cm⁻¹. - **EA** C₂₇H₂₅Cl₂O₂PRu (584.436): calcd. C 55.49, H 4.31; found C 54.76, H 5.06.

*[(η⁶-4'-butyric acid)(PPh₃)RuCl₂]* (**4g**):
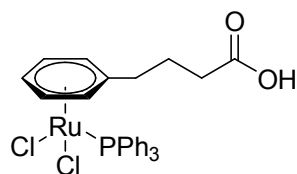


Red solid; - Yield: 144.8 mg (81%). - **¹H NMR** (400 MHz, 25 °C, CDCl₃): $\delta$ = 7.74-7.70 (m, 6 H, $C_{arom'}H$), 7.43-7.35 (m, 9 H, $C_{arom'}H$), 5.28 (d, $^3J$ = 7.2, 2 H, $C_{ortho}H$), 5.18 (t, $^3J$ = 5.0, 2 H, $C_{meta}H$), 4.59 (t, $^3J$ = 4.8, 1 H, $C_{para}H$), 2.69 (t, $^3J$ = 7.8, 2 H, 3'-$CH_2$), 2.48 (t, $^3J$ = 7.4, 2 H, 1'-$CH_2$), 1.98 (tt, $^3J$ = 8.0, $^3J$ = 6.8, 2 H, 2'-$CH_2$). - **¹³C NMR** (100.5 MHz, 25 °C, CDCl₃): $\delta$ = 176.9 ($C$OOH), 134.3 (d, $J_{PC}$ = 9.2 Hz, $C_{PPh3}$), 133.6 (d, $J_{PC}$ = 47.7 Hz, $C_{ortho'}$), 130.6 (s, $C_{para'}$), 128.3 (d, $J_{PC}$ = 10.8 Hz, $C_{meta'}$), 111.2 (d, $^2J_{PC}$ = 6.2 Hz, $C_{arom}$), 88.8 (d, $^2J_{PC}$ = 6.2 Hz, $C_{arom}$), 88.4 (s, $C_{arom}$), 82.1 (s, $C_{arom}$), 33.2 (1'-$CH_2$), 32.0 (3'-$CH_2$), 24.0 (2'-$CH_2$). - **³¹P NMR** (161.8 MHz, 25 °C, CDCl₃): $\delta$ = 28.34 (s). - **IR** (KBr): $\tilde{v}$ = 1740 vs (C=O), 1481 w, 1433 vs, 1394 w, 1262 w, 1150 s, 1093 s cm⁻¹. - **EA** C₂₈H₂₇Cl₂O₂PRu (598.463): calcd. C 56.19, H 4.55; found C 57.46, H 4.59.

*[(η⁶-5'-valeric acid)(PPh₃)RuCl₂]* (**4h**):
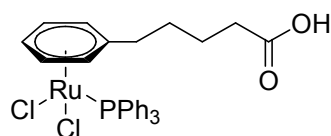


Red solid; - Yield: 111.5 mg (61%). - **¹H NMR** (400 MHz, 25 °C, CDCl₃): $\delta$ = 7.75-7.70 (m, 6 H, C$_{arom'}$H), 7.41-7.36 (m, 9 H, C$_{arom'}$H), 5.25 (d, $^3J$ = 5.6, 2 H, C$_{ortho}$H), 5.18 (t, $^3J$ = 4.8, 2 H, C$_{meta}$H), 4.57 (m, 1 H, C$_{para}$H), 2.63 (m, 2 H, 4'-CH₂), 2.39 (t, $^3J$ = 6.0, 2 H, 1'-CH₂), 1.70 (m, 4 H, 2'-CH₂, 3'-CH₂). - **¹³C NMR** (67.9 MHz, 25 °C, CDCl₃): $\delta$ = 178.2 (COOH), 134.3 (d, $J_{PC}$ = 9.9 Hz, C$_{PPh3}$), 133.6 (d, $J_{PC}$ = 47.8 Hz, C$_{ortho'}$), 130.6 (d, $J_{PC}$ = 1.6 Hz, C$_{para'}$), 128.3 (d, $J_{PC}$ = 9.9 Hz, C$_{meta'}$), 111.9 (d, $^2J_{PC}$ = 6.2 Hz, C$_{arom}$), 88.5 (m, C$_{arom}$), 82.0 (s, C$_{arom}$), 33.7 (1'-CH₂), 32.4 (4'-CH₂), 28.4 (3'-CH₂), 24.4 (2'-CH₂). - **³¹P NMR** (161.8 MHz, 25 °C, CDCl₃): $\delta$ = 28.34 (s). - **IR** (KBr): $\tilde{v}$ = 1726 vs sh (C=O), 1481 w, 1434 s, 1413 w, 1262 vs, 1185 w, 1093 vs, 1025 vs cm$^{-1}$. - **EA** C₂₉H₂₉Cl₂O₂PRu (612.489): calcd. C 56.87, H 4.77; found C 56.93, H 5.83.

*[(η⁶-benzylammonium)(PPh₃)RuCl₂]Cl* (**4i**):
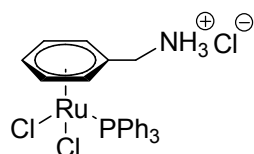


Red solid; - Yield: 136.3 mg (79%). - **¹H NMR** (400 MHz, 25 °C, CD₃OD): $\delta$ = 8.70 (s, 3 H, NH₃⁺), 7.65-7.60 (m, 6 H, C$_{arom'}$H), 7.51-7.43 (m, 9 H, C$_{arom'}$H), 5.80 (d, $^3J$ = 5.8, 2 H, C$_{ortho}$H), 5.52 (t, $^3J$ = 5.0, 2 H, C$_{meta}$H), 4.99 (t, $^3J$ = 5.0 1 H, C$_{para}$H), 3.83 (s, CH₂). - **¹³C NMR** (100.5 MHz, 25 °C, CD₃OD): $\delta$ = 143.3 (d, $J_{PC}$ = 9.2 Hz, C$_{PPh3}$), 142.6 (d, $J_{PC}$ = 46.9 Hz, C$_{ortho'}$), 139.9 (s, C$_{para'}$), 137.5 (d, $J_{PC}$ = 10.0 Hz, C$_{meta'}$), 108.8 (d, $^2J_{PC}$ = 6.9 Hz, C$_{arom}$), 99.6 (d, $^2J_{PC}$ = 5.4 Hz, C$_{arom}$), 97.7 (s, C$_{arom}$), 92.3 (s, C$_{arom}$), 50.1 (CH₂). - **³¹P NMR** (161.8 MHz, 25 °C, DMSO-d₆): $\delta$ = 28.41 (s). - **IR** (KBr): $\tilde{v}$ = 1600 w, 1481 s, 1434 vs, 1093 s, 746 s cm$^{-1}$. - **EA** C₂₅H₂₅Cl₃NPRu (577.875): calcd. C 51.96, H 4.36, N 2.42; found C 51.98, H 4.56, N 2.33.

*[(η⁶-2'-phenylethylammonium)(PPh₃)RuCl₂]Cl* (**4j**): [12,13]
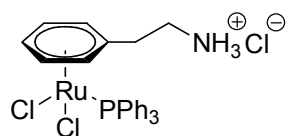


The residue was washed with a small amount of dichloromethane to yield a red solid (105.6 mg, 59%). - **¹H NMR** (400 MHz, 25 °C, CD₃OD): $\delta$ = 7.69-7.65 (m, 6 H, $C_{arom'}H$), 7.51-7.39 (m, 9 H, $C_{arom'}H$), 5.78 (d, $^3J$ = 6.0, 2 H, $C_{ortho}H$), 5.10 (t, $^3J$ = 4.6, 1 H, $C_{para}H$), 5.06 (t, $^3J$ = 5.4 2 H, $C_{meta}H$), 3.53 (t, $^3J$ = 6.8, 2 H, 1'-$CH_2$), 3.08 (dt, $^3J$ = 6.8, 2 H, 2'-$CH_2$). - **¹³C NMR** (100.5 MHz, 25 °C, CD₃OD): $\delta$ = 135.5 (d, $J_{PC}$ = 9.2 Hz, $C_{PPh3}$), 134.3 (d, $J_{PC}$ = 47.7 Hz, $C_{ortho'}$), 131.8 (s, $C_{para'}$), 129.2 (d, $J_{PC}$ = 10.0 Hz, $C_{meta'}$), 104.0 (d, $^2J_{PC}$ = 10.8 Hz, $C_{arom}$), 94.9 (d, $^2J_{PC}$ = 3.8 Hz, $C_{arom}$), 86.4 (s, $C_{arom}$), 85.3 (s, $C_{arom}$), 38.6 (1'-$CH_2$), 30.9 (2'-$CH_2$). - **³¹P NMR** (161.8 MHz, 25 °C, CD₃OD): $\delta$ = 28.86 (s). - **IR** (KBr): $\tilde{v}$ = 1623 w, 1481 s, 1433 vs, 1094 s, 751 s cm$^{-1}$. - **EA** C₂₆H₂₇Cl₃NPRu (591.902): calcd. C 53.76, H 4.60, N 2.37; found C 53.65, H 4.67, N 2.33.

*[(η⁶-3'-phenylpropylammonium)(PPh₃)RuCl₂]Cl* (**4k**):
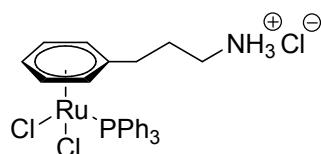


The residue was washed with a small amount of dichloromethane to yield a red solid (122.4 mg, 67%). - **¹H NMR** (400 MHz, 25 °C, CD₃OD): $\delta$ = 7.69-7.64 (m, 6 H, $C_{arom'}H$), 7.47-7.39 (m, 9 H, $C_{arom'}H$), 5.53 (d, $^3J$ = 6.0, 2 H, $C_{ortho}H$), 5.19 (t, $^3J$ = 5.8, 2 H, $C_{meta}H$), 4.79 (m, 1 H, $C_{para}H$), 3.17 (t, 3J = 2 H, 1'-$CH_2$), 2.77 (t, $^3J$ = 7.6, 2 H, 3'-$CH_2$), 2.12 (tt, $^3J$ = 7.4, $^3J$ = 7.6, 2 H, 2'-$CH_2$). - **¹³C NMR** (100.5 MHz, 25 °C, CD₃OD): $\delta$ = 135.5 (d, $J_{PC}$ = 9.2 Hz, $C_{PPh3}$), 134.6 (d, $J_{PC}$ = 47.7 Hz, $C_{ortho'}$), 131.7 (d, $J_{PC}$ = 2.3 Hz, $C_{para'}$), 129.2 (d, $J_{PC}$ = 10.0 Hz, $C_{meta'}$), 111.7 (d, $^2J_{PC}$ = 8.5 Hz, $C_{arom}$), 90.6 (d, $^2J_{PC}$ = 5.4 Hz, $C_{arom}$), 88.1 (s, $C_{arom}$), 84.0 (s, $C_{arom}$), 40.0 (1'-$CH_2$), 29.6 (3'-$CH_2$), 26.2 (2'-$CH_2$). - **³¹P NMR** (161.8 MHz, 25 °C, CD₃OD): $\delta$ = 29.63 (s). - **IR** (KBr): $\tilde{v}$ = 1570 w, 1482 s, 1434 vs, 1093 s, 745 s cm$^{-1}$. - **EA** C₂₇H₂₉Cl₃NPRu (605.929): calcd. C 53.52, H 4.82, N 2.31; found C 52.84, H 4.83, N 2.37.

*[(η⁶-4'-phenylbutylammonium)(PPh₃)RuCl₂]Cl* (**4l**):
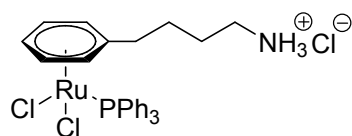


Red solid; - Yield: 163.7 mg (88%). - **¹H NMR** (400 MHz, 25 °C, CDCl₃): $\delta$ = 8.04 (s, 3 H, N$H_3^+$), 7.66-7.62 (m, 6 H, $C_{arom'}H$), 7.37-7.31 (m, 9 H, $C_{arom'}H$), 5.45 (d, $^3J$ = 5.6, 2 H, $C_{ortho}H$), 5.19 (t, $^3J$ = 4.4, 2 H, $C_{meta}H$), 4.40 (t, $^3J$ = 4.8, 1 H, $C_{para}H$), 3.05 (m, 2 H, 1'-$CH_2$), 2.60 (t, $^3J$ = 7.0, 2 H, 4'-$CH_2$), 1.86 (m, 2 H, 3'-$CH_2$), 1.76 (m, 2 H, 2'-$CH_2$). - **¹³C NMR** (100.5 MHz, 25 °C, CDCl₃): $\delta$ = 134.3 (d, $^1J_{PC}$ = 9.1, P$C$), 133.5 (d, $^2J_{PC}$ = 47.6, $C_{ortho'}$), 130.6 (s, $C_{para'}$), 128.3 (d, $^3J_{PC}$ = 9.9, $C_{meta'}$), 113.1 (d, $^2J_{PC}$ = 6.2 Hz, $C_{arom}$), 88.8 (s, $C_{arom}$), 87.9 (d, $^2J_{PC}$ = 5.4 Hz, $C_{arom}$), 81.6 (s, $C_{arom}$), 39.7 (1'-$CH_2$), 32.2 (4'-$CH_2$), 27.0 (3'-$CH_2$), 25.9 (2'-$CH_2$). - **³¹P NMR** (161.8 MHz, 25 °C, CDCl₃): $\delta$ = 29.41 (s). - **IR** (KBr): $\tilde{v}$ = 1607 w, 1481 s, 1434 vs, 1093 s, 746 s cm⁻¹. – **EA** $C_{28}H_{31}Cl_3NPRu$ (619.955): calcd. C 54.25, H 5.04, N 2.26; found C 53.90, H 5.25, N 2.19. - **ESI-MS** m/z (%) = 285.9 [M-Cl-HCl-PPh₃]⁺ (85), 548.0 [M-Cl-HCl]⁺ (100), 1130.8 [2M-Cl-2HCl]⁺ (65), 1209.7 [2M-Cl-HCl+AcN]⁺ (45).

*[(η⁶-N-acetyl-benzylamine)(PPh₃)RuCl₂]* (**4m**):
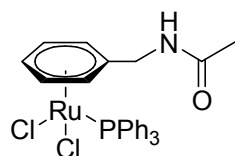


Red solid; - Yield: 175 mg (93%). - **¹H NMR** (400 MHz, 25 °C, CDCl₃): $\delta$ = 7.74-7.69 (m, 6 H, $C_{arom'}H$), 7.44-7.37 (m, 9 H, $C_{arom'}H$), 7.29 (m, 1 H, N$H$), 5.42 (d, $^3J$ = 6.0, 2 H, $C_{ortho}H$), 5.22 (t, $^3J$ = 5.8, 2 H, $C_{meta}H$), 4.67 (t, $^3J$ = 5.3, 1 H, $C_{para}H$), 4.51 (d, $^3J$ = 5.6, 2 H, C$H_2$), 2.08 (s, 3 H, C$H_3$). - **¹³C NMR** (100.5 MHz, 25 °C, CDCl₃): $\delta$ = 171.1 ($C$ONH), 134.2 (d, $J_{PC}$ = 9.2 Hz, $C_{PPh3}$), 133.2 (d, $J_{PC}$ = 46.9 Hz, $C_{ortho'}$), 130.8 (d, $J_{PC}$ = 2.3 Hz, $C_{para'}$), 128.4 (d, $J_{PC}$ = 10.0 Hz, $C_{meta'}$), 108.2 (d, $^2J_{PC}$ = 6.9 Hz, $C_{arom}$), 88.6 (s, $C_{arom}$), 86.9 (d, $^2J_{PC}$ = 5.4 Hz, $C_{arom}$), 81.6 (s, $C_{arom}$), 40.7 ($CH_2$), 23.3 ($CH_3$). - **³¹P NMR** (161.8 MHz, 25 °C, CDCl₃): $\delta$ = 27.36 (s). - **IR** (KBr): $\tilde{v}$ = 1645 vs (C=O), 1554 w, 1482 w, 1435 s, 1300 w, 1093 w, 1025 w cm⁻¹. - **EA** $C_{27}H_{26}Cl_2NOPRu$ (583.451): calcd. C 55.58, H 4.49, N 2.40; found C 54.38, H 4.39, N 2.36.

*[(η⁶-N-acetyl-2'-phenylethylamine)(PPh₃)RuCl₂]₂* (**4n**):
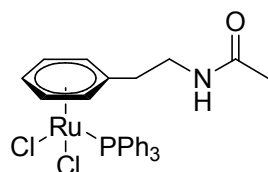


Red solid; - Yield: 177.5 mg (99%). - **¹H NMR** (400 MHz, 25 °C, CDCl₃): $\delta$ = 7.72-7.68 (m, 6 H, $C_{arom'}H$), 7.42-7.36 (m, 9 H, $C_{arom'}H$), 5.58 (t, $^3J$ = 6.0, 2 H, $C_{ortho}H$), 5.00 (t, $^3J$ = 5.0, 2 H, $C_{meta}H$), 4.62 (m, 1 H, $C_{para}H$), 3.73 (m, 2 H, 1'-C$H_2$), 2.95 (m, 2 H, 2'-C$H_2$), 1.93 (s, 3 H, C$H_3$). - **¹³C NMR** (100.5 MHz, 25 °C, CDCl₃): $\delta$ = 171.4 ($C$ONH), 134.3 (d, $J_{PC}$ = 9.2 Hz, $C_{PPh3}$), 133.3 (d, $J_{PC}$ = 46.9 Hz, $C_{ortho'}$), 130.7 (d, $J_{PC}$ = 1.5 Hz, $C_{para'}$), 128.3 (d, $J_{PC}$ = 10.0 Hz, $C_{meta'}$), 109.5 (d, $^2J_{PC}$ = 8.5 Hz, $C_{arom}$), 91.0 (d, $^2J_{PC}$ = 4.6 Hz, $C_{arom}$), 85.9 (s, $C_{arom}$), 82.9 (s, $C_{arom}$), 37.0 (2'-$CH_2$), 31.8 (1'-$CH_2$), 23.5 ($CH_3$). - **³¹P NMR** (161.8 MHz, 25 °C, CDCl₃): $\delta$ = 29.18 (s). - **IR** (KBr): $\tilde{v}$ = 1653 vs (C=O), 1540 w, 1482 w, 1435 vs, 1093 s, 746 w cm⁻¹. - **EA** C₂₈H₂₈Cl₂NOPRu (597.478): calcd. C 56.29, H 4.72, N 2.34; found C 56.21, H 4.84, N 2.10. - **ESI-MS** m/z (%) = 299.9 [M-Cl-PPh₃]⁺ (100), 561.9 [M-Cl]⁺ (60).

*[(η⁶-N-acetyl-3'-phenylpropylamine)(PPh₃)RuCl₂]* (**4o**):
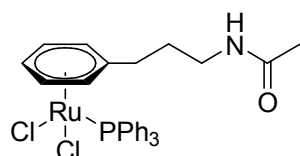


Red solid; - Yield: 143 mg (78%). - **¹H NMR** (400 MHz, 25 °C, CDCl₃): $\delta$ = 7.72-7.68 (m, 6 H, $C_{arom'}H$), 7.42-7.35 (m, 9 H, $C_{arom'}H$), 6.46 (m, 1 H, N$H$), 5.40 (d, $^3J$ = 6.0, 2 H, $C_{ortho}H$), 5.07 (t, $^3J$ = 5.7, 2 H, $C_{meta}H$), 4.47 (t, $^3J$ = 5.8, 1 H, $C_{para}H$), 3.40 (dt, $^3J$ = 6.4, $^3J$ = 5.6, 2 H, 1'-C$H_2$), 2.75 (t, $^3J$ = 6.8, 2 H, 3'-C$H_2$), 1.98 (tt, $^3J$ = 7.2, $^3J$ = 6.8, 2 H, 2'-C$H_2$), 1.95 (s, 3 H, C$H_3$). - **¹³C NMR** (100.5 MHz, 25 °C, CDCl₃): $\delta$ = 170.8 ($C$ONH), 134.3 (d, $J_{PC}$ = 9.2 Hz, $C_{PPh3}$), 133.5 (d, $J_{PC}$ = 50.7 Hz, $C_{ortho'}$), 130.7 (s, $C_{para'}$), 128.3 (d, $J_{PC}$ = 10.0 Hz, $C_{meta'}$), 112.6 (d, $^2J_{PC}$ = 7.7 Hz, $C_{arom}$), 88.9 (d, $^2J_{PC}$ = 5.4 Hz, $C_{arom}$), 87.1 (s, $C_{arom}$), 82.3 (s, $C_{arom}$), 38.3 (1'-$CH_2$), 28.7 (2'-$CH_2$), 26.6 (3'-$CH_2$), 23.5 ($CH_3$). - **³¹P NMR** (161.8 MHz, 25 °C, CDCl₃): $\delta$ = 28.95 (s). – **IR** (KBr): $\tilde{v}$ = 1671 vs (C=O), 1533 s, 1481 w, 1434 s, 1373 w, 1280 w, 851 s, 752 s cm⁻¹. - **EA** C₂₉H₃₀Cl₂NOPRu (611.504): calcd. C 56.29, H 4.72, N 2.34; found C 56.59, H 4.85, N 2.12.

*[(η⁶-N-acetyl-4'-phenylbutylamine)(PPh₃)RuCl₂]₂* (**4p**):
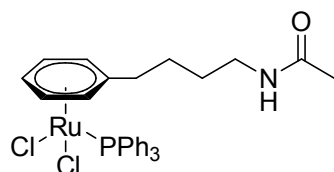


Red solid; - Yield: 167 mg (89%). - **$^1$H NMR** (400 MHz, 25 °C, CDCl₃): $\delta$ = 7.74-7.69 (m, 6 H, $C_{arom'}H$), 7.43-7.35 (m, 9 H, $C_{arom'}H$), 6.13 (m, 1 H, N$H$), 5.33 (d, $^3J$ = 5.6, 2 H, $C_{ortho}H$), 5.11 (t, $^3J$ = 5.6, 2 H, $C_{meta}H$), 4.57 (t, $^3J$ = 5.2, 1 H, $C_{para}H$), 3.30 (dt, $^3J$ = 6.8, $^3J$ = 6.0, 2 H, 1'-$CH_2$), 2.67 (t, $^3J$ = 7.8, 2 H, 4'-$CH_2$), 1.93 (s, 3 H, $CH_3$), 1.76 (tt, 2 H, $^3J$ = 8.0, $^3J$ = 6.8, 2 H, 3'-$CH_2$), 1.64 (tt, 2 H, $^3J$ = 6.8, 2'-$CH_2$). - **$^{13}$C NMR** (100.5 MHz, 25 °C, CDCl₃): $\delta$ = 170.6 ($C$ONH), 134.3 (d, $J_{PC}$ = 9.2 Hz, $C_{PPh3}$), 133.5 (d, $J_{PC}$ = 43.8 Hz, $C_{ortho'}$), 130.6 (s, $C_{para'}$), 128.3 (d, $J_{PC}$ = 10.0 Hz, $C_{meta'}$), 112.2 (d, $^2J_{PC}$ = 6.9 Hz, $C_{arom}$), 89.0 (d, $^2J_{PC}$ = 5.4 Hz, $C_{arom}$), 87.8 (s, $C_{arom}$), 81.9 (s, $C_{arom}$), 38.5 (1'-$CH_2$), 31.4 (4'-$CH_2$), 28.7 (3'-$CH_2$), 24.9 (2'-$CH_2$), 23.5 ($CH_3$). - **$^{31}$P NMR** (161.8 MHz, 25 °C, CDCl₃): $\delta$ = 28.44 (s). - **IR** (KBr): $\tilde{v}$ = 1652 (C=O), 1449 s, 1482 s, 1435 vs, 1370 w, 1291 w, 1093 s, 848 w, 748 s cm⁻¹. - **EA** C₃₀H₃₂Cl₂NOPRu (625.531): calcd. C 57.60, H 5.16, N 2.24; found C 57.78, H 5.29, N 2.09.

*[(η⁶-2'-phenyl acetyl ethyl ester)(PPh₃)RuCl₂]* (**4q**):
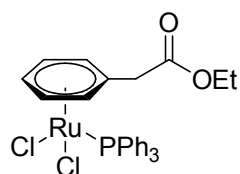


Red solid; - Yield: 148.7 mg (83%). - **$^1$H NMR** (400 MHz, 25 °C, CDCl₃): $\delta$ = 7.74-7.70 (m, 6 H, $C_{arom'}H$), 7.43-7.35 (m, 9 H, $C_{arom'}H$), 5.37 (d, $^3J$ = 6.0, 2 H, $C_{ortho}H$), 5.21 (t, $^3J$ = 5.2, 2 H, $C_{meta}H$), 4.70 (t, $^3J$ = 4.6, 1 H, $C_{para}H$), 4.16 (q, $^3J$ = 7.1, 2 H, $CH_2$-CH₃), 3.64 (s, 2 H, 1'-$CH_2$), 1.26 (t, $^3J$ = 7.0, 3 H, CH₂-$CH_3$). - **$^{13}$C NMR** (100.5 MHz, 25 °C, CDCl₃): $\delta$ = 170.2 ($C$OOEt), 134.2 (d, $J_{PC}$ = 9.2 Hz, $C_{PPh3}$), 133.4 (d, $J_{PC}$ = 48.4 Hz, $C_{ortho'}$), 130.6 (d, $J_{PC}$ = 1.5 Hz, $C_{para'}$), 128.3 (d, $J_{PC}$ = 10.0 Hz, $C_{meta'}$), 102.7 (d, $^2J_{PC}$ = 6.9 Hz, $C_{arom}$), 91.1 (d, $^2J_{PC}$ = 5.4 Hz, $C_{arom}$), 88.1 (s, $C_{arom}$), 82.8 (s, $C_{arom}$), 61.6 ($CH_2$-CH₃), 38.4 (1'-$CH_2$), 14.2 (CH₂-$CH_3$). - **$^{31}$P NMR** (161.8 MHz, 25 °C, CDCl₃): $\delta$ = 28.38 (s). - **IR** (KBr): $\tilde{v}$ = 1733 vs (C=O), 1483 s, 1435 s, 1216 w, 1175 w, 1161 w, 1094 s cm⁻¹. - **EA** C₂₈H₂₇Cl₂O₂PRu (598.463): calcd. C 56.19, H 4.55; found C 56.19, H 4.49.

*[(η⁶-3'-phenyl propanoic acid ethyl ester)(PPh₃)RuCl₂]* (**4r**):
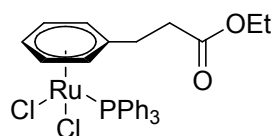


Red solid; - Yield: 86.4 mg (47%). - **¹H NMR** (400 MHz, 25 °C, CDCl₃): $\delta$ = 7.76-7.71 (m, 6 H, $C_{arom'}H$), 7.42-7.37 (m, 9 H, $C_{arom'}H$), 5.30 (d, $^3J$ = 8.4, 2 H, $C_{ortho}H$), 5.16 (t, $^3J$ = 4.8, 2 H, $C_{meta}H$), 4.61 (t, $^3J$ = 5.2, 1 H, $C_{para}H$), 4.09 (q, $^3J$ = 7.1, 2 H, $CH_2$-CH₃), 2.96 (t, $^3J$ = 7.0, 2'-$CH_2$), 2.74 (t, $^3J$ = 7.0, 1'-$CH_2$), 1.22 (t, $^3J$ = 7.4, 3 H, CH₂-$CH_3$). - **¹³C NMR** (100.5 MHz, 25 °C, CDCl₃): $\delta$ = 172.4 ($C$OOEt), 134.3 (d, $J_{PC}$ = 9.2 Hz, $C_{PPh3}$), 133.6 (d, $J_{PC}$ = 47.7 Hz, $C_{ortho'}$), 130.6 (d, $J_{PC}$ = 2.3 Hz, $C_{para'}$), 128.3 (d, $J_{PC}$ = 10.0 Hz, $C_{meta'}$), 110.1 (d, $^2J_{PC}$ = 6.9 Hz, $C_{arom}$), 89.1 (d, $^2J_{PC}$ = 6.2 Hz, $C_{arom}$), 88.2 (s, $C_{arom}$), 82.2 (s, $C_{arom}$), 60.9 ($CH_2$-CH₃), 33.0 (2'-$CH_2$), 27.9 (1'-$CH_2$), 14.3 (CH₂-$CH_3$). - **³¹P NMR** (161.8 MHz, 25 °C, CDCl₃): $\delta$ = 28.10 (s). - **IR** (KBr): $\tilde{v}$ = 1728 vs (C=O), 1481 s, 1435 s, 1262 s, 1093 s cm⁻¹. - **EA** C₂₉H₂₉Cl₂O₂PRu (612.489): calcd. C 56.87, H 4.77; found C 56.32, H 4.88. - **ESI-MS** m/z (%) = 315.0 [M-Cl-PPh₃]⁺ (90), 541.1 [M-Cl-HCl]⁺ (95), 355.7 [M-PPh₃-Cl+AcN]⁺ (85), 576.9 [M-Cl]⁺ (100).

*[(η⁶-4'-butyric acid ethyl ester)(PPh₃)RuCl₂]* (**4s**):
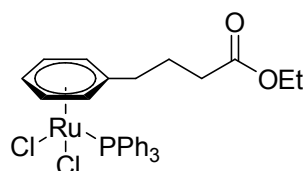


Red solid; - Yield: 171.1 mg (91%). - **¹H NMR** (400 MHz, 25 °C, CDCl₃): $\delta$ = 7.75-7.71 (m, 6 H, $C_{arom'}H$), 7.43-7.35 (m, 9 H, $C_{arom'}H$), 5.26 (d, $^3J$ = 6.0, 2 H, $C_{ortho}H$), 5.18 (t, $^3J$ = 5.7, 2 H, $C_{meta}H$), 4.58 (t, $^3J$ = 5.2, $C_{para}H$), 4.11 (q, $^3J$ = 7.2, 2 H, $CH_2$-CH₃), 2.66 (t, $^3J$ = 7.8, 2 H, 3'-$CH_2$), 2.40 (t, $^3J$ = 7.4, 2 H, 1'-$CH_2$), 1.96 (tt, $^3J$ = 7.6, $^3J$ = 7.2, 2 H, 2'-$CH_2$), 1.25 (t, $^3J$ = 7.2, 3 H, CH₂-$CH_3$). - **¹³C NMR** (100.5 MHz, 25 °C, CDCl₃): $\delta$ = 173.1 ($C$OOEt), 134.4 (d, $J_{PC}$ = 9.2 Hz, $C_{PPh3}$), 133.6 (d, $J_{PC}$ = 47.7 Hz, $C_{ortho'}$), 130.6 (d, $J_{PC}$ = 1.5 Hz, $C_{para'}$), 128.3 (d, $J_{PC}$ = 10.0 Hz, $C_{meta'}$), 111.4 (s, $C_{arom}$), 88.7 (d, $^2J_{PC}$ = 5.4 Hz, $C_{arom}$), 88.5 (s, $C_{arom}$), 82.0 (s, $C_{arom}$), 60.7 ($CH_2$-CH₃), 33.8 (3'-$CH_2$), 32.2 (1'-$CH_2$), 24.5 (2'-$CH_2$), 14.4 (CH₂-$CH_3$). - **³¹P NMR** (161.8 MHz, 25 °C, CDCl₃): $\delta$ = 28.26 (s). - **IR** (KBr): $\tilde{v}$ = 1727 vs (C=O), 1481 w, 1434 s, 1261 w, 1092 s cm⁻¹. - **EA** C₃₀H₃₁Cl₂O₂PRu (626.516): calcd. C 57.51, H 4.99; found C 56.79, H 5.15.

*[(η$^6$-5'-valeric acid ethyl ester)(PPh$_3$)RuCl$_2$]* (**4t**):
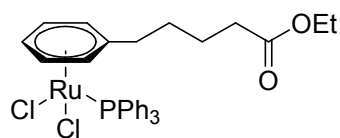


Red solid; - Yield: 173.7 mg (90%). - **$^1$H NMR** (400 MHz, 25 °C, CDCl$_3$): δ = 7.75-7.70 (m, 6 H, C$_{arom'}$H), 7.43-7.34 (m, 9 H, C$_{arom'}$H), 5.23 (d, $^3J$ = 6.0, 2 H, C$_{ortho}$H), 5.17 (t, $^3J$ = 5.6, 2 H, C$_{meta}$H), 4.56 (t, $^3J$ = 4.8, 1 H, C$_{para}$H), 4.10 (q, $^3J$ = 7.2, 2 H, CH$_2$-CH$_3$), 2.63 (t, $^3J$ = 7.0, 2 H, 4'-CH$_2$), 2.32 (t, $^3J$ = 6.8, 2 H, 1'-CH$_2$), 1.68 (m, 4 H, 2'-CH$_2$, 3'-CH$_2$), 1.23 (t, $^3J$ = 7.2, 3 H, CH$_2$-CH$_3$). - **$^{13}$C NMR** (100.5 MHz, 25 °C, CDCl$_3$): δ = 173.5 (COOEt), 134.3 (d, $J_{PC}$ = 10.0 Hz, C$_{PPh3}$), 133.7 (d, $J_{PC}$ = 49.2 Hz, C$_{ortho'}$), 130.6 (d, $J_{PC}$ = 2.3 Hz, C$_{para'}$), 128.3 (d, $J_{PC}$ = 10.0 Hz, C$_{meta'}$), 112.0 (d, $^2J_{PC}$ = 6.2 Hz, C$_{arom}$), 88.5 (m, C$_{arom}$), 82.0 (s, C$_{arom}$), 60.5 (CH$_2$-CH$_3$), 34.1 (4'-CH$_2$), 32.5 (1'-CH$_2$), 28.6 (3'-CH$_2$), 24.6 (2'-CH$_2$), 14.4 (CH$_2$-CH$_3$). - **$^{31}$P NMR** (161.8 MHz, 25 °C, CDCl$_3$): δ = 28.27 (s). - **IR** (KBr): $\tilde{v}$ = 1726 vs (C=O), 1482 w, 1435 s, 1183 s, 1093 s cm$^{-1}$. - **EA** C$_{31}$H$_{33}$Cl$_2$O$_2$PRu (640.542): calcd. C 58.13, H 5.19; found C 57.99, H 4.97.

*Immobilization of [(η$^6$-benzylammonium)(PPh$_3$)RuCl$_2$]Cl* (**5**):
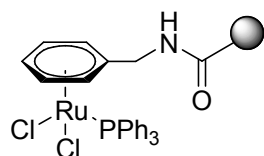


Carboxy functionalized PEG/PS resin (200 mg, 0.3 mmol/g) and EDCI (34.5 mg, 0.18 mmol) were suspended in dichloromethane (5 mL) and stirred gently for 2h at 0°C. Then, a solution of pentafluorophenole (22.1 mg, 0.12 mmol) and dichloromethane (1 mL) were added within 15 minutes to the reaction mixture and stirred 1 h at 0°C and at room temperature over night. The suspension was filtered and washed with diethylether (3*10 mL), and dried under reduced pressure, before it was resuspended in dichloromethane (15 mL) and [(η$^6$-benzylammonium)(PPh$_3$)RuCl$_2$]Cl (**3i**) (69.4 mg, 0.12 mmol) and triethylamine (20 μL, 0.12 mmol) added and stirred for 2 h. Solvents were filtered off and the resin washed with dichloromethane, diethylether and hexane. Solvent residues were removed under reduced pressure, yielding an orange solid (204.4 mg; 0.2 mmol/g; 66%). - **$^{31}$P MAS NMR** (121.496 MHz, HPDEC, 4mm ZrO$_2$ rotor): δ = 28.6 (s). - **EA** (0.2 mmol/g): calcd. Ru 2.0, Cl 1.4, P 0.6; found Ru 1.8, Cl 1.5, P 0.5.

*Synthesis of [(η⁶-4'-phenylbutanole)OsCl₂]₂ (**6**):*
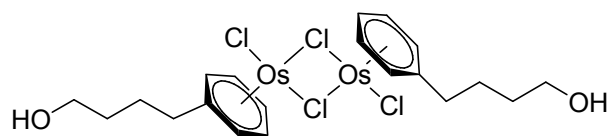


4'-(2,5-dihydrophenyl)butanole (282 mg, 1.85 mmol) was added to a suspension of $OsCl_3 \cdot n\ H_2O$ (109 mg, 0.37 mmol) dry ethanol (20 mL). The resulting slurry was heated to reflux and subsequently cooled to -78°C. The precipitate was filtered off, washed with cold ethanol and pentane (each 2 x 2.5 mL) and the brown product was dried *in vacuo*. Yield:

107 mg (0.13 mmol, 70%). - **¹H NMR** (400 MHz; 25 °C; DMSO-$d_6$): $\delta$ = 6.19 (t, $^3J$ = 5.4, 2 H, $C_{meta}H$), 6.02 (t, $^3J$ = 5.2, 2 H, $C_{ortho}H$), 5.95 (d, 1 H, $^3J$ = 5.8, $C_{para}H$), 3.80 (br, 1H, O$H$), 3.41 (t, $^3J$ = 6.4, 2 H, $C_{(1)}H_2$), 2.37 (t, $^3J$ = 7.7, 2 H, $C_{(4)}H_2$), 1.61 ("quint", $^3J$ = 7.2, $^3J$ = 7.6, 2 H, $C_{(3)}H_2$), 1.47 ("quint", $^3J$ = 7.6, $^3J$ = 6.8, 2 H, $C_{(2)}H_2$). - **¹³C NMR** (100.5 MHz; 25 °C; DMSO-$d_6$): $\delta$ = 100.5, 80.8, 76.3, 74.9 ($C_{arom}$), 60.3 ($C_{(1)}H_2$), 32.2 / 32.1 / 25.9 ($C_{(2)}H_2$ / $C_{(3)}H_2$ / $C_{(4)}H_2$). - **IR** (KBr): $\tilde{v}$ = 2930 vs, 2875 vs, 1455 s, 1433 s, 1399 s, 1184 w, 1137 w, 1074 vs, 1026 w, 980 s, 950 w, 874 s cm⁻¹. - **EA** $C_{20}H_{28}Cl_4O_2Os_2$ (822.7): calcd. C 29.20, H 3.43; found C 28.66, H 3.52.

*Synthesis of (2,5-dihydrobenzyl ammonium)₄[OsCl₆]₂ (**7**):*

2,5-dihydrobenzyl amine (280 mg, 1.93 mmol) was stirred with a solution of 20 mL of HCl in ethyl acetate (approx. 2 M). To this solution, $OsCl_3 \cdot n\ H_2O$ (150 mg, 0.51 mmol) in 20 mL of EtOH was added and subsequently heated to reflux for 16 h. The resulting suspension was reduced to half the volume under reduced pressure, cooled to -10°C for 48 h and filtered. The precipitate was washed with cold pentane and ethanol (each 3 x 5 mL) and the red powder dried *in vacuo*. Yield: 201 mg (63%). - **¹H NMR** (400 MHz, 25 °C, DMSO-$d_6$): $\delta$ = 7.76 (s, 3 H, N$H_3^+$), 5.75-5.66 (m, 3 H, $C_{(3)}H$ / $C_{(5)}H$ / $C_{(6)}H$), 3.36 (s, 2 H, $C_{(1)}H_2$), 2.70-2.60 (m, 4 H, $C_{(4)}H_2$ / $C_{(7)}H_2$). - **¹³C NMR** (100.5 MHz, 25 °C, CD₃OD): $\delta$ = 129.2 / 127.4 / 124.6 / 124.3 ($C_{(2)}$ / $C_{(3)}H$ / $C_{(5)}H$ / $C_{(6)}H$), 51.0 ($C_{(1)}H_2$), 29.6 / 27.4 ($C_{(4)}H_2$ / $C_{(7)}H_2$). - **IR** (KBr): $\tilde{v}$ = 2878 s, 2817 s, 1572 vs, 1469 vs, 1422 s, 1100 w, 1062 w, 960 s, 930 s, 669 s. - **EA** $C_{28}H_{48}Cl_{12}N_4Os_2$ (1246.5): calcd. C 26.98, H 3.88, N 4.49; found C 27.07, H 3.96, N 4.49.

*[(η⁶-N-trifluoroacetyl-benzylamine)RuCl₂]₂* (**8**):
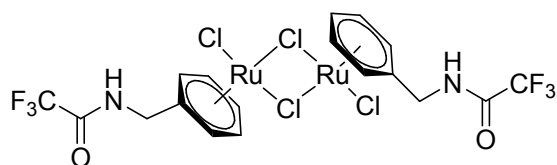


To a stirred, degassed solution N-Trifluoroacetyl-1',4'-cyclohexadiene-1-benzyl amine **2** (288 mg, 1.51 mmol) in ethanol (10 mL) $RuCl_3 \cdot 3\ H_2O$ (68 mg, 0.26 mmol) was added and the resulting solution heated for 16 h at 80°C. The reaction mixture was, cooled to -10°C for 24 h, filtered and the precipitate washed with a small amount of ethanol and dichloromethane. The reaction product was dried in vacuo, yielding an ochre powder. Yield: 66% (64.3 mg, 0.09 mmol).

- **¹H NMR** (400 MHz, 25 °C, DMSO-d₆): $\delta$ = 9.95 (m, 1 H, N$H$), 6.08 (t, 2 H, $^3J$ = 5.0, C$_{meta}H$), 5.93 (d, 2 H, $^3J$ = 5.0, C$_{ortho}H$), 5.88 (d, 1 H, $^3J$ = 5.0, C$_{para}H$), 4.26 (d, 2 H, $^3J$ = 4.6, C$H_2$), 1.87 (s, 3 H, C$H_3$). - **¹³C NMR** (100.5 MHz, 25 °C, DMSO-d₆): $\delta$ = 157.3 (q, $^2J_{FC}$ = 36.6, C(1)), 116.3 (q, $^1J_{FC}$ = 287.5, C(2)), 99.7, 88.6, 87.4, 86.0 (C$_{arom}$), 41.5 (C$_3$). - **¹⁹F NMR** (376.2 MHz; 25 °C; CDCl₃): $\delta$ = -74.17. – **IR** (KBr): $\tilde{\nu}$ = 3244 s, 3073 m, 1736 vs (C=O), 1555 m, 1449 m, 1423 m, 1227 vs, 1193 m, 1159 vs, 989 m cm⁻¹. - **EA** $C_{18}H_{16}Cl_4F_6N_2O_2Ru_2$ (750.27): calcd. C 28.82, H 2.15, N 3.73; found C 28.71, H 2.24, N 3.72.

## 2.5. η⁶- and η⁶:η¹-arene ruthenium phenylalanine complexes

*2,5-dihydro-phenylalanine hydrochloride* (**13**):[14]
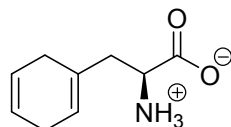


L-Phenylalanine **11** (12 g, 72.6 mmol) was placed in a flask fitted with gas inlet, and pressure relief valve and cooled to -78 °C. Then, liquid ammonia (600 mL) was condensed in the flask under constant stirring, before lithium (6 g) was added slowly to the reaction mixture. The deep blue mixture was maintained at -78°C for 30 minutes, before cold dry ethanol was carefully added until the blue color vanished (approx. 100 mL). The ammonia was allowed to evaporate overnight and the remaining volatiles removed in vacuo. The residual white solid was dissolved in a minimum amount of water (approx. 150 mL), acidified with hydrochloric acid (pH 4), and recrystallized at -18°C over night. The resulting product was collected by filtration and dried in vacuo, giving the title compound **13** (9.11 g, 59.5 mmol, 82%) as a white crystalline solid. - **¹H NMR** (400 MHz; 25 °C; $D_2O$): $\delta$ = 5.75 (s, 2H, -$CH_2CH$=$CH$-$CH_2$-), 5.67 (s, 1H, -$CH_2$-$CH$-C-), 3.99 (dd, $^3J_{(H,H)}$ = 9.6, $^3J_{(H,H)}$ = 4.8, 1H, $\alpha$-$CH$), 2.65 (m, 5H, $\beta$-$CHH'$ / CH-$CH_2$ / C-$CH_2$), 2.49 (m, 1H, $\beta$-$CHH'$). - **¹³C NMR** (100.5 MHz; 25 °C; $D_2O$): $\delta$ = 173.6 ($C_{(1)}$), 128.9 ($C_{(4)}$), 125.3 ($C_{(8)}$), 124.6 ($C_{(7)}$), 124.3 ($C_{(5)}$), 51.9 ($C_{(2)}$), 38.5 ($C_{(3)}$), 27.8 ($C_{(9)}$), 26.4 ($C_{(6)}$). - **IR** (KBr): $\tilde{v}$ = 1691 vs, 1626 vs, 1475 s, 1434 w, 1394 s, 1261 w, 1159 w 961 s, 654 s cm⁻¹. - **FAB-MS:** m/z = 168.0 [m+H]⁺.

*2,5-dihydro-phenylglycine hydrochloride* (**14**):[14]
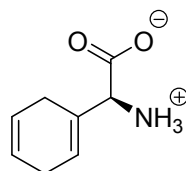


L-Phenylglycine **12** (11 g, 72.6 mmol) was placed in a flask fitted with gas inlet, and pressure relief valve and cooled to -78 °C. Then, liquid ammonia (600 mL) was condensed in the flask under constant stirring, before lithium (6 g) was added slowly to the reaction mixture. The deep blue mixture was maintained at -78°C for 30 minutes,

before cold dry ethanol was carefully added until the blue color vanished (approx. 100 mL). The ammonia was allowed to evaporate overnight and the remaining volatiles removed in vacuo. The residual white solid was dissolved in a minimum amount of water (approx. 150 mL), acidified with hydrochloric acid (pH 4), and recrystallized at -18°C over night. The resulting product was collected by filtration and dried in vacuo, giving the title compound **14** (7.90 g, 52.3 mmol, 72%) as a white crystalline solid. - **$^1$H NMR** (400 MHz; 25 °C; $D_2O$): $\delta$ = 5.72 / 5.38 (m, 3H, -$CH_2CH$=$CH$-$CH_2$- / -$CH_2$-$CH$-C-), 4.25 (s, 1H, $\alpha$-$CH$), 2.40-2.20 (m, 4H, CH-$CH_2$ / C-$CH_2$). - **$^{13}$C NMR** (100.5 MHz; 25 °C; $D_2O$): $\delta$ = 170.5 ($C_{(1)}$), 130.7 / 126.2 / 124.1 / 123.2 ($C_{(3)}$ / $C_{(4)}$ / $C_{(6)}$ / $C_{(7)}$), 58.3 ($C_{(2)}$), 26.5 ($C_{(5)}$), 25.2 ($C_{(8)}$).

*N-p-toluenesulfonyl ethylenediamine* (**15**): [15]
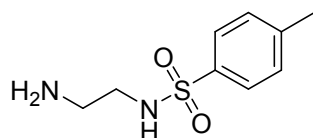


To a vigorously stirred solution of ethylene diamine (6 g, 100 mmol) in dichloromethane (25 mL), a suspension of *p*-toluenesulfonyl chloride (1.9 g, 10 mmol) in dichloromethane (50 mL) was added within 20 minutes. The reaction mixture was stirred at room temperature for 15 minutes and washed twice with deionized water. The organic phase was dried over $CaH_2$ and dried in vacuo. The title compound **15** was obtained as a white powder in 53% yield (1.14 g, 5.3 mmol). - **$^1$H NMR** (400 MHz; 25 °C; $CDCl_3$): $\delta$ = 7.75 (d, , $^3J_{(H,H)}$ = 7.8, 2H, $C_{(arom)}H$, $C_{(arom)}H$), 7.31 (d, $^3J_{(H,H)}$ = 7.8, 2H, $C_{(arom)}H$, $C_{(arom)}H$), 2.95 (t, $^3J_{(H,H)}$ = 5.9, 2H, $C_{(2)}H_2$), 2.78 (t, $^3J_{(H,H)}$ = 5.9, 2H, $C_{(3)}H_2$), 2.422 (s, 3H, $C_{(12)}H_3$. - **$^{13}$C NMR** (100.5 MHz; 25 °C; $CDCl_3$): $\delta$ = 142.9 ($C_{(9arom)}$), 137.0 ($C_{(6arom)}$), 129.0 ($C_{(8arom)}$, $C_{(10arom)}$), 127.3 ($C_{(7arom)}$, $C_{(11arom)}$), 45.2 ($C_{(3)}$), 40.7 ($C_{(2)}$), 20.9 ($C_{(12)}$). - **IR** (KBr): $\tilde{v}$ = 1597 w, 1385 w 1315 s, 1298 s, 1290 sh, 1149 vs, 1096 s, 1045, w, 816 w, 773 w, 660 s, 553 s, 498 w, 466 w, 454 w, 443 w, 427 w, 418 w cm$^{-1}$. - **EA** $C_9H_{14}N_2O_2S$ (214.3): calcd. C 50.45, H 6.59, N 13.07; found C 48.78, H 6.42, N 12.48. - **ESI-MS** m/z = 215.1 [M+H]$^+$; 429.0 [2M+H]$^+$; 451.0 [2M+Na]$^+$.

*1,4-Di-p- toluenesulfonyl ethylenediamine* (**16**): [16]
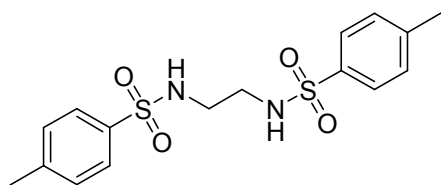


To a stirred mixture of ethylene diamine (3 g, 50 mmol) and KOH (5.6 g, 100 mmol) in dichloromethane (200 mL), a suspension of *p*-toluenesulfonyl chloride (19 g, 100 mmol) in dichloromethane (75 mL) was added within 40 minutes. The reaction mixture was stirred at room temperature over night minutes and washed twice with deionized water (50 mL). The organic phase was dried over $CaH_2$ and dried in vacuo. The title compound **16** was obtained as a white powder in 83% yield (15.3 g, 42 mmol). - **$^1$H NMR** (400 MHz; 25 °C; CDCl$_3$): $\delta$ = 7.70 (d, $^3J_{(H,H)}$ = 8, 4H, C$_{(5arom)}$*H*, C$_{(9arom)}$*H*), 7.30 (d, $^3J_{(H,H)}$ = 8, 4H, C$_{(6arom)}$*H*, C$_{(8arom)}$*H*), 3.05 (s, 4H, C$_{(1)}$*H*$_2$), 2.42 (s, 6H, C$_{(10)}$*H*$_3$), 1.24 (s, 2H, N*H*). - **$^{13}$C NMR** (100.5 MHz; 25 °C; CDCl$_3$): $\delta$ = 143.9 (C$_{(7arom)}$), 136.5 (C$_{(4arom)}$), 129.9 (C$_{(6arom)}$, C$_{(8arom)}$), 127.2 (C$_{(5arom)}$, C$_{(9arom)}$), 43.1 (C$_{(1)}$), 21.6 (C$_{(10)}$). - **IR** (KBr): $\tilde{\nu}$ = 1928 w, 1816 w, 1664, w, 1598, s, 1496 s, 1465 s, 1410 s, 1383 s, 1291 w, 1240 s, 1213 w, 1188 s, 1148 vs, 1093 s, 1061 vs, 1020 s, 959 w, 877 s, 820 s, 799 sh, 752 s, 710 sh, 610 s, 410 w cm$^{-1}$. - **EA** C$_{16}$H$_{20}$N$_2$O$_4$S$_2$ (368.5): calcd. C 52.15, H 5.47, N 7.60; found C 52.14, H 5.47, N 7.58.

*[($\eta^6$-PheOEt)RuCl$_2$]$_2$ · 2 HCl* (**20**):
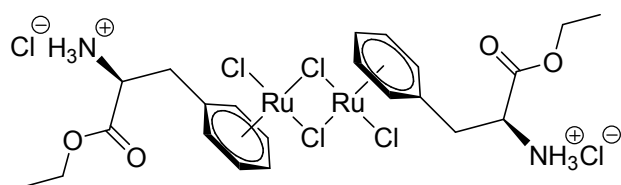


*(R)*-2,5-dihydrophenylalanine (1.02 g, 6.12 mmol) was stirred with 16 mL of a solution of HCl$_{conc.}$ in ethyl acetate (approx. 2M) for 1h. To this suspension RuCl$_3$ · 3 H$_2$O (400 mg, 1.53 mmol) and 60 mL of ethanol were added and the resulting mixture heated at 80°C for 16 h. The resulting suspension was cooled (-78°C) the precipitate was filtered off, washed with cold ethanol and dichloromethane (each 2 x 5 mL) and thereafter dried in under reduced pressure. The pure product **20** (553 mg, 0.69 mmol, 90%) was obtained as an orange powder. - **$^1$H NMR** (400 MHz, 25 °C, DMSO-d$_6$) $\delta$ = 8.92 (s, 6H, -N*H*$_3$$^+$), 6.08-5.87 (m, 10H, C$_{arene}$*H*), 4.39 (dd, $^3J$ = 6.8 Hz,

2H, *α-CH*), 4.23-4.14 (m, 4H, C*H₂*-CH₃), 3.05-2.90 (m, 4H, *β-CH₂*), 1.17 (t, $^3J$ = 7.0, 6H, CH₂-C*H₃*). - **$^{13}$C NMR** (100.5 MHz, 25 °C, DMSO-d₆) *δ* =168.3 (*C*OO), 97.9 / 88.5 / 88.1 / 87.6 / 87.4 / 85.6 (*C*arene), 62.1 (*C*H₂-CH₃), 51.8 (*α-C*H), 33.8 C(*β-C*H₂), 13.9 C(CH₂-*C*H₃). - **IR** (KBr): $\tilde{v}$ = 1724vs (CO), 1487s, 1250s, 1073w, 856w cm$^{-1}$. - **EA** C₂₂H₃₂Cl₆N₂O₄Ru₂ (803.4): calcd. C 32.9, H 4.0, N 3.5; found C 32.9, H 4.0, N 3.4.

*[(η⁶-PheGlyOEt)RuCl₂]₂ · 2 HCl* (**21**):[17]



*(R)*-2,5-dihydrophenylglycine (1.2 g, 6.12 mmol) was stirred with 16 mL of a solution of HCl$_{conc.}$ in ethyl acetate (approx. 2M) for 1h. To this suspension RuCl₃ • 3 H₂O (410 mg, 1.53 mmol) and 60 mL of ethanol were added and the resulting mixture heated at 80°C for 16 h. The resulting suspension was cooled (-78°C) the precipitate was filtered off, washed with cold ethanol and dichloromethane (each 2 x 5 mL) and thereafter dried in under reduced pressure. The pure product **21** (250 mg, 0.32 mmol, 42%) was obtained as an orange powder. - **$^1$H NMR** (400 MHz, 25 °C, DMSO-d₆) *δ* = 9.26 (s, 6H, -N*H₃$^+$*), 6.49-6.16 (m, 10H, C$_{arene}$*H*), 5.16 (s, 2H, *α-CH*), 4.27-4.18 (m, 4H, C*H₂*-CH₃), 1.21 (t, $^3J$ = 7.1, 6H, CH₂-C*H₃*). - **$^{13}$C NMR** (100.5 MHz, 25 °C, DMSO-d₆) *δ* = 165.3 (*C*OO), 91.3 / 91.0 / 89.6 / 86.8 / 85.7 (*C*arene), 62.9 (*C*H₂-CH₃), 56.0 (*α-C*H), 13.7 C(CH₂-*C*H₃).
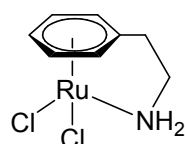
*[(η⁶-benzylammonium)RuCl₂]₂Cl₂* (**3i**):



*(R)*-2,5-dihydrophenylglycine (1.17 g, 7.65 mmol) was added to 20 mL of a solution of HCl$_{conc.}$ in *tert*-butyl alcohol (approx. 2M). Thereafter, RuCl₃ • 3 H₂O (400 mg, 1.53 mmol) in 70 mL of *tert*-butyl alcohol were added and the resulting mixture heated at 80°C for 16 h. The precipitate formed was filtered off, washed with cold ethanol and

dichloromethane (each 2 x 5 mL) and residue dried under reduced pressure. The pure product (666.3 mg, 1.06 mmol, 69%) was yielded as an ochre powder. - $^1$**H NMR** (400 MHz, 25 °C, DMSO-d$_6$) $\delta$ =8.80 (br s, 3 H, N$H_3^+$), 6.23 (d, $^3J$ = 6.0, 2 H, C$_{ortho}H$), 6.13 (t, $^3J$ = 5.8, 2 H, C$_{meta}H$), 5.98 (t, $^3J$ = 5.6 1 H, C$_{para}H$), 3.81 (s, 2 H, C$H_2$). - $^{13}$**C NMR** (100.5 MHz, 25 °C, DMSO-d$_6$) $\delta$ =93.4, 89.3, 87.3, 86.9 (C$_{arene}$), 40.6 (C$H_2$). - **IR** (KBr): $\tilde{v}$ = 3052 vs, 2912 vs, 1594 s, 1489 s, 1455 m, 1384 m, 1203 w, 1111 w, 1088 w, 876 s cm$^{-1}$. - **EA** C$_{14}$H$_{20}$Cl$_6$N$_2$Ru$_2$ (631.18): calcd. C 26.6, H 3.2, N 4.4; found C 26.9, H 3.4, N 4.3.

*[($\eta^6$:$\eta^1$-PheOH)RuCl$_2$]* (**22**):



*(R)*-2,5-dihydrophenylalanine (1.00 g, 6.25 mmol) was added to 20 mL of a solution of HCl$_{conc.}$ in *tert*-butyl alcohol (approx. 2M). Thereafter, RuCl$_3$ • 3 H$_2$O (342 mg, 1.25 mmol) in 100 mL of *tert*-butyl alcohol were added and the resulting mixture heated at 80°C for 16 h. The precipitate formed was filtered off, washed with 2-propanole (2 x 10 mL) and residue dried under reduced pressure. The pure product **22** (438 mg, 1.30 mmol, 52%) was obtained as a yellow powder. - $^1$**H NMR** (400 MHz, 25 °C, CDCl$_3$) $\delta$ = 5.85 (t, 1 H, $^3J_{HH}$ = 5.4 Hz, C$_{meta}H_a$), 5.80 (t, 1 H, $^3J_{HH}$ = 5.6 Hz, C$_{meta}H_b$), 5.63 (d, 1 H, $^3J_{HH}$ = 5.8 Hz, C$_{ortho}H_a$), 5.52 (t, 1 H, $^3J_{HH}$ = 5.8 Hz, C$_{para}H$), 5.39 (d, 1 H, $^3J_{HH}$ = 5.8 Hz, C$_{ortho}H_b$), 4.75-4.62 (m, 2 H, C$H$ / N$H_a$H$_b$), 4.06 (m, 1 H, NH$_a$$H_b$), 3.14 (dd, 1 H, $^3J_{HH}$ = 13.3 Hz, $^3J_{HH}$ = 6.2 Hz, CHC$H_a$H$_b$), 2.84 (dd, 1 H, $^3J_{HH}$ = 12.9 Hz, $^3J_{HH}$ = 12.0 Hz, CHCH$_a$$H_b$). - $^{13}$**C MAS NMR** (12 kHz, CPMAS, HPDEC, 4mm ZrO$_2$ rotor) $\delta$ = 171.4 / 168.6 (CO), 104.1 / 97.2 / 95.3 / 93.4 / 77.0 / 74.4 / 70.9 / 68.9 (C$_{arene}$ / $\alpha$-CH), 40.2 / 39.1 ($\beta$-CH$_2$). – **IR** (KBr): $\tilde{v}$ = 1747vs and 1739vs (CO) cm$^{-1}$. - **EA** C$_9$H$_{11}$Cl$_2$NO$_2$Ru (337.2): calcd. C 32.1, H 3.3, N 4.15, Cl 21.0; found C 32.1, H 3.7, N 4.1, Cl 20.9.

*[(η⁶-PheOH)RuCl₂(Me₂SO)]₂* (**23**):



[(η⁶:η¹-PheOH)RuCl₂]₂ **22** (20 mg, 0.06 mmol) was dissolved in a solution of concentrated hydrochloric acid and deuterated dimethylsulfoxide (520 µL, HCl/DMSO-d₆ = 1/25) and stirred until the complex was completely dissolved, before product complex **23** (quantitative) was analyzed in NMR. - **Opt. Rot.:** $[\alpha]_D^{22}$ +44.0 (c 0.58 in HCl$_{conc}$ / DMSO = 1 / 25). - **¹H NMR** (400 MHz, 25 °C, CDCl₃) $\delta$ = 8.72 (br s, 3 H, NH₃⁺), 6.05-5.96 (m, 3 H, C$_{arene}$H), 5.88 (d, 1 H, $^3J_{HH}$ = 5.8 Hz, C$_{ortho}$H), 5.84 (t, 1 H, $^3J_{HH}$ = 5.6 Hz, C$_{arene}$H), 4.28 (m, 1 H, CHCH₂), 2.95 (d, 1 H, $^3J_{HH}$ = 6.6 Hz, CHCH₂). - **¹³C NMR** (100.5 MHz, 25 °C, CDCl₃) $\delta$ = 169.8 (COO), 98.4 / 88.7 / 88.3 / 87.8 / 87.7 / 85.8 (C$_{arene}$), 52.1 (CH), 33.9 (CHCH₂).

*[(η⁶:η¹-C₆H₅(CH₂)₂NH₂)RuCl₂]* (**24**):



In a standard NMR tube, [(η⁶-C₆H₅(CH₂)₂NH₂)RuCl₂] **9** (20 mg, 0.03 mmol) was dissolved in a solution of triethylamine and deuterated dimethylsulfoxide (520 µL, Et₃N/DMSO-d₆ = 1/25) and immediately analyzed in NMR. - **¹H NMR** (400 MHz, 25 °C, CDCl₃) $\delta$ = 5.74 (t, 2 H, $^3J_{HH}$ = 5.4 Hz, C$_{meta}$H), 5.47 (t, 1 H, $^3J_{HH}$ = 5.4 Hz, C$_{para}$H), 5.29 (d, 2 H, $^3J_{HH}$ = 5.4 Hz, C$_{ortho}$H), 4.39 (m, 2 H, NH₂), 3.59 (t, 2 H, $^3J_{HH}$ = 5.2 Hz, CH₂CH₂NH₂), 2.67 (t, 2 H, $^3J_{HH}$ = 6.2 Hz, CH₂ CH₂NH₂).

*[(η⁶-PheOEt)RuCl₂(PPh₃)]* (**25**):

To a suspension of $[(\eta^6\text{-PheOEt})RuCl_2]_2 \cdot 2\,HCl$ 3 (39 mg, 0.05 mmol) in a solution of methanol / dichloromethane (4 mL, MeOH / DCM = 1 / 1), triphenylphosphine was added (31 mg, 0.12 mmol) and the mixture stirred at RT for 1.5 h, the solvent evaporated under reduced pressure and thereafter the residue redissolved in dichloromethane (1.5 mL) and diethylether (9 mL) added. The precipitate was filtered off and washed with diethylether and hexane. The pure product **25** (62.8 mg, 0.09 mmol, 97%) was obtained as a red solid. - **$^1$H NMR** (400 MHz, 25 °C, DMSO-$d_6$) $\delta$ = 8.77 (br s, 3 H, -N$H_3{}^+$), 7.62 (m, 6 H, $C_{PPh3}H$), 7.32 (m, 9 H, $C_{PPh3}H$), 6.02 (m, 1 H, $C_{ortho}H_a$), 5.80 (m, 1 H, $C_{ortho}H_b$), 5.28 (m, 1 H, $C_{meta}H_a$), 5.18 (m, 1 H, $C_{meta}H_b$), 4.60 (m, 1 H, $\alpha$-C$H$), 4.46 (m, 1 H, $C_{ortho}H$), 4.10 (m, 2 H, C$H_2$CH$_3$), 3.53 (m, 1 H, $\beta$-C$H_a$H$_b$), 3.40 (m, 1 H, $\beta$-CH$_a$$H_b$), 1.03 (m, 3 H, CH$_2$C$H_3$). - **$^{13}$C NMR** (100.5 MHz, 25 °C, DMSO-$d_6$) $\delta$ = 168.2 ($C$OO), 134.2 (d, $J_{PC}$ = 9.2 Hz, $C_{PPh3}$), 133.1 (d, $J_{PC}$ = 56.9 Hz, $C_{PPh3}$), 130.5 (s, $C_{PPh3}$), 128.3 (d, $J_{PC}$ = 9.2 Hz, $C_{PPh3}$), 105.2 / 90.8 / 90.6 / 88.5 / 87.7 / 82.8 ($C_{arene}$), 63.1 ($C$H$_2$CH$_3$), 53.3 ($\alpha$-CH), 33.8 ($\beta$-CH$_2$), 14.1 C(CH$_2$$C$H$_3$). – **$^{31}$P NMR** (161.8 MHz, 25 °C, CDCl$_3$): $\delta$ = 29.52 (s). - **IR** (KBr): $\tilde{v}$ = 1744vs (CO) cm$^{-1}$. - **EA** $C_{29}H_{31}Cl_3NO_2PRu$ (664.0): calcd. C 52.5, H 4.7, N 2.1; found C 52.3, H 4.6, N 2.1. - **ESI-MS:** m/z 592.1 ([M-H-2Cl]$^+$, 100%), 627.9 ([M-Cl]$^+$, 35).
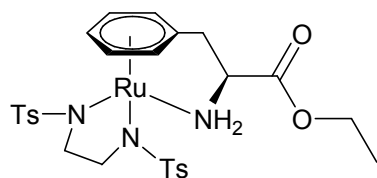
*$[(\eta^6{:}\eta^1\text{-PheOEt})RuCl_2]$* (**26**):



$[(\eta^6\text{-PheOEt})RuCl_2]_2 \cdot 2\,HCl$ **20** (100 mg, 0.12 mmol) suspended in dichloromethane (3 mL). After addition of triethylamine (174 µL, 1.24 mmol), the reaction mixture stirred at room temperature for 2 h, filtered, washed with a small amount of cold dichloromethane and dried under reduced pressure to give the bright yellow powder **26** (30 mg, 0.08 mmol, 33%). - **$^1$H NMR** (400 MHz, 25 °C, CDCl$_3$) $\delta$ = 6.03 (t, 1 H, $^3J_{HH}$ = 5.6 Hz, $C_{meta}H_a$), 5.91 (t, 1 H, $^3J_{HH}$ = 5.4 Hz, $C_{meta}H_b$), 5.50 (t, 1 H, $^3J_{HH}$ = 5.6 Hz, $C_{para}H$), 5.37 (d, 1 H, $^3J_{HH}$ = 5.4 Hz, $C_{ortho}H_b$), 5.26 (d, 1 H, $^3J_{HH}$ = 5.8 Hz, $C_{ortho}H_a$), 4.69 (m, 1 H, C$H$), 4.57 (t, 1 H, $^3J_{HH}$ = 10.4 Hz, N$H_a$H$_b$), 4.30 (q, 2 H, $^3J_{HH}$ = 7.1 Hz, C$H_2$CH$_3$), 3.82 (m, 1 H, NH$_a$$H_b$), 3.28 (dd, 1 H, $^3J_{HH}$ = 14.1 Hz, $^3J_{HH}$ = 6.2 Hz, CHC$H_a$H$_b$), 2.96 (dd, 1 H, $^3J_{HH}$ = 14.1 Hz, $^3J_{HH}$ = 11.2 Hz, CHCH$_a$$H_b$), 1.34 (t, 3 H, $^3J_{HH}$ = 7.0 Hz, CH$_2$C$H_3$). - **$^{13}$C NMR** (100.5 MHz, 25 °C, CDCl$_3$) $\delta$ = 169.9 ($C$OO),
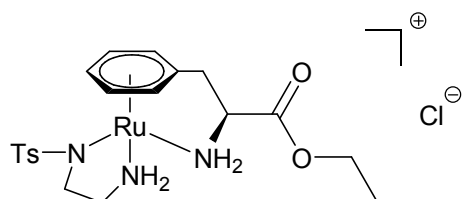
99.9 / 93.9 / 93.4 /78.5 / 75.8 / 72.4 ($C_{arene}$), 68.1 ($CH_2CH_3$), 63.0 ($CH$), 39.1 ($CHCH_2$), 14.3 ($CH_2CH_3$). - **IR** (KBr): $\tilde{v}$ = 1734vs and 1726vs (CO), 1575w, 1384w, 1288s, 1263s, 1206s cm$^{-1}$. - **IR** (nujol): $\tilde{v}$ = 1733vs and 1725vs (CO) cm$^{-1}$. - **IR** (CHCl$_3$): $\tilde{v}$ = 1741vs (CO) cm$^{-1}$. - **EA** C$_{11}$H$_{15}$Cl$_2$NO$_2$Ru (365.2): calcd. C 36.2, H 4.1, N 3.8; found C 35.8, H 4.1, N 3.55.

*[($\eta^6$:$\eta^1$-PheOEt)Ru(enTs$_2$)]* (**27**).



Triethylamine (103 µL, 0.74 mmol) was added to a suspension of [($\eta^6$-PheOEt)RuCl$_2$]$_2$ · 2 HCl (100 mg, 0.14 mmol) and N,N'-di-*p*-tosylethylenediamine (101 mg, 0.24 mmol) in ethanol (15 mL) and heated to reflux for 80 min. The solvent was evaporated under reduced pressure, the crude compound dissolved in dichloromethane (30 mL) and extracted with distilled water and brine (each 3 x 30 mL). The organic phase was dried over MgSO$_4$ and solvent removed under reduced pressure to give the yellow solid **27** (yield: 131 mg, 0.20 mmol, 73%). - **$^1$H NMR** (400 MHz, 25 °C, CDCl$_3$) $\delta$ = 7.67 (d, 4 H, $^3J_{HH}$ = 7.9 Hz, C$_{Ts}H$), 7.19 (m, 4 H, C$_{Ts}H$), 5.89 (t, 1 H, $^3J_{HH}$ = 5.4 Hz, C$_{meta}H_a$), 5.67 (t, 1 H, $^3J_{HH}$ = 5.4 Hz, C$_{meta}H_b$), 5.44 (d, 1 H, $^3J_{HH}$ = 7.0 Hz, C$_{ortho}H_a$), 5.42 (d, 1 H, $^3J_{HH}$ = 6.2 Hz, C$_{ortho}H_b$), 4.80 (t, 1 H, $^3J_{HH}$ = 5.6 Hz, C$_{para}H$), 4.75 (m, 1 H, $\alpha$-C$H$), 4.36 (m, 1 H, $\alpha$-CH-N$H_aH_b$), 4.20 (q, 2 H, $^3J_{HH}$ = 7.2 Hz, C$H_2$CH$_3$), 3.60 (m, 1 H, $\alpha$-CH-NH$_a$$H_b$), 3.26 (dd, 1 H, $^3J_{HH}$ = 13.7, $^3J_{HH}$ = 5.8, $\beta$-C$H_a$H$_b$), 2.70-2.34 (m, 5H, N-C$H_2$ / $\beta$-CH$_a$$H_b$), 2.33 (s, 6 H, C$_{Ts}$C$H_3$), 1.27 (t, 3 H, $^3J_{HH}$ = 6.9 Hz, CH$_2$C$H_3$). - **$^{13}$C NMR** (100.5 MHz, 25 °C, CDCl$_3$) $\delta$ = 170.1 (*C*OO), 141.5 / 141.4 (C$_{Ts}$CH$_3$), 140.8 / 140.1 (C$_{Ts}$SO$_2$), 129.4 / 129.3 / 126.9 / 126.6 (C$_{Ts}$H), 103.4 (*C*$_{arene}$CH$_2$), 93.3 / 91.8 / 80.3 / 77.3 / 69.3 (*C*$_{arene}$H), 67.5 ($\alpha$-*C*H), 62.3 (*C*H$_2$CH$_3$), 53.0 / 52.2 (-N-*C*H$_2$-), 38.4 ($\beta$-*C*H$_2$), 21.4 (C$_{Ts}$*C*H$_3$), 14.1 (CH$_2$*C*H$_3$). – **IR** (KBr): $\tilde{v}$ = 1738vs (CO), 1261vs, 1133vs, 1091vs, 814vs, 662s cm$^{-1}$. - **EA** C$_{27}$H$_{33}$N$_3$O$_6$RuS$_2$ (662.8): calcd. C 49.1, H 5.0, N 6.4; found C 49.0, H 5.0, N 5.9. - **ESI-MS**: m/z = 662.1 ([M+H]$^+$, 100%), 1322.6 ([2M+H]$^+$, 45).

*[($\eta^6$:$\eta^1$-PheOEt)Ru(enTs)]Cl* (**28**):



Triethylamine (103 µL, 0.74 mmol) was added to a suspension of [($\eta^6$-PheOEt)RuCl$_2$]$_2$ · 2 HCl (100 mg, 0.14 mmol) and N-*p*-tosylethylenediamine (59 mg, 0.24 mmol) in ethanol (15 mL) and refluxed for 80 min. Solvent was evaporated under reduced pressure, the crude product was suspended in sodium-dried tetrahydrofurane and left at -20°C for 16 h. Triethylammoniumchloride was filtered and tetrahydrofurane evaporated under reduced pressure. The crude compound was dissolved in dichloromethane, precipitated by adding diethylether, washed with diethylether and hexane and dried in vacuo to give the yellow solid **28** (yield: 81.3 mg, 0.15 mmol, 62%). - **$^1$H NMR** (400 MHz, 25 °C, CDCl$_3$) $\delta$ = 7.74 (d, 4 H, $^3J_{HH}$ = 7.9 Hz, C$_{Ts}$*H* / C̃$_{Ts}$*H̃*), 7.28 (d, 2 H, $^3J_{HH}$ = 7.8 Hz C$_{Ts}$*H* / C̃$_{Ts}$*H̃*), 7.21 (m, 1 H, CH$_2$-N*H$_a$*H$_b$), 6.77 (m, 1 H, C̃H$_2$-ÑH̃$_a$H̃$_b$), 6.66 (m, 1 H, C$_{meta}$*H$_a$*), 6.56 (m, 1 H, C̃$_{meta}$*H̃$_a$*), 6.44 (m, 1 H, $\alpha$-CH-N*H$_a$*H$_b$), 6.03 (t, 1 H, $^3J_{HH}$ = 5.5 Hz, C$_{meta}$*H$_b$*), 5.88 (t, 1 H, $^3J_{HH}$ = 5.4 Hz, C̃$_{meta}$*H̃$_b$*), 5.77 (m, 1 H, C̃H$_2$-ÑH̃$_a$H̃$_b$), 5.73 (m, 1 H, $\alpha$-C̃H-ÑH̃$_a$H̃$_b$), 5.60 (d, 1 H, $^3J_{HH}$ = 5.4 Hz, C̃$_{ortho}$*H̃$_b$*), 5.58 (m, 1 H, C$_{ortho}$*H$_a$*), 5.54 (d, 1 H, C̃$_{ortho}$*H̃$_a$*), 5.48 (d, 1 H, $^3J_{HH}$ = 5.7 Hz, C$_{ortho}$*H$_b$*), 5.41 (m, 1 H, CH$_2$-NH$_a$*H$_b$*), 5.20 (dd, 1 H, $^3J_{HH}$ = 4.4 Hz, $^3J_{HH}$ = 4.4 Hz, C̃$_{para}$*H̃*), 5.11 (dd, 1 H, $^3J_{HH}$ = 4.5 Hz, $^3J_{HH}$ = 4.5 Hz, C$_{para}$*H*), 4.84 (m, 2 H, $\alpha$-C*H* / $\alpha$-C̃*H̃*), 4.25 (m, 5 H, C*H$_2$*CH$_3$ / C̃*H̃$_2$*C̃H̃$_3$ / $\alpha$-C̃H-ÑH̃$_a$*H̃$_b$*), 3.61 (m, 1 H, $\alpha$-CH-NH$_a$*H$_b$*), 3.28 (dd, 1 H, $^3J_{HH}$ = 5.5 Hz, $^3J_{HH}$ = 14.5 Hz, $\beta$-CH$_a$*H$_b$*), 3.25 (dd, 1 H, $^3J_{HH}$ = 5.6 Hz, $^3J_{HH}$ = 14.2 Hz, $\beta$-C̃H̃$_a$*H̃$_b$*), 2.93 (dd, 1 H, $^3J_{HH}$ = 13.1 Hz, $^3J_{HH}$ = 13.1 Hz, $\beta$-C̃H̃$_a$*H̃$_b$*), 2.74-2.53 (m, 8 H, C*H$_2$*C*H$_2$* / C̃*H̃$_2$*C̃*H̃$_2$*), 2.67 (m, 1 H, $\beta$-CH$_a$*H$_b$*), 2.43 (s, 6 H, C$_{Ts}$C*H$_3$*), 1.34 (t, 3 H, $^3J_{HH}$ = 7.0 Hz, CH$_2$C*H$_3$*), 1.33 (t, 3 H, $^3J_{HH}$ = 6.9 Hz, C̃H̃$_2$C̃*H̃$_3$*). - **$^{13}$C NMR** (100.5 MHz, 25 °C, DMSO-d$_6$) $\delta$ = 170.5 / 170.4 (*C*OO / *C̃*ÕÕ), 141.3 / 141.1 / 140.9 / 140.7 (*C*$_{Ts}$SO$_2$ / *C̃*$_{Ts}$S̃Õ$_2$), 129.5 / 129.3 (*C*$_{Ts}$H / *C̃*$_{Ts}$H̃), 126.3 / 126.0 (*C*$_{Ts}$H / *C̃*$_{Ts}$H̃), 105.1 / 104.5 (*C*$_{arene}$CH$_2$ / *C̃*$_{arene}$CH̃$_2$), 94.7 / 93.0 / 90.8 / 90.2 / 80.0 / 77.7 / 77.3 / 74.5 / 70.2 / 69.5 / 68.1 / 67.1 (*C*$_{arene}$H / *C̃*$_{arene}$H̃ / $\alpha$-*C*H / $\alpha$-*C̃*H̃), 61.4 (*C*H$_2$CH$_3$ / *C̃*H̃$_2$C̃H̃$_3$), 50.2 / 46.2 / 46.1 (N*C*H$_2$ / Ñ*C̃*H̃$_2$), 36.9 / 36.8 ($\beta$-*C*H$_2$ / $\beta$-*C̃*H̃$_2$), 20.9 / 20.8 (C$_{Ts}$*C*H$_3$ / C̃$_{Ts}$*C̃*H̃$_3$), 14.0 (CH$_2$-*C*H$_3$ / C̃H̃$_2$-*C̃*H̃$_3$). - **$^1$H$^{15}$N-HSQC** (500 MHz, 25 °C, CDCl$_3$) $\delta$ = {6.9, -1.0} / {5.8, -1.0} / {7.2, -0.1} / {5.4, -0.1} (CH$_2$*N*H$_a$H$_b$ / CH$_2$*N*H$_a$H$_b$ / C̃H̃$_2$*Ñ*H̃$_a$H̃$_b$ / C̃H̃$_2$*Ñ*H̃$_a$H̃$_b$), {5.7, 13.2} / {4.3, 13.2} / {6.4, 15.3} / {3.6,

15.3} (CH*NH*$_a$H$_b$ / CH*NH$_a$H*$_b$ / C̃H̃*ÑH̃$_a$*H̃$_b$ / C̃H̃*ÑH̃$_a$H̃*$_b$). - **IR** (KBr): $\tilde{v}$ = 1736vs (CO), 1263vs, 1133vs, 1079vs, 832s, 662s cm$^{-1}$. - **EA** C$_{20}$H$_{28}$ClN$_3$O$_4$RuS · H$_2$O (563.1): calcd. C 42.8, H 5.4, N 7.5, Cl 6.3; found C 42.3, H 5.4, N 7.3, Cl 6.1. - **ESI-MS:** m/z = 508.1 ([M+H]$^+$, 80%), 1050.9 ([2M+HCl+H]$^+$, 100).

*[(η$^6$:η$^1$-PheO$^-$)Ru(enTs$_2$)] HNEt$_3$$^+$* (**29**):
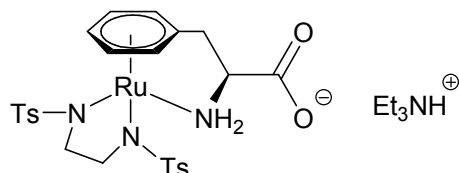


[(η$^7$-PheOEt)Ru(enTs$_2$)] **3** (72 mg, 0.11 mmol) was dissolved in a mixture of triethylamine, water and acetonitrile (10 mL, Et$_3$N:H$_2$O:AcN = 1:1:4.5) and stirred at room temperature for 16 h before removing volatiles under reduced pressure. The crude product was dissolved in dichloromethane (20 mL) and extracted with distilled water (3 x 10 mL). The aqueous phase was lyophilized, giving the bright yellow solid **29** (yield: 39.8 mg, 0.07 mmol, 64%). - **$^1$H NMR** (400 MHz, 25 °C, CDCl$_3$) δ = 7.69 (m, 4 H, C$_{Ts}$*H*), 7.19 (d, 4 H, $^3J_{HH}$ = 7.5 Hz, CTs*H*), 5.89 (t, 1 H, $^3J_{HH}$ = 5.4 Hz, C$_{meta}$*H*$_a$), 5.72 (t, 1 H, $^3J_{HH}$ = 5.2 Hz, C$_{meta}$*H*$_b$), 5.43 (d, 1 H, $^3J_{HH}$ = 5.4 Hz, C$_{ortho}$*H*$_a$), 5.39 (d, 1 H, $^3J_{HH}$ = 5.4 Hz, C$_{ortho}$*H*$_b$), 4.80 (t, 1 H, $^3J_{HH}$ = 5.4 Hz, C$_{para}$*H*), 4.61 (m, 1 H, α-C*H*), 4.33 (t, 1 H, $^3J_{HH}$ = 10.4 Hz, α-CH-N*H*$_a$H$_b$), 3.31 (m, 1 H, α-CH-NH$_a$*H*$_b$), 3.27 (m, 1 H, β-C*H*$_a$H$_b$), 3.04 (q, 6 H, $^3J_{HH}$ = 12.8 Hz, $^3J_{HH}$ = 6.1 Hz, N-C*H*$_2$CH$_3$), 2.75 (dd, 5H, $^3J_{HH}$ = 12.4 Hz, β-CH$_a$*H*$_b$), 2.58 (m, 2 H, NC*H*$_2$CH'$_2$N'), 2.50 (m, 2 H, NCH$_2$-C*H*'$_2$N'), 2.35 (s, 6 H, C$_{Ts}$C*H*$_3$), 1.27 (t, 9 H, $^3J_{HH}$ = 7.0 Hz, NCH$_2$C*H*$_3$). - **$^{13}$C NMR** (100.5 MHz, 25 °C, CDCl$_3$) δ = 175.3 (*C*OO), 141.2 / 141.1 / 141.0 (C$_{Ts}$CH$_3$ / C$_{Ts}$SO$_2$), 129.3 / 127.0 / 126.9 (C$_{Ts}$H), 106.2 (C$_{arene}$CH$_2$), 92.8 / 91.6 / 79.4 / 77.0 / 71.6 (C$_{arene}$), 69.7 (α-*C*H), 52.8 / 52.2 (N*C*H$_2$*C*H'$_2$N'), 45.4 (N(*C*H$_2$CH$_3$)$_3$), 39.7 (β-*C*H$_2$), 21.5 (C$_{arom\ tosyl}$*C*H$_3$), 9.0 (N(CH$_2$*C*H$_3$)$_3$). - **IR** (KBr): $\tilde{v}$ = 1610s (CO), 1259s, 1131vs, 1091vs, 815s, 661s cm$^{-1}$. - **EA** C$_{31}$H$_{46}$N$_4$O$_6$RuS$_2$ · 2 H$_2$O (772.0): calcd. C 48.2, H 6.5, N 7.3; found C 47.9, H 5.9, N 7.0. - **ESI-MS:** m/z = 634.1 ([M+H]$^+$, 100), 899.0.

*[(η⁶:η¹-Phe)Ru(enTs)]* (**30**):
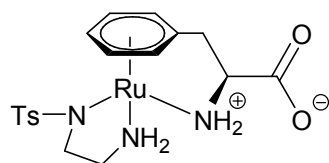


[(η⁷-PheOEt)Ru(enTs)]Cl 4 (44 mg, 0.08 mmol) was dissolved in a mixture of triethylamine, water and acetonitrile (7 mL, Et₃N:H₂O:AcN = 1:1:4.5) and stirred at room temperature for 16 h before removing volatiles under reduced pressure. The residue was washed with diethylether, dichloromethane and methanol, giving the citric powder **30** (yield: 22.8 mg, 39.8 mg, 0.05 mmol, 60%). - **¹H NMR** (400 MHz, 25 °C, 90 % DMSO-d₆, 10 % CD₃COOD) $\delta$ = 7.66 / 7.64 (d, 2 H, $^3J_{HH}$ = 7.5 Hz, d, 2 H, $^3J_{HH}$ = 7.0 Hz, C$_{Ts}$H / C$_{Ts}$H̃), 7.30 / 7.28, (d, 2 H, $^3J_{HH}$ = 6.2 Hz, d, 2 H, $^3J_{HH}$ = 7.1 Hz, C$_{Ts}$H / C$_{Ts}$H̃), 6.49 (m, 2 H, CH₂-NH$_a$H$_b$ / CH̃₂-NH̃$_a$H̃$_b$), 5.97 (t, 1 H, $^3J_{HH}$ = 5.4 Hz, C$_{meta}$H$_a$), 5.94 (t, 1 H, $^3J_{HH}$ = 5.0 Hz, C̃$_{meta}$H̃$_a$), 5.87 (t, 1 H, $^3J_{HH}$ = 5.0 Hz, C$_{meta}$H$_b$), 5.72 (t, 1 H, $^3J_{HH}$ = 4.1 Hz, C̃$_{meta}$H̃$_b$), 5.53 (d, 1 H, $^3J_{HH}$ = 6.2 Hz, C̃$_{ortho}$H̃$_a$), 5.51 (d, 1 H, $^3J_{HH}$ = 5.8 Hz, C̃$_{ortho}$H̃$_b$), 5.45 (d, 1 H, $^3J_{HH}$ = 5.8 Hz, C$_{ortho}$H$_a$), 5.26 (d, 1 H, $^3J_{HH}$ = 5.4 Hz, C$_{ortho}$H$_b$), 5.10 (t, 1 H, $^3J_{HH}$ = 5.2 Hz, C̃$_{para}$H̃), 5.04 (t, 1 H, $^3J_{HH}$ = 5.4 Hz, C$_{para}$H), 4.79 (m, 2 H, α-CH-NH$_a$H$_b$), 4.71 (m, 2 H, α-CH̃-NH̃$_a$H̃$_b$), 4.61 / 4.26 (m, 2 H, CH₂-NH$_a$H$_b$ / CH̃₂-NH̃$_a$H̃$_b$), 4.26 (m, 2 H, α-CH / α-CH̃), 3.61 (m, 2 H, α-CH̃-NH̃$_a$H̃$_b$), 3.52 (m, 2 H, α-CH-NH$_a$H$_b$), 3.13 (dd, 1 H, $^3J_{HH}$ = 13.7 Hz, $^3J_{HH}$ = 5.8 Hz, β-CH$_a$H$_b$), 3.05 (dd, 1 H, $^3J_{HH}$ = 13.7 Hz, $^3J_{HH}$ = 6.2 Hz, β-CH̃$_a$H̃$_b$), 2.68 (m, 1 H, β-CH̃$_a$H̃$_b$), 2.50 (m, 1 H, β-CH$_a$H$_b$), 2.60 (m, 2 H, CH₂CH₂-NH$_a$H$_b$ / CH̃₂CH̃₂-NH̃$_a$H̃$_b$), 2.20 (m, 2 H, CH₂CH₂-NH$_a$H$_b$ / CH̃₂CH̃₂-NH̃$_a$H̃$_b$). - **¹³C NMR** (100.5 MHz, 25 °C, 90 % DMSO-d₆, 10 % CD₃COOD) $\delta$ = 173.1 / 173.0 (COO / CÕÕ), 141.3 / 141.1 / 141.0 (C$_{Ts}$CH₃ / C̃$_{Ts}$CH̃₃), 129.7 / 129.4 (C$_{Ts}$SO₂ / C̃$_{Ts}$SÕ₂), 126.5 / 126.2 (C$_{Ts}$H / C̃$_{Ts}$H̃), 108.1 / 106.9 (C$_{arene}$CH₂ / C̃$_{arene}$CH̃₂), 94.7 / 93.3 / 90.8 / 90.2 / 79.8 / 77.7 / 76.2 / 74.5 (C$_{arene}$H / C̃$_{arene}$H̃), 71.9 / 71.8 / 71.7 / 71.5 / 71.4 / 71.3 (α-CH / α-CH̃), 70.6 / 70.0 (C$_{arene}$H / C̃$_{arene}$H̃), 50.3 / 46.7 / 46.5 (NCH₂ / ÑCH̃₂), 38.2 / 38.0 (β-CH₂ / β-CH̃₂), 21.0 (C$_{Ts}$CH₃ / C̃$_{Ts}$CH̃₃); m/z (ESI-MS) 480.2 ([M+H]⁺, 100). - **IR** (KBr): $\tilde{v}$ = 1619s and 1597s (CO), 1399s, 1385s, 1247s, 1126s, 1092vs, 834vs, 593s cm⁻¹. – **EA** C₁₈H₂₃N₃O₄RuS · 4 H₂O (551.6) calcd. C 39.3, H 5.7, N 7.6; found C 39.3, H 5.0, N 7.2.

## 2.6. η⁵-arene complexes of rhodium and iridium

*2,3,5,6-tetrahydro-2,3,5,6-tetramethyl-4-pyrone* (**40**):[18]
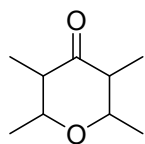


Under argon atmosphere, 38 g KOH (677 mmol) were dissolved in dry methanol (240 mL) and cooled to 0 °C. 3-pentanone (200 mL, 162.6 g, 1.89 mol) was added and within 8 h acetic aldehyde added (425 mL, 333.6 g; 7.57 mol). The reaction mixture was stirred at 0 °C for 14 h, before cold hydrochloric acid (HCl$_{conc.}$ 60 mL) was slowly added. The solution was filtered and extracted with diethylether (4 x 250 mL). The combined organic phases were washed trice with 2 N HCl (each 100 mL) and once with deionized water (100 mL), before the organic solvent was removed in vacuo. The reddish oil was distilled in vacuo (29-37 °C) to give the title compound **40** in 25% yield (74.02 g, 474 mmol) as a slightly yellowish clear oil. - **¹H NMR** (400 MHz, 25 °C, CDCl₃): $\delta$ = 3.30 (m; 2 H; OC*H*CH₃), 2.26 (m; 2 H; COC*H*), 0.85-1.33 (m; 12 H; COCHC*H₃*, COCHCC*H₃*).

*Tetramethylcyclopent-2-enone* (**41**):[18]
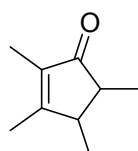


To a stirred solution of formic acid (305 mL) and sulfuric acid (105 mL), 2,3,5,6-tetrahydro-2,3,5,6-tetramethyl-4-pyrone **40** (74-02 g, 474 mmol) was quickly added and heated to 80°C for 18 h. Thereafter, the reaction mixture was poured into ice (1 kg) and extracted with diethylether (5 x 200 mL). The organic phase was washed with 2 N KOH (6 times, until the extracted aqueous phase is neutral) and brine (2 x 150 mL). Thereafter, solvent was removed in vacuo. The yellowish oil was distilled in vacuo (71-81 °C) to give the title compound **41** in 77% yield (50.63 g, 366 mmol) as a slightly yellowish clear oil. - **¹H NMR** (400 MHz, 25 °C, CDCl₃): $\delta$ = 2.22 (m; 1 H; COC*H*), 1.95 (s; 3 H; COCC*H₃*), 1.85 (m; 1 H; COCHC*H*) 1.65 (s; 3 H; COCCC*H₃*), 0.98-1.14 (m; 6 H; COCHC*H₃*, COCHCHC*H₃*).

*Tetramethylcylopent-2-ene methylene nitrile* (**42**):[19]
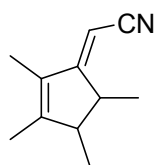


Under argon atmosphere, dry acetonitrile (2.65 mL, 3.56 g, 86.7 mmol) was dissolved in THF (100 mL) and cooled to -78 °C. Thereafter, $^t$BuLi (2M in cyclohexane; 43.4 mmol) was added and the reaction mixture stirred for 30 min. Then, a solution of tetramethylcyclopent-2-enone **41** (5.0 g, 36.2 mmol) in THF (15 mL) was added within 45 min and thereafter the reaction mixture stirred for 3 h. Then, degassed water (20 mL) was added and the mixture stirred vigorously for several minutes. The organic phase was separated, washed twice with degassed water (each 20 mL) and 2 N HCl$_{aq.}$ added, before the reaction mixture was stirred for further 20 h. Thereafter, the organic phase was separated, washed with brine (2 x 50 mL) dried over MgSO$_4$ and the solvent removed in vacuo. The yellow oil was distilled in vacuo to give the title compound **42** in 83% yield (4.86 g, 30.1 mmol) as a clear oil. - **$^1$H NMR** (400 MHz, 25 °C, CDCl$_3$): $\delta$ = 4.88 (d, $^4J_{H,H}$ = 1.7 Hz, 1H, C*H*CN), 2.61 (m, 1H, C*H*Me), 2.13 (m, 1H, CHC*H*Me), 1.82 (s, 3 H, CCC*H$_3$*), 1.65 (s, 3 H, CCCC*H$_3$*), 1.26 (d, $^3J_{H,H}$ = 7 Hz, CCHC*H$_3$*), 1.05 (d, $^3J_{H,H}$ = 7 Hz, 3H, CHCHC*H$_3$*).

*Tetramethylcyclopent-2-ene ethylene amine* (**43**):[19]
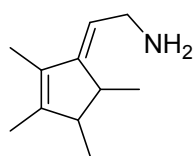


Under argon atmosphere, LiAlH$_4$ (1.72 g, 45.3 mmol) was suspended in dry diethylether (200 mL). Thereafter, tetramethylcylopent-2-ene methylene nitrile **43** (4.86 g, 30.1 mmol) were added within 80 min and the reaction mixture refluxed for 3 h. Then, degassed water (10 mL) was added and the mixture stirred for 8 h at room temperature, before 13 g MgSO$_4$ were added and stirred for 1h. The reaction mixture was filtered and extracted with diethylether (5 x 25 mL). The organic phases were combined and volatiles removed in vacuo. The yellow oil was distilled in vacuo to give the title compound **43** in 74% yield (3.66 g, 22.1 mmol) as a clear oil. - **$^1$H NMR** (400 MHz, 25 °C, CDCl$_3$): $\delta$ = 5.14 (t, 1 H, $^3J_{H,H}$ = 7.2 Hz; C*H*CH$_2$NH$_2$), 3.38 (t, 2 H; $^3J_{H,H}$ = 7.2 Hz;

CHC$H_2$NH$_2$), 2.43 (m, 1 H, CC*H*CH$_3$), 2.06 (m, 1 H, CCHC*H*CH$_3$), 1.82 (m, 2 H, N*H*$_2$), 1.68 (s, 3 H, CCC*H*$_3$), 1.64 (s, 3 H, CCCC*H*$_3$), 1.00 (d, 3 H, $^3J_{H,H}$ = 7.2 Hz, CCHC*H*$_3$), 0.96 (d, 2 H, $^3J_{H,H}$ = 7.2 Hz; CCHCHC*H*$_3$).

*[($\eta^5$-Me$_4$Cp(CH$_2$)$_2$NH$_3$)RhCl$_2$]$_2$Cl$_2$* (**50**):
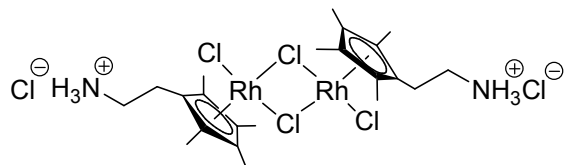


2-(2,3,4,5-Tetramethylcyclopentadienyl)ethylamine tautomere **43** (496 mg, 3.00 mmol) was dissolved in diethylether (10 mL) and treated with hydrochloric acid (1.47 mL, 5.9 mmol, 4 M in dioxane). Hexane (20 mL) was added to this solution until a white precipitate formed, which was filtered off and washed twice with hexane. The white solid was dissolved in ethanol (50 mL) and RhCl$_3$ · n H$_2$O (184 mg, 0.70 mmol) was added. The reaction mixture was refluxed for 4 days and thereafter stored at -20 °C over night. The precipitate was filtered off and washed with hexane, diethylether and cold ethanol to yield 190 mg of the pure product (0.25 mmol; 72 %) as an orange powder. - **$^1$H NMR** (400 MHz, 25 °C, DMSO-d$_6$): $\delta$ = 8.10 (br s, 3H, -N*H*$_3$), 2.94 (t, 2H, $^3J_{HH}$ = 7.5 Hz, CH$_2$C*H*$_2$NH$_3$), 2.48 (t, 2H, $^3J_{HH}$ = 7.5 Hz, C*H*$_2$CH$_2$NH$_3$), 1.74 / 1.65 (s, 12H, C*H*$_3$). - **$^{13}$C NMR** (125.8 MHz, 25 °C, DMSO-d$_6$): $\delta$ = 102.6 (d, $^1J_{RhC}$ = 7.3 Hz, *C*$_{Cp}$), 99.0 (d, $^1J_{RhC}$ = 7.5 Hz, *C*$_{Cp}$), 93.8 (d, $^1J_{RhC}$ = 8.1 Hz, *C*$_{Cp}$), 36.4 (s, *C*H$_2$CH$_2$NH$_3$), 22.0 (s, CH$_2$*C*H$_2$NH$_3$), 9.2 / 8.9 (2x s, *C*H$_3$). - **IR** (KBr): $\tilde{v}$ = 3114 s, 3019 m, 2920 m, 2852 w, 2360 w, 1622 s, 1464 s, 1376 m, 1262 w, 1132 m, 1024 m, 930 w, 817 w, 763 w cm$^{-1}$. - **EA** C$_{22}$H$_{38}$N$_2$Cl$_6$Rh$_2$ (749.1): C 35.27, H 5.11, N 3.74. Found: C 35.01, H 5.19, N 3.55. - **ESI-MS** m/z (%) = 302.1 (100) [½M-Cl-HCl]$^+$, 639.0 (55) [M-Cl-2HCl]$^+$.

*[($\eta^5$-Me$_4$Cp(CH$_2$)$_2$NH$_3$)IrCl$_2$]$_2$Cl$_2$* (**51**):
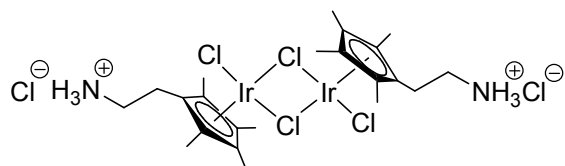


2-(2,3,4,5-Tetramethylcyclopentadienyl)ethylamine tautomere **43** (100 mg, 0.60 mmol) was dissolved in diethylether (2.5 mL) and treated with hydrochloric acid (0.29 mL, 1.2

mmol, 4 M in dioxane). To this solution, hexane (5 mL) was added until a white precipitate formed which was filtered of and washed two times with hexane. The white solid was dissolved in dry ethanol (10 mL) and $IrCl_3 \cdot n\ H_2O$ (55.7 mg, 0.19 mmol) was added. The reaction mixture was refluxed for 16 h after which the solution was filtered. Volatiles were evaporated under reduced pressure and t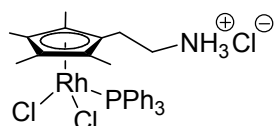he residue washed with diethylether and hexane, yielding 15.8 mg of the pure product (0.04 mmol, 21 %) as a yellow powder. - **$^1$H NMR** (400 MHz, 25 °C, DMSO-$d_6$): $\delta$ = 8.12 (br s, 3H, -N$H_3$), 2.90 (m, 2H, $CH_2CH_2NH_3$), 2.39 (t, 2H, $^3J_{HH}$ = 8.1 Hz, $CH_2CH_2NH_3$), 1.74 / 1.64 (s, 12H, $CH_3$). - **$^{13}$C NMR** (100.5 MHz, 25 °C, DMSO-$d_6$): $\delta$ = 97.1 / 92.2 / 85.8 ($C_{Cp}$), 36.8 ($CH_2CH_2NH_3$), 22.1 ($CH_2CH_2NH_3$), 8.9 / 8.8 ($CH_3$). - **EA** $C_{22}H_{38}N_2Cl_6Ir_2$ (927.7): C 28.48, H 4.13, N 3.02. Found: C 28.16, H 4.22, N 2.96.

*[($\eta^5$-Me$_4$Cp(CH$_2$)$_2$NH$_3$)RhCl$_2$(PPh$_3$)]* (**52**):



[($\eta^5$-Me$_4$Cp(CH$_2$)$_2$NH$_3$)RhCl$_2$]$_2$Cl$_2$ **50** (40 mg, 0.05 mmol) and triphenylphosphine (28 mg, 0.11 mmol) were dissolved in dimethylsulfoxide (1.2 mL) and vigorously stirred for 1 h. The solvent was removed under reduced pressure and the residue washed with diethylether. The product was obtained as a red powder in quantitative yield (68 mg). - **$^1$H NMR** (400 MHz, 25 °C, DMSO-$d_6$): $\delta$ = 8.18 (br s, 3H, N$H_3$), 7.72 (m, 6 H, C$_{PPh3}H$), 7.48 (m, 9H, C$_{PPh3}H$), 2.86 (t, 2H, $^3J_{HH}$ = 7.5 Hz, CH$_2$C$H_2$NH$_3$), 2.34 (t, 2H, $^3J_{HH}$ = 7.5 Hz, C$H_2$CH$_2$NH$_3$), 1.38 (d, 6H, $^4J_{PH}$ = 3.1 Hz, $CH_3$), 1.13 (d, 6H, $^4J_{PH}$ = 2.9 Hz, $CH_3$). - **$^{13}$C NMR** (125.6 MHz, 25 °C, DMSO-$d_6$): $\delta$ = 134.7 (d, $J_{PC}$ = 9.7 Hz, $C_{PPh3}$), 131.0 / 128.4 (2x br, $C_{PPh3}$), 101.3 (dd, $^1J_{RhC}$ = 6.3 Hz, $^2J_{PC}$ = 2.9 Hz, $C_{Cp}$), 98.6 (dd, $^1J_{RhC}$ = 6.8 Hz, $^2J_{PC}$ = 1.5 Hz, $C_{Cp}$), 98.2 (dd, $^1J_{RhC}$ = 5.9 Hz, $^2J_{PC}$ = 5.9 Hz, Cp), 36.3 (d, $^4J_{PC}$ = 4.9 Hz, CH$_2$CH$_2$NH$_3$), 22.3 (s, $CH_2CH_2NH_3$), 8.9 (d, $^3J_{PC}$ = 1.4 Hz, $CH_3$), 8.7 (d, $^3J_{PC}$ = 0.7 Hz, $CH_3$). - **$^{31}$P NMR** (161.8 MHz, 25 °C, DMSO-$d_6$): $\delta$ = 30.27 (d, $^1J_{P,Rh}$ = 144 Hz). – **IR** (KBr): $\tilde{v}$ = 2959 w, 1725 w, 1622 w, 1482 s, 1435 vs, 1384 vs, 1269 w, 1094 w, 1020 w, 745 m, 687 s, 525 s cm$^{-1}$. - **EA** $C_{29}H_{34}NCl_3PRh \cdot 0.5\ Me_2SO$ (675.9): C 53.31, H 5.52, N 2.07. Found: C 52.71, H 5.34, N 2.03. - **ESI-MS** m/z (%) = 302.1 (100) [M-PPh$_3$-Cl-HCl]$^+$, 564.0 (54) [M-Cl-HCl]$^+$.

*[(η⁵-Me₄Cp(CH₂)₂NHCO(CH₂)₂COOH)RhCl₂(PPh₃)]* (**53**):
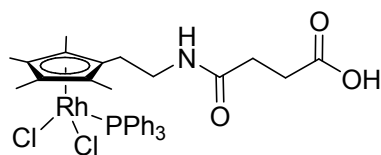


[(η⁵-Me₄Cp(CH₂)₂NH₃)RhCl₂PPh₃]Cl **52** (100 mg, 0.16 mmol) was dissolved in dichloromethane (5 mL), and succinic anhydride (20 mg, 0.16 mmol) and triethylamine (440 µL, 3.2 mmol) were added. The mixture was stirred at room temperature for 24 h and subsequently washed with 0.1 M HCl and brine (each 3 x 10 mL). The organic phase was dried over MgSO₄ and concentrated under reduced pressure to about 20 % of the original volume. Addition of hexane led to precipitation of the product as a red powder, which was filtered of and dried *in vacuo* (60.5 mg, 0.84 mmol, 54 %). - **¹H NMR** (400 MHz, 25 °C, CDCl₃): $\delta$ = 7.75 (m, 6H, C$_{PPh3}$*H*), 7.60 (m, 1H, N*H*), 7.37 (m, 9 H, C$_{PPh3}$*H*), 3.47 (m, 2H, CH₂C*H₂*NH), 2.47-2.35 (m, 4H C*H₂*CO), 3.46 (m, 2H, C*H₂*CH₂NH), 1.36 (d, 6H, ⁴$J_{PH}$ = 1.3 Hz, C*H₃*), 1.05 (d, 6H, ⁴$J_{PH}$ = 2.9 Hz, C*H₃*). - **¹³C NMR** (100.5 MHz, 25 °C, CDCl₃): $\delta$ = 174.7 / 174.4 (2x s, *C*O), 134.8 (d, $J_{PC}$ = 9.2 Hz, *C*$_{PPh3}$), 130.7 / 128.1 (2x br, *C*$_{PPh3}$), 103.2 (d, ¹$J_{RhC}$ = 3.8 Hz, *C*$_{Cp}$), 101.2 (dd, ¹$J_{RhC}$ = 8.5, ²$J_{PC}$ = 6.2 Hz, *C*$_{Cp}$), 96.2 (d, ¹$J_{RhC}$ = 6.1 Hz, *C*$_{Cp}$), 36.4 (d, ⁴$J_{PC}$ = 4.6 Hz, *C*H₂CH₂NH), 31.0 / 30.4 (2x s, *C*H₂CO), 24.7 (s, *C*H₂CH₂NH₃), 9.7 / 8.7 (2x s, *C*H₃). - **³¹P NMR** (CDCl₃): $\delta$ = 30.07 (d, ¹$J_{RhP}$ = 143 Hz). - **IR** (KBr): $\tilde{v}$ = 3057 m, 2957 sh, 2925 m, 1730 m, 1647 s, 1545 m, 1483 m, 1435 vs, 1384 vs, 1095 m, 1022 w, 748 m, 698 s, 525 s cm⁻¹. - **EA** C₃₃H₃₇NCl₂O₃PRh · H₂O (718.5): C 55.17, H 5.47, N 1.95. Found: C 54.93, H 5.68, N 1.95. - **ESI-MS** m/z (%) = 366.0 (100) [M-PPh₃-Cl-HCl]⁺, 402.0 (75) [M-PPh₃-Cl]⁺, 663.9 (42) [M-Cl]⁺.

*[(Cp*)RhCl₂(PPh₃)]* (**54**): [20]
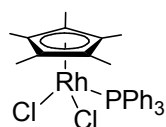


To a suspension of dinuclear rhodium(III) complex [(Cp*)RhCl₂] (124 mg, 0.2 mmol) in dichloromethane, triphenylphosphine was added (105 mg, 0.4 mmol) and the mixture stirred at RT for 1.0 h. The suspension was filtered, the solvent removed, the residue washed with diethyl ether (3 x 5 mL) and dried in vacuo, giving the title compound **54** as an orange powder (229 mg, 0.4 mmol, quantitative). -**¹H NMR** (400 MHz, 25 °C, CDCl₃): $\delta$ = 7.81 (t, $J$ = 8.6 Hz, 6 H), 7.35 (br s, 9 H), 1.35 (d, $J$ = 3.4 Hz, 15 H). - **³¹P NMR** (400 MHz, 25 °C, CDCl₃): $\delta$ = 30.63 (d, ¹$J_{RhP}$ = 144 Hz).

## 2.7. Metalla affinity labels for cysteine proteases

### 2.7.1. Organic precursors

*Boc-Leu-NH-Bzl* (**60**): [21]
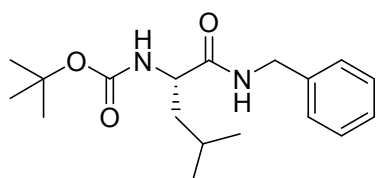


To a stirred solution of Boc-L-Leucine (4.83 g, 20.9 mmol) in Dichloromethane (150 mL), benzylamine **1i** (2.24 g, 20.9 mmol) was added and the reaction mixture cooled to 0°C. Thereafter, EDCI (4.98 g, 25.1 mmol) was added within 15 minutes. The reaction mixture was stirred for 1 h at 0 °C and then over night at room temperature. Then, it was washed with water (3 x 50 mL) and aqueous 1 M citric acid (4 x 40 mL). The organic phase was dried over $MgSO_4$ and volatiles removed under reduced pressure, giving the title compound in 79 % yield (5.30 g, 16.6 mmol) as a white solid. - **$^1$H NMR** (400 MHz, 25 °C, $CDCl_3$): $\delta$ = 7.19-7.32 (m, 5H, $H_{arom}$), 6.63 (s, 1H, N*H*CH$_2$Ph), 4.96 (d, $^3J_{HH}$ = 8.4 Hz, 1H, NHC*H*CO), 4.40 (d, $^3J_{HH}$ = 4.8 Hz, 2H, C*H$_2$*Ph), 4.13 (s, 1H, N*H*CH), 1.66-1.72 (m, 2H, CHC*H$_2$*CH), 1.46-1.54 (m, 1H, CH$_3$C*H*), 1.39 (s, 9H, C*H$_3$*), 0.90-0.93 (m, 6H, C*H$_3$*). - **$^{13}$C NMR** (101 MHz, 25 °C, $CDCl_3$): $\delta$ = 172.6 (CH*C*ONH), 155.9 (O*C*ONH), 138.2 ($C_{arom}$), 128.7 ($C_{arom}$), 127.7 ($C_{arom}$), 127.5 ($C_{arom}$), 80.2 ($C_{quart}$), 53.3 (NH*C*HCO), 43.5 (*C*H$_2$Ph), 41.2 (*C*HCH$_2$CH), 28.3 (*C*H$_{3 \text{ tert-Butyl}}$), 24.9 (*C*H$_3$CHCH$_3$), 23.0 (*C*H$_3$CH), 22.1 (*C'*H$_3$CH). - **IR** (KBr): $\tilde{v}$ = 2956 w, 1652 br vs, 1532 m, 1497 sh w, 1455 m 1386 m, 1367 m, 1256 w, 1029 m, 734 s, 699 vs cm$^{-1}$. - **EA** $C_{18}H_{28}N_2O_3$ (320.4): C 67.47, H 8.81, N 8.74. Found: C 67.32, H 8.89, N 8.80.

*NH$_2$-Leu-NHBz* (**61**): [21]
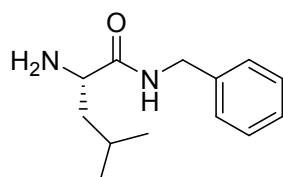


To a vigorously stirred solution of Boc-Leu-NH-Bzl **60** (1.56 g, 4.87 mmol) in dichloromethane (10 mL) trifluoro acetic acid (8 mL) was added. The reaction mixture

was stirred for 40 minutes, before saturated aqueous $Na_2CO_3$ was carefully added (until a pH value of 9 is reached). The mixture was then stirred for further 20 min, before the organic phase was separated, dried over $MgSO_4$ and volatiles removed in vacuo. The pure product **61** was obtained after silica column chromatography (silica gel 60; Merck; acetic acid ethyl ether / methanol = 15 / 1; 1% $Et_3N$) as a white solid (1.0 g, 4.6 mmol, 95 %). - **$^1$H NMR** (400 MHz, 25 °C, CDCl$_3$): $\delta$ = 7.68 (t, $^3J_{HH}$ = 5.6 Hz, 1H, CON*H*), 7.35-7.11 (m, 5H, *H*$_{arom.}$), 4.42 (d, $^3J_{HH}$ = 5.6 Hz, 2H, C*H*$_2$Ph), 3.49 (dd, $^3J_{HH}$ = 3.6 Hz, $^3J_{HH}$ = 10 Hz, 1H, C*H*NH$_2$) 1.79-1.67 (m, 1H, CHC*H*$_2$CH), 1.45-1.34 (m, 1H, CH$_3$C*H*), 0.95 (d, $^3J_{HH}$ = 6.0 Hz, 3H, C*H*$_3$), 0.92 (d, $^3J_{HH}$ = 6.0 Hz, 3H, C*H'*$_3$). - **$^{13}$C NMR** (101 MHz, 25 °C, CDCl$_3$): $\delta$ = 175.0 (*C*O), 138.6 (*C*$_{arom}$), 128.8 (*C*$_{arom}$), 128.0 (*C*$_{arom}$), 127.5 (*C*$_{arom}$), 53.6 (NH$_2$*C*H), 44.0 (*C*H$_2$Ph), 43.3 (CH*C*H$_2$CH), 25.0 (CH$_3$*C*HCH$_3$), 23.5 (*C*H$_3$CH), 21.6 (*C'*H$_3$CH). - **EA** C$_{13}$H$_{20}$N$_2$O (220.3): C 70.87, H 9.15, N 12.72. Found: C 70.44, H 9.04, N 12.17. - **ESI-MS** m/z = 221.3 [M+H$^+$]$^+$.

*2-acetoxy-3-bromo-succinic acid diethylester* (**62**): [22]
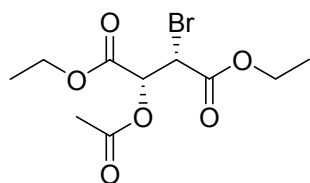


D-(-)-tartaric acid (10 g, 48 mmol) were placed in a 100 mL round bottom flask and cooled to 0 °C. Thereafter, HBr in AcOH (40 mL, 33% HBr in AcOH) were added within 30 min. The solution was stirred for 15 min at 0 °C and over night at room temperature. Then, the reaction mixture was poured over ice (100 g) and extracted with diethylether (3x  50 mL). The combined organic phases were washed with water (3x 50 mL) and brine (50 mL), dried over $MgSO_4$ and the solvent removed in vacuo, giving the title compound **62** as a yellowish oil (13.7 g, 43.2 mmol, 90 %). - **$^1$H NMR** (400 MHz, 25 °C, CDCl$_3$): $\delta$ = 5.56 (d, 1H, $^3J_{(H-H)}$ = 4.9 Hz, C*H*OAc), 4.75 (d, 1H, $^3J_{(H-H)}$ = 4.9 Hz, C*H*Br), 4.25 (dq, 4H, $^3J_{(H-H)}$ = 7.0 Hz, 2.1 Hz, C*H*$_2$CH$_3$), 2.06 (s, 3H, C(O)C*H*$_3$), 1.28 (t, 6H, $^3J_{(H-H)}$ = 7.3 Hz, CH$_2$C*H*$_3$). - **$^{13}$C NMR** (100.5 MHz, 25 °C, CDCl$_3$): $\delta$ = 169.5, 166.6, 166.3, 72.7, 63.0, 62.3, 20.3, 13.9.

*2-bromo-3-hydroxy-succinic acid diethylester* (**63**): [22]
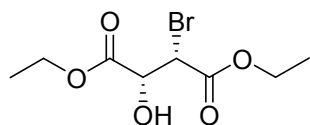


To a stirred solution of 2-acetoxy-3-bromo-succinic acid diethylester **62** (13.7 g, 43.2 mmol) in ethanol (50 mL), acetylchloride (1.6 mL, 1.77 g, 22.5 mmol) were added and the reaction mixture refluxed for 5 h. Thereafter, the reaction was allowed to cool down to room temperature, before the solvent was removed in vacuo. The title compound **63** (10.7 g, 39.8 mmol, 92 %) was used without further purification.

*Diethyl(2S,3S)-(+)-2,3-epoxysuccinate* (**64**): [22]
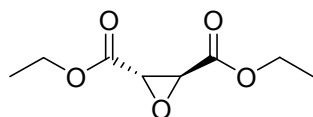


To a cooled solution (0 °C) of 2-bromo-3-hydroxy-succinic acid diethylester **63** (10.7 g, 39.8 mmol) in diethylether (60 mL), a solution of DBU (7.1 mL, 7.0 g, 45.8 mmol) in diethylether (30 mL) was added dropwise within 90 min. Thereafter, the reaction mixture was stirred for additional 60 min at 0 °C. Then, deionized water (10 mL) were added and the organic phase separated. The organic phase was washed with an aqueous 1 M solution of KHSO$_4$ (2 x 10 mL) and water (2 x 10 mL). Thereafter, it was dried over MgSO4 and the solvent removed under reduced pressure, yielding the title compound **64** as a clear oil (4.8 g, 25.5 mmol, 64%). - **$^1$H NMR** (400 MHz, 25 °C, CDCl$_3$): $\delta$ = 4.29 (m, 4H, C$H_2$CH$_3$), 3.65 (s, 2H, C$H_{Epx}$), 1.32 (t, 6H, $^3J_{HH}$ = 7.1 Hz, CH$_2$C$H_3$). - **$^{13}$C NMR** (100.5 MHz, 25 °C, CDCl$_3$): $\delta$ = 166.9 (*C*O), 62.4 (*C*H$_2$), 52.2 (*C*H(O)*C*H), 14.2 (*C*H$_3$).

*Monoethyl(2S,3S)-(+)-2,3-Epoxisuccinat* (**65**): [22]
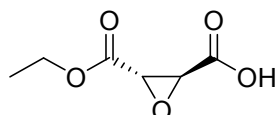


Diethyl(2S,3S)-(+)-2,3-epoxysuccinate **64** (2.3 g, 12.3 mmol) was dissolved in absolute EtOH (33 mL) and placed in an ice-bath. A solution of KOH (688 mg, 12.3 mmol) in absolute EtOH (16 mL) was added dropwise over 15 min to the colorless solution. The reaction mixture was then allowed to stir at 0 °C for 1.5 h, and then 1.5 h at RT. After

evaporation of solvent in vacuo, water (50 mL) was added and the solution extracted with $CH_2Cl_2$ (3 x 30 mL). The aqueous phase was acidified with $HCl_{conc.}$ (1.7 mL) and NaCl added (15 g). Thereafter, the reaction solution was extracted with AcOEt (4 x 30 mL). The combined organic phases were dried over $MgSO_4$ and the solvent removed in vacuo, giving the title compound **65** (1.75 g, 10.9 mmol, 89 %) as a colorless oil. - **$^1$H NMR** (400 MHz, 25 °C, $CDCl_3$): $\delta$ = 7.59 (br s, 1H, COO*H*), 4.32-4.34 (m, 2H, C*H$_2$*CH$_3$), 3.71 (d, 1H, $^3J_{HH}$ = 1.2 Hz, C*H*(O)C'H), 3.70 (d, 1H, $^3J_{HH}$ = 1.2 Hz, CH(O)C'*H*), 1.32 (t, 3H, $^3J_{(H-H)}$ = 7.3 Hz, CH$_2$C*H$_3$*). - **$^{13}$C NMR** (100.5 MHz, 25 °C, $CDCl_3$): $\delta$ = 171.5 / 166.5 (*C*OOEt / *C*OOH), 62.7 (*C*H$_2$), 52.4 / 51.6 (*C*H(O)C'H / CH(O)*C*'H), 14.2 (*C*H$_3$).

*EtO-Eps-Leu-NH-Bzl* (**66**): [21]
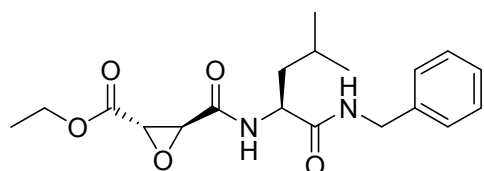


Ethyl-expoxysuccinate **65** (2.30 g, 14.3 mmol) and EDCI (3.67 g, 19.1 mmol) were dissolved in dichloromethane (70 mL), placed in an ice-bath and stirred for 30 min. Thereafter, a solution of H$_2$N-Leu-Bz (2.11 g, 9.6 mmol) in dichloromethane (70 mL) was added dropwise over 20 min to the colorless solution. The reaction mixture was then allowed to stir at 0 °C for 3 h, and then over night at room temperature. The reaction mixture was extracted with water (4x 45 mL) and thereafter with aqueous citric acid (4x 45 mL, 1 M in H$_2$O). The organic phase was dried (MgSO$_4$) and volatiles removed in vacuo, and washed with a small amount of hexane, and diethylether, yielding the title compound as a white solid. Yield: 1.12 g, 2.92 mmol, 31%. - **$^1$H NMR** (400 MHz, 25 °C, $CDCl_3$): $\delta$ = 7.34-7.22 (m, 5H, C$_{arom}$*H*), 6.62 (d, 1H, $^3J_{HH}$ = 8.7 Hz, N*H*CH), 6.44 (t, 1H, $^3J_{HH}$ = 5.2 Hz, N*H*CH$_2$), 4.46-4.19 (m, 5H, NHC*H* / NHC*H$_2$* / C*H$_2$*CH$_3$), 3.61 (d, 1H, $^3J_{HH}$ = 2.1, C*H*(O)CH'), 3.43 (d, 1H, $^3J_{HH}$ = 2.1, CH(O)*CH*'), 1.70-1.50 (m, 3H, CH$_2$C*H*(CH$_3$)$_2$ / C*H$_2$*CH(CH$_3$)$_2$), 1.30 (t, 3H, $^3J_{HH}$ = 7.3 Hz, CH$_2$C*H$_3$*), 0.91 (d, 3H, $^3J_{HH}$ = 6.6 Hz, CHC*H$_3$*), 0.90 (d, 3H, $^3J_{HH}$ = 6.6 Hz, CHC*H'$_3$*). - **$^{13}$C NMR** (100.52 MHz, 25 °C, $CDCl_3$): $\delta$ = 171.5 / 166.5 / 166.2 (*C*OO), 138.2 (*C*$_{arom}$), 62.5 (*C*H$_2$CH$_3$), 54.5 / 54.1 (*C*H(O)C'H / CH(O)*C*'H), (*C*H$_2$CH$_3$), 51.8 (*C*HCH$_2$), 43.5 (NH*C*H$_2$), 41.0 (CH*C*H$_2$), 24.8 (*C*H(CH$_3$)$_2$), 23.0 / 22.1 (*C*H$_3$ / *C*'H$_3$), 14.2 (CH$_2$*C*H$_3$). - **IR** (KBr): $\tilde{v}$ =3087 m, 2956 m, 2929 m, 2872 m, 1750 vs, 1641 vs, 1552 s, 1455 m, 1370 m, 1344 m, 1223 m, 1201 s, 1029 m, 897 m cm$^{-1}$.

*HO-Eps-Leu-NH-Bzl* (**67**): [21]
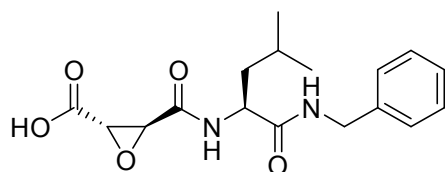


EtO-Eps-Leu-NH-Bzl **66** (363 mg, 3.0 mmol) was dissolved in absolute EtOH (10 mL) and placed in an ice-bath. A solution of KOH (168 mg, 3.0 mmol) in absolute EtOH (4 mL) was added dropwise over 15 min to the colorless solution. The reaction mixture was then allowed to stir at 0 °C for 3 h, and then 2 h at RT. After evaporation of solvent in vacuo, $CHCl_3$ (10 mL) was added to the resulting white solid and the resulting suspension was cooled to -20 °C for 4 h. Thereafter, the precipitate was collected by filtration, washed with a small amount of $CHCl_3$ and dried in vacuo, yielding the title compound as a white powder. Yield: 676 mg, 2.1 mmol, 68%. - **$^1$H NMR** (400 MHz, 25 °C, $CDCl_3$): $\delta$ = 7.34-7.20 (m, 6H, $C_{arom}H$ / N*H*C*H*$_2$), 7.06 (d, 1H, $^3J_{HH}$ = 7.9 Hz, N*H*CH), 4.40-4.33 (m, 3H, NHC*H* / NHC*H*$_2$), 3.57 (d, 1H, $^3J_{HH}$ = 2.1, C*H*(O)CH'), 3.51 (d, 1H, $^3J_{HH}$ = 2.1, CH(O)C*H*'), 1.66-1.56 (m, 3H, CH$_2$C*H*(CH$_3$)$_2$ / C*H*$_2$CH(CH$_3$)$_2$), 0.91 (d, 3H, $^3J_{HH}$ = 5.8 Hz, CHC*H*$_3$), 0.88 (d, 3H, $^3J_{HH}$ = 6.2 Hz, CHC*H*'$_3$). - **$^{13}$C NMR** (100.52 MHz, 25 °C, $CDCl_3$): $\delta$ = 172.7 / 168.8 / 166.7 (*C*OO), 140.0 / 129.4 / 128.2 / 128.0 (*C*$_{arom}$), 54.4 / 52.8 (*C*H(O)C'H), 52.8 / 52.7 (*C*HCH$_2$ / CH(O)*C*'H), 43.5 (NH*C*H$_2$), 41.8 (CH*C*H$_2$), 25.5 (*C*H(CH$_3$)$_2$), 23.3 / 21.8 (*C*H$_3$ / *C*'H$_3$). - **IR** (KBr): $\tilde{v}$ =3107 s, 2960 s, 2930 s, 2903 s, 1724 vs, 1684 vs, 1634 vs, 1563 vs, 1468 m, 1454 m, 1328 m, 1232 s, 1219 s, cm$^{-1}$. - **EA** $C_{17}H_{22}N_2O_5$ (334.4): calcd. C 61.1., H 6.6, N 8.4; found C 61.2, H 6.6, N 8.4.


*HOOC-CH$_2$CH$_2$-CO-NH-Leu-Bz* (**68**):
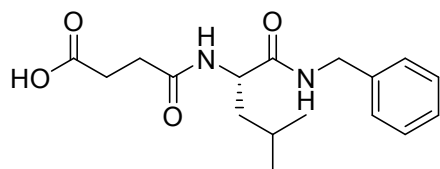


Succinic anhydride (245 mg, 2.45 mmol) and pyridine (166 µL 2.04 mmol) were dissolved in dichloromethane (75 mL) and HO-Leu-NH-Bzl **61** (450 mg, 2.04 mmol) added. The reaction mixture was stirred for 24 h at room temperature. Volatiles were removed under reduced pressure and the crude product chromatographed over silica (ethyl acetate / Methanol = 15 / 1), yielding a white solid (537 mg, 1.68 mmol, 82%). - **$^1$H NMR** (400 MHz, 25 °C, $CDCl_3$): $\delta$ = 9.17 (s, 1H, COO*H*), 7.71-7.61 (m, 1H, N*H*CHH'),

7.55 (d, 1H, $^3J_{HH}$ = 8.1 Hz, N*H*CH), 7.29-7.11 (m, 5H, C$_{arom}$*H*), 4.65-4.52 (m, 1H, NHC*H*), 4.35 (dd, 1H, $^2J_{HH}$ = 14.9 Hz, $^3J_{HH}$ = 5.8 Hz, NHC*H*H'), 4.19 (dd, 1H, $^2J_{HH}$ = 14.9 Hz, $^3J_{HH}$ = 5.0 Hz, NHCH*H'*), 2.62-2.28 (m, 4H, C*H$_2$*C*H$_2$*), 1.68-1.46 (m, 3H, C*H$_2$*C*H*(CH$_3$)$_2$), 0.88 (d, $^3J_{HH}$ = 4.7 Hz, C*H$_3$*), 0.85 (d, $^3J_{HH}$ = 4.6 Hz, C*H'$_3$*). - $^{13}$**C NMR** (101 MHz, 25 °C, CDCl$_3$): $\delta$ = 176.3 (*C*OO), 173.2 / 172.5 (*C*ON), 137.9 (*C*$_{arom}$), 128.6 (*C*$_{arom}$H), 127.6 (*C*$_{arom}$H), 127.5 (*C*$_{arom}$H), 52.0 (*C*HCH$_2$), 43.5 (NH*C*H$_2$), 41.3 (CH*C*H$_2$), 30.6 / 29.6 (*C*H$_2$C'H$_2$ / *C*H$_2$C'H$_2$), 24.9 (*C*H(CH$_3$)$_2$), 22.8 / 22.3 (*C*H$_3$ / *C'*H$_3$). - **IR** (KBr): $\tilde{v}$ = 3066 s, 2954 vs, 1696 vs (CO), 1644 vs, 1633 vs, 1539 vs, 1436 s, 1418 s, 1386 s, 1295 s, 1199 s. - **EA** C$_{17}$H$_{24}$N$_2$O$_4$ (320.4): calcd. C 63.7, H 7.6, N 8.7; found C 63.4, H 7.4, N 8.6. - **ESI-MS** m/z (%) = 679.3 [2M+K]$^+$ (100), 321.1[M+H]$^+$ (76), 663.4 [2M+Na]$^+$ (51), 343.3 [M+Na]$^+$ (32).

## 2.7.2. Catalyst synthesis

*[($\eta^6$-Me$_4$Cp(CH$_2$)$_2$NH-(I))RhCl$_2$PPh$_3$]* (**70**):
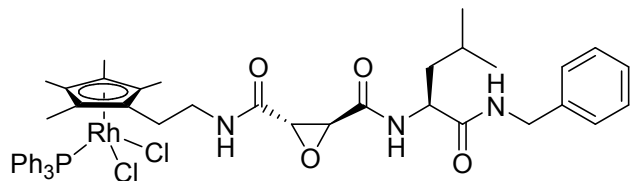


Dichloromethane (10 mL) was added to polystyrene bound cyclohexyl carbodiimide (182 mg, 1.3 mmol/g, 0.24 mmol) at 0°C and the resin allowed to swell for several minutes. HO-Eps-Leu-NH-Bzl **66** (40 mg, 0,12 mmol) was added to the gently stirred mixture, before pentafluorophenol (43 mg, 0.24 mmol) was slowly added and the reaction mixture stirred at 0°C for 1h and then at room temperature over night. The mixture was filtered, triethylamine (43 µL, 0.36 mmol) and then [Me$_4$Cp(CH$_2$)$_2$NH$_3$)RhCl$_2$PPh$_3$]Cl **52** (50 mg, 0.08 mmol) added, stirred vigorously stirred for 1 h and extracted with water and brine (each 3 x 10 mL), dried over MgSO$_4$ and volatiles removed under reduced pressure. The crude product was washed with diethylether and hexane, yielding a bright red solid (43 mg, 0.05 mmol, 63%). - **$^1$H NMR** (400 MHz, 25 °C, CDCl$_3$): $\delta$ = 7.82-7.72 (m, 6H, C$_{arom\ PPh3}$*H*), 7.50-7.17 (m, 15H, C$_{arom\ PPh3}$*H* / C$_{arom\ Bz}$*H* / CH$_2$CH$_2$N*H*), 7.09-6.95 (m, 2H, N*H*CH$_2$(C$_6$H$_5$) / N*H*CH), 4.48-4.40 (m, 1H, NHC*H*), 4.35 (dd, 1H, $^2J_{HH}$ = 14.9 Hz, $^3J_{HH}$ = 5.8 Hz, NHC*H*H'Ph), 4.27 (dd, 1H, $^2J_{HH}$ = 14.9 Hz, $^3J_{HH}$ = 5.8 Hz, NHCH*H*'Ph), 3.55 (d, 1H, $^3J_{HH}$ = 1.9, C*H*(O)CH'), 3.53 (d, 1H, $^3J_{HH}$ = 1.9, CH(O)C*H*'), 3.38 (m, 2H, CH$_2$C*H$_2$*NH), 2.26 (m, 2H, C*H$_2$*CH$_2$NH), 1.69-1.50 (m, 3H, C*H$_2$*C*H*(CH$_3$)$_2$), 1.49 (d, 3H, $^4J_{PH}$ = 2.9 Hz, C$_{Cp}$C*H$_3$*), 1.48 (d, 3H, $^4J_{PH}$ = 3.1 Hz, C$_{Cp}$C*H$_3$*), 1.09 (d, 6H, $^4J_{PH}$ = 2.9 Hz, C$_{Cp}$C*H$_3$*), 0.83 (d, 3H, $^3J_{HH}$ = 3.1 Hz, CHC*H$_3$*), 0.81 (d, 3H, $^3J_{HH}$ = 3.1 Hz, CHC*H'$_3$*). - **$^{13}$C NMR** (101 MHz, 25 °C, CDCl$_3$): $\delta$ = 171.5 / 166.5 / 166.2 (each s, *C*ON), 138.2 (s, *C*$_{arom\ Bzl}$), 134.8 (d, $^3J_{PC}$ = 9.7 Hz, *C*$_{PPh3}$), 130.7 (br s, *C*$_{PPh3}$), 128.7 (s, *C*$_{Bzl}$), 128.1 (br s, *C*$_{PPh3}$), 127.7 (s, *C*$_{Bzl}$H), 127.4 (s, *C*$_{Bz}$ H), 102.5 (d, $^1J_{RhC}$ = 5.5 Hz, *C*$_{Cp}$), 102.3 (d, $^2J_{RhC}$ = 4.3 Hz, *C*$_{Cp}$), 100.3 (dd, $^2J_{RhC}$ = 6.6 Hz, $^3J_{PC}$ = 6.6 Hz, *C*$_{Cp}$), 97.1 (m, *C*$_{Cp}$), 54.5 / 54.1 (each s, *C*H(O)C'H / CH(O)*C*'H), 51.8 (s, *C*HCH$_2$), 43.5 (s, NH*C*H$_2$), 41.0 (s, CH*C*H$_2$), 36.3 (d, $^4J_{PC}$ = 4.3 Hz, *C*H$_2$CH$_2$NH), 24.8 (s, *C*H(CH$_3$)$_2$), 24.6 (s, CH$_2$*C*H$_2$NH), 23.0 / 22.1 (each s, *C*H$_3$ / *C*'H$_3$), 9.5 (s, Cp$_{arom}$*C*H$_3$), 8.7 (s, Cp$_{arom}$*C*H$_3$). - **$^{31}$P NMR** (162 MHz, 25 °C, CDCl$_3$): $\delta$ = 30.0 (d, $^1J_{PRh}$ = 143 Hz). - **IR** (KBr): $\tilde{v}$ =3060 s, 2957 s, 2926 s, 2870 s, 1664 vs (br, CO), 1533 vs 1436 vs, 1368

w, 1260 w, 1095 s cm$^{-1}$. - **EA** C$_{46}$H$_{53}$Cl$_2$N$_3$O$_4$PRh (916.7): calcd. C 60.3, H 5.8, N 4.6; found C 60.2, H 6.1, N 4.3. - **ESI-MS** m/z (%) = 880.1 [M-Cl]$^+$ (100), 618.2 [M-PPh$_3$-Cl]$^+$ (70).

*[(η$^6$-C$_6$H$_5$CH$_2$NH-Eps-Leu-Bz)RuCl$_2$PPh$_3$]* (**71**):
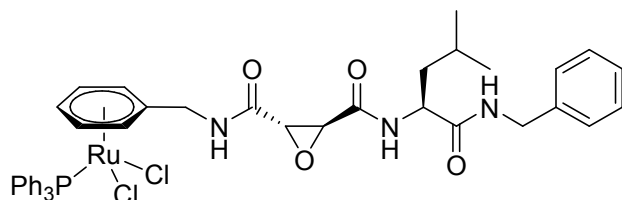


Dichloromethane (10 mL) was added to polystyrene bound cyclohexyl carbodiimide (230 mg, 1.3 mmol/g, 0.30 mmol) at 0°C and the resin allowed to swell for several minutes. HO-Eps-NH-Leu-Bzl **66** (50 mg, 0.15 mmol) was added to the gently stirred mixture, before pentafluorophenol (28 mg, 0.15 mmol) was slowly added and the reaction mixture stirred at 0°C for 1 h and then at room temperature over night. The mixture was filtered, triethylamine (50 μL, 0.35 mmol) and then [(η$^6$-benzyl-ammonium)(PPh$_3$)RuCl$_2$]Cl **4i** (58 mg, 0.10 mmol) added, vigorously stirred for 1 h and washed with water and brine (each 3 x 10 mL), dried over MgSO$_4$ and volatiles removed under reduced pressure. The crude product was washed with diethylether and hexane, yielding a bright red solid (60 mg, 0.07 mmol, 69%). - **$^1$H NMR** (400 MHz, 25 °C, CDCl$_3$): $\delta$ = 7.97 (t, 1H, $^3J_{HH}$ = 5.4 Hz, N*H*CH$_2$), 7.76-7.65 (m, 6H, C$_{PPh3}$*H*), 7.51-7.22 (m, 14H, C$_{PPh3}$*H* / C$_{Bzl}$*H*), 6.76 (d, 1H, $^3J_{HH}$ = 8.3 Hz, N*H*CH), 6.50 (t, 1 H, $^3J_{HH}$ = 5.4 Hz, N*H*CH$_2$), 5.61 (d, 1H, $^3J_{HH}$ = 5.6 Hz, C$_{ortho}$*H*), 5.35-5.31 (m, 1H, C$_{meta}$*H*), 5.29 (d, 1H, $^3J_{HH}$ = 6.1 Hz, C$_{ortho}$*H*), 5.12-5.04 (m, 1H, C$_{meta}$*H*), 4.68 (dd, 1H, $^2J_{HH}$ = 15.4 Hz, $^3J_{HH}$ = 6.2 Hz, C*H*H'), 4.61-4.55 (m, 1H, C$_{para}$*H*), 4.52-4.30 (m, 5H, PhC*H$_2$* / CH*H'* / C*H$_2$*Ph), 3.93 (s, 1 H, C*H*(O)CH'), 3.57 (s, 1 H, CH(O)C*H'*), 1.73-1.50 (m, 3 H, C*H$_2$$^i$*Pr / CH$_2$C*H*(CH$_3$)$_2$), 0.89 (d, 6H, $^3J_{HH}$ = 6.0 Hz). - **$^{13}$C NMR** (101 MHz, 25 °C, CDCl$_3$): $\delta$ = 171.4 / 167.1 / 166.3 (each s, *C*ON), 138.2 (s, *C*$_{Bz}$), 134.2 (d, $J_{PC}$ = 9.2 Hz, *C*$_{PPh3}$), 133.0 (d, $J_{PC}$ = 47.7 Hz, *C*$_{PPh3}$), 130.8 (d, $J_{PC}$ = 2.5 Hz, *C*$_{PPh3}$), 128.7 (s, *C*$_{Bzl}$H), 128.4 (d, $J_{PC}$ = 10.1 Hz, *C*$_{PPh3}$), 127.8 (s, *C*$_{Bzl}$H), 127.5 (s, *C*$_{Bzl}$H), 107.6 (d, $^2J_{PC}$ = 6.7 Hz, *C*$_{arom}$), 89.5 (s, *C*$_{arom}$), 88.0 (d, $^2J_{PC}$ = 6.5 Hz, *C*$_{arom}$), 87.6 (s, *C*$_{arom}$), 86.2 (s, *C*$_{arom}$), 82.0 (s, *C*$_{arom}$), 54.54 / 54.46 / 51.9 (each s, *C*H(O)C'H / CH(O)*C'*H / *C*HCH2), 43.5 / 41.0 / 40.6 (each s, NH*C*H$_2$C$_{arom}$ / NH*C*H$_2$C$_{Bzl}$ / *C*HCH$_2$), 24.9 / 23.0 / 22.1 (each s, *C*H(CH$_3$)(C'H$_3$) / CH(*C*H$_3$)(C'H$_3$) / CH(CH$_3$)(*C'*H$_3$)). - **$^{31}$P NMR** (162 MHz, 25 °C, CDCl$_3$): $\delta$ = 27.8 (s). - **IR**

(KBr): $\tilde{v}$ =3060 w, 2956 w, 2927 w, 1669 vs (CO), 1526 vs, 1482 w, 1435 s, 1243 w, 1093 w, 697 s, 527 s cm$^{-1}$. - **EA** $C_{42}H_{44}Cl_2N_3O_4PRu$ (857.8): calcd. C 58.8, H 5.2, N 4.9; found C 58.4, H 5.0, N 4.6. - **ESI-MS** m/z (%) = 822.1 [M-Cl]$^+$ (100), 1679.8 [2M-PPh$_3$-Cl]$^+$ (20), 1415.8 [2M-PPh$_3$-Cl]$^+$ (8).

*[($\eta^5$-Me$_4$Cp(CH$_2$)$_2$NH-Suc-Leu-Bz)RhCl$_2$PPh$_3$]* (**72**):
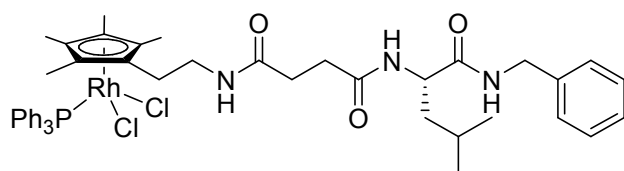


Dichloromethane (10 mL) was added to polystyrene bound cyclohexyl carbodiimide (182 mg, 1.3 mmol/g, 0.24 mmol) at 0°C and the resin allowed to swell for several minutes. HO-Suc-Leu-Bz **68** (38 mg, 0,12 mmol) was added to the gently stirred mixture, before pentafluorophenol (43 mg, 0.24 mmol) was slowly added and the reaction mixture stirred at 0°C for 1h and then at room temperature over night. The mixture was filtered, triethylamine (43 µL, 0.36 mmol) and then [Me$_4$Cp(CH$_2$)$_2$NH$_3$)RhCl$_2$PPh$_3$]Cl **52** (50 mg, 0.08 mmol) added, stirred vigorously stirred for 1 h and extracted with water and brine (each 3 x 10 mL), dried over MgSO$_4$ and volatiles removed under reduced pressure. The crude product was washed with diethylether and hexane, yielding a bright red solid (54 mg, 0.06 mmol, 80%). - **$^1$H NMR** (400 MHz, 25 °C, CDCl$_3$): $\delta$ = 7.82-7.74 (m, 6H, C$_{PPh3}$*H*), 7.48-7.11 (m, 16H, N*H*CH$_2$ / C$_{PPh3}$*H* / C$_{Bzl}$*H* / N*H*CH$_2$), 6.46 (d, 1H, $^3J_{HH}$ = 8.1 Hz, N*H*CH), 4.49-4.40 (m, 1H, NHC*H*), 4.36 (d, 2H, $^3J_{HH}$ = 5.9 Hz, NHC*H*$_2$(C$_6$H$_5$)), 3.52-3.33 (m, 2H, CH$_2$C*H*$_2$NH), 2.60-2.38 (m, 4H, COC*H*$_2$C*H*$_2$CO), 2.30-2.20 (m, 2H, C*H*$_2$CH$_2$NH), 1.83-1.50 (m, 3H, C*H*$_2$C*H*(CH$_3$)$_2$), 1.49 (d, 3H, $^4J_{PH}$ = 2.8 Hz, C$_{Cp}$C*H*$_3$), 1.48 (d, 3H, $^4J_{PH}$ = 2.5 Hz, C$_{Cp}$C*H*$_3$), 1.03 (d, 3H, $^4J_{PH}$ = 3.3 Hz, C$_{Cp}$C*H*$_3$), 0.99 (d, 3H, $^4J_{PH}$ = 2.9 Hz, C$_{Cp}$C*H*$_3$), 0.89 (d, $^3J_{HH}$ = 4.6 Hz, CHC*H*$_3$), 0.87 (d, $^3J_{HH}$ = 4.6 Hz, CHC*H'*$_3$). - **$^{13}$C NMR** (101 MHz, 25 °C, CDCl$_3$): $\delta$ = 172.9 / 172.7 / 172.4 (each s, *C*ON), 138.9 (s, *C*$_{Bz}$), 134.8 (d, $^3J_{PC}$ = 9.5 Hz, C$_{PPh3}$), 130.7 (br s, C$_{PPh3}$), 128.6 (s, *C*$_{Bzl}$H), 128.2 (br s, C$_{PPh3}$), 127.7 (s, *C*$_{Bzl}$H), 127.2 (s, *C*$_{Bzl}$H), 104.0 (d, $^1J_{RhC}$ = 6.0 Hz, *C*$_{Cp}$), 102.9 (d, $^2J_{RhC}$ = 6.0 Hz, *C*$_{Cp}$), 101.0-101.3 (m, *C*$_{Cp}$), 96.0 (d, $^2J_{RhC}$ = 6.9 Hz, *C*$_{Cp}$), 95.4 (d, $^1J_{RhC}$ = 7.6 Hz, *C*$_{Cp}$), 52.2 (s, *C*HCH$_2$), 43.4 (s, NH*C*H$_2$), 40.7 (s, CH*C*H$_2$), 36.1 (d, $^4J_{PC}$ = 4.7 Hz, *C*H$_2$CH$_2$NH), 32.1 / 31.7 (each s, CH$_2$*C'*H$_2$ / CH$_2$*C'*H$_2$), 25.0 (s, *C*H(CH$_3$)$_2$), 24.7 (d, $^4J_{PC}$ = 2.3 Hz, CH$_2$*C*H$_2$NH), 23.2 / 21.9 (each s, *C*H$_3$ / *C'*H$_3$), 9.7 / 9.6 / 8.7 / 8.6 (each s, C$_{Cp}$*C*H$_3$). - **$^{31}$P NMR** (162 MHz, 25 °C, CDCl$_3$): $\delta$ = 29.8 (d, $J_{PRh}$ = 142 Hz). - **IR** (KBr): $\tilde{v}$ = 3030 s, 3058 w, 2956 s, 1652 vs, (br,

CO), 1522 s, 1435 vs, 1384 vs, 1257 w, 1095 w cm$^{-1}$. - **EA** C$_{46}$H$_{57}$N$_3$O$_4$PRh (919.3): calcd. C 60.00, H 6.2, N 4.6; found C 59.5, H 5.6, N 4.4. - **ESI-MS** m/z (%) = 604.2 [M-PPh$_3$-Cl]$^+$ (100), 866.0 [M-Cl]$^+$ (20).

## 2.8. Metalla labels for serine proteases

### 2.8.1. Organic precursors

*1-tosyl-10-undecene* (**80**): [23]

TsO⌇⌇⌇⌇⌇⌇
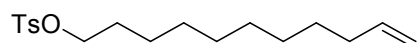
10-Undecenole (8.0 g, 47.2 mmol) was dissolved in pyridine (55 mL) and placed in an ice-bath. To this solution, *p*-toluenesulfonyl chloride were added (18.0 g, 94.4 mmol) and the reaction mixture stirred for 1 h at 0 °C and then for 20 h at room temperature. Thereafter, EtOAc (150 mL) and water (150 mL) were added. The organic phase was separated, and the aqueous phase extracted with EtOAc (2 x 50 mL). The combined organic phases were washed with 1 M aqueous hydrochloric acid (2 x 100 mL) and brine (2 x 100 mL), dried over $MgSO_4$ and the solvent removed in vacuo, giving the title compound **80** (11.25 g, 34.7 mmol, 74 %) as a colorless oil. - **$^1$H NMR** ($CDCl_3$, RT, 399.8 MHz): $\delta$ = 7.78 (d, 2 H, $^3J_{H,H}$ = 8.0 Hz, $C_{arom}H$), 7.33 (d, 2 H, $^3J_{H,H}$ = 8.0 Hz, $C_{arom}H$), 5.79 (m, 1 H, C$H$CH$_2$), 4.93 (m, 2 H, CHC$H_2$), 4.01 (t, 2 H, $^3J_{H,H}$ = 6.4 Hz, SOC$H_2$), 2.44 (s, 3 H, $C_{arom}CH_3$), 2.03-2.01 (m, 2 H, C$H_2$CHCH$_2$), 1.65-1.58 (m, 2 H, SOCH$_2$C$H_2$), 1.37-1.22 (m, 12 H).

*1-iodo-10-undecene* (**81**): [23]

I⌇⌇⌇⌇⌇⌇
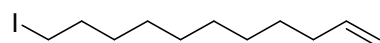
To a solution of 1-tosyl-10-undecene **80** (11.25 g, 34.7mmol) in acetone (70 mL), NaI (10.6 g, 69.5 mmol) was added and the mixture refluxed for 2 h. Thereafter, the reaction mixture was allowed to cool down to room temperature. Thereafter, EtOAc (150 mL) and water (150 mL) were added. The organic phase was separated, and the aqueous phase extracted with EtOAc (2 x 50 mL). The combined organic phases were washed with saturated aqueous $NaS_2O_3$ (100 mL) and brine (100 mL), dried over $MgSO_4$ and the solvent removed in vacuo, giving the title compound **81** (9.53 g, 34.0 mmol, 98 %) as a colorless oil. - **$^1$H NMR** ($CDCl_3$, RT, 400 MHz): $\delta$ = 5.83-5.76 (m, 1 H, C$H$CH$_2$), 5.00-4.91 (m, 2 H, CHC$H_2$), 3.16 (t, 2 H, $^3J_{H,H}$ = 10 Hz, IC$H_2$), 2.02 (m, 2 H, C$H_2$CHCH$_2$), 1.81 (m, 2 H, ICH$_2$C$H_2$), 1.37-1.28 (m, 12 H).

*1-diethoxy phosphinyl-10-undecene* (**82**): [23]
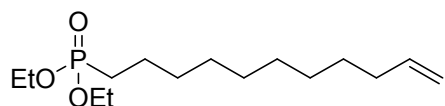


A mixture of triethylphosphite (27.15 mL, 158 mmol) and 1-iodo-10-undecene **81** (4.45 g, 15.8 mmol) were refluxed at 160 °C for 13 h. Then, the reaction mixture was allowed to cool to room temperature. Excess triethylphosphite was removed at 40 °C in vacuo. The yellowish residue was purified by column chromatography (silica gel 60; 3 x 20 cm; hexane / EtOAc; Gradient 75 % to 0 % hexane; $R_f$ = 0.55 (EtOAc)), giving the title compound **82** (3.64 g, 12.5 mmol, 79 %) as a colorless oil. - **¹H NMR** (CDCl₃, RT, 400 MHz): $\delta$ = 5.95–5.75 (m, 1 H, C*H*CH₂), 5.03–4.90 (m, 2 H, CHC*H₂*), 4.05 (m, 4 H, PC*H₂*), 2.02 (m, 2 H, C*H₂*CHCH₂), 1.80–1.20 (m, 22 H).

*1-ethoxyhydroxy phosphinyl-10-undecene* (**83**): [23]
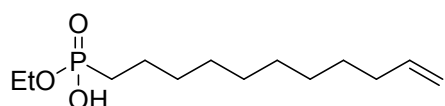


A solution of 1-diethoxy phosphinyl-10-undecene **82** (3.45 g, 11.9 mmol) were dissolved in dry dichloromethane (45 mL) and trimethylsilylbromide (1.88 mL, 2.18 g, 14.3 mmol) slowly added and the reaction mixture stirred for 30 min. Thereafter, an aqueous solution of KHSO4 (5%, 65mL) was added and the reaction stirred for another 45 min, before AcOEt (250 mL) and water (120 mL) were added. The organic phase was separated, washed with brine (2 x 150 mL), dried over MgSO₄ and the solvent removed under reduced pressure, and the raw product purified via column chromatography (silica gel 60; 3 x 25 cm; CHCl₃ / MeOH / NH₃ (aqueous solution, 25%) = 32 /8 / 1; Rf = 0,19), giving the title compound **83** (1.68 g, 6.40 mmol, 54 %) as a white semisolid. - **¹H NMR** (CDCl₃, RT, 400 MHz): $\delta$ = 5.95–5.75 (m, 1 H, C*H*CH₂), 5.03–4.90 (m, 2 H, CHC*H₂*), 4.05 (m, 2 H, POC*H₂*CH₃), 2.02 (m, 2 H, C*H₂*CHCH₂), 1.80–1.20 (m, 22 H).

*10-ethoxyhydroxy phosphinyl decanoic acid* (**84**): [23]
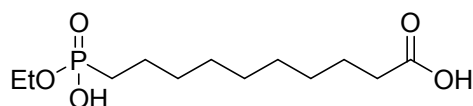
1-Ethoxyhydroxy phosphinyl-10-undecene **83** (1.30 g, 4.94 mmol) was dissolved in a mixture of $CCl_4$, AcN and $H_2O$ (46 mL, $CCl_4$ / AcN / $H_2O$ = 13 / 13 / 20) and $RuCl_3 \cdot$ n $H_2O$ added (26 mg, 0.11 mmol). To the vigorously stirred solution, $NaIO_4$ (4.03 g, 20.28 mmol) was added slowly and the reaction solution stirred for 2 h. Thereafter, dichloromethane (50 mL) and aqueous hydrochloric acid were added (50 mL, 1 M), the aqueous phase separated and extracted with dichloromethane (50 mL). The combined organic phases were filtered, washed with brine (50 mL), dried over $MgSO_4$ and volatiles removed in vacuo. The raw product was redissolved in diethylether (50 mL) and filtered three times over celite. The solvent was removed in vacuo. Recrystallization from AcN gave the title compound **84** (0.60 g, 2.14 mmol, 43 %) as a white solid. - **$^1$H NMR** ($CDCl_3$, RT, 400 MHz): $\delta$ = 9.20-9.08 (m, 2 H, -COO$H$, P-O$H$), 4.12-4.04 (m, 2 H, POC$H_2$CH$_3$), 2.32 (t, 2 H, $^3J_{H,H}$ = 7.6 Hz, C$H_2$COOH), 1.77-1.58 (m, 6 H, PC$H_2$, PCH2C$H_2$, C$H_2$CH$_2$COOH),  1.36-1.28 (m, 13 H). - **$^{13}$C NMR** ($CDCl_3$, RT, 101 MHz): $\delta$ = 179.77 (*C*OOH), 61.04 (d, $^2J_{C,P}$ = 6,9 Hz, PO*C*), 34.18 (*C*COOH), 30.37 (d, $^1J_{C,P}$ = 16,2 Hz,  P*C*H$_2$), 29.10, 29.04, 28.97, 26.62, 25.21, 24.71, 22.14 (d, $^2J_{C,P}$ = 3,8 Hz, P$CH_2$*C*H$_2$), 16.39 (d, J = 6,2 Hz, POCH$_2$*C*H$_3$). - **$^{31}$P NMR** ($CDCl_3$, RT, 161 MHz): $\delta$ = 36.87.

*Diphenyl-[(N-benzoyloxycarbonyl)aminobenzyl]phosphonate* (**85**): [24]
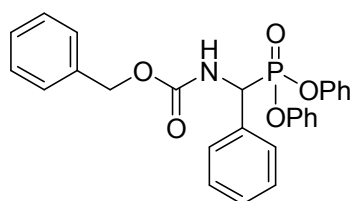


A mixture of benzaldehyde (31.0 g, 100 mmol), benzylcarbamate (15.1 g, 150 mmol) and triphenylphosphite (15.9 g, 100 mmol) were stirred for approx. 1 h or to the end of the exothermic reaction. The mixture was then heated for 1 h to 80-85 °C. Thereafter, volatiles were removed under reduced pressure. The residue was recrystallized (-10 °C) from methanol (~100 mL), giving the title compound **85** (22.7 g, 48 mmol, 48 %)as a white powder. - **$^1$H NMR** (400 MHz, 25 °C, $CDCl_3$): $\delta$ = 7.80-7.30 (m, 20H, H$_{arom}$), 6.10 (d, $^3J_{HH}$ = 9.6 Hz, 1H, N$H$), 5.58 (dd, $^3J_{HH}$ = 9.6 Hz, $^2J_{PH}$ = 22 Hz, 1H, C$H$P), 5.40 (s, 2H, C$H_2$). - **$^{13}$C NMR** (101 MHz, 25 °C, $CDCl_3$): $\delta$  = 155.8 (d, $^3J_{PC}$ = 13 Hz, O*C*ONH), 150.5 (d, $^3J_{PC}$ = 8.7 Hz, *C*$_{arom\ gem\ OPh}$), 150.2 (d, $^3J_{PC}$ = 8.7 Hz, *C*$_{arom\ gem\ OPh}$), 136.1 (*C*$_{arom.}$), 134.3 (*C*$_{arom.}$), 129.9 (d, $J_{PC}$ = 11 Hz, *C*$_{arom.}$), 129.0 (*C*$_{arom.}$), 128.9 (*C*$_{arom.}$), 128.7 (*C*$_{arom.}$),

128.4 (d, $J_{PC}$ = 9.0 Hz, $C_{arom.}$), 125.6 (d, $J_{PC}$ = 8.1 Hz, $C_{arom.}$), 120.6 (d, $J_{PC}$ = 16 Hz, $C_{arom.}$), 120.5 (d, $J_{PC}$ = 16 Hz, $C_{arom.}$), 67.7 ($CH_2$), 53.1 (d, $^1J_{PC}$ = 159 Hz). - **$^{31}$P NMR** (162 MHz, 25 °C, CDCl$_3$): $\delta$ = 15.0.

*Diphenyl-(aminobenzyl)phosphonate* (**86**): [24]
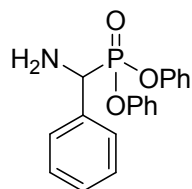


Diphenyl-[(N-benzoyloxycarbonyl)aminobenzyl]phosphonate **85** (1.39 g, 2.94 mmol) was suspended in a solution of hydrobromic acid and acetic acid (30 mL, 48% HBr in AcOH). The reaction mixture was stirred for 1.5 h, before volatiles were removed in vacuo. The remaining residue was washed with diethylether. Thereafter, the white solid was suspended in diethylether and gaseous ammonia bubbled through the mixture for about 10-15 min. The precipitate was filtered off and solvent removed in vacuo, yielding the title compound **86** (0.93 g, 2.73, 93 %) as a white crystalline solid. - **$^1$H NMR** (400 MHz, 25 °C, CDCl$_3$): $\delta$ = 7.80-6.80 (m, 20H, H$_{arom}$), 4.64 (d, $^2J_{PH}$ = 16 Hz, 1H, C*H*Ph), 2.06 (s, 2H, N*H$_2$*). - **$^{13}$C NMR** (101 MHz, 25 °C, CDCl$_3$): $\delta$ = 150.3-150.8 (m, $C_{arom\ gem\ OPh}$), 136.4 (d, $^1J_{PC}$ = 2.3 Hz, $C_{arom\ gem\ Ph}$), 129.7 (d, $J_{PC}$ = 10 Hz, $C_{arom}$), 129.4 ($C_{arom}$), 129.1-128.4 (m, $C_{arom}$), 128.2 (d, $J_{PC}$ = 6.9 Hz, $C_{arom}$), 125.2 (d, $J_{PC}$ = 9.9 Hz, $C_{arom}$), 120.6 (d, $J_{PC}$ = 13 Hz, $C_{arom}$), 120.5 (d, $J_{PC}$ = 13 Hz, $C_{arom}$), 54.4 (d, $^1J_{PC}$ = 151 Hz, Ph*C*H). - **$^{31}$P NMR** (162 MHz, 25 °C, CDCl$_3$): $\delta$ = 18.4. - **IR** (KBr): $\tilde{v}$ = 3360, 3280, 2830, 1590, 1485, 1455, 1265, 1215, 1190, 1160, 1070, 1030, 1010, 940 cm$^{-1}$.

*Suc-P(OPh)$_2$* (**87**):
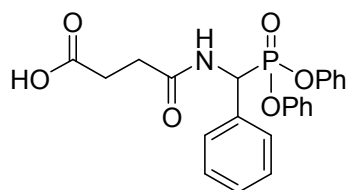


Succinic acid anhydride (354 mg, 3.54 mmol) and diphenyl-(aminobenzyl)phosphonate **86** (1.00 g, 2.95 mmol) were dissolved in dichloromethane (75 mL). Then, pyridine

(237 µL, 2.95 mmol) was added and the reaction mixture stirred for 24 h. Thereafter, the mixture was washed with water (3 x 40 mL) and brine (2 x 40 mL), dried over MgSO$_4$ and volatiles removed under reduced pressure. The raw product was redissolved in AcOEt and precipitated with diethylether to give the pure title compound **87** (1.06 g, 2.41 mmol, 68 %) as a white solid. - **$^1$H NMR** (400 MHz, 25 °C, CDCl$_3$): $\delta$ = 8.36 (dd, $^3J_{HP}$ = 13 Hz, $^3J_{HH}$ = 9.6 Hz, 1H, N*H*), 7.54-6.63 (m, 15H, *H*$_{arom}$), 5.96 (dd, $^3J_{HH}$ = 9.6 Hz $^2J_{PH}$ = 22 Hz, 2H, NH-C*H*Ph), 2.64–2.39 (m, 4H, C*H$_2$*C*H$_2$*COOH). - **$^{13}$C NMR** (101 MHz, 25 °C, CDCl$_3$): $\delta$ = 176.3 (*C*OOH), 171.8 (d, $^3J_{PC}$ = 9.2 Hz, NH*C*O), 150.3 (d, $J_{PC}$ = 9.9 Hz, *C*$_{arom}$), 150.1 (d, $J_{PC}$ = 11 Hz, *C*$_{arom.}$), 133.8 (*C*$_{arom.}$), 130.0 (d, $J_{PC}$ = 27 Hz, *C*$_{arom.}$), 129.4-128.4 (m, 2 *C*$_{arom.}$), 125.6 (d, $J_{PC}$ = 24 Hz, *C*$_{arom.}$), 120.6 (d, $J_{PC}$ = 3.8 Hz, *C*$_{arom.}$), 120.2 (d, $J_{PC}$ = 3.8 Hz, *C*$_{arom.}$), 50.7 (d, $^1J_{PC}$ = 159 Hz Ph*C*H), 30.5 (*C*H$_2$*C'*H$_2$), 29.4 (*C*H$_2$*C'*H$_2$). - **$^{31}$P NMR** (162 MHz, 25 °C, CDCl$_3$): $\delta$ = 15.1. – **IR** (KBr): $\tilde{v}$ = 3261 m, 3060 m, 2917 w, 1719 m, 1701 sh w, 1677 m, 1653 s, 1589 m, 1550 m, 1492 s, 1202 m, 1179 m, 942 vs cm$^{-1}$. - **EA** C$_{23}$H$_{22}$NO$_6$P (439.4): calcd. C 63.87, H 5.05, N 3.19; found C 62.46, H 4.95, N 3.04. - **ESI-MS** m/z = 462.2 [M+Na$^+$]$^+$, 901.1 [2M+Na$^+$]$^+$, 917.1 [2M+K$^+$]$^+$.

## 2.8.2. Catalyst synthesis

*[Rh]-FP* (**90**):
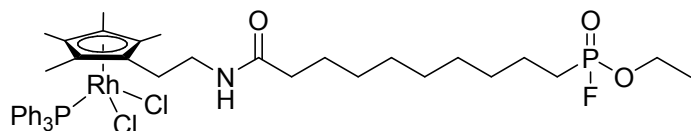


10-(ethoxyhydroxyphosphinyl)-decanoic acid **84** (72 mg, 0.26 mmol) was dissolved in a teflon-flask in dichloromethane (5 mL) at -78°C. To this solution, DAST was added (135 µL, 1.02 mmol) and the solution stirred for 15 min at -78°C and then for 10 min at room temperature. Water (10 mL, small portions) was added and the solution vigorously stirred for 5 min, before ethyl acetate (30 mL) was added, the organic phase separated, washed with brine, dried over $MgSO_4$, and volatiles removed under reduced pressure. The residual yellowish oil was dissolved in a teflon-flask in dichloromethane (5 mL) and triethylamine (143 µL, 1.02 mmol) and $Me_4Cp(CH_2)_2NH_3)RhCl_2PPh_3]Cl$ **52** (30 mg, 0.05 mmol) added. The reaction solution was stirred at room temperature for 3 h before volatiles were removed in vacuo. The red crude reaction product was dissolved in dichloromethane (3 mL) and precipitated with hexane (50 mL) at -20°C over night. Supernatant was filtered off, the red precipitate washed with hexane and dried in vacuo, yielding a bright red solid (35 mg, 0.04 mmol, 86 %). - **$^1$H NMR** (400 MHz, 25 °C, $CDCl_3$): $\delta$ = 7.82-7.78 (m, 6H, $C_{arom\ PPh3}H$), 7.37 (m, 9H, $C_{arom\ PPh3}H$), 6.40 (t, 1H, $^3J_{HH}$ = 5.8 Hz, N$H$), 4.23 (m, 2H, OC$H_2$CH$_3$), 3.85 (dt, 2H, $^3J_{HH}$ = 6.2 Hz, CH$_2$C$H_2$NH), 2.24 (m, 2H, C$H_2$CH$_2$NH), 2.12 (t, 2H, $^3J_{HH}$ = 7.9 Hz, COC$H_2$CH$_2$), 1.90-1.81 / 1.68-1.59 (m, 4H, C$H_2$CH$_2$P / CH$_2$C$H_2$P), 1.56-1.52 (m, 2H, COCH$_2$C$H_2$), 1.52 (d, 6H, $^4J_{PH}$ = 1.7, C$H_3$), 1.36 (t, 3H, $^3J_{HH}$ = 7.1 Hz, COCH$_2$C$H_2$), 1.25 (m, 10H, (CH$_2$)$_2$(C$H_2$)$_5$(CH$_2$)$_2$), 1.11 (d, 6H, $^4J_{PH}$ = 2.9, C'$H_3$). - **$^{13}$C NMR** ($CDCl_3$, 25 °C, 125 MHz): $\delta$ = 173.5 (*C*ON), 134.8 (d, $J_{PC}$ = 9.2 Hz, $C_{arom\ PPh3}H$), 130.6 ($C_{arom\ PPh3}H$), 128.1 ($C_{arom\ PPh3}H$), 102.7 (d, $^2J_{RhC}$ = 6.9 Hz, $C_{arom\ Cp*}$), 100.3 (dd, $^2J_{RhC}$ = 6.9 Hz, $^3J_{PC}$ = 6.9 Hz, $C_{arom\ Cp*}$), 96.6 (d, $^2J_{RhC}$ = 6.2, $C_{arom\ Cp*}$), 63.11 (d, $^2J_{PC}$ = 7.7 Hz, OCH$_2$), 36.6, 36.3 (d, $^4J_{PC}$ = 5.4 Hz, CH$_2$CH$_2$NH), 30.3 (d, 16.9 Hz), 29.3 (d, 3.1 Hz), 29.0 (d, 17.7 Hz), 25.6, 25.2, 25.0, 24.9, 23.7 (d, 22.3 Hz), 21.9 (d, 5.4 Hz), 16.4 (d, 5.4 Hz), 9.5 / 8.6 (CH$_3$). - **$^{31}$P NMR** ($CDCl_3$, 25 °C, 161.8 MHz): $\delta$ = 32.54 (d, $^3J_{PF}$ = 1.07 kHz), 29.82 (d, $^1J_{PRh}$ = 142 Hz). - **$^{19}$F NMR** ($CDCl_3$, 25 °C, 376.2 MHz): $\delta$ = -64.57 (d, $^3J_{PF}$ = 1.07 kHz). - **IR** (KBr): $\tilde{v}$ = 2922 s, 2851 s, 1645 w, 1435 w, 1384 vs, 1262 w, 1095 w, 1035 w cm$^{-1}$. - **EA** $C_{41}H_{57}FNO_4P_2Rh$ (881.22): calcd.

C 55.79, H 6.51, N 1.59; found C 55.37, H 6.51, N 1.56. - **ESI-MS** m/z (%) = 566.1 [M-PPh$_3$-Cl]$^+$ (100), 530.2 [M-PPh$_3$-HCl-Cl]$^+$ (21), 827.9 [M-Cl]$^+$ (6), 792.1 [M-Cl-HCl]$^+$ (3).

*[Rh]-SF* (**91**):
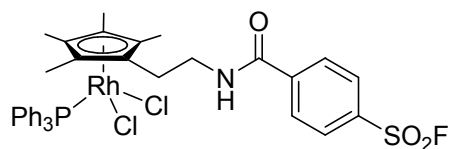


Synthetic route A)

Dichloromethane (10 mL) was added to polystyrene bound cyclohexyl carbodiimide (182 mg, 1.3 mmol/g, 0.24 mmol) at 0°C and the resin allowed to swell for several minutes. 4-(fluorosulfonyl)-benzoic acid (25 mg, 0.12 mmol) was added to the gently stirred mixture, before pentafluorophenole (43 mg, 0.24 mmol) was slowly added and the reaction mixture stirred at 0°C for 1h and then at room temperature over night. The mixture was filtered, triethylamine (43 µL, 0.36 mmol) and thereafter [Me$_4$Cp(CH$_2$)$_2$NH$_3$)RhCl$_2$PPh$_3$]Cl **52** (50 mg, 0.08 mmol) added. The mixture was stirred vigorously for 1 h and extracted with water and brine (each 3 x 10 mL), dried over MgSO$_4$ and volatiles removed under reduced pressure. The crude product was washed with diethylether and hexane, yielding a bright red solid (36 mg, 0.05 mmol, 59%).

Synthetic route B)

4-(fluorosulfonyl)-benzoic acid (42 mg, 0.21 mmol) was dissolved in a teflon-flask in dichloromethane (5 mL) at -78°C. To this solution, DAST was added (107 µL, 133 mg, 0.82 mmol) and the solution stirred for 2 h at -78°C and then for 10 min at room temperature. Water (10 mL, small portions) was added and the solution vigorously stirred for 15 min, before ethyl acetate (30 mL) was added, the organic phase separated, washed with brine (3 x 5 mL), dried over MgSO$_4$, and volatiles removed under reduced pressure. The residual yellowish oil was dissolved in a teflon-flask in dichloromethane (5 mL) and triethylamine (83 µL, 0.82 mmol) and [Me$_4$Cp(CH$_2$)$_2$NH$_3$)RhCl$_2$PPh$_3$]Cl **52** (148 mg, 0.19 mmol) added. The reaction solution was stirred at room temperature for 3 h before volatiles were removed in vacuo. The red crude reaction product was dissolved in dichloromethane (3 mL) and precipitated with

hexane (50 mL). The supernatant was filtered off, the red precipitate washed with hexane and dried in vacuo, yielding an orange (141 mg, 0.18 mmol, 95 %).

**$^1$H NMR** (400 MHz, 25 °C, CDCl$_3$): $\delta$ = 8.12 (t, 1H, $^3J_{HH}$ = 5.8, N*H*), 8.03 (d, $^3J_{HH}$ = 8.3, C$_{arom\ SO2F}$*H*), 7.80-7.72 (m, 8H, C$_{arom\ SO2F}$*H* / C$_{arom\ PPh3}$*H*), 7.33 (m, 9H, C$_{arom\ PPh3}$*H*), 3.85 (dt, 2H, $^3J_{HH}$ = 5.8, CH$_2$C*H$_2$*NH), 2.67 (m, 2H, C*H$_2$*CH$_2$NH), 1.60 (d, $^4J_{PH}$ = 2.1, C*H$_3$*), 0.98 (d, $^4J_{PH}$ = 2.9, C'*H$_3$*). - **$^{13}$C NMR** (CDCl$_3$, 25 °C, 125 MHz): $\delta$ = 165.0 (*C*ON), 140.2 (*C*$_{arom\ SO2F}$), 134.7 (d, $J_{PC}$ = 9.2, *C*$_{arom\ PPh3}$H), 130.7 (*C*$_{arom\ PPh3}$H), 129.1 (*C*$_{arom\ SO2F}$H), 128.4 (*C*$_{arom\ SO2F}$H), 128.2 (*C*$_{arom\ PPh3}$H), 103.3 (d, $^2J_{RhC}$ = 6.2, *C*$_{arom\ Cp*}$), 103.1 (m, *C*$_{arom\ Cp*}$), 95.5 (d, $^2J_{RhC}$ = 7.7, *C*$_{arom\ Cp*}$), 37.1 (d, $^4J_{PC}$ =4.6, *C*H$_2$CH$_2$NH), 25.3 (CH$_2$*C*H$_2$NH), 9.8 / 8.6 (*C*H$_3$). - **$^{31}$P NMR** (CDCl$_3$, 25 °C, 161.8 MHz): $\delta$ = 30.04 (d, $^3J_{PRh}$ = 143 Hz). – **$^{19}$F NMR** (CDCl$_3$, RT, 376.2 MHz): $\delta$ = 85.86. - **IR** (KBr): $\tilde{v}$ = 3056 s, 2920 s, 2815 w, 1664 s, 1532 w, 1483 w, 1435 vs, 1411 vs, 1213 vs, 1095 s cm$^{-1}$. - **EA** C$_{36}$H$_{36}$FNO$_3$PRhS · H$_2$O (785.1): calcd. C 54.97, H 4.61, N 1.78; found C 54.48, H 5.29, N 1.84. - **ESI-MS** m/z (%) = 488.0 [M-PPh$_3$-Cl]$^+$ (100), 749.9 [M-Cl]$^+$ (37).

*[Ru]-SF* (**92**):
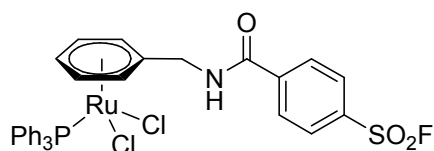


Dichloromethane (10 mL) was added to polystyrene bound cyclohexyl carbodiimide (182 mg, 1.3 mmol/g, 0.24 mmol) at 0°C and the resin allowed to swell for several minutes. 4-(fluorosulfonyl)-benzoic acid **2** (25 mg, 0.12 mmol) was added to the gently stirred mixture, before pentafluorophenole (43 mg, 0.24 mmol) was slowly added and the reaction mixture stirred at 0°C for 1h and then at room temperature over night. The mixture was filtered, triethylamine (43 µL, 0.36 mmol) and thereafter [(η$^6$-benzyl-ammonium)(PPh$_3$)RuCl$_2$]Cl **4i** (50 mg, 0.08 mmol) added. The reaction mixture was stirred vigorously for 1 h and extracted with water and brine (each 3 x 10 mL), dried over MgSO$_4$ and volatiles removed under reduced pressure. The crude product was washed with diethylether and hexane, yielding a bright red solid (27 mg, 0.03 mmol, 43%). - **$^1$H NMR** (400 MHz, 25 °C, CDCl$_3$): $\delta$ = 8.76 (m, N*H*), 8.26 (d, $^3J_{HH}$ = 8.3, C$_{arom\ SO2F}$*H*), 8.04 (d, $^3J_{HH}$ = 8.3, C$_{arom\ SO2F}$*H*), 7.71-7.26 (m, 6H, C$_{arom\ PPh3}$*H*), 7.43-7.37 (m, 9H, C$_{arom\ PPh3}$*H*), 5.61 (d, 2H, $^3J_{HH}$ = 5.0, C$_{arom\ ortho\ Rh}$*H*), 5.26 (m, 2H, C$_{arom\ meta\ Rh}$*H*), 4.75

(d, 2H, $^3J_{HH}$ = 2.5, C$H_2$). - $^{13}$**C NMR** (CDCl$_3$, 25 °C, 125 MHz): $\delta$ = 165.4 (s, $C$ON), 139.9 (s, $C_{arom\ SO2F}$), 135.6 (d, $^2J_{FC}$ = 25.4 Hz, $C$SO$_2$F), 134.2 (d, $J_{PC}$ = 10.0 Hz, $C_{arom\ PPh3}$), 132.9 (d, $J_{PC}$ = 47.7 Hz, $C_{arom\ PPh3}$), 130.9 (d, $J_{PC}$ = 1.5 Hz, $C_{arom\ PPh3}$), 129.1 (s, $C_{arom\ SO2F}$H), 128.9 (s, $C_{arom\ SO2F}$H), 128.4 (d, $J_{PC}$ = 10.0 Hz, $C_{arom\ PPh3}$), 105.9 (d, $^2J_{PRu}$ = 7.7, $C_{arom\ C6H5}$), 88.8 (d, $^2J_{PRu}$ = 5.4, $C_{arom\ C6H5}$), 87.9 (m, $C_{arom\ C6H5}$), 82.4 (m, $C_{arom\ C6H5}$), 41.9 (s, C$H_2$NH). - $^{31}$**P NMR** (CDCl$_3$, 25 °C, 161.8 MHz): $\delta$ = 28.03. - $^{19}$**F NMR** (CDCl$_3$, 25 °C, 376.2 MHz): $\delta$ = 66.28. – **IR** (KBr): $\tilde{v}$ = 3059 m, 2920 m, 2851 m, 1666 s sh, 1528 m, 1482 m, 1435 s, 1412 s, 1213 vs, 1094 s, 697 s cm$^{-1}$. - **EA** C$_{32}$H$_{27}$FNO$_3$PRhS (727.57): calcd. C 51.36, H 3.59, N 2.00; found C 51.98, H 3.88, N 2.03. - **ESI-MS** m/z (%) = 691.9 [M-Cl]$^+$ (100).


*[Rh]-P(OPh)$_2$* (**93**):



Dichloromethane (20 mL) was added to polystyrene bound cyclohexyl carbodiimide (182 mg, 1.3 mmol/g, 0.24 mmol) at 0°C and the resin allowed to swell for several minutes. Suc-Leu-P(OPh)$_2$ **87** (51.7 mg, 118 µmol) was added to the gently stirred mixture, before pentafluorophenole (43 mg, 0.24 mmol) was slowly added and the reaction mixture stirred at 0°C for 1h and then at room temperature over night. The mixture was filtered, triethylamine (43 µL, 0.36 mmol) and thereafter [Me$_4$Cp(CH$_2$)$_2$NH$_3$)RhCl$_2$PPh$_3$]Cl **52** (50 mg, 0.08 mmol) added. The reaction mixture was stirred vigorously for 1 h and extracted with water and brine (each 3 x 10 mL), dried over MgSO$_4$ and volatiles removed under reduced pressure. The crude product was redissolved in dichloromethane (5 mL) precipitated with diethylether and washed with diethylether and hexane, yielding a bright red solid (82 mg, 0.08 mmol, 68%). - $^1$**H NMR** (400 MHz, 25 °C, CDCl$_3$): $\delta$ = 8.23 (d, $^3J_{HH}$ = 10 Hz, 1H, CH$_2$N$H$) 8.07 - 7.04 (m, 28H, $H_{arom}$), 7.00 (t, $^3J_{HH}$ = 5.6 Hz, 1H, N$H$CH), 6.84 (d, $^3J_{HH}$ = 8.0 Hz, 2H, $H_{arom}$), 5.90 (dd, $^2J_{PH}$ = 22 Hz, $^3J_{HH}$ = 9.7 Hz, 1H, C$H$), 3.30-3.48 (m, 2H, C$H_2$NH), 2.48–2.26 (m, 4H, COC$H_2$C$H_2$), 2.26-2.16 (m, 2H, C$H_{2\ Cp}$), 1.46 (dd, $^3J_{RhH}$ = 5.6 Hz, $^4J_{PH}$ = 2.4 Hz, 6H, C$H_3$) 1.07 (dd, $^3J_{RhH}$ = 4.2 Hz, $^4J_{HP}$ = 4.2 Hz, 6H, C$H_3$'). - $^{13}$**C NMR** (101 MHz, 25 °C, CDCl$_3$): $\delta$ = 172.6 ($C$O), 172.0 (d, $^4J_{RhC}$ = 7.7 Hz, $C$O), 150.6 (d, $^3J_{PC}$ = 9.9 Hz,

$C_{arom\ gem\ Ph}$), 150.2 (d, $^4J_{PC}$ = 9.2 Hz, $C_{arom\ gem\ OPh}$), 134.8 (d, $^3J_{PC}$ = 9.9 Hz, $C_{arom\ gem\ PPh3}$), 134.2 ($C_{arom}$), 130.6 (br, $C_{arom}$), 129.7 (d, $J_{PC}$ = 11 Hz, $C_{arom}$), 128.8 ($C_{arom}$), 128.5 (d, $J_{PC}$ = 6.1 Hz, $C_{arom}$), 128.1 (br, $C_{arom}$), 125.3 (d, $J_{PC}$ = 4.6 Hz, $C_{arom}$), 120.6 (d, $J_{PC}$ = 3.9 Hz, $C_{arom}$), 120.5 (d, $J_{PC}$ = 4.2 Hz, $C_{arom}$), 102.5 (dd, $^1J_{RhC}$ = 6.9 Hz, $^3J_{PC}$ = 6.9 Hz, $C_{Cp}$) , 100.5 (dd, $^1J_{RhC}$ = 6.9 Hz, $^3J_{PC}$ = 6.9 Hz, $C_{Cp}$), 96.8 (d, $^1J_{RhC}$ = 6.9 Hz, $C_{Cp}$), 96.6 (d, $^1J_{RhC}$ = 6.1 Hz, $C_{Cp}$), 50.8 (d, $^1J_{PC}$ = 156 Hz, $CH$), 36.3 (d, $^4J_{PC}$ = 4.6 Hz, $CH_{2\ Cp}$), 31.8 ($COCH_2$), 31.5 ($COCH_2$), 24.7 ($NHCH_2$), 9.5 ($CH_3$), 8.6 ($CH_3$). - **$^{31}$P NMR** (162 MHz, 25 °C, CDCl$_3$): $\delta$ = 29.9 (d, $^1J_{RhP}$ = 143 Hz, $PPh_3$), 14.8 (s, O$P$(OPh)$_2$C). - **IR** (KBr): $\tilde{v}$ = 3295 w, 3057 m, 2920 m, 2360 w, 2225 w, 1670 s, 1589 m, 1522 m, 1489 vs, 1435 vs, 1384 s, 1266 m, 1186 vs, 1161 s, 1095 m, 1025 m, 041 vs cm$^{-1}$. - **EA** C$_{52}$H$_{53}$F Cl$_2$ N$_2$ O$_5$P$_2$Rh (1021.8): calcd. C 61.13, H 5.23, N 2.74; found C 60.18, H 5.51, N 3.00. - **ESI-MS** m/z = 687.1 [M-PPh$_3$-2Cl$^-$-H$^+$]$^+$, 723.1 [M-PPh$_3$-Cl$^-$]$^+$, 949.1 [2M-2Cl$^-$-H$^+$]$^+$, 984.8 [2M-Cl$^-$]$^+$.
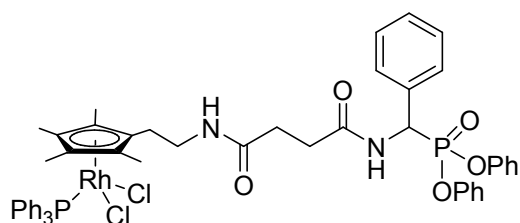
*[Rh]-OSu* (**94**):



Dichloromethane (5 mL) was added to polystyrene bound cyclohexyl carbodiimide (63 mg, 1.3 mmol/g, 0.06 mmol) at 0°C and the resin allowed to swell for several minutes. [($\eta^5$-Me$_4$Cp(CH$_2$)$_2$NHCO(CH$_2$)$_2$COOH)RhCl$_2$(PPh$_3$)] **53** (19 mg, 0.03 mmol) and the mixture stirred gently for 1 h, before N-hydroxy-succinimide (5 mg, 0.04 mmol) was added and the reaction mixture stirred at 0°C for 1h and then at room temperature over night. The mixture was filtered, washed with water and brine (each 3 x 5 mL) and dried over MgSO$_4$. Thereafter, the volume of the reaction solution was reduced under reduced pressure (~ 1mL) and the diethylether added (~4 mL). The raw product was filtered off and washed with diethylether and hexane to give the title compound **94** (10.3 mg, 15 µmol, 54%) as an orange solid. - **$^1$H NMR** (400 MHz, 25 °C, CDCl$_3$): $\delta$ (ppm) = 7.95–7.19 (m, 15H, $H_{arom\ PPh3}$), 6.78-6.70 (m, 1H, CH$_2$N$H$CO), 3.42–3.50 (m, 2H, CH$_2$C$H_2$NH), 2.86 (t, $^3J_{HH}$ = 6.8 Hz, 2H, COCH$_2$C$H_2$CO $_{Succinimide}$), 2.80 (s, 4H, C$H_{2\ Succinimide}$), 2.50 (t, $^3J_{HH}$ = 6.8 Hz, 2H, COC$H_2$CH$_2$CO $_{Succinimide}$), 2.30–2.21 (m, 2H, CH$_2$C$H_2$NH), 1.51 (d, $^3J_{RhH}$ = 2.4 Hz, 6H, C$H_3$), 1.10 (d, $^3J_{RhH}$ = 3.1 Hz, 6H, C$H_3$). - **$^{13}$C NMR** (101 MHz, 25 °C, CDCl$_3$): $\delta$ = 170.3 ($C$ONH), 169.2 ($CO_{\ Succinimide}$), 168.2

($C$OON), 134.8 (d, $^3J_{PC}$ = 9.9 Hz, $C_{arom\ PPh3}$), 130.6 ($C_{arom\ PPh3}$), 128.1 ($C_{arom\ PPh3}$), 102.6 (d, $^1J_{RhC}$ = 5.3 Hz, $Cp_{arom}$), 100.5 (m, $Cp_{arom}$), 96.7 (d, $^1J_{RhC}$ = 6.1 Hz, $Cp_{arom}$), 36.4 (d, $^5J_{PC}$ = 3.9 Hz, $CH_2CH_2NH$), 30.5 ($CH_2CH_2COON$), 26.8 ($CH_2CH_2COON$), 25.6 ($CH_{2\ Succinimide}$), 24.8 ($CH_2CH_2NH$), 9.5 (Me), 8.6 (Me). - $^{31}$**P NMR** (162 MHz, 25 °C, CDCl$_3$): $\delta$ = 30.0 (d, $^1J_{RhP}$ = 143 Hz). - **IR** (KBr): $\tilde{v}$ = 2923 w, 1813 w, 1738 s, 1665 br w, 1435 m, 1384 s cm$^{-1}$. - **ESI-MS** m/z = 760.9 [M-Cl]$^+$, 498.9 [M-Cl$^-$-PPh$_3$]$^+$.

## 2.8.3. Synthesis of a ferrocene-labeled fluoro sulfonic acid metalla label

*1-(Methylcarbamoylbenzyl-4-sulfonylfluorid)ferrocene* (**95**):
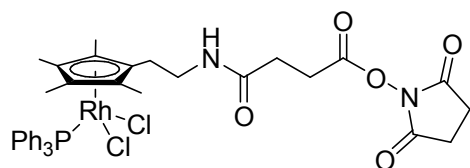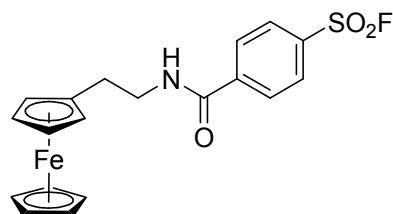


Dichloromethane (20 mL) was added to polystyrene bound cyclohexyl carbodiimide (168 mg, 1.9 mmol/g, 0.24 mmol) at 0°C and the resin allowed to swell for several minutes. 4-(fluorosulfonyl)-benzoic acid (67 mg, 0.32 mmol) was added to the gently stirred mixture, before pentafluorophenole (121 mg, 0.66 mmol) was slowly added and the reaction mixture stirred at 0°C for 1h and then at room temperature over night. The mixture was filtered, triethylamine (110 mg, 1.09 mmol) and thereafter ferrocenylethylamine (50 mg, 0.22 mmol) added. The reaction mixture was stirred vigorously for 1 h and washed with water and brine (each 3 x 10 mL), dried over $MgSO_4$ and volatiles removed under reduced pressure. The crude product was purified via column chromatography (silica gel 60, hexane / dichloromethane = 5 / 1 → 1 / 5) to give the title compound as a yellow solid (24 mg, 0.06 mmol, 18 %). - **$^1$H NMR** (400 MHz, 25 °C, $CDCl_3$): $\delta$ = 8.06 (d, 2H, $^3J_{H-H}$ = 7.7Hz, Ar), 7.97 (d, 2H, $^3J_{H-H}$ = 7.7Hz, Ar), 6.36 (s, 1H, N*H*), 4.35 (s, 2H, C*H$_2$*), 4.27 (s, 4H, Cp) 4.20 (s, 5H, Cp). - **$^{13}$C NMR** (100 MHz, 25 °C, $CDCl_3$): $\delta$ = 164.6, 141.2, 135.5, 128.2, 84.0, 68.9, 68.7, 40.0. – **$^{19}$F NMR** ($CDCl_3$, 25 °C, 376.2 MHz): $\delta$ = 66.08. - **ESI-MS** m/z = 401.2 [M+H]$^+$.

## 2.9. Stability tests of $\eta^6$-arene Ru(II) complexes

**Catalyst stability tests under catalysis conditions.** Catalysts (0.016 mmol) were added to a biphasic solution of water (0.5 mL) and styrene (0.4 mmol, 42 mg) in Cyclohexane/Dichloromethane (1/1 total volume of 0.5 mL). Bis(ethyleneglycole)-dibutylether (0.4 mmol, 87 mg) was added as GC-standard. The mixture was heated to 70-80 °C and pressurized ($H_2$, 50 bar) for 35 min. The organic and inorganic phase were analyzed by ESI MS to detect organometallic species present in catalytic runs.

**Table C5:** Masses and species observed for selected catalysts after catalytic runs in ESI MS spectra.

| entry | catalyst | masses obs. [m/z] | species obs. [m/z] | abundance [%] |
|-------|----------|-------------------|--------------------|---------------|
| 1 | **3b** | 952.9[b] | [3M-HCl-3Cl+2OH+$\eta^6$-ligand]$^+$ | 35 |
| | | 764.9[b] | [2M-HCl-2Cl+OH+$\eta^6$-ligand+styrene]$^+$ | 20 |
| | | 730.0[b] | [2M-2HCl-2Cl+OH+$\eta^6$-ligand+styrene]$^+$ | 15 |
| 2 | **3f** | 1061.9[b] | [4Ru+7OH+3styrene+2$\eta^6$-ligand]$^+$ | 50 |
| | | 1000.9[b] | [4Ru+7OH+3styrene+$\eta^6$-ligand]$^+$ | 50 |
| | | 942.9[b] | [4Ru+7OH+4styrene]$^+$ | 40 |
| 3 | **3l** | 625.1[a] | [2M-2PPh$_3$-2HCl-Cl+$H_2O$]$^+$ | 100 |
| | | 879.0[b] | [2M-PPh$_3$-4HCl-Cl+2OH+2Na+$H_2$] | 100 |
| | | 913.8[b] | [2M-PPh$_3$-2HCl-3Cl+4OH+2Na] | 85 |
| 4 | **3n** | 576.9[a] | [M-Cl]$^+$ | 10 |
| | | 1189.5[a] | [2M-Cl]$^+$ | 10 |
| | | 541.1[a] | [M-Cl-HCl]$^+$ | 5 |
| | | 1121.8[b] | [3M-3PPh$_3$-5Cl-3CH$_2$CH$_3$+Na+3styrene]$^+$ | 100 |
| | | 890.9[b] | [3M-3PPh$_3$-4Cl-3CH$_2$CH$_3$+2$H_2O$]$^+$ | 40 |
| | | 857.9[b] | [3M-3PPh$_3$-6Cl-3CH$_2$CH$_3$+2OH+styrene]$^+$ | 40 |
| | | 609.0[b] | [2M-2PPh$_3$-Cl-2CH$_2$CH$_3$+2H]$^+$ | 20 |
| 5 | **3q** | 1021.8[a] | [2M-Cl+$H_2O$]$^+$ | 20 |
| | | 975.8[b] | [3M-3PPh$_3$-2Cl+OH+styrene]$^+$ | 15 |

Catalyst/Styrene = 1/25. Catalysts were employed in a concentration of 16 mM. (a) ESI MS spectrum of organic phase (b) ESI MS spectrum of aqueous phase. Main metal containing peaks are displayed. Organic peaks observed (e.g. PPh$_3$O are omitted for clarity).

## 2.10. Hydrogenation and transfer hydrogenation experiments

## 2.10.1. Biphasic hydrogenations with homogenous catalysts

**Hydrogenation of styrene in unbuffered solution.** The catalyst (**3a**-**3t**, 0.016 mmol) was added to a biphasic solution of distilled water (20 mL) and styrene (16 mmol, 1.666 g) in Cyclohexane/Dichloromethane (1/1 total volume of 20 mL) was added. Bis(ethyleneglycole)-dibutylether (0.016 mol, 3.493 g) was added as GC-standard. The mixture was heated (80°C) and pressurized (50 bar $H_2$). According to reaction conditions, small amounts of the biphasic system were taken periodically. The organic layer was analyzed by GC to determine the amount of styrene and ethyl benzene.

***Table C6:*** Catalytic runs employing different mononuclear ruthenium complexes.

| entry | catalyst | FG | $(CH_2)_n$ | $TOF_{max}$ [h$^{-1}$] | $t_{ini}$ [min] | $t_{max}$ [min] | yield [%] |
|---|---|---|---|---|---|---|---|
| 1 | **3a** | -OH | 2 | 1280 | 30 | 73 | 100 |
| 2 | **3b** | -OH | 3 | 1940 | 0 | 41 | 96 |
| 3 | **3c** | -OH | 4 | 800 | 55 | 80[a] | 76 |
| 4 | **3d** | -OH | 5 | 1330 | 114 | 120[a] | 92 |
| 5 | **3e** | -NHAc | 1 | 2730 | 0 | 52 | 100 |
| 6 | **3f** | -NHAc | 2 | 4290 | 0 | 32 | 100 |
| 7 | **3g** | -NHAc | 3 | 1580 | 43 | 73 | 99 |
| 8 | **3h** | -NHAc | 4 | 1710 | 27 | 56 | 100 |
| 9 | **3i** | -NH$_3^+$Cl$^-$ | 1 | 3330 | 0 | 89 | 99 |
| 10 | **3j** | -NH$_3^+$Cl$^-$ | 2 | 950 | 56 | 101[a] | 68 |
| 11 | **3k** | -NH$_3^+$Cl$^-$ | 3 | 1540 | 0 | 101[a] | 35 |
| 12 | **3l** | -NH$_3^+$Cl$^-$ | 4 | 2220 | 0 | 80 | 100 |
| 13 | **3m** | -COOEt | 1 | 2070 | 34 | 64 | 100 |
| 14 | **3n** | -COOEt | 2 | 1370 | 0 | 120[a] | 91 |
| 15 | **3o** | -COOEt | 3 | 2500 | 0 | 40 | 100 |
| 16 | **3p** | -COOEt | 4 | 920 | 46 | 79 | 100 |
| 17 | **3q** | -COOH | 1 | 4290 | 0 | 120 | 96 |
| 18 | **3r** | -COOH | 2 | 2000 | 0 | 100[a] | 97 |
| 19 | **3s** | -COOH | 3 | 700 | 55 | 100[a] | 92 |
| 20 | **3t** | -COOH | 4 | 1360 | 0 | 59 | 100 |

Temperature was in all cases 80°C. Pressure ($H_2$) was 50 bar. Product formation and educt consumption were monitored via GC-FID. (a) in these cases $t_{max}$ marks the last data point measured. The reaction was not necessarily complete.

**Hydrogenation of styrene at different temperatures.** The catalyst (**3f**, 0.016 mmol) was added to a biphasic solution of distilled water (20 mL) and styrene (0.016 mol, 1.666 g) in Cyclohexane/Dichloromethane (1/1 total volume of 20 mL) was added. Bis(ethyleneglycole)-dibutylether (0.016 mol, 3.493 g) was added as GC-standard. The mixture was heated (80 - 60 °C) and pressurized (50 bar $H_2$). According to reaction conditions, small amounts von of the biphasic system were taken periodically. The organic layer was analyzed by GC to determine the amount of styrene and ethyl benzene.

***Table C7:*** Catalytic runs at different temperatures.

| entry | catalyst | T [°C] | $TOF_{max}$ [h$^{-1}$] | $t_{ini}$ [min] | $t_{max}$ [min] | yield [%] |
|-------|----------|--------|-----------------------|-----------------|-----------------|-----------|
| 1 | **3f** | 80 | 4290 | 0 | 23 | 100 |
| 2 | **3f** | 60 | 470 | 69 | 181 | 100 |
| 3 | **3f** | 50 | 370 | 0 | 314 | 100 |

Pressure was 50 bar in all cases. Product formation and educt consumption were monitored via GC-FID.

**Hydrogenation of styrene at different pressures.** The catalyst (**3f**, 0.016 mmol) was added to a biphasic solution of distilled water (20 mL) and styrene (0.016 mol, 1.666 g) in Cyclohexane/Dichloromethane (1/1 total volume of 20 mL) was added. Bis(ethyleneglycole)-dibutylether (0.016 mol, 3.493 g) was added as GC-standard. The mixture was heated (80 °C) and pressurized (50 – 10 bar $H_2$). According to reaction conditions, small amounts von of the biphasic system were taken periodically. The organic layer was analyzed by GC to determine the amount of styrene and ethyl benzene.

***Table C8:*** Catalytic runs at different pressures.

| entry | catalyst | p ($H_2$) [bar] | $TOF_{max}$ [h$^{-1}$] | $t_{ini}$ [min] | $t_{max}$ [min] | yield [%] |
|-------|----------|-----------------|-----------------------|-----------------|-----------------|-----------|
| 1 | **3f** | 50 | 4290 | 0 | 23 | 100 |
| 2 | **3f** | 30 | 1760 | 70 | 73 | 100 |
| 3 | **3f** | 10 | 640 | 0 | 170 | 100 |

Temperature was in all cases was 80°C. Product formation and educt consumption were monitored via GC-FID.

**Hydrogenation of styrene in buffered solutions:** The catalyst (**3b** and **3l**, 0.016 mmol) was added to a biphasic buffered aqueous solution or (20 mL, 0.1 M phosphate) and styrene (0.016 mol, 1.666 g) in Cyclohexane/Dichloromethane (1/1 total volume of 20 mL) was added. Bis(ethyleneglycole)-dibutylether (0.016 mol, 3.493 g) was added as GC-standard. The mixture was heated and pressurized (H$_2$). According to reaction conditions, small amounts von of the biphasic system were taken periodically. The organic layer was analyzed by GC to determine the amount of styrene and ethyl benzene.

**Table C9:** Catalytic runs employing buffered aqueous solutions.

| entry | catalyst | pH | TOF$_{max}$ [h$^{-1}$] | t$_{ini}$ [min] | t$_{max}$ [min] | yield [%] |
|:---:|:---:|:---:|:---:|:---:|:---:|:---:|
| 1 | **3b** | 2.5 | n.o. | n.o. | 120[a] | 10 |
| 2 | **3b** | 6.5 | 440 | 62 | 120[a] | 66 |
| 3 | **3b** | 10.5 | 5450 | 19 | 31 | 100 |
| 4 | **3l** | 2.5 | n.o. | n.o. | 120[a] | 42 |
| 5 | **3l** | 6.5 | 1880 | 26 | 45 | 96 |
| 6 | **3l** | 10.5 | 1360 | 20 | 51 | 98 |

Temperature was in all cases was 80°C. Product formation and educt consumption were monitored via GC-FID. (a) in these cases t$_{max}$ marks the last data point measured. The reaction was not necessarily complete.

**Hydrogenation of different olefins:** The catalyst (**3b**, 0.016 mmol) was added to a biphasic buffered aqueous solution or (20 mL, 0.1 M phosphate) and 1-octene or cyclooctene (0.016 mol, 1.666 g) in Cyclohexane/Dichloromethane (1/1 total volume of 20 mL) were added. Bis(ethyleneglycole)-dibutylether (0.016 mol, 3.493 g) was added as GC-standard. The mixture was heated and pressurized (H$_2$). According to reaction conditions, small amounts von of the biphasic system were taken periodically. The organic layer was analyzed by GC to determine the amount of styrene and ethyl benzene.

**Table C10:** Catalytic runs employing different substrates

| entry | catalyst | substrate | TOF$_{max}$ | t$_{ini}$ [min] | t$_{max}$ [min] | yield [%] |
|:---:|:---:|:---:|:---:|:---:|:---:|:---:|
| 1 | **3b** | 1-octene | 3160 | 36 | 50 | 100 |
| 2 | **3b** | cyclooctene | 6670 | 35 | 49 | 98 |

Temperature was in all cases was 80°C. Pressure (H$_2$) was 50 bar. Product formation and educt consumption were monitored via GC-FID.

## 2.10.2. Transfer hydrogenations with homogenous catalysts

**General procedure for the transfer hydrogenation of Acetophenone employing complexes 12, 14, 15:** Organometallic complex (10 μmol) was added to dry $^i$PrOH (5 mL). Thereafter, bis(ethyleneglycole)-dibutylether (10 mmol, 1.24 mL) and acetophenone (10 mmol, 1.17 mL) were added and the reaction started upon addition of KOH (100 μmol) in $^i$PrOH (1 mL). Yields and ees were analyzed via chiral GC (Varian capillary column, fused silica 25 m x 0.25 mm, coated cp chirasil-dex CB df = 0.25).

***Table C11:*** Hydrogenation results for the catalytic hydrogenation of acetophenone.[a]

| entry | complex | time [d] | yield [%] | ee [%] |
|-------|---------|----------|-----------|--------|
| 1 | **3** | 12.5 | <2 | 20 (*S*) |
| 2 | **12** | 12.5 | <2 | 17 (*S*) |
| 3 | **14** | 12.5 | <2 | 52 (*S*) |
| 4 | **15** | 12.5 | 27 | 1 (*R*) |

(a) Conditions: The reaction was carried out at room temperature using a 1.4 M. solution of acetophenone (10 mM) in 2-propanole. Reaction time = 12.5 d. Yield was determined by gas chromatography. Complex **3**: substrate:KOH:catalyst = 1000/100/1; Complexes **12**,**14**,**15**: substrate/KOH/catalyst = 1000/100/2; Ees were determined by chiral gas chromatography.[25]

## 2.10.3. Hydrogenations with organometallic enzyme hybrids

**General procedure for asymmetric hydrogenation of ketones catalyzed by organometallic enzyme hybrids:** A small glass vial, equipped with a stirring bar is charged with 200 µL papain suspension and 260 µL buffered solution (120 mM $PO_4^{2-}$) containing DTT (0 to 7.7 mM). After incubating for 1 h, 50 µL DMSO and 5 µL of the metalla label (20 mM in DMSO) are added and the solution is stirred gently for 3 h. Subsequently 5 µL HO-Eps-Leu-NH-Bzl **67** (20 mM in DMSO) is added and the reaction solution stirred for another 3 h, before 5 µL of ketone (1 M in DMSO) are added. The vial is placed in a standard multivial autoclave and pressurized with $H_2$ (10 to 75 bar) at the desired temperature (20 to 40 °C). After the desired amount of time, pressure is released and the reaction solution is extracted with dichloromethane (600 µL, 2.5 h). Yields were determined either with $^{19}F$ NMR spectroscopy or gas chromatography. Enantiomeric excesses were determined by chiral GC (Varian capillary column, fused silica 25 m x 0.25 mm, coated cp chirasil-dex CB df = 0.25).



| A | B | C | D | E |
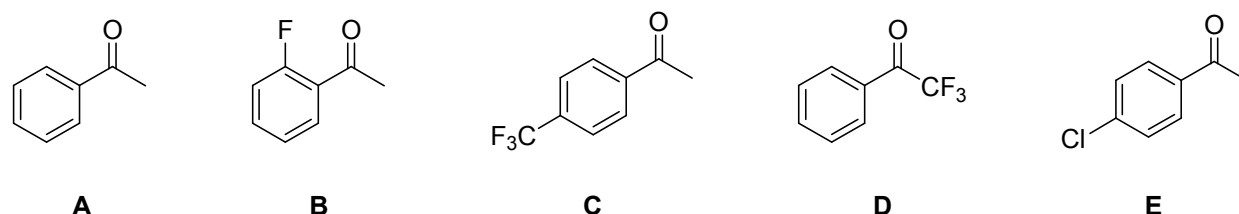
*Figure C1.* Substrates employed in the catalytic hydrogenation of ketones with OMEHs.

*Table C12:* Variations in temperature.

| entry | organometallic enzyme hybrid | T [°C] | DTT [mM] | substrate | t [h] | yield [%] | ee [%] |
|-------|------------------------------|--------|----------|-----------|-------|-----------|--------|
| 1 | [Rh]-Epx@papain **101** | 20 | 3.8 | **D** | 65 | 10 | 24 (*R*) |
| 2 | [Rh]-Epx@papain **101** | 30 | 3.8 | **D** | 65 | 16 | 24 (*R*) |
| 3 | [Rh]-Epx@papain **101** | 40 | 3.8 | **D** | 65 | 53 | 24 (*R*) |
| 4 | [Rh]-Deox@papain **102** | 20 | 3.8 | **D** | 65 | 2 | 5 (*R*) |
| 5 | [Rh]-Deox@papain **102** | 40 | 3.8 | **D** | 65 | 14 | 9 (*R*) |
| 6 | [Rh]-Epx@bromelain **103** | 20 | 3.8 | **D** | 65 | 3 | 4 (*R*) |
| 7 | [Rh]-Epx@bromelain **103** | 40 | 0.95 | **D** | 96 | 11 | 12 (*S*) |
| 8 | [Rh]-Epx **70** | 20 | 3.8 | **D** | 65 | < 1 | 1 (*S*) |
| 9 | [Rh]-Deox **72**- | 20 | 3.8 | **D** | 65 | < 1 | < 1 (*R*) |
| 10 | [Rh]-Epx **70** | 40 | 0 | **D** | 65 | 4 | 3 (*R*) |
| 11 | [Rh]-Deox **72**- | 40 | 0 | **D** | 65 | 4 | 3 (*R*) |

In all cases, DMSO concentration was 12.4 %, the pH value was 6.5 and p($H_2$) was 25 bar.

**Table C13:** 2.4. Variations in pressure.

| entry | organometallic enzyme hybrid | p (H$_2$) [bar] | DTT [mM] | substrate | t [h] | yield [%] | ee [%] |
|---|---|---|---|---|---|---|---|
| 1 | [Rh]-Epx@papain **101** | 10 | 0.95 | **D** | 65 | 10 | 11 (*R*) |
| 2 | [Rh]-Epx@papain **101** | 25 | 0.95 | **D** | 65 | 81 | 23 (*R*) |
| 3 | [Rh]-Epx@papain **101** | 75 | 0.95 | **D** | 65 | 89 | 20 (*R*) |
| 4 | [Rh]-Deox@papain **102** | 10 | 0.95 | **D** | 65 | 6 | 4 (*R*) |
| 5 | [Rh]-Deox@papain **102** | 25 | 0.95 | **D** | 65 | 26 | 6 (*R*) |
| 6 | [Rh]-Deox@papain **102** | 75 | 0.95 | **D** | 65 | 21 | 3 (*R*) |

In all cases, DMSO concentration was 12.4 %, the pH value was 6.5 and T was 40 °C.

**Table C14:** Variations in DTT concentration.

| entry | organometallic enzyme hybrid | p (H$_2$) [bar] | DTT [mM] | substrate | t [h] | yield [%] | ee [%] |
|---|---|---|---|---|---|---|---|
| 1 | [Rh]-Epx@papain **101** | 25 | 3.8 | **D** | 65 | 53 | 24 (*R*) |
| 2 | [Rh]-Epx@papain **101** | 25 | 2.9 | **D** | 65 | 57 | 22 (*R*) |
| 3 | [Rh]-Epx@papain **101** | 25 | 1.9 | **D** | 65 | 58 | 22 (*R*) |
| 4 | [Rh]-Epx@papain **101** | 25 | 0.95 | **D** | 65 | 81 | 23 (*R*) |
| 5 | [Rh]-Epx@papain **101** | 25 | 0.48 | **D** | 65 | 19 | 10 (*R*) |
| 6 | [Rh]-Epx@papain **101** | 25 | 0.19 | **D** | 65 | 36 | 2 (*R*) |
| 7 | [Rh]-Epx@papain **101** | 25 | 0.01 | **D** | 65 | 21 | 2 (*S*) |
| 8 | [Rh]-Epx@papain **101** | 25 | 0 | **D** | 65 | 49 | 7 (*S*) |
| 9 | [Rh]-Deox@papain **102** | 25 | 3.8 | **D** | 65 | 14 | 9 (*R*) |
| 10 | [Rh]-Deox@papain **102** | 25 | 2.9 | **D** | 65 | 20 | 5 (*R*) |
| 11 | [Rh]-Deox@papain **102** | 25 | 1.9 | **D** | 65 | 15 | 4 (*S*) |
| 12 | [Rh]-Deox@papain **102** | 25 | 0.95 | **D** | 65 | 27 | 2 (*S*) |
| 13 | [Rh]-Deox@papain **102** | 25 | 0 | **D** | 65 | 30 | 4 (*S*) |

In all cases, DMSO concentration was 12.4 %, the pH value was 6.5 and T was 40 °C.

**Table C15:** Variations in DMSO concentration.

| entry | organometallic enzyme hybrid | p (H$_2$) [bar] | DMSO [%] | substrate | t [h] | yield [%] | ee [%] |
|---|---|---|---|---|---|---|---|
| 1 | [Rh]-Epx@papain **101** | 25 | 12.4 | **D** | 65 | 16 | 23 (*R*) |
| 2 | [Rh]-Epx@papain **101** | 25 | 8.0 | **D** | 65 | 4 | 21 (*R*) |
| 3 | [Rh]-Epx@papain **101** | 25 | 5.2 | **D** | 65 | 3 | 15 (*R*) |
| 4 | [Rh]-Epx@papain **101** | 25 | 3.2 | **D** | 65 | < 1% | 14 (*R*) |

In all cases, DTT concentration was 19.0 mM, the pH value was 6.5 and T was 30 °C.

**Table C16:** Variations in affinity label concentration.

| entry | organometallic enzyme hybrid | [Rh]-Epx **70** [mM] | substrate | t [h] | yield [%] | ee [%] |
|-------|------------------------------|----------------------|-----------|-------|-----------|--------|
| 1 | [Rh]-Epx@papain **101** | 0.37 | **D** | 65 | 21 | 6 (*R*) |
| 2 | [Rh]-Epx@papain **101** | 0.28 | **D** | 65 | 3 | 18 (*R*) |
| 3 | [Rh]-Epx@papain **101** | 0.19 | **D** | 65 | 81 | 23 (*R*) |
| 4 | [Rh]-Epx@papain **101** | 0.10 | **D** | 65 | 60 | 22 (*R*) |
| 5 | [Rh]-Epx@papain **101** | 0.04 | **D** | 65 | 34 | 21 (*R*) |

In all cases, DMSO concentration was 12.4 %, DTT concentration was 0.95 mM, the pH value was 6.5 and T was 40 °C.

**Table C17:** Variations of the pH value.

| entry | organometallic enzyme hybrid | pH | DTT [mM] | substrate | t [h] | yield [%] | ee [%] |
|-------|------------------------------|-----|----------|-----------|-------|-----------|--------|
| 1 | [Rh]-Epx@papain **101** | 6.0 | 0.95 | **D** | 65 | 33 | 20 (*R*) |
| 2 | [Rh]-Epx@papain **101** | 6.5 | 0.95 | **D** | 65 | 81 | 23 (*R*) |
| 3 | [Rh]-Epx@papain **101** | 7.0 | 0.95 | **D** | 65 | 39 | 19 (*R*) |
| 4 | [Rh]-Epx@papain **101** | 7.5 | 0.95 | **D** | 65 | 42 | 15 (*R*) |
| 5 | [Rh]-Deox@papain **102** | 6.0 | 0.95 | **D** | 65 | 7 | < 1 (*R*) |
| 6 | [Rh]-Deox@papain **102** | 6.5 | 0.95 | **D** | 65 | 26 | 7 (*R*) |
| 7 | [Rh]-Deox@papain **102** | 7.0 | 0.95 | **D** | 65 | 37 | 7 (*R*) |
| 8 | [Rh]-Deox@papain **102** | 7.5 | 0.95 | **D** | 65 | 33 | 6 (*R*) |

In all cases, DMSO concentration was 12.4 %, $p(H_2)$ was 25 bar and T was 40 °C.

**Table C18:** Different substrates.

| entry | organometallic enzyme hybrid | $p(H_2)$ [bar] | DTT [mM] | substrate | t [h] | yield [%] | ee [%] |
|-------|------------------------------|----------------|----------|-----------|-------|-----------|--------|
| 1 | [Rh]-Epx@papain **101** | 75 | 0.95 | **A** | 96 | 2 | 37 (*R*) |
| 2 | [Rh]-Epx@papain **101** | 75 | 0.95 | **B** | 96 | 8 | 29 (*R*) |
| 3 | [Rh]-Epx@papain **101** | 75 | 0.95 | **C** | 96 | 16 | 45 (*R*) |
| 4 | [Rh]-Epx@papain **101** | 75 | 0.95 | **D** | 96 | 92 | 20 (*R*) |
| 5 | [Rh]-Epx@papain **101** | 75 | 0.95 | **E** | 96 | 12 | 64 (*R*) |

In all cases, DMSO concentration was 12.4 %, the pH value was 6.5 and T was 40 °C.

**Table C19:** Longer [M]-AL inhibition time.[a]

| entry | organometallic enzyme hybrid | $p(H_2)$ [bar] | DTT [mM] | substrate | t [h] | yield [%] | ee [%] |
|-------|------------------------------|----------------|----------|-----------|-------|-----------|--------|
| 1 | [Rh]-Epx@papain **101** | 25 | 0.95 | **D** | 65 | 100 | 26 (*R*) |
| 2 | [Rh]-Deox@papain **102** | 25 | 0.95 | **D** | 65 | 63 | 8 (*R*) |

In all cases, DMSO concentration was 12.4 %, the pH value was 6.5 and T was 40 °C. (a) [M]-AL inhibition time = 96 h; RT.

***Table C20:*** Various experiments.

| entry | organometallic enzyme hybrid | p (H$_2$) [bar] | DTT [mM] | substrate | t [h] | yield [%] | ee [%] |
|-------|------------------------------|-----------------|----------|-----------|-------|-----------|--------|
| 1 | [Rh]-Epx@bromelain **103** | 75 | 3.8 | **D** | 96 | 36 | < 1 (*S*) |
| 2 | [Rh]-Epx@bromelain **103** | 25 | 0.95 | **D** | 65 | 11 | 12 (*S*) |
| 3 | [Ru]-Epx@bromelain **105** | 75 | 0.95 | **D** | 96 | 40 | 10 (*S*) |
| 4 | [Ru]-Epx@bromelain **105** | 25 | 0.95 | **D** | 65 | 12 | 18 (*S*) |
| 5 | [Ru]-Epx@bromelain **104** | 75 | 0.95 | **D** | 96 | 44 | 20 (*S*) |
| 6 | [Ru]-Epx@bromelain **104** | 25 | 0.95 | **D** | 65 | 18 | 25 (*S*) |
| 7 | [Cp*RhPPh$_3$Cl$_2$] **54**+papain | 75 | 0.95 | **D** | 96 | 31 | 4 (*R*) |
| 8 | [Cp*RhPPh$_3$Cl$_2$] **54** | 75 | 0.95 | **D** | 96 | < 1 | < 1 (*S*) |
| 9 | [Rh]-Epx **70** | 25 | 0.95 | **D** | 65 | 7 | 2 (*S*) |
| 10 | [Rh]-Epx **70** | 25 | 0 | **D** | 65 | 4 | 3 (*R*) |
| 11 | [Ru]-Epx **71** | 25 | 0.95 | **D** | 65 | 5 | < 1 (*S*) |
| 12 | [Rh]-Deox **72** | 25 | 0 | **D** | 65 | 5 | 3 (*R*) |

In all cases, DMSO concentration was 12.4 %, the pH value was 6.5 and T was 40 °C.

## 2.10.4. Transfer hydrogenations with organometallic enzyme hybrids

**General procedure for the asymmetric hydrogenation of ketones catalyzed by organometallic enzyme hybrids:** In a small glass vial equipped with a magnetic stirbar, 250 μL protease (0.1 μMol) in aqueous buffered solution (5 mM $PO_4^{2-}$, pH 7.5), were added to 95 μL of DMSO. 5 μL of metalla label were added (20 mM in DMSO) and stirred gently for 1.5 h. Then, 5 μL of PMSF were added and stirred gently for 1.5 h, before 5 μL of ketone (1 M in DMSO) and 250 μL of aqueous formiate buffer were added and the glass vial sealed. After the desired amount of time, the reaction solution was extracted for 2.5 h with 600 μL of dichloromethane. Yields were determined by $^{19}F$ NMR or chiral GC. In every case, the organic phase was then reduced to a minimum volume and the enantiomeric excess determined by chiral GC (Varian capillary column, fused silica 25 m x 0.25 mm, coated cp chirasil-dex CB df = 0.25).
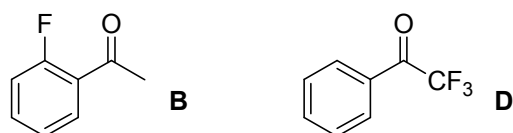


**Figure C1.** Substrates employed in the catalytic hydrogenation of ketones with OMEHs.

**Table C21:** Variations of pH-values.

| entry | organometallic enzyme hybrid | [M]-L | pH | substrate | t [h] | yield [%] | ee [%] |
|---|---|---|---|---|---|---|---|
| 1 | [Rh]-SF@α-chymotrypsin **107** | **4** | 8 | **D** | 48 | 32 | 13 (*S*) |
| 2 | [Rh]-SF@α-chymotrypsin **107** | **4** | 7 | **D** | 48 | 33 | 17 (*S*) |
| 3 | [Rh]-SF@α-chymotrypsin **107** | **4** | 6 | **D** | 48 | 30 | 15 (*S*) |
| 4 | [Rh]-SF@α-chymotrypsin **107** | **4** | 5 | **D** | 48 | 24 | 20 (*S*) |
| 5 | [Rh]-SF@α-chymotrypsin **107** | **4** | 4 | **D** | 48 | 18 | 13 (*S*) |
| 6 | [Rh]-SF@α-chymotrypsin **107** | **4** | 3 | **D** | 48 | 4 | 3 (*S*) |

Total volume of the reaction was 610 μL, substrate / catalyst ratio = 50 / 1. The content of DMSO was 17 vol%. The reaction was carried out at room temperature.

*Table C22:* Variations of formiate concentration.

| entry | organometallic enzyme hybrid | formiate [M] | pH | substrate | t [h] | yield [%] | ee [%] |
|-------|------------------------------|--------------|----|-----------|-------|-----------|--------|
| 1 | [Rh]-SF@α-chymotrypsin **107** | 1.0 | 5 | **D** | 48 | 24 | 20 (*S*) |
| 2 | [Rh]-SF@α-chymotrypsin **107** | 0.4 | 5 | **D** | 48 | 18 | 14 (*S*) |
| 3 | [Rh]-SF@α-chymotrypsin **107** | 0.1 | 5 | **D** | 48 | 10 | 11 (*S*) |
| 4 | [Rh]-SF@α-chymotrypsin **107** | 0.04 | 5 | **D** | 48 | 6 | 8 (*S*) |

Total volume of the reaction was 610 µL, substrate / catalyst ratio = 50 / 1. The content of DMSO was 17 vol%. The reaction was carried out at room temperature. Reaction time was 48 h.

*Table C23:* Comparison of different enzyme hybrid catalysts and substrates.

| entry | organometallic enzyme hybrid | pH | formiate [M] | substrate | t [h] | yield [%] | ee [%] |
|-------|------------------------------|----|--------------|-----------|-------|-----------|--------|
| 1 | [Rh]-SF@trypsin **109** | 5 | 1.0 | **D** | 48 | 29 | 5 (*S*) |
| 2 | [Rh]-PF@α-chymotrypsin **106** | 5 | 1.0 | **D** | 48 | 22 | 9 (*S*) |
| 3 | [Rh]-PF@α-chymotrypsin **106** | 5 | 1.0 | **B** | 48 | 5 | 13 (*S*) |

Total volume of the reaction was 610 µL, substrate / catalyst ratio = 50 / 1. The content of DMSO was 17 vol%. The reaction was carried out at room temperature. Reaction time was 48 h.

*Table C24:* Comparison of catalyst performances in dependence of anchoring moiety and presence of enzyme.

| entry | catalyst | substrate | enzyme | linker | yield[a] [%] | ee[a] [%] |
|-------|----------|-----------|--------|--------|-----------|--------|
| 1 | [Rh]-SF@α-chymotrypsin **107** | **D** | yes | yes | 24 | 20 (*S*) |
| 2 | [Rh]-SF **91** | **D** | no | yes | 5 | <1 (*S*) |
| 3 | [Cp*RhCl$_2$PPh$_3$]+α-chymotrypsin **110** | **D** | yes | no | 4 | <1 (*S*) |
| 4 | [Cp*RhCl$_2$PPh$_3$] **54** | **D** | no | no | 3 | <1 (*S*) |

Total volume of the reaction was 610 µL, substrate / catalyst ratio = 50 / 1. The content of DMSO was 17 %. Reaction time was 48 h. The reaction was carried out at room temperature. (a) 2,2,2-trifluoro acetophenone was used as substrate

***Table C25:*** Time-dependent measurements.

| entry | organometallic enzyme hybrid | pH | substrate | t [h] | yield [%] | ee [%] |
|---|---|---|---|---|---|---|
| 1 | [Rh]-SF@α-chymotrypsin **107** | 5 | **B** | 1 | 0.3 | n.d.[a] |
| 2 | [Rh]-SF@α-chymotrypsin **107** | 5 | **B** | 3 | 1 | n.d.[a] |
| 3 | [Rh]-SF@α-chymotrypsin **107** | 5 | **B** | 6 | 1.4 | n.d.[a] |
| 4 | [Rh]-SF@α-chymotrypsin **107** | 5 | **B** | 12 | 3.0 | n.d.[a] |
| 5 | [Rh]-SF@α-chymotrypsin **107** | 5 | **B** | 24 | 4.4 | n.d.[a] |
| 6 | [Rh]-SF@α-chymotrypsin **107** | 5 | **B** | 48 | 6.4 | 18 (S) |
| 7 | [Rh]-SF@α-chymotrypsin **107** | 5 | **B** | 72 | 9.5 | 17 (S) |
| 8 | [Rh]-SF@α-chymotrypsin **107** | 5 | **B** | 109 | 9.2 | 17 (S) |
| 9 | [Rh]-SF@α-chymotrypsin **107** | 5 | **B** | 144 | 12.3 | 16 (S) |
| 10 | [Rh]-SF@α-chymotrypsin **107** | 5 | **B** | 193 | 10.9 | 16 (S) |
| 11 | [Rh]-SF@α-chymotrypsin **107** | 5 | **B** | 253 | 11.6 | 16 (S) |
| 12 | [Rh]-SF@α-chymotrypsin **107** | 5 | **B** | 305 | 12.4 | 15 (S) |
| 13 | [Rh]-SF@α-chymotrypsin **107** | 5 | **D** | 1 | 0.8 | n.d.[a] |
| 14 | [Rh]-SF@α-chymotrypsin **107** | 5 | **D** | 3 | 2.6 | n.d.[a] |
| 15 | [Rh]-SF@α-chymotrypsin **107** | 5 | **D** | 6 | 5.5 | n.d.[a] |
| 16 | [Rh]-SF@α-chymotrypsin **107** | 5 | **D** | 12 | 11.6 | n.d.[a] |
| 17 | [Rh]-SF@α-chymotrypsin **107** | 5 | **D** | 24 | 15.5 | n.d.[a] |
| 18 | [Rh]-SF@α-chymotrypsin **107** | 5 | **D** | 48 | 24.0 | 20 (S) |
| 19 | [Rh]-SF@α-chymotrypsin **107** | 5 | **D** | 72 | 33.4 | 17 (S) |
| 20 | [Rh]-SF@α-chymotrypsin **107** | 5 | **D** | 144 | 49.5 | 17 (S) |
| 21 | [Rh]-SF@α-chymotrypsin **107** | 5 | **D** | 200 | 52.7 | 16 (S) |
| 22 | [Rh]-SF@α-chymotrypsin **107** | 5 | **D** | 259 | 59.6 | 15 (S) |
| 23 | [Rh]-SF@α-chymotrypsin **107** | 5 | **D** | 310 | 67.1 | 16 (S) |

Total volume of the reaction was 610 µL, substrate / catalyst ratio = 50 / 1. The content of DMSO was 17 vol%. The reaction was carried out at room temperature. Reaction time was 48 h. (a) enantiomeric excesses were not listed due to the detection limit of the chiral GC-FID.

# 2.11. Preparation of OMEHs for MALDI-TOF measurements

## 2.11.1. MALDI-TOF measurements of cysteine proteases

**Procedure for the inhibition of Papain by [Rh]-Epx 70 and [Rh]-Deox 72 for MALDI-TOF mass spectra measurements:** To 1.15 mL of an aqueous buffered solution (40 mM $PO_4^{3-}$, pH 7.0), 50 μL papain suspension and 50 μL aqueous buffered TCEP solution were added (12.5 mM, dissolved in phosphate buffer, 40 mM $PO_4^{3-}$, pH 7.0) and stirred gently for 1 h. Thereafter, 70.5 μL of a solution containing the complex **1^Rh** or **2^Rh** were added (0.55 mM in DMSO). The reaction solution was stirred gently for 3 h and without further purification analyzed via MALDI-TOF.

*Table C26:* Table of species observed in MALDI-TOF spectra in comparison to the native enzymes employed.

| entry | enzyme species | obs. Mass [kDa] | $\Delta_{native\ enzyme}$[Da] | species |
|---|---|---|---|---|
| 1 | papain | 23.418 | | $[M]^+$ |
| | | 11.710 | | $[M]^{2+}$ |
| 2 | [Rh]-Epx@papain **101** | 24015 | 597 | $[M-2Cl-PPh_3]^+$ |
| | | 12006 | 296 | $[M-2Cl-PPh_3]^{2+}$ |
| | | 12065 | 355 | $[M-2Cl-PPh_3+Cys]^{2+}$ |
| 3 | [Rh]-Deox+papain **102** | 23.418 | 0 | no covalent inhibition |
| | | 11.710 | 0 | no covalent inhibition |

## 2.11.2. MALDI-TOF measurements of serine proteases

**General procedure for the inhibition of trypsin by 1 and 2 for MALDI-TOF mass spectra measurements:** 5 µL organometallic linker (0.02 M in DMSO) were added to 50 µL aqueous buffered trypsin solution (5 mg / mL trypsin in phosphate buffer, 39 mM, pH 8) and stirred gently for 3 h. Thereafter, the reaction mixture was diluted with 495 µL distilled water, filtered and without further purification analyzed via MALDI-TOF.

**General procedure for the inhibition of α-chymotrypsin by 1 and 2 for MALDI-TOF mass spectra measurements:** 5 µL organometallic linker (20 mM in DMSO) were added to 50 µL aqueous buffered α-chymotrypsin solution (5.2 mg / mL trypsin in phosphate buffer, 39 mM, pH 8, 25 mM $CaCl_2$) and stirred gently for 3 h. Thereafter, the reaction mixture was diluted with 495 µL distilled water, filtered and without further purification analyzed via MALDI-TOF.

***Table C27:*** Table of species observed in MALDI-TOF spectra in comparison to the native enzymes employed.

| entry | enzyme species | obs. Mass [kDa] | $\Delta_{native\ enzyme}$[Da] | species |
|---|---|---|---|---|
| 1 | α-chymotrypsin | 25.443 | | $[M]^+$ |
| | | 12.729 | | $[M]^{2+}$ |
| 2 | [Rh]-SF@α-chymotrypsin **107** | 26.135 | 692 | $[M-2Cl-F]^+$ |
| | | 13.080 | 351 | $[M-2Cl-F]^{2+}$ |
| 3 | [Rh]-PF@α-chymotrypsin **106** | 25.946 | 503 | $[M-PPh_3-Cl-OEt-F]^+$ |
| | | 12.979 | 250 | $[M-PPh_3-Cl-OEt-F]^{2+}$ |
| 4 | Trypsin | 23.303 | | $[M]^+$ |
| | | 11.661 | | $[M]^{2+}$ |
| 5 | [Rh]-SF@trypsin **109** | 23.733 | 430 | $[M-PPh_3-2Cl-F]^+$ |
| | | 11.879 | 218 | $[M-PPh_3-2Cl-F]^{2+}$ |
| | | 24.003 | 700 | $[M-2Cl-F]^+$ |
| | | 12.018 | 357 | $[M-2Cl-F]^{2+}$ |
| 6 | [Rh]-PF@trypsin **108** | 23.803 | 500 | $[M-PPh_3-Cl-OEt-F]^+$ |
| | | 11.911 | 250 | $[M-PPh_3-Cl-OEt-F]^{2+}$ |

## 2.12. Chromogenic inhibition assays of proteases

### 2.12.1. Chromogenic assays of cysteine proteases

**Procedure for the measurement of photometric assays for the detection of enzyme activity in presence of different concentrations of metalla affinity label:** To 100 µL buffered aqueous solution (100 mM, $PO_4^{2-}$, pH 7.0), 100 µL activated papain solution were added (1 µL papain suspension an 1 µL DTT solution (1 mM in buffered aqueous suspension, 100 mM $PO_4^{2-}$, pH 7.0) were added to 98 µL buffered aqueous solution (100 mM $PO_4^{2-}$, pH 7.0), incubated for 45 min). Then, 5 µL metalla label was added (concentration varying from 0 to 88 µM, solution in DMSO). The reaction solution was allowed to react for 3 h, before enzyme activity was tested by adding 10 µL of BAPNA (0.2 mM in DMSO). Absorptions of the reaction solution were measured immediately after addition of the substrate and after 125 min at a wavelength of 405 nm.

**Table C28:** Activities observed in chromogenic assays of papain, employing different concentrations of [Rh]-Epx **70** or [Rh]-Deox **72**.

| entry | [M]-Al | enzyme | conc. [M]-Al [µM] | $\Delta_{abs.}$ | activity (%)[a] |
|-------|--------|--------|-------------------|------------|-----------------|
| 1 | [Rh]-Epx **70** | Papain | 0 | 0.2965 | 1 |
| 2 | [Rh]-Epx **70** | Papain | 0.06 | 0.2845 | 96 |
| 3 | [Rh]-Epx **70** | Papain | 0.26 | 0.2582 | 87 |
| 4 | [Rh]-Epx **70** | Papain | 0.51 | 0.1860 | 63 |
| 5 | [Rh]-Epx **70** | Papain | 0.77 | 0.1315 | 44 |
| 6 | [Rh]-Epx **70** | Papain | 1.02 | 0.0555 | 19 |
| 7 | [Rh]-Epx **70** | Papain | 1.53 | 0.0047 | 2 |
| 8 | [Rh]-Epx **70** | Papain | 2.04 | 0.0005 | 0 |
| 9 | [Rh]-Deox **72** | Papain | 0 | 0.3666 | 1 |
| 10 | [Rh]-Deox **72** | Papain | 0.06 | 0.3448 | 94 |
| 11 | [Rh]-Deox **72** | papain | 0.26 | 0.3594 | 98 |
| 12 | [Rh]-Deox **72** | papain | 0.51 | 0.3609 | 98 |
| 13 | [Rh]-Deox **72** | papain | 0.77 | 0.3521 | 96 |
| 14 | [Rh]-Deox **72** | papain | 1.02 | 0.3620 | 99 |
| 15 | [Rh]-Deox **72** | papain | 1.53 | 0.3803 | 103 |
| 16 | [Rh]-Deox **72** | papain | 2.04 | 0.3631 | 99 |

Data points were collected after 125 min reaction time. A baseline correction was carried out. (a) relative to initial activity.

## 2.12.2. Chromogenic assays of serine proteases

**Procedure for the measurement of photometric assays for the detection of enzyme activity in presence of different concentrations of metalla affinity label:** To 180 µL buffered aqueous solution (68 mM, $PO_4^{2-}$, pH 7.6), of trypsin (0.2 g / 1 mL, 8.6 µM),  different concentrations of [Rh]-FP **90** were added (10 µL, 0 µM - 158 µM in DMSO) and the reaction mixture incubated for 10 min. Thereafter, BAPNA was added (10 µL, 0.2 mM in DMSO). Absorptions of the reaction solution were measured immediately after addition of the substrate and after 15 min at a wavelength of 405 nm.

**Table C29:** Activities observed in chromogenic assays of trypsin, employing different concentrations of [Rh]-PF **90**.

| entry | [M]-L | enzyme | conc. [M]-Al [µM][a] | $\Delta_{abs.}$ | activity (%)[b] |
|-------|-------|--------|----------------------|------------------|------------------|
| 1 | [Rh]-FP **90** | trypsin | 0 | 1.6226 | 100 |
| 2 | [Rh]-FP **90** | trypsin | 1.3 | 1.4979 | 92 |
| 3 | [Rh]-FP **90** | trypsin | 2.6 | 1.0221 | 63 |
| 4 | [Rh]-FP **90** | trypsin | 4.0 | 0.8238 | 51 |
| 5 | [Rh]-FP **90** | trypsin | 5.3 | 0.7439 | 46 |
| 6 | [Rh]-FP **90** | trypsin | 6.6 | 0.5903 | 36 |
| 7 | [Rh]-FP **90** | trypsin | 7.9 | 0.3312 | 20 |

Data points were collected after 125 min reaction time. A baseline correction was carried out. (a) overall concentration in the reaction mixture (b) relative to initial activity.

## 2.13. X-Ray spectroscopical data

*Table C30:* Crystal data and details for the structure determination of compound **3i**.

| formula | $C_9H_{16}Cl_3N_1O_1Ru_1S_1$ |
|---|---|
| formula wt | 393.71 |
| space group | $P2_1/c$ |
| $a$ (Å) | 7.660(5) |
| $b$ (Å) | 21.030(5) |
| $c$ (Å) | 8.260(5) |
| $\alpha$ (deg) | 90 |
| $\beta$ (deg) | 91.264(5) |
| $\gamma$ (deg) | 90 |
| $V$ (Å$^3$) | 1330.3(12) |
| $Z$ | 4 |
| $D_{calcd}$ (g cm$^{-3}$) | 1.966 |
| temperature [K] | 150 |
| $\lambda$ [Å] | 0.71073 |
| no. of indep rflns | 2465 |
| no. of params | 147 |
| R1 ($I > 2\sigma(I)$) | 0.0494 |
| wR2 (all data) | 0.0944 |
| goodness of fit | 0.690 |
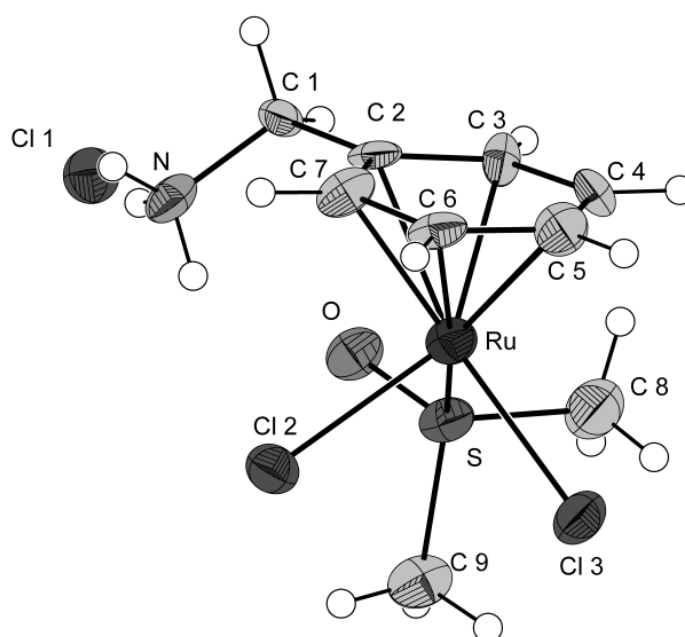
*Table C31:* Crystal data and details for the structure determination of compound **4r**.

| | |
|---|---|
| formula | $C_{27}H_{25}Cl_2O_2P_1Ru_1$; $C_1H_1Cl_3$ |
| formula wt | 703.78 |
| space group | $P2_1/n$ |
| $a$ (Å) | 11.5173(3) |
| $b$ (Å) | 13.9418(3) |
| $c$ (Å) | 20.2221(4) |
| $\alpha$ (deg) | 90 |
| $\beta$ (deg) | 91.3023(10) |
| $\gamma$ (deg) | 90 |
| $V$ (Å$^3$) | 3246.26(13) |
| $Z$ | 4 |
| $D_{calcd}$ (g cm$^{-3}$) | 1.440 |
| temperature [K] | 103 |
| $\lambda$ [Å] | 0.71073 |
| no. of indep rflns | 5686 |
| no. of params | 438 |
| R1 ($I > 2\sigma(I)$) | 0.0275 |
| wR2 (all data) | 0.0655 |
| goodness of fit | 1.09 |
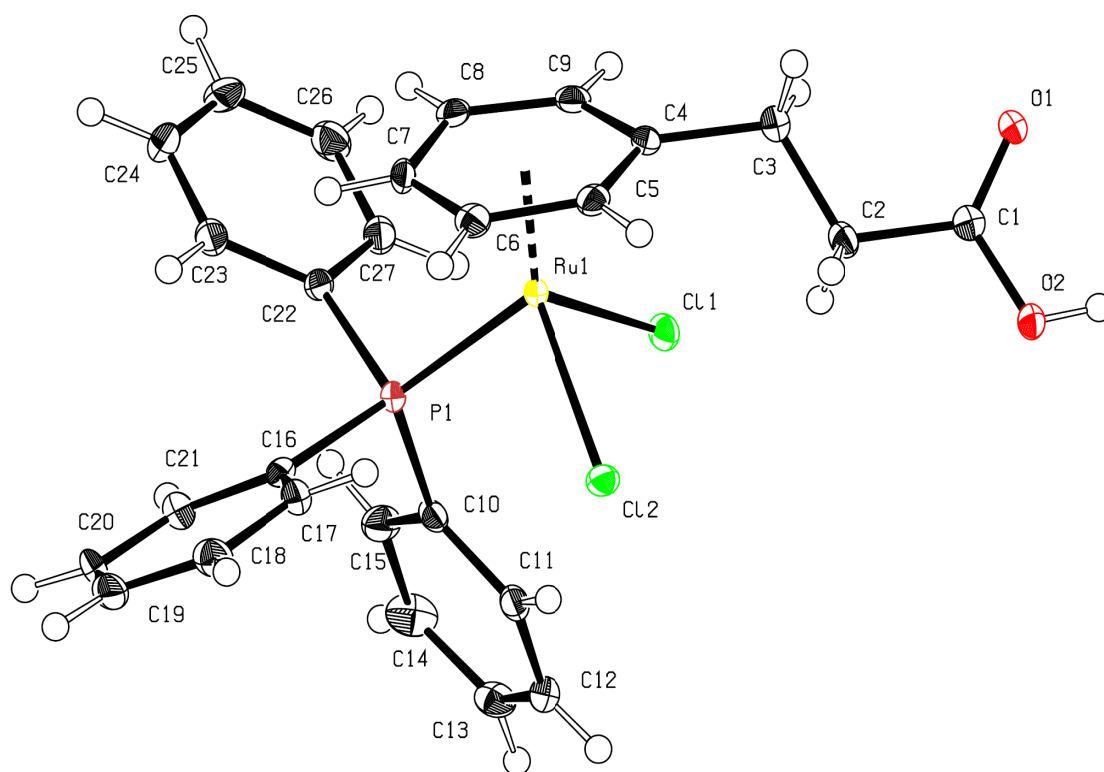
*Table C32:* Crystal data and details for the structure determination of compound **6**.

| | |
|---|---|
| formula | $C_{28}H_{48}Cl_{12}N_4Os_2$ |
| formula wt | 1246.50 |
| space group | $P2_1/c$ |
| $a$ (Å) | 12.228(2) |
| $b$ (Å) | 13.715(3) |
| $c$ (Å) | 24.472(5) |
| $\alpha$ (deg) | 90 |
| $\beta$ (deg) | 97.69(3) |
| $\gamma$ (deg) | 90 |
| $V$ (Å$^3$) | 4067.3(14) |
| $Z$ | 4 |
| $D_{calcd}$ (g cm$^{-3}$) | 2.036 |
| temperature [K] | 150 |
| $\lambda$ [Å] | 0.71073 |
| no. of indep rflns | 7420 |
| no. of params | 410 |
| R1 ($I > 2\sigma(I)$) | 0.0327 |
| wR2 (all data) | 0.0708 |
| goodness of fit | 0.992 |
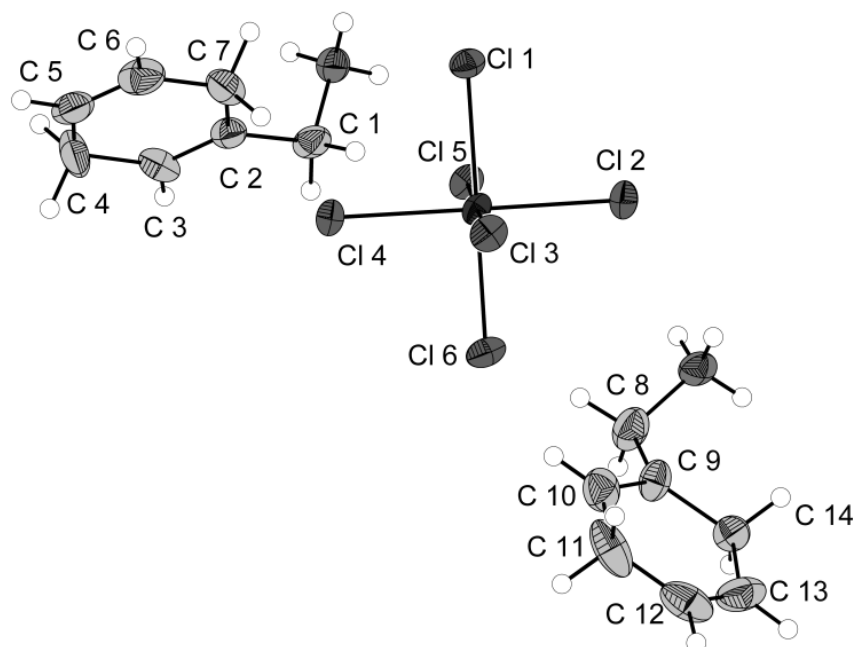
**Table C33:** Crystal data and details for the structure determination of compound **13**.

| | |
|---|---|
| formula | $2(C_9H_{13}NO_2) \cdot HCl$ |
| formula wt | 370.87 |
| space group | $P2_1$ |
| $a$ (Å) | 1157.81(9) |
| $b$ (Å) | 508.28(4) |
| $c$ (Å) | 1584.93(13) |
| $\alpha$ (deg) | 90 |
| $\beta$ (deg) | 98.471(7) |
| $\gamma$ (deg) | 90 |
| $V$ (Å$^3$) | 922.54(13) |
| $Z$ | 2 |
| $D_{calcd}$ (g cm$^{-3}$) | 1.335 |
| temperature [K] | 173 |
| $\lambda$ [Å] | 0.71073 |
| no. of indep rflns | 1395 |
| no. of params | 240 |
| R1 ($I > 2\sigma(I)$) | 0.0614 |
| wR2 (all data) | 0.1335 |
| goodness of fit | 1.085 |
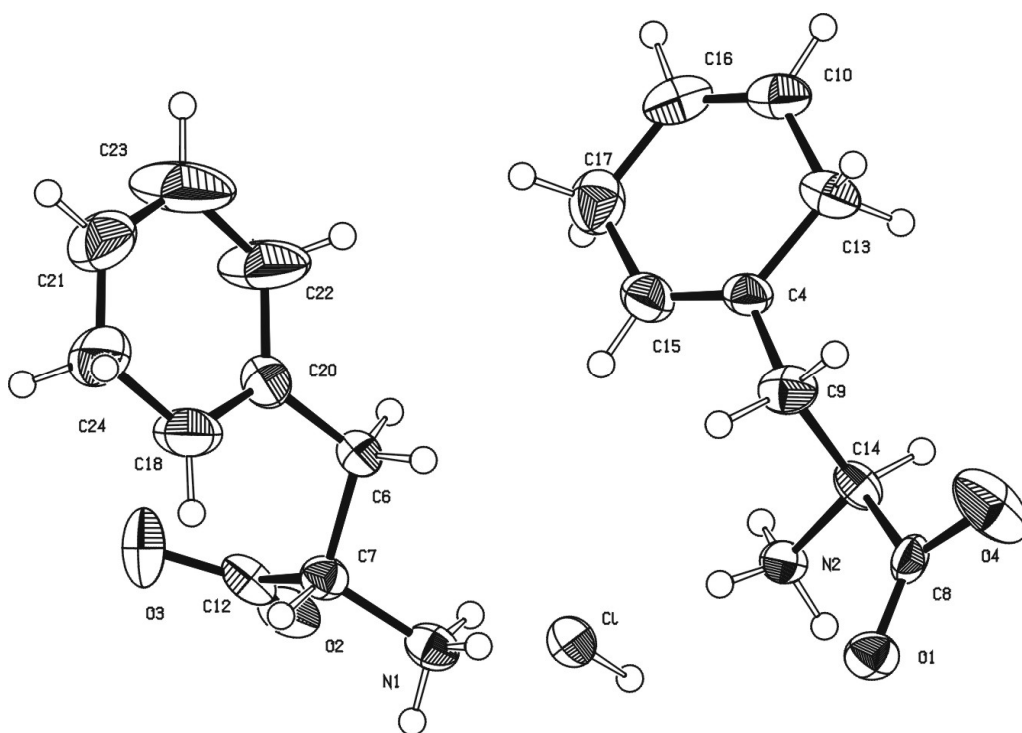
***Table C34:*** Crystal data and details for the structure determination of compound **12**.

| | |
|---|---|
| formula | $C_{16}H_{20}N_2O_4S_2$ |
| formula wt | 368.48 |
| space group | $P2_1/c$ |
| $a$ (Å) | 5.764(1) |
| $b$ (Å) | 8.109(2) |
| $c$ (Å) | 18.24(4) |
| $\alpha$ (deg) | 90 |
| $\beta$ (deg) | 97.81(8) |
| $\gamma$ (deg) | 90 |
| $V$ (Å$^3$) | 844.81(3) |
| $Z$ | 2 |
| $D_{calcd}$ (g cm$^{-3}$) | 1.449 |
| temperature [K] | 173 |
| $\lambda$ [Å] | 0.71073 |
| no. of indep rflns | 1535 |
| no. of params | 149 |
| R1 ($I > 2\sigma(I)$) | 0.0331 |
| wR2 (all data) | 0.0828 |
| goodness of fit | 1.05 |
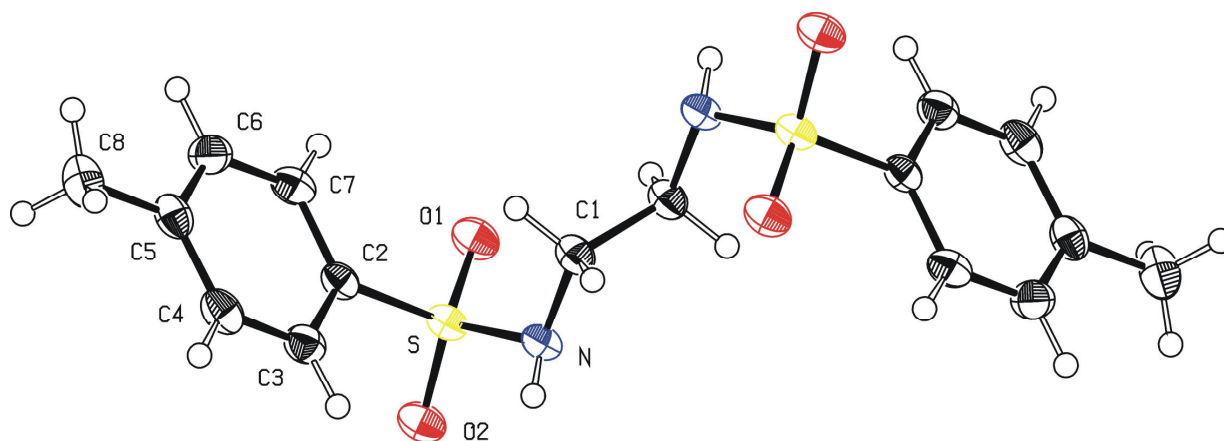
*Table C35:* Crystal data and details for the structure determination of compound **20^Py**.

| | |
|---|---|
| formula | $C_{26}H_{30}Cl_2N_4O_2Ru$ |
| formula wt | 602.51 |
| space group | $P2(1)2(1)2(1)$ |
| $a$ (Å) | 9.0078(18) |
| $b$ (Å) | 9.5536(19) |
| $c$ (Å) | 31.245(6) |
| $\alpha$ (deg) | 90 |
| $\beta$ (deg) | 90 |
| $\gamma$ (deg) | 90 |
| $V$ (Å$^3$) | 2688.9(9) |
| $Z$ | 4 |
| $D_{calcd}$ (g cm$^{-3}$) | 1.488 |
| temperature [K] | 150 |
| $\lambda$ [Å] | 0.71073 |
| no. of indep rflns | 4868 |
| no. of params | 318 |
| R1 ($I > 2\sigma(I)$) | 0.0323 |
| wR2 (all data) | 0.0957 |
| goodness of fit | 1.184 |
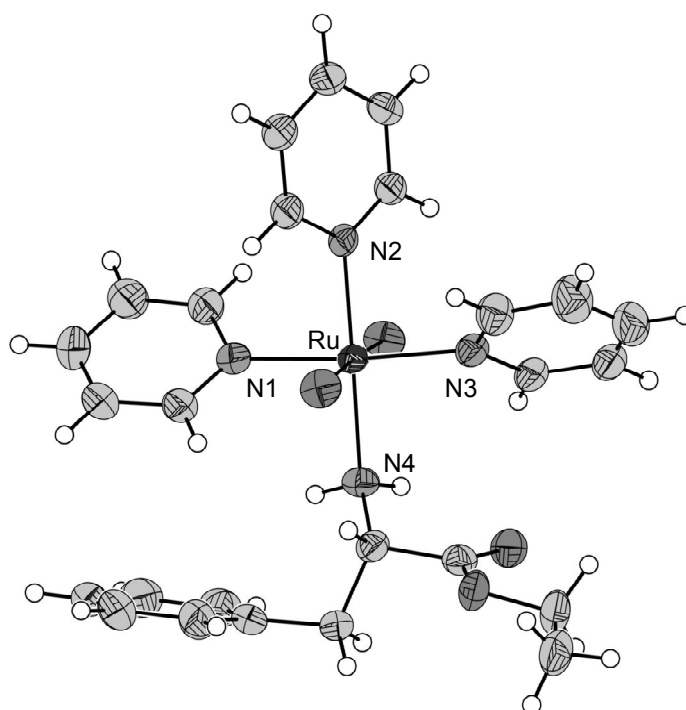
***Table C36:*** Crystal data and details for the structure determination of compound **30**.

| | |
|---|---|
| formula | $C_{44}H_{68}N_6O_{12}Ru_2S_6$ |
| formula wt | 1267.54 |
| space group | $P1$ |
| $a$ (Å) | 10.390(1) |
| $b$ (Å) | 12.136(1) |
| $c$ (Å) | 12.916(1) |
| $\alpha$ (deg) | 103.59(1) |
| $\beta$ (deg) | 111.66(1) |
| $\gamma$ (deg) | 108.65(1) |
| $V$ (Å$^3$) | 1313.9(2) |
| $Z$ | 1 |
| $D_{calcd}$ (g cm$^{-3}$) | 1.602 |
| temperature [K] | 150 |
| $\lambda$ [Å] | 0.71073 |
| no. of indep rflns | 8468 |
| no. of params | 631 |
| R1 ($I > 2\sigma(I)$) | 0.0401 |
| wR2 (all data) | 0.0952 |
| goodness of fit | 1.004 |
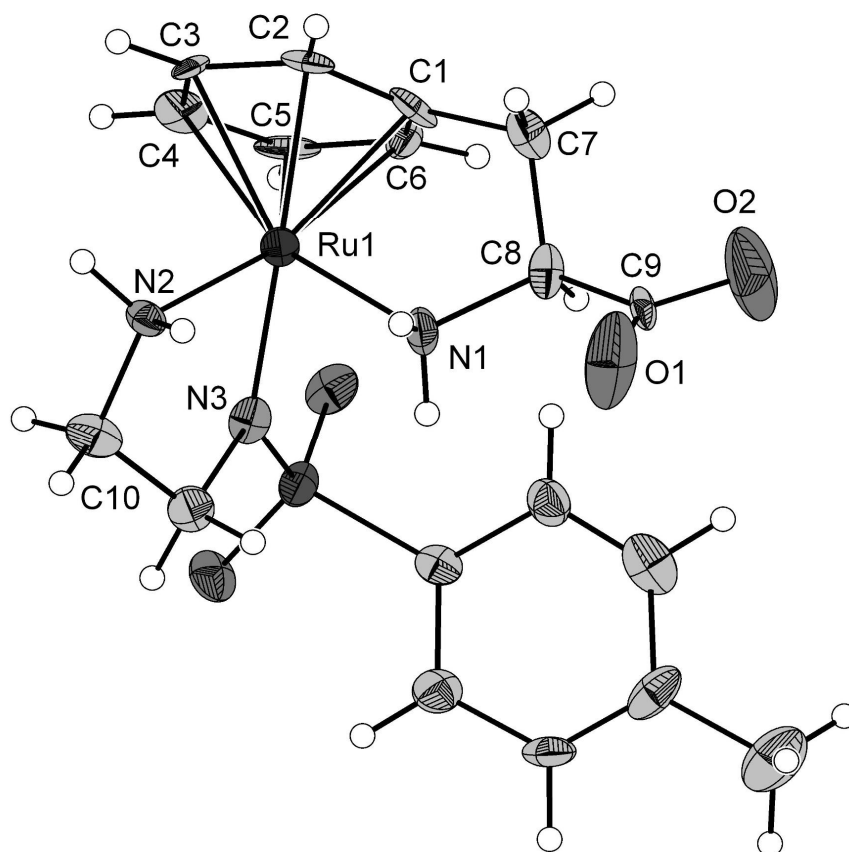
*Table C37:* Crystal data and details for the structure determination of compound **70**.

| | |
|---|---|
| formula | $C_{46}H_{53}Cl_2N_3O_4P_1Rh_1$ |
| formula wt | 916.69 |
| space group | $P2_1$ |
| $a$ (Å) | 8.7620(3) |
| $b$ (Å) | 32.5384(10) |
| $c$ (Å) | 8.8665(3) |
| $\alpha$ (deg) | 90.00 |
| $\beta$ (deg) | 109.700(2) |
| $\gamma$ (deg) | 90.00 |
| $V$ (Å$^3$) | 2379.90(14) |
| $Z$ | 2 |
| $D_{calcd}$ (g cm$^{-3}$) | 1.279 |
| temperature [K] | 296(2) |
| $\lambda$ [Å] | 0.71073 |
| no. of indep rflns | 9041 |
| no. of params | 501 |
| R1 ($I > 2\sigma(I)$) | 0.0527 |
| wR2 (all data) | 0.1472 |
| goodness of fit | 1.249 |
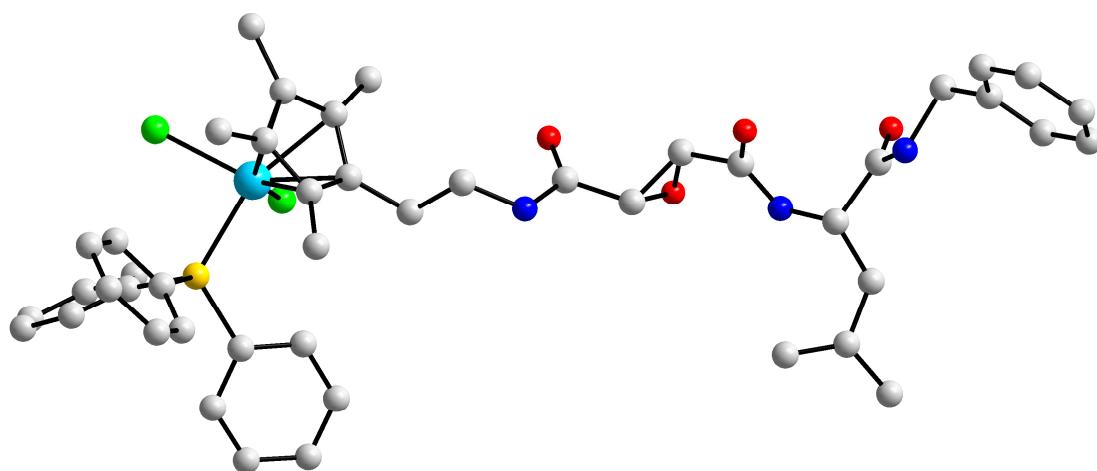
*Table C38:* Crystal data and details for the structure determination of compound **91**.

| | |
|---|---|
| formula | 2 ($C_{36}H_{36}Cl_2F_1N_1O_3P_1Rh_1S_1$), 3 ($C_1H_1Cl_3$) |
| formula wt | 1931.12 |
| space group | *P*-1 |
| *a* (Å) | 15.0745(9) |
| *b* (Å) | 16.9192(10) |
| *c* (Å) | 18.5003(12) |
| α (deg) | 69.352(3) |
| β (deg) | 73.986(4) |
| γ (deg) | 69.983(3) |
| *V* (Å$^3$) | 4083.5(4) |
| *Z* | 2 |
| $D_{calcd}$ (g cm$^{-3}$) | 1.571 |
| temperature [K] | 123 |
| λ [Å] | 0.71073 |
| no. of indep rflns | 11695 |
| no. of params | 945 |
| R1 (*I* > 2σ(*I*)) | 0.0410 |
| wR2 (all data) | 0.1146 |
| goodness of fit | 1.05 |
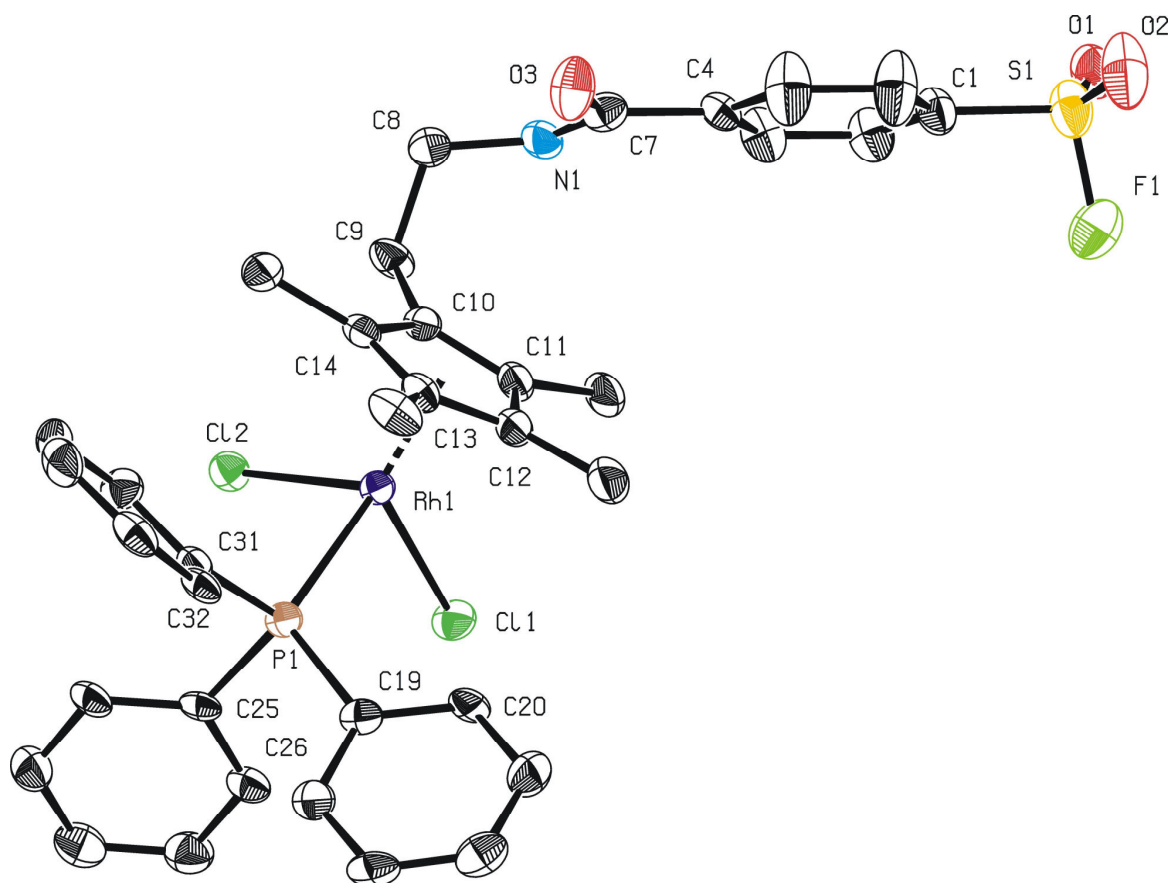
# 3. References

[1]     For a comprehesive list for solvent drying procedures, please see: http://www.chm.tu-dresden.de/oc/bauer/Trocknung%20von%20L%C3%B6sungsmitteln.pdf

[2]     Bruker AXS Shelxtl, Version 6.14, **2000**.

[3]     G. B. Sheldrick, *"SHELXS-86"*, Universität Göttingen**1986**.

[4]     A. L. Spek, *"The "EUCLID" Package"*, in *"Computional Crystallography"*, Clarendon Press, Oxford **1982**.

[5]     (a) A. J. Birch, *Pure Appl. Chem.* **1996**, *68*, 553-556; (b) P. W. Rabideau, Z. Marcinow, *The Birch reduction of aromatic compounds. Organic Reactions*, New York, **1992**, *42*, 1-334.

[6]     F. K. Cheung, C. Lin, F. Minissi, A. L. Criville, M. A. Graham, D. J. Fox, M. Wills, *Org. Lett.* **2007**, *9*, 4659-4662.

[7]     W. H. Ang, E. Daldini, L. Juillerat-Jeanneret, P. J. Dyson, *Inorg. Chem.* **2007**, *46*, 9048-9050.

[8]     this compound was prepared similar to the route described before; S. Sugasawa, R. Tachikawa *Tetrahedron* **1958**, *4*, 205-212.

[9]     T. Onishi, Y. Miyaki, H. Asano and H. Kurosawa, *Chem. Lett.* **1999**, *28*, 809.

[10]    Y. Miyaki, T. Onishi, H. Kurosawa, *Inorg. Chim. Acta* **2000**, *300-302*, 369-377.

[11]    A. Casini, C. Gabbiani, F. Sorrentino, M. P. Rigobello, A. Bindoli, T. J. Geldbach, A. Marrone, N. Re, C. G. Hartinger, P. J. Dyson, L. Messori, *J. Med. Chem.* **2008**, *51*, 6773-6781.

[12]    C. Scolaro, T. J. Geldbach, S. Rochat, A. Dorcier, C. Gossens, A. Bergamo, M. Cocchietto, I. Tavernelli, G. Sava, U. Rothilsberger, P. J. Dyson, *Organometallics*, **2006**, *25*, 756-765.

[13]    Y. Miyaki, T. Onishi, H. Kurosawa, *Inorg. Chim. Acta* **2000**, *300-302*, 369-377.

[14]    A. Skolaut, J. Rétey, *Arch. Biochem. Biophys.* **2001**, *393*, 187-191.

[15]    A. Dijksman, J.M. Elzinga, Y.-X. Li, I. W. C. E. Arends, R. A. Sheldon *Tetrahedron: Asymmetry* **2002**, *13*, 879-884.

[16]    Y. Fukudome, H. Naito, T. Hata, H. Urabe, *J. Am. Chem. Soc.* **2008**, *130*, 1820-1821.

[17]    H. Dialer, P. Mayer, K. Polborn, W. Beck, *Eur. J. Inorg. Chem.* **2001**, 1051-1055.

[18] C. M. Fendrick, L. D. Schertz, V. W. Day, T. J. Marks, *Organometallics* **1988**, *7*, 1828-1838.

[19] D. van Leusen, D. J. Beetstra, B. Hessen, J. H. Teuben, *Organometallics* **2000**, *19*, 4084-4089.

[20] (a) J. W. Kang, K. Moseley, P. M. Maitlis, *J. Am. Chem. Soc.* **1969**, *91*, 5970-5977; (b) B. L. Booth, R. N. Haszeldine, M. Hill, *J. Organomet. Chem.* **1969**, *16*, 491-496; (c) B. Paz-Michel, M. Cervantes-Vazquez, M. A. Paz-Sandoval, *Inorg. Chim. Acta* **2008**, *361*, 3094-3102; (d) V. Tedesco, W. von Philipsborn, *Mag. Res. Chem.* **1996**, *34*, 373-376; (e) W. D. Jones, V. L. Kuykendall, *Inorg. Chem.* **1991**, *30*, 2615-2622, and references therein.

[21] (a) B. J. Gour-Salin, P. Lachance, M.-C. Magny, C. Plouffe, R. Ménard, A. C. Storer, *Biochem. J.* **1994**, *299*, 389-392; (b) K. A. H. Chehade, A. Baruch, S. H. L. Verhelst, M. Bogyo, *Synthesis* **2005**, *2*, 240-244; (c) F. Sarabia, A. Sánchez-Ruiz, S. Chammaa, *Bioorg. Med. Chem.* **2005**, *13*, 1691-1705.

[22] K. A. H. Chehade, A. Baruch, S. H. L. Verhelst, M. Bogyo, *Synthesis* **2005**, *2*, 240-244.

[23] Y. Liu, M. P. Paricelli, B. F. Cravatt, *PNAS* **1999**, *96*, *26*, 14694-14699.

[24] (a) J. Oleksyszyn, L. Subotkowska, P. Mastalerz, *Synthesis* **1979**, 985; (b) H. Hoffmann, H. Förster, *Mh. Chem.* **1968**, *99*, 380-388.

[25] Enantiomer separations were carried out using a Varian capillary column, fused silica 25 m x 0.25 mm, coated cp chirasil-dex CB df = 0.25.

# D | Summary

# Synthesis of organometallic enzyme hybrids via metalla affinity labels

The objective of this thesis was to establish the new concept of metalla affinity label based organometallic enzyme hybrids as enantioselective catalysts. The investigation presented resulted in three major achievements:

(I)     The synthesis of a broad range of catalytically active metalla affinity labels, which represent a new class of compounds.

(II)    The synthesis and characterization of organometallic enzyme hybrids generated from the conversion of enzymes with these metalla affinity labels.

(III)   The identification of factors influencing the catalytical performance of the organometallic enzyme hybrids based on the new concept.

Metalla affinity labels can be seen as trifunctional organometallic complexes, consisting of a homogeneous catalyst with pendant linker, reactive functional group and a peptidic part. The metalla affinity labels and metalla linkers synthesized in this thesis are covalent inhibitors. They specifically target the catalytically active amino acid of serine or cysteine proteases, giving covalently linked organometallic enzyme hybrids. During this reaction, the peptidic part guarantees selective formation of an enzyme-inhibitor complex. The catalytically active and initially achiral transition metal center is thereby being embedded in the chiral environment of the enzyme active center. Through this directed and covalent ancourage, chiral information is transferred to the catalytically active transition metal center, facilitating asymmetric catalysis (figure D1).
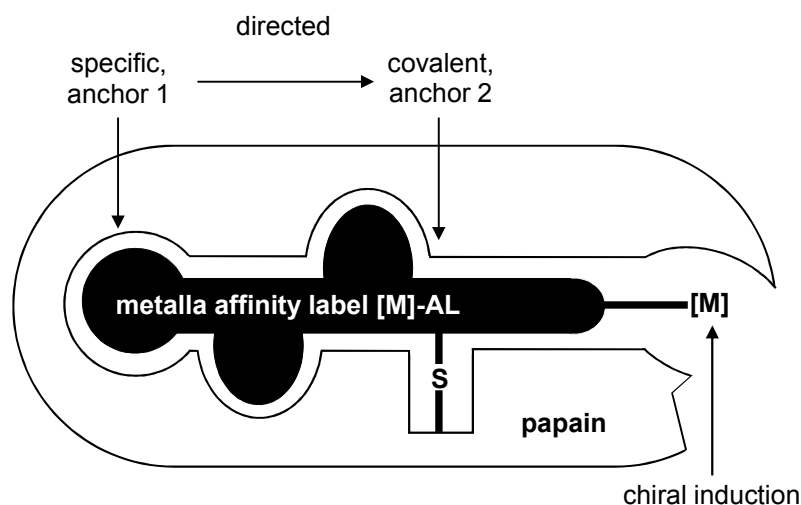


***Figure D1:*** Schematic representation of a metalla affinity label in the active center of a cysteine protease.

## Synthesis of organometallic catalysts with pendant linkers

The first step in the synthesis of organometallic enzyme hybrids was to identify suitable catalyst motives comprising pendant functional groups, which are stable under peptide coupling conditions and catalytically active in aqueous buffered solutions. Therefore, half sandwich complexes of group 8 and group 9 metals were investigated.

## $\eta^6$-arene ruthenium(II) und osmium (II) complexes

In the case of ruthenium(II) complexes with pendant linkers, a library of different functional groups and linker lengths was synthesized by optimizing the reaction sequence illustrated in scheme D1. The library contains carboxylic acids, amines, amino acids, alcohols, amides and carboxylic acid esters. Furthermore, linker lengths varied between 1 and 4 $CH_2$-groups.



n   = 1-4
FG  = $NH_2$, NHR, $CH_2OH$, COOH
FG' = $NH_2$, NHR, $CH_2OH$ COOH, COOR
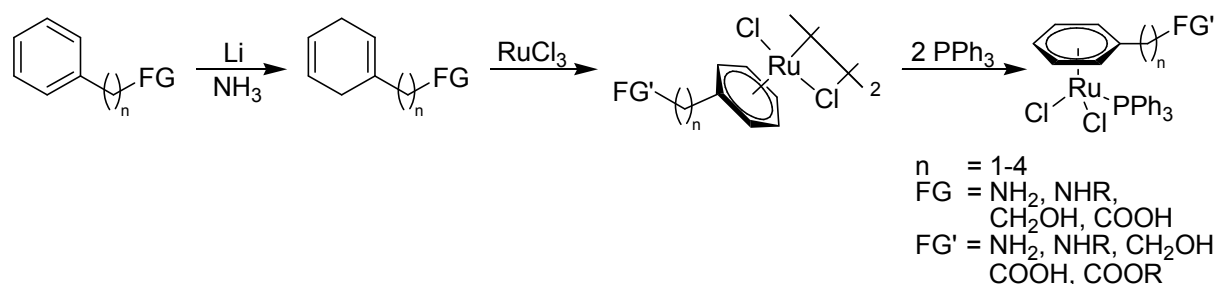
**Scheme D1:** Synthesized $\eta^6$-arene ruthenium(II) complexes.

Ruthenium(II) complexes comprising amide and carboxylic acid pendant functional groups were synthesized as test molecules to mimic the properties of the catalysts after their conjugation with organic molecules. Besides ruthenium chloride, the respective osmium chloride was successfully applied in this synthetic strategy (scheme D2), resulting in the first literature known $\eta^6$-arene osmium(II) complex comprising a pendant linker.
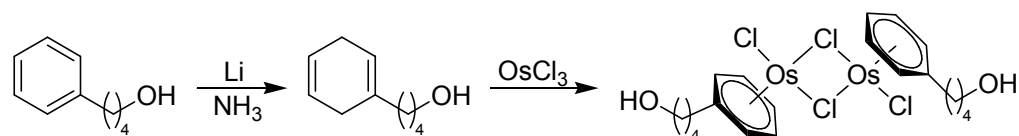


**Scheme D2:** Synthesized $\eta^6$-arene osmium(II) species.

Furthermore, L-phenylalanine was employed to synthesize $\eta^6$-arene ruthenium(II) complexes. Detailed studies were carried out, investigating the behavior of carboxylic acid ethyl ester and amino group under various solvent conditions and with different nucleophiles. L-phenylalanine $\eta^6$-arene complexes were further converted with ethylene diamine derivatives. This results in the formation of diastereotopic or diastereomeric $\eta^6$:$\eta^1$-ruthenium complexes. The structures of this class of compounds was confirmed via two-dimensional heteronuclear NMR-techniques as well as X-Ray diffractometry. (figure D2).
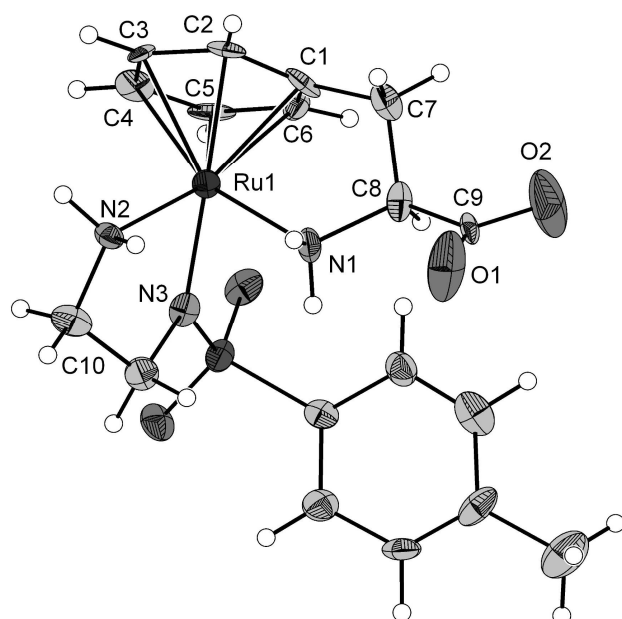


**Figure D2:** ORTEP-representation of a $\eta^6$:$\eta^1$-arene phenylalanine coordinated ruthenium(II) complex.

The catalytic activity of the $\eta^6$-arene ruthenium(II) library was confirmed in the biphasic hydrogenation of olefins. Herefore, TOFs of the organometallic complexes with different functional groups and linker lengths were compared. Furthermore, the influence of different temperatures, pressures and pH values was tested. Investigation of the catalyst structures prior and after catalytic runs showed, that not only the complex activity is sufficient for their employment as metalla affinity label precursors, but also the stability of the arene systems is high enough to facilitate linkage to organic molecules via this ligand, as cleavage during catalytical runs is not a dominant process.

## $\eta^5$-Cp* rhodium(III) and iridium (III) complexes

Besides ruthenium and osmium, also rhodium and iridium were applied for the generation of catalysts comprising pendant functionalizeable linkers. In this case, a

ethylamine Cp* tautomere was used instead of 1,4-cyclohexadiene derivatives. The Cp* tautomere can be reacted with Rh(III) and Ir(III) chlorides, yielding dinuclear halide Cp* coordinated complexes with a pendant ethylamine group (scheme D3).



M = Rh, Ir
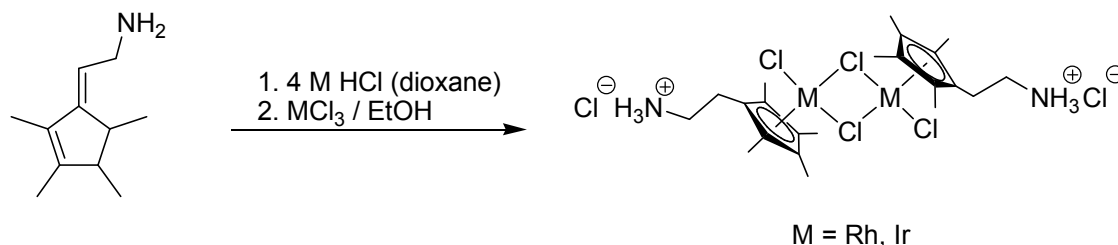
**Scheme D3:** Synthesis of rhodium(III) and iridium(III) complexes with functionalizeable pendant linkers.

The rhodium species was further converted into its respective mononuclear triphenylphosphine coordinated complex with pendant functional group. Consecutive reaction with carboxylic acid anhydrides showed, that the inner coordination sphere of the metal center remains unaltered, whereas the outer sphere pendant amino group opens the anhydride, resulting in peptide bond formation (scheme D4).
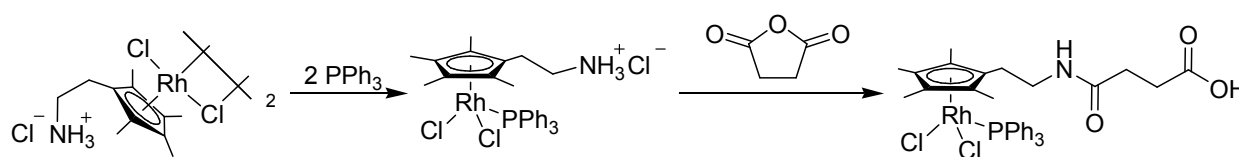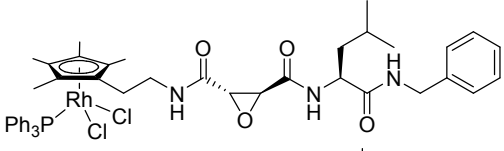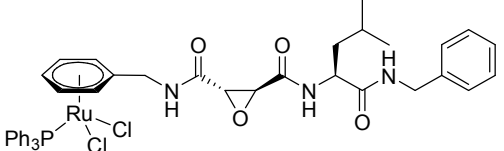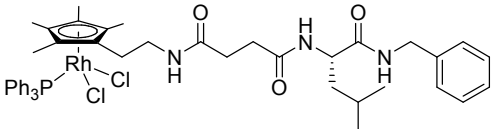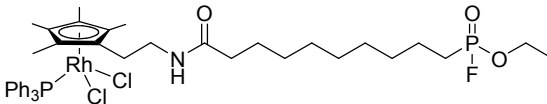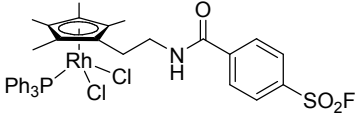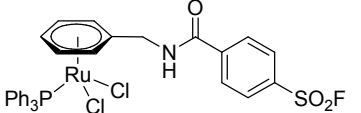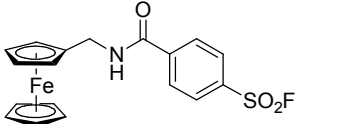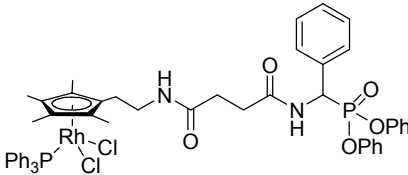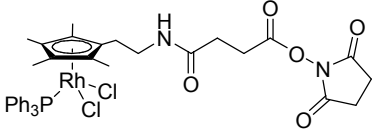


**Scheme D4:** Selective functionalization of a Rhodium(III) catalyst.

The possibility to selectively react halide-bridged transition metal complexes at the metal center (triphenylphosphine) or at the functional group of the pendant linker (carboxylic acid anhydride), confirms the applicability of this class of compounds as a building block in the synthesis of metalla affinity labels.

## Synthesis of metalla affinity labels and metalla linkers

Besides using carboxylic acid anhydrides, conjugation of metal center and peptidic affinity label was achieved via pentafluorophenole active esters or carboxylic acid fluorides, which then can be converted due to their electrophilicity by amines. All three methods result in peptide bond formation between the organometallic complex and the organic molecule which is to be conjugated.

**Table D1:** Metalla affinity labels and metalla linkers exhibiting peptidyl epoxides, their non-covalent analogue, phosphonyl fluorides, sulfonyl fluorides, diphenyl phosphonates or non-specific linkers synthesized within this thesis.

| entry | reactive group | inhibited class of enzyme | Lewis-structure |
|-------|----------------|---------------------------|-----------------|
| 1 | peptidyl epoxide | cysteine protease |  |
| 2 | non-covalent peptidyl epoxide analogue | cysteine protease |  |
| 3 | phosphonyl fluoride | serine protease |  |
| 4 | sulfonyl fluoride | serine protease |  |
| 5 | diphenyl phosphonate | serine protease |  |
| 6 | non-specific linker | not specified |  |

All conjugation methods developed leave the metal coordination sphere unaltered. The synthetic strategies via pentafluorophenole active esters or carboxylic acid fluorides are extremely mild. They tolerate labile groups such as epoxides, sulfonic acid fluorides, phosphonic acid fluorides or diphenyl phosphonates. Table D1 has a list of the metalla affinity labels and metalla linkers designed within this thesis. Figure D3 (part a) shows the ORTEP-representation of [Rh]-SF (table D1, entry 4), illustrating the unaltered inner coordination sphere as well as the intact sulfonic acid fluoride moiety.

Also of the metalla affinity label [Rh]-Epx a crystal structure was obtained (table D1, entry 1). A stick-representation clearly shows the different segments, of which the metalla affinity label has been built up (figure D3, part b): The peptidic affinity part, the central reactive epoxide group as well the organometallic catalyst motive.
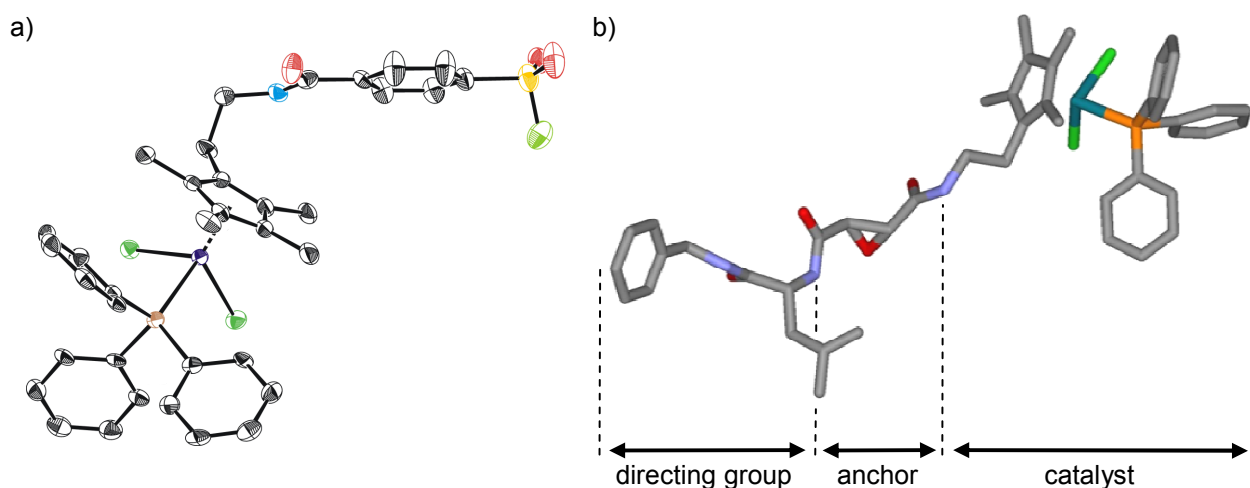


**Figure D3:** (a) ORTEP-representation of [Rh]-SF **91**, one of the metalla linkers designed within this thesis. (b) Stick-representation of the peptidyl epoxide metalla affinity label [Rh]-Epx **70** crystal structure.

Scheme D5 summarizes the synthetic route to a metalla affinity label ([Rh]-Epx). It visualizes the advantages of the modular system, which was developed during this thesis. The synthetic route itself has 15 different reaction steps. In spite of this overall high number of steps which are crucial to yield the metalla affinity label, the schematic representation clearly shows, that only the last three steps are necessary for the conjugation of homogeneous catalyst, reactive group and peptidic part. If for example the metal centre is to be exchanged from rhodium to ruthenium, this means only one single additional step. Therefore, by applying combinatorial synthesis, in spite of the quite complex synthetic strategies necessary for the particular components, different metalla affinity labels can be designed with low synthetic effort and time necessary.

**Conversion of metalla affinity labels to organometallic enzyme hybrids**

The generation of organometallic enzyme hybrids was achieved by reacting the different metalla affinity labels with the appropriate enzymes (bromelain, papain, α-chymotrypsin or trypsin) in aqueous buffered solutions. Following this reaction procedure, different organometallic enzyme hybrids can be generated with one single metalla affinity label or metalla linker. Due to the different environments in the active centers of different enzymes, the embedded catalysts show diverse properties in asymmetric catalysis.
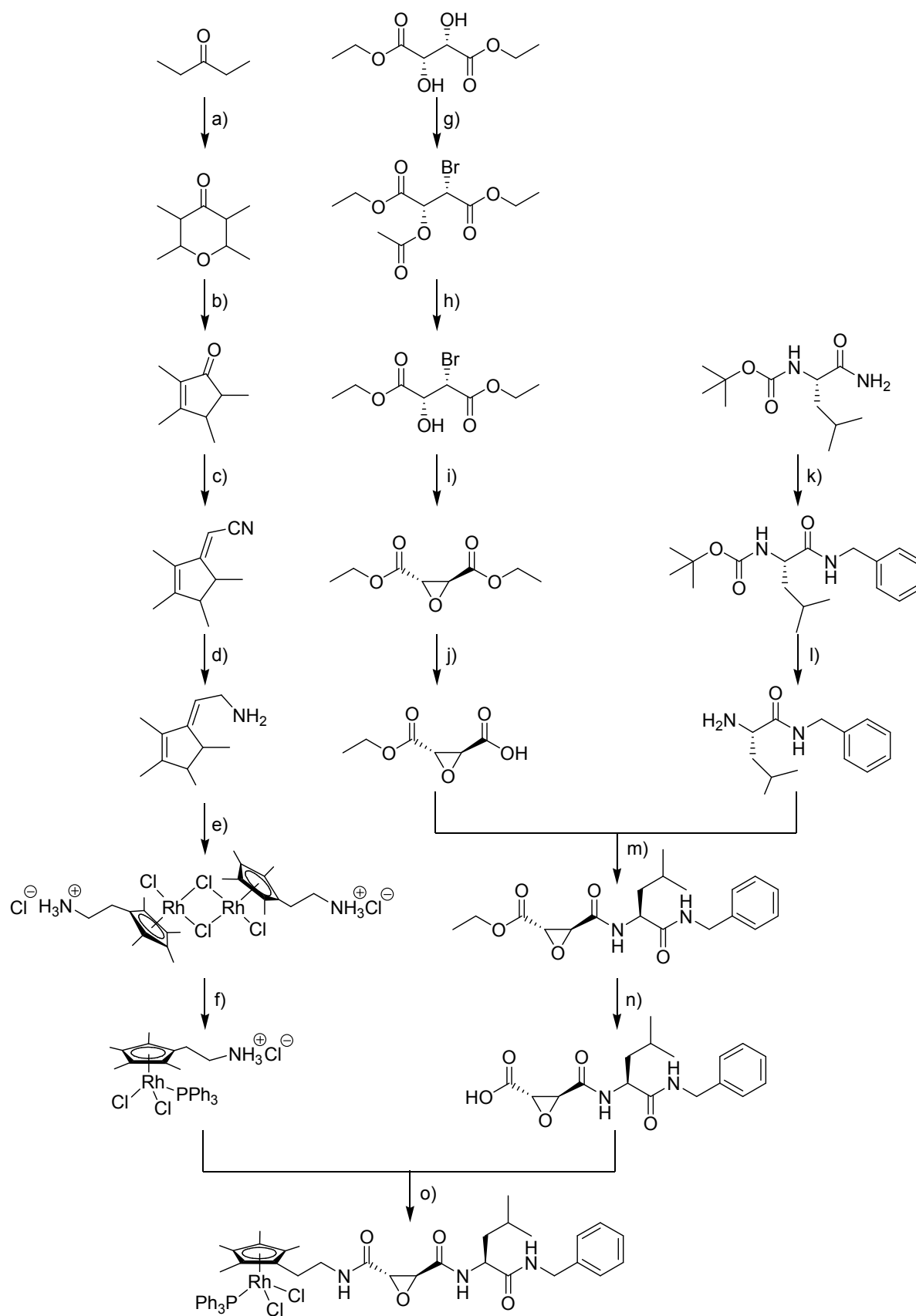
**Scheme D5:** Synthetic route to [Rh]-Epx, a peptidyl epoxide metalla affinity label. (a) KOH, CH₃COH, 0 °C, (MeOH); (b) 80°C (H₂CO, H₂SO₄); (c) AcN, ᵗBuLi (THF); (d) LiAlH₄, 55°C, (Et₂O); (e) RhCl₃, HCl, reflux, (EtOH); (f) PPh₃, RT, (DMSO); (g) HBr, 0 °C, (AcOH); (h) CH₃COCl, reflux, (EtOH); (i) DBU, 0°C, (Et₂O); (j) 1eq. KOH, 0°C, (EtOH_abs.); (k) C₆H₅CH₂NH₂, EDCI, 0°C, (DCM); (l) TFA, (DCM); (m) EDCI, 0°C, (DCM); (n) 1eq. KOH, 0°C, (EtOH_abs.); (o) 1. SS-DCC, HOPfp, 0 °C (DCM), 2. Et₃N, RT, (DCM).

The covalent inhibition of the employed enzymes was confirmed by various analytical tools, for example chromogenic activity assays or MALDI-TOF measurements. To exclude the possibility, that inhibition is mediated via the Lewis acidic transition metal centers instead of the reactive moieties, a non-covalent analogue of the peptidyl epoxide [Rh]-Epx was applied (table D1, entries 1-2). It was shown with MALDI-TOF mass spectra and chromogenic activity assays, that in absence of a reactive epoxide moiety, no inhibition of the enzyme takes place (figure D4). These results confirmed the conceptual binding mode of metalla affinity labels (figure D1).
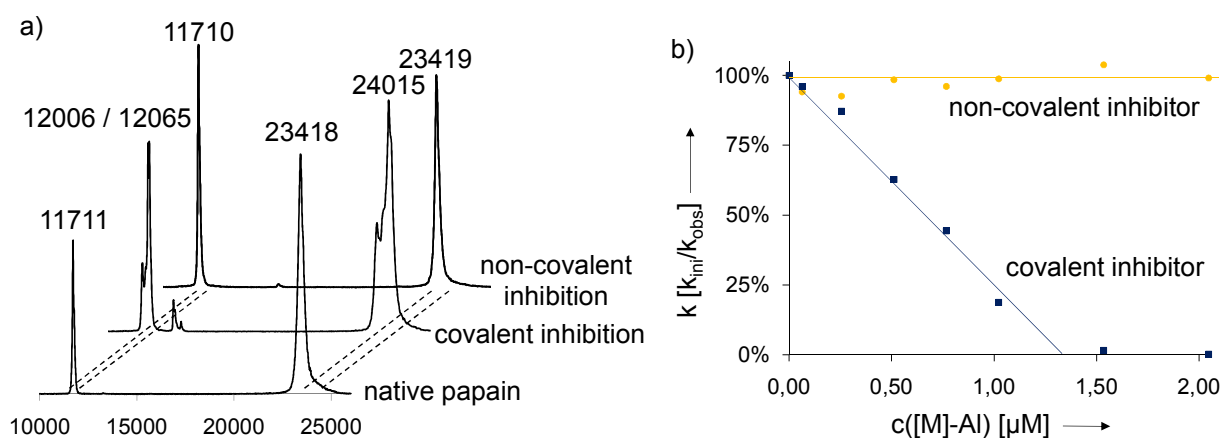


**Figure D4:** (a) MALDI-TOF mass spectra of native papain, covalently inhibited papain ([Rh]-Epx) and papain in presence of a non-covalent inhibitor ([Rh]-Deox). (b) Chromogenic activity assay employing a covalent inhibitor ([Rh]-Epx) and a non-covalent inhibitor ([Rh]-Deox).

## Application of organometallic enzyme hybrids in asymmetric catalysis

The synthesized organometallic enzyme hybrids were applied in the asymmetric hydrogenation (cysteine proteases) or transfer hydrogenation (serine proteases). Their properties were optimized in screenings. For this purpose variations in pH values of the aqueous buffered solutions, temperature, pressure (in the case of transfer hydrogenations: formiate concentration) and substrates were carried out. Additionally, kinetic measurements were carried out to monitor changes in enantioselectivity of the catalysts at long reaction times. These experiments confirmed the modularity of the concept. Enantioselectivities and activities are influenced by the nature of enzyme and metalla affinity label applied. Selectivity even inverts, when [Rh]-Epx@papain instead of [Ru]-Epx@papain is employed. Upon application of non-covalent binding metal centers, both for cysteine as well as serine proteases, racemic mixtures or significantly decreased enantiomeric excesses are obtained. In the optimal case, the hydrogenation of 4-chloro acetophenone, enantiomeric excesses of 64 % (*R*) were yielded

(12 % yield). The best yields were obtained for the conversion of 2,2,2-trifluoro-acetophenone (92 %) with an enantioselectivity of 20 %. Besides asymmetric hydrogenations, organometallic enzyme hybrids were also successfully tested in asymmetric transfer hydrogenations, yielding enantiomeric excesses of up to 20 %.

Overall, the new concept for the generation of organometallic enzyme hybrids via metalla affinity labels, which was investigated within this thesis, could be established and successfully applied for asymmetric catalysis. It was possible to generate a library of organometallic enzyme hybrids with a modular building block system. The synthesized hybrid species showed varying enantioselectivities, dependent on the chiral environment, in which the catalytically active centers were embedded in (figure D5). This confirmed, that a modular concept is crucial to the generation of organometallic enzyme hybrids, as it allows to generate and screen a large number of hybrids in a short amount of time, giving the possibility to further optimize the most promising candidates by directed evolution.
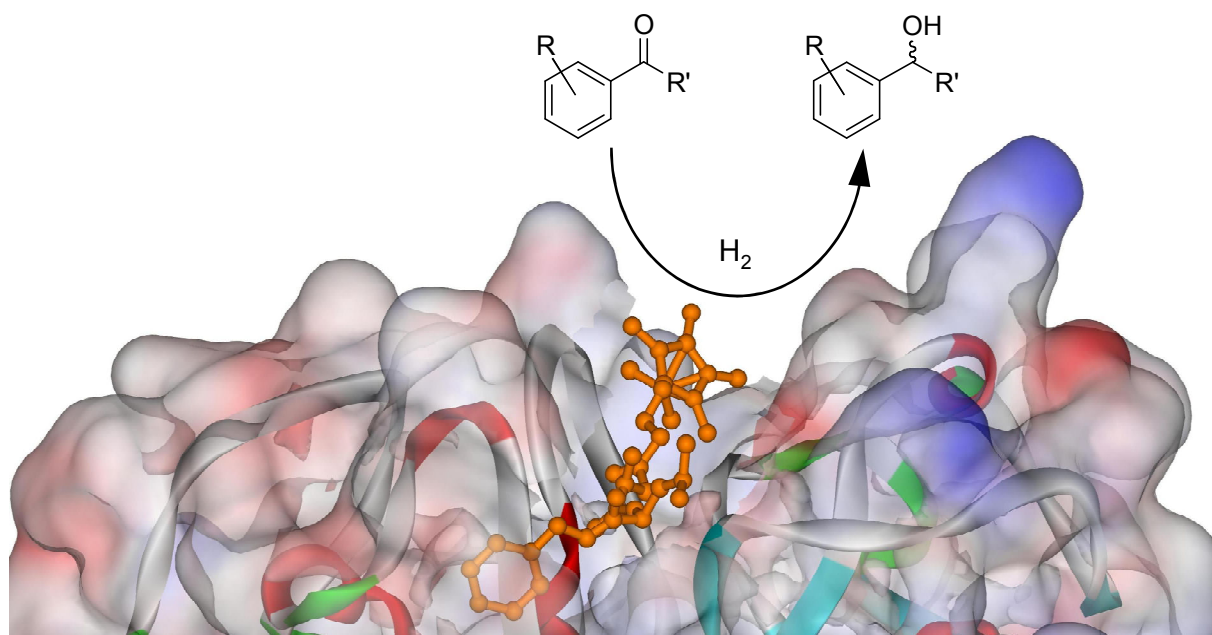


**Figure D5:** Embedded metalla affinity label in the active site of papain.

# E | Zusammenfassung

# Die Synthese von Organometall-Enzym-Hybriden mit Hilfe von Metalla-Affinitätsmarkern

Das Ziel dieser Arbeit war es, ein neues Konzept zur Generierung von Metalla-Affinitätsmarker basierten Organometall-Enzym-Hybriden zu etablieren. Die hier beschriebenen Untersuchungen führten zu drei verschiedenen Hauptresultaten:

(I)     Die Synthese eines breiten Spektrums verschiedener katalytisch aktiver Metalla-Affinitätsmarker, einer neuen Verbindungsklasse.

(II)    Die Synthese und Charakterisierung von Organometall-Enzym-Hybriden, welche aus der Umsetzung von Enzymen mit Metalla-Affinitätsmarkern gewonnen wurden.

(III)   Die Identifizierung von Faktoren, welche die katalytischen Eigenschaften der auf diesem Konzept basierenden Organometall-Enzym-Hybride beeinflussen.

Bei Metalla-Affinitätsmarkern handelt es sich um trifunktionelle organometallische Komplexe, bestehend aus einem homogenen Katalysator mit nicht-koordinierendem Linker, reaktiven funktionellen Gruppen und einem peptidischen Teil. Die im Rahmen dieser Arbeit synthetisierten Metalla-Affinitätsmarker sind kovalente Inhibitoren. Sie reagieren spezifisch und mit Serin- oder Cysteinproteasen unter Bildung von kovalent verankerten Organometall-Enzym-Hybriden. Bei der Umsetzung mit Enzymen sorgt der peptidische Teil für eine selektive Bildung eines Enzym-Inhibitor-Komplexes. Das katalytisch aktive und an sich achirale Metallzentrum des Metalla-Affinitätsmarkers wird dadurch in die chirale Umgebung des aktiven Zentrums des Enzyms eingebettet. Durch
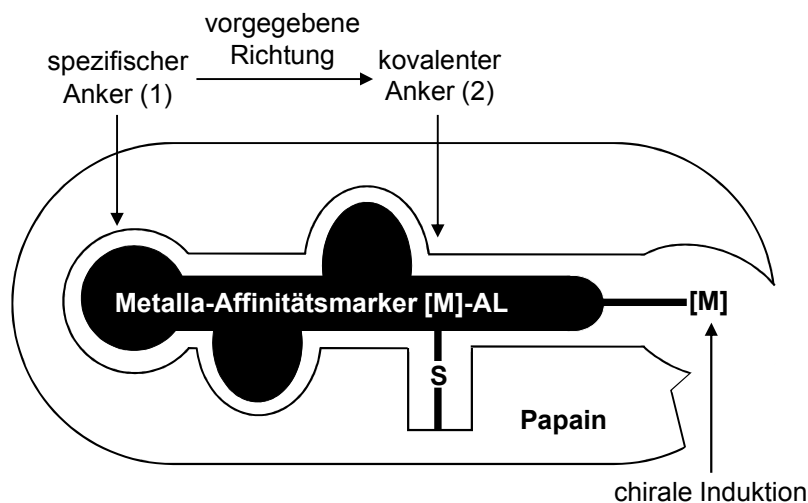


**Abbildung E1:** Schematische Darstellung eines Metalla-Affinitätsmarkers im aktiven Zentrum einer Cystein-Protease.

diese chirale Umgebung ist es möglich, Organometall-Enzym-Hybride in der asymmetrischen Katalyse einzusetzen (Abbildung E1).

**Synthese organometallischer Katalysatoren mit nicht-koordinierten Linkern**

Der erste Schritt auf dem Weg zu Organometall-Enzym-Hybriden war es, geeignete Katalysatoren mit nicht koordinierender funktioneller Gruppe zu identifizieren, welche unter Peptidkupplungsbedingungen stabil und in wässrigen Pufferlösungen aktiv sind.

Deswegen wurden Klavierstuhl-Komplexe der Gruppe 8 und Gruppe 9 mit funktionalisierbaren nicht-koordinierenden Linkern verwendet.

### $\eta^6$-Aren Ruthenium(II) und Osmium (II) Komplexe

Im Falle von Ruthenium(II)-Komplexen mit nicht-koordinierenden Linkern wurde durch Optimierung der in Schema E1 dargestellten Reaktionssequenz eine Bibliothek von Ru(II)-Komplexen mit verschiedenen funktionellen Gruppen synthetisiert. Die Bibliothek beinhaltet Carbonsäuren, Amine, Aminosäuren, Alkohole, Amide und Carbonsäureester. Des Weiteren wurden die Linker-Längen zwischen 1 und 4 $CH_2$-Gruppen variiert.
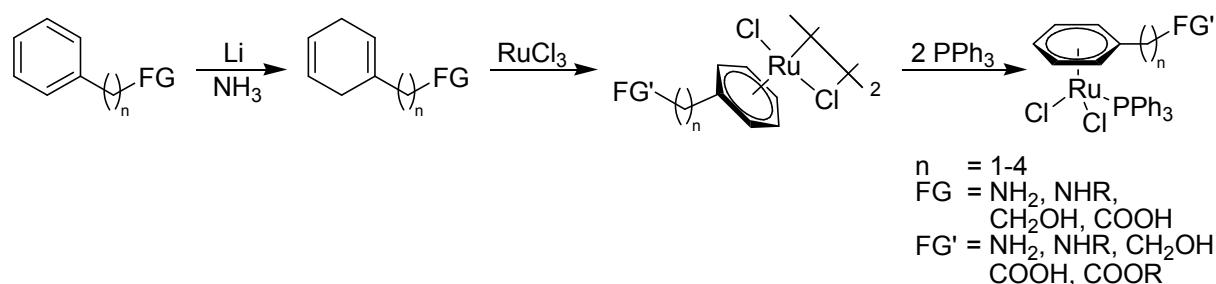


*Schema E1:* Synthetisierte $\eta^6$-Aren Ruthenium(II) Komplexe.

Ruthenium(II) Komplexe mit Amid- und Carbonsäure-Linkern wurden als Probemoleküle synthetisiert, um die Eigenschaften der Katalysatoren nach ihrer Kupplung abzubilden. Neben Ruthenium(III)chloriden wurden auch die entsprechenden Osmium(III)chloride im Rahmen dieser Synthesestrategie eingesetzt (Schema E2). Hierbei konnte der erste literaturbekannte $\eta^6$-Aren Osmium(II) Komplex mit funktionellem Linker synthetisiert werden.
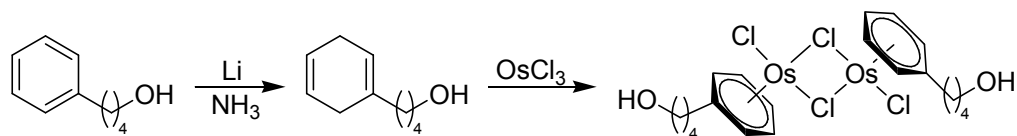
***Schema E2:*** Synthetisierte η⁶-Aren Osmium(II) Spezies.

Auch L-Phenylalanin wurde als Ligand für η⁶-Aren Ruthenium(II)-Komplexe eingesetzt. Es wurden detaillierte Studien durchgeführt, wie sich Amino- und Carbonsäure-Funktionalität unter verschiedenen Lösungsmittelbedingungen beziehungsweise in Anwesenheit verschiedener Nukleophile verhalten. L-Phenylalanin η⁶-Aren Komplexe wurden auch mit Ethylendiamin-Derivaten umgesetzt. Hierbei entstehen diastereotope oder diastereomere η⁶:η¹-Ruthenium-Komplexe. Die Struktur der Verbindungen wurde mit Hilfe heteronuklearer zweidimensionaler NMR-Techniken sowie Röntgendiffraktometrie bestimmt (Abbildung E2).
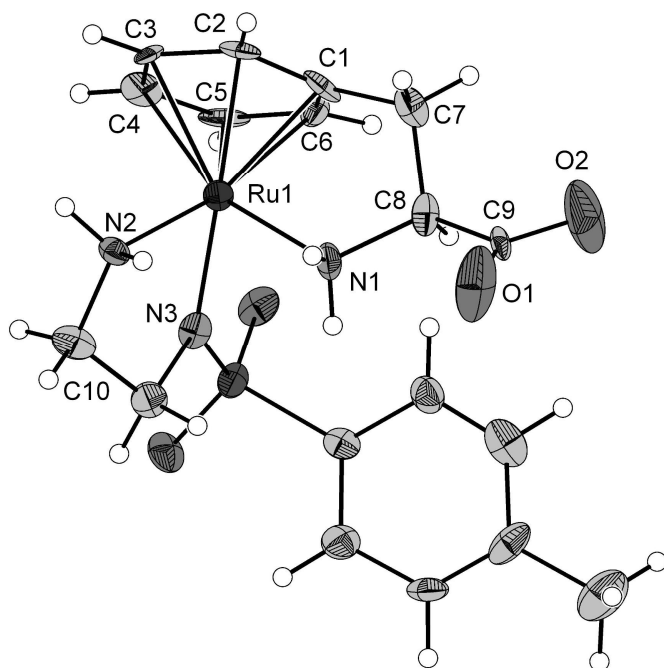


***Abbildung E2:*** ORTEP-Darstellung eines η⁶:η¹-Aren Phenylalanin-koordinierten Ruthenium(II)-Komplexes.

Die katalytische Aktivität der η⁶-Aren Ru(II)-Bibliothek wurde in der katalytischen zweiphasigen Hydrierung von Olefinen bestimmt. Hierbei wurden die TOFs der verschiedenen funktionellen Gruppen und Linker-Längen verglichen. Auch der Einfluss verschiedener Temperaturen, Drücke und pH-Werte wurde bestimmt. Studien der Komplex-Strukturen vor und nach der Katalyse zeigten, dass nicht nur die Aktivität der Systeme hinreichend für einen Einsatz als Metalla-Affinitätsmarker sind, sondern dass auch die Stabilität der η⁶-Aren Liganden groß genug ist, um Konjugation über sie zu ermöglichen.

# η⁵-Cp* Rhodium(III) und Iridium (III) Komplexe

Neben Ruthenium und Osmium wurden auch Rhodium und Iridium verwendet, um nicht koordinierte funktionalisierte Katalysatoren zu generieren. Hier wurde statt 1,4-Cyclohexadien-Derivaten ein Ethylamin Cp*-Tautomeres verwendet, welches mit Rh(III) und Ir(III) Chloriden zu den entsprechenden halogenverbrückten dinuklearen Ethylamin funktionalisierten Cp*-Derivaten reagiert (Schema E3).
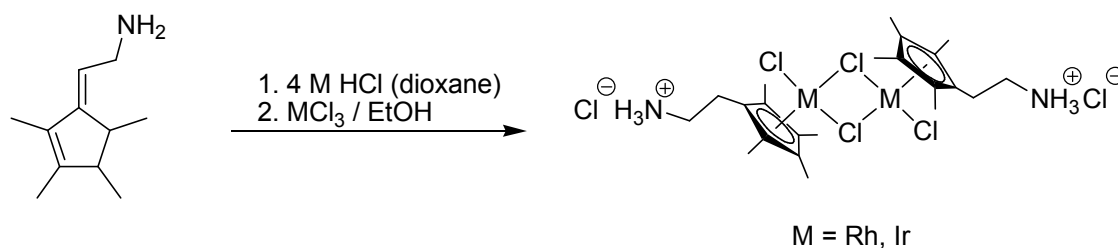


**Schema E3:** Synthese von Rhodium(III) und Iridium(III)-Komplexen mit nicht-koordinierten funktionalisierbaren Linkern.

Die Rhodium-Spezies kann mit Triphenylphosphan zu ihrem einkernigen Analogon umgesetzt werden. Anschließende Umsetzung dieser Spezies mit organischen Anhydriden hat keine Änderung der inneren Koordinationssphäre des Metallzentrums zur Folge. Vielmehr wird das Anhydrid selektiv vom Amin-Linker des Metallkomplexes angegriffen und so der Katalysator ausschließlich in seiner äußeren Koordinationssphäre modifiziert (Schema E4).
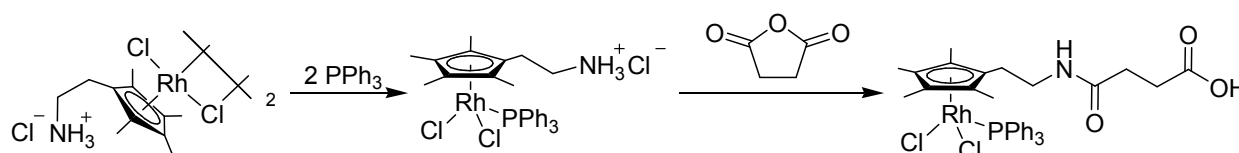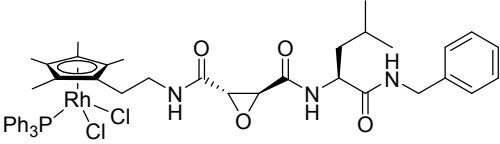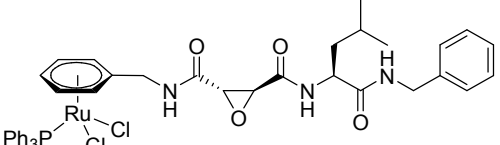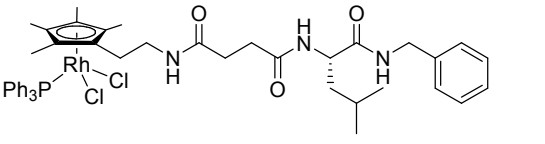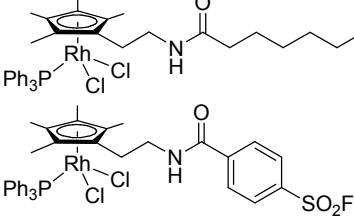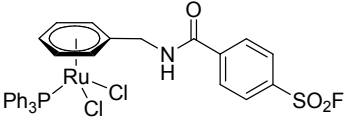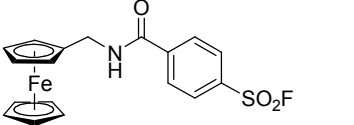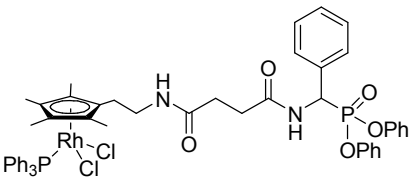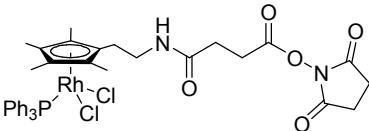


**Schema E4:** Selektive Funktionalisierung eines Rhodium(III)-Katalysators.

Die Möglichkeit, halogen-verbrückte Metallkomplexe selektiv am Metallzentrum (Triphenylphosphan) oder an der funktionalisierten Gruppe des Rings (Carbonsäureanhydrid) zu modifizieren, bestätigt die Eignung dieser Klasse von Verbindungen als Baustein für die Synthese von Metalla-Affinitätsmarkern.

## Synthese von Metalla-Affinitätsmarkern und Metalla-Linkern

Neben Carbonsäureanhydriden kann eine Konjugation von Metallzentrum und peptidischem Affinitätsmarker auch über Pentafluorphenol-Aktivester und Carbonsäurefluoride realisiert werden, welche aufgrund ihrer Elektrophilie von Aminen

**Tabelle E1:** Metalla-Affinitätsmarker und Metalla-Linker, die im Rahmen dieser Arbeit synthetisiert wurden. Als reaktive Gruppen wurden Peptidyl-Epoxide, Phosphonsäurefluoride, Sulfonsäurefluoride oder Phosphonsäure Diphenylester verwendet. Auch nicht-kovalent bindende Analoga der Peptidyl-Epoxide und unspezifisch bindende Succinimid-Linker wurden dargestellt.

| Nr. | Reaktive Gruppe | Inhibierte Enzymklasse | Lewis-Strukturformel |
|-----|-----------------|------------------------|----------------------|
| 1 | Peptidyl-Epoxid | Cystein Protease |  |
| 2 | Nicht-kovalentes Analogon von Peptidyl-Epoxiden | Cystein Protease |  |
| 3 | Phosphonsäurefluorid | Serin Protease |  |
| 4 | Sulfonsäurefluorid | Serin Protease |  |
| 5 | Phosphonsäure Diphenylester | Serin Protease |  |
| 6 | Unspezifischer Linker | Nicht spezifisch |  |

angegriffen werden können. Im Rahmen aller drei Methoden wurden Peptidbindungen zwischen dem Metallkomplex und dem zu konjugierenden organischen Rest erzeugt.

Bei allen im Rahmen dieser Arbeit entwickelten Methoden bleibt die innere Koordinationssphäre des Metallzentrums intakt. Die Syntheserouten über Pentafluorphenol-Aktivester oder Carbonsäurefluoride sind extrem mild. Sie tolerieren leicht zu spaltende Gruppen wie Epoxide, Sulfonsäurefluoride, Phosphonsäurefluoride

oder Phosphonsäure Diphenylester. Tabelle E1 zeigt eine Aufstellung der im Rahmen dieser Arbeit synthetisierbaren Metalla-Affinitätslabel und Metalla-Linker. Abbildung E3 (Teil a) zeigt die ORTEP-Darstellung von [Rh]-SF (Tabelle E1, Nr. 4), welcher im Rahmen dieser Arbeit kristallisiert wurde. Die Struktur bestätigt, dass sowohl die innere Koordinationssphäre des Katalysators als auch das Sulfonsäurefluorid intakt erhalten wurden.
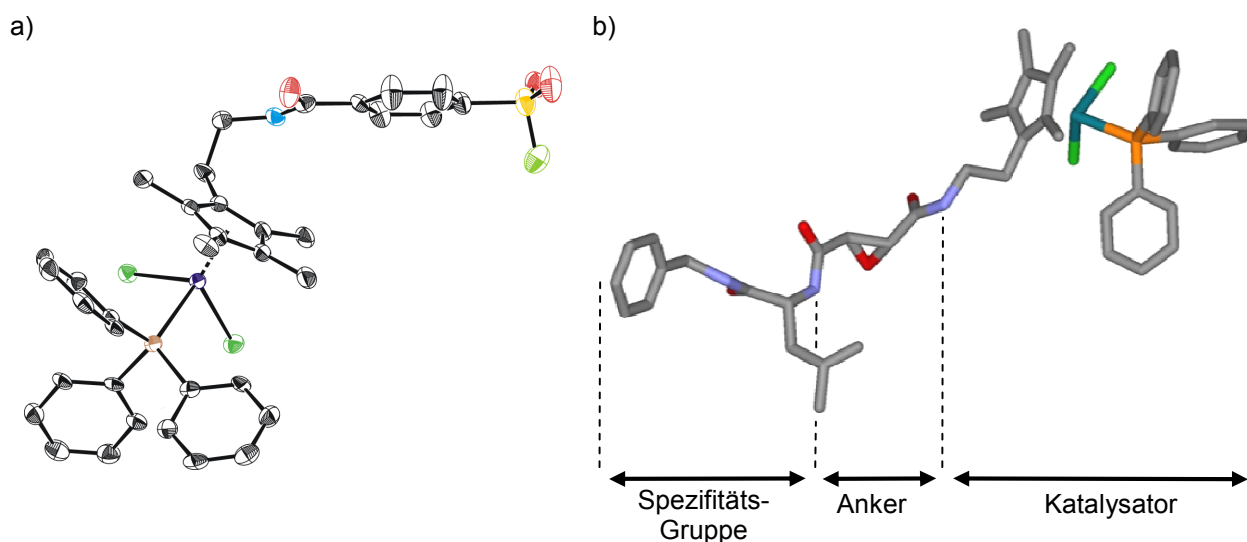
a)         b)



**Abbildung E3:** (a) ORTEP-Darstellung von [Rh]-SF **91**, einer der im Rahmen dieser Arbeit synthetisierten Metalla-Linker. (b) Stabdarstellung der Kristallstruktur des Peptidyl-Epoxid Metalla-Affinitätsmarkers [Rh]-Epx **70**.

Eine weitere Kristallstruktur wurde von dem Metalla-Affinitätsmarker [Rh]-Epx (Tabelle E1, Nr. 1) erhalten. Eine Darstellung der Kristallstruktur in Stabdarstellung zeigt deutlich die verschiedenen Segmente, aus denen der Metalla-Affinitätsmarker aufgebaut ist (Abbildung E3, Teil b). Der peptidische Affinitäts-Teil, die zentrale reaktive Epoxid-Gruppe und der organometallische Katalysator.

Schema E5 stellt die Syntheseroute des Metalla-Affinitätsmarkers ([Rh]-Epx) dar. Hier zeigen sich die Vorteile des Baukastensystems, über welches diese Verbindungsklasse aufgebaut werden kann (15 Schritte). Trotz der insgesamt hohen Zahl verschiedener Reaktionsschritte, die notwendig sind, um diesen Metalla-Affinitätsmarker zu synthetisieren, ist aus dem Schema klar ersichtlich, dass nur die letzten drei Reaktionsschritte für die Kupplung der verschiedenen Teilsegmente verantwortlich sind. Soll zum Beispiel das Metallzentrum (Ruthenium statt Rhodium) variiert werden, ist nur ein zusätzlicher Reaktionsschritt notwendig. So können mit Hilfe kombinatorischer Synthese trotz der aufwändigen Synthese einzelner Komponenten viele verschiedene Metalla-Affinitätsmarker in kurzer Zeit und mit geringem synthetischen Aufwand dargestellt werden.
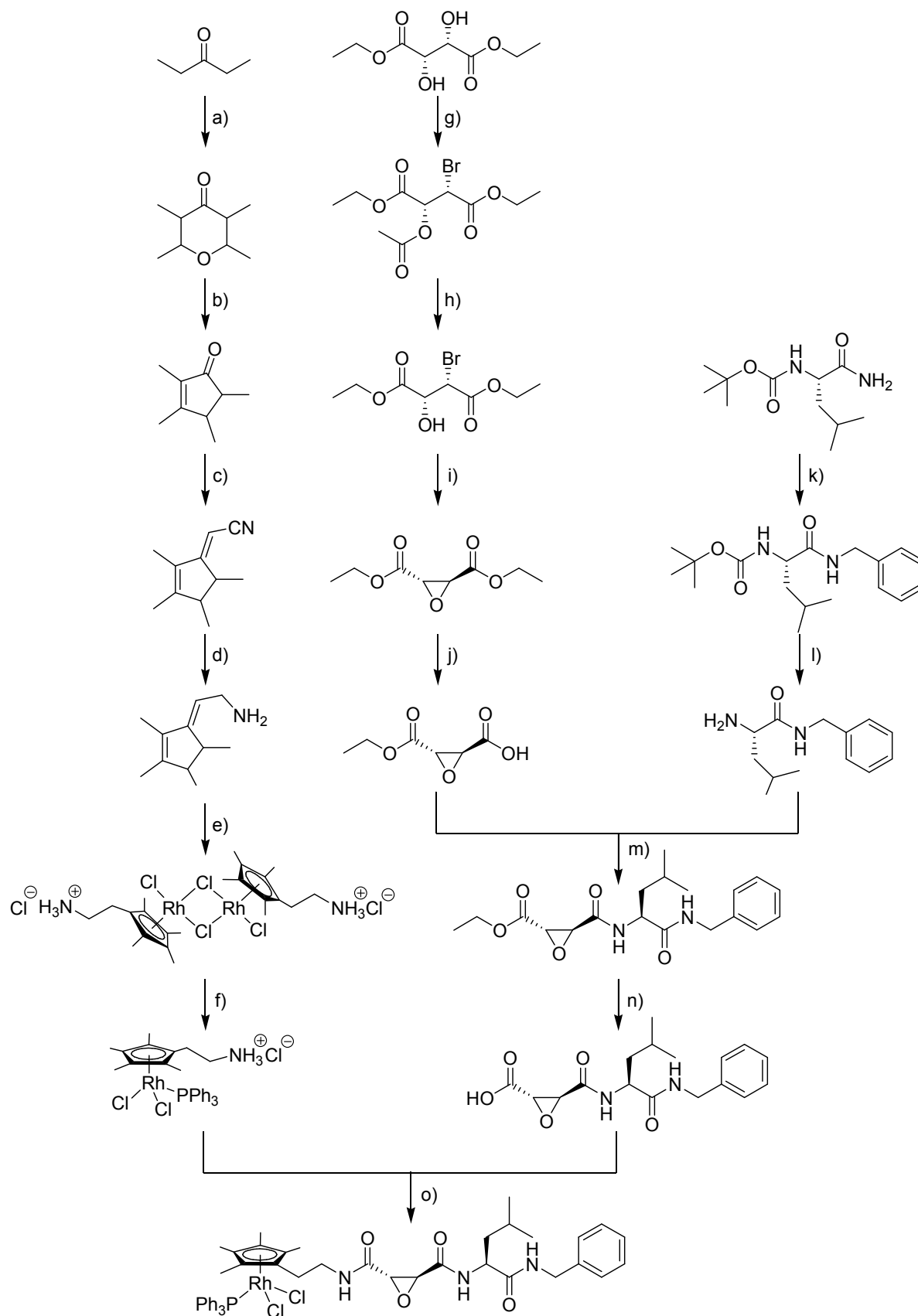
***Schema E5:*** Syntheseroute zur Darstellung von [Rh]-Epx, ein Peptidyl-Epoxid Metalla-Affinitätsmarker. (a) KOH, CH$_3$COH, 0 °C, (MeOH); (b) 80°C (H$_2$CO, H$_2$SO$_4$); (c) AcN, $^t$BuLi (THF); (d) LiAlH$_4$, 55°C, (Et$_2$O); (e) RhCl$_3$, HCl, reflux, (EtOH); (f) PPh$_3$, RT, (DMSO); (g) HBr, 0 °C, (AcOH); (h) CH$_3$COCl, reflux, (EtOH); (i) DBU, 0°C, (Et$_2$O); (j) 1eq. KOH, 0°C, (EtOH$_{abs.}$); (k) C$_6$H$_5$CH$_2$NH$_2$, EDCI, 0°C, (DCM); (l) TFA, (DCM); (m) EDCI, 0°C, (DCM); (n) 1eq. KOH, 0°C, (EtOH$_{abs.}$); (o) 1. SS-DCC, HOPfp, 0 °C (DCM), 2. Et$_3$N, RT, (DCM).

## Umsetzung von Metalla-Affinitätsmarkern zu Organometall-Enzym-Hybriden

Die Synthese von Organometall-Enzym-Hybriden gelang, indem die verschiedenen Metalla-Affinitätsmarker und Metalla-Linker zusammen mit ihren entsprechenden Enzymen (Bromelain, Papain, α-Chymotrypsin oder Trypsin) in wässrigen Pufferlösungen umgesetzt wurden. Auf diese Art und Weise können mit einem Metalla-Affinitätsmarker oder Metalla-Linker verschiedene Organometall-Enzym-Hybride entworfen werden. Aufgrund der unterschiedlichen Umgebungen im aktiven Zentrum haben die eigebetteten Katalysatoren dabei unterschiedliche Eigenschaften in der asymmetrischen Katalyse. Die kovalente Inhibition der Enzyme wurde durch verschiedene Methoden bestätigt, unter anderem durch chromogene Inihbitionsassays oder MALDI-TOF-Messungen. Um auszuschließen, dass eine Inhibition über die Lewis-Sauren Metallzentren statt der reaktiven Gruppen erfolgt, wurde auch ein nicht-kovalentes Analogon des Peptidyl-Epoxids [Rh]-Epx (Tabelle E1, Nr. 1-2) verwendet. Hierbei zeigte sich, dass sowohl in MALDI-TOF Messungen als auch bei chromogenen Aktivitätsassays keine Inhibition des Enzyms auftritt, wenn die reaktive Epoxid-Gruppe nicht vorhanden ist (Abbildung E4). Dies bestätigte den konzeptionellen Bindungsmechanismus der Metalla-Aktivitätsmarker (Abbildung E1).
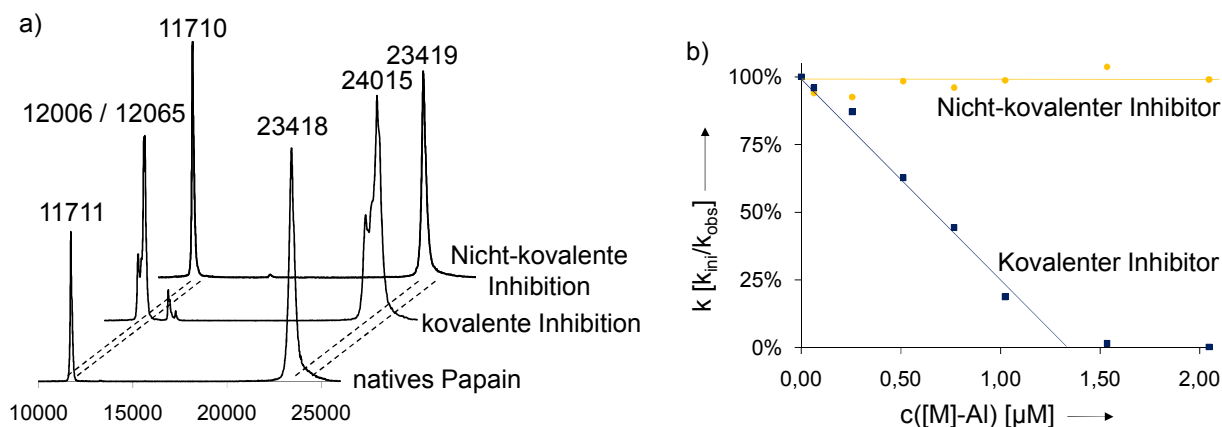


**Abbildung E4:** (a) MALDI-TOF Massenspektren von nativem Papain, kovalent inhibiertem Papain ([Rh]-Epx) und Papain in Anwesenheit eines nicht-kovalenten Inhibitors ([Rh]-Deox). (b) Chromogenes Inhibitionsassay mit kovalentem Inhibitor ([Rh]-Epx) und nicht-kovalentem Inhibitor ([Rh]-Deox).

## Anwendung von Organometall-Enzym-Hybriden in der asymmetrischen Katalyse

Die synthetisierten Organometall-Enzym-Hybride wurden in der asymmetrischen Hydrierung (Cystein-Proteasen) oder Transferhydrierung (Serin-Proteasen) eingesetzt. Ihre Eigenschaften wurden in screenings optimiert, wobei unterschiedliche pH-Werte der Pufferlösungen, Katalysatorkonzentrationen, Temperaturen, Drücke (im Falle von

Transferhydrierungen: Formiatkonzentrationen) und Substrate getestet wurden. Zusätzlich wurden Kinetiken erstellt, um Änderungen der Enantioselektivität bei langen Reaktionszeiten zu beobachten. Hierbei wurde die Modularität der Generierung von Organometall-Enzym-Hybriden bestätigt. Enantioselektivitäten und Aktivitäten hängen hierbei von den unterschiedlichen eingesetzten Metalla-Affinitätsmarkern ab. Zum Beispiel invertiert sich die Selektivität, wenn [Rh]-Epx@Papain anstelle von [Ru]-Epx@Papain verwendet wird. Werden nicht-kovalent bindende Metallzentren eingesetzt, werden sowohl bei Serin als auch bei Cystein-Proteasen keine oder nur sehr geringe Enantioselektivitäten erreicht. Im besten Falle wurden Enantiomerenüberschüsse von 64% (*R*) bei der Hydrierung von 4-Chlor-Acetophenon erreicht (12% Umsatz). Die besten Umsätze lieferte 2,2,2-Trifluoroacetophenon (92%) bei gleichzeitigen Enantioselektivitäten von 20% (*R*). Neben asymmetrischen Hydrierungen wurden Organometall-Enzym-Hybride auch erfolgreich in der asymmetrischen Transferhydrierung getestet, wobei Enantioselektivitäten von bis zu 20 % erreicht werden konnten.

Grundsätzlich konnte das im Rahmen dieser Arbeit erarbeitete Konzept zur Darstellung von Organometall-Enzym-Hybriden umgesetzt und erfolgreich in der enantioselektiven Katalyse getestet werden (Abbildung E5). Es war möglich, mit Hilfe eines Baukastensystems kombinatorisch eine Bibliothek von Organometall-Enzym-Hybriden zu generieren, welche abhängig von der chiralen Enzymumgebung unterschiedliche Enantioselektivitäten zeigen. Dabei wurde bestätigt, dass bei der Generierung von Organometall-Enzym-Hybriden ein modulares Konzept von essentieller Bedeutung ist, um in kurzer Zeit eine große Menge von Organometall-Enzym-Hybriden zu screenen und im Rahmen möglicher nachfolgender gerichteter Evolution vielversprechendere Optimierungsergebnisse zu erzielen.
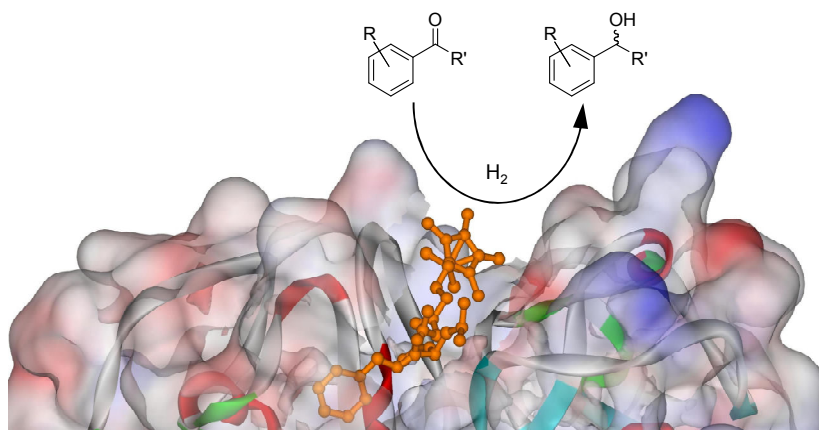


**Abbildung E5:** Eingebetteter Metalla-Affinitätsmarker im aktiven Zentrum von Papain.

# F | List of Publications

## Publications

1. *Side chain functionalized η$^5$-tetramethyl cyclopentadienyl complexes of Rh and Ir with a pendant primary amine group*, Thomas Reiner, Dominik Jantke, Andreas Raba, Alexander N. Marziale, Jörg Eppinger, *J. Organomet. Chem.* **2009**, *in press,* doi:10.1016/j.tetasy.2009.01.022.

2. *$^{31}$P NMR assays for rapid determination of enantiomeric excess in catalytic hydrosilylations and transfer hydrogenations*, Thomas Reiner, Frederik N. Naraschewski, Jörg Eppinger, *Tetrahedron: Asymmetry*, **2009**, *in press,* doi:10.1016/j.jorganchem.2009.01.056.

3. *η$^6$-Arene Half-Sandwich Complexes of Ruthenium and Osmium with a Pendant Donor Functionality*, Thomas Reiner, Markus Waibel, Florian J. Kiefer, Jörg Eppinger, *submitted*.

4. *Metalla affinity labels - a new approach to organometallic enzyme hybrids,* Thomas Reiner, Andreas Raba, Dominik Jantke, Alexander N. Marziale, Jörg Eppinger, *submitted.*

5. *A new and facile protocol for Suzuki coupling at room temperature in aqueous solution*, Alexander N. Marziale, Stefan Faul, Thomas Reiner, Sven Schneider, Jörg Eppinger, *submitted.*

6. *Enantioselective Transfer Hydrogenation of Ketones mediated via activation of anchored achiral organometallic moieties and serine proteases*, Thomas Reiner, Dominik Jantke, Andreas Raba, Jörg Eppinger, *submitted.*

## Presentations and Posters

1. *A New Route Towards Organometallic Enzyme Hybrid Catalysts*, Thomas Reiner, Dominik Jantke, Markus Waibel, Jörg Eppinger, International Symposium on Metallomics 2007, Nagoya, Nov. 28th- Dec. 1st 2007.

2. *Metalla Affinity Labels - A New Route to Organometallic Enzyme Hybrid Catalysts*, Jörg Eppinger, Thomas Reiner, Dominik Jantke, Chemiedozententagung, Kaiserslautern, Apr. 1st 2008.

3. *Metalla Affinity Labels - A New Route to Organometallic Enzyme Hybrid Catalysts*, Thomas Reiner, Jörg Eppinger, NanoCat Evaluation Meeting, Tutzing, June 5th 2008.

4. *Metalla Affinity Labels - A Highly Efficient Route to Organometallic Enzyme Hybrid Catalysts*, Thomas Reiner, Jörg Eppinger, 1st Joint Nano Workshop, München, June 10th 2008.

5. *Synthesis and application of organometallic enzyme hybrid catalysts based on metalla-affinity labels*, Jörg Eppinger, Thomas Reiner, Alexander N. Marziale, Dominik Jantke, Andreas Raba, 236th ACS National Meeting, Philadelphia, PA, USA, Aug. 17th- 21st 2008, INOR-041.

6. *Synthesis and application of organometallic enzyme hybrid catalysts based on metalla-affinity labels*, Thomas Reiner, Alexander N. Marziale, Dominik Jantke, Jörg Eppinger, 14. Vortragstagung der Wöhler-Vereinigung, Garching/München, Oct. 8th- 10th 2008.

# G | Curriculum Vitae

## CURRICULUM VITAE OF THOMAS REINER

### ACADEMIC WORK EXPERIENCE

| | |
|---|---|
| 10.2006 – present | Technical University of Munich, Department of Chemistry, Chair of Inorganic Chemistry (Lichtenbergstrasse 4, 85747 Garching b. München, Germany)<br>Research and Teaching Assistant in form of a PhD position<br><br>• Responsible for a research project in the field of bioorganometallic chemistry;<br>Title: Metalla Affinity Labels – a New Route to Organometallic Enzyme Hybrids<br>• Supervising PhD student for the chair's NMR spectrometers<br>• Supervision of three Bachelor Theses, several student research projects and supervisor for the education of laboratory assistants. |

### ACADEMIC EDUCATION

| | |
|---|---|
| 05.2007 – present | Member of "Nano Cat", an interdisciplinary graduate school<br>Principal subjects: Heterogeneous Catalysis / Homogeneous Catalysis |
| 04.2005 – 04.2006 | Technische Universität München<br>(Lichtenbergstr. 4, 85748 Garching b. München, Germany)<br>M.Sc. in Chemistry<br>Principal subjects: Inorganic Chemistry, Organic Chemistry<br>Thesis Title: Synthesis and Functionalization of Catalytically Active $\eta^6$-Labelled Metalla-Amino Acids<br>Supervisors: Prof. Dr. Dr. h. c. mult. W. A. Herrmann, Dr. Jörg Eppinger |
| 09.2004 – 10.2004 | Successful participation at the summer school programme "Innovation in Science and Technology", Indian Institute of Technology Bombay, Mumbai, India<br>Subjects covered: Technical Chemistry, Physical Chemistry, Organic Chemistry |
| 10.2003 – 03.2004 | University of Oxford; Fellow at St. Anne's College<br>(Woodstock Road, Oxford, OX2 6HS, United Kingdom)<br>2nd and 3rd year lectures in:<br>Subjects covered: Inorganic Chemistry, Organic Chemistry, Organometallic Chemistry |

| | |
|---|---|
| 10.2001 – 04.2005 | Technische Universität München<br>(Lichtenbergstr. 4, 85748 Garching b. München, Germany)<br>B.Sc. in Chemistry<br>Subjects covered: Technical Chemistry, Theoretical Chemistry, Inorganic Chemistry,<br>Organic Chemistry, Physical Chemistry<br>Thesis Title: New Routes to Thiosemicarbazone and Thiosemicarbazide Ligands<br>Supervisors: Prof. Dr. Jon Dilworth (University of Oxford),<br>Prof. Dr. W. Hiller (Technische Universität München) |

**AWARDS AND FELLOWSHIPS**

| | |
|---|---|
| 12.2007 | Poster award at the "International Symposium on Metallomics", Nagoya, Japan |
| 05.2007 | Scholarship granted by the Bavarian Academy of Excellence (ENB-Scholarship) |
| 10.2004 | Bavarian-Swabian award of literature 2004 |
| 10.2003 | European University Exchange Fellowship (Erasmus Fellowship) |
| 06.2003 | Award of literature 2003, granted by the city of Augsburg |

**OTHER WORK EXPERIENCE**

| | |
|---|---|
| 09.2000 – 07.2001 | Bayerisches Rotes Kreuz – Kreisverband Augsburg Land<br>(Gabelsbergerstraße 20, 86199 Augsburg)<br>Compulsory civilian service<br>Responsibility: Organization and assistance at Red Cross blood donation events |
| 07.2000 – 09.2000 | Augsburger Allgemeine Zeitung<br>(Curt-Frenzel-Str. 2, 86167 Augsburg)<br>Occupation: Trainee in the editorial division<br>Responsibility: Evaluating topics and writing articles for the editorial division |